ISSN 1948-5204 (online)

World Journal of *Gastrointestinal Oncology*

World J Gastrointest Oncol 2024 December 15; 16(12): 4532-4781

Published by Baishideng Publishing Group Inc

World Journal of Gastrointestinal Oncology

Contents

Monthly Volume 16 Number 12 December 15, 2024

EDITORIAL

4532 Mixed neuroendocrine non-neuroendocrine tumors: The quest for evidence

Cives M, Porta C, Palmirotta R

4537 Is nutritional status a new indicator to use in clinical practice for colorectal cancer patients?

Berardi R, Chiariotti R, Mentrasti G

4543 Gene targets with therapeutic potential in hepatocellular carcinoma

Shodry S, Hasan YTN, Ahdi IR, Ulhaq ZS

4548 Estimating prognosis of gastric neuroendocrine neoplasms using machine learning: A step towards precision medicine

Wang HN, An JH, Zong L

4553 Exploring Xiaojianzhong decoction's potential in gastric cancer treatment: Integrative insights and experimental validation

Cheng CH, Hao WR, Cheng TH

4559 Critical considerations for the management of gastrointestinal mixed neuroendocrine non-neuroendocrine neoplasms and pure neuroendocrine carcinomas

Pavlidis ET, Galanis IN, Pavlidis TE

REVIEW

4565 Unraveling the role of cancer-associated fibroblasts in colorectal cancer

Cui JY, Ma J, Gao XX, Sheng ZM, Pan ZX, Shi LH, Zhang BG

ORIGINAL ARTICLE

Case Control Study

4579 Prognostic utility of gamma-glutamyl transpeptidase to platelet ratio in patients with solitary hepatitis B virus-related hepatocellular carcinoma after hepatectomy

Yang CK, Wei ZL, Shen XQ, Jia YX, Wu QY, Wei YG, Su H, Qin W, Liao XW, Zhu GZ, Peng T

Retrospective Cohort Study

4597 Prognostic prediction models for postoperative patients with stage I to III colorectal cancer based on machine learning

Ji XL, Xu S, Li XY, Xu JH, Han RS, Guo YJ, Duan LP, Tian ZB

4614 Local excision for middle-low rectal cancer after neoadjuvant chemoradiation: A retrospective study from a single tertiary center

Chen N, Li CL, Wang L, Yao YF, Peng YF, Zhan TC, Zhao J, Wu AW

World Journal of Gastrointestinal Oncology

Monthly Volume 16 Number 12 December 15, 2024

Contents

Retrospective Study

4625 Risk factors for hepatocellular carcinoma in cirrhosis: A comprehensive analysis from a decade-long study

Zhou DQ, Liu JY, Zhao F, Zhang J, Liu LL, Jia JR, Cao ZH

4636 Prognosis of radiotherapy for esophageal cancer in elderly patients exceeding seventy-five years old

Hu LL, Rong F, Liu L, Zhang L, Zhang LL, Yang Q, Xia ZL, Wang H

4650 Nomogram model based on γ-glutamyl transferase to albumin ratio predicts survival in hepatocellular carcinoma patients with transarterial chemoembolization treatment

Wu ZY, Li H, Chen JL, Su K, Weng ML, Han YW

4663 Deep learning model combined with computed tomography features to preoperatively predicting the risk stratification of gastrointestinal stromal tumors

Li Y, Liu YB, Li XB, Cui XN, Meng DH, Yuan CC, Ye ZX

4675 Temozolomide and capecitabine regimen as first-line treatment in advanced gastroenteropancreatic neuroendocrine tumors at a Latin American reference center

Cruz-Diaz WE, Paitan V, Medina J, Flores R, Haro-Varas J, Mantilla R, Castro-Oliden V

Basic Study

4685 Vitamin D 1,25-Dihydroxyvitamin D_3 reduces lipid accumulation in hepatocytes by inhibiting M1 macrophage polarization

Luo WJ, Dong XW, Ye H, Zhao QS, Zhang QB, Guo WY, Liu HW, Xu F

4700 Matrine promotes colorectal cancer apoptosis by downregulating shank-associated RH domain interactor expression

Zhou YC, Wang QQ, Zhou GYJ, Yin TF, Zhao DY, Sun XZ, Tan C, Zhou L, Yao SK

4716 Enhancing the radiosensitivity of colorectal cancer cells by reducing spermine synthase through promoting autophagy and DNA damage

Guo YB, Wu YM, Lin ZZ

META-ANALYSIS

4728 Efficacy and safety of transhepatic arterial chemoembolization with drug-loaded microspheres in unresectable primary liver cancer

Deng J, Mi YH, Xie L, Sun XX, Liu DH, Long HJ, He LY, Wu DH, Shang HC

CASE REPORT

4738 Mixed pancreatic ductal adenocarcinoma and well-differentiated neuroendocrine tumor: A case report

Zhao X, Bocker Edmonston T, Miick R, Joneja U

4746 Signet-ring cell carcinoma of the transverse colon in a 10-year-old girl: A case report

Lv L, Song YH, Gao Y, Pu SQ, A ZX, Wu HF, Zhou J, Xie YC

World Journal of Gastrointestinal Oncology

Monthly Volume 16 Number 12 December 15, 2024

Contents

LETTER TO THE EDITOR

4753 Combinations of lenvatinib and immune checkpoint inhibitors plus transarterial chemoembolization, is it the prime time for unresectable hepatocellular carcinoma?

Centrone N, Serrano Uson Junior PL

4757 Advancing hepatocellular carcinoma treatment with hepatic arterial infusion chemotherapy

Caliskan Yildirim E, Ergun Y

4762 Timely identification and treatment of uterine artery pseudoaneurysm after hysteroscopic procedures

Byeon H

4766 Current efficacy of hepatic arterial infusion chemotherapy in hepatocellular carcinoma

Dias E Silva D, Borad M, Uson Junior PLS

4770 Use of traditional Chinese medicine bezoars and bezoar-containing preparations in hepatocarcinoma

Li DH, Wen QE, Feng RQ, Qiao C, Tian XT

4778 Crosslink among cyclin-dependent kinase 9, ATP binding cassette transporter G2 and Beclin 1 in colorectal cancer

Shao ZB, He K, Su YB, Shi Z

World Journal of Gastrointestinal Oncology

Monthly Volume 16 Number 12 December 15, 2024

Contents

ABOUT COVER

AIMS AND SCOPE

The primary aim of *World Journal of Gastrointestinal Oncology* (*WJGO*, *World J Gastrointest Oncol*) is to provide scholars and readers from various fields of gastrointestinal oncology with a platform to publish high-quality basic and clinical research articles and communicate their research findings online.

WJGO mainly publishes articles reporting research results and findings obtained in the field of gastrointestinal oncology and covering a wide range of topics including liver cell adenoma, gastric neoplasms, appendiceal neoplasms, biliary tract neoplasms, hepatocellular carcinoma, pancreatic carcinoma, cecal neoplasms, colonic neoplasms, colorectal neoplasms, duodenal neoplasms, esophageal neoplasms, gallbladder neoplasms, *etc*.

INDEXING/ABSTRACTING

The *WJGO* is now abstracted and indexed in PubMed, PubMed Central, Science Citation Index Expanded (SCIE, also known as SciSearch®), Journal Citation Reports/Science Edition, Scopus, Reference Citation Analysis, China Science and Technology Journal Database, and Superstar Journals Database. The 2024 edition of Journal Citation Reports® cites the 2023 journal impact factor (JIF) for *WJGO* as 2.5; JIF without journal self cites: 2.5; 5-year JIF: 2.8; JIF Rank: 72/143 in gastroenterology and hepatology; JIF Quartile: Q3; and 5-year JIF Quartile: Q2. The *WJGO*'s CiteScore for 2023 is 4.2 and Scopus CiteScore rank 2023: Gastroenterology is 80/167; Oncology is 196/404.

RESPONSIBLE EDITORS FOR THIS ISSUE

Production Editor: *Si Zhao*; **Production Department Director:** *Xiang Li*; **Cover Editor:** *Jia-Ru Fan*.

NAME OF JOURNAL
World Journal of Gastrointestinal Oncology

ISSN
ISSN 1948-5204 (online)

LAUNCH DATE
February 15, 2009

FREQUENCY
Monthly

EDITORS-IN-CHIEF
Monjur Ahmed, Florin Burada

EDITORIAL BOARD MEMBERS
https://www.wjgnet.com/1948-5204/editorialboard.htm

PUBLICATION DATE
December 15, 2024

INSTRUCTIONS TO AUTHORS
https://www.wjgnet.com/bpg/gerinfo/204

GUIDELINES FOR ETHICS DOCUMENTS
https://www.wjgnet.com/bpg/GerInfo/287

GUIDELINES FOR NON-NATIVE SPEAKERS OF ENGLISH
https://www.wjgnet.com/bpg/gerinfo/240

PUBLICATION ETHICS
https://www.wjgnet.com/bpg/GerInfo/288

PUBLICATION MISCONDUCT
https://www.wjgnet.com/bpg/gerinfo/208

ARTICLE PROCESSING CHARGE
https://www.wjgnet.com/bpg/gerinfo/242

STEPS FOR SUBMITTING MANUSCRIPTS
https://www.wjgnet.com/bpg/GerInfo/239

ONLINE SUBMISSION
https://www.f6publishing.com

World Journal of Gastrointestinal Oncology

Submit a Manuscript: https://www.f6publishing.com

World J Gastrointest Oncol 2024 December 15; 16(12): 4532-4536

DOI: 10.4251/wjgo.v16.i12.4532

ISSN 1948-5204 (online)

EDITORIAL

Mixed neuroendocrine non-neuroendocrine tumors: The quest for evidence

Mauro Cives, Camillo Porta, Raffaele Palmirotta

Specialty type: Oncology

Provenance and peer review: Invited article; Externally peer reviewed.

Peer-review model: Single blind

Peer-review report's classification

Scientific Quality: Grade A, Grade C, Grade D

Novelty: Grade A, Grade B, Grade C

Creativity or Innovation: Grade A, Grade C, Grade C

Scientific Significance: Grade A, Grade B, Grade B

P-Reviewer: Lu H; Wang D; Zhu X

Received: April 8, 2024

Revised: July 16, 2024

Accepted: July 22, 2024

Published online: December 15, 2024

Processing time: 218 Days and 0.8 Hours

Mauro Cives, Camillo Porta, Raffaele Palmirotta, Interdisciplinary Department of Medicine, University of Bari "Aldo Moro", Bari 70124, Italy

Mauro Cives, Camillo Porta, Department of Medical Oncology, AOU Consorziale Policlinico di Bari, Bari 70124, Italy

Corresponding author: Raffaele Palmirotta, MD, PhD, Associate Professor, Senior Researcher, Interdisciplinary Department of Medicine, University of Bari "Aldo Moro", Piazza G. Cesare 11, Bari 70124, Italy. raffaelepalmirotta@gmail.com

Abstract

Mixed neuroendocrine non-neuroendocrine neoplasms (MiNENs) are rare mixed tumors containing both neuroendocrine and non-neuroendocrine components that occupy at least 30% of the whole tumor. Biologically, both components appear to derive from an identical cellular precursor undergoing early dual differentiation or late transdifferentiation. While our understanding of MiNENs has improved in recent years, many areas of uncertainty remain. In this context, setting diagnostic criteria capable of capturing the continuum of disease biology while providing clinically meaningful information in terms of prognosis and response to treatments appears vital to advance the field and improve patients' outcomes. Evidence is needed to generate robust classification schemes, and multi-institutional cooperation will likely play a crucial role in building adequately powered cohorts to address some of the most pressing questions discussed in this Editorial. What is the minimum representation for each component needed to define MiNENs? How can the epidemiology of MiNENs change according to different diagnostic definitions? How can we generate the clinical evidence nee-ded to optimize the management of MiNENs?

Key Words: Mixed neuroendocrine non-neuroendocrine neoplasms; Neuroendocrine neoplasm; Neuroendocrine carcinoma; Mixed tumors; Digestive; Gastroenteropancreatic

Core Tip: In this Editorial, we highlight potential pitfalls in the current classification of mixed neuroendocrine non-neuroendocrine neoplasms and comment on challenges in the management of this heterogeneous group of malignancies in light of the paucity of evidence in the field. Improved biological and clinical knowledge is needed to generate robust classification schemes that will in turn provide clarity on the epidemiology of the disease, prognosis of affected patients and guidance for treatment tailoring.

Citation: Cives M, Porta C, Palmirotta R. Mixed neuroendocrine non-neuroendocrine tumors: The quest for evidence. *World J Gastrointest Oncol* 2024; 16(12): 4532-4536
URL: https://www.wjgnet.com/1948-5204/full/v16/i12/4532.htm
DOI: https://dx.doi.org/10.4251/wjgo.v16.i12.4532

INTRODUCTION

In their timely review in this issue of *World Journal of Gastrointestinal Oncology*, Díaz-López *et al*[1] provide a comprehensive description of the biology and clinical management of mixed neuroendocrine non-neuroendocrine neoplasms (MiNENs). According to the 2022 World Health Organization (WHO) classification[2], MiNENs consist of both a neuroendocrine component and an adenocarcinoma, signet ring cell carcinoma or, more rarely, squamous cell carcinoma component, with each component exceeding 30%. While knowledge of this group of malignancies has evolved in recent years, the emergence of new data has perhaps raised as many questions as it has answered.

One key theme around MiNENs is how we exactly define them. "All models are wrong, but some are useful" is an aphorism attributed to the statistician George Box. While histopathological classifications are imperfect per se, they provide crucial information in oncology. However, a priori evidence (*i.e.* survival rates according to different groups) is needed to build models (histopathological classifications) capable of conveying useful information. Where is the evidence when it comes to the WHO classification of MiNENs? Non-neuroendocrine components are present in approximately 40% of gastroenteropancreatic neuroendocrine carcinomas[3], a figure way larger than the perceived frequency of MiNENs. Indeed, only a proportion of such malignancies (namely those tumors harboring neuroendocrine and non-neuroendocrine components exceeding the arbitrarily established 30% cut-off) are currently captured as MiNENs according to the 2022 WHO classification[2]. Is thus a scattered minor neuroendocrine or non-neuroendocrine component irrelevant in terms of clinical behavior, treatment response or prognosis? Possibly no, at least according to studies showing that a neuroendocrine component > 20% or even > 10% can affect patients' prognosis[4-7]. Not only do these data question the appropriateness of the arbitrarily chosen 30% cut-off, they also indicate that divergent lineage differentiation (namely the presence of neuroendocrine component in non-neuroendocrine cancers and vice versa) has profound prognostic (and perhaps therapeutic) implications per se. Notably, such concept has been already incorporated in the last edition of the WHO classification of thoracic tumors where "combined neuroendocrine/non-neuroendocrine lung tumors" refer to mixed entities combining high-grade neoplasms representing at least 10% of the whole tumor[8]. While the arbitrarily chosen 30% cut-off will be probably revisited in the upcoming WHO classifications of digestive tumors, quantification and reporting of the neuroendocrine and non-neuroendocrine components in mixed tumors is presently advisable. Why relatively small foci of neuroendocrine components in non-neuroendocrine cancers may dictate an aggressive clinical behavior remains largely unknown.

Building a model upon high-level evidence is key to render the model itself relevant and useful. While a relevant model should be able to precisely capture the biology of the disease in its entirety, a useful model should be able to set the criteria needed for defining the epidemiology of the disease, predicting prognosis and, ideally, response to treatments.

BUILDING A RELEVANT MODEL

So far, fundamental research investigating the molecular alterations of MiNENs has relied on the WHO classification criteria. This means that molecular investigations have been carried out on samples selected within the boundaries imposed by the WHO classification. By doing so, several distinctive traits of MiNENs have been identified. First, multiple studies[9-11] have shown that neuroendocrine and non-neuroendocrine components share a common trunk of mutations, with passenger mutations showing segregation in a specific component. Second, the spectrum of shared mutations is typically similar to that observed in pure adenocarcinomas of the specific anatomic site[11]. Third, allelic imbalances and chromosomal aberrations are more frequent in the neuroendocrine component rather than in the non-neuroendocrine component[12]. While these observations support the hypothesis that the neuroendocrine and non-neuroendocrine components of MiNENs have a monoclonal origin and then undergo an early dual differentiation or a late subclonal transdifferentiation, whether such a biological process could be confined within the boundaries of a percent threshold is disputable. In this context, whether divergent molecular alterations could be found in mixed tumors with different neuroendocrine/non-neuroendocrine percent representation (including representation below the 30% threshold) is currently unknown. A critical appraisal of the molecular underpinnings of mixed tumors of the digestive tract according to the relative component distribution is needed to inform future classification schemes.

BUILDING A USEFUL MODEL

Inconsistent reporting and varying nomenclature over the past several decades make it difficult to estimate the actual incidence of MiNENs. However, it is likely that the frequency of MiNENs is currently underestimated, primarily as result of challenges in diagnosis. Well-curated multi-institutional analyses from tertiary centers managing high volumes of patients with NENs might provide a better snapshot than tumor registries, although representativeness of the sample would be matter of concern. What would be the impact of lowering the percent threshold for each component in mixed tumors of the digestive tract in terms of incidence and prevalence? No answer can be given at present.

As pointed out by Díaz-López and colleagues in their review[1], the neuroendocrine component of MiNENs dictates patients' prognosis. Several lines of evidence support this conclusion. First, survival outcomes of MiNENs compare similarly to those of NEC patients, diverging from those of non-neuroendocrine cancers[13]. Second, the neuroendocrine component is almost always responsible for the metastatic process[14,15]. Third, the Ki-67 index of the neuroendocrine component determines the natural history of the disease[16,17]. Nevertheless, these concepts represent an oversimplification of the MiNEN reality. Indeed, MiNENs can contain tumor entities with variable degrees of biological aggressiveness in the neuroendocrine and non-neuroendocrine component, and a widely accepted grading system is presently lacking. Although La Rosa's proposal[3] to subdivide MiNENs into low-grade, intermediate-grade and high-grade entities according to the most aggressive component appears valuable to inform management decisions (Table 1), its prognostic relevance remains to be evaluated by large series studies. In this regard, caution should be posed when interpreting survival outcomes in MiNEN patients. Indeed, only lower stage tumors are likely to undergo surgery and can be consequently diagnosed as MiNENs, whereas advanced tumors are more likely to undergo biopsy and can be possibly categorized based on a sample where the dual component is not represented. As result, while observational studies may overestimate the benefit of surgery in MiNENs, comparisons between MiNENs and other tumor entities such as pure NECs or pure non-neuroendocrine cancers hold a substantial risk of selection bias and immortal time bias.

Table 1 Proposed grading and systemic management of mixed neuroendocrine non-neuroendocrine neoplasms

Grades	Neuroendocrine component	Non-neuroendocrine component	Systemic management
Low	Well-differentiated NET, Grade 1 Ki-67 < 3%, MI < 2/10 HPF, Grade 2 Ki-67 3-20, MI 2-20/10 HPF	Adenoma	Somatostatin analogs; Radiolabeled somatostatin analogs (when $SSTR^+$); Everolimus; Sunitinib (pancreatic primaries); Temozolomide-based chemotherapy
Intermediate	Well-differentiated NET, Grade 1 Ki-67 < 3%, MI < 2/10 HPF, Grade 2 Ki-67 3-20, MI 2-20/10 HPF	Adenocarcinoma, signet ring cell carcinoma, mucinous neoplasm	5-FU-based regimens (*i.e.* FOLFIRINOX, FOLFIRI, FOLFOX, *etc*), Targeted therapies according to molecular profiling
High	NEC (small/large cell)	Adenocarcinoma, squamous cell carcinoma, acinar cell carcinoma, adenosquamous carcinoma, mucinous carcinoma, signet ring cell carcinoma	Etoposide/Platinum 5-FU-based regimens (*i.e.* FOLFIRINOX, FOLFIRI, FOLFOX, *etc*), Targeted therapies according to molecular profiling

HPF: High power field; MI: Mitotic index; NEC: Neuroendocrine carcinoma; NET: Neuroendocrine tumor.

Evidence on MiNEN treatment is very limited, and guidelines[18] often extrapolate data from neuroendocrine and non-neuroendocrine space. In most institutions, when a poorly differentiated neuroendocrine component is present, the etoposide/platinum regimen is recommended; on the other hand, when the non-neuroendocrine component is the most aggressive one, 5-FU-based combinations are preferred[19]. Whether etoposide/platinum combination is the most effective option for the upfront treatment of high-grade NENs has been recently questioned[20], and prospective evidence, possibly generated by using innovative clinical trial designs[21], is needed to guide the management of patients with MiNEN.

CONCLUSION

The frequency of MiNENs appears very low at present, but future changes to the WHO classification as well as improved recognition of these entities among both pathologists and clinicians might change the epidemiology of the disease, allowing a better understanding of their biology, natural history and clinical management. While the need of the hour is how we exactly define MiNENs, questing for high-level evidence through collaborative studies will certainly be instrumental to improve patients' outcomes.

FOOTNOTES

Author contributions: Cives M, Porta C and Palmirotta R contributed to this paper; Palmirotta R designed the overall concept and outline

of the manuscript; Cives M and Palmirotta R contributed to the discussion and design of the manuscript; Cives M, Porta C and Palmirotta R contributed to the writing and editing of the manuscript, and review of literature.

Supported by The Associazione Italiana per la Ricerca sul Cancro, No. 23583; and The Apulia Region ("Il Team Oncogenomico: Modello operativo per la riduzione dei costi dell'assistenza sanitaria in Oncologia" Project).

Conflict-of-interest statement: Authors declare no conflicts of interest.

Country of origin: Italy

ORCID number: Mauro Cives 0000-0002-3013-1816; Camillo Porta 0000-0003-2412-1563; Raffaele Palmirotta 0000-0002-9401-7377.

S-Editor: Liu H
L-Editor: Filipodia
P-Editor: Zhao YQ

REFERENCES

1 **Díaz-López S**, Jiménez-Castro J, Robles-Barraza CE, Ayala-de Miguel C, Chaves-Conde M. Mixed neuroendocrine non-neuroendocrine neoplasms in gastroenteropancreatic tract. *World J Gastrointest Oncol* 2024; **16**: 1166-1179 [PMID: 38660639 DOI: 10.4251/wjgo.v16.i4.1166]
2 **WHO Classification of Tumours Editorial Board**. WHO classification of endocrine and neuroendocrine tumours. Available from: https://tumourclassification.iarc.who.int/welcome/
3 **La Rosa S**, Sessa F, Uccella S. Mixed Neuroendocrine-Nonneuroendocrine Neoplasms (MiNENs): Unifying the Concept of a Heterogeneous Group of Neoplasms. *Endocr Pathol* 2016; **27**: 284-311 [PMID: 27169712 DOI: 10.1007/s12022-016-9432-9]
4 **Park JY**, Ryu MH, Park YS, Park HJ, Ryoo BY, Kim MG, Yook JH, Kim BS, Kang YK. Prognostic significance of neuroendocrine components in gastric carcinomas. *Eur J Cancer* 2014; **50**: 2802-2809 [PMID: 25201164 DOI: 10.1016/j.ejca.2014.08.004]
5 **Lewin K**. Carcinoid tumors and the mixed (composite) glandular-endocrine cell carcinomas. *Am J Surg Pathol* 1987; **11** Suppl 1: 71-86 [PMID: 3544888 DOI: 10.1097/00000478-198700111-00007]
6 **de Mestier L**, Cros J, Neuzillet C, Hentic O, Egal A, Muller N, Bouché O, Cadiot G, Ruszniewski P, Couvelard A, Hammel P. Digestive System Mixed Neuroendocrine-Non-Neuroendocrine Neoplasms. *Neuroendocrinology* 2017; **105**: 412-425 [PMID: 28803232 DOI: 10.1159/000475527]
7 **La Rosa S**. Challenges in High-grade Neuroendocrine Neoplasms and Mixed Neuroendocrine/Non-neuroendocrine Neoplasms. *Endocr Pathol* 2021; **32**: 245-257 [PMID: 33786701 DOI: 10.1007/s12022-021-09676-z]
8 **WHO classification of tumors Editorial Board**. Thoracic Tumours WHO Classification of Tumours, 5th ed. 2021
9 **Sun L**, Zhang J, Wang C, Zhao S, Shao B, Guo Y, Liu Y, Sun Y. Chromosomal and molecular pathway alterations in the neuroendocrine carcinoma and adenocarcinoma components of gastric mixed neuroendocrine-nonneuroendocrine neoplasm. *Mod Pathol* 2020; **33**: 2602-2613 [PMID: 32461621 DOI: 10.1038/s41379-020-0579-z]
10 **Yuan W**, Liu Z, Lei W, Sun L, Yang H, Wang Y, Ramdas S, Dong X, Xu R, Cai H, Li JZ, Ke Y. Mutation landscape and intra-tumor heterogeneity of two MANECs of the esophagus revealed by multi-region sequencing. *Oncotarget* 2017; **8**: 69610-69621 [PMID: 29050228 DOI: 10.18632/oncotarget.18678]
11 **Jesinghaus M**, Konukiewitz B, Keller G, Kloor M, Steiger K, Reiche M, Penzel R, Endris V, Arsenic R, Hermann G, Stenzinger A, Weichert W, Pfarr N, Klöppel G. Colorectal mixed adenoneuroendocrine carcinomas and neuroendocrine carcinomas are genetically closely related to colorectal adenocarcinomas. *Mod Pathol* 2017; **30**: 610-619 [PMID: 28059096 DOI: 10.1038/modpathol.2016.220]
12 **Fujita Y**, Uesugi N, Sugimoto R, Eizuka M, Matsumoto T, Sugai T. Gastric mixed neuroendocrine-non-neuroendocrine neoplasm (MiNEN) with pancreatic acinar differentiation: a case report. *Diagn Pathol* 2019; **14**: 38 [PMID: 31077220 DOI: 10.1186/s13000-019-0815-3]
13 **Lin J**, Zhao Y, Zhou Y, Tian Y, He Q, Lin J, Hao H, Zou B, Jiang L, Zhao G, Lin W, Xu Y, Li Z, Xue F, Li S, Fu W, Li Y, Xu Z, Li Y, Chen J, Zhou X, Zhu Z, Cai L, Li E, Li H, Zheng C, Li P, Huang C, Xie J. Comparison of Survival and Patterns of Recurrence in Gastric Neuroendocrine Carcinoma, Mixed Adenoneuroendocrine Carcinoma, and Adenocarcinoma. *JAMA Netw Open* 2021; **4**: e2114180 [PMID: 34313744 DOI: 10.1001/jamanetworkopen.2021.14180]
14 **Sahnane N**, Furlan D, Monti M, Romualdi C, Vanoli A, Vicari E, Solcia E, Capella C, Sessa F, La Rosa S. Microsatellite unstable gastrointestinal neuroendocrine carcinomas: a new clinicopathologic entity. *Endocr Relat Cancer* 2015; **22**: 35-45 [PMID: 25465415 DOI: 10.1530/ERC-14-0410]
15 **Li Y**, Yau A, Schaeffer D, Magliocco A, Gui X, Urbanski S, Waghray R, Owen D, Gao ZH. Colorectal glandular-neuroendocrine mixed tumor: pathologic spectrum and clinical implications. *Am J Surg Pathol* 2011; **35**: 413-425 [PMID: 21317713 DOI: 10.1097/PAS.0b013e3182093657]
16 **Milione M**, Maisonneuve P, Pellegrinelli A, Grillo F, Albarello L, Spaggiari P, Vanoli A, Tagliabue G, Pisa E, Messerini L, Centonze G, Inzani F, Scarpa A, Papotti M, Volante M, Sessa F, Fazio N, Pruneri G, Rindi G, Solcia E, La Rosa S, Capella C. Ki67 proliferative index of the neuroendocrine component drives MANEC prognosis. *Endocr Relat Cancer* 2018; **25**: 583-593 [PMID: 29592868 DOI: 10.1530/ERC-17-0557]
17 **Milione M**, Maisonneuve P, Grillo F, Mangogna A, Centonze G, Prinzi N, Pusceddu S, Garzone G, Cattaneo L, Busico A, Bossi P, Spaggiari P, Pellegrinelli A, Del Gobbo A, Ferrero S, Kankava K, Pruneri G, Rolli L, Roca E, Bercich L, Tironi A, Benvenuti MR, Gallazzi MS, Romano

R, Berruti A, Pastorino U, Capella C. Ki-67 Index of 55% Distinguishes Two Groups of Bronchopulmonary Pure and Composite Large Cell Neuroendocrine Carcinomas with Distinct Prognosis. *Neuroendocrinology* 2021; **111**: 475-489 [PMID: 32365350 DOI: 10.1159/000508376]

18 **Sorbye H**, Grande E, Pavel M, Tesselaar M, Fazio N, Reed NS, Knigge U, Christ E, Ambrosini V, Couvelard A, Tiensuu Janson E. European Neuroendocrine Tumor Society (ENETS) 2023 guidance paper for digestive neuroendocrine carcinoma. *J Neuroendocrinol* 2023; **35**: e13249 [PMID: 36924180 DOI: 10.1111/jne.13249]

19 **Cives M**, Strosberg JR. Gastroenteropancreatic Neuroendocrine Tumors. *CA Cancer J Clin* 2018; **68**: 471-487 [PMID: 30295930 DOI: 10.3322/caac.21493]

20 **Hadoux J**, Afchain P, Walter T, Tougeron D, Hautefeuille V, Monterymard C, Lorgis V, Thuillier F, Baudin E, Scoazec JY, Lepage C, Desgrippes R. FOLFIRINEC: a randomized phase II trial of mFOLFIRINOX vs platinum-etoposide for metastatic neuroendocrine carcinoma of gastroenteropancreatic or unknown origin. *Dig Liver Dis* 2021; **53**: 824-829 [PMID: 33994125 DOI: 10.1016/j.dld.2021.04.016]

21 **Beckman RA**, Natanegara F, Singh P, Cooner F, Antonijevic Z, Liu Y, Mayer C, Price K, Tang R, Xia A, Apostolaros M, Granville C, Michaels D. Advancing innovative clinical trials to efficiently deliver medicines to patients. *Nat Rev Drug Discov* 2022; **21**: 543-544 [PMID: 35760887 DOI: 10.1038/d41573-022-00109-y]

World Journal of Gastrointestinal Oncology

Submit a Manuscript: https://www.f6publishing.com

World J Gastrointest Oncol 2024 December 15; 16(12): 4537-4542

DOI: 10.4251/wjgo.v16.i12.4537

ISSN 1948-5204 (online)

EDITORIAL

Is nutritional status a new indicator to use in clinical practice for colorectal cancer patients?

Rossana Berardi, Rebecca Chiariotti, Giulia Mentrasti

Specialty type: Oncology

Provenance and peer review: Invited article; Externally peer reviewed.

Peer-review model: Single blind

Peer-review report's classification

Scientific Quality: Grade C
Novelty: Grade B
Creativity or Innovation: Grade B
Scientific Significance: Grade B

P-Reviewer: Yan B

Received: April 30, 2024
Revised: June 20, 2024
Accepted: July 15, 2024
Published online: December 15, 2024
Processing time: 195 Days and 19.7 Hours

Rossana Berardi, Rebecca Chiariotti, Giulia Mentrasti, Department of Medical Oncology, Università Politecnica delle Marche, Azienda Ospedaliero-Universitaria delle Marche, Ancona 60126, Marche, Italy

Co-first authors: Rossana Berardi and Rebecca Chiariotti.

Corresponding author: Rossana Berardi, MD, PhD, Professor, Department of Medical Oncology, Università Politecnica delle Marche, Azienda Ospedaliero-Universitaria delle Marche, Via Conca 71, Ancona 60126, Marche, Italy. r.berardi@univpm.it

Abstract

In this editorial we comment on the interesting article by Liu *et al*. The topic of discussion is the need for a cost-effective and easy-to-use scoring system for predicting the prognosis of colorectal cancer patients. In this context, nutritional assessment plays a crucial role in the multimodal evaluation of patients. In particular, the controlling nutritional status score was found to be an effective tool in the clinical decision-making process, in order to customize treatment strategies and to improve patient outcomes.

Key Words: Controlling nutritional status score; Colorectal cancer; Nutritional status; Clinical outcome; Nutritional biomarkers; Tailored-medicine; Personalized therapies

Core Tip: The controlling nutritional status (CONUT) score is significantly associated with the prognosis of colorectal cancer patients, as supported by a large body of literature. Compared with other nutritional scores, the CONUT score may be introduced in clinical practice as an optimal prognostic nutritional index to predict patient outcome.

Citation: Berardi R, Chiariotti R, Mentrasti G. Is nutritional status a new indicator to use in clinical practice for colorectal cancer patients? *World J Gastrointest Oncol* 2024; 16(12): 4537-4542
URL: https://www.wjgnet.com/1948-5204/full/v16/i12/4537.htm
DOI: https://dx.doi.org/10.4251/wjgo.v16.i12.4537

INTRODUCTION

Colorectal cancer (CRC) represents a significant global health and financial burden, and is currently ranked the third most common cancer in the world and the second leading cause of cancer-related death[1] in both sexes. Over a million new cases of CRC have been diagnosed globally every year in the past decade[2].

Cancer patients usually experience malnutrition and weight loss, especially those with gastrointestinal tumors. Previous studies have shown that malnutrition and cachexia are responsible for 20% of cancer-related deaths, rather than cancer itself[3].

Malnutrition is linked to an increased risk of postoperative complications and to prolonged hospitalization, with a considerable burden in terms of health care costs[4]. Besides, a compromised nutritional status reduces patient's tolerance to radiation and chemotherapy, resulting in a poor response to treatment and worse prognosis[5]. Thus, nutritional assessment of CRC patients should become a part of routine clinical practice to determine its impact on treatment efficacy and survival[6,7].

Patients with good nutritional status at diagnosis and during treatments are expected to have a better quality of life and longer survival[8], but it has also been postulated that nutritional status may impact the activity of immune cells against cancer in patients receiving treatments with chemotherapy, targeted therapy or immune checkpoint inhibitors (ICIs)[4]. The matter of discussion is how systemic inflammation and body composition (BC) influence prognosis, and the identification of nutritional and immunological signatures able to predict clinical outcome and response to therapies, with the aim of better stratification of patients and personalized treatments.

Systemic inflammation status

Tumor growth has been essentially linked to cancer-associated systemic inflammatory response. A consistent body of literature has identified several circulating inflammatory indicators as potentially helpful for prognosis prediction. Serum markers associated with inflammation can be divided into two categories: Upregulated in disease progression (neutrophils, platelets, monocytes, and C-reactive protein), and downregulated in disease progression (lymphocytes and albumin). Their combination can be used as inflammation-related markers.

In this regard, Yamamoto *et al*[9] reviewed the prognostic impact of inflammation-related markers in CRC and their use in clinical practice.

They divided the markers into five groups: Neutrophil-related markers, albumin-related markers, monocyte-related markers, C-reactive protein-related markers[10] and platelet-related markers. The most relevant in CRC are reported in the Table 1.

Nutritional status and body composition

In the issue of the *World Journal of Gastrointestinal Oncology* Liu *et al*[6], published a valuable paper. This case control study highlights the role of preoperative nutritional status as an independent prognostic factor to predict the outcome of CRC patients who underwent potentially curative resection. In particular, the study addresses the role of the Controlling Nutritional Status (CONUT) score, an immune-nutritional screening tool based on serum albumin, total cholesterol, and lymphocyte count, in predicting CRC patients' prognosis[11]. According to the study, a pre-operative CONUT score ≥ 5, characterizing patients with moderate or severe malnutrition, was independently associated with poorer overall survival (OS) and relapse-free survival (RFS) compared to those with a CONUT score ≤ 4, who showed significantly longer RFS and OS (Table 2).

Recent studies have confirmed that the CONUT score is an easy-to-use parameter to prognosticate cancer response during treatment[12-14]. A review published by Chen *et al*[7] including 62 studies involving a total of 25224 patients showed the value of the CONUT score, assessed before surgical or medical treatment. A high CONUT was correlated with shorter OS, cancer-specific survival, progression and recurrence-free survival, disease-free survival and a higher incidence of postoperative complications and mortality.

WHAT IS INNOVATIVE ABOUT CONUT COMPARED TO OTHER SCORES?

The CONUT score is a cost-effective immuno-metabolic tool evaluated from three peripheral blood parameters routinely assessed in clinical practice. Compared to the abovementioned biomarkers, derived from a maximum of two serum markers, the CONUT score provides a more comprehensive representation of both the nutritional and immunological status of patients[14].

Albumin, the main component of serum proteins, is highly correlated with body cell mass and inflammation. The presence of an ongoing inflammatory response contributes to sarcopenia, with repercussions on patients' prognosis[15]. The albumin level reflects nutritional and metabolic status in cancer patients.

Lymphopenia is independently associated with poorer survival outcomes in cancer patients, as the lymphocyte count suggests the grade of immunological and systemic inflammatory response in these patients[16,17].

The neutrophil-to-lymphocyte ratio (NLR) describes tumor inflammation. According to many studies, a high NLR is linked to poor survival in different solid tumors, including colon cancer[18,19].

Lymphocytes and the NLR play a crucial role in cancer immune evasion and surveillance, in addition to the tumor microenvironment, and this seems to be related to response to immunotherapy[20].

Table 1 Most frequently reported inflammation-related biomarkers for the prediction of prognosis in colorectal cancer patients as shown in previous reports[9]

Inflammation-related biomarkers	
Neutrophil-related markers	NLR: Low NLR was related to better CSS and DFS, with different cut-off values depending on the study: The smallest was 2, while the largest was 5
Albumin-related markers	GPS that includes serum CRP levels and serum albumin levels: High GPS indicated systemic inflammation (elevated CRP) and low nutritional state (hypoalbuminemia), that was associated with lower CSS and DFS
Monocyte-related markers	Monocyte count: Elevated monocyte count was significantly associated with poor OS and DFS, with variable cut off values depending on the study. LMR: Low LMR was independently associated with worse OS and DFS. The cutoff value depended on the study
C-reactive protein-related markers	CAR: Elevated CAR was significantly associated with worse OS and RFS in patients who underwent curative resection. The cutoff value varied between 0.025 and 0.22 according to the study. LCR: Low LCR (cut off between 12980 and 6000 depending on the study) was most significantly and independently correlated with worse OS and DFS. CLR: Was reported as an independent and significant indicator of poor long-term outcomes in patients with CRCm after hepatic resection, with a cutoff level of 62.8×10^{-6}[10]
Platelet-related markers	PLR: High PLT reflects both an increase in PLT count and a decrease in lymphocyte count and was negatively related to OS in previous reports on colorectal cancer. The cutoff value varied among studies from 150 to 246.36

CSS: Cancer-specific survival; DFS: Disease-free survival; GPS: Glasgow prognostic score; CRP: C-reactive protein; OS: Overall survival; LMR: Lymphocyte–monocyte ratio; CAR: C-reactive protein–albumin ratio; LCR: Lymphocyte–C-reactive protein ratio; CLR: C-reactive protein–lymphocyte ratio; CRCm: Metastatic colorectal cancer; PLR: Platelet–lymphocyte ratio; PLT: Platelet.

Table 2 Definition of controlling nutritional status score

Variable	Normal	Light	Moderate	Severe
Albumin (g/dL)	3.5-4.5	3.0-3.49	2.5-2.9	< 2.5
Albumin score	0	2	4	6
Total lymphocyte count (mm^3)	≥ 1600	1200-1599	800-1199	< 800
Total lymphocyte count score	0	1	2	3
Total cholesterol (mg/dL)	< 180	140-180	100-139	< 100
Total cholesterol score	0	1	2	3
CONUT score	0-1	2-4	5-8	9-12
Assessment	Normal	Light	Moderate	Severe

Low controlling nutritional status (CONUT) score includes: Normal (0-1) and light (2-4) subgroups. High CONUT score includes: Moderate (5-8) and severe (9-12) subgroups[6]. CONUT: Controlling nutritional status.

With regard to the CONUT score, high serum cholesterol levels have been shown to enhance the anticancer activity of natural killer cells in mice[21], and in solid cancers treated with ICIs, high cholesterol has been demonstrated to correlate with better clinical outcomes[22].

Another element worth mentioning is the relationship between the CONUT score and BC.

In the study of Liu *et al*[6], no significant association was observed between body mass index (BMI) and the CONUT score. BMI is a crude measure, does not adequately discriminate the percentage of fat-free mass and does not rule out sarcopenia in cancer patients.

By contrast, in their study an inverse correlation between the CONUT score and skeletal muscle mass index (SMI) was shown (Liu *et al*[6], Figure 4C). The incidence of sarcopenia was higher in the high CONUT group. Moreover, comparing the time-dependent curves of CONUT + tumor-node-metastasis (TNM) stage and SMI + TNM stage, they showed concordance in both 3-year OS (Liu *et al*[6], Figure 4A) and 3-year RFS (Liu *et al*[6], Figure 4B), suggesting that the CONUT score is as reliable as SMI in predicting the postoperative prognosis of CRC. This association likely relies on both the CONUT score and SMI reflecting the body protein reserves.

KEY POINTS

The SMI was obtained by dividing the skeletal muscle area (SMA) (cm^2) by the square of height (m). The SMA was evaluated in a cross-section of the third lumbar vertebrae on CT, by measuring the areas of psoas major, paraspinal

muscles, transverse abdominis, external oblique, internal oblique, and rectus abdominis muscles. Sarcopenia was defined as SMI < 40.8 (cm^2/m^2) in men and SMI < 34.9 (cm^2/m^2) in women.

Sarcopenia is a multifactorial condition that is frequently seen in cancer patients. It is characterized by a degenerative and systemic loss of skeletal muscle mass (SMM) and function[23].

Previous studies have demonstrated that a decreased SMM in cancer patients, as well as proven sarcopenia/cachexia, have negative effects on response to treatments, both in surgical and oncological treatments[24,25].

In addition, a SMM assessed by CT seems to be associated with increased chemotherapy and radiotherapy toxicity[26].

Several studies in advanced tumors treated with ICIs have confirmed the key prognostic role of SMM and the importance of patients' assessment, at baseline and during treatment, to actively assess the efficacy and tolerance of immunotherapy[27].

One of the potential limitations of the paper written by Liu *et al*[6] is that the authors focused on the CONUT score, neglecting other nutritional markers, such as the NLR, Glasgow prognostic score (GPS/modified GPS, (mGPS)) and prognostic nutritional index, which have been largely validated in previous studies[9]. However, their choice to focus on the CONUT score could be justified considering that it represents a more comprehensive prognostic indicator, as it combines nutritional parameters (albumin, and cholesterol) with immunologic status (including lymphocyte count), whose interplay validated by a body of literature, is significant in prognosis[7].

Nutritional assessment has an essential role in gastrointestinal tumors, particularly in CRC, that has generally a low survival rate due to its high prevalence, delayed diagnosis and elevated rate of local recurrence or metastasis, despite continuous therapeutic progress.

A multidisciplinary team-based approach has improved clinical outcomes, but substantial disparities between patients are still often observed in terms of disease presentation, response to treatments and prognosis. Therefore, it is necessary to identify new biological indicators to improve the accuracy of prognostic prediction and patient outcome[25,28].

In this context, nutritional evaluation could have a key role, representing a cost-effective and modifiable chance of therapeutic intervention for clinicians. In fact, various effective nutritional assessment tools have already been described, especially in the pre-operative setting, but there is no gold standard and they have not been routinely implemented in clinical practice[29,30].

Shan *et al*[25] suggested a prognostic model based on multiple parameters such as psoas muscle index in stage II-III CRC patients, highlighting how the presence of sarcopenia before adjuvant chemotherapy affects RFS and OS[25].

A recent study by Wang *et al*[31] including 5014 CRC patients indicated white blood cells, neutrophils, monocytes, eosinophils, alkaline phosphatase, and lactate dehydrogenase levels as additional indicators to be included in the CONUT scoring system, to provide a more accurate assessment of the clinical prognosis for patients with CRC.

Considering the concordance between the CONUT score and SMI, both resonating with TNM staging in CRC patients undergoing surgery, the two indicators could be combined in an innovative prognostic index to better stratify patients before and during treatments. In this regard, in the pre- and post-operative setting it could help in selecting patients with an increased risk of relapse, who would benefit from a more intensive adjuvant and neo-adjuvant treatment, from those who do not require oncological therapy after curative resection. The role of the CONUT score together with TNM stage in predicting the risk of relapse in the study by Liu *et al*[6], suggests that the data recently observed on circulating tumor DNA in the adjuvant setting of CRC could be replicated with nutritional and metabolic tools in the future[32].

Therefore, in the era of immuno-oncology a new body of research is attempting to clarify the mechanism of resistance to immunotherapy in proficient mismatch repair CRC patients to enhance sensitivity to ICIs[8]. Ongoing clinical trials are focusing on this matter especially in the peri-operative setting[32]. Given its immune-metabolic dimension and the relationship to immunotherapy outcome[33], the CONUT score could also be considered in this setting as a stratification factor to evaluate patients.

CONCLUSION

The role of the CONUT score, as an independent prognostic factor in patients undergoing surgery for CRC and in advanced disease, is well established. Based on the abovementioned evidence and the valuable findings of Liu *et al*[6], use of the CONUT score should also be encouraged and considered in clinical practice due to its affordability[34]. Further studies are needed to validate the relevance of this promising score in the clinical decision-making process, and to suggest when early nutritional interventions are indicated; thus, implementing personalized oncology from a supportive care perspective[8].

FOOTNOTES

Author contributions: Berardi R, Chiariotti R, and Mentrasti G contributed to conception, design and manuscript writing.

Conflict-of-interest statement: Professor Rossana Berardi: Astra Zeneca, Advisory Board, Personal; Bayer, Advisory Board, Personal; Boehringer Ingelheim, Advisory Board, Personal; EISAI, Advisory Board, Personal; Incyte, Advisory Board, Personal; Lilly, Advisory Board, Personal; Menarini, Advisory Board, Personal; Merck, Advisory Board, Personal; MSD, Advisory Board, Personal; Gilead, Invited Speaker, Personal; Astra Zeneca, Funding, Institutional; Pfizer, Funding, Institutional; Roche, Funding, Institutional. The other authors indicated no financial relationships.

Country of origin: Italy

ORCID number: Rossana Berardi 0000-0002-9529-2960; Rebecca Chiariotti 0009-0009-1465-7154.

S-Editor: Li L
L-Editor: Webster JR
P-Editor: Zhao YQ

REFERENCES

1 **Bray F**, Laversanne M, Sung H, Ferlay J, Siegel RL, Soerjomataram I, Jemal A. Global cancer statistics 2022: GLOBOCAN estimates of incidence and mortality worldwide for 36 cancers in 185 countries. *CA Cancer J Clin* 2024; **74**: 229-263 [PMID: 38572751 DOI: 10.3322/caac.21834]
2 **Siegel RL**, Miller KD, Goding Sauer A, Fedewa SA, Butterly LF, Anderson JC, Cercek A, Smith RA, Jemal A. Colorectal cancer statistics, 2020. *CA Cancer J Clin* 2020; **70**: 145-164 [PMID: 32133645 DOI: 10.3322/caac.21601]
3 **Wu BW**, Yin T, Cao WX, Gu ZD, Wang XJ, Yan M, Liu BY. Clinical application of subjective global assessment in Chinese patients with gastrointestinal cancer. *World J Gastroenterol* 2009; **15**: 3542-3549 [PMID: 19630112 DOI: 10.3748/wjg.15.3542]
4 **Vidhya K**, Gupta S, R L, Rs N, Velumani Y, Raina D, Kumari K, Gupta A. Assessment of Nutritional Status and Correlation of Factors With Body Mass Index of Cancer Patients: A Cross-Sectional Study. *Cureus* 2024; **16**: e54146 [PMID: 38496132 DOI: 10.7759/cureus.54146]
5 **Hill A**, Kiss N, Hodgson B, Crowe TC, Walsh AD. Associations between nutritional status, weight loss, radiotherapy treatment toxicity and treatment outcomes in gastrointestinal cancer patients. *Clin Nutr* 2011; **30**: 92-98 [PMID: 20719409 DOI: 10.1016/j.clnu.2010.07.015]
6 **Liu LX**, Wang H, Gao B, Xu TT, Yuan QG, Zhou SZ, Ding C, Miao J, Guan WX. Preoperative controlling nutritional status as an optimal prognostic nutritional index to predict the outcome for colorectal cancer. *World J Gastrointest Oncol* 2024; **16**: 343-353 [PMID: 38425394 DOI: 10.4251/wjgo.v16.i2.343]
7 **Chen J**, Song P, Peng Z, Liu Z, Yang L, Wang L, Zhou J, Dong Q. The Controlling Nutritional Status (CONUT) Score and Prognosis in Malignant Tumors: A Systematic Review and Meta-Analysis. *Nutr Cancer* 2022; **74**: 3146-3163 [PMID: 35382655 DOI: 10.1080/01635581.2022.2059091]
8 **Ziętarska M**, Krawczyk-Lipiec J, Kraj L, Zaucha R, Małgorzewicz S. Nutritional status assessment in colorectal cancer patients qualified to systemic treatment. *Contemp Oncol (Pozn)* 2017; **21**: 157-161 [PMID: 28947886 DOI: 10.5114/wo.2017.68625]
9 **Yamamoto T**, Kawada K, Obama K. Inflammation-Related Biomarkers for the Prediction of Prognosis in Colorectal Cancer Patients. *Int J Mol Sci* 2021; **22** [PMID: 34360768 DOI: 10.3390/ijms22158002]
10 **Taniai T**, Haruki K, Hamura R, Fujiwara Y, Furukawa K, Gocho T, Shiba H, Yanaga K. The Prognostic Significance of C-reactive Protein-To-Lymphocyte Ratio in Colorectal Liver Metastases. *J Surg Res* 2021; **258**: 414-421 [PMID: 33109402 DOI: 10.1016/j.jss.2020.08.059]
11 **Zhang Y**, Kong FF, Zhu ZQ, Shan HX. Controlling Nutritional Status (CONUT) score is a prognostic marker in III-IV NSCLC patients receiving first-line chemotherapy. *BMC Cancer* 2023; **23**: 225 [PMID: 36894927 DOI: 10.1186/s12885-023-10682-z]
12 **Kuroda D**, Sawayama H, Kurashige J, Iwatsuki M, Eto T, Tokunaga R, Kitano Y, Yamamura K, Ouchi M, Nakamura K, Baba Y, Sakamoto Y, Yamashita Y, Yoshida N, Chikamoto A, Baba H. Controlling Nutritional Status (CONUT) score is a prognostic marker for gastric cancer patients after curative resection. *Gastric Cancer* 2018; **21**: 204-212 [PMID: 28656485 DOI: 10.1007/s10120-017-0744-3]
13 **Zhang Y**, Zhang X. Controlling nutritional status score, a promising prognostic marker in patients with gastrointestinal cancers after surgery: A systematic review and meta-analysis. *Int J Surg* 2018; **55**: 39-45 [PMID: 29783000 DOI: 10.1016/j.ijsu.2018.05.018]
14 **Niu X**, Zhu Z, Bao J. Prognostic significance of pretreatment controlling nutritional status score in urological cancers: a systematic review and meta-analysis. *Cancer Cell Int* 2021; **21**: 126 [PMID: 33608012 DOI: 10.1186/s12935-021-01813-2]
15 **McMillan DC**, Watson WS, O'Gorman P, Preston T, Scott HR, McArdle CS. Albumin concentrations are primarily determined by the body cell mass and the systemic inflammatory response in cancer patients with weight loss. *Nutr Cancer* 2001; **39**: 210-213 [PMID: 11759282 DOI: 10.1207/S15327914nc392_8]
16 **Mehrazin R**, Uzzo RG, Kutikov A, Ruth K, Tomaszewski JJ, Dulaimi E, Ginzburg S, Abbosh PH, Ito T, Corcoran AT, Chen DY, Smaldone MC, Al-Saleem T. Lymphopenia is an independent predictor of inferior outcome in papillary renal cell carcinoma. *Urol Oncol* 2015; **33**: 388.e19-388.e25 [PMID: 25027688 DOI: 10.1016/j.urolonc.2014.06.004]
17 **Li S**, Yao W, Liu R, Lu Y, Zhang H, Liang X. Severe lymphopenia as a prognostic factor in rectal cancer patients receiving adjuvant chemoradiotherapy: a retrospective study. *Sci Rep* 2023; **13**: 7566 [PMID: 37161043 DOI: 10.1038/s41598-023-34145-4]
18 **Banna GL**, Friedlaender A, Tagliamento M, Mollica V, Cortellini A, Rebuzzi SE, Prelaj A, Naqash AR, Auclin E, Garetto L, Mezquita L, Addeo A. Biological Rationale for Peripheral Blood Cell-Derived Inflammatory Indices and Related Prognostic Scores in Patients with Advanced Non-Small-Cell Lung Cancer. *Curr Oncol Rep* 2022; **24**: 1851-1862 [PMID: 36255605 DOI: 10.1007/s11912-022-01335-8]
19 **Templeton AJ**, McNamara MG, Šeruga B, Vera-Badillo FE, Aneja P, Ocaña A, Leibowitz-Amit R, Sonpavde G, Knox JJ, Tran B, Tannock IF, Amir E. Prognostic role of neutrophil-to-lymphocyte ratio in solid tumors: a systematic review and meta-analysis. *J Natl Cancer Inst* 2014; **106**: dju124 [PMID: 24875653 DOI: 10.1093/jnci/dju124]
20 **Alturki NA**. Review of the Immune Checkpoint Inhibitors in the Context of Cancer Treatment. *J Clin Med* 2023; **12** [PMID: 37445336 DOI: 10.3390/jcm12134301]
21 **Qin WH**, Yang ZS, Li M, Chen Y, Zhao XF, Qin YY, Song JQ, Wang BB, Yuan B, Cui XL, Shen F, He J, Bi YF, Ning G, Fu J, Wang HY. High Serum Levels of Cholesterol Increase Antitumor Functions of Nature Killer Cells and Reduce Growth of Liver Tumors in Mice.

Gastroenterology 2020; **158**: 1713-1727 [PMID: 31972238 DOI: 10.1053/j.gastro.2020.01.028]

22 **Pecci F**, Cantini L, Cognigni V, Perrone F, Mazzaschi G, Agostinelli V, Mentrasti G, Favari E, Maffezzoli M, Cortellini A, Rossi F, Chiariotti R, Venanzi FM, Lo Russo G, Galli G, Proto C, Ganzinelli M, Tronconi F, Morgese F, Campolucci C, Moretti M, Vignini A, Tiseo M, Minari R, Rocchi MLB, Buti S, Berardi R. Prognostic Impact of Blood Lipid Profile in Patients With Advanced Solid Tumors Treated With Immune Checkpoint Inhibitors: A Multicenter Cohort Study. *Oncologist* 2024; **29**: e372-e381 [PMID: 37796838 DOI: 10.1093/oncolo/oyad273]

23 **Deer RR**, Volpi E. Protein intake and muscle function in older adults. *Curr Opin Clin Nutr Metab Care* 2015; **18**: 248-253 [PMID: 25807346 DOI: 10.1097/MCO.0000000000000162]

24 **Lobo DN**, Gianotti L, Adiamah A, Barazzoni R, Deutz NEP, Dhatariya K, Greenhaff PL, Hiesmayr M, Hjort Jakobsen D, Klek S, Krznaric Z, Ljungqvist O, McMillan DC, Rollins KE, Panisic Sekeljic M, Skipworth RJE, Stanga Z, Stockley A, Stockley R, Weimann A. Perioperative nutrition: Recommendations from the ESPEN expert group. *Clin Nutr* 2020; **39**: 3211-3227 [PMID: 32362485 DOI: 10.1016/j.clnu.2020.03.038]

25 **Shan L**, Li T, Gu W, Gao Y, Zuo E, Qiu H, Li R, Cheng X. Application of Prognostic Models Based on Psoas Muscle Index, Stage, Pathological Grade, and Preoperative Carcinoembryonic Antigen Level in Stage II-III Colorectal Cancer Patients Undergoing Adjuvant Chemotherapy. *J Oncol* 2022; **2022**: 6851900 [PMID: 35154320 DOI: 10.1155/2022/6851900]

26 **Güner G**, Özçakar L, Baytar Y, Onur MR, Demir M, Aktaş BY, Aktepe OH, Güven DC, Taban H, Yıldırım HÇ, Akın S, Aksoy S, Kara M, Dizdar Ö. Sonographic Measurements of Rectus Femoris Muscle Thickness Strongly Predict Neutropenia in Cancer Patients Receiving Chemotherapy. *Cancers (Basel)* 2024; **16** [PMID: 38473418 DOI: 10.3390/cancers16051061]

27 **Li S**, Wang T, Tong G, Li X, You D, Cong M. Prognostic Impact of Sarcopenia on Clinical Outcomes in Malignancies Treated With Immune Checkpoint Inhibitors: A Systematic Review and Meta-Analysis. *Front Oncol* 2021; **11**: 726257 [PMID: 34513704 DOI: 10.3389/fonc.2021.726257]

28 **Abbass T**, Tsz Ho YT, Horgan PG, Dolan RD, McMillan DC. The relationship between computed tomography derived skeletal muscle index, psoas muscle index and clinical outcomes in patients with operable colorectal cancer. *Clin Nutr ESPEN* 2020; **39**: 104-113 [PMID: 32859302 DOI: 10.1016/j.clnesp.2020.07.010]

29 **Silva TH**, Sillos André JC, Orlando Correa Schilithz A, Borges Murad L, Arantes Ferreira Peres W. Prediction of survival of preoperative colorectal patients: A new tool to assess the interaction of nutritional status and inflammation. *Clin Nutr ESPEN* 2023; **56**: 230-236 [PMID: 37344078 DOI: 10.1016/j.clnesp.2023.05.018]

30 **Misiewicz A**, Dymicka-Piekarska V. Fashionable, but What is Their Real Clinical Usefulness? NLR, LMR, and PLR as a Promising Indicator in Colorectal Cancer Prognosis: A Systematic Review. *J Inflamm Res* 2023; **16**: 69-81 [PMID: 36643953 DOI: 10.2147/JIR.S391932]

31 **Wang Z**, Bian J, Yuan J, Zhao S, Huang S, Wu R, Fei F. Study on the correlation between controlling nutritional status score and clinical biochemical indicators in patients with colorectal cancer. *Heliyon* 2024; **10**: e27202 [PMID: 38486724 DOI: 10.1016/j.heliyon.2024.e27202]

32 **Nair KG**, Kamath SD, Chowattukunnel N, Krishnamurthi SS. Preoperative Strategies for Locally Advanced Colon Cancer. *Curr Treat Options Oncol* 2024; **25**: 376-388 [PMID: 38349502 DOI: 10.1007/s11864-024-01184-6]

33 **Zhang J**, Li M, Zhang L, Kuang T, Yu J, Wang W. Prognostic value of controlling nutritional status on clinical and survival outcomes in cancer patients treated with immunotherapy. *Sci Rep* 2023; **13**: 17715 [PMID: 37853186 DOI: 10.1038/s41598-023-45096-1]

34 **Ko K**, Park YH, Lee JW, Ku JH, Kwak C, Kim HH. Influence of nutritional deficiency on prognosis of renal cell carcinoma (RCC). *BJU Int* 2013; **112**: 775-780 [PMID: 24028765 DOI: 10.1111/bju.12275]

World Journal of Gastrointestinal Oncology

Submit a Manuscript: https://www.f6publishing.com

World J Gastrointest Oncol 2024 December 15; 16(12): 4543-4547

DOI: 10.4251/wjgo.v16.i12.4543

ISSN 1948-5204 (online)

EDITORIAL

Gene targets with therapeutic potential in hepatocellular carcinoma

Syifaus Shodry, Yuliono Trika Nur Hasan, Iwal Reza Ahdi, Zulvikar Syambani Ulhaq

Specialty type: Oncology

Provenance and peer review: Invited article; Externally peer reviewed.

Peer-review model: Single blind

Peer-review report's classification

Scientific Quality: Grade C
Novelty: Grade B
Creativity or Innovation: Grade B
Scientific Significance: Grade B

P-Reviewer: Tchilikidi KY

Received: June 27, 2024
Revised: August 3, 2024
Accepted: August 13, 2024
Published online: December 15, 2024
Processing time: 138 Days and 8.4 Hours

Syifaus Shodry, Yuliono Trika Nur Hasan, Iwal Reza Ahdi, Faculty of Medicine and Health Sciences, Maulana Ibrahim Islamic State University of Malang, Malang 65144, Jawa Timur, Indonesia

Zulvikar Syambani Ulhaq, Research Center for Preclinical and Clinical Medicine, National Research and Innovation Agency Republic of Indonesia, Cibinong 16911, Indonesia

Corresponding author: Zulvikar Syambani Ulhaq, MD, PhD, Research Scientist, Research Center for Preclinical and Clinical Medicine, National Research and Innovation Agency Republic of Indonesia, Cibinong Science Center, Jl. Raya Jakarta-Bogor, Cibinong 16911, Indonesia. zulvikar.syambani.ulhaq@brin.go.id

Abstract

Hepatocellular carcinoma (HCC) is the third leading cause of cancer-related deaths worldwide. Major treatments include liver transplantation, resection, and chemotherapy, but the 5-year recurrence rate remains high. Late diagnosis often prevents surgical intervention, contributing to poor patient survival rates. Carcinogenesis in HCC involves genetic alterations that drive the transformation of normal cells into malignant ones. Enhancer of zeste homolog 2 (EZH2), a key regulator of cell cycle progression, is frequently upregulated in HCC and is associated with advanced stages and poor prognosis, making it a potential biomarker. Additionally, signal transducer and activator of transcription 3, which binds to EZH2, affects disease staging and outcomes. Targeting EZH2 presents a promising therapeutic strategy. On the other hand, abnormal lipid metabolism is a hallmark of HCC and impacts prognosis. Fatty acid binding protein 5 is highly expressed in HCC tissues and correlates with key oncogenes, suggesting its potential as a biomarker. Other genes such as guanine monophosphate synthase, cell division cycle associated 5, and epidermal growth factor receptor provide insights into the molecular mechanisms of HCC, offering potential as biomarkers and therapeutic targets.

Key Words: Hepatocellular carcinoma; Enhancer of zeste homolog 2; Target genes; Biomarkers; Potential therapeutic

Core Tip: Hepatocellular carcinoma (HCC) is one of the leading causes of cancer-related deaths due to late diagnosis and high recurrence rates. Key biomarkers such as enhancer of zeste homolog 2 and fatty acid binding protein 5, along with other genetic biomarkers provide insights into HCC progression and potential therapeutic targets.

Citation: Shodry S, Hasan YTN, Ahdi IR, Ulhaq ZS. Gene targets with therapeutic potential in hepatocellular carcinoma. *World J Gastrointest Oncol* 2024; 16(12): 4543-4547
URL: https://www.wjgnet.com/1948-5204/full/v16/i12/4543.htm
DOI: https://dx.doi.org/10.4251/wjgo.v16.i12.4543

INTRODUCTION

Hepatocellular carcinoma (HCC) is the most common form of primary liver cancer, accounting for 80% of all cases[1,2]. HCC imposes a substantial health and economic burden worldwide, especially in Asia[3]. Moreover, HCC is the third leading cause of cancer-related deaths globally, with a 5-year survival rate around 18%[3]. In 2020, there were about 906000 new cases and 830000 deaths from HCC, with Asia bearing 80% of the global disease burden[4]. Various treatments are available for managing HCC, including transcatheter arterial chemoembolization, liver transplantation (LT) or resection, transarterial radioembolization, radiofrequency ablation, and targeted systemic chemotherapy[5]. While surgical treatment is often viewed as the standard curative option for early-stage HCC[6-8], it is not a complete solution since the majority of patients are diagnosed at a more advanced stage with poor prognoses. Despite various treatment efforts, the 5-year recurrence rate remains high at approximately 70% following surgery[9]. Consequently, there is a critical need for more effective treatments to enhance the long-term survival of HCC patients.

Indeed, HCC is prevalent and frequently linked to a poor prognosis for patients[2]. The disease's incidence and mortality rates have been rising globally, particularly in regions such as eastern and southeastern Asia and Africa[10]. Chronic infections with hepatitis B virus (HBV) and hepatitis C virus (HCV) are well-established primary contributors to liver cirrhosis and HCC. Furthermore, exposure to aflatoxin B1 and long-term alcohol abuse are notable risk factors for the development of HCC[11,12]. Despite advancements in surgical techniques that have improved overall survival (OS) rates among patients with HCC, the 5-year OS remains low at 15%, and cancer-specific survival is less than 20%[13]. This is likely because many patients are not eligible for surgical resection or LT, primarily due to late diagnosis[14]. Furthermore, the disease is marked by a significant recurrence rate, with more than 40%-70% of patients experiencing a relapse within 5 years of surgical intervention[15]. The process of cancer development is generally understood to be a multistep phenomenon, driven by the accumulation of genetic changes that activate multiple signaling pathways, and ultimately leading to the transformation of normal cells into cancerous ones[16].

Genetics plays a crucial role in understanding the structure and function of organisms and have been widely applied in clinical diagnosis, drug development, and disease prediction[17-19]. Genes that play a role in DNA replication and maintaining proper sister chromatid cohesion are crucial for cell division, and any disruptions in these processes can greatly influence the onset and progression of malignant diseases[20]. In HCC, the genes related to this condition, along with their interacting counterparts, create a network of gene interactions[21]. Several molecules in this network are integral to the development and progression of HCC. For example, genes such as signal transducer and activator of transcription 3 (STAT3) and centrosomal protein of 55 kDa (CEP55) are involved in cell migration and invasion[22,23]. Additionally, EZH2, the catalytic subunit of polycomb repressive complex 2, is functionally associated with cell cycle regulation. Abnormal regulation of EZH2 can accelerate cell proliferation and extend cell survival, which may contribute to the onset and progression of cancer[24]. Study indicates that EZH2 is overexpressed in other cancers, including breast and prostate cancers, and its presence is linked to advanced disease and unfavorable outcomes[25].

The correlation between EZH2 and lymph node metastasis is more pronounced in EZH2-expressing tumor cells within lymph nodes compared to their matched primary tumor cells[25]. This suggests that elevated EZH2 expression is linked to higher tumor grade and increased likelihood of lymph node metastasis[25]. EZH2 also interacts with CEP55, worsening the prognosis in HCC[22]. Moreover, STAT3 causes carcinogenesis by binding to and being activated by EZH2 [26,27]. STAT3 and EZH2 are both promising molecular biomarkers for tumor progression and are associated with poor prognosis[25]. Their activation shows a strong correlation with tumor-node-metastasis (TNM) stage and patient survival, indicating that the combined expression of STAT3 and EZH2 may aid in determining the clinical TNM stage and predicting disease outcomes. STAT3 can be downregulated by EZH2 knockdown, making EZH2 a potential therapeutic target and biomarker for HCC diagnosis and prognosis[25].

Given the liver's crucial role in lipid metabolism, including the synthesis of most of the body's cholesterol and fatty acids[28,29], disrupted lipid metabolism is a key feature of metabolic reprogramming in HCC and significantly impacts its prognosis[30]. In HCC, this disruption is characterized by alterations in lipid oxidation processes, increased cholesterol esterification, elevated endogenous lipid synthesis, and changes in lipid uptake and efflux[30]. These changes closely correlate with tumor survival, growth, proliferation, and metastasis[30]. It is notable that FABP5 is highly expressed in human HCC tissues and cell lines compared with normal liver tissues and hepatocytes. FABP5, a specific isoform of FABPs, binds various long-chain fatty acids and retinoids. It is involved in transporting lipids to cellular compartments for membrane synthesis, storage, trafficking, and transcriptional regulation[31,32]. FABP5 increases the activity of the nuclear receptor peroxisome proliferator-activated receptor β/δ, which drives cell migration, growth, and survival, thus

displaying tumor-promoting properties[33]. High FABP5 expression correlates with cancer hallmarks and oncogenes such as polo like kinase 1 and baculoviral IAP repeat containing, which are master regulators in cell cycle progression and inhibition of cell death[32]. Positive FABP5 expression is associated with worse prognoses and higher recurrence rates[32]. Together, these data strongly suggest that both EZH2 and FABP5 may be useful as markers and novel therapeutic targets for treating HCC, providing valuable insights for potential therapeutic development.

OTHER POTENTIAL THERAPEUTIC GENE TARGET FOR HCC

The pathomechanism of liver cancer involves a complex interplay of various risk factors, including race, age, HBV, and HCV, which all contribute to abnormal gene expression linked to the onset and progression of HCC. Current research is focused on identifying key genes crucial for the initiation as well as the progression of HCC as a potential treatment strategy. With the advancement of genomics, numerous gene sequencing data have been stored in public databases, providing valuable resources for bioinformatic mining of gene expression profiles related to cancer[34]. In 2017, Zhang *et al*[35] identified key genes and pathways related to HCC through bioinformatic analysis of differentially expressed genes (DEGs) between HCC samples and normal samples. In HCC, 10 deregulated genes include: KRAS proto-oncogene, GTPase (KRAS), epidermal growth factor receptor (EGFR), B-cell lymphoma 2, acetyl-CoA carboxylase alpha, cluster of differentiation 8A, guanine monophosphate synthase (GMPS), transforming growth factor beta 1, STAT3, human epidermal growth factor receptor 2. Among these, albumin combined with bilirubin (albumin–bilirubin grade) displayed higher prognostic value. GMPS, essential for the synthesis of purines, has been recognized as a significant target for repression by p53, and its upregulation disrupts the tumor-suppressive p53 network in liver cancer, making GMPS a potential therapeutic target. EGFR overexpression contributes to HCC progression by enhancing cell proliferation, migration, and invasion, establishing it as an effective drug target and prognostic biomarker.

On the other hand, in 2021, Li and Xu[36] identified six genes that serve as potential therapeutic targets for HCC. Among these, cell division cycle associated 5 (CDCA5) plays a crucial role in the accurate separation of sister chromatids during the S and G2/M phases of the cell cycle[37,38]. Overexpression of CDCA5 has been clinically associated with a poor prognosis in HCC patients[39]. Opa interacting protein 5 (OIP5) regulates HCC growth and metastasis through the AKT/mammalian target of rapamycin signaling pathways[40]. DNA topoisomerase 2 alpha (TOP2A) is highly expressed in HCC tumors and is associated with shorter patient survival and increased resistance to chemotherapy[41]. Protein regulator of cytokinesis 1 (PRC1) overexpression enhances chemoresistance and inhibits apoptosis in HCC patients undergoing chemotherapy[42]. Abnormal spindle-like microcephaly-associated protein (ASPM) overexpression serves as a marker for increased metastatic potential and poor prognosis in HCC[43]. Additionally, nucleolar and spindle-associated protein 1 (NUSAP1) overexpression is associated with significantly lower survival rates in patients with HCC [44], with microRNA 193a-5p implicated in hepatocarcinogenesis suppression by regulating NUSAP1 Levels. Cyclin A2 (CCNA2) and kinesin family member 20A (KIF20A) also demonstrate elevated expression levels in HCC tissues compared to normal tissues[45].

In 2018, Hu *et al*[46] identified 56 upregulated and 8 downregulated DEGs in HCC. Their analysis revealed significant enrichment of genes involved in cell cycle arrest, transcription regulation, protein amino acid phosphorylation, cell cycle, and apoptosis. They proposed JUN, early growth response protein 1 (EGR1), MYC, and cyclin-dependent kinase inhibitor 1A (CDKN1A) as potential diagnostic and therapeutic molecular biomarkers for HCC. c-JUN prevents apoptosis by antagonizing p53 activity, contributing to early-stage HCC[47]. EGR1 contributes to HCC radio resistance by upregulating autophagy-related 4B, yet paradoxically, its upregulation by beta-lapachone inhibits hepatoma cell progression and metastasis[48]. MYC controls various cellular processes, including cell cycle progression, proliferation, and apoptosis, with miR-320a acting as a tumor suppressor by targeting MYC in HCC[49]. CDKN1A, a prominent cell cycle inhibitor, arrests cell cycle progression at the G1/S and G2/M transitions by blocking the activity of CDK4/6-cyclin D and CDK2-cyclin E complexes[28,50]. In summary, ongoing research continues to uncover crucial genes and pathways involved in HCC, offering new insights into potential therapeutic targets and prognostic biomarkers.

CONCLUSION

In conclusion, both EZH2 and FABP5 serve as biomarkers for poor outcomes in HCC and show potential as therapeutic targets for patients with this disease. Additionally, other markers such as GMPS, CDCA5, EGFR, OIP5, TOP2A, PRC1, ASPM, NUSAP1, CCNA2, JUN, EGR1, MYC, and CDKN1A contribute to a detailed understanding of the molecular mechanisms underlying HCC occurrence and progression. These molecules hold promise as both biomarkers and therapeutic targets.

FOOTNOTES

Author contributions: Shodry S wrote the original manuscript; Hasan YTN and Ahdi IR supervised the project; Ulhaq ZS conceived the study, wrote the original draft and revised the manuscript, and supervised the study; Ulhaq ZS was the main contributor to this manuscript.

Conflict-of-interest statement: The authors have no conflicts of interest to declare.

Country of origin: Indonesia

ORCID number: Zulvikar Syambani Ulhaq 0000-0002-2659-1940.

S-Editor: Lin C
L-Editor: Filipodia
P-Editor: Zhao S

REFERENCES

1 **Foglia B**, Turato C, Cannito S. Hepatocellular Carcinoma: Latest Research in Pathogenesis, Detection and Treatment. *Int J Mol Sci* 2023; **24** [PMID: 37569600 DOI: 10.3390/ijms241512224]
2 **Ladju RB**, Ulhaq ZS, Soraya GV. Nanotheranostics: A powerful next-generation solution to tackle hepatocellular carcinoma. *World J Gastroenterol* 2022; **28**: 176-187 [PMID: 35110943 DOI: 10.3748/wjg.v28.i2.176]
3 **Kim DY**. Changing etiology and epidemiology of hepatocellular carcinoma: Asia and worldwide. *J Liver Cancer* 2024; **24**: 62-70 [PMID: 38523466 DOI: 10.17998/jlc.2024.03.13]
4 **Sim YK**, Chong MC, Gandhi M, Pokharkar YM, Zhu Y, Shi L, Lequn L, Chen CH, Kudo M, Lee JH, Strasser SI, Chanwat R, Chow PKH; Asia-Pacific Hepatocellular Carcinoma Trials Group. Real-World Data on the Diagnosis, Treatment, and Management of Hepatocellular Carcinoma in the Asia-Pacific: The INSIGHT Study. *Liver Cancer* 2024; **13**: 298-313 [PMID: 38756144 DOI: 10.1159/000534513]
5 **Kotsifa E**, Vergadis C, Vailas M, Machairas N, Kykalos S, Damaskos C, Garmpis N, Lianos GD, Schizas D. Transarterial Chemoembolization for Hepatocellular Carcinoma: Why, When, How? *J Pers Med* 2022; **12** [PMID: 35330436 DOI: 10.3390/jpm12030436]
6 **Lin S**, Hoffmann K, Schemmer P. Treatment of hepatocellular carcinoma: a systematic review. *Liver Cancer* 2012; **1**: 144-158 [PMID: 24159579 DOI: 10.1159/000343828]
7 **Tabori NE**, Sivananthan G. Treatment Options for Early-Stage Hepatocellular Carcinoma. *Semin Intervent Radiol* 2020; **37**: 448-455 [PMID: 33328700 DOI: 10.1055/s-0040-1720950]
8 **Cucchetti A**, Elshaarawy O, Han G, Chong CCN, Serra C, O'Rourke JM, Crew R, Felicani C, Ercolani G, Shah T, Vogel A, Lai PBS, Johnson PJ. 'Potentially curative therapies' for hepatocellular carcinoma: how many patients can actually be cured? *Br J Cancer* 2023; **128**: 1665-1671 [PMID: 36807338 DOI: 10.1038/s41416-023-02188-z]
9 **Llovet JM**, Kelley RK, Villanueva A, Singal AG, Pikarsky E, Roayaie S, Lencioni R, Koike K, Zucman-Rossi J, Finn RS. Hepatocellular carcinoma. *Nat Rev Dis Primers* 2021; **7**: 6 [PMID: 33479224 DOI: 10.1038/s41572-020-00240-3]
10 **Yang JD**, Hainaut P, Gores GJ, Amadou A, Plymoth A, Roberts LR. A global view of hepatocellular carcinoma: trends, risk, prevention and management. *Nat Rev Gastroenterol Hepatol* 2019; **16**: 589-604 [PMID: 31439937 DOI: 10.1038/s41575-019-0186-y]
11 **Chu YJ**, Yang HI, Wu HC, Lee MH, Liu J, Wang LY, Lu SN, Jen CL, You SL, Santella RM, Chen CJ. Aflatoxin B(1) exposure increases the risk of hepatocellular carcinoma associated with hepatitis C virus infection or alcohol consumption. *Eur J Cancer* 2018; **94**: 37-46 [PMID: 29533866 DOI: 10.1016/j.ejca.2018.02.010]
12 **El-Serag HB**. Epidemiology of viral hepatitis and hepatocellular carcinoma. *Gastroenterology* 2012; **142**: 1264-1273.e1 [PMID: 22537432 DOI: 10.1053/j.gastro.2011.12.061]
13 **Orcutt ST**, Anaya DA. Liver Resection and Surgical Strategies for Management of Primary Liver Cancer. *Cancer Control* 2018; **25**: 1073274817744621 [PMID: 29327594 DOI: 10.1177/1073274817744621]
14 **Abdelhamed W**, El-Kassas M. Hepatocellular carcinoma recurrence: Predictors and management. *Liver Res* 2023; **7**: 321-332 [DOI: 10.1016/j.livres.2023.11.004]
15 **Wen T**, Jin C, Facciorusso A, Donadon M, Han HS, Mao Y, Dai C, Cheng S, Zhang B, Peng B, Du S, Jia C, Xu F, Shi J, Sun J, Zhu P, Nara S, Millis JM; MDT of West China Hospital*. Multidisciplinary management of recurrent and metastatic hepatocellular carcinoma after resection: an international expert consensus. *Hepatobiliary Surg Nutr* 2018; **7**: 353-371 [PMID: 30498711 DOI: 10.21037/hbsn.2018.08.01]
16 **Niu ZS**, Niu XJ, Wang WH. Genetic alterations in hepatocellular carcinoma: An update. *World J Gastroenterol* 2016; **22**: 9069-9095 [PMID: 27895396 DOI: 10.3748/wjg.v22.i41.9069]
17 **Ulhaq ZS**, Garcia CP. Estrogen receptor beta (ESR2) gene polymorphism and susceptibility to dementia. *Acta Neurol Belg* 2021; **121**: 1281-1293 [PMID: 32335869 DOI: 10.1007/s13760-020-01360-z]
18 **Ulhaq ZS**, Nurputra DK, Soraya GV, Kurniawati S, Istifiani LA, Pamungkas SA, Tse WKF. A systematic review on Treacher Collins syndrome: Correlation between molecular genetic findings and clinical severity. *Clin Genet* 2023; **103**: 146-155 [PMID: 36203321 DOI: 10.1111/cge.14243]
19 **Ulhaq ZS**, Garcia CP. Inflammation-related gene polymorphisms associated with Parkinson's disease: an updated meta-analysis. *Egypt J Med Hum Genet* 2020; **21**: 14 [DOI: 10.1186/s43042-020-00056-6]
20 **Ulhaq ZS**, Soraya GV, Milliana A, Tse WKF. Association between GPER gene polymorphisms and GPER expression levels with cancer predisposition and progression. *Heliyon* 2021; **7**: e06428 [PMID: 33748487 DOI: 10.1016/j.heliyon.2021.e06428]
21 **Su SG**, Li QL, Zhang MF, Zhang PW, Shen H, Zhang CZ. An E2F1/DDX11/EZH2 Positive Feedback Loop Promotes Cell Proliferation in Hepatocellular Carcinoma. *Front Oncol* 2020; **10**: 593293 [PMID: 33614480 DOI: 10.3389/fonc.2020.593293]
22 **Li M**, Gao J, Li D, Yin Y. CEP55 Promotes Cell Motility *via* JAK2–STAT3–MMPs Cascade in Hepatocellular Carcinoma. *Cells* 2018; **7** [PMID: 30096813 DOI: 10.3390/cells7080099]
23 **Ulhaq ZS**, Tse WKF. PFHxS Exposure and the Risk of Non-Alcoholic Fatty Liver Disease. *Genes (Basel)* 2024; **15** [PMID: 38254982 DOI:

10.3390/genes15010093]
24 **Yu TY**, Zhan ZJ, Lin Q, Huang ZH. Computed tomography-based radiomics predicts the fibroblast-related gene *EZH2* expression level and survival of hepatocellular carcinoma. *World J Clin Cases* 2024; **12**: 5568-5582 [DOI: 10.12998/wjcc.v12.i24.5568]
25 **Bae AN**, Jung SJ, Lee JH, Lee H, Park SG. Clinical Value of EZH2 in Hepatocellular Carcinoma and Its Potential for Target Therapy. *Medicina (Kaunas)* 2022; **58** [PMID: 35208478 DOI: 10.3390/medicina58020155]
26 **Kim E**, Kim M, Woo DH, Shin Y, Shin J, Chang N, Oh YT, Kim H, Rheey J, Nakano I, Lee C, Joo KM, Rich JN, Nam DH, Lee J. Phosphorylation of EZH2 activates STAT3 signaling *via* STAT3 methylation and promotes tumorigenicity of glioblastoma stem-like cells. *Cancer Cell* 2013; **23**: 839-852 [PMID: 23684459 DOI: 10.1016/j.ccr.2013.04.008]
27 **Park SH**, Fong KW, Mong E, Martin MC, Schiltz GE, Yu J. Going beyond Polycomb: EZH2 functions in prostate cancer. *Oncogene* 2021; **40**: 5788-5798 [PMID: 34349243 DOI: 10.1038/s41388-021-01982-4]
28 **Ulhaq ZS**, Tse WKF. Perfluorohexanesulfonic acid (PFHxS) induces oxidative stress and causes developmental toxicities in zebrafish embryos. *J Hazard Mater* 2023; **457**: 131722 [PMID: 37263022 DOI: 10.1016/j.jhazmat.2023.131722]
29 **Ulhaq ZS**, Boncan DAT, Chan TF, Tse WKF. Insights from metabolomics and transcriptomics studies on Perfluorohexanesulfonic acid (PFHxS) exposed zebrafish embryos. *Sci Total Environ* 2023; **904**: 166833 [PMID: 37673246 DOI: 10.1016/j.scitotenv.2023.166833]
30 **Feng XC**, Liu FC, Chen WY, Du J, Liu H. Lipid metabolism of hepatocellular carcinoma impacts targeted therapy and immunotherapy. *World J Gastrointest Oncol* 2023; **15**: 617-631 [PMID: 37123054 DOI: 10.4251/wjgo.v15.i4.617]
31 **Ohira M**, Yokoo H, Ogawa K, Fukai M, Kamiyama T, Sakamoto N, Taketomi A. Serum fatty acid-binding protein 5 is a significant factor in hepatocellular carcinoma progression independent of tissue expression level. *Carcinogenesis* 2021; **42**: 794-803 [PMID: 33754641 DOI: 10.1093/carcin/bgab025]
32 **Ohata T**, Yokoo H, Kamiyama T, Fukai M, Aiyama T, Hatanaka Y, Hatanaka K, Wakayama K, Orimo T, Kakisaka T, Kobayashi N, Matsuno Y, Taketomi A. Fatty acid-binding protein 5 function in hepatocellular carcinoma through induction of epithelial-mesenchymal transition. *Cancer Med* 2017; **6**: 1049-1061 [PMID: 28374947 DOI: 10.1002/cam4.1020]
33 **Kawaguchi K**, Senga S, Kubota C, Kawamura Y, Ke Y, Fujii H. High expression of Fatty Acid-Binding Protein 5 promotes cell growth and metastatic potential of colorectal cancer cells. *FEBS Open Bio* 2016; **6**: 190-199 [PMID: 27047747 DOI: 10.1002/2211-5463.12031]
34 **Xu H**, Huang J, Hua S, Liang L, He X, Zhan M, Lu L, Chu J. Interactome analysis of gene expression profiles identifies CDC6 as a potential therapeutic target modified by miR-215-5p in hepatocellular carcinoma. *Int J Med Sci* 2020; **17**: 2926-2940 [PMID: 33173413 DOI: 10.7150/ijms.51145]
35 **Zhang C**, Peng L, Zhang Y, Liu Z, Li W, Chen S, Li G. The identification of key genes and pathways in hepatocellular carcinoma by bioinformatics analysis of high-throughput data. *Med Oncol* 2017; **34**: 101 [PMID: 28432618 DOI: 10.1007/s12032-017-0963-9]
36 **Li C**, Xu J. Identification of Potentially Therapeutic Target Genes in Ovarian Cancer via Bioinformatic Approach. 2021 IEEE 9th International Conference on Bioinformatics and Computational Biology (ICBCB); 2021 May 25-27 [DOI: 10.1109/icbcb52223.2021.9459203]
37 **Shen A**, Liu L, Chen H, Qi F, Huang Y, Lin J, Sferra TJ, Sankararaman S, Wei L, Chu J, Chen Y, Peng J. Cell division cycle associated 5 promotes colorectal cancer progression by activating the ERK signaling pathway. *Oncogenesis* 2019; **8**: 19 [PMID: 30808873 DOI: 10.1038/s41389-019-0123-5]
38 **Hu H**, Xiang Y, Zhang XY, Deng Y, Wan FJ, Huang Y, Liao XH, Zhang TC. CDCA5 promotes the progression of breast cancer and serves as a potential prognostic biomarker. *Oncol Rep* 2022; **48** [PMID: 36004470 DOI: 10.3892/or.2022.8387]
39 **Tian Y**, Wu J, Chagas C, Du Y, Lyu H, He Y, Qi S, Peng Y, Hu J. CDCA5 overexpression is an Indicator of poor prognosis in patients with hepatocellular carcinoma (HCC). *BMC Cancer* 2018; **18**: 1187 [PMID: 30497429 DOI: 10.1186/s12885-018-5072-4]
40 **Li H**, Zhang J, Lee MJ, Yu GR, Han X, Kim DG. OIP5, a target of miR-15b-5p, regulates hepatocellular carcinoma growth and metastasis through the AKT/mTORC1 and β-catenin signaling pathways. *Oncotarget* 2017; **8**: 18129-18144 [PMID: 28184024 DOI: 10.18632/oncotarget.15185]
41 **Meng J**, Wei Y, Deng Q, Li L, Li X. Study on the expression of TOP2A in hepatocellular carcinoma and its relationship with patient prognosis. *Cancer Cell Int* 2022; **22**: 29 [PMID: 35033076 DOI: 10.1186/s12935-021-02439-0]
42 **Wang Y**, Shi F, Xing GH, Xie P, Zhao N, Yin YF, Sun SY, He J, Wang Y, Xuan SY. Protein Regulator of Cytokinesis PRC1 Confers Chemoresistance and Predicts an Unfavorable Postoperative Survival of Hepatocellular Carcinoma Patients. *J Cancer* 2017; **8**: 801-808 [PMID: 28382142 DOI: 10.7150/jca.17640]
43 **Zhang H**, Yang X, Zhu L, Li Z, Zuo P, Wang P, Feng J, Mi Y, Zhang C, Xu Y, Jin G, Zhang J, Ye H. ASPM promotes hepatocellular carcinoma progression by activating Wnt/β-catenin signaling through antagonizing autophagy-mediated Dvl2 degradation. *FEBS Open Bio* 2021; **11**: 2784-2799 [PMID: 34428354 DOI: 10.1002/2211-5463.13278]
44 **Roy S**, Hooiveld GJ, Seehawer M, Caruso S, Heinzmann F, Schneider AT, Frank AK, Cardenas DV, Sonntag R, Luedde M, Trautwein C, Stein I, Pikarsky E, Loosen S, Tacke F, Ringelhan M, Avsaroglu SK, Goga A, Buendia MA, Vucur M, Heikenwalder M, Zucman-Rossi J, Zender L, Roderburg C, Luedde T. microRNA 193a-5p Regulates Levels of Nucleolar- and Spindle-Associated Protein 1 to Suppress Hepatocarcinogenesis. *Gastroenterology* 2018; **155**: 1951-1966.e26 [PMID: 30165047 DOI: 10.1053/j.gastro.2018.08.032]
45 **Wu C**, Qi X, Qiu Z, Deng G, Zhong L. Low expression of KIF20A suppresses cell proliferation, promotes chemosensitivity and is associated with better prognosis in HCC. *Aging (Albany NY)* 2021; **13**: 22148-22163 [PMID: 34491228 DOI: 10.18632/aging.203494]
46 **Hu WQ**, Wang W, Fang DL, Yin XF. Identification of Biological Targets of Therapeutic Intervention for Hepatocellular Carcinoma by Integrated Bioinformatical Analysis. *Med Sci Monit* 2018; **24**: 3450-3461 [PMID: 29795057 DOI: 10.12659/MSM.909290]
47 **Eferl R**, Ricci R, Kenner L, Zenz R, David JP, Rath M, Wagner EF. Liver tumor development. c-Jun antagonizes the proapoptotic activity of p53. *Cell* 2003; **112**: 181-192 [PMID: 12553907 DOI: 10.1016/s0092-8674(03)00042-4]
48 **Peng WX**, Wan YY, Gong AH, Ge L, Jin J, Xu M, Wu CY. Egr-1 regulates irradiation-induced autophagy through Atg4B to promote radioresistance in hepatocellular carcinoma cells. *Oncogenesis* 2017; **6**: e292 [PMID: 28134935 DOI: 10.1038/oncsis.2016.91]
49 **Xie F**, Yuan Y, Xie L, Ran P, Xiang X, Huang Q, Qi G, Guo X, Xiao C, Zheng S. miRNA-320a inhibits tumor proliferation and invasion by targeting c-Myc in human hepatocellular carcinoma. *Onco Targets Ther* 2017; **10**: 885-894 [PMID: 28243124 DOI: 10.2147/OTT.S122992]
50 **Khan MGM**, Boufaied N, Yeganeh M, Kandhi R, Petkiewicz S, Sharma A, Yoshimura A, Ferbeyre G, Labbé DP, Ramanathan S, Ilangumaran S. SOCS1 Deficiency Promotes Hepatocellular Carcinoma *via* SOCS3-Dependent CDKN1A Induction and NRF2 Activation. *Cancers (Basel)* 2023; **15** [PMID: 36765862 DOI: 10.3390/cancers15030905]

World Journal of Gastrointestinal Oncology

Submit a Manuscript: https://www.f6publishing.com

World J Gastrointest Oncol 2024 December 15; 16(12): 4548-4552

DOI: 10.4251/wjgo.v16.i12.4548

ISSN 1948-5204 (online)

EDITORIAL

Estimating prognosis of gastric neuroendocrine neoplasms using machine learning: A step towards precision medicine

Hong-Niu Wang, Jia-Hao An, Liang Zong

Specialty type: Gastroenterology and hepatology

Provenance and peer review: Invited article; Externally peer reviewed.

Peer-review model: Single blind

Peer-review report's classification
Scientific Quality: Grade C
Novelty: Grade B
Creativity or Innovation: Grade B
Scientific Significance: Grade B

P-Reviewer: Xie YF

Received: July 17, 2024
Revised: August 5, 2024
Accepted: August 12, 2024
Published online: December 15, 2024
Processing time: 118 Days and 10.5 Hours

Hong-Niu Wang, Jia-Hao An, Graduate School of Medicine, Changzhi Medical College, Changzhi 046000, Shanxi Province, China

Liang Zong, Department of Gastrointestinal Surgery, Changzhi People's Hospital, Changzhi 046000, Shanxi Province, China

Co-first authors: Hong-Niu Wang and Jia-Hao An.

Corresponding author: Liang Zong, PhD, Doctor, Department of Gastrointestinal Surgery, Changzhi People's Hospital, No. 502 Changxing Middle Road, Changzhi 046000, Shanxi Province, China. 250537471@qq.com

Abstract

Survival rates following radical surgery for gastric neuroendocrine neoplasms (g-NENs) are low, with high recurrence rates. This fact impacts patient prognosis and complicates postoperative management. Traditional prognostic models, including the Cox proportional hazards (CoxPH) model, have shown limited predictive power for postoperative survival in gastrointestinal neuroectodermal tumor patients. Machine learning methods offer a unique opportunity to analyze complex relationships within datasets, providing tools and methodologies to assess large volumes of high-dimensional, multimodal data generated by biological sciences. These methods show promise in predicting outcomes across various medical disciplines. In the context of g-NENs, utilizing machine learning to predict survival outcomes holds potential for personalized postoperative management strategies. This editorial reviews a study exploring the advantages and effectiveness of the random survival forest (RSF) model, using the lymph node ratio (LNR), in predicting disease-specific survival (DSS) in postoperative g-NEN patients stratified into low-risk and high-risk groups. The findings demonstrate that the RSF model, incorporating LNR, outperformed the CoxPH model in predicting DSS and constitutes an important step towards precision medicine.

Key Words: Machine learning; Artificial intelligence; Gastric neuroendocrine neoplasm; Random survival forest model; Disease-specific survival

Core Tip: Liu *et al*'s study addresses a critical issue in determining the postoperative prognosis of gastric neuroendocrine tumors by identifying the significance of lymph node ratio. Moreover, the random survival forest model, a machine-learning approach, surpasses traditional Cox proportional hazards models by enhancing predictive accuracy, clinical utility, and overall performance. This model's ability to stratify patient risks and personalize survival predictions can aid in formulating targeted postoperative strategies, thus realizing an important aspect of personalized "precision medicine".

Citation: Wang HN, An JH, Zong L. Estimating prognosis of gastric neuroendocrine neoplasms using machine learning: A step towards precision medicine. *World J Gastrointest Oncol* 2024; 16(12): 4548-4552
URL: https://www.wjgnet.com/1948-5204/full/v16/i12/4548.htm
DOI: https://dx.doi.org/10.4251/wjgo.v16.i12.4548

INTRODUCTION

Liu *et al*[1] published a study titled "Combining lymph node ratio to develop prognostic models for postoperative gastric neuroendocrine neoplasm patients". Their study utilized machine learning techniques to identify risk factors associated with disease-specific survival (DSS) in postoperative gastric neuroendocrine neoplasm (g-NEN) patients, and succeeded in constructing an efficient and precise prognostic model based on lymph node ratio (LNR), defined as the ratio of the number of positive lymph nodes to the number examined. It also shows off one of the most promising features of artificial intelligence or machine learning, its capacity to identify patterns from multidimensional data sets such as those found in medicine. They researched a field that is in sore need of a reliable prognostic model to guide postoperative management. g-NENs represent a rare and challenging type of gastric malignancy in oncology. These neoplasms are classified into three types: Well-differentiated neuroendocrine tumors (NETs), poorly differentiated neuroendocrine carcinomas (NEC), and mixed neuroendocrine-non-NETs. While gastric NETs typically exhibit an indolent growth pattern and are often benign, gastric NECs (g-NECs) are highly malignant, aggressive, and associated with a poor prognosis[2], showing lower postoperative survival rates and higher recurrence rates[3,4]. Currently, there are no highly effective treatment options for NENs. Various clinical characteristics significantly influence the prognosis of NEN patients[5-7]. In resected g-NECs, the presence of more than two metastatic lymph nodes, metastatic disease in over 10% of resected lymph nodes, and involvement of station 2 lymph nodes have all been demonstrated as significant prognostic indicators associated with poorer outcomes[8]. Due to its incorporation of the number of lymph nodes examined during surgery, LNR turns out to be a more advantageous parameter for prognostic estimation in such patients. Indeed, many studies have shown that the prognostic value of LNR exceeds that of the absolute number of involved lymph nodes[9] for various types of cancer. The present editorial explores the promise of machine learning as a pathway toward precision medicine, particularly in its capacity to predict postoperative outcomes for NEN patients. The advent of such artificial intelligence techniques offers unique opportunities to identify subtle patterns and factors that traditional prognostic methods might overlook[10,11].

MACHINE LEARNING IN G-NEN RESEARCH

Machine learning models can analyze complex relationships within datasets and has shown promise in predicting various medical outcomes[10]. In the context of g-NENs, machine learning has the potential to predict postoperative prognosis and tailor personalized postoperative management strategies.

Traditionally, predictive models such as the Cox proportional hazards (CoxPH) model have been employed[12,13]. However, their limitations have spurred the exploration of innovative approaches[11,14]. Liu *et al*'s study critically compared the performance of the random survival forest (RSF) and CoxPH models in predicting DSS for patients after g-NEN surgery[1]. This greater certainty regarding outcomes allow physicians to tailor the postoperative management strategies for their patients, avoiding the pitfalls and discomfort that can be inherent to end-of-life treatment.

Inspired by a comprehensive cohort consisting of 286 patients from the Surveillance, Epidemiology, and End Results (SEER) database and 92 g-NEN patients from the First Affiliated Hospital of Soochow University, Liu *et al*[1] constructed a RSF model using 14 key features. These features encompass demographic, clinicopathologic, and tumor-specific factors. The RSF model underwent rigorous evaluation in terms of discrimination, calibration, clinical utility, and overall performance, and its performance was compared with that of traditional models.

This study analyzed data from 7685 patients in the SEER database from 2000 to 2019, of which 286 met the inclusion criteria. Included patients had primary g-NEN, underwent curative surgery, and had complete pathological information. The exclusion criteria (n = 7399) included: (1) Cases without histopathological evidence; (2) History of other malignancies; (3) Cases lacking detailed clinical data such as differentiation grade, tumor size, or tumor node metastasis (TNM) stage; (4) Cases without information on survival duration or those who died within one month; (5) Cases that did not undergo surgery or had only local surgery; and (6) Cases without information on the number of examined lymph nodes and positive lymph nodes. Patients from the SEER database were randomly divided into a training set and an internal validation set at a ratio of 8:2. The external test cohort consisted of 92 patients from the First Affiliated Hospital of Soochow University, covering the period from 2011 to 2020.

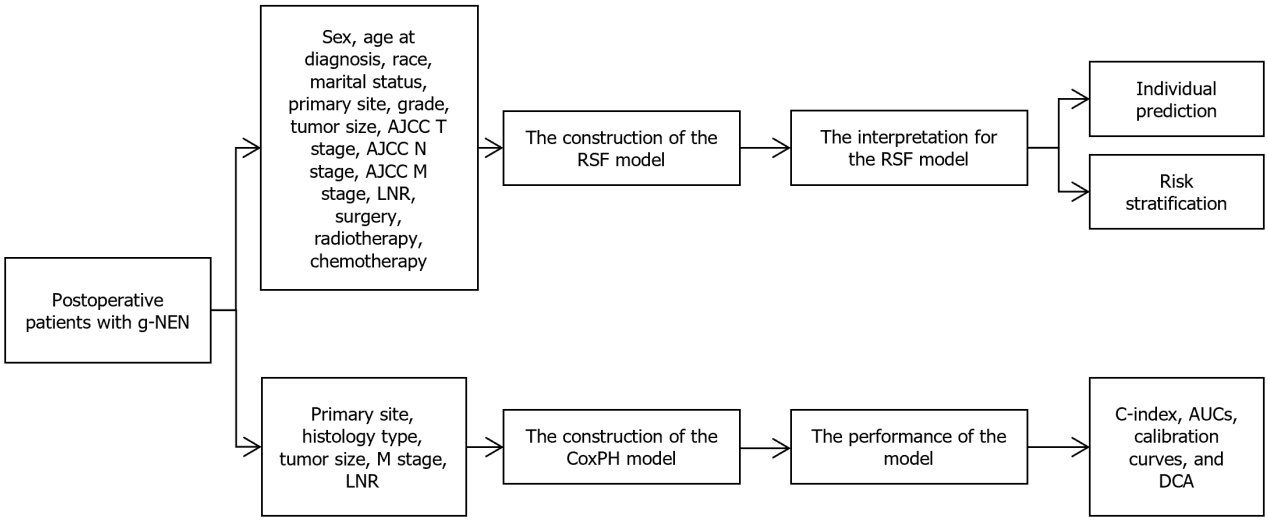

Figure 1 Construction of random survival forest model and Cox proportional hazards model. g-NEN: Gastric neuroendocrine neoplasm; AJCC: American Joint Committee on Cancer; LNR: Lymph node ratio; C-index: Concordance Index; AUC: Area under the curve; DCA: Decision curve analysis; RSF: Random survival forest; CoxPH: Cox proportional hazards.

Both RSF and CoxPH models were constructed. For the CoxPH model, univariate and multivariate regression analyses identified primary site, histologic type, size, M stage, and LNR as independent risk factors. These selected independent risk factors were then used to develop the CoxPH model, which was visualized using a nomogram. The RSF model, utilizing random forest techniques such as feature and sample bootstrapping, demonstrated faster training times and reduced estimation bias. This model was built using 14 factors: Sex, age at diagnosis, race, marital status, primary site, differentiation grade, tumor size, American Joint Committee on Cancer (AJCC) T stage, AJCC N stage, AJCC M stage, LNR, surgery at the primary site, radiotherapy, and chemotherapy. Optuna was used to determine the optimal hyperparameters for the RSF model: 330 estimators, a minimum of 5 samples per split, and a minimum of 1 sample per leaf. Shapley additive explanations (SHAP) plots were used to interpret the RSF model. Patients were then assigned risk scores and divided into low-risk, medium-risk, and high-risk groups, providing valuable insights for identifying high-risk populations and facilitating timely clinical interventions. Kaplan-Meier analysis confirmed the stratification for all cohorts ($P < 0.0001$) (Figure 1). Additionally, individualized survival predictions were made, allowing for a clear prediction of the impact of all admission variables on each patient's prognosis.

The performance of the 8th edition AJCC TNM staging system, CoxPH model, and RSF model was evaluated using the C-index, areas under the receiver operating characteristic curves (AUCs), calibration curves, and decision curve analysis (DCA). The RSF model was further interpreted using SHAP values. In an external test set, the RSF model outperformed the 8th AJCC TNM staging system and the CoxPH model, with C-index values of 0.769, 0.744, and 0.723, respectively.

The 1-, 3-, and 5-year AUCs for the 8th AJCC TNM staging system were 0.690, 0.769, and 0.770, respectively. For the CoxPH model, the AUCs were 0.786, 0.834, and 0.810. The RSF model achieved AUCs of 0.803, 0.895, and 0.869 at 1, 3, and 5 years, respectively. DCA indicated that the RSF model had a higher net benefit compared to the other models (Table 1).

SHAP analysis indicated that histologic type was the most significant variable in the RSF model, followed by LNR, T stage, and M stage. Elevated LNR levels were linked to worse patient outcomes.

The study's limitations include selection bias from its retrospective design and the SEER database's primary focus on the United States population, which may not generalize to Asian, especially Chinese, populations. Additionally, the lack of multi-center external validation reduces the robustness of the findings.

In the study by Song *et al*[12], a survival nomogram for g-NECs was constructed. Yang *et al*[15] developed a prognostic nomogram for g-NEN patients using computed tomography radiomic features. However, both studies failed to demonstrate that LNR is an independent risk factor. Padwal *et al*[16] and Jiang *et al*[17] employed machine learning to build prognostic models for pancreatic NEN patients, while Liu *et al*[1] were the first to use a random forest survival model for g-NENs. This study, through multivariable regression analysis, identified LNR as an independent risk factor, providing higher statistical power and significance.

CONCLUSION

The RSF model has become a key tool for precise postoperative prognostic estimation and optimized management of g-NENs, showing advantages over traditional models. Its capability to stratify risks and predict individual survival marks a new era of personalized prediction and optimized prognostic strategies. Artificial intelligence, particularly machine learning algorithms, holds great promise in transforming the diagnosis, treatment, and prognosis of gastric diseases by analyzing extensive medical data to identify patterns and anomalies. We predict that artificial intelligence's role in personalized, prognosis-based management in gastric diseases will be crucial, aiding healthcare professionals in selecting

Table 1 Performance of the Cox proportional hazards model and the random survival forest model

Model	Cohort	C-index	AUC		
			1-year	3-year	5-year
CoxPH	Training	0.834 (0.789-0.879)	0.848 (0.763-0.930)	0.881 (0.831-0.932)	0.875 (0.822-0.927)
	Internal	0.871 (0.802-0.940)	0.843 (0.717-0.969)	0.948 (0.892-1.000)	0.990 (0.969-1.000)
	External	0.744 (0.665-0.822)	0.786 (0.622-0.889)	0.834 (0.735-0.934)	0.810 (0.688-0.931)
RSF	Training	0.940 (0.924-0.956)	0.962 (0.938-0.989)	0.979 (0.963-0.995)	0.971 (0.951-0.992)
	Internal	0.870 (0.818-0.921)	0.867 (0.761-0.973)	0.955 (0.899-1.000)	0.986 (0.960-1.000)
	External	0.769 (0.691-0.846)	0.803 (0.608-0.891)	0.895 (0.814-0.976)	0.869 (0.769-0.970)

CoxPH: Cox proportional hazards; RSF: Random survival forest; AUC: Area under receiver operating characteristic curve; C-index: Concordance Index.

the right intervention for each patient. The RSF model is expected to redefine g-NEN prognosis and guide more precise, individualized patient management.

ACKNOWLEDGEMENTS

We are grateful to those researchers who provided study data.

FOOTNOTES

Author contributions: Wang HN and An JH drafted the initial manuscript; Zong L reviewed the manuscript; all three authors contributed to this editorial work.

Conflict-of-interest statement: The authors declare that they have no conflict of interest to disclose.

Country of origin: China

ORCID number: Hong-Niu Wang 0000-0003-2572-4868; Jia-Hao An 0009-0006-3018-4295; Liang Zong 0000-0003-4139-4571.

S-Editor: Fan M
L-Editor: Wang TQ
P-Editor: Chen YX

REFERENCES

1 **Liu W**, Wu HY, Lin JX, Qu ST, Gu YJ, Zhu JZ, Xu CF. Combining lymph node ratio to develop prognostic models for postoperative gastric neuroendocrine neoplasm patients. *World J Gastrointest Oncol* 2024; **16**: 3507-3520 [DOI: 10.4251/wjgo.v16.i8.3507]
2 **Zi M**, Ma Y, Chen J, Pang C, Li X, Yuan L, Liu Z, Yu P. Clinicopathological characteristics of gastric neuroendocrine neoplasms: A comprehensive analysis. *Cancer Med* 2024; **13**: e7011 [PMID: 38457192 DOI: 10.1002/cam4.7011]
3 **Iwasaki K**, Barroga E, Enomoto M, Tsurui K, Shimoda Y, Matsumoto M, Miyoshi K, Ota Y, Matsubayashi J, Nagakawa Y. Long-term surgical outcomes of gastric neuroendocrine carcinoma and mixed neuroendocrine-non-neuroendocrine neoplasms. *World J Surg Oncol* 2022; **20**: 165 [PMID: 35610656 DOI: 10.1186/s12957-022-02625-y]
4 **Exarchou K**, Stephens NA, Moore AR, Howes NR, Pritchard DM. New Developments in Gastric Neuroendocrine Neoplasms. *Curr Oncol Rep* 2022; **24**: 77-88 [PMID: 35059996 DOI: 10.1007/s11912-021-01175-y]
5 **Sackstein PE**, O'Neil DS, Neugut AI, Chabot J, Fojo T. Epidemiologic trends in neuroendocrine tumors: An examination of incidence rates and survival of specific patient subgroups over the past 20 years. *Semin Oncol* 2018; **45**: 249-258 [PMID: 30348533 DOI: 10.1053/j.seminoncol.2018.07.001]
6 **Panzuto F**, Campana D, Massironi S, Faggiano A, Rinzivillo M, Lamberti G, Sciola V, Lahner E, Manuzzi L, Colao A, Annibale B. Tumour type and size are prognostic factors in gastric neuroendocrine neoplasia: A multicentre retrospective study. *Dig Liver Dis* 2019; **51**: 1456-1460 [PMID: 31175013 DOI: 10.1016/j.dld.2019.04.016]

7 **Song W**, Tian C. The Effect of Marital Status on Survival of Patients with Gastrointestinal Stromal Tumors: A SEER Database Analysis. *Gastroenterol Res Pract* 2018; **2018**: 5740823 [PMID: 29483926 DOI: 10.1155/2018/5740823]

8 **Tang X**, Chen Y, Guo L, Zhang J, Wang C. Prognostic significance of metastatic lymph node number, ratio and station in gastric neuroendocrine carcinoma. *J Gastrointest Surg* 2015; **19**: 234-241 [PMID: 25394386 DOI: 10.1007/s11605-014-2691-1]

9 **Widschwendter P**, Polasik A, Janni W, de Gregorio A, Friedl TWP, de Gregorio N. Lymph Node Ratio Can Better Predict Prognosis than Absolute Number of Positive Lymph Nodes in Operable Cervical Carcinoma. *Oncol Res Treat* 2020; **43**: 87-95 [PMID: 31935729 DOI: 10.1159/000505032]

10 **Ngiam KY**, Khor IW. Big data and machine learning algorithms for health-care delivery. *Lancet Oncol* 2019; **20**: e262-e273 [PMID: 31044724 DOI: 10.1016/S1470-2045(19)30149-4]

11 **Christou CD**, Tsoulfas G. Challenges and opportunities in the application of artificial intelligence in gastroenterology and hepatology. *World J Gastroenterol* 2021; **27**: 6191-6223 [PMID: 34712027 DOI: 10.3748/wjg.v27.i37.6191]

12 **Song X**, Xie Y, Lou Y. A novel nomogram and risk stratification system predicting the cancer-specific survival of patients with gastric neuroendocrine carcinoma: a study based on SEER database and external validation. *BMC Gastroenterol* 2023; **23**: 238 [PMID: 37452300 DOI: 10.1186/s12876-023-02875-4]

13 **Hu P**, Bai J, Liu M, Xue J, Chen T, Li R, Kuai X, Zhao H, Li X, Tian Y, Sun W, Xiong Y, Tang Q. Trends of incidence and prognosis of gastric neuroendocrine neoplasms: a study based on SEER and our multicenter research. *Gastric Cancer* 2020; **23**: 591-599 [PMID: 32026156 DOI: 10.1007/s10120-020-01046-8]

14 **Pickett KL**, Suresh K, Campbell KR, Davis S, Juarez-Colunga E. Random survival forests for dynamic predictions of a time-to-event outcome using a longitudinal biomarker. *BMC Med Res Methodol* 2021; **21**: 216 [PMID: 34657597 DOI: 10.1186/s12874-021-01375-x]

15 **Yang ZH**, Han YJ, Cheng M, Wang R, Li J, Zhao HP, Gao JB. Prognostic value of computed tomography radiomics features in patients with gastric neuroendocrine neoplasm. *Front Oncol* 2023; **13**: 1143291 [PMID: 37409252 DOI: 10.3389/fonc.2023.1143291]

16 **Padwal MK**, Basu S, Basu B. Application of Machine Learning in Predicting Hepatic Metastasis or Primary Site in Gastroenteropancreatic Neuroendocrine Tumors. *Curr Oncol* 2023; **30**: 9244-9261 [PMID: 37887568 DOI: 10.3390/curroncol30100668]

17 **Jiang C**, Wang K, Yan L, Yao H, Shi H, Lin R. Predicting the survival of patients with pancreatic neuroendocrine neoplasms using deep learning: A study based on Surveillance, Epidemiology, and End Results database. *Cancer Med* 2023; **12**: 12413-12424 [PMID: 37165971 DOI: 10.1002/cam4.5949]

World Journal of Gastrointestinal Oncology

Submit a Manuscript: https://www.f6publishing.com

World J Gastrointest Oncol 2024 December 15; 16(12): 4553-4558

DOI: 10.4251/wjgo.v16.i12.4553

ISSN 1948-5204 (online)

EDITORIAL

Exploring Xiaojianzhong decoction's potential in gastric cancer treatment: Integrative insights and experimental validation

Chun-Han Cheng, Wen-Rui Hao, Tzu-Hurng Cheng

Specialty type: Oncology

Provenance and peer review: Invited article; Externally peer reviewed.

Peer-review model: Single blind

Peer-review report's classification

Scientific Quality: Grade C, Grade C

Novelty: Grade B, Grade C

Creativity or Innovation: Grade B, Grade C

Scientific Significance: Grade B, Grade B

P-Reviewer: Cao J; Xing QC

Received: July 24, 2024

Revised: September 2, 2024

Accepted: September 5, 2024

Published online: December 15, 2024

Processing time: 110 Days and 17.1 Hours

Chun-Han Cheng, Department of Medical Education, Linkou Chang Gung Memorial Hospital, Taoyuan 33305, Taiwan

Wen-Rui Hao, Division of Cardiology, Department of Internal Medicine, Shuang Ho Hospital, Ministry of Health and Welfare, Taipei Medical University, Taipei 23561, Taiwan

Wen-Rui Hao, Division of Cardiology, Department of Internal Medicine, School of Medicine, College of Medicine, Taipei Medical University, Taipei 11002, Taiwan

Tzu-Hurng Cheng, Department of Biochemistry, School of Medicine, College of Medicine, China Medical University, Taichung 404328, Taiwan

Co-first authors: Chun-Han Cheng and Wen-Rui Hao.

Corresponding author: Tzu-Hurng Cheng, PhD, Professor, Department of Biochemistry, School of Medicine, College of Medicine, China Medical University, No. 91 Xueshi Road, North District, Taichung 404328, Taiwan. thcheng@mail.cmu.edu.tw

Abstract

Gastric cancer (GC) remains a formidable global health concern with significant morbidity and mortality rates, despite the fact that numerous advances have been made to improve conventional therapies. Xiaojianzhong decoction (XJZ), a traditional Chinese medicine, has garnered academic attention as a multicomponent, multitarget approach to managing GC. The present editorial explores the potential of XJZ in the treatment of GC through a comprehensive analysis of network pharmacology and experimental validation. Network pharmacology was used to identify key molecular targets of XJZ, including interleukin 6, prostaglandin-endoperoxide synthase 2, and matrix metalloproteinase 9, and *in vitro* experiments were used to confirm the efficacy of XJZ in inhibiting cell proliferation, inducing apoptosis, and modulating gene expression associated with GC progression. This editorial highlights XJZ as a promising therapeutic strategy for GC and indicates a need for further clinical exploration and validation of its efficacy.

Key Words: Xiaojianzhong decoction; Gastric cancer; Network pharmacology; Traditional Chinese medicine; Experimental validation

Core Tip: This editorial integrates network pharmacology insights with rigorous experimental validation to highlight the potential of Xiaojianzhong decoction as a multifaceted therapeutic approach for gastric cancer.

Citation: Cheng CH, Hao WR, Cheng TH. Exploring Xiaojianzhong decoction's potential in gastric cancer treatment: Integrative insights and experimental validation. *World J Gastrointest Oncol* 2024; 16(12): 4553-4558
URL: https://www.wjgnet.com/1948-5204/full/v16/i12/4553.htm
DOI: https://dx.doi.org/10.4251/wjgo.v16.i12.4553

INTRODUCTION

Gastric cancer (GC) remains a formidable global health challenge because of its high morbidity and mortality rates. The effectiveness of conventional treatments, such as those involving surgery, chemotherapy, and molecular targeting agents, is often limited because of the treatments' severe adverse effects and the emergence of drug resistance. Consequently, traditional Chinese medicine (TCM) has increasingly gained attention as a complementary approach to managing GC; it offers a holistic approach to treatment that contrasts with the reductionist approach of conventional medicine. In TCM, health and disease are viewed through the lens of syndrome differentiation, which involves identifying patterns of disharmony within the body's organ systems. In the context of GC, relevant TCM syndromes include spleen qi deficiency, damp-heat in the stomach, and blood stasis. These syndromes correspond to specific symptoms and underlying imbalances that contribute to the development and progression of gastric malignancies. For example, spleen qi deficiency is characterized by symptoms such as fatigue, poor appetite, and abdominal distention, which are common in patients with GC. Spleen qi deficiency is believed to weaken the digestive system, leading to the accumulation of dampness and the subsequent development of phlegm and blood stasis, which creates an internal environment conducive to tumor growth[1].

Xiaojianzhong (XJZ) decoction, a classical TCM formulation, was reported to produce promising results in the treatment of GC[1]. XJZ is traditionally used to treat spleen qi deficiency with cold in the middle jiao, a condition that manifests as abdominal pain, loose stools, and a preference for warmth and pressure on the abdomen. XJZ comprises a synergistic combination of herbs, with each playing a unique role in restoring balance. The key ingredients of XJZ are *Bai Shao* (*Paeonia lactiflora*), *Gui Zhi* (*Cinnamomum cassia*), *Zhi Gan Cao* (*Glycyrrhiza uralensis*), *Sheng Jiang* (*Zingiber officinale*), *Da Zao* (*Ziziphus jujuba*), and *Yi Tang* (*Saccharum Granorum*)[1]. *Bai Shao* and *Gui Zhi* are the core ingredients of the formula, working together to harmonize the interior and alleviate pain by warming and nourishing the spleen and stomach. *Zhi Gan Cao* and *Sheng Jiang* support the digestive system, enhancing the body's ability to absorb nutrients and expel dampness. *Da Zao* and *Yi Tang* have nourishing and strengthening effects, replenishing the qi and blood[1].

The components of XJZ have been studied for their potential anticancer effects from a modern pharmacological perspective. *Bai Shao* was discovered to exert anti-inflammatory and antiproliferative effects, which may help inhibit the growth of gastric tumors by modulating immune responses and mitigating oxidative stress. *Gui Zhi*, known for its warming properties, was demonstrated to enhance blood circulation and reduce inflammation, potentially counteracting the hypoxic and acidic microenvironment that supports cancer cell survival. *Zhi Gan Cao*, a widely studied herb in TCM, contains glycyrrhizin, a compound that exerts anticancer activities by inducing apoptosis and inhibiting proliferation of various cancer cell lines[2].

Recent research has provided further insights into the mechanisms underlying the efficacy of XJZ in treating GC. Studies utilizing network pharmacology and experimental validation have elucidated the multicomponent, multitarget activities of this decoction. For instance, XJZ was discovered to alleviate aspirin-induced gastric mucosal injury through the phosphoinositide 3-kinase (PI3K)/AKT/mammalian target of rapamycin (mTOR)/Unc-51-like autophagy-activating kinase 1 (ULK1) pathway and the AMP-activated protein kinase/ULK1 pathway, both of which are crucial in regulating cell survival, autophagy, and metabolism[2]. This suggests that XJZ not only protects the gastric mucosa from damage but also modulates key signaling pathways involved in cancer progression. XJZ was also revealed to prevent the growth of gastric precancerous lesions by inhibiting autophagy and glycolysis—pathways often hijacked by cancer cells to support their growth under nutrient-limiting conditions—in gastric mucosal cells[3]. Moreover, the ability of the decoction to activate the p62/Keap1/nuclear factor erythroid 2–related factor 2 signaling pathway and inhibit ferroptosis underscores its potential in GC treatment[4]. Ferroptosis, a type of regulated cell death driven by iron-dependent lipid peroxidation, has been implicated in cancer development and resistance to therapy. By inhibiting this pathway, XJZ may protect cells from oxidative stress and inflammation, both of which are key drivers of gastric carcinogenesis[4].

In generally, XJZ exemplifies the holistic approach of many forms of TCM in treating complex diseases such as GC. Its traditional use for addressing spleen qi deficiency and related syndromes aligns with the modern understanding of its pharmacological activities, which include anti-inflammatory, antiproliferative, and cytoprotective effects[1,3]. These findings highlight the potential of XJZ as an adjunct to conventional GC therapies and as a multifaceted strategy that targets the disease from both a symptomatic and mechanistic standpoint. As researchers continue to explore the integration of TCM with modern medicine, formulations such as XJZ may play an increasingly pivotal role in the comprehensive management of GC[5].

NETWORK PHARMACOLOGY INSIGHTS

Network pharmacology has emerged as a crucial approach for deciphering the complex mechanisms through which XJZ treats GC. By integrating computational analysis with extensive data available from databases, researchers have elucidated the active ingredients in XJZ and their molecular targets, thereby uncovering its broad therapeutic potential in treating GC. XJZ is a formulation composed of several herbs (Table 1), each of which contributes unique active compounds that collectively influence various biological pathways related to GC[1]. The key constituents of XJZ are paeoniflorin from *P. lactiflora*, cinnamaldehyde from *C. cassia*, and glycyrrhizic acid from *G. uralensis*. These compounds modulate critical processes such as inflammation, cell proliferation, and metastasis. Paeoniflorin inhibits the nuclear factor kappa-light-chain-enhancer of the activated B cells signaling pathway, thereby reducing inflammation and enhancing the sensitivity of GC cells to chemotherapy[6]. Cinnamaldehyde targets the PI3K/AKT signaling pathway, which is central to tumor growth and survival[2]. Glycyrrhizic acid, known for its anti-inflammatory properties, modulates the Toll-like receptor 4 pathway, thereby reducing the levels of proinflammatory cytokines and ameliorating gastric mucosal injury[4,7].

Network pharmacology studies have identified genes encoding interleukin (IL)-6, prostaglandin-endoperoxide synthase 2, matrix metalloproteinase (MMP) 9, and MMP2 as the primary targets of XJZ. IL-6, a proinflammatory and protumor cytokine, is a vital target in GC treatment. Prostaglandin-endoperoxide synthase 2 facilitates cancer progression by contributing to inflammation and angiogenesis within the tumor microenvironment[8-12]. MMP9 and MMP2 enable cancer cell invasion and metastasis by degrading extracellular matrix components[3,13]. These network pharmacological insights highlight the holistic therapeutic potential of XJZ. Unlike conventional treatments that often target single mechanisms, XJZ involves multiple targets, offering a comprehensive approach to managing GC by addressing its complexity and heterogeneity. This multitarget approach is particularly advantageous for preventing resistance and addressing the multifactorial nature of GC[1]. Moreover, the network pharmacological approach provides a deeper understanding of the interactions and pathways through which XJZ exerts its effects. This thorough analysis supports the optimization of XJZ formulations and the identification of potential biomarkers for evaluating treatment efficacy and patient responses. Network pharmacology can considerably enhance the understanding of the mechanisms of action of XJZ in GC treatment and supports its integration into contemporary GC management strategies[2,3].

IN VITRO EXPERIMENTAL VALIDATION

The results of *in vitro* experiments on XJZ further indicate its therapeutic potential against GC, complementing the insights gained through network pharmacological analysis. XJZ significantly inhibits the proliferation of various GC cell lines, including MKN-45, AGS, and SGC-7901, in a dose-dependent manner. These cell lines represent different subtypes and stages of GC, suggesting that the decoction exerts broad anticancer activities across different GC contexts. Control experiments were performed on normal gastric epithelial cell lines, such as GES-1, to assess the specificity and potential toxicity of the components of XJZ. The results confirmed that XJZ preferentially targets cancerous cells, indicating its potential as a selective therapeutic agent[2]. Further experiments revealed that XJZ induces apoptosis and causes cell cycle arrest at the G_0/G_1 phase in GC cell lines, which is crucial for tumor suppression because it prevents cancer cells from proliferating and facilitates programmed cell death. These effects were consistently observed across the GC cell lines that were used, suggesting that the mechanisms of XJZ are not specific to a particular GC subtype[3]. Molecular assays provided deeper insights into the effects of XJZ on gene expression within GC cells. Notably, XJZ treatment resulted in the downregulation of oncogenic markers such as IL-6 and MMP9, which are associated with tumor growth, inflammation, and metastasis. Furthermore, protective factors such as heme oxygenase 1 (HMOX1) were upregulated, reflecting a shift toward a more regulated and less malignant cellular environment. HMOX1, known for its cytoprotective and anti-inflammatory properties, contributes significantly to the overall anticancer effects of XJZ[4,13]. To enhance the generalizability of these findings, additional experiments were conducted on a broader range of GC cell lines, including MGC-803 and BGC-823. The consistent antiproliferative, proapoptotic, and gene regulatory effects observed across these diverse cell lines underscore the potential of XJZ as a broad-spectrum therapeutic agent against GC[14,15].

Overall, these *in vitro* experiments have robustly substantiated the therapeutic potential of XJZ in GC treatment. The dose-dependent inhibition of GC cell proliferation, induction of apoptosis, cell cycle arrest, and significant alterations in gene expression profiles collectively validate the multifaceted mechanisms through which XJZ exerts its anticancer effects. These findings highlight the importance of integrating experimental validation with network pharmacology to fully understand and optimize the therapeutic applications of traditional formulations such as XJZ in modern oncology [11,16].

IMMUNE MODULATION BY XJZ IN THE TUMOR MICROENVIRONMENT

XJZ has garnered attention for its potential to modulate the tumor microenvironment of GC. The tumor microenvironment, comprising a complex network of cancer cells, immune cells, stromal cells, and signaling molecules, plays a pivotal role in cancer progression, metastasis, and response to therapy[1,16]. In addition to exerting direct cytotoxic effects on GC cells, XJZ modulates the immune response within the tumor microenvironment, which is crucial for effective anticancer therapy[1,3]. Studies have highlighted the ability of XJZ to modulate immune responses in GC. For example, research reported that XJZ can enhance the activity of cytotoxic T lymphocytes while reducing the immunosup-

Table 1 Key components of Xiaojianzhong decoction and their pharmacological activities in gastric cancer treatment[1]

Component	Herb source	Pharmacological activity	Ref.
Cinnamaldehyde	*Cinnamomum cassia*	Exhibits anti-inflammatory and antiulcer effects by modulating NF-kB and MAPK pathways. Prevents *Helicobacter pylori* infection and enhances mucosal healing	Chen *et al*[1], 2024; Li *et al*[7], 2024; Han *et al*[17], 2023
Galangin	*Alpinia officinarum*	Protects gastric mucosa by mediating the TLR4/NF-κB and transient receptor potential vanilloid 1 signaling pathways, promoting healing of gastric lesions	Lin *et al*[12], 2023; Lin *et al*[18], 2024
Gingerol	*Zingiber officinale*	Possesses anti-inflammatory and antioxidant properties. Protects gastric mucosa by inhibiting lipid peroxidation and cytokine production	al-Yahya *et al*[8], 1989; Gumbarewicz *et al*[9], 2022
Glycyrrhizin	*Glycyrrhiza uralensis*	Modulates immune responses, reduces oxidative stress, and prevents gastric ulcer formation, playing a role in the suppression of gastric cancer cell proliferation	Yang *et al*[10], 2017; Chen *et al*[13], 2024
Liquiritigenin	*Glycyrrhiza uralensis*	Protects against gastric mucosal injury by activating the PI3K/AKT pathway. Exhibits antiulcerative and anticancer properties through antiapoptotic and anti-inflammatory mechanisms	Yang *et al*[10], 2017; Guo *et al*[11], 2024
Paeoniflorin	*Paeonia lactiflora*	Inhibits multidrug resistance in gastric cancer cells by suppressing NF-κB activation. Modulates autophagy and exerts protective effects against gastric mucosal injury	Chen *et al*[1], 2024; Asai *et al*[5], 2011; Fang *et al*[6], 2012
Honey	Natural source	Demonstrates gastroprotective effects through antioxidant activity. Promotes mucosal healing and reduces inflammation in gastric lesions	Chen *et al*[2], 2023; Zheng *et al*[16], 2024

[1]Key components of Xiaojianzhong decoction (XJZ) and their pharmacological activities in gastric cancer treatment.
The table highlights the primary herbal components of XJZ, their active constituents, and the associated pharmacological activities that contribute to gastric cancer treatment, including modulation of key signaling pathways, inhibition of cancer cell proliferation, induction of apoptosis, and enhancement of gastric mucosal protection. The information is synthesized from studies that explore both the network pharmacology and experimental validations of XJZ in gastric cancer contexts.

pressive effects of regulatory T cells within the tumor microenvironment. This dual action not only supports the body's natural immune response against cancer cells but also helps overcome the immune evasion strategies employed by tumors[16]. Furthermore, XJZ was indicated to modulate key signaling pathways involved in immune regulation, such as the PI3K/AKT and mTOR pathways, which are critical for maintaining immune cell homeostasis and function[2]. By influencing these pathways, XJZ may strengthen the efficacy of immune-based therapies, making it a valuable adjunct to conventional treatments[1].

Although *in vitro* studies have provided substantial evidence of the immunomodulatory and anticancer properties of XJZ, comprehensive *in vivo* studies are required to validate these findings. Animal models of GC can be employed to evaluate the effects of XJZ on both the immune microenvironment and tumor progression. Studies employing such models should focus on assessing the direct cytotoxic effects of XJZ on GC cells and its ability to modulate immune responses within the tumor microenvironment in a living organism[1,3]. Future research should also investigate the potential synergistic effects of XJZ when it is combined with other immunotherapies or conventional chemotherapies. Understanding the interactions between XJZ and existing treatments could pave the way for more effective and personalized therapeutic strategies for GC[15]. Overall, although XJZ has been demonstrated to act as a potent immunomodulator in the tumor microenvironment of GC, comprehensive *in vivo* studies are required to fully evaluate its therapeutic potential and optimize its use in clinical settings. Such research will be crucial for establishing XJZ as a cornerstone in the fight against GC and establishing its potential to improve patient outcomes through a multifaceted approach to tumor suppression.

CLINICAL IMPLICATIONS AND FUTURE DIRECTIONS

XJZ has received considerable recognition for its holistic anticancer effects, particularly against GC. Conventional monotherapies target specific molecular pathways; XJZ likely has higher efficacy because of the synergistic interactions among multiple bioactive compounds within the decoction (Table 1). Network pharmacology has revealed that XJZ influences a broad spectrum of molecular targets involved in GC progression, including key signaling pathways such as PI3K/AKT/mTOR and AMP-activated protein kinase/ULK1, which are critical for regulating cell proliferation, apoptosis, autophagy, and glycolysis[2,13]. This network-based interaction suggests that the therapeutic effects of XJZ are likely due to the synergistic activity of its constituents, which work together to disrupt cancer cell survival and growth more effectively than any individual component could. Furthermore, the p62/Keap1/nuclear factor erythroid 2-related factor 2 signaling pathway, which plays a prominent role in mitigating oxidative stress and ferroptosis in GC cells, is another crucial target of XJZ. The ability of XJZ to activate this pathway highlights its potential for protecting cells from

oxidative damage, which is often implicated in cancer progression[4]. This multifaceted mechanism of action reinforces the idea that XJZ exerts its anticancer effects through a network of interactions rather than through the isolated actions of individual compounds. In addition to directly targeting cancer cells, XJZ may modulate the tumor immune microenvironment, which could further enhance its anticancer efficacy. The tumor microenvironment is a complex ecosystem that comprises cancer cells, various immune cells, stromal cells, and signaling molecules. The effects of XJZ on this microenvironment, particularly through the regulation of immune responses, may contribute to its ability to suppress tumor growth and improve overall treatment outcomes[16]. By modulating immune pathways, XJZ might bolster the body's natural ability for immune surveillance and attacking cancer cells, with this involving a dual mechanism of action: Direct cytotoxicity against cancer cells and indirect immune system modulation to promote anticancer activity. Integrating network pharmacology data with experimental outcomes reveals the potential of XJZ as a complementary or alternative therapy in the management of GC. *In vitro* studies have robustly demonstrated the ability of XJZ to inhibit GC cell proliferation and induce apoptosis through various molecular pathways, suggesting that XJZ could effectively supplement conventional treatments by targeting multiple pathways simultaneously. This multifaceted approach may reduce side effects and overcome drug resistance[1,2,16].

However, translating these promising preclinical findings into clinical practice requires careful consideration and further research. Rigorous clinical trials must be conducted to validate the efficacy and safety of XJZ in human patients, with such trials focusing on optimal dosing regimens, pharmacokinetic profiles, and potential interactions with conventional cancer therapies to ensure therapeutic synergy without adverse effects[1,14]. Moreover, identifying biomarkers that predict patient responses to XJZ could facilitate the development of personalized treatment approaches, enabling clinicians to tailor therapies to patients' genetic and molecular profiles and thereby maximize efficacy while minimizing toxicity. Longitudinal studies are also warranted to assess the long-term effects of XJZ on patients with GC, including the potential benefits and risks associated with its prolonged use[15]. Future research should delve deeper into the precise molecular mechanisms that mediate the effects of XJZ, particularly its effects on various cellular processes and its interactions with other therapeutic agents. Elucidating these mechanisms would improve the understanding of the therapeutic potential of XJZ and guide future drug development efforts. Moreover, exploring different treatment combinations and protocols is essential to optimizing therapeutic strategies and improving patient outcomes. Although preclinical evidence strongly supports the efficacy of XJZ as a treatment for GC, substantial additional efforts are required to translate these findings into clinical practice. XJZ presents a unique opportunity for bridging TCM and modern oncology and may reshape the landscape of cancer treatment with a more personalized and comprehensive approach to GC management[1,16].

CONCLUSION

XJZ has a rich history in TCM and has been validated through modern scientific methodologies as a promising therapeutic option for GC. Network pharmacology has unveiled the intricate mechanisms responsible for the efficacy of XJZ, highlighting its ability to modulate critical pathways involved in GC progression. Network pharmacology has identified key molecular targets and pathways affected by XJZ, including inflammation, cell proliferation, and metastasis, which are crucial in the context of cancer[1]. Experimental validation has reinforced these findings, demonstrating the potential of XJZ to inhibit cell proliferation, induce apoptosis, and alter gene expression profiles in GC cells. Studies have indicated that XJZ can inhibit GC cell growth in a dose-dependent manner, induce cell cycle arrest at the G_0/G_1 phase, and downregulate oncogenic markers such as IL-6 and MMP9 while upregulating protective factors such as HMOX1[2,3]. Moving forward, integrating XJZ into clinical practice holds considerable potential for enhancing current GC treatment paradigms. Its multicomponent, multitarget approach addresses the limitations of conventional therapies, such as adverse side effects and drug resistance. This holistic alternative offers a more comprehensive treatment strategy by targeting multiple pathways and processes involved in cancer progression[4]. However, in-depth clinical studies are imperative to validate these preclinical findings and determine optimal dosing regimens. Rigorous clinical trials will be crucial for establishing the safety, efficacy, and pharmacokinetic profile of XJZ in human patients. Elucidating potential drug interactions and optimizing personalized treatment protocols will also be vital steps toward integrating XJZ into conventional oncological practice. In conclusion, XJZ represents a convergence of ancient wisdom and modern scientific rigor, presenting a compelling avenue for advancing personalized and integrative approaches to GC therapy. By bridging TCM and contemporary oncology, XJZ paves the way for innovative strategies that prioritize efficacy, safety, and patient-centered care in the management of GC. Such integration holds promise for improving treatment outcomes and quality of life for patients with GC, exemplifying the potential benefits of combining traditional and modern medical practices.

FOOTNOTES

Author contributions: Cheng CH, Hao WR, and Cheng TH have contributed to this editorial; Cheng CH and Hao WR primarily responsible for writing, and Cheng TH overseeing revisions. All authors have read and approved the final manuscript.

Conflict-of-interest statement: The authors declare having no conflicts of interest.

Country of origin: Taiwan

ORCID number: Tzu-Hurng Cheng 0000-0002-9155-4169.

S-Editor: Liu H
L-Editor: A
P-Editor: Zhang L

REFERENCES

1 **Chen GQ**, Nan Y, Ning N, Huang SC, Bai YT, Zhou ZY, Qian G, Li WQ, Yuan L. Network pharmacology study and in vitro experimental validation of Xiaojianzhong decoction against gastric cancer. *World J Gastrointest Oncol* 2024; **16**: 3932-3954 [PMID: 39350988 DOI: 10.4251/wjgo.v16.i9.3932]

2 **Chen T**, Bao S, Chen J, Zhang J, Wei H, Hu X, Liang Y, Li J, Yan S. Xiaojianzhong decoction attenuates aspirin-induced gastric mucosal injury *via* the PI3K/AKT/mTOR/ULK1 and AMPK/ULK1 pathways. *Pharm Biol* 2023; **61**: 1234-1248 [PMID: 37602379 DOI: 10.1080/13880209.2023.2243998]

3 **Zhang JX**, Bao SC, Chen J, Chen T, Wei HL, Zhou XY, Li JT, Yan SG. Xiaojianzhong decoction prevents gastric precancerous lesions in rats by inhibiting autophagy and glycolysis in gastric mucosal cells. *World J Gastrointest Oncol* 2023; **15**: 464-489 [PMID: 37009319 DOI: 10.4251/wjgo.v15.i3.464]

4 **Chen J**, Zhang J, Chen T, Bao S, Li J, Wei H, Hu X, Liang Y, Liu F, Yan S. Xiaojianzhong decoction attenuates gastric mucosal injury by activating the p62/Keap1/Nrf2 signaling pathway to inhibit ferroptosis. *Biomed Pharmacother* 2022; **155**: 113631 [PMID: 36122518 DOI: 10.1016/j.biopha.2022.113631]

5 **Asai M**, Kawashima D, Katagiri K, Takeuchi R, Tohnai G, Ohtsuka K. Protective effect of a molecular chaperone inducer, paeoniflorin, on the HCl- and ethanol-triggered gastric mucosal injury. *Life Sci* 2011; **88**: 350-357 [PMID: 21167840 DOI: 10.1016/j.lfs.2010.12.014]

6 **Fang S**, Zhu W, Zhang Y, Shu Y, Liu P. Paeoniflorin modulates multidrug resistance of a human gastric cancer cell line *via* the inhibition of NF-κB activation. *Mol Med Rep* 2012; **5**: 351-356 [PMID: 22051979 DOI: 10.3892/mmr.2011.652]

7 **Li CY**, Liao LJ, Yang SX, Wang LY, Chen H, Luo P, Huang GR, Huang YQ. Cinnamaldehyde: An effective component of Cinnamomum cassia inhibiting Helicobacter pylori. *J Ethnopharmacol* 2024; **330**: 118222 [PMID: 38663778 DOI: 10.1016/j.jep.2024.118222]

8 **al-Yahya MA**, Rafatullah S, Mossa JS, Ageel AM, Parmar NS, Tariq M. Gastroprotective activity of ginger zingiber officinale rosc., in albino rats. *Am J Chin Med* 1989; **17**: 51-56 [PMID: 2589236 DOI: 10.1142/S0192415X89000097]

9 **Gumbarewicz E**, Jarząb A, Stepulak A, Kukula-Koch W. Zingiber officinale Rosc. in the Treatment of Metabolic Syndrome Disorders-A Review of In Vivo Studies. *Int J Mol Sci* 2022; **23** [PMID: 36555184 DOI: 10.3390/ijms232415545]

10 **Yang Y**, Wang S, Bao YR, Li TJ, Yang GL, Chang X, Meng XS. Anti-ulcer effect and potential mechanism of licoflavone by regulating inflammation mediators and amino acid metabolism. *J Ethnopharmacol* 2017; **199**: 175-182 [PMID: 28159726 DOI: 10.1016/j.jep.2017.01.053]

11 **Guo Y**, Wu Y, Huang T, Huang D, Zeng Q, Wang Z, Hu Y, Liang P, Chen H, Zheng Z, Liang T, Zhai D, Jiang C, Liu L, Zhu H, Liu Q. Licorice flavonoid ameliorates ethanol-induced gastric ulcer in rats by suppressing apoptosis *via* PI3K/AKT signaling pathway. *J Ethnopharmacol* 2024; **325**: 117739 [PMID: 38301986 DOI: 10.1016/j.jep.2024.117739]

12 **Lin K**, Deng T, Qu H, Ou H, Huang Q, Gao B, Li X, Wei N. Gastric protective effect of Alpinia officinarum flavonoids: mediating TLR4/NF-κB and TRPV1 signalling pathways and gastric mucosal healing. *Pharm Biol* 2023; **61**: 50-60 [PMID: 36541204 DOI: 10.1080/13880209.2022.2152058]

13 **Chen T**, Chen J, Bao SC, Zhang JX, Wei HL, Zhou XY, Hu X, Liang Y, Li JT, Yan SG. Mechanism of Xiaojianzhong decoction in alleviating aspirin-induced gastric mucosal injury revealed by transcriptomics and metabolomics. *J Ethnopharmacol* 2024; **318**: 116910 [PMID: 37453623 DOI: 10.1016/j.jep.2023.116910]

14 **Jiang Y**, Liu B, Fu L, Li F. UBE2C regulates the KEAP1/NRF2 signaling pathway to promote the growth of gastric cancer by inhibiting autophagy. *Int J Biol Macromol* 2024; **276**: 134011 [PMID: 39032892 DOI: 10.1016/j.ijbiomac.2024.134011]

15 **Leylek O**, Honeywell ME, Lee MJ, Hemann MT, Ozcan G. Functional genomics reveals an off-target dependency of drug synergy in gastric cancer therapy. *Gastric Cancer* 2024 [PMID: 39033209 DOI: 10.1007/s10120-024-01537-y]

16 **Zheng J**, Feng H, Lin J, Zhou J, Xi Z, Zhang Y, Ling F, Liu Y, Wang J, Hou T, Xing F, Li Y. KDM3A Ablation Activates Endogenous Retrovirus Expression to Stimulate Antitumor Immunity in Gastric Cancer. *Adv Sci (Weinh)* 2024; e2309983 [PMID: 39031630 DOI: 10.1002/advs.202309983]

17 **Han YM**, Song MY, Lee DY, Lee SW, Ahn HR, Yoo J, Kim HJ, Kim EH. Gastric Mucosal Protective Effects of Cinnamomum cassia in a Rat Model of Ethanol-Induced Gastric Injury. *Nutrients* 2023; **16** [PMID: 38201885 DOI: 10.3390/nu16010055]

18 **Lin K**, Wang Z, Wang E, Zhang X, Liu X, Feng F, Yu X, Yi G, Wang Y. Targeting TRPV1 signaling: Galangin improves ethanol-induced gastric mucosal injury. *J Ethnopharmacol* 2024; **335**: 118605 [PMID: 39047882 DOI: 10.1016/j.jep.2024.118605]

World Journal of Gastrointestinal Oncology

Submit a Manuscript: https://www.f6publishing.com

World J Gastrointest Oncol 2024 December 15; 16(12): 4559-4564

DOI: 10.4251/wjgo.v16.i12.4559

ISSN 1948-5204 (online)

EDITORIAL

Critical considerations for the management of gastrointestinal mixed neuroendocrine non-neuroendocrine neoplasms and pure neuroendocrine carcinomas

Efstathios T Pavlidis, Ioannis N Galanis, Theodoros E Pavlidis

Specialty type: Oncology

Provenance and peer review: Invited article; Externally peer reviewed.

Peer-review model: Single blind

Peer-review report's classification

Scientific Quality: Grade B, Grade C, Grade C

Novelty: Grade B, Grade B, Grade C

Creativity or Innovation: Grade B, Grade B, Grade C

Scientific Significance: Grade B, Grade C, Grade C

P-Reviewer: Jeong KY; Kontogeorgos G; Tajiri K

Received: August 10, 2024

Revised: September 25, 2024

Accepted: October 18, 2024

Published online: December 15, 2024

Processing time: 94 Days and 7.5 Hours

Efstathios T Pavlidis, Ioannis N Galanis, Theodoros E Pavlidis, The 2nd Department of Propaedeutic Surgery, Hippokration General Hospital, School of Medicine, Aristotle University of Thessaloniki, Thessaloniki 54642, Greece

Corresponding author: Theodoros E Pavlidis, Doctor, PhD, Emeritus Professor, Surgeon, The 2nd Department of Propaedeutic Surgery, Hippokration General Hospital, School of Medicine, Aristotle University of Thessaloniki, Konstantinoupoleos 49, Thessaloniki 54642, Greece. pavlidth@auth.gr

Abstract

Mixed neuroendocrine non-neuroendocrine neoplasms constitute rare tumors that are located mainly in the gastrointestinal (GI) tract and have high degrees of malignancy, and the frequency of these tumors has been increasing. They consist of a neuroendocrine neoplastic component with another component of adenocarcinoma usually and have a dismal prognosis. The rare GI pure neuroendocrine carcinoma is highly aggressive and requires complex and extensive management since a genetic distinction exists between it and GI non-neuroendocrine neoplasms, which are generally slow-growing lesions. The most common GI-mixed neuroendocrine non-neuroendocrine neoplasms are colorectal, followed by gastric, mainly in the gastroesophageal junction. Current imaging modalities of nuclear medicine and radiology play important roles in the accuracy of diagnosis. Liquid biopsy may contribute to early detection and timely diagnosis. Ultrasonography, either endoscopic or abdominal, is a technique that contributes to a diagnosis; additionally, contrast-enhanced ultrasonography is very helpful in follow-up appointments. Histopathology establishes a definite diagnosis and stage by evaluating the cell differentiation grade and the cell proliferation index Ki67. The genetic profile can be valuable in diagnosis and gene therapy. Surgical resection with wide lymphadenectomy, whenever possible, and adjuvant chemotherapy constitute the main therapeutic management strategies. Targeted therapy and immunotherapy achieve encouraging results.

Key Words: Neuroendocrine neoplasms; Gastrointestinal neuroendocrine neoplasms; Mixed gastrointestinal neuroendocrine neoplasms; Gastrointestinal neuroendocrine carcinomas; Neuroendocrine carcinoma; Neuroendocrine non-neuroendocrine neoplasms

Core Tip: The rare but steadily increasing number of gastrointestinal mixed neuroendocrine non-neuroendocrine neoplasms and pure neuroendocrine carcinomas require more radical treatment than slow-growing neuroendocrine neoplasms do and they are related to poor prognosis. They constitute a complicated diagnostic and therapeutic challenge. The current management strategy begins with surgery and is followed by chemotherapy. New chemotherapeutics and novel biological agents for targeted therapy, along with immunotherapy broaden the range of therapeutic options, providing promising outcomes. Effective management should be individualized and multidisciplinary.

Citation: Pavlidis ET, Galanis IN, Pavlidis TE. Critical considerations for the management of gastrointestinal mixed neuroendocrine non-neuroendocrine neoplasms and pure neuroendocrine carcinomas. *World J Gastrointest Oncol* 2024; 16(12): 4559-4564
URL: https://www.wjgnet.com/1948-5204/full/v16/i12/4559.htm
DOI: https://dx.doi.org/10.4251/wjgo.v16.i12.4559

INTRODUCTION

Recently, in the *World Journal of Gastrointestinal Oncology*, the editorial by Cives *et al*[1] and previously the review by Díaz-López *et al*[2] presented the current aspects of the interesting issue of mixed neuroendocrine non-neuroendocrine neoplasms (MiNENs) of the gastroenteropancreatic tract in precise detail. These rare neoplasms consist of heterogeneous lesions of combined neuroendocrine neoplasms with epithelial carcinoma (at least 30% of each component) that exhibit high malignancy with rapid progression and a dismal prognosis[3]. The pathogenetic mechanism of MiNENs and neuroendocrine carcinoma (NEC) is still unclear. It seems that a possible association with Crohn's disease exists with more gene disorders and greater aggressiveness[4]. They are increasing in prevalence in the gastrointestinal (GI) tract, and their incidence is increasing every year[5]. A tenfold increase was reported between 2000 and 2017[6]. Although MiNENs were initially called mixed adenoneuroendocrine cancers, the recent World Health Organization (WHO) update established the current terminology[7].

Although MiNENs are rare entities, there is particular interest in their diagnosis and treatment. The usual aggressive behavior of these cells is influenced by poor cell differentiation and an increased Ki67 cell proliferation index according to histopathology assessment[8-11]. Pure NECs merit specific preoperative evaluation and wide operative management by radical surgery, including extended lymphadenectomy, followed by proper adjuvant therapy. This carcinoma is a subgroup that usually affects the GI tract in more than 35% of patients[12].

The most common GI-MiNENs are those of the colorectal region[13], followed by those of the gastroesophageal junction and stomach[14,15]. Colorectal MiNENs constitute the majority of poorly differentiated cells and should be managed as adenocarcinomas[13]. Gastric MiNENs differ biologically, histopathologically and clinically from stomach adenocarcinomas, represent the least common gastric neoplasms and are located more often in the gastroesophageal junction[16]. Ampullary MiNENs are extremely rare[17], and proper management constitutes a therapeutic extended operative excision and adjuvant chemotherapy[9]. Less common sites of GI-MiNENs include the appendix[18], which are associated with the best prognosis[6], small intestine, esophagus, liver, pancreas[19], biliary tree, and gallbladder (gallbladder NEC represents 0.5% of all NENs and 2.1% of gallbladder malignancies)[20]. GI-MiNENs may present apart from the neuroendocrine component, another epithelial neoplasm, instead of adenocarcinoma[3]. The histological types of MiNENs include collision, combined and amphicrine types[17].

When distant and high-grade metastases are present in GI-MiNENs, a treatment plan consisting of chemotherapy and targeted therapy, including novel biological agents and immunotherapy, can replace an otherwise ineffective and risky extended surgical resection[10]. Among various GI-MiNENs, different clinical and pathological manifestations may be found, but in any case, these manifestations do not substantially affect the prognosis[21]. The prognosis depends on histological grade, cell differentiation, mitotic rate and Ki67 proliferation index. The Ki67 proliferation index is the most reliable prognostic factor, with a crucial value of 55%[10,21].

DIAGNOSIS

Genetic profile analysis may be valuable in precise diagnosis and in novel targeted gene therapy. It has been postulated that, genetically, GI-NECs are different from GI-NETs. Mutations in the *TP53* gene and *RB1* gene are common in GI-NECs, as are mutations in the *CCNE1* gene and MYC proto-oncogene, BHLH transcription factor (*MYC*) gene. Nonpancreatic GI-NECs are the only ones characterized by mutations in the *Notch* gene family. Transcription factors, mainly the *SOX2* gene, are overexpressed in most GI-NECs[22]. In gastric and colorectal NECs, mutations in the *TP53*, *RB1*, and *KRAS* genes have been detected. However, *BRAF* gene mutations have been found only in colorectal NECs[23].

The identification of molecular biomarkers in circulation is a new diagnostic challenge. Recently, they have been used for precise assessment in ambiguous cases, including tumor cells, tumor DNA, microRNAs, and NETest. Another valuable current diagnostic test in serum is the so-called liquid biopsy, which depends on mRNA assessment, which

contributes to timely diagnosis and treatment monitoring[24-27]. The development and application of the above molecular biomarkers can accurately classify these neoplasms, ensuring their more effective management[28].

Current imaging modalities of nuclear medicine and radiology play important roles in accurate and timely diagnosis. These methods include fluorodeoxyglucose positron emission computed tomography (PET-CT) and, more precisely, gallium^{68} PET-CT or the novel most accurate 18F-fluoro-dihydroxyphenylalanine PET-CT, which is specific for distinguishing NENs, and single photon emission computed tomography[29-32]. The novel endoscopic and abdominal ultrasonography (US) technique contributes to diagnosis, and contrast-enhanced US is very helpful in follow-up appointments [26].

There are no specific reliable tumor markers, only the abovementioned biomarkers[26]. They are typically diagnosed by fine needle biopsy under imaging guidance or biopsy endoscopy (EUS-fine needle biopsy) for upper GI and colorectal neoplasms which are the gold standard for the preoperative diagnosis of MiNENs and NECs[26]. The staging in the definite histopathological assessment of the specimen must be accurate according to the WHO guidelines, which provide precise terminology, particularly the rate of mitoses and the necessary cell proliferation index Ki67[10,33]. In the majority (60%) of samples, the neuroendocrine component has a Ki67 proliferation index equal to or greater than 55%[21]. The WHO staging and recommendations must be followed precisely to reduce the risks of misdiagnosis.

MANAGEMENT

Compared with slow-growing NENs, mixed MiNENs and pure NECs require more radical treatment, ensuring necessary R0 resection without residual NENs. This means that in mixed neoplasms and pure carcinomas if a more advanced disease (mainly hepatic metastases) exists that cannot exclude any residual focal neoplastic lesion after attempting potentially curative operative excision, the disease should be characterized as inoperable. In contrast, for functional hypersecreting NENs, there is an indication for debulking surgery (90% resection of the tumor burden) for better control and alleviation of persistent symptoms; consequently, NENs with hepatic metastases are not characterized as inoperable a priori[34]. It is also well known for NENs that curative surgical management of the primary site is highly important, but the management of hepatic metastatic spread must be individualized, and meticulous long-term follow-up is imperative. The current management policy for NEN hepatic metastases includes systemic therapy as first-line therapy and hepatectomy only if systemic therapy fails[35].

In operable cases, whenever feasible, the ideal basic management for both MiNENs and NECs is a radically wide operation with extended lymphadenectomy followed by chemotherapy[36]. The physical status, age and comorbidities of a patient are the primary factors associated with extended surgical procedure outcomes. Therapeutic radical surgery includes complete excision (colectomy, gastrectomy, esophagectomy, proximal pancreatoduodenectomy, or enterectomy) with extended lymphadenectomy according to the location of the primary tumor. It is more risky and complicated but may offer a reasonable chance of cure. In inoperable advanced metastatic cases, any palliative treatment must be aimed at the predominant responsible metastatic component, either the neuroendocrine neoplasm or epithelial carcinoma[28]; this palliation may be achieved by debulking surgery; microwave or radiofrequency ablation; chemotherapy; drugs that suppress tumor growth, mainly in relapse after surgery; novel targeted therapy; and immunotherapy[24,25]. Although approximately 40% of patients have distant hepatic metastases at the time of diagnosis, 88% of all patients undergo some operative procedures[6].

For advanced MiNENs, first-line chemotherapy with 5-fluorouracil or capecitabine plus oxaliplatin has been used as treatment. However, it might differ according to the primary site or the proportion of tumor. The median overall survival was 14 months, depending on the Ki67 proliferation index. Survival was better (35.3 months *vs* 11.9 months) in patients whose Ki67 index was < 55%[37].

Novel targeted therapies include: (1) Toripalimab, a programmed cell death protein inhibitor, and surufatinib, a tyrosine kinase inhibitor that has been used with encouraging early results in advanced solid tumors, including MiNENs, NECs and NENs[38]; (2) Sunitinib, a tyrosine kinase inhibitor, and everolimus, an mechanistic target of rapamycin inhibitor[39]; and (3) Bevacizumab, an anti-vascular endothelial growth factor monoclonal antibody, and atezolizumab, a programmed cell death ligand 1 inhibitor, for advanced cases, also providing encouraging results[40].

The biological behavior of GI-MiNENs does not differ from that of pure GI-NECs, and the prognosis is similarly poor in both[41]. The median overall survival of all patients with colorectal MiNENs and NECs is 38 months and 42 months, respectively, whereas for those with stage III disease, it is 30 months and 25 months, respectively. Patients with stage III disease and less lymph node involvement have better survival after adjuvant chemotherapy, as determined by multivariate analysis[13].

The prognosis of GI-MiNENs is poorer than that of pure GI-NENs. The former is an independent risk factor for cancer-specific survival in terms of the size of the tumor, degree of lymph node involvement, degree of distant metastasis and applied surgical procedure[5]. The most commonly used chemotherapy for aggressive pure NECs is cisplatin plus etoposide, but the median overall survival time is one year[42]. Rectal NECs are rare and highly aggressive and have a poor prognosis, especially high-grade NECs with poor differentiation. Surgical resection and chemoradiotherapy may be helpful[43].

Apart from symptom palliation, treatment with somatostatin analogs may be beneficial in suppressing tumor growth. Thorough evaluation of somatostatin receptors, including the five subtypes identified by their immunohistochemical expression, is highly important for determining the effectiveness of applied therapy and predicting patient outcome. Somatostatin receptor antagonist targeted therapy has been used recently for its antineoplastic activity[44]. The newest such drug, pasireotide, which binds subtype 1 and 4 receptors, may be more effective[45].

Given that pure NECs constitute a subgroup of poorly differentiated NENs with a mitotic rate > 20%, a Ki67 proliferation index > 20%[34] and clear genetic distinction (gene alterations are prevalent in NECs and rare in NENs)[46], they are more aggressive and require wider radical excision than NENs, which are generally slow-growing lesions[34]. The evaluation of genetic profiles is important in determining the application of targeted therapy and immunotherapy in the usual advanced inoperable patients[46,47]. The characteristic endoscopic features (submucosal tumor elevation, such as white coating and ulceration) lead to accurate biopsies for histopathological and molecular analysis, contributing to proper management[48]. Cisplatin and etoposide or irinotecan have been used as first-line chemotherapies in advanced inoperable NECs and as second-line immunotherapies with nivolumab, a monoclonal antibody against programmed cell death protein 1 with satisfactory results[49,50]. Folinic acid, 5-fluorouracil, irinotecan and capecitabine, temozolomide were used as second-line chemotherapies for metastatic NECs in a multicenter study, with encouraging results (1-year overall survival of 28.4% for folinic acid, 5-fluorouracil, irinotecan and 32.4% for capecitabine, temozolomide)[51].

In any case, the effective treatment of GI-MiNENs and GI-pure NECs is difficult, since the prognosis is poor for these high malignancy neoplasms and different genetic factors are implicated. The novel treatment must be individualized, multidisciplinary and targeted. New chemotherapeutics and novel biological agents for targeted therapy, along with immunotherapy, broaden the range of therapeutic options mainly in inoperable cases, providing promising outcomes[10,21,34].

CONCLUSION

The current management of GI MiNENs and pure NECs constitutes a challenging multidisciplinary task that must be personalized for each patient. Early and accurate diagnosis has an important contribution to proper management. Apart from diagnostic and therapeutic modern endoscopic modalities, the role of gastroenterologists is also crucial, in diagnosis and scheduled follow-up appointments. Surgery is the cornerstone of any curative treatment accompanied by chemotherapy and novel drugs. Future perspectives should open new horizons in novel chemotherapies, targeted gene therapy and immunotherapy.

FOOTNOTES

Author contributions: Pavlidis TE, Galanis IN, and Pavlidis ET analyzed data, reviewed and approved the paper; Pavlidis TE designed research and contributed new analytic tools; Pavlidis ET performed research.

Conflict-of-interest statement: All the authors report no relevant conflicts of interest for this article.

Country of origin: Greece

ORCID number: Efstathios T Pavlidis 0000-0002-7282-8101; Ioannis N Galanis 0009-0001-4283-0788; Theodoros E Pavlidis 0000-0002-8141-1412.

S-Editor: Wang JJ
L-Editor: A
P-Editor: Wang WB

REFERENCES

1 **Cives M**, Porta C, Palmirotta R. Mixed neuroendocrine non-neuroendocrine tumors: The quest for evidence. *World J Gastrointest Oncol* 2024; **16**: 4532-4536 [DOI: 10.4251/wjgo.v16.i12.4532]

2 **Díaz-López S**, Jiménez-Castro J, Robles-Barraza CE, Ayala-de Miguel C, Chaves-Conde M. Mixed neuroendocrine non-neuroendocrine neoplasms in gastroenteropancreatic tract. *World J Gastrointest Oncol* 2024; **16**: 1166-1179 [PMID: 38660639 DOI: 10.4251/wjgo.v16.i4.1166]

3 **Shenoy S**. Mixed neuroendocrine and adenocarcinoma of gastrointestinal tract: A complex diagnosis and therapeutic challenge. *World J Gastrointest Oncol* 2024; **16**: 2295-2299 [PMID: 38994166 DOI: 10.4251/wjgo.v16.i6.2295]

4 **Liao X**, Schmidt AL, Zhang D, Li P, Wang X, Ko HM, Choi WT, Alpert L, Hao Y, Kovar-Peltz S, Polydorides AD, Wanjari P, Mastro J, Wang P. Clinicopathologic and Molecular Characterization of Inflammatory Bowel Disease-Associated Neuroendocrine Carcinomas and Mixed Neuroendocrine-Non-Neuroendocrine Neoplasms. *Mod Pathol* 2024; **37**: 100566 [PMID: 39025404 DOI: 10.1016/j.modpat.2024.100566]

5 **Xu B**, Zhang F, Wu R, Peng Y, Mao Z, Tong S. Incidence, survival, and prognostic factors for patients with gastrointestinal mixed neuroendocrine non-neuroendocrine neoplasms: a SEER population-based study. *J Cancer Res Clin Oncol* 2023; **149**: 15657-15669 [PMID: 37656242 DOI: 10.1007/s00432-023-05356-z]

6 **Song H**, Yang S, Zhang Y, Hua Y, Kleeff J, Liu Q, Liao Q. Comprehensive analysis of mixed neuroendocrine non-neuroendocrine neoplasms (MiNENs): A SEER database analysis of 767 cases. *Front Oncol* 2022; **12**: 1007317 [PMID: 36698410 DOI: 10.3389/fonc.2022.1007317]

7 **Bosman FT**, Carneiro F, Hruban RH, Theise ND. Digestive system tumours. In: WHO classification of tumours, 5th ed. Lyon: IARC Press, 2019

8 **Guerrera LP**, Suarato G, Napolitano R, Perrone A, Caputo V, Ventriglia A, Martini G, Della Corte CM, Orditura M, Martinelli E, Ciardiello F, Montella M, Franco R, Troiani T, Napolitano S. Mixed Neuroendocrine Non-Neuroendocrine Neoplasms of the Gastrointestinal Tract: A Case Series. *Healthcare (Basel)* 2022; **10** [PMID: 35455885 DOI: 10.3390/healthcare10040708]

9 **Wang Y**, Zhang Z, Wang C, Xi SH, Wang XM. Mixed neuroendocrine-nonneuroendocrine neoplasm of the ampulla: Four case reports. *World J Clin Cases* 2022; **10**: 2268-2274 [PMID: 35321159 DOI: 10.12998/wjcc.v10.i7.2268]

10 **Elpek GO**. Mixed neuroendocrine-nonneuroendocrine neoplasms of the gastrointestinal system: An update. *World J Gastroenterol* 2022; **28**: 794-810 [PMID: 35317101 DOI: 10.3748/wjg.v28.i8.794]

11 **Pellat A**, Cottereau AS, Terris B, Coriat R. Neuroendocrine Carcinomas of the Digestive Tract: What Is New? *Cancers (Basel)* 2021; **13** [PMID: 34359666 DOI: 10.3390/cancers13153766]

12 **Dasari A**, Shen C, Devabhaktuni A, Nighot R, Sorbye H. Survival According to Primary Tumor Location, Stage, and Treatment Patterns in Locoregional Gastroenteropancreatic High-grade Neuroendocrine Carcinomas. *Oncologist* 2022; **27**: 299-306 [PMID: 35380711 DOI: 10.1093/oncolo/oyab039]

13 **Suraju MO**, Freischlag K, Jacob D, Thompson D, Mckeen A, Tran C, Sherman SK, Goffredo P, Weigel RJ, Hassan I. Epidemiology and survival outcomes of colorectal mixed neuroendocrine-non-neuroendocrine neoplasms and neuroendocrine carcinoma. *Surgery* 2024; **175**: 735-742 [PMID: 37867105 DOI: 10.1016/j.surg.2023.09.019]

14 **Qiu MZ**, Chen Q, Zheng DY, Zhao Q, Wu QN, Zhou ZW, Yang LQ, Luo QY, Sun YT, Lai MY, Yuan SS, Wang FH, Luo HY, Wang F, Li YH, Zhang HZ, Xu RH. Precise microdissection of gastric mixed adeno-neuroendocrine carcinoma dissects its genomic landscape and evolutionary clonal origins. *Cell Rep* 2023; **42**: 112576 [PMID: 37285266 DOI: 10.1016/j.celrep.2023.112576]

15 **Cheng Y**, Zhang X, Zhou X, Xu K, Lin M, Huang Q. Differences in clinicopathology and prognosis between gastroesophageal junctional and gastric non-cardiac neuroendocrine carcinomas: a retrospective comparison study of consecutive 56 cases from a single institution in China. *Am J Cancer Res* 2022; **12**: 4737-4750 [PMID: 36381336]

16 **Liu L**, Li Q, Liu W, Qiu Z, Wu Z, Yu D, Deng W. Gastric mixed neuroendocrine non-neuroendocrine neoplasms. *Front Oncol* 2024; **14**: 1335760 [PMID: 38655135 DOI: 10.3389/fonc.2024.1335760]

17 **Ziogas IA**, Rallis KS, Tasoudis PT, Moris D, Schulick RD, Del Chiaro M. Management and outcomes of mixed adenoneuroendocrine carcinoma of the ampulla of Vater: A systematic review and pooled analysis of 56 patients. *Eur J Surg Oncol* 2023; **49**: 682-687 [PMID: 36646615 DOI: 10.1016/j.ejso.2023.01.005]

18 **Xing X**, Zhang Y, Wang L, Wang Y, Zhang Z, Li Z, Li M. Discussion on the benefits of different treatment strategies in elderly and non-elderly patients with appendix MiNEN: a retrospective study based on SEER database. *Int J Colorectal Dis* 2023; **38**: 93 [PMID: 37039889 DOI: 10.1007/s00384-023-04384-y]

19 **Dhakre VW**, Galande ST, Patil VG, Shah NC, Rathod C, Sethna KS, Amrapurkar AD. Mixed Neuroendocrine and Non-Neuroendocrine Neoplasm of Pancreas: What Do We Know, What Have We Learnt? *Gastrointest Tumors* 2023; **10**: 14-18 [PMID: 37102120 DOI: 10.1159/000528759]

20 **Yao X**, Wu K, Lu B, Lin F. Neuroendocrine carcinoma of the gallbladder: A case report and literature review. *Medicine (Baltimore)* 2024; **103**: e39147 [PMID: 39093760 DOI: 10.1097/MD.0000000000039147]

21 **Jiang C**, Yao H, Zhang Q, Shi H, Lin R. Clinicopathological characteristics of mixed neuroendocrine-non-neuroendocrine neoplasms in gastrointestinal tract. *Pathol Res Pract* 2023; **243**: 154373 [PMID: 36791563 DOI: 10.1016/j.prp.2023.154373]

22 **Yachida S**, Totoki Y, Noë M, Nakatani Y, Horie M, Kawasaki K, Nakamura H, Saito-Adachi M, Suzuki M, Takai E, Hama N, Higuchi R, Hirono S, Shiba S, Kato M, Furukawa E, Arai Y, Rokutan H, Hashimoto T, Mitsunaga S, Kanda M, Tanaka H, Takata S, Shimomura A, Oshima M, Hackeng WM, Okumura T, Okano K, Yamamoto M, Yamaue H, Morizane C, Arihiro K, Furukawa T, Sato T, Kiyono T, Brosens LAA, Wood LD, Hruban RH, Shibata T. Comprehensive Genomic Profiling of Neuroendocrine Carcinomas of the Gastrointestinal System. *Cancer Discov* 2022; **12**: 692-711 [PMID: 34880079 DOI: 10.1158/2159-8290.CD-21-0669]

23 **Mafficini A**, Scarpa A. Genetics and Epigenetics of Gastroenteropancreatic Neuroendocrine Neoplasms. *Endocr Rev* 2019; **40**: 506-536 [PMID: 30657883 DOI: 10.1210/er.2018-00160]

24 **Yin F**, Wu ZH, Lai JP. New insights in diagnosis and treatment of gastroenteropancreatic neuroendocrine neoplasms. *World J Gastroenterol* 2022; **28**: 1751-1767 [PMID: 35633912 DOI: 10.3748/wjg.v28.i17.1751]

25 **Fernandez CJ**, Agarwal M, Pottakkat B, Haroon NN, George AS, Pappachan JM. Gastroenteropancreatic neuroendocrine neoplasms: A clinical snapshot. *World J Gastrointest Surg* 2021; **13**: 231-255 [PMID: 33796213 DOI: 10.4240/wjgs.v13.i3.231]

26 **Takayanagi D**, Cho H, Machida E, Kawamura A, Takashima A, Wada S, Tsunoda T, Kohno T, Shiraishi K. Update on Epidemiology, Diagnosis, and Biomarkers in Gastroenteropancreatic Neuroendocrine Neoplasms. *Cancers (Basel)* 2022; **14** [PMID: 35267427 DOI: 10.3390/cancers14051119]

27 **Maurer E**, Heinzel-Gutenbrunner M, Rinke A, Rütz J, Holzer K, Figiel J, Luster M, Bartsch DK. Relevant prognostic factors in patients with stage IV small intestine neuroendocrine neoplasms. *J Neuroendocrinol* 2022; **34**: e13076 [PMID: 34964186 DOI: 10.1111/jne.13076]

28 **Cattaneo L**, Centonze G, Sabella G, Lagano V, Angerilli V, Pardo C, Bertani E, Spada F, Prinzi N, Pusceddu S, Fassan M, Fazio N, Milione M. Digestive MiNENs: Could histological classification and molecular characterization drive clinical outcome and therapeutic approach? *Crit Rev Oncol Hematol* 2023; **188**: 104044 [PMID: 37268174 DOI: 10.1016/j.critrevonc.2023.104044]

29 **Gherghe M**, Lazăr AM, Stanciu AE, Mutuleanu MD, Sterea MC, Petroiu C, Galeș LN. The New Radiolabeled Peptide (99m)TcEDDA/HYNIC-TOC: Is It a Feasible Choice for Diagnosing Gastroenteropancreatic NETs? *Cancers (Basel)* 2022; **14** [PMID: 35681704 DOI: 10.3390/cancers14112725]

30 **Inaba Y**, Hijioka S, Iwama I, Asai T, Miyamura H, Chatani S, Hasegawa T, Murata S, Kato M, Sato Y, Yamaura H, Onaya H, Shimizu J, Hara K. Clinical usefulness of Somatostatin Receptor Scintigraphy in the Diagnosis of Neuroendocrine Neoplasms. *Asia Ocean J Nucl Med Biol* 2022; **10**: 1-13 [PMID: 35083344 DOI: 10.22038/AOJNMB.2021.56254.1390]

31 **Ramzan A**, Tafti D. Nuclear Medicine PET/CT Gastrointestinal Assessment, Protocols, and Interpretation. 2023 May 22. In: StatPearls [Internet]. Treasure Island (FL): StatPearls Publishing; 2024 Jan- [PMID: 35593839]

32 **Morland D**, Jallerat P, Brixi H, Cadiot G, Papathanassiou D, Deguelte S. Performances of 18F-FDOPA PET/CT in the Preoperative Evaluation of the Peritoneal Cancer Index in Small Intestine Neuroendocrine Tumors. *Clin Nucl Med* 2022; **47**: 294-298 [PMID: 35067541 DOI:

10.1097/RLU.0000000000004057]
33 **Fang JM**, Li J, Shi J. An update on the diagnosis of gastroenteropancreatic neuroendocrine neoplasms. *World J Gastroenterol* 2022; **28**: 1009-1023 [PMID: 35431496 DOI: 10.3748/wjg.v28.i10.1009]
34 **Pavlidis ET**, Pavlidis TE. Molecular factors, diagnosis and management of gastrointestinal tract neuroendocrine tumors: An update. *World J Clin Cases* 2022; **10**: 9573-9587 [PMID: 36186187 DOI: 10.12998/wjcc.v10.i27.9573]
35 **Zhang H**, Tsuchikawa T, Takeuchi S, Deng H, Tanaka K, Matsui A, Nakanishi Y, Asano T, Noji T, Nakamura T, Takeuchi S, Wada M, Xu J, Zhang Y, Hirano S. Distinct clinicopathological features of neuroendocrine liver metastases originating from the pancreas and rectum. *World J Surg Oncol* 2024; **22**: 209 [PMID: 39097743 DOI: 10.1186/s12957-024-03476-5]
36 **Zhang S**, Zheng C, Chen Y, Xu Q, Ma J, Yuan W, Jiang Q, Zhao Y, Zhang J, Che X, Wang C, Huang X, Chen F, Wang N, Ma X, Lan Z. Clinicopathologic features, surgical treatments, and outcomes of small bowel tumors: A retrospective study in China. *Int J Surg* 2017; **43**: 145-154 [PMID: 28583893 DOI: 10.1016/j.ijsu.2017.05.076]
37 **Spada F**, Milione M, Maisonneuve P, Prinzi N, Smiroldo V, Bolzacchini E, Pusceddu S, Carnaghi C, Sessa F, La Rosa S, Uccella S, Fazio N. An Italian real-world multicenter study of patients with advanced mixed neuroendocrine non-neuroendocrine neoplasms (MiNENs) of the gastro-entero-pancreatic system treated with chemotherapy. *J Endocrinol Invest* 2024; **47**: 2279-2294 [PMID: 38402360 DOI: 10.1007/s40618-024-02314-5]
38 **Zhang P**, Shi S, Xu J, Chen Z, Song L, Zhang X, Cheng Y, Zhang Y, Ye F, Li Z, Yin F, Ji D, Gao H, Li Y, Chen W, Yang M, Weng D, Wu C, Ma Y, Sheng W, Zhao Y, Yin X, Shen W, Su W, Shi M, Fan S, Tan P, Xu Q, Lu M, Shen L. Surufatinib plus toripalimab in patients with advanced neuroendocrine tumours and neuroendocrine carcinomas: An open-label, single-arm, multi-cohort phase II trial. *Eur J Cancer* 2024; **199**: 113539 [PMID: 38237373 DOI: 10.1016/j.ejca.2024.113539]
39 **Zhu L**, Ye X, She Y, Liu W, Hasegawa K, Rossi RE, Du Q, Zhai Q. Assessing the effectiveness and safety of surufatinib versus everolimus or sunitinib in advanced neuroendocrine neoplasms: insights from a real-world, retrospective cohort study using propensity score and inverse probability treatment weighting analysis. *J Gastrointest Oncol* 2024; **15**: 689-709 [PMID: 38756630 DOI: 10.21037/jgo-24-218]
40 **Halperin DM**, Liu S, Dasari A, Fogelman D, Bhosale P, Mahvash A, Estrella JS, Rubin L, Morani AC, Knafl M, Overeem TA, Fu SC, Solis LM, Parra Cuentas E, Verma A, Chen HL, Gite S, Subashchandrabose P, Dervin S, Schulze K, Darbonne WC, Yun C, Wistuba II, Futreal PA, Woodman SE, Yao JC. Assessment of Clinical Response Following Atezolizumab and Bevacizumab Treatment in Patients With Neuroendocrine Tumors: A Nonrandomized Clinical Trial. *JAMA Oncol* 2022; **8**: 904-909 [PMID: 35389428 DOI: 10.1001/jamaoncol.2022.0212]
41 **Toor D**, Loree JM, Gao ZH, Wang G, Zhou C. Mixed neuroendocrine-non-neuroendocrine neoplasms of the digestive system: A mini-review. *World J Gastroenterol* 2022; **28**: 2076-2087 [PMID: 35664032 DOI: 10.3748/wjg.v28.i19.2076]
42 **Espinosa-Olarte P**, La Salvia A, Riesco-Martinez MC, Anton-Pascual B, Garcia-Carbonero R. Chemotherapy in NEN: still has a role? *Rev Endocr Metab Disord* 2021; **22**: 595-614 [PMID: 33843007 DOI: 10.1007/s11154-021-09638-0]
43 **Erstad DJ**, Dasari A, Taggart MW, Kaur H, Konishi T, Bednarski BK, Chang GJ. Prognosis for Poorly Differentiated, High-Grade Rectal Neuroendocrine Carcinomas. *Ann Surg Oncol* 2022; **29**: 2539-2548 [PMID: 34787737 DOI: 10.1245/s10434-021-11016-8]
44 **Popa O**, Taban SM, Pantea S, Plopeanu AD, Barna RA, Cornianu M, Pascu AA, Dema ALC. The new WHO classification of gastrointestinal neuroendocrine tumors and immunohistochemical expression of somatostatin receptor 2 and 5. *Exp Ther Med* 2021; **22**: 1179 [PMID: 34475969 DOI: 10.3892/etm.2021.10613]
45 **Ohmoto A**, Morizane C. Genomic Profiles and Current Therapeutic Agents in Neuroendocrine Neoplasms. *Curr Drug Targets* 2020; **21**: 389-405 [PMID: 31633473 DOI: 10.2174/1389450119666191014105211]
46 **Dai Q**, Zhang J, Long W, Haybaeck J, Yang Z. Genetic alterations of GI-NECs involving three main signaling pathways. *Cancer Med* 2023; **12**: 8238-8250 [PMID: 36653904 DOI: 10.1002/cam4.5633]
47 **McDonald A**, Avadhani V, Oprea-Ilies G, Zakka K, Lesinski GB, Gbolahan OB, Alese O. A pilot study of the immune microenvironment of GI neuroendocrine carcinoma. *Endocr Relat Cancer* 2024; **31** [PMID: 39045861 DOI: 10.1530/ERC-24-0046]
48 **Matsueda K**, Uedo N, Kitamura M, Shichijo S, Maekawa A, Kanesaka T, Takeuchi Y, Higashino K, Ishihara R, Michida T, Kawano S, Kawahara Y. Endoscopic features of gastric neuroendocrine carcinoma. *J Gastroenterol Hepatol* 2023; **38**: 1808-1817 [PMID: 37527834 DOI: 10.1111/jgh.16309]
49 **Hanzawa S**, Asami S, Kanazawa T, Oono S, Takakura N. Multimodal Treatment With Nivolumab Contributes to Long-Term Survival in a Case of Unresectable Esophagogastric Junction Neuroendocrine Carcinoma. *Cureus* 2024; **16**: e65981 [PMID: 39221328 DOI: 10.7759/cureus.65981]
50 **Seyama Y**, Yamada T, Suzuki H, Fukuda S, Tsuji M, Niisato Y, Hirose S, Yamamoto Y, Moriwaki T, Hyodo I. Gastric neuroendocrine carcinoma presenting complete durable response by nivolumab treatment for multiple metastases and radiotherapy to oligoprogressive metastasis. *Int Cancer Conf J* 2023; **12**: 268-273 [PMID: 37577341 DOI: 10.1007/s13691-023-00611-z]
51 **Bongiovanni A**, Liverani C, Foca F, Bergamo F, Leo S, Pusceddu S, Gelsomino F, Brizzi MP, Di Meglio G, Spada F, Tamberi S, Lolli I, Cives M, Marconcini R, Pucci F, Berardi R, Antonuzzo L, Badalamenti G, Santini D, Recine F, Vanni S, Tebaldi M, Severi S, Rudnas B, Nanni O, Ranallo N, Crudi L, Calabrò L, Ibrahim T. A randomized phase II trial of Captem or Folfiri as second-line therapy in neuroendocrine carcinomas. *Eur J Cancer* 2024; **208**: 114129 [PMID: 39002347 DOI: 10.1016/j.ejca.2024.114129]

World Journal of Gastrointestinal Oncology

Submit a Manuscript: https://www.f6publishing.com

World J Gastrointest Oncol 2024 December 15; 16(12): 4565-4578

DOI: 10.4251/wjgo.v16.i12.4565

ISSN 1948-5204 (online)

REVIEW

Unraveling the role of cancer-associated fibroblasts in colorectal cancer

Jia-Yu Cui, Jing Ma, Xin-Xin Gao, Zhi-Mei Sheng, Zi-Xin Pan, Li-Hong Shi, Bao-Gang Zhang

Specialty type: Oncology

Provenance and peer review: Unsolicited article; Externally peer reviewed.

Peer-review model: Single blind

Peer-review report's classification

Scientific Quality: Grade B, Grade C

Novelty: Grade B, Grade B

Creativity or Innovation: Grade B, Grade C

Scientific Significance: Grade B, Grade B

P-Reviewer: Liu H

Received: June 18, 2024

Revised: August 30, 2024

Accepted: September 19, 2024

Published online: December 15, 2024

Processing time: 146 Days and 19.9 Hours

Jia-Yu Cui, Jing Ma, Xin-Xin Gao, Zi-Xin Pan, Affiliated Hospital of Shandong Second Medical University, School of Clinical Medicine, Shandong Second Medical University, Weifang 261053, Shandong Province, China

Zhi-Mei Sheng, Affiliated Hospital of Shandong Second Medical University, Department of Pathology, Shandong Second Medical University, Weifang 261053, Shandong Province, China

Li-Hong Shi, School of Rehabilitation Medicine, Shandong Second Medical University, Weifang 261053, Shandong Province, China

Bao-Gang Zhang, Department of Pathology, Shandong Second Medical University, Weifang 261053, Shandong Province, China

Co-corresponding authors: Li-Hong Shi and Bao-Gang Zhang.

Corresponding author: Bao-Gang Zhang, MD, PhD, Doctor, Teacher, Department of Pathology, Shandong Second Medical University, No. 4948 East Shengli Street, Quewen District, Weifang 261000, Shandong Province, China. zbg0903@hotmail.com

Abstract

Within the intricate milieu of colorectal cancer (CRC) tissues, cancer-associated fibroblasts (CAFs) act as pivotal orchestrators, wielding considerable influence over tumor progression. This review endeavors to dissect the multifaceted functions of CAFs within the realm of CRC, thereby highlighting their indispensability in fostering CRC malignant microenvironment and indicating the development of CAFs-targeted therapeutic interventions. Through a comprehensive synthesis of current knowledge, this review delineates insights into CAFs-mediated modulation of cancer cell proliferation, invasiveness, immune evasion, and neovascularization, elucidating the intricate web of interactions that sustain the pro-tumor metabolism and secretion of multiple factors. Additionally, recognizing the high level of heterogeneity within CAFs is crucial, as they encompass a range of subtypes, including myofibroblastic CAFs, inflammatory CAFs, antigen-presenting CAFs, and vessel-associated CAFs. Innovatively, the symbiotic relationship between CAFs and the intestinal microbiota is explored, shedding light on a novel dimension of CRC pathogenesis. Despite remarkable progress, the orchestrated dynamic functions of CAFs remain incompletely deciphered, underscoring the need for continued research endeavors for therapeutic advancements in CRC management.

Key Words: Colorectal cancer; Cancer-associated fibroblasts; Therapeutic strategies; Microbiota; Neovascularization

Core Tip: Within the intricate milieu of colorectal cancer (CRC) tissues, cancer-associated fibroblasts (CAFs) act as pivotal orchestrators, wielding considerable influence over tumor progression. This review endeavors to dissect the multifaceted functions of CAFs within the realm of CRC, thereby highlighting their indispensability in fostering CRC malignant microenvironment and indicating the development of CAFs-targeted therapeutic interventions. Through a comprehensive synthesis of current knowledge, this review delineates insights into CAFs-mediated modulation of cancer cell proliferation, invasiveness, immune evasion, and neovascularization, elucidating the intricate web of interactions that sustain the pro-tumor metabolism and secretion of multiple factors. Additionally, recognizing the high level of heterogeneity within CAFs is crucial, as they encompass a range of subtypes, including myofibroblastic CAFs, inflammatory CAFs, antigen-presenting CAFs, and vessel-associated CAFs. Innovatively, the symbiotic relationship between CAFs and the intestinal microbiota is explored, shedding light on a novel dimension of CRC pathogenesis. Despite remarkable progress, the orchestrated dynamic functions of CAFs remain incompletely deciphered, underscoring the need for continued research endeavors for therapeutic advancements in CRC management.

Citation: Cui JY, Ma J, Gao XX, Sheng ZM, Pan ZX, Shi LH, Zhang BG. Unraveling the role of cancer-associated fibroblasts in colorectal cancer. *World J Gastrointest Oncol* 2024; 16(12): 4565-4578
URL: https://www.wjgnet.com/1948-5204/full/v16/i12/4565.htm
DOI: https://dx.doi.org/10.4251/wjgo.v16.i12.4565

INTRODUCTION

Malignant tumors have become a significant factor affecting the mortality worldwide, with colorectal cancer (CRC) being among the crucial types of malignancies. CRC is the third most common cancer and the second leading cause of cancer-related death worldwide[1]. It is well known that the development of tumors is not solely due to changes of genes within tumor cells, and the alterations in the surrounding microenvironment also play a significant role in tumor progression.

Over 100 years ago, Paget and others elucidated the importance of the tumor microenvironment (TME) with the "seed and soil" hypothesis which implied a synergistic interaction between tumors and their microenvironment[2]. Numerous studies have confirmed that the stromal components of the TME have crucial impacts on the occurrence and evolution of tumors. As the most abundant non-cancerous stromal cell type, cancer-associated fibroblasts (CAFs) play vital roles in the development of CRC by influencing the proliferation, invasion, and metastasis of cancer cells as well as angiogenesis and immune response through reshaping the extracellular matrix (ECM), secreting soluble factors (chemokines and growth factors), and modulating the microbial community[3,4].

In this review, we aim to delve into the crucial role of CAFs in the progression and treatment of CRC. Additionally, we provide a comprehensive overview of the diverse functions of CAFs, including their impact on cancer cell proliferation, invasiveness, immune evasion, and neovascularization, as well as their role in shaping the TME and influencing tumor growth and metastasis. This exploration highlights the intricate network between CRC and CAFs and clarifies how these interactions affect the disease's prognosis and treatment efficacy. Moreover, we introduce a novel perspective on the symbiotic relationship between CAFs and the intestinal microbiota, potentially opening new avenues for targeting CAFs.

ORIGIN OF CAFS

Function of fibroblasts

Normal fibroblasts (NFs) are spindle-shaped mesenchymal cells possessing non-epithelial, non-endothelial, and non-immunological characteristics[5,6] which commonly locate in the connective tissue and help to maintain tissue homeostasis[7]. Functionally, fibroblasts synthesize and secrete laminin, type IV collagen, and other basement membrane-related proteins under normal physiological conditions. Particularly, fibroblasts in intestinal tissue exhibit specialized functions that are crucial for supporting epithelial cells and maintaining barrier integrity[8]. Their roles in ECM production, tissue remodeling, cell communication, immunoregulation, and wound healing collectively contribute to the maintenance of the intestinal epithelial function. In addition, fibroblasts exhibit inhibitory effects on the occurrence, development, invasion, and metastasis of tumor cells through various mechanisms including direct cell-to-cell contact, secretion of soluble factors, and preservation of an intact ECM environment[9]. However, in the context of malignant tumors, changes in the structure and function of the TME lead fibroblasts to transition from their initial anti-tumor characteristics to pro-tumor preference[10].

Origins of CAFs

CAFs are generally considered to be all fibroblasts embedded within and around cancerous tissues, representing a crucial component of TME[11]. Progenitor cells of CAFs are recruited from several sources and developed by distinct pathways [12], and most of the available evidence supports that the majority of CAFs may originate from the activation of locally resident fibroblasts[13]. Tissue-resident quiescent fibroblasts can be activated by various factors including inflammatory cytokines, constipation, microorganisms, and chemokines [interleukin (IL)-6], as well as growth factors such as transforming growth factor-β (TGF-β)[14] (Figure 1). Persisted activation tends to cause morphological and functional transformations of NFs into CAFs which are involved in cancer initiation, progression, and chemoresistance[15]. It should be noted that CAFs and NFs are interconvertible, although the underlying mechanism is still poorly understood. Fibrocytes represent a quiescent fibroblast state, which are also considered as one of the sources of CAFs[16,17]. For example, fibrocytes derived from hepatic stellate cells (HSCs) expressing fibroblast growth factor receptor 2 were identified as the origin of CAFs in esophageal squamous cell carcinoma[18].

Mesenchymal stem cells (MSCs) are proposed as potential precursors for CAFs, and Notch and Akt signaling pathways have been reported to be involved in the differentiation of bone marrow MSCs into CAFs[19,20] (Figure 1). In addition, MSCs could acquire CAF-like characteristics while stimulated by TGF-β, tumor necrosis factor-α, and IL-1β[21]. Intriguingly, macrophages can assist MSCs in developing CAF-like features[22]. Stellate cells are also an alternative origin of CAFs in certain tumors[23,24] (Figure 1). Insufficient vitamin A can trigger the transformation of pancreatic stellate cells into CAFs[25], and insulin-like growth factor-1 (IGF-1) signaling is crucial for activating HSCs into CAFs[26]. Adipocytes are recognized as another category of CAFs precursors[17,27] (Figure 1). Adipocytes may play a role in tumorigenesis through a mechanism of adipocyte-fibroblast transition[28]. Tumor cells could induce morphological changes and, meanwhile, decrease lipid content and marker expression of adipocytes. Bochet *et al*[29] found that adipocytes may dedifferentiate into cancer-associated adipocytes, and cancer-associated adipocytes become less adipocyte-like and phenotypically mirror fibroblasts with increased expression of ECM components. Moreover, epithelial and endothelial cells can differentiate into CAFs through epithelial-to-mesenchymal transition (EMT) and endothelial-to-mesenchymal transition[30-33]. Through the TGF-β-mediated EMT, epithelial cells are able to differentiate into functional CAFs expressing ferroptosis suppressor protein 1 and α-fibroblast activation protein (FAP)[34], whereas during the endothelial-to-mesenchymal transition, endothelial cells acquire a mesenchymal-like phenotype as well as invasive and migratory properties[35]. Cell types, including pericytes[36], monocytes[37], mesothelial cells[38], hematopoietic stem cells[39], circulating bone marrow cells[40], and smooth muscle cells[41], are also identified as potential precursors for CAFs. Understanding the origins of CAFs can provide new targets for cancer stromal remodeling process.

HETEROGENEITY OF CAFS

Heterogeneity transcends not only between individuals with the same tumor but also manifests as striking variations within a single tumor[42]. This dynamic variability evolves continuously over time and across spatial dimensions, interacting intricately with the surrounding microenvironment, making it a perpetually shifting and complex process. Distinct subtypes of CAFs are characterized by unique biological markers. In CRC, commonly identified CAF biomarkers include α-smooth muscle actin (α-SMA), FAP, vimentin, fibroblast specific protein 1, podoplanin, and platelet-derived growth factor receptors α/β (PDGFRα/β)[43]. With the advent of sequencing technologies, researchers have begun to analyze CAF populations at the single-cell level and revealed substantial heterogeneity among CAFs[44]. Single-cell sequencing has identified two principal CAF subsets named CAF-A and CAF-B in human CRC: CAF-A expresses high levels of FAP, matrix metalloproteinase-2 (MMP-2), and collagen type I alpha 2 while CAF-B is characterized by the expression of myofibroblastic markers such as α-SMA, transgelin, and PDGFα[45].

Additionally, recent studies have revealed two distinct subpopulations of CAFs in CRC: Myofibroblastic CAFs (myCAFs), characterized by high α-SMA and IL-6 expression, and inflammatory CAFs (iCAFs), which exhibit low α-SMA and high IL-6 expression[23,46-51]. myCAFs are primarily involved in regulating the ECM, collagen deposition, cellular contraction, and adhesion, whereas iCAFs are distinguished by their secretion of cytokines and chemokines and their interactions with immune cells[50,51]. Interestingly, we discovered that iCAFs were particularly concentrated around dilated blood vessels at the colonic luminal margin and demonstrated greater activity than myCAFs in mismatch repair-deficient tumors[46].

As research continues to deepen, the classification of CAF subtypes has become increasingly nuanced. Khaliq *et al*[51] utilized large-scale single-cell sequencing across diverse ethnic groups to achieve a more detailed categorization of myCAF and iCAF subtypes in CRC tissue, drawing on classification methods previously used in breast cancer[49]. The myCAF group was further subdivided into ecm-myCAFs, associated with ECM proteins; wound-myCAFs, linked to wound healing signaling; and TGFβ-myCAFs, dependent on the TGFβ pathway[51]. Similarly, the iCAF group was refined to include IL-iCAFs, related to IL signaling, and detox-iCAFs, associated with detoxification pathways. In addition to myCAFs and iCAFs, a type of vascular-associated CAFs expressing pericyte markers and hypoxia-inducible factor 2 has also been identified in CRC, participating in angiogenesis and vascular development and potentially contributing to tumor invasion and metastasis[51-53].

CAFs are frequently linked to the promotion of CRC, but recent studies have also uncovered their potential role in inhibiting CRC growth[54,55]. Kobayashi *et al*[56] discovered that CAFs can polarize into GREM1$^+$ CAFs, which promote tumor progression, and ISLR$^+$ CAFs, which inhibit tumor progression, under the regulation of the TGFβ-FOXL1-GREM1/ISLR axis. Although the specific mediators secreted by ISLR$^+$ CAFs that inhibit CRC progression remain unidentified, it is clear that these mediators contribute to activating bone morphogenetic protein signaling in CRC cells.

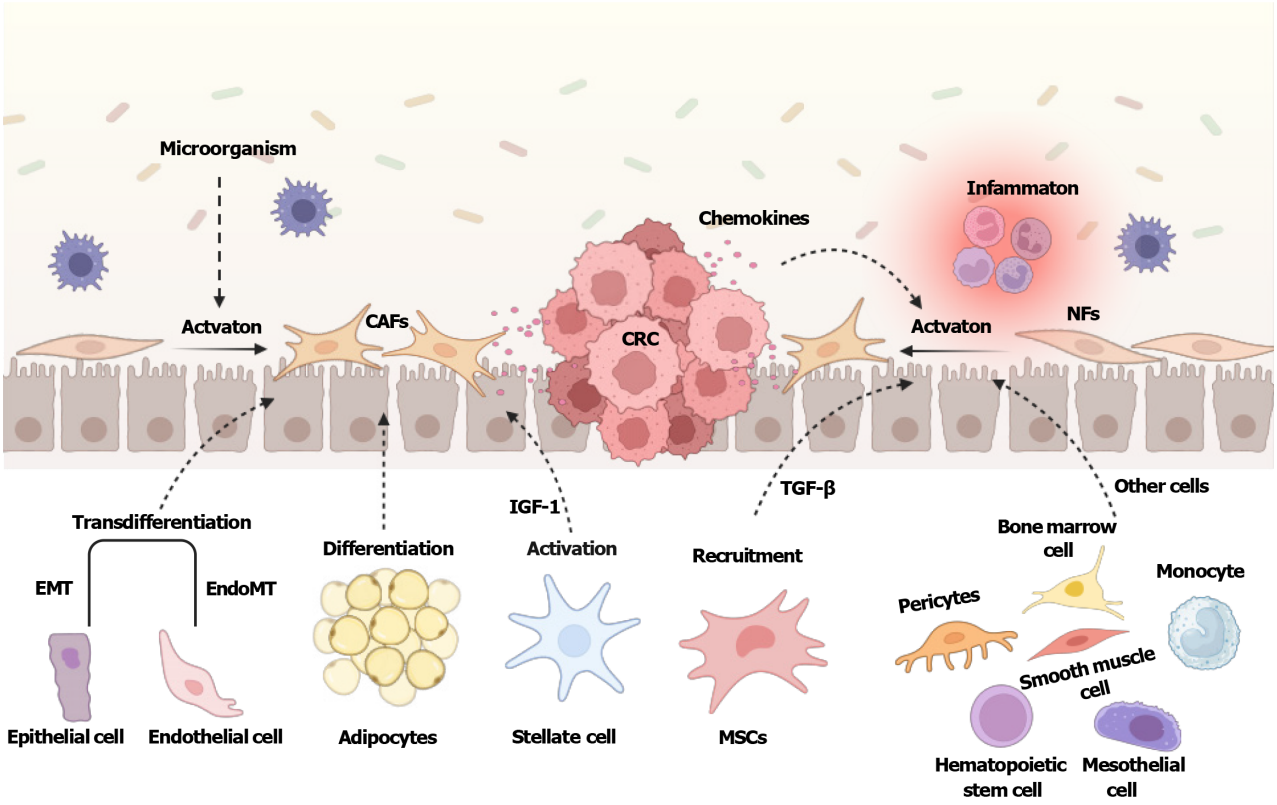

Figure 1 Origins of cancer-associated fibroblasts in colorectal cancer. Normal fibroblasts can be activated by various factors including inflammation, microorganisms, and chemokines, and transform into cancer-associated fibroblasts. In addition, epithelial cells, endothelial cells, hepatic stellate cells, adipocytes, mesenchymal stem cells, pericytes, monocytes, mesothelial cells, hematopoietic stem cells, bone marrow cells, and smooth muscle cells, are all potential precursors of cancer-associated fibroblasts. Created with BioRender.com (Supplementary material). CAFs: Cancer-associated fibroblasts; CRC: Colorectal cancer; TGF-β: Transforming growth factor-β; NFs: Normal fibroblasts; EMT: Epithelial-to-mesenchymal transition; IGF-1: Insulin-like growth factor-1; MSCs: Mesenchymal stem cells.

The heterogeneity of CAFs is continuously evolving with technological and temporal advancements. Single-cell sequencing and spatial transcriptomics have significantly enhanced our understanding of CAFs' diversity. However, a thorough classification of the functional diversity among different CAF subtypes in CRC remains incomplete, and more effective approaches for elucidating the identities and states of CAF subtypes are urgently needed[57,58].

ROLES OF CAFS IN CRC

CAFs and tumor proliferation and migration

In recent years, an increasing awareness has emerged regarding the pre-existing tumorigenic state of fibroblasts even prior to the onset of malignant cell transformation[13]. To delve deeper into the pathogenic intricacies of CRC, investigators isolated CAFs and NFs from fresh surgical specimens of colorectal adenocarcinoma patients. Additionally, co-culturing of these cells with colorectal tumor cells unveiled that tumor cells in conjunction with CAFs exhibited heightened proliferative and migrative capacities[59]. Mechanically, CAFs facilitate CRC proliferation and migration by secreting a variety of cytokines and small extracellular vesicles containing microRNAs (miRNAs), long noncoding RNAs (lncRNAs), and circular RNAs (circRNAs)[60] (Figure 2). Furthermore, Hirashima *et al*[61] revealed that gene sets related to the Wnt signaling pathway were highly enriched in colorectal CAFs by analyzing the expression profiles of paired CAFs and NFs from CRC tissue. Subsequent *in vitro* experiment showed that cancer cell proliferation and migration were significantly stimulated by both recombinant Wnt5a protein and CAFs-secreted Wnt2 through activating Wnt signaling [62]. Interestingly, the strategic collaboration between CAFs and tumor-associated macrophages amplifies the migratory prowess of CRC cells[63], which indicates that the immune microenvironment including various immune cells may serve as pivotal orchestrators in propelling the biological function of CAFs.

CAFs and tumor immune suppression

On the other hand, the intricate crosstalks between CAFs and immune cells also lead to tumor immune evasion by mediating immune cell recruitment and functional differentiation within the TME[64] (Figure 2). In the context of CRCs, the MSCs, as precursors to CAFs, exacerbate tumor progression by intensifying the inhibition of immune cells. Studies found that the sialylation profile of stromal cells is an important mechanism by which MSCs/CAFs modulate T cell

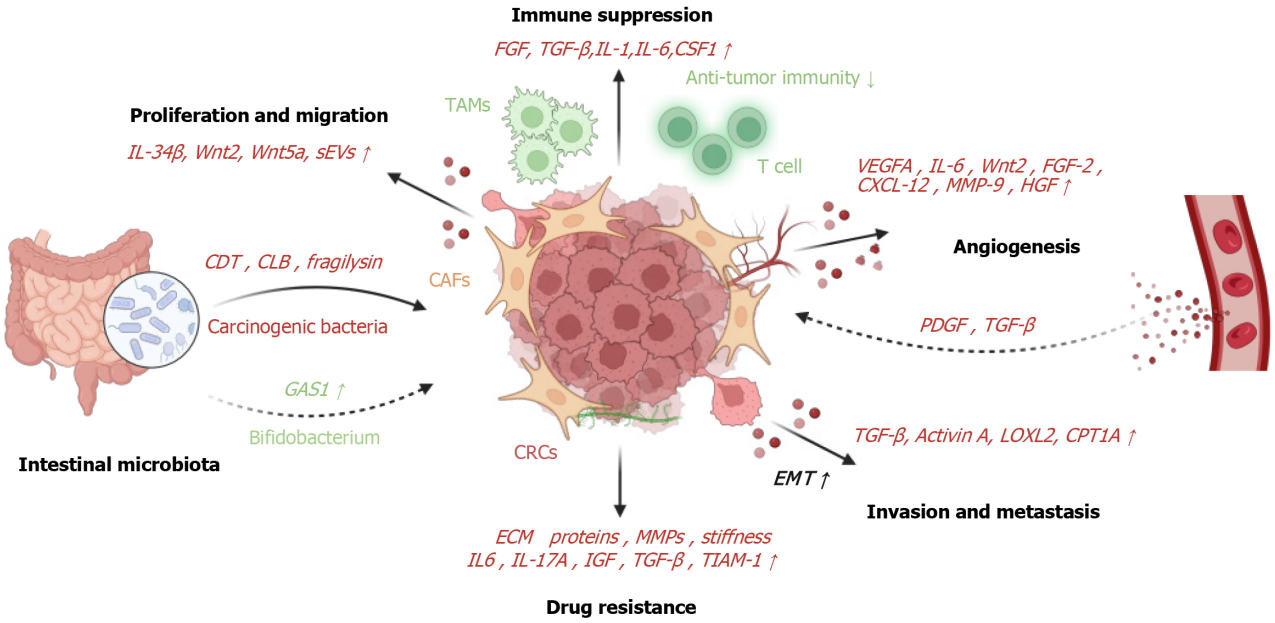

Figure 2 Roles of cancer-associated fibroblasts. Cancer-associated fibroblasts (CAFs) secrete a variety of cytokines, including interleukin (IL)-34, Wnt2, Wnt5a, and small extracellular vesicles, which actively promote colorectal cancer proliferation and migration. Additionally, CAFs intricately manage tumor immune evasion through a range of complex mechanisms, including the secretion of diverse cytokines and chemokines such as fibroblast growth factor, transforming growth factor-β (TGF-β), IL-1, IL-6, and colony-stimulating factor 1. And CAFs contribute to tumor initiation by releasing pro-tumor factors that stimulate angiogenesis, including vascular endothelial growth factor A, IL-6, Wnt2, fibroblast growth factor 2, CXC motif chemokine ligand 12, matrix metalloproteinase-9, and hepatocyte growth factor. In turn, the leaky vasculature within tumors releases pro-angiogenic factors such as platelet-derived growth factor and TGF-β through degranulation, which further activates fibroblasts. The secretion of TGF-β, activin A, and lysyl oxidase-like 2 by CAFs, along with the upregulation of carnitine palmitoyl-transferase 1A expression, promotes epithelial-to-mesenchymal transition in colorectal cancer, thereby enhancing the invasion and metastasis of colorectal cancer. Moreover, CAFs produce ECM proteins and remodel the matrix *via* matrix metalloproteinases, creating a physical barrier and increasing matrix stiffness and interstitial pressure. And CAFs secrete key soluble factors, including IL-6, IL-17A, and insulin-like growth factor-1. "Carcinogenic bacteria" secrete bacterial toxins such as cytolethal distending toxin, colibactin, and fragilysin, influencing the tumor microenvironment to foster tumor progression and immune evasion. Meanwhile, Bifidobacterium exhibits anticancer effects by activating CD143+ CAFs. Created with BioRender.com (Supplementary material). IL: Interleukin; sEVs: Small extracellular vesicles; FGF: Fibroblast growth factor; TGF-β: Transforming growth factor-β; CSF1: Colony-stimulating factor 1; TAMs: Tumor-associated macrophages; VEGFA: vascular endothelial growth factor A; CXCL-12: CXC motif chemokine ligand 12; MMP: Matrix metalloproteinase; HGF: Hepatocyte growth factor; CDT: Cytolethal distending toxin; CLB: Colibactin; CAFs: Cancer-associated fibroblasts; PDGF: Platelet-derived growth factor; GAS1: Growth arrest specific 1; CRC: Colorectal cancer; IGF: Insulin-like growth factor; TIAM-1: T-lymphoma invasion and metastasis-inducing protein-1; EMT: Epithelial-to-mesenchymal transition; LOLX2: Lysyl oxidase-like 2; CPT1A: Carnitine palmitoyl-transferase 1A.

exhaustion. Targeting stromal cell sialylation may overcome immunosuppression in the CRC TME[65]. The investigations spearheaded by Yang *et al*[66] illuminated the exacerbation of CAFs' pro-tumor role with the loss of the *BCL9* gene, culminating in the aberrant activation of the Wnt/β-catenin signaling pathway, thereby impeding T-cell-mediated anti-tumor immune responses.

Tumor-associated macrophages contribute to all aspects of tumor progression. Colony-stimulating factor 1 produced by tumor cells caused histone deacetylase 2-mediated downregulation of granulocyte-specific chemokine expression in CAFs. Treatment with colony-stimulating factor 1 receptor inhibitors disrupted this crosstalk and triggered a profound increase in granulocyte recruitment to tumors[67]. Moreover, colony-stimulating factor 1 receptor inhibitors have been utilized as agents targeting tumor-associated macrophages in clinical trials for solid tumors, including intestinal cancers [68]. However, their efficacy has been limited. This limitation has been attributed to CAFs' capability to counteract the therapeutic effects of these agents by recruiting polymorphonuclear myeloid-derived suppressor cells to tumor sites, thereby shaping an immunosuppressive TME[67]. Concomitantly, the involvement of pentraxin 3, fostering M2-like polarization of macrophages, surfaces in the context of CAF-mediated immune suppression, with elevated pentraxin 3 expression correlating positively with fibroblasts and inflammatory response signals in CRC patients, prognosticating unfavorable survival outcomes[69]. The pervasive influence of CAFs also extends to shaping the cytotoxicity of T lymphocytes, fortifying tumor cells in their evasion of the body's immune response[70].

A noteworthy revelation surfaces from recent research, underscoring the tumor-suppressive function of α-SMA+ CAFs within a genetically engineered mouse model of metastatic CRC. The α-SMA(+) CAFs in CRC exert tumor-restraining functions *via* bone morphogenetic protein 4/TGF-β1 paracrine signaling that serves to suppress Lgr5(+) CSCs and promote anti-tumor immunity, ultimately limiting CRC progression[71]. However, the nuanced impact of the depletion strategy, predominantly targeting α-SMA+ CAFs, on other α-SMA+ cells dispersed throughout the body, introduces an element of uncertainty regarding its potential perturbation of the observed outcomes. While there is a growing interest in cancer immunology, our comprehension of how CAFs participate in tumor immune surveillance is still in its infancy. More extensive investigations into CAFs are imperative to pinpoint promising target molecules or subsets of CAFs and to devise innovative therapies that can enhance the clinical efficacy of existing immunotherapies.

CAFs and tumor angiogenesis

Angiogenesis stands out as a pivotal step throughout diverse stages of tumor progression, playing a crucial role in the invasive growth of CRC. The significance lies in its ability to provide abundant blood vessels, furnishing oxygen and nutrients indispensable for the proliferation of tumor tissues. As a hallmark of malignant tumors, angiogenesis is closely associated with tumor growth, metastasis, and patient prognosis and is promoted by the most potent pro-angiogenic factor, vascular endothelial growth factor (VEGF), which stimulates angiogenesis by binding to its corresponding receptor VEGF receptor 2 (VEGFR2) on endothelial cells[72-74].

Neovascularization in cancer is governed not solely by tumor cells but also by stromal cells[75]. In fact, CAFs directly foster tumor angiogenesis by releasing pro-angiogenic factors and indirectly by generating the ECM[5,75]. In the context of CRC, cancer cells exhibit minimal VEGF secretion whereas CAFs represent a significant origin of VEGFA through the abundant release of IL-6[75,76]. The intricate interplay between colon cancer cells and the TME facilitates the transformation of NFs into CAFs, positively modulating IL-6 secretion, thereby amplifying VEGF secretion and fostering tumor angiogenesis[77]. Additionally, Unterleuthner *et al*[78] discovered that WNT2 secreted by CAFs plays a pivotal role in promoting the formation of tumor blood vessels in CRC. Silencing WNT2 in CAFs significantly diminishes the angiogenic potential of tumor vessels, highlighting that elevated WNT2 expression in CAFs renders tumors more susceptible to invasion and metastasis. Moreover, CAFs promote tumor initiation by secreting pro-tumor factors (Figure 2) that enhance angiogenesis, including VEGF-α, fibroblast growth factor 2, CXC motif chemokine ligand 12, MMP-9, and hepatocyte growth factor (HGF)[79]. In turn, the permeable vasculature within tumors leads to platelet extravasation and the subsequent release of pro-angiogenic factors such as PDGF and TGFβ through degranulation, which further activate fibroblasts[80]. Collectively, these studies offer a compelling rationale for considering CAFs as a viable therapeutic target to modify tumor vasculature.

CAFs promote tumor invasion and metastasis

In the intricate landscape of tumorigenesis, CAFs stand as instrumental architects, actively promoting the insidious progression of tumor invasion and metastasis[81,82]. As a substantial component of the TME, CAFs wield their influence in fostering the malignant behaviors of cancer cells. The multifaceted role of CAFs is underscored by their ability to induce EMT, a pivotal process that endows cancer cells with the traits essential for invasion and metastasis. Research illuminates the mechanistic intricacies, revealing that factors (Figure 2) such as TGF-β activation of colonic stromal fibroblasts and the secretion of activin A contribute to the heightened migratory capacity and EMT in colonic epithelial cells, thereby rendering CRC cells more prone to metastasis[83].

The dynamic interplay extends to specific molecular signaling pathways, as evidenced by studies elucidating the stimulation of EMT in CRC cells through the secretion of lysyl oxidase-like 2 by CAFs (Figure 2), activating the focal adhesion kinase signaling pathway[84]. Inhibition of this process presents a potential avenue for curtailing CRC cell invasion and metastasis. Additionally, the orchestration of EMT by CAFs involves regulatory elements such as myosin light chain 9, which influences the secretion of C-C motif ligand 2 and TGF-β, thereby shaping the TME and impacting CRC invasion and metastasis[85].

Beyond their involvement in EMT, CAFs exert a substantial impact on the metabolic landscape of CRC cells, enhancing their invasion and metastasis. Through the upregulation of key factors like carnitine palmitoyl-transferase 1A (Figure 2) [86], CAFs promote fatty acid oxidation while minimizing glycolysis, ultimately fostering a milieu conducive to tumor growth and invasion. Woven into this intricate narrative is the expression of WNT2 in CAFs, contributing to the invasion of CRC cells and unveiling additional dimensions to the role of CAFs in promoting metastasis[87]. As the exploration of CAFs' influence on tumor invasion and metastasis unfolds, their capacity to produce signaling molecules, including TGF-β, leukemia inhibitory factor, and HGF, emerges as another crucial facet[88]. These molecules act as potent drivers, propelling cancer cell proliferation and invasion behaviors. TGF-β, in particular, emerges as an effective inducer of EMT through paracrine signaling, endowing premalignant cells with mesenchymal properties that facilitate invasion and metastasis[89]. Furthermore, CAFs play a pivotal role in the colonization of distant organs during metastasis, either by creating a supportive microenvironment for cancer cells or by accompanying them in their journey[90].

Examining factors that foster invasion and metastasis through the lenses of EMT and metabolism is imperative. Concurrently, we need to delve into the repercussions of cancer cell EMT on CAFs subtypes. A crucial aspect to explore involves comprehending the influence of EMT-inducing transcription factors on stromal cells. Existing studies underscore a direct correlation between the expression of EMT transcription factors and the presence of CAFs[91]. Noteworthy is the work of Franci *et al*[92], who discerned predominant Snail expression in fibroblasts proximate to tumor cells in CRC. Furthermore, CRCs exhibiting mesenchymal gene expression traits display a heightened proclivity for distant metastasis, marked by the accumulation of CAFs in the stromal milieu. And findings indicate that fibroblasts within epithelial tumors exhibit elevated miR-200 expression and reduced levels of actin alpha 2 and fibronectin 1 compared to their mesenchymal counterparts[93]. This discovery unveils a novel mechanism for the heterogeneity of CRC CAFs, elucidating how miRNA transfer *via* extracellular vesicles contributes to this phenomenon. It also offers insights into why CRCs with augmented metastatic potential boast an abundance of CAFs.

CAFs and tumor drug resistance

Recent investigations underscore the pivotal role of the TME in shaping tumor cell resistance, elucidating the substantial impact of CAFs in promoting drug resistance across diverse cancers, notably CRC[94]. The intricate interplay involves CAFs's production of ECM proteins and matrix remodeling MMPs, forming both a physical barrier and elevating matrix stiffness and interstitial pressure (Figure 2). This dual effect impedes the efficient penetration of chemotherapy drugs and targeted therapies, contributing significantly to drug resistance[95]. Moreover, the secretion of key soluble factors

(Figure 2) by CAFs, including IL-6, IL-17A, and IGF, intricately mediates chemotherapy resistance and amplifies cytokine secretion post-treatment, consequently intensifying drug resistance[96,97].

Beyond their physical and soluble influences, CAFs play a pivotal role in immune suppression within the TME[13]. The accumulation of aberrant ECM components exacerbates immune suppression, adversely impacting the efficacy of immune checkpoint inhibitors. The involvement of the TGF-β signaling pathway is particularly noteworthy in the context of immune therapy resistance. It is intriguing to observe that the blockade of TGF-β signaling, in conjunction with receptor kinase inhibitors and anti-programmed cell death protein 1/programmed cell death ligand 1 immunotherapy, exhibits a synergistic effect in a murine model of CRC liver metastasis[98,99]. Notably, an elevated compound stromal score, characterized by three stromal components (CAFs, leukocytes, and endothelial cells), has the potential to anticipate resistance to radiotherapy in rectal cancer patients[100].

Regarding molecularly targeted medications, the release of HGF and IGF2 by CAFs plays a role in conferring resistance to tyrosine kinase inhibitors[101]. Notably, the concurrent inhibition of epidermal growth factor receptor (EGFR) and MET, or insulin receptor and IGF1 receptor, which facilitate the IGF2/insulin receptor/IGF1 receptor signaling pathway, has been shown to augment the therapeutic efficacy of an EGFR inhibitor in xenograft models of colon cancer, respectively[102]. In the realm of CRC, CAFs further exhibit their intricate influence by secreting IL-17A, which acts on the IL-17A receptor on CSCs. This action maintains CSPDCs' stem cell characteristics, upregulates nuclear factor-κB expression, and induces resistance in cancer cells[97]. Additionally, the secretion of exosomes by CAFs is implicated in promoting the stemness and chemotherapy resistance of CRC. The interaction with eukaryotic initiation factor 4A-III and the exosomal miR-625-3p blockade of the CELF2/WWOX pathway underscore the multifaceted mechanisms through which CAFs potentiate drug resistance[103,104]. Furthermore, CAFs contribute to chemotherapy resistance in CRC cells by inducing the overexpression of T-lymphoma invasion and metastasis-inducing protein-1, presenting T-lymphoma invasion and metastasis-inducing protein-1 as a promising therapeutic target[105]. In a co-culture setting, CAF-conditioned medium induces the overexpression of the *RBCK1* gene, augmenting the stemness and resistance of CRC cells[106]. This intricate web of interactions emphasizes the significant and varied roles of CAFs in fueling drug resistance in CRC, urging further exploration for targeted therapeutic interventions.

Relationship between CAFs and intestinal microbiota

As a crucial component of the intestinal barrier, the intestinal microbiota intricately weaves a biofilm, actively participating in intestinal functions and establishing a conducive survival environment for intestinal cells. Notably, this microbial consortium is implicated in various stages of CRC, ranging from benign precursor lesions (polyps) to *in situ* growth and metastasis. The concept of "carcinogenic bacteria" introduced in 2018, encompasses species like *Escherichia coli*, *Fusobacterium nucleatum*, and enterotoxigenic *Bacteroides fragilis*, underscoring their pivotal role in CRC pathogenesis. Concurrently, bacterial toxins such as cytolethal distending toxin, colibactin, and fragilysin exert their influence on the TME, fostering tumor development and immune escape. Noteworthy insights illuminate the intricate interplay between *Helicobacter pylori*, fibroblasts, and cancer cells, leading to the induction of Serpin E1 expression. This induction propels the transformation of NFs into CAFs, contributing to the onset of gastric cancer[107]. The complexity of these interactions emphasizes the multifaceted role of the intestinal microbiota in orchestrating the TME and influencing cancer progression.

Crucially, the nuanced roles of distinct intestinal bacteria must be acknowledged, as some confer beneficial effects on the human body. For instance, the work of Chen *et al*[108] highlights the positive impact of youth-associated Bifidobacterium, activating CD143+ CAFs, thereby initiating the Wnt signaling pathway and upregulating growth arrest specific 1 expression. This cascade of events manifests in anticancer effects, unveiling a promising therapeutic target for CRC[108]. These findings underscore the dynamic nature of the interactions between the intestinal microbiota, fibroblasts, and cancer cells, offering a profound understanding of the intricate molecular mechanisms shaping the TME and presenting potential avenues for therapeutic interventions.

TREATMENT OF CAFS IN CRC

Alongside surgical resection, the most current clinical approaches to treating CRC involve chemotherapy and radiotherapy, which exert diverse effects on the various cellular constituents of the TME[109]. A comparative study of CRC specimens from patients before and after undergoing cytotoxic treatment revealed a marked rise in CAFs[97]. CAFs exposed to chemotherapy were observed to prolong tumor cell survival and accelerate growth compared to untreated CAFs, indicating that CAFs may shield tumor cells from the growth-inhibitory effects of chemotherapy[109]. In contrast to the genetic instability often observed in malignant tumor cells of CRC, CAFs exhibit genetic stability. This characteristic distinction prompts the exploration of combined therapies targeting both CRC cells and CAFs, envisaged as a novel strategy to augment treatment effectiveness and overcome resistance in CRC. These strategies encompass three primary methods: (1) The elimination of "harmful" CAFs[110]; (2) The reprogramming of CAFs into "normal" fibroblasts or anti-tumor "beneficial" CAF subtypes[111]; and (3) The blockade of signals or ECM components derived from CAFs [112,113]. Successful implementation of these approaches necessitates a precise definition and classification of CAFs, coupled with an enhanced understanding of their diverse functions. Despite extensive research endeavors, several strategies targeting CAFs are yet to yield satisfactory clinical outcomes[14,114,115].

Currently, numerous anticancer drugs targeting CAFs are undergoing preclinical research or clinical trial phases. These drugs predominantly exert direct damage to CAFs by targeting specific surface molecules or impede the secretion of pro-cancer factors and associated signaling pathways in CAFs. The inaugural phase I clinical trial targeting

gastrointestinal cancers, employing autologous MSCs genetically modified to express herpes simplex virus-thymidine kinase, has demonstrated acceptable safety and tolerability. These MSCs facilitate the conversion of the pro-drug ganciclovir into its active cytotoxic metabolite. Furthermore, researchers are exploring the combination of TGF-β inhibitors or Hedgehog inhibitors with standard chemotherapies or immunotherapies[116]. This combination strategy aims to obstruct pro-tumorigenic signaling pathways pertinent to CAFs in gastrointestinal cancers[99,117,118]. Moreover, the differentiation of HSCs into CAFs *via* the C-X-C chemokine receptor type 4/TGF-β1 signaling axis promotes CRC liver metastasis. Consequently, blocking the C-X-C chemokine receptor type 4/TGF-β1 signaling axis emerges as a beneficial strategy for anti-metastasis treatment in CRC[119].

As research on the TME advances, exosomes have emerged as a promising avenue for therapeutic development. Among many miRNA molecules, miRNA-20a was found to inhibit the secretion of CXC motif chemokine ligand 8 from CAFs, thereby inhibiting tumor growth[120]. CAFs are also capable of secreting the lncRNAs CCAL and H19, thereby inducing drug resistance in cancer cells through the activation of β-catenin signaling[121,122]. Furthermore, CAFs release exosomal circSLC7A6 to stimulate the proliferation of CRC cells, an effect that can be inhibited by matrine, a compound derived from *Sophora flavescens*[123]. Additionally, CAFs secrete exosomal miR-93-5p and miR-21, which are transferred into CRC cells, consequently enhancing tumor resistance to chemotherapy[124-126].

Diverse attempts have been made to directly target specific subsets of CAFs. Some researchers have encapsulated drugs within lipid nanocapsules to directly target CAFs in the TME, discovering that paclitaxel and acetylcholinesterase are particularly promising for inhibiting CAF development[127]. Notably, a DNA vaccine inducing CD8 T cell killing of FAP+ CAFs has demonstrated the depletion of FAP+ CAFs and the inhibition of tumor progression in a CRC mouse model[128]. However, clinical trials evaluating anti-FAP monoclonal antibodies have not yielded the anticipated efficacy in advanced CRC patients[129]. Combining the chemotherapeutic drug oxaliplatin with the inhibitor PT-100 in a CRC mouse model significantly increased the sensitivity of tumor tissue to chemotherapy, concurrently reducing the recruitment of pro-tumor cells and angiogenesis[130]. Additionally, calcium/calmodulin-dependent protein kinase II has emerged as a pivotal mediator of TFG-β1-induced CAFs activation and participation in CRC cell signaling, positioning calcium/calmodulin-dependent protein kinase II as a promising target for future CRC treatment[131]. Furthermore, CAFs enhance the chemotherapy resistance of CRC cells by receiving signals through their receptor C-C motif chemokine receptor 5, suggesting that targeting C-C motif chemokine receptor 5 may offer a potential approach for treating CRC [132]. In the meanwhile, phosphorylated signal transducer and activator of transcription 3 in CAFs can be used as a tool to judge the prognosis of patients with CRC, and the activation of CAFs may be a therapeutic target for CRC[133]. Moreover, inhibitors of HGF activation, such as SRI 31215, offer a novel strategy to disrupt autocrine and paracrine oncogenic HGF/MET signaling, thereby preventing HGF-dependent cancer cell proliferation, EMT, and migration[134]. Simultaneously targeting HGF and EGFR can effectively block both primary and acquired fibroblast-mediated resistance to EGFR inhibitors in colon cancer cells.

CONCLUSION

In CRC, CAFs predominantly reside within the tumor or adjacent tissues, secreting factors that fuel tumor initiation, progression, invasion, and metastasis. Notably, CAFs play a pivotal role in aiding tumor cells in evading the body's immune responses, thereby fortifying resistance to radiation and chemotherapy. Consequently, the targeting of CAFs has emerged as an innovative and promising approach in the treatment landscape of CRC.

Anticipating future developments in the realm of CAFs, particularly in CAF subpopulation biology, there has been rapid and significant progress. A growing body of evidence underscores the crucial roles played by specific subgroups of CAFs in tumor initiation, development, metastasis, and resistance to treatment. Nevertheless, the heterogeneity in phenotype and function exhibited by CAFs introduces variability in their roles across different types of tumors and at various stages of the same tumor. Therefore, further exploration is imperative to unravel the nuanced functions of CAFs in different pathological subtypes of CRC and at distinct developmental stages.

Recent reports add an intriguing layer to our understanding, revealing that CAFs not only promote tumor cell development but also exhibit inhibitory effects on tumors. Investigating the underlying mechanisms and pathways through which CAFs themselves exert inhibitory effects represents a promising avenue for future research. The advent of modern scientific technologies, such as single-cell sequencing and spatial transcriptomics, has empowered researchers to delve into the study of CAFs subgroups at unprecedented levels. However, despite the valuable insights gained from single-cell technologies in identifying CAFs subgroups, comprehensive characterization and in-depth functional analyses remain essential to validate data and establish meaningful connections.

In the future trajectory of research, dedicated efforts should be directed towards comprehending the dynamic nature of CAFs, exploring their plasticity, deciphering the factors influencing their transformation, and investigating the potential reversibility of these changes. This concerted endeavor holds the promise of offering more precise and effective strategies for cancer treatment, ultimately paving the way for improved therapeutic outcomes and enhanced well-being for patients.

ACKNOWLEDGEMENTS

We sincerely thank our colleagues for their valuable suggestions and technical assistance for this research. We thank BioRender.com for expert assistance in the pattern drawing.

FOOTNOTES

Author contributions: Cui JY wrote the manuscript; Ma J, Gao XX, Sheng ZM, and Pan ZX collected the data; Shi LH and Zhang BG reviewed this review. All authors reviewed, edited, and approved the final manuscript and revised it critically for important intellectual content, gave final approval of the version to be published, and agreed to be accountable for all aspects of the work. The collaboration between Shi LH and Zhang BG is crucial for the publication of this manuscript and other manuscripts still in preparation, and they contributed equally to this work.

Conflict-of-interest statement: All the authors report no relevant conflicts of interest for this article.

Country of origin: China

ORCID number: Zi-Xin Pan 0009-0004-2225-5845; Bao-Gang Zhang 0000-0002-2355-6461.

S-Editor: Wang JJ
L-Editor: Wang TQ
P-Editor: Zhang L

REFERENCES

1 **Xi Y**, Xu P. Global colorectal cancer burden in 2020 and projections to 2040. *Transl Oncol* 2021; **14**: 101174 [PMID: 34243011 DOI: 10.1016/j.tranon.2021.101174]
2 **Paget S**. The distribution of secondary growths in cancer of the breast. 1889. *Cancer Metastasis Rev* 1989; **8**: 98-101 [PMID: 2673568]
3 **Wang W**, Li Q, Yamada T, Matsumoto K, Matsumoto I, Oda M, Watanabe G, Kayano Y, Nishioka Y, Sone S, Yano S. Crosstalk to stromal fibroblasts induces resistance of lung cancer to epidermal growth factor receptor tyrosine kinase inhibitors. *Clin Cancer Res* 2009; **15**: 6630-6638 [PMID: 19843665 DOI: 10.1158/1078-0432.CCR-09-1001]
4 **Gaggioli C**, Hooper S, Hidalgo-Carcedo C, Grosse R, Marshall JF, Harrington K, Sahai E. Fibroblast-led collective invasion of carcinoma cells with differing roles for RhoGTPases in leading and following cells. *Nat Cell Biol* 2007; **9**: 1392-1400 [PMID: 18037882 DOI: 10.1038/ncb1658]
5 **Kalluri R**. The biology and function of fibroblasts in cancer. *Nat Rev Cancer* 2016; **16**: 582-598 [PMID: 27550820 DOI: 10.1038/nrc.2016.73]
6 **Tarin D**, Croft CB. Ultrastructural features of wound healing in mouse skin. *J Anat* 1969; **105**: 189-190 [PMID: 5803198]
7 **Li B**, Wang JH. Fibroblasts and myofibroblasts in wound healing: force generation and measurement. *J Tissue Viability* 2011; **20**: 108-120 [PMID: 19995679 DOI: 10.1016/j.jtv.2009.11.004]
8 **Davidson S**, Coles M, Thomas T, Kollias G, Ludewig B, Turley S, Brenner M, Buckley CD. Fibroblasts as immune regulators in infection, inflammation and cancer. *Nat Rev Immunol* 2021; **21**: 704-717 [PMID: 33911232 DOI: 10.1038/s41577-021-00540-z]
9 **Alkasalias T**, Moyano-Galceran L, Arsenian-Henriksson M, Lehti K. Fibroblasts in the Tumor Microenvironment: Shield or Spear? *Int J Mol Sci* 2018; **19** [PMID: 29883428 DOI: 10.3390/ijms19051532]
10 **Kise K**, Kinugasa-Katayama Y, Takakura N. Tumor microenvironment for cancer stem cells. *Adv Drug Deliv Rev* 2016; **99**: 197-205 [PMID: 26362921 DOI: 10.1016/j.addr.2015.08.005]
11 **Öhlund D**, Elyada E, Tuveson D. Fibroblast heterogeneity in the cancer wound. *J Exp Med* 2014; **211**: 1503-1523 [PMID: 25071162 DOI: 10.1084/jem.20140692]
12 **Biffi G**, Tuveson DA. Diversity and Biology of Cancer-Associated Fibroblasts. *Physiol Rev* 2021; **101**: 147-176 [PMID: 32466724 DOI: 10.1152/physrev.00048.2019]
13 **Abudukelimu S**, de Miranda NFCC, Hawinkels LJAC. Fibroblasts in Orchestrating Colorectal Tumorigenesis and Progression. *Cell Mol Gastroenterol Hepatol* 2024; **17**: 821-826 [PMID: 38307492 DOI: 10.1016/j.jcmgh.2024.01.013]
14 **Koliaraki V**, Pallangyo CK, Greten FR, Kollias G. Mesenchymal Cells in Colon Cancer. *Gastroenterology* 2017; **152**: 964-979 [PMID: 28111227 DOI: 10.1053/j.gastro.2016.11.049]
15 **Feng B**, Wu J, Shen B, Jiang F, Feng J. Cancer-associated fibroblasts and resistance to anticancer therapies: status, mechanisms, and countermeasures. *Cancer Cell Int* 2022; **22**: 166 [PMID: 35488263 DOI: 10.1186/s12935-022-02599-7]
16 **Sahai E**, Astsaturov I, Cukierman E, DeNardo DG, Egeblad M, Evans RM, Fearon D, Greten FR, Hingorani SR, Hunter T, Hynes RO, Jain RK, Janowitz T, Jorgensen C, Kimmelman AC, Kolonin MG, Maki RG, Powers RS, Puré E, Ramirez DC, Scherz-Shouval R, Sherman MH, Stewart S, Tlsty TD, Tuveson DA, Watt FM, Weaver V, Weeraratna AT, Werb Z. A framework for advancing our understanding of cancer-associated fibroblasts. *Nat Rev Cancer* 2020; **20**: 174-186 [PMID: 31980749 DOI: 10.1038/s41568-019-0238-1]
17 **Xu Y**, Li W, Lin S, Liu B, Wu P, Li L. Fibroblast diversity and plasticity in the tumor microenvironment: roles in immunity and relevant therapies. *Cell Commun Signal* 2023; **21**: 234 [PMID: 37723510 DOI: 10.1186/s12964-023-01204-2]
18 **Qiu H**, Zhang X, Qi J, Zhang J, Tong Y, Li L, Fu L, Qin YR, Guan X, Zhang L. Identification and characterization of FGFR2(+) hematopoietic stem cell-derived fibrocytes as precursors of cancer-associated fibroblasts induced by esophageal squamous cell carcinoma. *J Exp Clin Cancer Res* 2022; **41**: 240 [PMID: 35941662 DOI: 10.1186/s13046-022-02435-w]
19 **Friedman G**, Levi-Galibov O, David E, Bornstein C, Giladi A, Dadiani M, Mayo A, Halperin C, Pevsner-Fischer M, Lavon H, Mayer S, Nevo R, Stein Y, Balint-Lahat N, Barshack I, Ali HR, Caldas C, Nili-Gal-Yam E, Alon U, Amit I, Scherz-Shouval R. Cancer-associated fibroblast compositions change with breast cancer progression linking the ratio of S100A4(+) and PDPN(+) CAFs to clinical outcome. *Nat Cancer* 2020;

1: 692-708 [PMID: 35122040 DOI: 10.1038/s43018-020-0082-y]

20 **Quante M**, Tu SP, Tomita H, Gonda T, Wang SS, Takashi S, Baik GH, Shibata W, Diprete B, Betz KS, Friedman R, Varro A, Tycko B, Wang TC. Bone marrow-derived myofibroblasts contribute to the mesenchymal stem cell niche and promote tumor growth. *Cancer Cell* 2011; **19**: 257-272 [PMID: 21316604 DOI: 10.1016/j.ccr.2011.01.020]

21 **Rubinstein-Achiasaf L**, Morein D, Ben-Yaakov H, Liubomirski Y, Meshel T, Elbaz E, Dorot O, Pichinuk E, Gershovits M, Weil M, Ben-Baruch A. Persistent Inflammatory Stimulation Drives the Conversion of MSCs to Inflammatory CAFs That Promote Pro-Metastatic Characteristics in Breast Cancer Cells. *Cancers (Basel)* 2021; **13** [PMID: 33806906 DOI: 10.3390/cancers13061472]

22 **Zhang Q**, Chai S, Wang W, Wan C, Zhang F, Li Y, Wang F. Macrophages activate mesenchymal stem cells to acquire cancer-associated fibroblast-like features resulting in gastric epithelial cell lesions and malignant transformation in vitro. *Oncol Lett* 2019; **17**: 747-756 [PMID: 30655826 DOI: 10.3892/ol.2018.9703]

23 **Öhlund D**, Handly-Santana A, Biffi G, Elyada E, Almeida AS, Ponz-Sarvise M, Corbo V, Oni TE, Hearn SA, Lee EJ, Chio II, Hwang CI, Tiriac H, Baker LA, Engle DD, Feig C, Kultti A, Egeblad M, Fearon DT, Crawford JM, Clevers H, Park Y, Tuveson DA. Distinct populations of inflammatory fibroblasts and myofibroblasts in pancreatic cancer. *J Exp Med* 2017; **214**: 579-596 [PMID: 28232471 DOI: 10.1084/jem.20162024]

24 **Trivedi P**, Wang S, Friedman SL. The Power of Plasticity-Metabolic Regulation of Hepatic Stellate Cells. *Cell Metab* 2021; **33**: 242-257 [PMID: 33232666 DOI: 10.1016/j.cmet.2020.10.026]

25 **Zhou Y**, Zhou J, Sun B, Xu W, Zhong M, Li Y, He C, Chen Y, Wang X, Jones PM, Sun Z. Vitamin A deficiency causes islet dysfunction by inducing islet stellate cell activation *via* cellular retinol binding protein 1. *Int J Biol Sci* 2020; **16**: 947-956 [PMID: 32140064 DOI: 10.7150/ijbs.37861]

26 **Xie Z**, Gao Y, Ho C, Li L, Jin C, Wang X, Zou C, Mao Y, Wang X, Li Q, Fu D, Zhang YF. Exosome-delivered CD44v6/C1QBP complex drives pancreatic cancer liver metastasis by promoting fibrotic liver microenvironment. *Gut* 2022; **71**: 568-579 [PMID: 33827783 DOI: 10.1136/gutjnl-2020-323014]

27 **Zhang Y**, Daquinag A, Traktuev DO, Amaya-Manzanares F, Simmons PJ, March KL, Pasqualini R, Arap W, Kolonin MG. White adipose tissue cells are recruited by experimental tumors and promote cancer progression in mouse models. *Cancer Res* 2009; **69**: 5259-5266 [PMID: 19491274 DOI: 10.1158/0008-5472.CAN-08-3444]

28 **Downer MA**, Griffin MF, Morgan AG, Parker JB, Li DJ, Berry CE, Liang NE, Kameni L, Cotterell AC, Akras D, Valencia C, Longaker MT, Wan DC. Understanding the Role of Adipocytes and Fibroblasts in Cancer. *Ann Plast Surg* 2023; **91**: 779-783 [PMID: 37553786 DOI: 10.1097/SAP.0000000000003658]

29 **Bochet L**, Lehuédé C, Dauvillier S, Wang YY, Dirat B, Laurent V, Dray C, Guiet R, Maridonneau-Parini I, Le Gonidec S, Couderc B, Escourrou G, Valet P, Muller C. Adipocyte-derived fibroblasts promote tumor progression and contribute to the desmoplastic reaction in breast cancer. *Cancer Res* 2013; **73**: 5657-5668 [PMID: 23903958 DOI: 10.1158/0008-5472.CAN-13-0530]

30 **Fischer KR**, Durrans A, Lee S, Sheng J, Li F, Wong ST, Choi H, El Rayes T, Ryu S, Troeger J, Schwabe RF, Vahdat LT, Altorki NK, Mittal V, Gao D. Epithelial-to-mesenchymal transition is not required for lung metastasis but contributes to chemoresistance. *Nature* 2015; **527**: 472-476 [PMID: 26560033 DOI: 10.1038/nature15748]

31 **Rhim AD**, Mirek ET, Aiello NM, Maitra A, Bailey JM, McAllister F, Reichert M, Beatty GL, Rustgi AK, Vonderheide RH, Leach SD, Stanger BZ. EMT and dissemination precede pancreatic tumor formation. *Cell* 2012; **148**: 349-361 [PMID: 22265420 DOI: 10.1016/j.cell.2011.11.025]

32 **Potenta S**, Zeisberg E, Kalluri R. The role of endothelial-to-mesenchymal transition in cancer progression. *Br J Cancer* 2008; **99**: 1375-1379 [PMID: 18797460 DOI: 10.1038/sj.bjc.6604662]

33 **Morgan A**, Griffin M, Kameni L, Wan DC, Longaker MT, Norton JA. Medical Biology of Cancer-Associated Fibroblasts in Pancreatic Cancer. *Biology (Basel)* 2023; **12** [PMID: 37626931 DOI: 10.3390/biology12081044]

34 **Chen PY**, Wei WF, Wu HZ, Fan LS, Wang W. Cancer-Associated Fibroblast Heterogeneity: A Factor That Cannot Be Ignored in Immune Microenvironment Remodeling. *Front Immunol* 2021; **12**: 671595 [PMID: 34305902 DOI: 10.3389/fimmu.2021.671595]

35 **Adjuto-Saccone M**, Soubeyran P, Garcia J, Audebert S, Camoin L, Rubis M, Roques J, Binétruy B, Iovanna JL, Tournaire R. TNF-α induces endothelial-mesenchymal transition promoting stromal development of pancreatic adenocarcinoma. *Cell Death Dis* 2021; **12**: 649 [PMID: 34172716 DOI: 10.1038/s41419-021-03920-4]

36 **Dulauroy S**, Di Carlo SE, Langa F, Eberl G, Peduto L. Lineage tracing and genetic ablation of ADAM12(+) perivascular cells identify a major source of profibrotic cells during acute tissue injury. *Nat Med* 2012; **18**: 1262-1270 [PMID: 22842476 DOI: 10.1038/nm.2848]

37 **Huang X**, He C, Hua X, Kan A, Mao Y, Sun S, Duan F, Wang J, Huang P, Li S. Oxidative stress induces monocyte-to-myofibroblast transdifferentiation through p38 in pancreatic ductal adenocarcinoma. *Clin Transl Med* 2020; **10**: e41 [PMID: 32508052 DOI: 10.1002/ctm2.41]

38 **Huang H**, Wang Z, Zhang Y, Pradhan RN, Ganguly D, Chandra R, Murimwa G, Wright S, Gu X, Maddipati R, Müller S, Turley SJ, Brekken RA. Mesothelial cell-derived antigen-presenting cancer-associated fibroblasts induce expansion of regulatory T cells in pancreatic cancer. *Cancer Cell* 2022; **40**: 656-673.e7 [PMID: 35523176 DOI: 10.1016/j.ccell.2022.04.011]

39 **McDonald LT**, Russell DL, Kelly RR, Xiong Y, Motamarry A, Patel RK, Jones JA, Watson PM, Turner DP, Watson DK, Soloff AC, Findlay VJ, LaRue AC. Hematopoietic stem cell-derived cancer-associated fibroblasts are novel contributors to the pro-tumorigenic microenvironment. *Neoplasia* 2015; **17**: 434-448 [PMID: 26025666 DOI: 10.1016/j.neo.2015.04.004]

40 **Direkze NC**, Forbes SJ, Brittan M, Hunt T, Jeffery R, Preston SL, Poulsom R, Hodivala-Dilke K, Alison MR, Wright NA. Multiple organ engraftment by bone-marrow-derived myofibroblasts and fibroblasts in bone-marrow-transplanted mice. *Stem Cells* 2003; **21**: 514-520 [PMID: 12968105 DOI: 10.1634/stemcells.21-5-514]

41 **Rinkevich Y**, Mori T, Sahoo D, Xu PX, Bermingham JR Jr, Weissman IL. Identification and prospective isolation of a mesothelial precursor lineage giving rise to smooth muscle cells and fibroblasts for mammalian internal organs, and their vasculature. *Nat Cell Biol* 2012; **14**: 1251-1260 [PMID: 23143399 DOI: 10.1038/ncb2610]

42 **Punt CJ**, Koopman M, Vermeulen L. From tumour heterogeneity to advances in precision treatment of colorectal cancer. *Nat Rev Clin Oncol* 2017; **14**: 235-246 [PMID: 27922044 DOI: 10.1038/nrclinonc.2016.171]

43 **Kobayashi H**, Gieniec KA, Lannagan TRM, Wang T, Asai N, Mizutani Y, Iida T, Ando R, Thomas EM, Sakai A, Suzuki N, Ichinose M, Wright JA, Vrbanac L, Ng JQ, Goyne J, Radford G, Lawrence MJ, Sammour T, Hayakawa Y, Klebe S, Shin AE, Asfaha S, Bettington ML, Rieder F, Arpaia N, Danino T, Butler LM, Burt AD, Leedham SJ, Rustgi AK, Mukherjee S, Takahashi M, Wang TC, Enomoto A, Woods SL, Worthley DL. The Origin and Contribution of Cancer-Associated Fibroblasts in Colorectal Carcinogenesis. *Gastroenterology* 2022; **162**: 890-906 [PMID: 34883119 DOI: 10.1053/j.gastro.2021.11.037]

44 **Chen Y**, Liang Z, Lai M. Targeting the devil: Strategies against cancer-associated fibroblasts in colorectal cancer. *Transl Res* 2024; **270**: 81-93 [PMID: 38614213 DOI: 10.1016/j.trsl.2024.04.003]

45 **Li H**, Courtois ET, Sengupta D, Tan Y, Chen KH, Goh JJL, Kong SL, Chua C, Hon LK, Tan WS, Wong M, Choi PJ, Wee LJK, Hillmer AM, Tan IB, Robson P, Prabhakar S. Reference component analysis of single-cell transcriptomes elucidates cellular heterogeneity in human colorectal tumors. *Nat Genet* 2017; **49**: 708-718 [PMID: 28319088 DOI: 10.1038/ng.3818]

46 **Pelka K**, Hofree M, Chen JH, Sarkizova S, Pirl JD, Jorgji V, Bejnood A, Dionne D, Ge WH, Xu KH, Chao SX, Zollinger DR, Lieb DJ, Reeves JW, Fuhrman CA, Hoang ML, Delorey T, Nguyen LT, Waldman J, Klapholz M, Wakiro I, Cohen O, Albers J, Smillie CS, Cuoco MS, Wu J, Su MJ, Yeung J, Vijaykumar B, Magnuson AM, Asinovski N, Moll T, Goder-Reiser MN, Applebaum AS, Brais LK, DelloStritto LK, Denning SL, Phillips ST, Hill EK, Meehan JK, Frederick DT, Sharova T, Kanodia A, Todres EZ, Jané-Valbuena J, Biton M, Izar B, Lambden CD, Clancy TE, Bleday R, Melnitchouk N, Irani J, Kunitake H, Berger DL, Srivastava A, Hornick JL, Ogino S, Rotem A, Vigneau S, Johnson BE, Corcoran RB, Sharpe AH, Kuchroo VK, Ng K, Giannakis M, Nieman LT, Boland GM, Aguirre AJ, Anderson AC, Rozenblatt-Rosen O, Regev A, Hacohen N. Spatially organized multicellular immune hubs in human colorectal cancer. *Cell* 2021; **184**: 4734-4752.e20 [PMID: 34450029 DOI: 10.1016/j.cell.2021.08.003]

47 **Sebastian A**, Hum NR, Martin KA, Gilmore SF, Peran I, Byers SW, Wheeler EK, Coleman MA, Loots GG. Single-Cell Transcriptomic Analysis of Tumor-Derived Fibroblasts and Normal Tissue-Resident Fibroblasts Reveals Fibroblast Heterogeneity in Breast Cancer. *Cancers (Basel)* 2020; **12** [PMID: 32455670 DOI: 10.3390/cancers12051307]

48 **Affo S**, Nair A, Brundu F, Ravichandra A, Bhattacharjee S, Matsuda M, Chin L, Filliol A, Wen W, Song X, Decker A, Worley J, Caviglia JM, Yu L, Yin D, Saito Y, Savage T, Wells RG, Mack M, Zender L, Arpaia N, Remotti HE, Rabadan R, Sims P, Leblond AL, Weber A, Riener MO, Stockwell BR, Gaublomme J, Llovet JM, Kalluri R, Michalopoulos GK, Seki E, Sia D, Chen X, Califano A, Schwabe RF. Promotion of cholangiocarcinoma growth by diverse cancer-associated fibroblast subpopulations. *Cancer Cell* 2021; **39**: 866-882.e11 [PMID: 33930309 DOI: 10.1016/j.ccell.2021.03.012]

49 **Kieffer Y**, Hocine HR, Gentric G, Pelon F, Bernard C, Bourachot B, Lameiras S, Albergante L, Bonneau C, Guyard A, Tarte K, Zinovyev A, Baulande S, Zalcman G, Vincent-Salomon A, Mechta-Grigoriou F. Single-Cell Analysis Reveals Fibroblast Clusters Linked to Immunotherapy Resistance in Cancer. *Cancer Discov* 2020; **10**: 1330-1351 [PMID: 32434947 DOI: 10.1158/2159-8290.CD-19-1384]

50 **Peng Z**, Ye M, Ding H, Feng Z, Hu K. Spatial transcriptomics atlas reveals the crosstalk between cancer-associated fibroblasts and tumor microenvironment components in colorectal cancer. *J Transl Med* 2022; **20**: 302 [PMID: 35794563 DOI: 10.1186/s12967-022-03510-8]

51 **Khaliq AM**, Erdogan C, Kurt Z, Turgut SS, Grunvald MW, Rand T, Khare S, Borgia JA, Hayden DM, Pappas SG, Govekar HR, Kam AE, Reiser J, Turaga K, Radovich M, Zang Y, Qiu Y, Liu Y, Fishel ML, Turk A, Gupta V, Al-Sabti R, Subramanian J, Kuzel TM, Sadanandam A, Waldron L, Hussain A, Saleem M, El-Rayes B, Salahudeen AA, Masood A. Correction: Refining colorectal cancer classification and clinical stratification through a single-cell atlas. *Genome Biol* 2022; **23**: 156 [PMID: 35831907 DOI: 10.1186/s13059-022-02724-9]

52 **Bartoschek M**, Oskolkov N, Bocci M, Lövrot J, Larsson C, Sommarin M, Madsen CD, Lindgren D, Pekar G, Karlsson G, Ringnér M, Bergh J, Björklund Å, Pietras K. Spatially and functionally distinct subclasses of breast cancer-associated fibroblasts revealed by single cell RNA sequencing. *Nat Commun* 2018; **9**: 5150 [PMID: 30514914 DOI: 10.1038/s41467-018-07582-3]

53 **Zhang M**, Yang H, Wan L, Wang Z, Wang H, Ge C, Liu Y, Hao Y, Zhang D, Shi G, Gong Y, Ni Y, Wang C, Zhang Y, Xi J, Wang S, Shi L, Zhang L, Yue W, Pei X, Liu B, Yan X. Single-cell transcriptomic architecture and intercellular crosstalk of human intrahepatic cholangiocarcinoma. *J Hepatol* 2020; **73**: 1118-1130 [PMID: 32505533 DOI: 10.1016/j.jhep.2020.05.039]

54 **Miyai Y**, Esaki N, Takahashi M, Enomoto A. Cancer-associated fibroblasts that restrain cancer progression: Hypotheses and perspectives. *Cancer Sci* 2020; **111**: 1047-1057 [PMID: 32060987 DOI: 10.1111/cas.14346]

55 **Wang Z**, Yang Q, Tan Y, Tang Y, Ye J, Yuan B, Yu W. Cancer-Associated Fibroblasts Suppress Cancer Development: The Other Side of the Coin. *Front Cell Dev Biol* 2021; **9**: 613534 [PMID: 33614646 DOI: 10.3389/fcell.2021.613534]

56 **Kobayashi H**, Gieniec KA, Wright JA, Wang T, Asai N, Mizutani Y, Lida T, Ando R, Suzuki N, Lannagan TRM, Ng JQ, Hara A, Shiraki Y, Mii S, Ichinose M, Vrbanac L, Lawrence MJ, Sammour T, Uehara K, Davies G, Lisowski L, Alexander IE, Hayakawa Y, Butler LM, Zannettino ACW, Din MO, Hasty J, Burt AD, Leedham SJ, Rustgi AK, Mukherjee S, Wang TC, Enomoto A, Takahashi M, Worthley DL, Woods SL. The Balance of Stromal BMP Signaling Mediated by GREM1 and ISLR Drives Colorectal Carcinogenesis. *Gastroenterology* 2021; **160**: 1224-1239.e30 [PMID: 33197448 DOI: 10.1053/j.gastro.2020.11.011]

57 **Mellman I**, Chen DS, Powles T, Turley SJ. The cancer-immunity cycle: Indication, genotype, and immunotype. *Immunity* 2023; **56**: 2188-2205 [PMID: 37820582 DOI: 10.1016/j.immuni.2023.09.011]

58 **Caligiuri G**, Tuveson DA. Activated fibroblasts in cancer: Perspectives and challenges. *Cancer Cell* 2023; **41**: 434-449 [PMID: 36917949 DOI: 10.1016/j.ccell.2023.02.015]

59 **Fernando-Macías E**, Fernández-García MT, García-Pérez E, Porrero Guerrero B, López-Arévalo C, Rodríguez-Uría R, Sanz-Navarro S, Vá zquez-Villa JF, Muñíz-Salgueiro MC, Suárez-Fernández L, Galván JA, Barneo-Caragol C, García-Ocaña M, de Los Toyos JR, Barneo-Serra L. A new aggressive xenograft model of human colon cancer using cancer-associated fibroblasts. *PeerJ* 2020; **8**: e9045 [PMID: 32547853 DOI: 10.7717/peerj.9045]

60 **Yang K**, Zhang F, Luo B, Qu Z. CAFs-derived small extracellular vesicles circN4BP2L2 promotes proliferation and metastasis of colorectal cancer *via* miR-664b-3p/HMGB3 pathway. *Cancer Biol Ther* 2022; **23**: 404-416 [PMID: 35722996 DOI: 10.1080/15384047.2022.2072164]

61 **Hirashima T**, Karasawa H, Aizawa T, Suzuki T, Yamamura A, Suzuki H, Kajiwara T, Musha H, Funayama R, Shirota M, Ohnuma S, Nakayama K, Unno M. Wnt5a in cancer-associated fibroblasts promotes colorectal cancer progression. *Biochem Biophys Res Commun* 2021; **568**: 37-42 [PMID: 34175688 DOI: 10.1016/j.bbrc.2021.06.062]

62 **Aizawa T**, Karasawa H, Funayama R, Shirota M, Suzuki T, Maeda S, Suzuki H, Yamamura A, Naitoh T, Nakayama K, Unno M. Cancer-associated fibroblasts secrete Wnt2 to promote cancer progression in colorectal cancer. *Cancer Med* 2019; **8**: 6370-6382 [PMID: 31468733 DOI: 10.1002/cam4.2523]

63 **Stadler M**, Pudelko K, Biermeier A, Walterskirchen N, Gaigneaux A, Weindorfer C, Harrer N, Klett H, Hengstschläger M, Schüler J, Sommergruber W, Oehler R, Bergmann M, Letellier E, Dolznig H. Stromal fibroblasts shape the myeloid phenotype in normal colon and colorectal cancer and induce CD163 and CCL2 expression in macrophages. *Cancer Lett* 2021; **520**: 184-200 [PMID: 34256095 DOI: 10.1016/j.canlet.2021.07.006]

64 **Musa M**, Ali A. Cancer-associated fibroblasts of colorectal cancer and their markers: updates, challenges and translational outlook. *Future Oncol* 2020; **16**: 2329-2344 [PMID: 32687721 DOI: 10.2217/fon-2020-0384]

65 **Egan H**, Treacy O, Lynch K, Leonard NA, O'Malley G, Reidy E, O'Neill A, Corry SM, De Veirman K, Vanderkerken K, Egan LJ, Ritter T, Hogan AM, Redmond K, Peng L, Che J, Gatlin W, Jayaraman P, Sheehan M, Canney A, Hynes SO, Kerr EM, Dunne PD, O'Dwyer ME, Ryan

AE. Targeting stromal cell sialylation reverses T cell-mediated immunosuppression in the tumor microenvironment. *Cell Rep* 2023; **42**: 112475 [PMID: 37167967 DOI: 10.1016/j.celrep.2023.112475]

66 **Yang M**, Wei Z, Feng M, Zhu Y, Chen Y, Zhu D. Pharmacological Inhibition and Genetic Knockdown of BCL9 Modulate the Cellular Landscape of Cancer-Associated Fibroblasts in the Tumor-Immune Microenvironment of Colorectal Cancer. *Front Oncol* 2021; **11**: 603556 [PMID: 34026600 DOI: 10.3389/fonc.2021.603556]

67 **Kumar V**, Donthireddy L, Marvel D, Condamine T, Wang F, Lavilla-Alonso S, Hashimoto A, Vonteddu P, Behera R, Goins MA, Mulligan C, Nam B, Hockstein N, Denstman F, Shakamuri S, Speicher DW, Weeraratna AT, Chao T, Vonderheide RH, Languino LR, Ordentlich P, Liu Q, Xu X, Lo A, Puré E, Zhang C, Loboda A, Sepulveda MA, Snyder LA, Gabrilovich DI. Cancer-Associated Fibroblasts Neutralize the Anti-tumor Effect of CSF1 Receptor Blockade by Inducing PMN-MDSC Infiltration of Tumors. *Cancer Cell* 2017; **32**: 654-668.e5 [PMID: 29136508 DOI: 10.1016/j.ccell.2017.10.005]

68 **Cannarile MA**, Weisser M, Jacob W, Jegg AM, Ries CH, Rüttinger D. Colony-stimulating factor 1 receptor (CSF1R) inhibitors in cancer therapy. *J Immunother Cancer* 2017; **5**: 53 [PMID: 28716061 DOI: 10.1186/s40425-017-0257-y]

69 **Chen FW**, Wu YL, Cheng CC, Hsiao YW, Chi JY, Hung LY, Chang CP, Lai MD, Wang JM. Inactivation of pentraxin 3 suppresses M2-like macrophage activity and immunosuppression in colon cancer. *J Biomed Sci* 2024; **31**: 10 [PMID: 38243273 DOI: 10.1186/s12929-023-00991-7]

70 **Monteran L**, Erez N. The Dark Side of Fibroblasts: Cancer-Associated Fibroblasts as Mediators of Immunosuppression in the Tumor Microenvironment. *Front Immunol* 2019; **10**: 1835 [PMID: 31428105 DOI: 10.3389/fimmu.2019.01835]

71 **McAndrews KM**, Vázquez-Arreguín K, Kwak C, Sugimoto H, Zheng X, Li B, Kirtley ML, LeBleu VS, Kalluri R. αSMA(+) fibroblasts suppress Lgr5(+) cancer stem cells and restrain colorectal cancer progression. *Oncogene* 2021; **40**: 4440-4452 [PMID: 34108617 DOI: 10.1038/s41388-021-01866-7]

72 **Lu Y**, Qin T, Li J, Wang L, Zhang Q, Jiang Z, Mao J. Correction: MicroRNA-140-5p inhibits invasion and angiogenesis through targeting VEGF-A in breast cancer. *Cancer Gene Ther* 2020; **27**: 838-839 [PMID: 33060838 DOI: 10.1038/s41417-020-00240-1]

73 **Ding C**, Luo J, Fan X, Li L, Li S, Wen K, Feng J, Wu G. Elevated Gab2 induces tumor growth and angiogenesis in colorectal cancer through upregulating VEGF levels. *J Exp Clin Cancer Res* 2017; **36**: 56 [PMID: 28420432 DOI: 10.1186/s13046-017-0524-2]

74 **Bagheri A**, Kumar P, Kamath A, Rao P. Association of angiogenic cytokines (VEGF-A and VEGF-C) and clinical characteristic in women with unexplained recurrent miscarriage. *Bratisl Lek Listy* 2017; **118**: 258-264 [PMID: 28516786 DOI: 10.4149/BLL_2017_051]

75 **De Palma M**, Biziato D, Petrova TV. Microenvironmental regulation of tumour angiogenesis. *Nat Rev Cancer* 2017; **17**: 457-474 [PMID: 28706266 DOI: 10.1038/nrc.2017.51]

76 **Fukumura D**, Xavier R, Sugiura T, Chen Y, Park EC, Lu N, Selig M, Nielsen G, Taksir T, Jain RK, Seed B. Tumor induction of VEGF promoter activity in stromal cells. *Cell* 1998; **94**: 715-725 [PMID: 9753319 DOI: 10.1016/s0092-8674(00)81731-6]

77 **Nagasaki T**, Hara M, Nakanishi H, Takahashi H, Sato M, Takeyama H. Interleukin-6 released by colon cancer-associated fibroblasts is critical for tumour angiogenesis: anti-interleukin-6 receptor antibody suppressed angiogenesis and inhibited tumour-stroma interaction. *Br J Cancer* 2014; **110**: 469-478 [PMID: 24346288 DOI: 10.1038/bjc.2013.748]

78 **Unterleuthner D**, Neuhold P, Schwarz K, Janker L, Neuditschko B, Nivarthi H, Crncec I, Kramer N, Unger C, Hengstschläger M, Eferl R, Moriggl R, Sommergruber W, Gerner C, Dolznig H. Cancer-associated fibroblast-derived WNT2 increases tumor angiogenesis in colon cancer. *Angiogenesis* 2020; **23**: 159-177 [PMID: 31667643 DOI: 10.1007/s10456-019-09688-8]

79 **Ben Baruch B**, Mantsur E, Franco-Barraza J, Blacher E, Cukierman E, Stein R. CD38 in cancer-associated fibroblasts promotes pro-tumoral activity. *Lab Invest* 2020; **100**: 1517-1531 [PMID: 32612286 DOI: 10.1038/s41374-020-0458-8]

80 **Yan M**, Jurasz P. The role of platelets in the tumor microenvironment: From solid tumors to leukemia. *Biochim Biophys Acta* 2016; **1863**: 392-400 [PMID: 26193075 DOI: 10.1016/j.bbamcr.2015.07.008]

81 **Drev D**, Harpain F, Beer A, Stift A, Gruber ES, Klimpfinger M, Thalhammer S, Reti A, Kenner L, Bergmann M, Marian B. Impact of Fibroblast-Derived SPARC on Invasiveness of Colorectal Cancer Cells. *Cancers (Basel)* 2019; **11** [PMID: 31554208 DOI: 10.3390/cancers11101421]

82 **Tommelein J**, Verset L, Boterberg T, Demetter P, Bracke M, De Wever O. Cancer-associated fibroblasts connect metastasis-promoting communication in colorectal cancer. *Front Oncol* 2015; **5**: 63 [PMID: 25853091 DOI: 10.3389/fonc.2015.00063]

83 **Bauer J**, Emon MAB, Staudacher JJ, Thomas AL, Zessner-Spitzenberg J, Mancinelli G, Krett N, Saif MT, Jung B. Increased stiffness of the tumor microenvironment in colon cancer stimulates cancer associated fibroblast-mediated prometastatic activin A signaling. *Sci Rep* 2020; **10**: 50 [PMID: 31919369 DOI: 10.1038/s41598-019-55687-6]

84 **Xuefeng X**, Hou MX, Yang ZW, Agudamu A, Wang F, Su XL, Li X, Shi L, Terigele T, Bao LL, Wu XL. Epithelial-mesenchymal transition and metastasis of colon cancer cells induced by the FAK pathway in cancer-associated fibroblasts. *J Int Med Res* 2020; **48**: 300060520931242 [PMID: 32588696 DOI: 10.1177/0300060520931242]

85 **Deng S**, Cheng D, Wang J, Gu J, Xue Y, Jiang Z, Qin L, Mao F, Cao Y, Cai K. MYL9 expressed in cancer-associated fibroblasts regulate the immune microenvironment of colorectal cancer and promotes tumor progression in an autocrine manner. *J Exp Clin Cancer Res* 2023; **42**: 294 [PMID: 37926835 DOI: 10.1186/s13046-023-02863-2]

86 **Peng S**, Chen D, Cai J, Yuan Z, Huang B, Li Y, Wang H, Luo Q, Kuang Y, Liang W, Liu Z, Wang Q, Cui Y, Wang H, Liu X. Enhancing cancer-associated fibroblast fatty acid catabolism within a metabolically challenging tumor microenvironment drives colon cancer peritoneal metastasis. *Mol Oncol* 2021; **15**: 1391-1411 [PMID: 33528867 DOI: 10.1002/1878-0261.12917]

87 **Kramer N**, Schmöllerl J, Unger C, Nivarthi H, Rudisch A, Unterleuthner D, Scherzer M, Riedl A, Artaker M, Crncec I, Lenhardt D, Schwarz T, Prieler B, Han X, Hengstschläger M, Schüler J, Eferl R, Moriggl R, Sommergruber W, Dolznig H. Autocrine WNT2 signaling in fibroblasts promotes colorectal cancer progression. *Oncogene* 2017; **36**: 5460-5472 [PMID: 28553956 DOI: 10.1038/onc.2017.144]

88 **Shi Y**, Gao W, Lytle NK, Huang P, Yuan X, Dann AM, Ridinger-Saison M, DelGiorno KE, Antal CE, Liang G, Atkins AR, Erikson G, Sun H, Meisenhelder J, Terenziani E, Woo G, Fang L, Santisakultarm TP, Manor U, Xu R, Becerra CR, Borazanci E, Von Hoff DD, Grandgenett PM, Hollingsworth MA, Leblanc M, Umetsu SE, Collisson EA, Scadeng M, Lowy AM, Donahue TR, Reya T, Downes M, Evans RM, Wahl GM, Pawson T, Tian R, Hunter T. Author Correction: Targeting LIF-mediated paracrine interaction for pancreatic cancer therapy and monitoring. *Nature* 2021; **600**: E18 [PMID: 34848876 DOI: 10.1038/s41586-021-04176-w]

89 **Massagué J**, Ganesh K. Metastasis-Initiating Cells and Ecosystems. *Cancer Discov* 2021; **11**: 971-994 [PMID: 33811127 DOI: 10.1158/2159-8290.CD-21-0010]

90 **Gonzalez-Zubeldia I**, Dotor J, Redrado M, Bleau AM, Manrique I, de Aberasturi AL, Villalba M, Calvo A. Co-migration of colon cancer cells and CAFs induced by TGFβ1 enhances liver metastasis. *Cell Tissue Res* 2015; **359**: 829-839 [PMID: 25557989 DOI:

10.1007/s00441-014-2075-6]
91 **Baulida J**. Epithelial-to-mesenchymal transition transcription factors in cancer-associated fibroblasts. *Mol Oncol* 2017; **11**: 847-859 [PMID: 28544627 DOI: 10.1002/1878-0261.12080]
92 **Francí C**, Takkunen M, Dave N, Alameda F, Gómez S, Rodríguez R, Escrivà M, Montserrat-Sentís B, Baró T, Garrido M, Bonilla F, Virtanen I, García de Herreros A. Expression of Snail protein in tumor-stroma interface. *Oncogene* 2006; **25**: 5134-5144 [PMID: 16568079 DOI: 10.1038/sj.onc.1209519]
93 **Bhome R**, Emaduddin M, James V, House LM, Thirdborough SM, Mellone M, Tulkens J, Primrose JN, Thomas GJ, De Wever O, Mirnezami AH, Sayan AE. Epithelial to mesenchymal transition influences fibroblast phenotype in colorectal cancer by altering miR-200 levels in extracellular vesicles. *J Extracell Vesicles* 2022; **11**: e12226 [PMID: 35595718 DOI: 10.1002/jev2.12226]
94 **Yan H**, Guo BY, Zhang S. Cancer-associated fibroblasts attenuate Cisplatin-induced apoptosis in ovarian cancer cells by promoting STAT3 signaling. *Biochem Biophys Res Commun* 2016; **470**: 947-954 [PMID: 26826383 DOI: 10.1016/j.bbrc.2016.01.131]
95 **Provenzano PP**, Cuevas C, Chang AE, Goel VK, Von Hoff DD, Hingorani SR. Enzymatic targeting of the stroma ablates physical barriers to treatment of pancreatic ductal adenocarcinoma. *Cancer Cell* 2012; **21**: 418-429 [PMID: 22439937 DOI: 10.1016/j.ccr.2012.01.007]
96 **Ireland L**, Santos A, Ahmed MS, Rainer C, Nielsen SR, Quaranta V, Weyer-Czernilofsky U, Engle DD, Perez-Mancera PA, Coupland SE, Taktak A, Bogenrieder T, Tuveson DA, Campbell F, Schmid MC, Mielgo A. Chemoresistance in Pancreatic Cancer Is Driven by Stroma-Derived Insulin-Like Growth Factors. *Cancer Res* 2016; **76**: 6851-6863 [PMID: 27742686 DOI: 10.1158/0008-5472.CAN-16-1201]
97 **Lotti F**, Jarrar AM, Pai RK, Hitomi M, Lathia J, Mace A, Gantt GA Jr, Sukhdeo K, DeVecchio J, Vasanji A, Leahy P, Hjelmeland AB, Kalady MF, Rich JN. Chemotherapy activates cancer-associated fibroblasts to maintain colorectal cancer-initiating cells by IL-17A. *J Exp Med* 2013; **210**: 2851-2872 [PMID: 24323355 DOI: 10.1084/jem.20131195]
98 **Hawinkels LJ**, Ten Dijke P. Exploring anti-TGF-β therapies in cancer and fibrosis. *Growth Factors* 2011; **29**: 140-152 [PMID: 21718111 DOI: 10.3109/08977194.2011.595411]
99 **Tauriello DVF**, Palomo-Ponce S, Stork D, Berenguer-Llergo A, Badia-Ramentol J, Iglesias M, Sevillano M, Ibiza S, Cañellas A, Hernando-Momblona X, Byrom D, Matarin JA, Calon A, Rivas EI, Nebreda AR, Riera A, Attolini CS, Batlle E. TGFβ drives immune evasion in genetically reconstituted colon cancer metastasis. *Nature* 2018; **554**: 538-543 [PMID: 29443964 DOI: 10.1038/nature25492]
100 **Isella C**, Terrasi A, Bellomo SE, Petti C, Galatola G, Muratore A, Mellano A, Senetta R, Cassenti A, Sonetto C, Inghirami G, Trusolino L, Fekete Z, De Ridder M, Cassoni P, Storme G, Bertotti A, Medico E. Stromal contribution to the colorectal cancer transcriptome. *Nat Genet* 2015; **47**: 312-319 [PMID: 25706627 DOI: 10.1038/ng.3224]
101 **Luraghi P**, Reato G, Cipriano E, Sassi F, Orzan F, Bigatto V, De Bacco F, Menietti E, Han M, Rideout WM 3rd, Perera T, Bertotti A, Trusolino L, Comoglio PM, Boccaccio C. MET signaling in colon cancer stem-like cells blunts the therapeutic response to EGFR inhibitors. *Cancer Res* 2014; **74**: 1857-1869 [PMID: 24448239 DOI: 10.1158/0008-5472.CAN-13-2340-T]
102 **Vaquero J**, Lobe C, Tahraoui S, Clapéron A, Mergey M, Merabtene F, Wendum D, Coulouarn C, Housset C, Desbois-Mouthon C, Praz F, Fouassier L. The IGF2/IR/IGF1R Pathway in Tumor Cells and Myofibroblasts Mediates Resistance to EGFR Inhibition in Cholangiocarcinoma. *Clin Cancer Res* 2018; **24**: 4282-4296 [PMID: 29716918 DOI: 10.1158/1078-0432.CCR-17-3725]
103 **Qu Z**, Yang KD, Luo BH, Zhang F. CAFs-secreted exosomal cricN4BP2L2 promoted colorectal cancer stemness and chemoresistance by interacting with EIF4A3. *Exp Cell Res* 2022; **418**: 113266 [PMID: 35752345 DOI: 10.1016/j.yexcr.2022.113266]
104 **Zhang Y**, Yin C, Wei C, Xia S, Qiao Z, Zhang XW, Yu B, Zhou J, Wang R. Exosomal miR-625-3p secreted by cancer-associated fibroblasts in colorectal cancer promotes EMT and chemotherapeutic resistance by blocking the CELF2/WWOX pathway. *Pharmacol Res* 2022; **186**: 106534 [PMID: 36336217 DOI: 10.1016/j.phrs.2022.106534]
105 **Izumi D**, Toden S, Ureta E, Ishimoto T, Baba H, Goel A. TIAM1 promotes chemoresistance and tumor invasiveness in colorectal cancer. *Cell Death Dis* 2019; **10**: 267 [PMID: 30890693 DOI: 10.1038/s41419-019-1493-5]
106 **Liu ML**, Zang F, Zhang SJ. RBCK1 contributes to chemoresistance and stemness in colorectal cancer (CRC). *Biomed Pharmacother* 2019; **118**: 109250 [PMID: 31545242 DOI: 10.1016/j.biopha.2019.109250]
107 **Chen X**, Chen W, Zhao Y, Wang Q, Wang W, Xiang Y, Yuan H, Xie Y, Zhou J. Interplay of Helicobacter pylori, fibroblasts, and cancer cells induces fibroblast activation and serpin E1 expression by cancer cells to promote gastric tumorigenesis. *J Transl Med* 2022; **20**: 322 [PMID: 35864535 DOI: 10.1186/s12967-022-03537-x]
108 **Chen S**, Fan L, Lin Y, Qi Y, Xu C, Ge Q, Zhang Y, Wang Q, Jia D, Wang L, Si J, Wang L. Bifidobacterium adolescentis orchestrates CD143(+) cancer-associated fibroblasts to suppress colorectal tumorigenesis by Wnt signaling-regulated GAS1. *Cancer Commun (Lond)* 2023; **43**: 1027-1047 [PMID: 37533188 DOI: 10.1002/cac2.12469]
109 **Yan L**, Zheng J, Wang Q, Hao H. Role of cancer-associated fibroblasts in colorectal cancer and their potential as therapeutic targets. *Biochem Biophys Res Commun* 2023; **681**: 127-135 [PMID: 37774570 DOI: 10.1016/j.bbrc.2023.09.065]
110 **Lo A**, Wang LS, Scholler J, Monslow J, Avery D, Newick K, O'Brien S, Evans RA, Bajor DJ, Clendenin C, Durham AC, Buza EL, Vonderheide RH, June CH, Albelda SM, Puré E. Tumor-Promoting Desmoplasia Is Disrupted by Depleting FAP-Expressing Stromal Cells. *Cancer Res* 2015; **75**: 2800-2810 [PMID: 25979873 DOI: 10.1158/0008-5472.CAN-14-3041]
111 **Ferrer-Mayorga G**, Gómez-López G, Barbáchano A, Fernández-Barral A, Peña C, Pisano DG, Cantero R, Rojo F, Muñoz A, Larriba MJ. Vitamin D receptor expression and associated gene signature in tumour stromal fibroblasts predict clinical outcome in colorectal cancer. *Gut* 2017; **66**: 1449-1462 [PMID: 27053631 DOI: 10.1136/gutjnl-2015-310977]
112 **Dufour A**, Overall CM. Missing the target: matrix metalloproteinase antitargets in inflammation and cancer. *Trends Pharmacol Sci* 2013; **34**: 233-242 [PMID: 23541335 DOI: 10.1016/j.tips.2013.02.004]
113 **Feig C**, Jones JO, Kraman M, Wells RJ, Deonarine A, Chan DS, Connell CM, Roberts EW, Zhao Q, Caballero OL, Teichmann SA, Janowitz T, Jodrell DI, Tuveson DA, Fearon DT. Targeting CXCL12 from FAP-expressing carcinoma-associated fibroblasts synergizes with anti-PD-L1 immunotherapy in pancreatic cancer. *Proc Natl Acad Sci U S A* 2013; **110**: 20212-20217 [PMID: 24277834 DOI: 10.1073/pnas.1320318110]
114 **Berlin J**, Bendell JC, Hart LL, Firdaus I, Gore I, Hermann RC, Mulcahy MF, Zalupski MM, Mackey HM, Yauch RL, Graham RA, Bray GL, Low JA. A randomized phase II trial of vismodegib versus placebo with FOLFOX or FOLFIRI and bevacizumab in patients with previously untreated metastatic colorectal cancer. *Clin Cancer Res* 2013; **19**: 258-267 [PMID: 23082002 DOI: 10.1158/1078-0432.CCR-12-1800]
115 **Winer A**, Adams S, Mignatti P. Matrix Metalloproteinase Inhibitors in Cancer Therapy: Turning Past Failures Into Future Successes. *Mol Cancer Ther* 2018; **17**: 1147-1155 [PMID: 29735645 DOI: 10.1158/1535-7163.MCT-17-0646]
116 **von Einem JC**, Guenther C, Volk HD, Grütz G, Hirsch D, Salat C, Stoetzer O, Nelson PJ, Michl M, Modest DP, Holch JW, Angele M, Bruns C, Niess H, Heinemann V. Treatment of advanced gastrointestinal cancer with genetically modified autologous mesenchymal stem cells:

Results from the phase 1/2 TREAT-ME-1 trial. *Int J Cancer* 2019; **145**: 1538-1546 [PMID: 30801698 DOI: 10.1002/ijc.32230]

117 **Vennin C**, Murphy KJ, Morton JP, Cox TR, Pajic M, Timpson P. Reshaping the Tumor Stroma for Treatment of Pancreatic Cancer. *Gastroenterology* 2018; **154**: 820-838 [PMID: 29287624 DOI: 10.1053/j.gastro.2017.11.280]

118 **Jia SN**, Han YB, Yang R, Yang ZC. Chemokines in colon cancer progression. *Semin Cancer Biol* 2022; **86**: 400-407 [PMID: 35183412 DOI: 10.1016/j.semcancer.2022.02.007]

119 **Tan HX**, Gong WZ, Zhou K, Xiao ZG, Hou FT, Huang T, Zhang L, Dong HY, Zhang WL, Liu Y, Huang ZC. CXCR4/TGF-β1 mediated hepatic stellate cells differentiation into carcinoma-associated fibroblasts and promoted liver metastasis of colon cancer. *Cancer Biol Ther* 2020; **21**: 258-268 [PMID: 31825725 DOI: 10.1080/15384047.2019.1685157]

120 **Signs SA**, Fisher RC, Tran U, Chakrabarti S, Sarvestani SK, Xiang S, Liska D, Roche V, Lai W, Gittleman HR, Wessely O, Huang EH. Stromal miR-20a controls paracrine CXCL8 secretion in colitis and colon cancer. *Oncotarget* 2018; **9**: 13048-13059 [PMID: 29560130 DOI: 10.18632/oncotarget.24495]

121 **Ren J**, Ding L, Zhang D, Shi G, Xu Q, Shen S, Wang Y, Wang T, Hou Y. Carcinoma-associated fibroblasts promote the stemness and chemoresistance of colorectal cancer by transferring exosomal lncRNA H19. *Theranostics* 2018; **8**: 3932-3948 [PMID: 30083271 DOI: 10.7150/thno.25541]

122 **Deng X**, Ruan H, Zhang X, Xu X, Zhu Y, Peng H, Zhang X, Kong F, Guan M. Long noncoding RNA CCAL transferred from fibroblasts by exosomes promotes chemoresistance of colorectal cancer cells. *Int J Cancer* 2020; **146**: 1700-1716 [PMID: 31381140 DOI: 10.1002/ijc.32608]

123 **Gu C**, Lu H, Qian Z. Matrine reduces the secretion of exosomal circSLC7A6 from cancer-associated fibroblast to inhibit tumorigenesis of colorectal cancer by regulating CXCR5. *Biochem Biophys Res Commun* 2020; **527**: 638-645 [PMID: 32423804 DOI: 10.1016/j.bbrc.2020.04.142]

124 **Bhome R**, Goh RW, Bullock MD, Pillar N, Thirdborough SM, Mellone M, Mirnezami R, Galea D, Veselkov K, Gu Q, Underwood TJ, Primrose JN, De Wever O, Shomron N, Sayan AE, Mirnezami AH. Exosomal microRNAs derived from colorectal cancer-associated fibroblasts: role in driving cancer progression. *Aging (Albany NY)* 2017; **9**: 2666-2694 [PMID: 29283887 DOI: 10.18632/aging.101355]

125 **Bullock MD**, Pickard KM, Nielsen BS, Sayan AE, Jenei V, Mellone M, Mitter R, Primrose JN, Thomas GJ, Packham GK, Mirnezami AH. Pleiotropic actions of miR-21 highlight the critical role of deregulated stromal microRNAs during colorectal cancer progression. *Cell Death Dis* 2013; **4**: e684 [PMID: 23788041 DOI: 10.1038/cddis.2013.213]

126 **Chen X**, Liu J, Zhang Q, Liu B, Cheng Y, Zhang Y, Sun Y, Ge H, Liu Y. Exosome-mediated transfer of miR-93-5p from cancer-associated fibroblasts confer radioresistance in colorectal cancer cells by downregulating FOXA1 and upregulating TGFB3. *J Exp Clin Cancer Res* 2020; **39**: 65 [PMID: 32293494 DOI: 10.1186/s13046-019-1507-2]

127 **Fourniols T**, Bastien E, Canevat A, Feron O, Préat V. Inhibition of colorectal cancer-associated fibroblasts by lipid nanocapsules loaded with acriflavine or paclitaxel. *Int J Pharm* 2020; **584**: 119337 [PMID: 32371002 DOI: 10.1016/j.ijpharm.2020.119337]

128 **Loeffler M**, Krüger JA, Niethammer AG, Reisfeld RA. Targeting tumor-associated fibroblasts improves cancer chemotherapy by increasing intratumoral drug uptake. *J Clin Invest* 2006; **116**: 1955-1962 [PMID: 16794736 DOI: 10.1172/JCI26532]

129 **Hofheinz RD**, al-Batran SE, Hartmann F, Hartung G, Jäger D, Renner C, Tanswell P, Kunz U, Amelsberg A, Kuthan H, Stehle G. Stromal antigen targeting by a humanised monoclonal antibody: an early phase II trial of sibrotuzumab in patients with metastatic colorectal cancer. *Onkologie* 2003; **26**: 44-48 [PMID: 12624517 DOI: 10.1159/000069863]

130 **Li M**, Li M, Yin T, Shi H, Wen Y, Zhang B, Chen M, Xu G, Ren K, Wei Y. Targeting of cancerassociated fibroblasts enhances the efficacy of cancer chemotherapy by regulating the tumor microenvironment. *Mol Med Rep* 2016; **13**: 2476-2484 [PMID: 26846566 DOI: 10.3892/mmr.2016.4868]

131 **Chen W**, Chen Y, Su J, Kang J, Ding Y, Ai W, Zhang J, Luo H, An P. CaMKII Mediates TGFβ1-Induced Fibroblasts Activation and Its Cross Talk with Colon Cancer Cells. *Dig Dis Sci* 2022; **67**: 134-145 [PMID: 33528688 DOI: 10.1007/s10620-021-06847-0]

132 **Tanabe Y**, Sasaki S, Mukaida N, Baba T. Blockade of the chemokine receptor, CCR5, reduces the growth of orthotopically injected colon cancer cells *via* limiting cancer-associated fibroblast accumulation. *Oncotarget* 2016; **7**: 48335-48345 [PMID: 27340784 DOI: 10.18632/oncotarget.10227]

133 **Heichler C**, Scheibe K, Schmied A, Geppert CI, Schmid B, Wirtz S, Thoma OM, Kramer V, Waldner MJ, Büttner C, Farin HF, Pešić M, Knieling F, Merkel S, Grüneboom A, Gunzer M, Grützmann R, Rose-John S, Koralov SB, Kollias G, Vieth M, Hartmann A, Greten FR, Neurath MF, Neufert C. STAT3 activation through IL-6/IL-11 in cancer-associated fibroblasts promotes colorectal tumour development and correlates with poor prognosis. *Gut* 2020; **69**: 1269-1282 [PMID: 31685519 DOI: 10.1136/gutjnl-2019-319200]

134 **Owusu BY**, Bansal N, Venukadasula PK, Ross LJ, Messick TE, Goel S, Galemmo RA, Klampfer L. Inhibition of pro-HGF activation by SRI31215, a novel approach to block oncogenic HGF/MET signaling. *Oncotarget* 2016; **7**: 29492-29506 [PMID: 27121052 DOI: 10.18632/oncotarget.8785]

World Journal of Gastrointestinal Oncology

Submit a Manuscript: https://www.f6publishing.com

World J Gastrointest Oncol 2024 December 15; 16(12): 4579-4596

DOI: 10.4251/wjgo.v16.i12.4579

ISSN 1948-5204 (online)

ORIGINAL ARTICLE

Case Control Study

Prognostic utility of gamma-glutamyl transpeptidase to platelet ratio in patients with solitary hepatitis B virus-related hepatocellular carcinoma after hepatectomy

Cheng-Kun Yang, Zhong-Liu Wei, Xiao-Qiang Shen, Yu-Xuan Jia, Qiong-Yuan Wu, Yong-Guang Wei, Hao Su, Wei Qin, Xi-Wen Liao, Guang-Zhi Zhu, Tao Peng

Specialty type: Oncology

Provenance and peer review: Unsolicited article; Externally peer reviewed.

Peer-review model: Single blind

Peer-review report's classification

Scientific Quality: Grade A, Grade B, Grade C

Novelty: Grade B, Grade B, Grade C

Creativity or Innovation: Grade A, Grade C, Grade C

Scientific Significance: Grade B, Grade B, Grade B

P-Reviewer: Suwanprinya C; Tao HS; Zhao Y

Received: February 28, 2024

Revised: September 12, 2024

Accepted: September 29, 2024

Published online: December 15, 2024

Processing time: 258 Days and 1.9 Hours

Cheng-Kun Yang, Zhong-Liu Wei, Xiao-Qiang Shen, Yu-Xuan Jia, Yong-Guang Wei, Hao Su, Wei Qin, Xi-Wen Liao, Guang-Zhi Zhu, Tao Peng, Department of Hepatobiliary Surgery, The First Affiliated Hospital of Guangxi Medical University, Nanning 530021, Guangxi Zhuang Autonomous Region, China

Cheng-Kun Yang, Zhong-Liu Wei, Xiao-Qiang Shen, Yu-Xuan Jia, Yong-Guang Wei, Hao Su, Wei Qin, Xi-Wen Liao, Guang-Zhi Zhu, Tao Peng, Guangxi Key Laboratory of Enhanced Recovery after Surgery for Gastrointestinal Cancer, Nanning 530021, Guangxi Zhuang Autonomous Region, China

Qiong-Yuan Wu, Department of Tuina, Nanning Hospital of Traditional Chinese Medicine, Nanning 530022, Guangxi Zhuang Autonomous Region, China

Corresponding author: Tao Peng, MD, PhD, Professor, Department of Hepatobiliary Surgery, The First Affiliated Hospital of Guangxi Medical University, No. 6 Shuangyong Road, Nanning 530021, Guangxi Zhuang Autonomous Region, China. pengtaogmu@163.com

Abstract

BACKGROUND

The prognostic impact of preoperative gamma-glutamyl transpeptidase to platelet ratio (GPR) levels in patients with solitary hepatitis B virus (HBV)-related hepatocellular carcinoma (HCC) following radical resection has not been established.

AIM

To examine the clinical utility of GPR for prognosis prediction in solitary HBV-related HCC patients.

METHODS

A total of 1167 solitary HBV-related HCC patients were retrospectively analyzed. GPR levels were compared with 908 non-HCC individuals. Overall survival (OS) and recurrence-free survival (RFS) were evaluated, and cox proportional hazard model analyses were performed to identify independent risk factors. Differences in characteristics were adjusted by propensity score matching (PSM). Subgroup and stratified survival analyses for HCC risks were performed, and a linear trend

of the hazard ratio (HR) according to GPR levels was constructed.

RESULTS

GPR levels of patients with solitary HBV-related HCC were higher than those with hepatic hemangiomas, chronic hepatitis B and healthy control (adjusted $P < 0.05$). Variable bias was diminished after the PSM balance test. The low GPR group had improved OS ($P < 0.001$) and RFS ($P < 0.001$) in the PSM analysis and when combined with other variables. Multivariate cox analyses suggested that low GPR levels were associated with a better OS (HR = 0.5, 95%CI: 0.36-0.7, $P < 0.001$) and RFS (HR = 0.57, 95%CI: 0.44-0.73, $P < 0.001$). This same trend was confirmed in subgroup analyses. Prognostic nomograms were constructed and the calibration curves showed that GPR had good survival prediction. Moreover, stratified survival analyses found that GPR > 0.6 was associated with a worse OS and higher recurrence rate (P for trend < 0.001).

CONCLUSION

Preoperative GPR can serve as a noninvasive indicator to predict the prognosis of patients with solitary HBV-related HCC.

Key Words: Gamma-glutamyl transpeptidase to platelet ratio; Hepatitis B virus; Hepatocellular carcinoma; Prognosis; Propensity score matching

Core Tip: In this study, we assessed the prognostic value of gamma-glutamyl transpeptidase to platelet ratio (GPR) in early hepatitis B virus (HBV)-related hepatocellular carcinoma (HCC) patients. We evaluated the clinical utility of preoperative GPR in predicting outcomes for solitary HBV-related HCC patients using propensity score matching, restricted cubic spline, survival analyses and stratified analyses. Preoperative GPR levels facilitate recurrence monitoring and inform treatment strategies, potentially enhancing the quality of life for HCC patients.

Citation: Yang CK, Wei ZL, Shen XQ, Jia YX, Wu QY, Wei YG, Su H, Qin W, Liao XW, Zhu GZ, Peng T. Prognostic utility of gamma-glutamyl transpeptidase to platelet ratio in patients with solitary hepatitis B virus-related hepatocellular carcinoma after hepatectomy. *World J Gastrointest Oncol* 2024; 16(12): 4579-4596
URL: https://www.wjgnet.com/1948-5204/full/v16/i12/4579.htm
DOI: https://dx.doi.org/10.4251/wjgo.v16.i12.4579

INTRODUCTION

Worldwide there are 782500 new cases and 745500 deaths per year due to hepatocellular carcinoma (HCC), the most common primary liver cancer[1]. Environmental and individual risk factors include male sex, advanced age, obesity, type 2 diabetes, infection with hepatitis B virus (HBV) or hepatitis C virus (HCV), cirrhosis, aflatoxin B1 exposure, alcohol abuse, smoking, and several metabolic factors[2,3]. Chronic HBV infection is an important risk factor for HCC, especially in Asia-Pacific regions, and accounts for > 50% of newly diagnosed HCC cases[4]. Although HBV can become inactive, chronic HBV infections can cause progressive liver fibrosis, which may evolve into HCC in patients with cirrhosis[5]. The annual incidence of HBV-related HCC in patients with chronic HBV infection ranges from 2% to 5% when cirrhosis is already established[6].

Surgical resection is regarded as a standard curative treatment for early and intermediate stages of HCC among appropriately selected patients[7]. However, 5-year recurrence rates of HCC patients after curative hepatectomy are as high as 70%–80%, which hinders their long-term survival[8,9]. Clinical outcomes following surgery differ widely and such large variation is mostly unexplained. This variation becomes an obstacle to finding effective therapies and strategies for cancer management. Therefore, it is important to identify risk factors associated with postoperative recurrence and death to avoid subsequent consequences after HCC resection.

Liver puncture biopsy is an invasive procedure and the gold standard for ascertaining the degree of liver fibrosis and damage. Previous studies have found that various non-invasive methods based on routine laboratory tests can predict liver fibrosis, cirrhosis, and even the risk of developing HCC, including the fibrosis-4 index[10], aspartate aminotransferase-platelet index[11], and albumin-bilirubin score[12]. Interestingly, a previous study demonstrated that the gamma-glutamyl transpeptidase to platelet ratio (GPR) is an accurate indicator of chronic hepatic fibrosis in patients with chronic HBV infection[13]. In addition, the relative risk of HCC development was significantly increased within chronic HBV patients with high GPR levels[14]. Dai *et al*[15] reported that preoperative GPR could be an effective non-invasive predictor for the prognosis of HCC patients after hepatectomy[15]. A meta-analysis encompassing 10 studies with 4706 patients indicated that HCC patients with higher GPR exhibited poorer clinical outcomes compared to those with lower GPR, suggesting that GPR is a valid prognostic biomarker for HCC. Furthermore, elevated GPR may signal a deteriorating prognosis in postoperative HCC patients[16]. According to the Chinese guidelines for the diagnosis and treatment

of primary liver cancer[17], Chinese patients with single nodule liver cancer are considered to be in the early stage, and surgical resection is the preferred treatment method. Previous research has demonstrated that the GPR value is a potential prognostic indicator for the occurrence of both overall postoperative and major complications following minor hepatectomy in patients with HCC[18]. However, no study has investigated the prognostic effect of preoperative GPR levels in patients with solitary HBV-related HCC after radical resection.

In the present study, we explored the critical importance of preoperative GPR as a prognosis factor for HBV-related HCC through propensity score matching (PSM), and survival and stratified analyses.

MATERIALS AND METHODS

Study population

We enrolled patients who underwent curative HCC resection between January 2012 and December 2018 at the Department of Hepatobiliary Surgery, The First Affiliated Hospital of Guangxi Medical University.

Inclusion criteria were as follows: (1) The 18 years of age or older; (2) Medical history of chronic HBV infection; (3) HBV-related HCC was confirmed histopathologically after initial hepatectomy, without previous treatment; (4) Patients presented solitary HCC without gross vascular invasion, bile duct tumor thrombosis, satellite nodules or extrahepatic metastasis upon preoperative clinical imaging and histopathological examination; (5) Child-Pugh classification A or B; and (6) Negative surgical margin observed microscopically or macroscopically upon resection.

Exclusion criteria: (1) Patients with concurrent malignancies; (2) Patients deemed unsuitable for surgery due to either poor tolerance or insufficient residual liver volume to ensure surgical feasibility; (3) Patients diagnosed with hepatic neoplasms of mixed histology; (4) Recurrent HCC; and (5) Non-HBV infection. A total of 1167 patients were enrolled, of whom 172 patients were Barcelona Clinic Liver Cancer (BCLC) stage 0, and 995 patients were BCLC stage A.

To evaluate GPR levels, a total of 908 participants (age ≥ 18 years and ≤ 80 years, males and females) were enrolled from the First Affiliated Hospital of Guangxi Medical University, including 28 patients with hepatic hemangiomas, 242 healthy control, 67 patients with nonalcoholic fatty liver, 224 patients with chronic hepatitis B, 84 patients with chronic hepatitis C, 245 patients with post-hepatitis cirrhosis, and 18 patients with alcoholic cirrhosis. Eligibility criteria were as follows: (1) Liver cirrhosis detected by liver biopsy or supported by two imaging techniques, with chronic hepatitis infection or alcoholism history; (2) Chronic hepatitis defined as hepatitis B surface antigen or hepatitis C antibodies positive for at least 6 months, with confirmed of HBV or HCV infection; (3) Nonalcoholic fatty liver and hepatic hemangiomas were diagnosed by two clinical imaging methods, in patients with no history of hepatitis infection; and (4) Healthy individuals were confirmed to have no liver or gastrointestinal diseases, no history of other malignancies, and were serologically negative for hepatitis viruses.

This study was approved by The Ethics Committee of The First Affiliated Hospital of Guangxi Medical University, China, No. 2024-E638-01. All participants signed written informed consent before study commencement.

Data acquisition and pre-processing

Medical records of HBV-related HCC were reviewed to extract information on baseline characteristics and pathological variables. Histopathological examination confirmed the diagnosis of cirrhosis. Tumor stage after operation was determined following the BCLC staging system. Cutoff values of continuous variables were based on those used commonly in upper and lower clinical limits or median values of subjects. GPR was defined as gamma-glutamyl transpeptidase (GGT) (U/L)/platelet count (× 10^9/L). The above indicators are derived from the latest preoperative clinical data of each patient. The x-tile program[19] was used to generate the optimal GPR cutoff point with minimum P values from χ^2 tests. Therefore, the cutoff value of GPR was set as 0.2. In particular, the tercile stratification thresholds for GPR were set at 0.2 and 0.6.

Follow-up

After surgery, all patients were followed-up for at least one year. During the first postoperative year, outpatient surveillance was conducted at 3-month intervals, and then every 6-month thereafter by outpatient visits or telephone calls until death or up to January 31, 2022. Serum alpha-fetoprotein (AFP) assay, ultrasonography, and chest radiography were routinely performed. Enhanced computed tomography was performed every 6 months. Based on this surveillance, the overall survival (OS) time was defined as the time from surgery to death (any cause) or to the interruption of follow-up. The recurrence-free survival (RFS) time was defined as the time from surgery to HCC recurrence, including the appearance of intrahepatic tumor nodule(s) with radiologic features consistent with HCC, with or without a rise in serum AFP levels, or follow-up interruption.

PSM

PSM analysis was used to adjust for differences in baseline characteristics and to minimize biases of variable selection. With a 0.05 standardized difference as the caliper, a 1:1 matching was performed using the nearest neighbor method. Standardized mean differences were used to assess the balanced distribution of matched patients within each group. A mean difference value higher than 0.1 was considered imbalanced. Matching variables included sex, age, body mass index, smoking history, drinking history, history of liver fluke disease, liver cirrhosis, alpha-fetoprotein, tumor size, liver function grade, microvascular imaging (MVI), *etc.* After PSM, both low and high GPR groups included 328 patients

(Figure 1). Three groups of PSM analysis were further matched by R packet TriMatch[20].

Statistical analysis

Descriptive analysis of clinicopathological features was assessed using Pearson's χ^2 and Wilcoxon rank sum tests, as appropriate. Survival analysis was performed through the Kaplan-Meier method to estimate the survival rates for different groups. The log-rank test was used to evaluate the statistical significance of the equivalences of the survival curves. To evaluate the association between variables and endpoints, a cox proportional hazards model was constructed for univariate and multivariate survival analyses to calculate the hazard ratio (HR) and 95%CI. In multivariable analyses, we used forward stepwise selection of covariates that were $P < 0.05$ in the univariate regression. Restricted cubic spline (RCS) analyses were performed to determine the association between continuous GPR levels and death/recurrence risks. Interaction analyses, combined analyses, and nomograms were utilized to explore the comprehensive effects of GPR levels and subgroup parameters on the prognosis of HCC. Statistical significance for a linear trend of HR across stratified GPR levels and clinical outcomes of patients was tested. $P < 0.05$ indicated a statistically significant difference.

All analyses were performed in x-tile (version 3.6.1), R (version 3.6.2, https://www.r-project.org/) and Statistical Package for the Social Sciences version 24.0 (IBMCorp., Chicago, IL, United States).

RESULTS

A flow diagram summarizing the present work is shown in Figure 1.

GPR level comparisons

Pairwise comparison of GPR levels revealed that GPR levels of solitary HBV-related HCC patients were higher than those of patients with hepatic hemangiomas, chronic hepatitis B and healthy controls (adjusted $P < 0.05$) (Figure 2). However, no significant difference was found between patients with HBV-related HCC and post-hepatitis cirrhosis.

PSM balance test

To adjust for differences in baseline characteristics, associated covariates were entered into the propensity model. After the PSM balance test, the distribution of propensity scores in the high and low GPR groups were similar (Figure 3A). Moreover, all variables were within a reasonable range (overall distance fell within the caliper) after adjusting for solitary HCC patients with GPR ≤ 0.2 and GPR > 0.2 (Figure 3B).

Characteristics of the study population

Comparisons of baseline characteristics and clinicopathological features among early-stage solitary HCC patients with GPR ≤ 0.2 and GPR > 0.2 before and after PSM are presented in Table 1. Before PSM, there were differences between the groups in several variables, including sex, smoking, drinking, liver flukes, cirrhosis, serum AFP level, total bilirubin, albumin, GGT, HBV DNA, tumor size and infiltrative growth ($P < 0.05$) (Table 1). After PSM, the clinicopathological variables of the two groups were balanced, and the two groups were comparable (Table 1). Although some differences in the serum AFP and total bilirubin, the overall distance of propensity scores is still within a reasonable range (Figure 3B).

Survival analysis

Survival curve and Cox proportional hazards model analyses showed that, compared with the high GPR group (GPR > 0.2), low GPR patients had a better OS time and risk value upon univariate analyses (log-rank $P < 0.001$, HR = 0.48, 95%CI: 0.36-0.64, $P < 0.001$) (Figure 3C and Table 2). After matching, the low GPR group was shown to have a better OS and risk than the high GPR group of patients with early-stage solitary HCC (log-rank $P < 0.001$, HR = 0.49, 95%CI: 0.35-0.69, $P < 0.001$) (Figure 3D and Table 2). Similarly, compared with the high GPR group (GPR > 0.2), patients in the low GPR group had improved RFS and risk values (log-rank $P < 0.001$, HR = 0.49, 95%CI: 0.4-0.6, $P < 0.001$) (Figure 3E and Table 3). Indeed, after matching, the low GPR group had improved RFS and risk (log-rank $P < 0.001$; HR = 0.56, 95%CI: 0.44-0.71, $P < 0.001$) (Figure 3F and Table 3). Moreover, some clinical features were related to tumor prognosis, such as tumor size, cirrhosis, and HBV-DNA (Table 2 and Table 3). Results from the multivariate analysis suggest that preoperative low GPR levels were independently associated with a better OS (HR = 0.5, 95%CI: 0.36-0.7, $P < 0.001$) and RFS (HR = 0.57, 95%CI: 0.44-0.73, $P < 0.001$) (Table 3).

Subgroup and combined analyses by baseline characteristics

To explore more deeply the predictive value of GPR levels for the prognosis of early-stage solitary HBV-related HCC patients, we performed subgroup analyses based on baseline characteristics. Patients in each group were divided into subgroups with low and high GPR levels. Among subgroups, low preoperative GPR levels were significantly associated with an improved OS when compared to those that had high GPR levels (Figure 4A). A strong interaction was found between GPR and HBV-DNA copies (P for interaction = 0.015) (Figure 4A). Indeed, the forest plot depict that the risk of RFS was improved in patients with low GPR values among each subgroup of baseline characteristics (Figure 4A). Importantly, a significant interaction between GPR and tumor size was observed (P for interaction = 0.032) (Figure 4A). Combined analyses showed that a low GPR coupled with a tumor size ≤ 5 cm, absence of cirrhosis, AFP < 200 ng/mL, and no MVI predicted a favorable OS after PSM (Figure 4B). Conversely, high GPR levels coupled with tumor size > 5 cm, AFP ≥ 200 ng/mL, the presence of cirrhosis and MVI predicted a shorter recurrence time (Figure 4C).

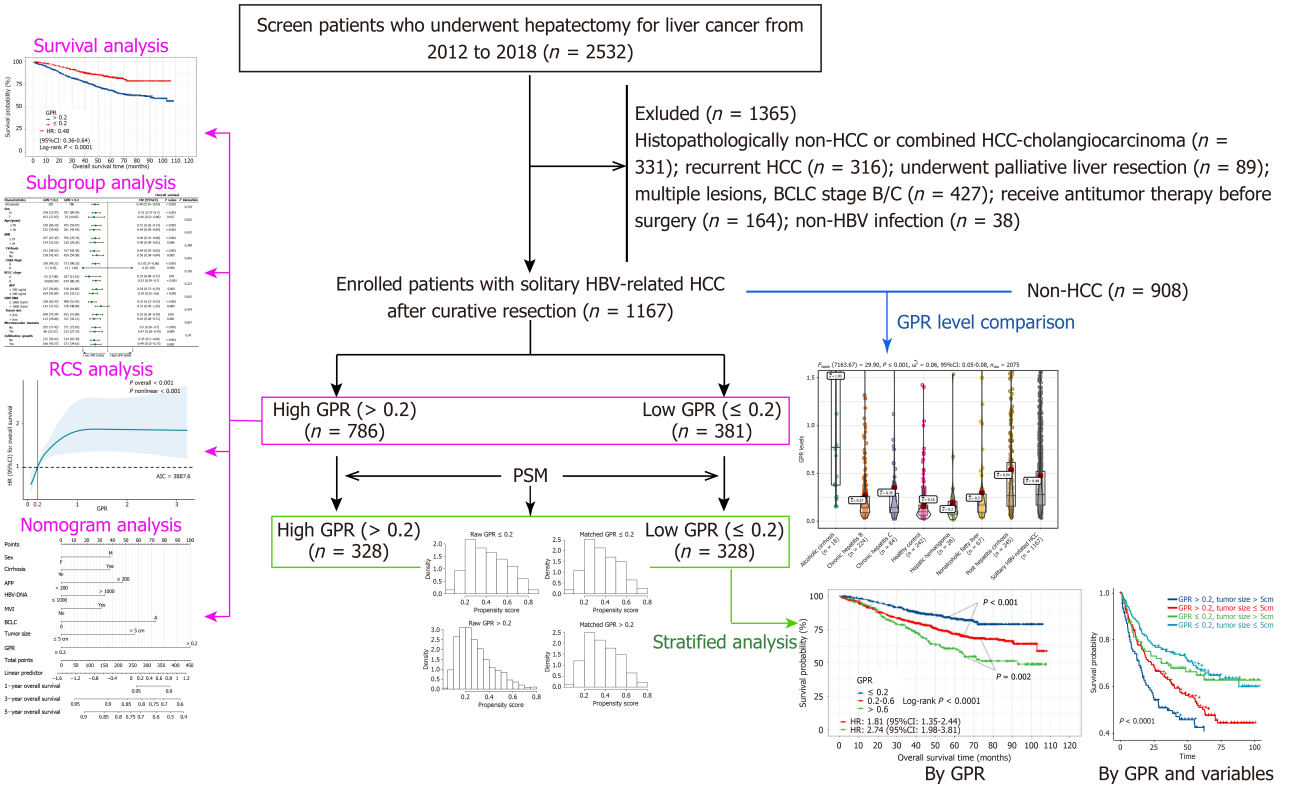

Figure 1 Flow diagram of the propensity score analysis for this study. GPR: Gamma-glutamyl transpeptidase-to-platelet ratio; RCS: Restricted cubic spline; HCC: Hepatocellular carcinoma; BCLC: Barcelona Clinic Liver Cancer.

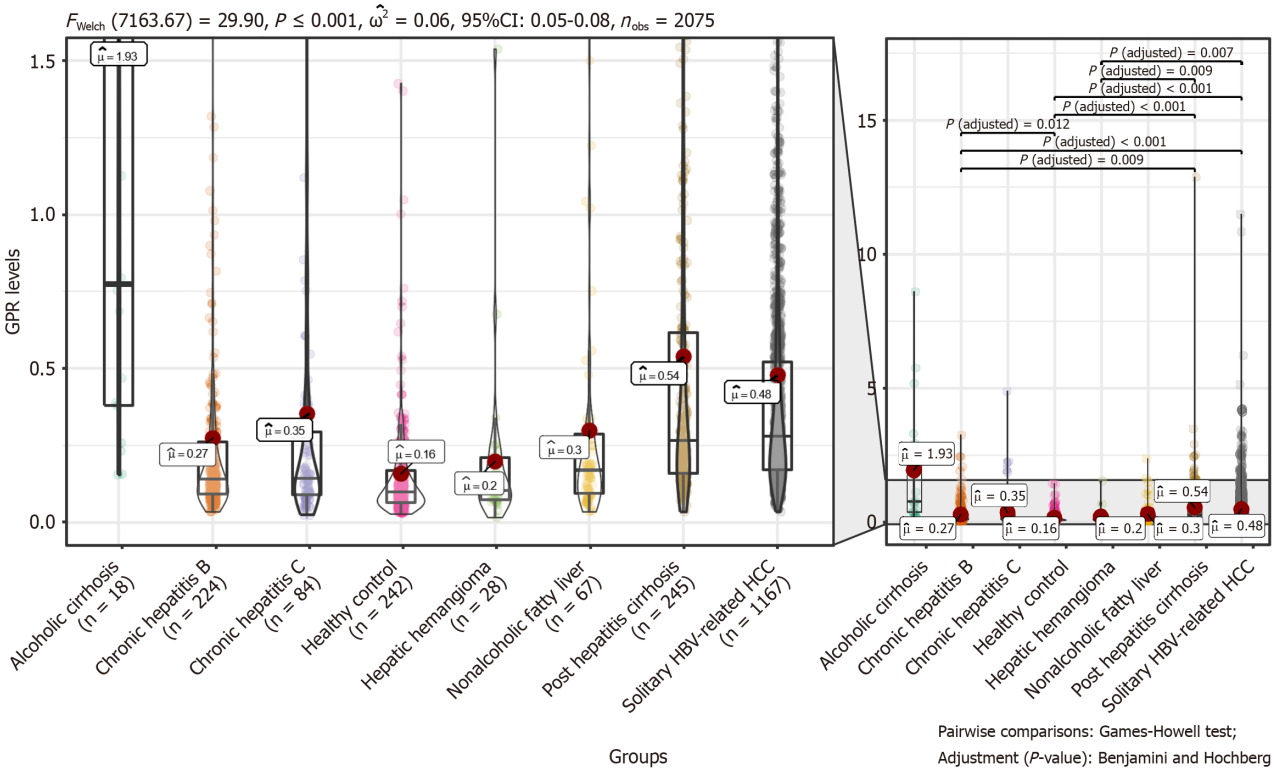

Figure 2 Violin plot analysis comparing the gamma-glutamyl transpeptidase-to-platelet ratio levels among hepatitis B virus-related hepatocellular carcinoma and other 7 non-hepatocellular carcinoma groups. Pairwise comparisons were performed by Games-Howell test, and *P* value was adjusted by Benjamini-Hochberg methods.

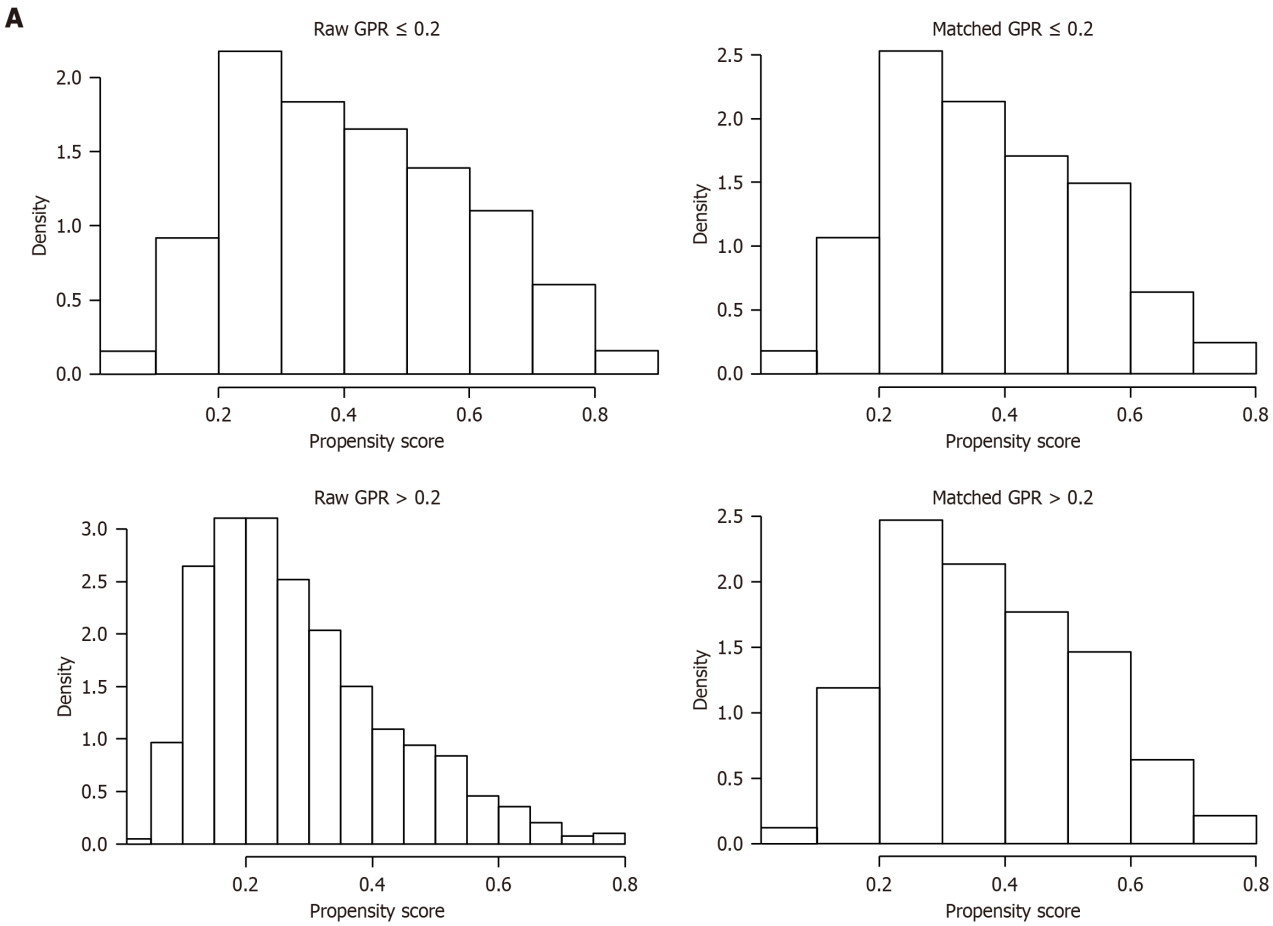
A
Raw GPR ≤ 0.2
Matched GPR ≤ 0.2
Raw GPR > 0.2
Matched GPR > 0.2
Density
Propensity score

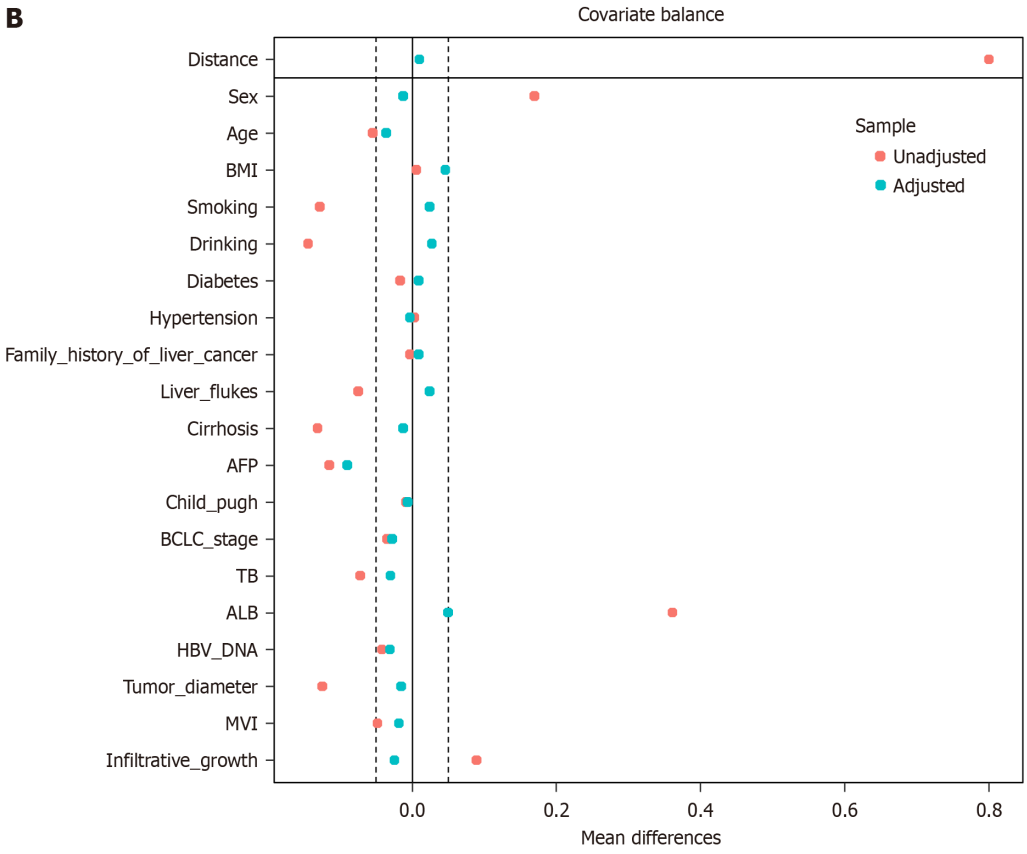
B
Covariate balance
Distance
Sex
Age
BMI
Smoking
Drinking
Diabetes
Hypertension
Family_history_of_liver_cancer
Liver_flukes
Cirrhosis
AFP
Child_pugh
BCLC_stage
TB
ALB
HBV_DNA
Tumor_diameter
MVI
Infiltrative_growth
Sample
Unadjusted
Adjusted
Mean differences

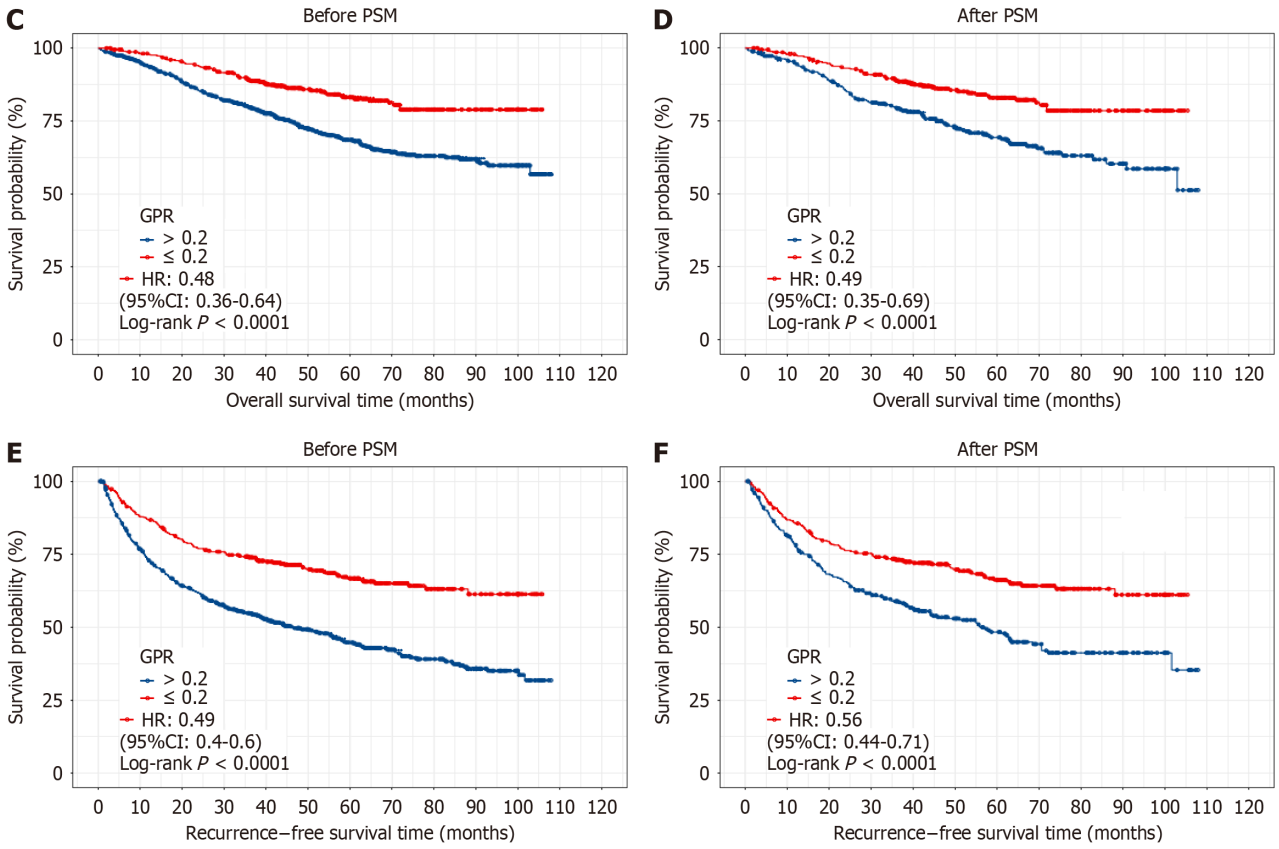

Figure 3 The balance test of propensity score matching and KaplanMeier analysis between gamma-glutamyl transpeptidase-to-platelet ratio level and prognosis of solitary hepatitis B virus-related hepatocellular carcinoma cohort. A: Distribution of propensity values before and after propensity score matching (PSM); B: Absolute standardized differences in covariates between solitary hepatocellular carcinoma (HCC) patients with gamma-glutamyl transpeptidase-to-platelet ratio (GPR) ≤ 0.2 and GPR > 0.2, before and after PSM; C and D: Kaplan-Meier survival curves of overall survival in patients with solitary HCC before and after PSM; E and F: Kaplan-Meier survival curves of RFS in patients with solitary HCC before and after PSM. PSM: Propensity score matching; GPR: Gamma-glutamyl transpeptidase-to-platelet ratio; BMI: Body mass index; HR: Hazard ratio; AFP: Alpha-fetoprotein; TB: Total bilirubin; ALB: Albumin; HBV: Hepatitis B virus; MVI: Microvascular imaging.

Stratified and RCS analyses by GPR levels

RCS curves demonstrated that the association between continuous GPR levels and death/recurrence risks presented as a non-linear trend, with or without variables adjustments ($P < 0.001$) (Figure 5A). Per standardized difference increased in GPR levels were associated with a 1.29 (1.18-1.42) HR increase in OS after PSM (Table 4). Moreover, the HR for RFS of HCC patients after hepatectomy was positively correlated with elevated GPR level per standardized difference change (HR = 1.20, 95%CI: 1.11-1.31, $P < 0.001$) (Table 4). To verify if GPR levels could predict the prognosis of patients with solitary HBV-related HCC, a GPR-based risk assessment divided patients into three groups, namely the GPR > 0.2 group was stratified as intermedial GPR levels (0.2 < GPR ≤ 0.6) and high GPR levels (GPR > 0.6). Compared with patients at the bottom tercile for preoperative GPR (GPR ≤ 0.2), patients in the middle tercile had worse OS and RFS ($P < 0.001$) (Figure 5B). Moreover, those in the top tercile group had even lower OS (HR = 2.74; 95%CI: 1.98–3.81, P for trend < 0.001) and RFS values (HR = 2.60; 95%CI: 2.04–3.31, P for trend < 0.001) (Figure 5B and Table 4). After matching analysis, the triangle chart showed the correlation among the matching items in each group, and the absolute standard deviation was well adjusted (Figure 5C). Indeed, after PSM, intermedial GPR level was associated with worse prognosis in terms of OS (HR = 1.52, 95%CI: 1.08–2.14, log-rank $P < 0.001$) and RFS (HR = 1.69, 95%CI: 1.25–2.17, log-rank $P < 0.001$) (Figure 5D). Furthermore, high GPR levels were associated with worse prognosis of postoperative patients with HCC, including shorter OS (HR = 2.33, 95%CI: 1.60–3.39, P for trend < 0.001) and RFS (HR = 2.35, 95% CI: 1.77–3.13, P for trend < 0.001) (Figure 5D and Table 4). We detected an increased linear trend for HR in patients stratified according to their GPR levels (P for trend < 0.001) (Table 4). Besides, Kaplan-Meier curves of OS and RFS were statistically different among GPR-stratified patients with or without adjusting for PSM (all $P < 0.05$) (Figure 5). Therefore, a high GPR level is enough to warrant HCC surveillance before liver resections.

Construction of prognostic nomograms

According to the univariate Cox analysis results of the variables and clinical prognosis before PSM, clinical variables that may be associated factors ($P < 0.05$) were included in the model construction. Thus, we developed two survival nomograms to predict OS (Figure 6A) and RFS (Figure 6B). The c-indexes of the OS and RFS nomograms were respectively 0.732 (95%CI: 0.669-0.795) and 0.756 (95%CI: 0.723-0.785). Moreover, calibration curves demonstrated that the nomograms predicted the 1-year, 3-years, and 5-years OS and RFS with a high resolution and accuracy.

A

Characteristics	GPR ≤ 0.2	GPR > 0.2	Overall survival HR (95%CI)	*P* value	*P* interaction	Recurrence-free survival HR (95%CI)	*P* value	*P* interaction
All parents	381	786	0.48 (0.36–0.64)	< 0.001		0.49 (0.4–0.6)	< 0.001	
Sex					0.793			0.359
M	278 (72.97)	707 (89.95)	0.51 (0.37–0.7)	< 0.001		0.47 (0.37–0.6)	< 0.001	
F	103 (27.03)	79 (10.05)	0.44 (0.22–0.86)	0.017		0.6 (0.38–0.95)	0.03	
Age (years)					0.622			0.849
≤ 50	229 (60.10)	425 (54.07)	0.51 (0.36–0.73)	< 0.001		0.5 (0.39–0.65)	< 0.001	
> 50	152 (39.90)	361 (45.93)	0.44 (0.28–0.69)	< 0.001		0.47 (0.34–0.64)	< 0.001	
BMI					0.957			0.473
≤ 24	257 (67.45)	556 (70.74)	0.49 (0.35–0.68)	< 0.001		0.47 (0.37–0.59)	< 0.001	
> 24	124 (32.55)	230 (29.26)	0.48 (0.28–0.81)	0.006		0.54 (0.38–0.78)	0.001	
Cirrhosis					0.384			0.15
Yes	223 (58.53)	357 (45.42)	0.44 (0.29–0.65)	< 0.001		0.43 (0.33–0.58)	< 0.001	
No	158 (41.47)	429 (54.58)	0.56 (0.38–0.84)	0.005		0.58 (0.44–0.77)	< 0.001	
Child-Pugh					0.991			0.987
A	378 (99.21)	773 (98.35)	0.5 (0.37–0.66)	< 0.001		0.49 (0.4–0.6)	< 0.001	
B	3 (0.79)	13 (1.65)	0 (0–Inf)	0.999		0 (0–Inf)	0.999	
BCLC stage					0.183			0.464
0	65 (17.06)	107 (13.61)	0.25 (0.09–0.72)	0.01		0.57 (0.34–0.96)	0.034	
A	316(82.94)	679 (86.39)	0.52 (0.39–0.7)	< 0.001		0.48 (0.38–0.59)	< 0.001	
AFP					0.227			0.339
< 200 ng/ml	217 (56.96)	510 (64.89)	0.54 (0.37–0.79)	0.001		0.51 (0.39–0.67)	< 0.001	
≥ 200 ng/ml	164 (43.04)	276 (35.11)	0.39 (0.25–0.6)	< 0.001		0.43 (0.32–0.58)	< 0.001	
HBV DNA					0.015			0.062
≤ 1000 IU/ml	238 (62.47)	408 (51.91)	0.35 (0.23–0.53)	< 0.001		0.42 (0.32–0.55)	< 0.001	
> 1000 IU/ml	143 (37.53)	378 (48.09)	0.72 (0.49–1.05)	0.089		0.61 (0.46–0.83)	0.001	
Tumor size					0.474			0.032
≤ 5cm	268 (70.34)	455 (57.89)	0.55 (0.38–0.79)	0.00		0.59 (0.46–0.76)	< 0.001	
> 5cm	113 (29.66)	331 (42.11)	0.45 (0.28–0.71)	0.001		0.39 (0.28–0.56)	< 0.001	
Microvascular invasion					0.827			0.476
No	295 (77.43)	571 (72.65)	0.5 (0.36–0.7)	< 0.001		0.47 (0.37–0.59)	< 0.001	
Yes	86 (22.57)	215 (27.35)	0.47 (0.28–0.79)	0.004		0.56 (0.39–0.81)	0.002	
Infiltrative growth					0.74			0.872
No	215 (56.43)	514 (65.39)	0.45 (0.3–0.66)	< 0.001		0.47 (0.35–0.61)	< 0.001	
Yes	166 (43.57)	272 (34.61)	0.49 (0.32–0.73)	0.001		0.48 (0.36–0.65)	< 0.001	

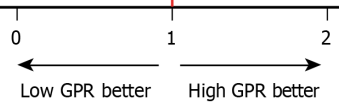

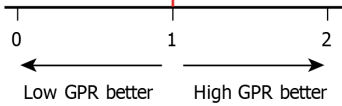

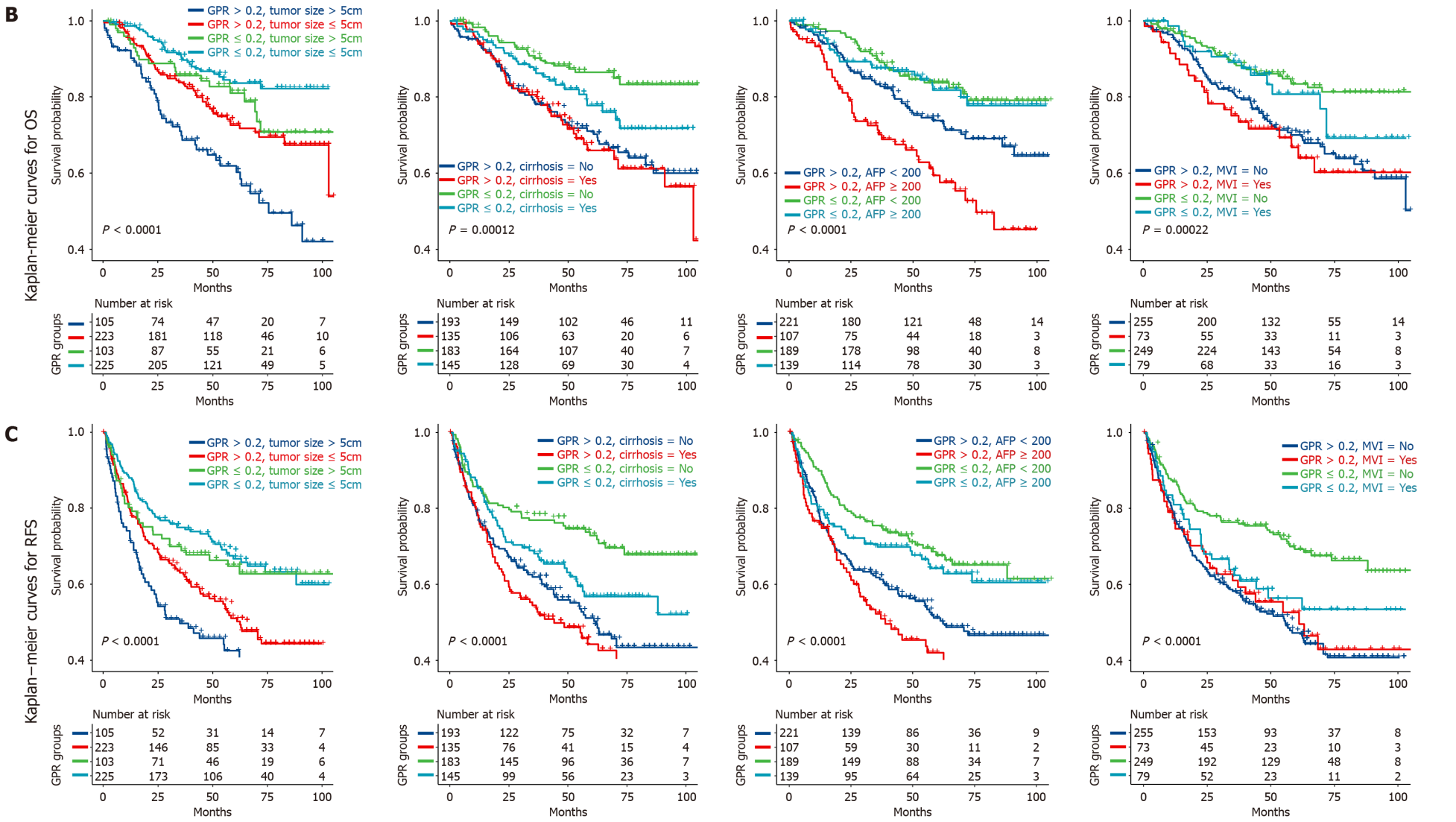

Figure 4 Subgroup analyses for gamma-glutamyl transpeptidase-to-platelet ratio level and combined analyses of gamma-glutamyl transpeptidase-to-platelet ratio levels and variables in overall survival and recurrence-free survival of solitary hepatitis B virus-related hepatocellular carcinoma. A: Subgroup analyses for overall survival (OS) and recurrence-free survival (RFS); B: Combined analyses with tumor size, cirrhosis, alpha-fetoprotein (AFP), and microvascular imaging (MVI) for OS; C: Combined analyses with tumor size, cirrhosis, AFP, and MVI for RFS. GPR: Gamma-glutamyl transpeptidase-to-platelet ratio; HR: Hazard ratio; OS: Overall survival; BMI: Body mass index; HR: Hazard ratio; AFP: Alpha-fetoprotein; HBV: Hepatitis B virus; BCLC: Barcelona Clinic Liver Cancer; F: Female; M: Male.

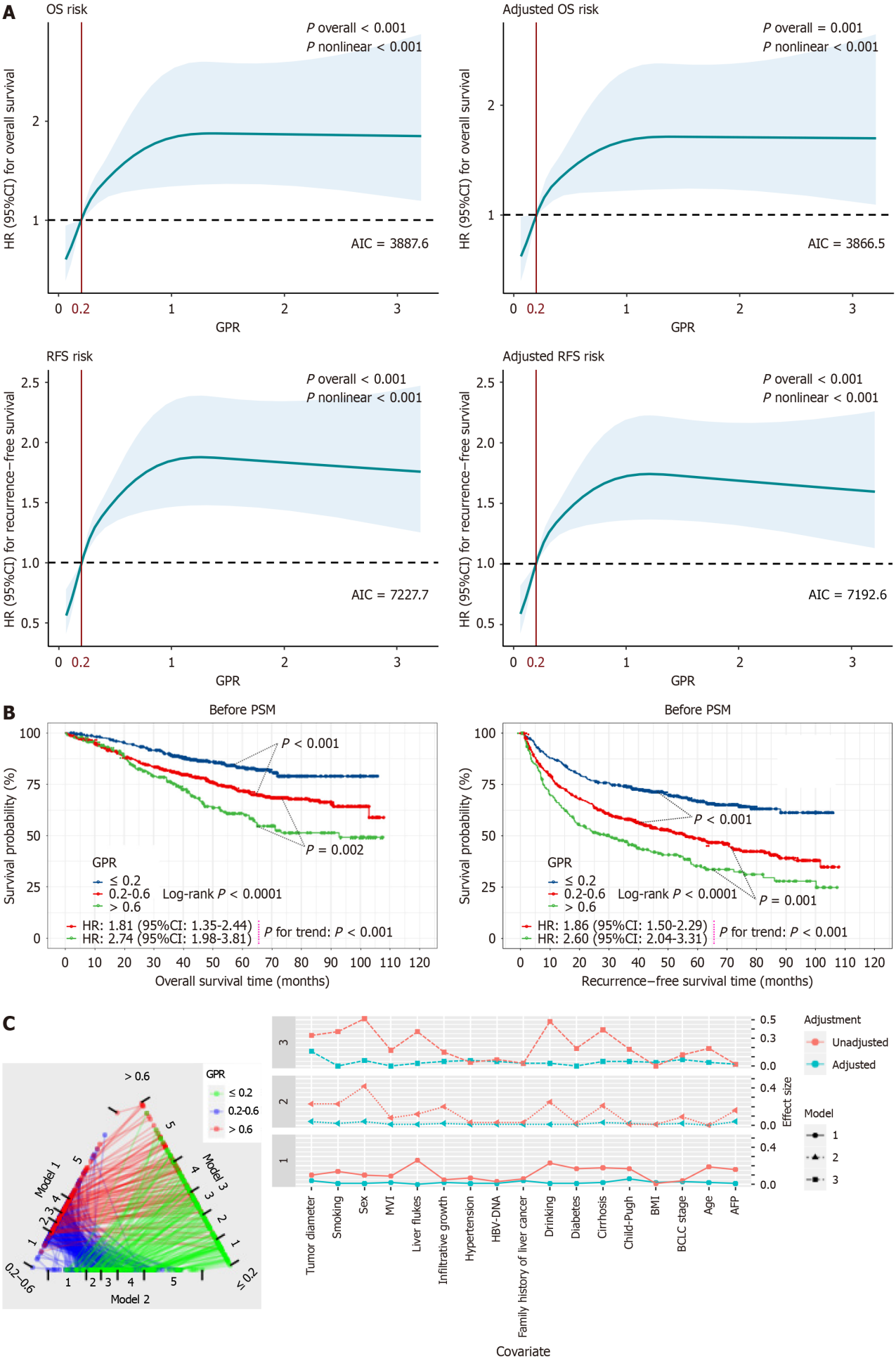
A
OS risk
P overall < 0.001
P nonlinear < 0.001
HR (95%CI) for overall survival
AIC = 3887.6
GPR
Adjusted OS risk
P overall = 0.001
P nonlinear < 0.001
AIC = 3866.5
RFS risk
P overall < 0.001
P nonlinear < 0.001
HR (95%CI) for recurrence−free survival
AIC = 7227.7
Adjusted RFS risk
P overall < 0.001
P nonlinear < 0.001
AIC = 7192.6
B
Before PSM
Survival probability (%)
P < 0.001
P = 0.002
GPR
≤ 0.2
0.2-0.6
> 0.6
Log-rank P < 0.0001
HR: 1.81 (95%CI: 1.35-2.44)
HR: 2.74 (95%CI: 1.98-3.81)
P for trend: P < 0.001
Overall survival time (months)
Before PSM
P < 0.001
P = 0.001
Log-rank P < 0.0001
HR: 1.86 (95%CI: 1.50-2.29)
HR: 2.60 (95%CI: 2.04-3.31)
P for trend: P < 0.001
Recurrence−free survival time (months)
C
GPR
≤ 0.2
0.2-0.6
> 0.6
Model 1
Model 2
Model 3
Adjustment
Unadjusted
Adjusted
Model
Effect size
Tumor diameter
Smoking
Sex
MVI
Liver flukes
Infiltrative growth
Hypertension
HBV-DNA
Family history of liver cancer
Drinking
Diabetes
Cirrhosis
Child-Pugh
BMI
BCLC stage
Age
AFP
Covariate

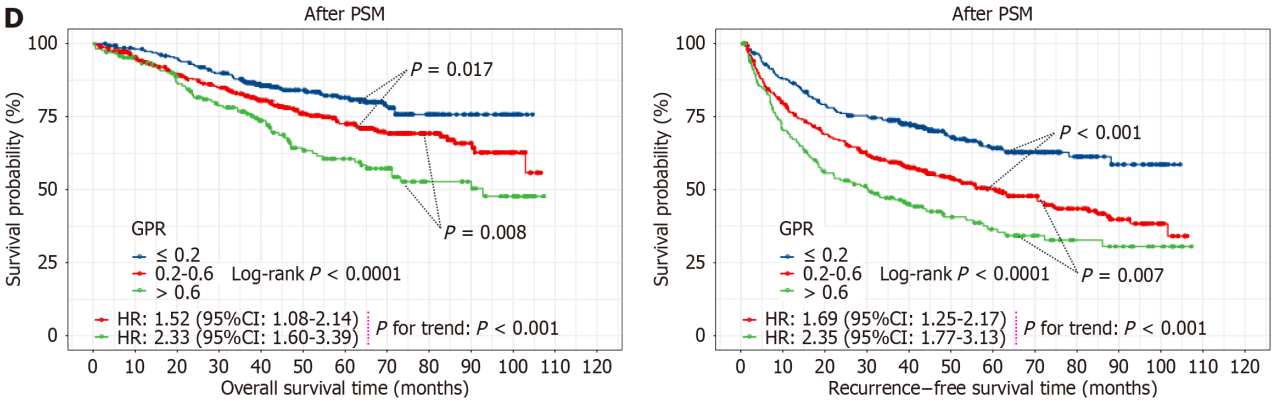

Figure 5 The association between gamma-glutamyl transpeptidase-to-platelet ratio and death/recurrence risk and Kaplan-Meier stratified analysis between gamma-glutamyl transpeptidase-to-platelet ratio levels and prognosis in the solitary hepatitis B virus-related hepatocellular carcinoma cohort. A: The restricted cubic spline curves of gamma-glutamyl transpeptidase-to-platelet ratio levels. The risk was adjusted by age, cirrhosis, hepatitis B virus-DNA, tumor size, microvascular imaging, and infiltrative growth; B: Kaplan-Meier survival curves of overall survival (OS) and recurrence-free survival (RFS) in patients with solitary hepatocellular carcinoma (HCC) before propensity score matching (PSM); C: Triangle plot and absolute standardized differences adjustment of three groups; D: Kaplan-Meier survival curves of OS and RFS in patients with solitary HCC after PSM. OS: Overall survival; PSM: Propensity score matching; GPR: Gamma-glutamyl transpeptidase-to-platelet ratio; MVI: Microvascular imaging; HBV: Hepatitis B virus; BCLC: Barcelona Clinic Liver Cancer; BMI: Body mass index; HR: Hazard ratio; AFP: Alpha-fetoprotein.

DISCUSSION

HCC is a common malignant tumor with high recurrence rates and cancer mortality. Previous studies have found that the ratio of routine blood tests and liver function tests have a good predictive value on the prognosis of liver cancer. In the current study, we explored the value of GPR to clinical prognosis by screening early HBV-related HCC patients. GPR levels were higher in these patients than in those with hepatic hemangiomas, chronic hepatitis B and healthy controls. Of note, when the preoperative GPR cutoff value was set at 0.2, HCC patients with high GPR levels had a poorer prognosis. In the entire cohort, patients in the high GPR group had a significantly increased risk after hepatectomy. We used PSM to balance baseline and clinicopathological characteristics. This analysis corroborated the correlation between GPR levels and clinical prognosis for HBV-related HCC patients. Subgroup and combined analyses suggested that, low GPR levels had a protective effect on patient prognosis after liver resection. These findings were supported when patients were stratified according to GPR terciles (*P* for trend < 0.001). Prognostic nomograms were constructed and the calibration curves showed that GPR can predict the OS and RFS well. This is the first study to examine the relationship between the GPR and surgical outcomes in solitary HBV-related HCC patients. Our results could provide useful information for preoperative planning and postoperative surveillance in these patients.

In this study, multivariate analyses before and after PSM found that, in patients with a single nodule HBV-related HCC, the tumor diameter was associated with OS after radical resection. In addition, the tumor size, aggressive tumor growth, and the presence of liver cirrhosis were associated with tumor recurrence. A Korean study noted that a tumor size > 3 cm, and microvascular invasion were closely associated with early recurrence after liver resection for solitary HCC[21]. A previous study noted that cancer recurrence and long-term survival were independently associated with a tumor size > 5 cm in cirrhotic patients undergoing curative hepatectomy for solitary HCC without macrovascular invasion[22]. Besides, compared with patients who underwent curative hepatectomy without liver cirrhosis, HCC patients with liver cirrhosis had a 6% to 15% higher annual risk of de novo recurrence[23]. Patients with HBV-related HCC often have a background of liver cirrhosis, so it is particularly important to evaluate the prognosis of patients before surgery. Some study suggested that GPR can be a good predictor for HCC development in chronic hepatitis B patients[14, 24]. A study has demonstrated that HBV-associated HCC patients with high GPR levels had significantly poorer survival outcomes, regardless of the specific treatment approaches administered[25].

GGT as a cell-membrane-bound enzyme plays a crucial role in modulating the metabolic process of glutathione, involved in nucleic acid metabolism and carcinogenesis. Previous study suggested that serum GGT levels strongly predicted HCC development in patients with chronic HBV infection who underwent nucleotide/nucleoside analogues, particularly non-cirrhotic patients[26]. The detection of serum GGT was previously reported to be associated with the prognosis of HCC patients who underwent hepatectomy[27], radiofrequency-ablation[28], adjuvant transarterial chemoembolization[29], and liver transplantation[30]. A plausible mechanism underlying the prognostic significance of GPR could involve its correlation with inflammatory processes. GGT, a constituent of the GPR, serves as a biomarker for hepatic injury and is indicative of the ongoing inflammatory response in HCC. Elevated GGT levels have been observed in individuals with conditions such as hepatitis, liver fibrosis, cirrhosis, and hepatic malignancies[16]. Elevated levels of GGT have been significantly associated with the presence of multiple intrahepatic micrometastases and vascular invasion in HCC[28,30]. Certain serum inflammatory cytokines, notably tumor necrosis factor-alpha and interferon-alpha, which are closely associated with the prognosis of HCC, may contribute to the upregulation of GGT expression[31]. Furthermore, GGT participates in oxidative reactions and serves as a biomarker for oxidative stress, which is an essential component of numerous chronic inflammation-associated responses[32-34]. Platelets, which are anuclear cytoplasmic

Table 1 Preoperative clinicopathologic data of patients with solitary hepatitis B virus-related hepatocellular carcinoma

Variables		Before PSM				After PSM			
		N (1167)	GPR ≤ 0.2 (*n* = 381)	GPR > 0.2 (*n* = 786)	*P* value	*N* (656)	GPR ≤ 0.2 (*n* = 328)	GPR > 0.2 (*n* = 328)	*P* value
Sex	Male	985	278	707	< 0.001	533	266	267	1
	Female	182	103	79		123	62	61	
Age (years)	≤ 50	654	229	425	0.059	377	196	181	0.269
	> 50	513	152	361		279	132	147	
Body mass index	> 24	354	124	230	0.282	205	107	98	0.5
	≤ 24	813	257	556		451	221	230	
Smoking	Yes	407	100	307	< 0.001	190	97	93	0.796
	No	760	281	479		466	231	235	
Drinking	Yes	386	89	297	< 0.001	179	87	92	0.726
	No	781	292	489		477	241	236	
Diabetes mellitus	Yes	59	15	44	0.284	33	15	18	0.721
	No	1108	366	742		623	313	310	
Hypertension	Yes	114	38	76	0.953	67	33	34	1
	No	1053	343	710		589	295	294	
Family history of liver cancer	Yes	128	41	87	0.954	72	39	33	0.532
	No	1039	340	699		584	289	295	
Liver flukes	Yes	221	53	168	0.003	112	51	61	0.35
	No	946	328	618		544	277	267	
Cirrhosis	Yes	587	158	429	< 0.001	280	145	135	0.477
	No	580	223	357		376	183	193	
Serum alpha-fetoprotein (ng/mL)	≥ 200	440	164	276	0.011	246	139	107	0.012
	< 200	727	217	510		410	189	221	
Child-Pugh	A	1151	378	773	0.355	649	325	324	1
	B	16	3	13		7	3	4	
Barcelona Clinic Liver Cancer stage	0	172	65	107	0.142	103	53	50	0.83
	A	995	316	679		553	275	278	
Total bilirubin (μmol/L)	> 20.5	128	31	97	0.04	73	28	45	0.047
	≤ 20.5	1039	350	689		583	300	283	
Albumin (g/L)	> 40	534	223	311	< 0.001	354	184	170	0.309
	≤ 40	633	158	475		302	144	158	
Gamma-glutamyl transpeptidase (U/L)	> 50	557	18	539	< 0.001	221	18	203	< 0.001
	≤ 50	610	363	247		435	310	125	
Hepatitis B virus DNA (IU/mL)	> 1000	521	143	378	0.001	277	126	151	0.058
	≤ 1000	646	238	408		379	202	177	
HBeAg status	-	299	619	918	0.914	259	252	511	0.510
	+	82	167	249		69	76	145	
Antiviral therapy	No	265	521	786	0.264	233	221	454	0.310

	Yes	116	265	381		95	107	202	
Surgical margin (cm)	< 2	169	308	477	0.092	146	127	273	0.132
	≥ 2	212	478	690		182	201	383	
Tumor size (cm)	> 5	444	113	331	< 0.001	208	103	105	0.933
	≤ 5	723	268	455		448	225	223	
Microvascular invasion	Yes	301	86	215	0.093	152	79	73	0.644
	No	866	295	571		504	249	255	
Infiltrative growth	Yes	438	166	272	0.004	270	137	133	0.812
	No	729	215	514		386	191	195	

P value: Calculated by Pearson's χ^2 test. PSM: Propensity score matching; GPR: Gamma-glutamyl transpeptidase-to-platelet ratio.

Table 2 Univariate and multivariate Cox-regression analyses predicting overall survival before and after propensity score matching

Variables	Before propensity matching				After propensity matching			
	Uni-HR (95%CI)	*P* value	Multi-HR (95%CI)	*P* value	Uni-HR (95%CI)	*P* value	Multi-HR (95%CI)	*P* value
Sex (male/female)	1.44 (1.01-2.05)	0.043	1.3 (0.9-1.87)	0.159	1.22 (0.79-1.87)	0.364		
Age (years) (> 50/≤ 50)	1.02 (0.81-1.29)	0.85			0.86 (0.63-1.19)	0.362		
Body mass index (> 24/≤ 24)	1.16 (0.9-1.49)	0.255			1.25 (0.88-1.79)	0.218		
Smoking (yes/no)	1.05 (0.83-1.34)	0.672			1.04 (0.74-1.48)	0.81		
Drinking (yes/no)	0.9 (0.7-1.15)	0.412			0.85 (0.59-1.23)	0.388		
Diabetes mellitus (yes/no)	0.75 (0.4-1.41)	0.372			0.46 (0.15-1.45)	0.186		
Hypertension (yes/no)	0.82 (0.54-1.24)	0.345			0.66 (0.36-1.23)	0.192		
Family cases (yes/no)	0.79 (0.53-1.17)	0.234			0.61 (0.34-1.1)	0.098		
Liver flukes (yes/no)	0.88 (0.65-1.19)	0.392			0.75 (0.47-1.18)	0.214		
Cirrhosis (yes/no)	1.21 (0.96-1.53)	0.1			1.24 (0.9-1.71)	0.18		
Child-Pugh (B/A)	2.16 (1.07-4.36)	0.032	1.78 (0.87-3.63)	0.115	1.34 (0.33-5.42)	0.679		
Barcelona Clinic Liver Cancer stage (A/0)	1.93 (1.31-2.83)	< 0.001	1.51 (1-2.26)	0.048	2.03 (1.19-3.45)	0.009	1.64 (0.94-2.86)	0.082
Total bilirubin (μmol/L) (> 20.5/≤ 20.5)	0.85 (0.6-1.21)	0.37			0.9 (0.55-1.45)	0.651		
Albumin (g/L) (> 40/≤ 40)	1.35 (1.07-1.71)	0.012	1.16 (0.91-1.48)	0.229	1.2 (0.87-1.65)	0.26		
Alpha-fetoprotein (ng/mL) (≥ 200/< 200)	1.38 (1.09-1.74)	0.006	1.35 (1.06-1.72)	0.013	1.37 (0.99-1.89)	0.055		
Hepatitis B virus DNA (IU/mL) (> 1000/≤ 1000)	0.73 (0.58-0.92)	0.008	0.83 (0.66-1.05)	0.123	0.72 (0.52-0.99)	0.042	0.82 (0.59-1.12)	0.213
Tumor size (cm) (≤ 5/> 5)	0.57 (0.46-0.72)	< 0.001	0.74 (0.57-0.95)	0.019	0.6 (0.43-0.82)	0.002	0.66 (0.48-0.93)	0.017
Microvascular invasion (yes/no)	1.55 (1.21-1.99)	< 0.001	1.19 (0.92-1.55)	0.186	1.2 (0.83-1.74)	0.322		
Infiltrative growth (yes/no)	1.29 (1.02-1.63)	0.032	1.35 (1.06-1.7)	0.014	1.2 (0.87-1.65)	0.272		
Gamma-glutamyl transpeptidase-to-platelet ratio (≤ 0.2/> 0.2)	0.48 (0.36-0.64)	< 0.001	0.52 (0.39-0.69)	< 0.001	0.49 (0.35-0.69)	< 0.001	0.5 (0.36-0.7)	< 0.001

Uni-HR: Hazard ratio for univariable Cox-regression analyses; Multi-HR: Hazard ratio for multivariable Cox-regression analyses.

fragments derived from bone marrow megakaryocytes, serve as critical agents in hemostasis. Upon vascular injury, they swiftly accumulate at the site of damage and discharge granule contents, including platelet-activating factors, to facilitate thrombus formation[35]. Additionally, platelets are implicated in multiple stages of tumorigenesis, including the promotion of tumor growth, intravasation of tumor cells, and metastatic spread. Furthermore, their ability to secrete substantial amounts of microparticles and exosomes is crucial for orchestrating effective communication between the

Table 3 Univariate and multivariate Cox-regression analyses predicting recurrence-free survival before and after propensity score matching

Variables	Before propensity matching				After propensity matching			
	Uni-HR (95%CI)	*P* value	Multi-HR (95%CI)	*P* value	Uni-HR (95%CI)	*P* value	Multi-HR (95%CI)	*P* value
Sex (male/female)	1.32 (1.03-1.69)	0.028	1.19 (0.92-1.54)	0.176	1.09 (0.8-1.49)	0.574		
Age (years) (> 50/≤ 50)	1.03 (0.87-1.22)	0.756			0.93 (0.73-1.19)	0.575		
Body mass index (> 24/≤ 24)	1.13 (0.94-1.36)	0.185			1 (0.77-1.29)	0.989		
Smoking (yes/no)	1.11 (0.93-1.32)	0.244			1.01 (0.78-1.31)	0.93		
Drinking (yes/no)	1 (0.84-1.2)	0.972			0.85 (0.64-1.11)	0.23		
Diabetes mellitus (yes/no)	1.4 (0.98-2)	0.067			1.22 (0.71-2.1)	0.461		
Hypertension (yes/no)	0.81 (0.6-1.09)	0.165			0.83 (0.54-1.26)	0.38		
Family cases (yes/no)	0.89 (0.68-1.16)	0.384			0.76 (0.51-1.14)	0.192		
Liver flukes (yes/no)	1.14 (0.93-1.4)	0.204			1.01 (0.74-1.38)	0.945		
Cirrhosis (yes/no)	1.27 (1.08-1.5)	0.005	1.25 (1.05-1.49)	0.012	1.3 (1.03-1.65)	0.03	1.33 (1.04-1.68)	0.021
Child-Pugh (B/A)	1.08 (0.54-2.18)	0.823			1.01 (0.32-3.14)	0.99		
Barcelona Clinic Liver Cancer stage (A/0)	1.4 (1.09-1.8)	0.008	1.14 (0.87-1.49)	0.348	1.39 (0.98-1.97)	0.061		
Total bilirubin (μmol/L) (> 20.5/≤ 20.5)	0.87 (0.67-1.13)	0.292			0.85 (0.6-1.22)	0.386		
Albumin (g/L) (> 40/≤ 40)	1.36 (1.15-1.61)	< 0.001	1.17 (0.98-1.4)	0.084	1.21 (0.96-1.54)	0.112		
Alpha-fetoprotein (ng/mL) (≥ 200/< 200)	1.31 (1.1-1.55)	0.002	1.29 (1.08-1.54)	0.005	1.22 (0.96-1.55)	0.111		
Hepatitis B virus DNA (IU/mL) (> 1000/≤ 1000)	0.8 (0.68-0.95)	0.009	0.9 (0.76-1.06)	0.214	0.76 (0.6-0.96)	0.023	0.8 (0.63-1.02)	0.067
Tumor size (cm) (≤ 5/> 5)	0.6 (0.51-0.71)	< 0.001	0.67 (0.55-0.81)	< 0.001	0.79 (0.62-1.02)	0.07		
Microvascular invasion (yes/no)	1.4 (1.16-1.68)	< 0.001	1.1 (0.9-1.33)	0.359	1.18 (0.9-1.56)	0.233		
Infiltrative growth (yes/no)	1.24 (1.05-1.47)	0.013	1.28 (1.08-1.53)	0.005	1.24 (0.97-1.57)	0.082		
Gamma-glutamyl transpeptidase-to-platelet ratio (≤ 0.2/> 0.2)	0.49 (0.4-0.6)	< 0.001	0.53 (0.43-0.65)	< 0.001	0.56 (0.44-0.71)	< 0.001	0.57 (0.44-0.73)	< 0.001

Uni-HR: Hazard ratio for univariable Cox-regression analyses; Multi-HR: Hazard ratio for multivariable Cox-regression analyses.

Table 4 Stratified analysis between gamma-glutamyl transpeptidase-to-platelet ratio levels and prognosis in the solitary hepatitis B virus-related hepatocellular carcinoma

Variables	Before propensity matching				After propensity matching			
	OS-HR (95%CI)	*P* value	RFS-HR (95%CI)	*P* value	OS-HR (95%CI)	*P* value	RFS-HR (95%CI)	*P* value
As continuous	1.12 (1.04-1.20)	0.002	1.11 (1.06-1.17)	< 0.001	1.29 (1.18-1.42)	< 0.001	1.20 (1.11-1.31)	< 0.001
By GPR cut-off								
GPR ≤ 0.2								
GPR > 0.2	2.07 (1.56-2.74)	< 0.001	2.05 (1.68-2.51)	< 0.001	2.04 (1.46-2.84)	< 0.001	1.79 (1.40-2.28)	< 0.001
By GPR tercile								
Bottom (≤ 0.2)								
Middle (> 0.2, ≤ 0.6)	1.81 (1.35-2.44)	< 0.001	1.85 (1.50-2.29)	< 0.001	1.52 (1.08-2.14)	0.017	1.69 (1.25-2.17)	< 0.001
Top (> 0.6)	2.74 (1.98-3.81)	< 0.001	2.60 (2.04-3.31)	< 0.001	2.33 (1.60-3.39)	< 0.001	2.35 (1.77-3.13)	< 0.001
P for trend[1]	< 0.001		< 0.001		< 0.001		< 0.001	
By interquartile								

Q1								
Q2	1.42 (0.98-2.06)	0.061	1.43 (1.10-1.86)	< 0.001	0.75 (0.43-1.28)	0.288	0.88 (0.60-1.29)	0.514
Q3	1.72 (1.20-2.46)	0.003	1.74 (1.35-2.24)	< 0.001	1.45 (0.90-2.34)	0.125	1.58 (1.12-2.23)	0.009
Q4	2.34 (1.66-3.29)	< 0.001	2.29 (1.79-2.93)	< 0.001	2.08 (1.33-3.24)	0.001	1.79 (1.27-2.51)	0.001
P for trend[1]	< 0.001		< 0.001		< 0.001		< 0.001	

[1]Test for trend based on variable containing median value for each classification.
HR: Hazard ratio; OS: Overall survival; RFS: Recurrence-free survival; GPR: Gamma-glutamyl transpeptidase-to-platelet ratio.

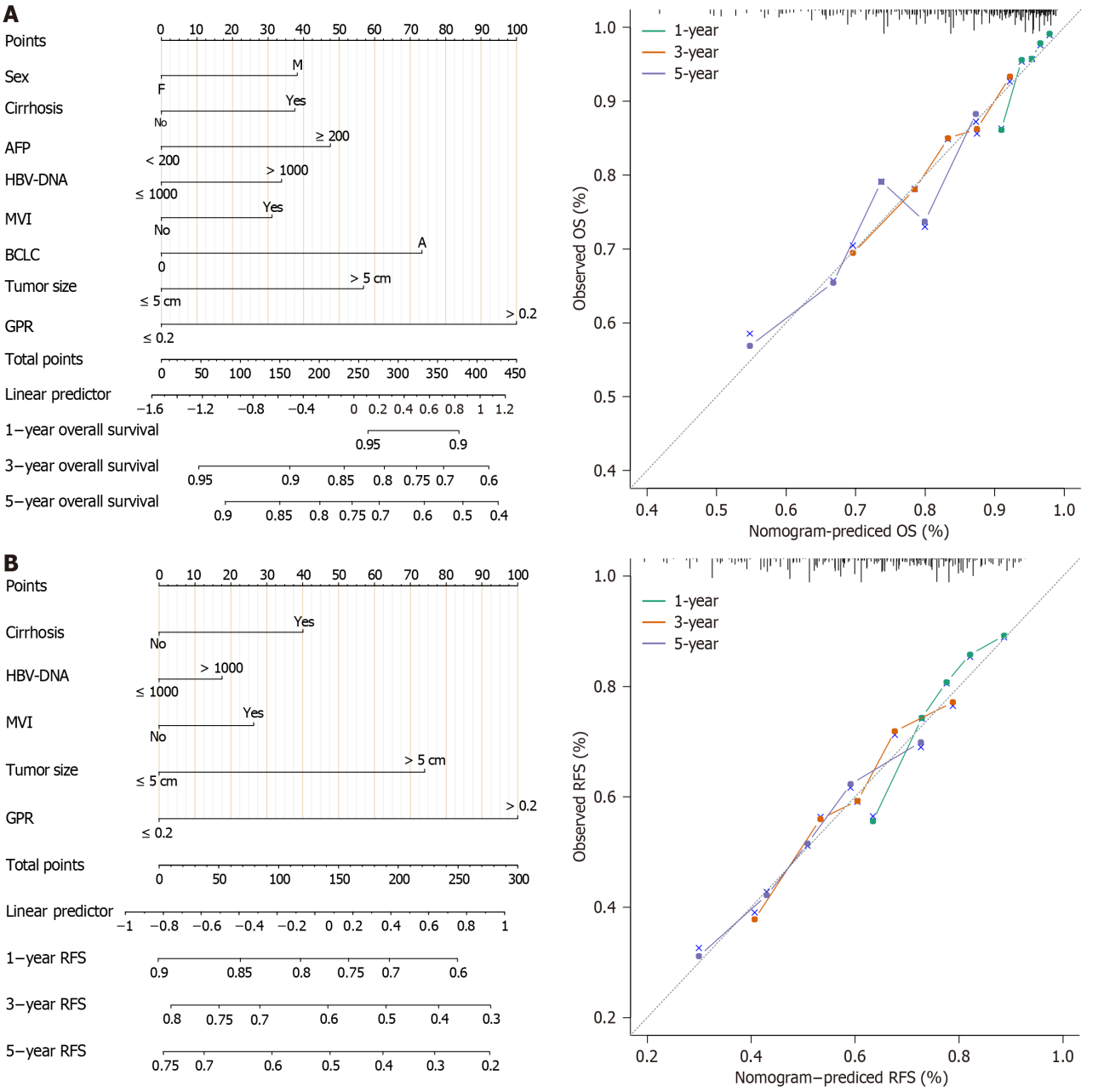

Figure 6 Prognostic nomograms for solitary hepatitis B virus-related hepatocellular carcinoma. A: Nomogram plot and calibration curves for overall survival; B: Nomogram plot and calibration curves for recurrence-free survival. AFP: Alpha-fetoprotein; HBV: Hepatitis B virus; MVI: Microvascular imaging; BCLC: Barcelona Clinic Liver Cancer; GPR: Gamma-glutamyl transpeptidase-to-platelet ratio; RFS: Recurrence-free survival; OS: Overall survival; F: Female; M: Male.

tumor and its host environment[36,37]. A study has explored the correlation between the GPR and inflammation-related signaling pathways, revealing that the expression of p38 mitogen-activated protein kinase exhibited a significant negative correlation with both the GPR and GGT[38]. In the present study, we explored the association of preoperative GPR and the prognosis of patients with single-lesion HBV-related HCC. First, we compared the enrolled subjects with the control group in different physiological states. The results showed that the GPR level of HCC patients was at the same level as that of post-hepatitis cirrhosis patients, and was at a high level compared with healthy subjects and patients with benign liver diseases. The above findings can more intuitively show the evaluation of the prognostic value of GPR level. We set a GPR cutoff value of 0.2 to distinguish the above-mentioned patients into high-risk and low-risk groups. After adjusting for baseline characteristics by PSM, HCC patients who underwent hepatectomy had a poor OS and elevated RFS rate when their preoperative GPR was > 0.2. Previously published studies[15,25,39,40] found that an increased GPR was associated with the prognosis of HCC patients, but the cutoff values varied widely, ranging from 0.3 to 0.84. These differences could be explained by different inclusion and exclusion criteria, differences in tumor staging, and background of liver cirrhosis and hepatitis. Indeed, some researchers have shown that GPR levels have a good prognostic value in HCC patients[41-43], even in AFP-negative HCC[44]. In this study, through subgroup and stratification analyses, we confirmed that a low preoperative GPR level predicts a good prognosis for HCC patients. Therefore, GPR may be a good noninvasive index to guide clinician decision-making.

Although preoperative GPR levels were shown to accurately predict surgical outcomes in patients with HBV-related HCC, the present study has several limitations. First, data were collected from one center in a confined area where HBV is prevalent, and only patients with solitary HCC who received curative resection were included. Although the sample size was modest and potential selection bias should be considered in subsequent analyses, further external validation by multicenter, large-sample, prospective studies is essential to determine the robustness of our findings in different patient populations. Our study is still unclear about the mechanisms linking GPR levels to tumor progression. Further research could provide additional insights to better understand the role of GPR in HCC progression. This study has preliminarily illuminated the role of GPR in predicting outcomes for HCC patients undergoing liver resection; the relationship between various noninvasive blood fibrosis indices and postoperative outcomes warrants further investigation. Moreover, it is unclear if preoperative GPR is useful for HCV-related HCC or nonalcoholic fatty liver disease-related HCC patients receiving radical resection.

CONCLUSION

GPR levels before surgery can be used as a new indicator to predict surgical outcomes in patients with solitary HBV-related HCC. This is a potentially helpful tool to monitor the recurrence and OS in clinical practice. A prognostic risk stratification based on GPR can objectively and accurately predict the postoperative prognosis of HCC patients. Therefore, preoperative GPR levels can be used for recurrence monitoring and treatment strategy based on risk stratification, and may contribute to improve the quality of life of solitary nodule HCC patients.

FOOTNOTES

Author contributions: Yang CK and Peng T designed the study; Yang CK, Wei ZL, Shen XQ, Jia YX, and Wu QY performed research; Yang CK, Wei ZL, Shen XQ, Jia YX, Wu QY and Wei XL provided sample collection and clinical support; Yang CK, Wei YG, Su H, Liao XW, Zhu GZ and Qin W contributed to data interpretation; Yang CK and Wei ZL wrote the manuscript; Peng T critically revised the manuscript and participated in the analysis and interpretation of the data; all of the authors read and approved the final version of the manuscript to be published.

Supported by The National Natural Science Foundation of China, No. 81560535, No. 81802874 and No. 81072321; and The Self-funded Scientific Research Project of Health Commission in Guangxi Zhuang Autonomous Region, China, No. Z20210977.

Institutional review board statement: This study was approved by The Ethics Committee of The First Affiliated Hospital of Guangxi Medical University, China.

Informed consent statement: All participants signed written informed consent before study commencement.

Conflict-of-interest statement: The authors declare that the research was conducted in the absence of any commercial or financial relationships that could be construed as a potential conflict of interest.

Data sharing statement: The datasets generated during and/or analyzed during the current study are available from the corresponding author on reasonable request.

STROBE statement: The authors have read the STROBE Statement-checklist of items, and the manuscript was prepared and revised according to the STROBE Statement-checklist of items.

Country of origin: China

ORCID number: Cheng-Kun Yang 0000-0001-6109-7334; Hao Su 0000-0003-2291-6071; Wei Qin 0000-0002-0512-6361; Xi-Wen Liao 0000-0002-1724-1463; Guang-Zhi Zhu 0000-0001-5958-7289; Tao Peng 0000-0001-6133-7078.

S-Editor: Luo ML
L-Editor: A
P-Editor: Zhang L

REFERENCES

1 **Bray F**, Ferlay J, Soerjomataram I, Siegel RL, Torre LA, Jemal A. Global cancer statistics 2018: GLOBOCAN estimates of incidence and mortality worldwide for 36 cancers in 185 countries. *CA Cancer J Clin* 2018; **68**: 394-424 [PMID: 30207593 DOI: 10.3322/caac.21492]
2 **El-Serag HB**, Rudolph KL. Hepatocellular carcinoma: epidemiology and molecular carcinogenesis. *Gastroenterology* 2007; **132**: 2557-2576 [PMID: 17570226 DOI: 10.1053/j.gastro.2007.04.061]
3 **Bruix J**, Reig M, Sherman M. Evidence-Based Diagnosis, Staging, and Treatment of Patients With Hepatocellular Carcinoma. *Gastroenterology* 2016; **150**: 835-853 [PMID: 26795574 DOI: 10.1053/j.gastro.2015.12.041]
4 **El-Serag HB**. Hepatocellular carcinoma. *N Engl J Med* 2011; **365**: 1118-1127 [PMID: 21992124 DOI: 10.1056/NEJMra1001683]
5 **European Association for the Study of the Liver**. EASL clinical practice guidelines: Management of chronic hepatitis B virus infection. *J Hepatol* 2012; **57**: 167-185 [PMID: 22436845 DOI: 10.1016/j.jhep.2012.02.010]
6 **Fattovich G**, Stroffolini T, Zagni I, Donato F. Hepatocellular carcinoma in cirrhosis: incidence and risk factors. *Gastroenterology* 2004; **127**: S35-S50 [PMID: 15508101 DOI: 10.1053/j.gastro.2004.09.014]
7 **Raza A**, Sood GK. Hepatocellular carcinoma review: current treatment, and evidence-based medicine. *World J Gastroenterol* 2014; **20**: 4115-4127 [PMID: 24764650 DOI: 10.3748/wjg.v20.i15.4115]
8 **Grazi GL**, Ercolani G, Pierangeli F, Del Gaudio M, Cescon M, Cavallari A, Mazziotti A. Improved results of liver resection for hepatocellular carcinoma on cirrhosis give the procedure added value. *Ann Surg* 2001; **234**: 71-78 [PMID: 11420485 DOI: 10.1097/00000658-200107000-00011]
9 **Lim KC**, Chow PK, Allen JC, Siddiqui FJ, Chan ES, Tan SB. Systematic review of outcomes of liver resection for early hepatocellular carcinoma within the Milan criteria. *Br J Surg* 2012; **99**: 1622-1629 [PMID: 23023956 DOI: 10.1002/bjs.8915]
10 **Kim M**, Lee Y, Yoon JS, Lee M, Kye SS, Kim SW, Cho Y. The FIB-4 Index Is a Useful Predictor for the Development of Hepatocellular Carcinoma in Patients with Coexisting Nonalcoholic Fatty Liver Disease and Chronic Hepatitis B. *Cancers (Basel)* 2021; **13**: 2301 [PMID: 34064988 DOI: 10.3390/cancers13102301]
11 **Maegawa FB**, Shehorn L, Aziz H, Kettelle J, Jie T, Riall TS. Association Between Noninvasive Fibrosis Markers and Postoperative Mortality After Hepatectomy for Hepatocellular Carcinoma. *JAMA Netw Open* 2019; **2**: e187142 [PMID: 30657533 DOI: 10.1001/jamanetworkopen.2018.7142]
12 **Johnson PJ**, Berhane S, Kagebayashi C, Satomura S, Teng M, Reeves HL, O'Beirne J, Fox R, Skowronska A, Palmer D, Yeo W, Mo F, Lai P, Iñarrairaegui M, Chan SL, Sangro B, Miksad R, Tada T, Kumada T, Toyoda H. Assessment of liver function in patients with hepatocellular carcinoma: a new evidence-based approach-the ALBI grade. *J Clin Oncol* 2015; **33**: 550-558 [PMID: 25512453 DOI: 10.1200/JCO.2014.57.9151]
13 **Lemoine M**, Shimakawa Y, Nayagam S, Khalil M, Suso P, Lloyd J, Goldin R, Njai HF, Ndow G, Taal M, Cooke G, D'Alessandro U, Vray M, Mbaye PS, Njie R, Mallet V, Thursz M. The gamma-glutamyl transpeptidase to platelet ratio (GPR) predicts significant liver fibrosis and cirrhosis in patients with chronic HBV infection in West Africa. *Gut* 2016; **65**: 1369-1376 [PMID: 26109530 DOI: 10.1136/gutjnl-2015-309260]
14 **Park YE**, Kim BK, Park JY, Kim DY, Ahn SH, Han KH, Han S, Jeon MY, Heo JY, Song K, Kim SU. Gamma-glutamyl transpeptidase-to-platelet ratio is an independent predictor of hepatitis B virus-related liver cancer. *J Gastroenterol Hepatol* 2017; **32**: 1221-1229 [PMID: 27859587 DOI: 10.1111/jgh.13653]
15 **Dai T**, Deng M, Ye L, Liu R, Lin G, Chen X, Li H, Liu W, Yang Y, Chen G, Wang G. Prognostic value of combined preoperative gamma-glutamyl transpeptidase to platelet ratio and fibrinogen in patients with HBV-related hepatocellular carcinoma after hepatectomy. *Am J Transl Res* 2020; **12**: 2984-2997 [PMID: 32655824]
16 **Zhang Y**, Jin F, Wu Y, Wang B, Xie J, Li Y, Pan Y, Liu Z, Shen W. Prognostic impact of gamma-glutamyl transpeptidase to platelets ratio on hepatocellular carcinoma patients who have undergone surgery: a meta-analysis and systematic review. *Eur J Gastroenterol Hepatol* 2023; **35**: 803-811 [PMID: 37395231 DOI: 10.1097/MEG.0000000000002572]
17 **Zhou J**, Sun H, Wang Z, Cong W, Zeng M, Zhou W, Bie P, Liu L, Wen T, Kuang M, Han G, Yan Z, Wang M, Liu R, Lu L, Ren Z, Zeng Z, Liang P, Liang C, Chen M, Yan F, Wang W, Hou J, Ji Y, Yun J, Bai X, Cai D, Chen W, Chen Y, Cheng W, Cheng S, Dai C, Guo W, Guo Y, Hua B, Huang X, Jia W, Li Q, Li T, Li X, Li Y, Li Y, Liang J, Ling C, Liu T, Liu X, Lu S, Lv G, Mao Y, Meng Z, Peng T, Ren W, Shi H, Shi G, Shi M, Song T, Tao K, Wang J, Wang K, Wang L, Wang W, Wang X, Wang Z, Xiang B, Xing B, Xu J, Yang J, Yang J, Yang Y, Yang Y, Ye S, Yin Z, Zeng Y, Zhang B, Zhang B, Zhang L, Zhang S, Zhang T, Zhang Y, Zhao M, Zhao Y, Zheng H, Zhou L, Zhu J, Zhu K, Liu R, Shi Y, Xiao Y, Zhang L, Yang C, Wu Z, Dai Z, Chen M, Cai J, Wang W, Cai X, Li Q, Shen F, Qin S, Teng G, Dong J, Fan J. Guidelines for the Diagnosis and Treatment of Primary Liver Cancer (2022 Edition). *Liver Cancer* 2023; **12**: 405-444 [PMID: 37901768 DOI: 10.1159/000530495]
18 **Ke MY**, Zhang M, Su Q, Wei S, Zhang J, Wang Y, Wu R, Lv Y. Gamma-glutamyl transpeptidase to platelet ratio predicts short-term outcomes in hepatocellular carcinoma patients undergoing minor liver resection. *J Surg Res* 2018; **231**: 403-410 [PMID: 30278960 DOI: 10.1016/j.jss.2018.05.049]
19 **Camp RL**, Dolled-Filhart M, Rimm DL. X-tile: a new bio-informatics tool for biomarker assessment and outcome-based cut-point

optimization. *Clin Cancer Res* 2004; **10**: 7252-7259 [PMID: 15534099 DOI: 10.1158/1078-0432.CCR-04-0713]

20 **Lee J**, Little TD. A practical guide to propensity score analysis for applied clinical research. *Behav Res Ther* 2017; **98**: 76-90 [PMID: 28153337 DOI: 10.1016/j.brat.2017.01.005]

21 **Jung SM**, Kim JM, Choi GS, Kwon CHD, Yi NJ, Lee KW, Suh KS, Joh JW. Characteristics of Early Recurrence After Curative Liver Resection for Solitary Hepatocellular Carcinoma. *J Gastrointest Surg* 2019; **23**: 304-311 [PMID: 30215196 DOI: 10.1007/s11605-018-3927-2]

22 **Liang BY**, Gu J, Xiong M, Zhang EL, Zhang ZY, Chen XP, Huang ZY. Tumor size may influence the prognosis of solitary hepatocellular carcinoma patients with cirrhosis and without macrovascular invasion after hepatectomy. *Sci Rep* 2021; **11**: 16343 [PMID: 34381132 DOI: 10.1038/s41598-021-95835-5]

23 **Sasaki K**, Shindoh J, Margonis GA, Nishioka Y, Andreatos N, Sekine A, Hashimoto M, Pawlik TM. Effect of Background Liver Cirrhosis on Outcomes of Hepatectomy for Hepatocellular Carcinoma. *JAMA Surg* 2017; **152**: e165059 [PMID: 28052155 DOI: 10.1001/jamasurg.2016.5059]

24 **Zhu YF**, Tan YF, Xu X, Zheng JL, Zhang BH, Tang HR, Yang JY. Gamma-glutamyl transpeptidase-to-platelet ratio and the fibrosis-4 index in predicting hepatitis B virus-related hepatocellular carcinoma development in elderly chronic hepatitis B patients in China: A single-center retrospective study. *Medicine (Baltimore)* 2019; **98**: e18319 [PMID: 31852119 DOI: 10.1097/MD.0000000000018319]

25 **Pang Q**, Bi JB, Wang ZX, Xu XS, Qu K, Miao RC, Chen W, Zhou YY, Liu C. Simple models based on gamma-glutamyl transpeptidase and platelets for predicting survival in hepatitis B-associated hepatocellular carcinoma. *Onco Targets Ther* 2016; **9**: 2099-2109 [PMID: 27110127 DOI: 10.2147/OTT.S101465]

26 **Huang CF**, Jang TY, Jun DW, Ahn SB, An J, Enomoto M, Takahashi H, Ogawa E, Yoon E, Jeong SW, Shim JJ, Jeong JY, Kim SE, Oh H, Kim HS, Cho YK, Kozuka R, Inoue K, Cheung KS, Mak LY, Huang JF, Dai CY, Yuen MF, Nguyen MH, Yu ML. On-treatment gamma-glutamyl transferase predicts the development of hepatocellular carcinoma in chronic hepatitis B patients. *Liver Int* 2022; **42**: 59-68 [PMID: 34687130 DOI: 10.1111/liv.15085]

27 **Long G**, Shen J, Zhou L. A-G Score Associated With Outcomes in Solitary Hepatocellular Carcinoma Patients After Hepatectomy. *Front Oncol* 2020; **10**: 1286 [PMID: 32850396 DOI: 10.3389/fonc.2020.01286]

28 **Ma H**, Zhang L, Tang B, Wang Y, Chen R, Zhang B, Chen Y, Ge N, Wang Y, Gan Y, Ye S, Ren Z. γ-Glutamyltranspeptidase is a prognostic marker of survival and recurrence in radiofrequency-ablation treatment of hepatocellular carcinoma. *Ann Surg Oncol* 2014; **21**: 3084-3089 [PMID: 24748164 DOI: 10.1245/s10434-014-3724-4]

29 **Guo J**, Liu S, Gao S, Kou F, Zhang X, Liu P, Yang R, Zhu X. γ-Glutamyltranspeptidase as a Prognostic Biomarker in Advanced Hepatocellular Carcinoma Treated with Transarterial Chemoembolization. *J Vasc Interv Radiol* 2021; **32**: 419-428 [PMID: 33067120 DOI: 10.1016/j.jvir.2020.07.020]

30 **Fu SJ**, Zhao Q, Ji F, Chen MG, Wu LW, Ren QQ, Guo ZY, He XS. Elevated Preoperative Serum Gamma-glutamyltranspeptidase Predicts Poor Prognosis for Hepatocellular Carcinoma after Liver Transplantation. *Sci Rep* 2016; **6**: 28835 [PMID: 27381639 DOI: 10.1038/srep28835]

31 **Carr BI**, Akkiz H, Bag HG, Karaoğullarından U, Yalçın K, Ekin N, Özakyol A, Altıntaş E, Balaban HY, Şimşek H, Uyanıkoğlu A, Balkan A, Kuran S, Üsküdar O, Ülger Y, Güney B, Delik A. Serum levels of gamma-glutamyl transpeptidase in relation to HCC human biology and prognosis. *J Transl Sci* 2021; **7**: 10.15761/jts.1000446 [PMID: 34540270 DOI: 10.15761/jts.1000446]

32 **Lee DS**, Evans JC, Robins SJ, Wilson PW, Albano I, Fox CS, Wang TJ, Benjamin EJ, D'Agostino RB, Vasan RS. Gamma glutamyl transferase and metabolic syndrome, cardiovascular disease, and mortality risk: the Framingham Heart Study. *Arterioscler Thromb Vasc Biol* 2007; **27**: 127-133 [PMID: 17095717 DOI: 10.1161/01.ATV.0000251993.20372.40]

33 **Lee DH**, Jacobs DR Jr. Association between serum gamma-glutamyltransferase and C-reactive protein. *Atherosclerosis* 2005; **178**: 327-330 [PMID: 15694941 DOI: 10.1016/j.atherosclerosis.2004.08.027]

34 **Pleiner J**, Mittermayer F, Schaller G, Marsik C, MacAllister RJ, Wolzt M. Inflammation-induced vasoconstrictor hyporeactivity is caused by oxidative stress. *J Am Coll Cardiol* 2003; **42**: 1656-1662 [PMID: 14607455 DOI: 10.1016/j.jacc.2003.06.002]

35 **Smyth SS**, McEver RP, Weyrich AS, Morrell CN, Hoffman MR, Arepally GM, French PA, Dauerman HL, Becker RC; 2009 Platelet Colloquium Participants. Platelet functions beyond hemostasis. *J Thromb Haemost* 2009; **7**: 1759-1766 [PMID: 19691483 DOI: 10.1111/j.1538-7836.2009.03586.x]

36 **Schlesinger M**. Role of platelets and platelet receptors in cancer metastasis. *J Hematol Oncol* 2018; **11**: 125 [PMID: 30305116 DOI: 10.1186/s13045-018-0669-2]

37 **Haemmerle M**, Stone RL, Menter DG, Afshar-Kharghan V, Sood AK. The Platelet Lifeline to Cancer: Challenges and Opportunities. *Cancer Cell* 2018; **33**: 965-983 [PMID: 29657130 DOI: 10.1016/j.ccell.2018.03.002]

38 **Luo D**, Li H, Hu J, Zhang M, Zhang S, Wu L, Han B. Development and Validation of Nomograms Based on Gamma-Glutamyl Transpeptidase to Platelet Ratio for Hepatocellular Carcinoma Patients Reveal Novel Prognostic Value and the Ratio Is Negatively Correlated With P38MAPK Expression. *Front Oncol* 2020; **10**: 548744 [PMID: 33344225 DOI: 10.3389/fonc.2020.548744]

39 **Wang WL**, Zheng XL, Zhang ZY, Zhou Y, Hao J, Tang G, Li O, Xiang JX, Wu Z, Wang B. Preoperative γ-glutamyl transpeptidase to platelet ratio (GPR) is an independent prognostic factor for HBV-related hepatocellular carcinoma after curative hepatic resection. *Medicine (Baltimore)* 2016; **95**: e4087 [PMID: 27399101 DOI: 10.1097/MD.0000000000004087]

40 **Yang D**, Wu H, Nong W, Zheng M, Li A, Wang Y, Li M, Chen Q, Yuan S, Yu J, Liao W. A new model based on gamma-glutamyl transpeptidase to platelet ratio (GPR) predicts prognostic outcome after curative resection of solitary hepatocellular carcinoma. *Clin Res Hepatol Gastroenterol* 2021; **45**: 101509 [PMID: 33744828 DOI: 10.1016/j.clinre.2020.07.014]

41 **Zhang J**, Wang T, Xu L, Wang P, Zhang M, Xu M. Development and validation of a prognostic model based on the albumin-to-fibrinogen ratio (AFR) and gamma-glutamyl transpeptidase-to-platelet ratio (GPR) in hepatocellular carcinoma patients. *Clin Chim Acta* 2020; **511**: 107-116 [PMID: 33035501 DOI: 10.1016/j.cca.2020.09.038]

42 **Gu Y**, Zheng F, Zhang Y, Qiao S. Novel Nomogram Based on Inflammatory Markers for the Preoperative Prediction of Microvascular Invasion in Solitary Primary Hepatocellular Carcinoma. *Cancer Manag Res* 2022; **14**: 895-907 [PMID: 35256861 DOI: 10.2147/CMAR.S346976]

43 **Wu W**, Wang Q, Han D, Li J, Nie Y, Guo D, Yang L, Tao K, Zhang X, Dou K. Prognostic value of preoperative inflammatory markers in patients with hepatocellular carcinoma who underwent curative resection. *Cancer Cell Int* 2021; **21**: 500 [PMID: 34535132 DOI: 10.1186/s12935-021-02204-3]

44 **Huang L**, Mo Z, Hu Z, Zhang L, Qin S, Qin X, Li S. Diagnostic value of fibrinogen to prealbumin ratio and gamma-glutamyl transpeptidase to platelet ratio in the progression of AFP-negative hepatocellular carcinoma. *Cancer Cell Int* 2020; **20**: 77 [PMID: 32190001 DOI: 10.1186/s12935-020-1161-y]

World Journal of Gastrointestinal Oncology

Submit a Manuscript: https://www.f6publishing.com

World J Gastrointest Oncol 2024 December 15; 16(12): 4597-4613

DOI: 10.4251/wjgo.v16.i12.4597

ISSN 1948-5204 (online)

ORIGINAL ARTICLE

Retrospective Cohort Study

Prognostic prediction models for postoperative patients with stage I to III colorectal cancer based on machine learning

Xiao-Lin Ji, Shuo Xu, Xiao-Yu Li, Jin-Huan Xu, Rong-Shuang Han, Ying-Jie Guo, Li-Ping Duan, Zi-Bin Tian

Specialty type: Oncology

Provenance and peer review: Unsolicited article; Externally peer reviewed.

Peer-review model: Single blind

Peer-review report's classification

Scientific Quality: Grade B, Grade C, Grade E

Novelty: Grade B, Grade B, Grade D

Creativity or Innovation: Grade B, Grade B, Grade D

Scientific Significance: Grade B, Grade B, Grade D

P-Reviewer: Cengiz F; Stabellini N; Wang Z

Received: March 19, 2024

Revised: September 7, 2024

Accepted: September 14, 2024

Published online: December 15, 2024

Processing time: 237 Days and 23.6 Hours

Xiao-Lin Ji, Li-Ping Duan, Department of Gastroenterology, Beijing Key Laboratory for Helicobacter Pylori Infection and Upper Gastrointestinal Diseases, Peking University Third Hospital, Beijing 100191, China

Shuo Xu, Beijing Aerospace Wanyuan Science Technology Co., Ltd., China Academy of Launch Vehicle Technology, Beijing 100176, China

Xiao-Yu Li, Rong-Shuang Han, Ying-Jie Guo, Zi-Bin Tian, Department of Gastroenterology, The Affiliated Hospital of Qingdao University, Qingdao 266003, Shandong Province, China

Jin-Huan Xu, Institute of Automation, Qilu University of Technology (Shandong Academy of Sciences), Jinan 250014, Shandong Province, China

Co-first authors: Xiao-Lin Ji and Shuo Xu.

Co-corresponding authors: Zi-Bin Tian and Li-Ping Duan.

Corresponding author: Li-Ping Duan, MD, PhD, Chief Physician, Professor, Department of Gastroenterology, Beijing Key Laboratory for Helicobacter Pylori Infection and Upper Gastrointestinal Diseases, Peking University Third Hospital, No. 49 Garden Road, Haidian District, Beijing 100191, China. duanlp@bjmu.edu.cn

Abstract

BACKGROUND

Colorectal cancer (CRC) is characterized by high heterogeneity, aggressiveness, and high morbidity and mortality rates. With machine learning (ML) algorithms, patient, tumor, and treatment features can be used to develop and validate models for predicting survival. In addition, important variables can be screened and different applications can be provided that could serve as vital references when making clinical decisions and potentially improving patient outcomes in clinical settings.

AIM

To construct prognostic prediction models and screen important variables for patients with stage I to III CRC.

METHODS

More than 1000 postoperative CRC patients were grouped according to survival time (with cutoff values of 3 years and 5 years) and assigned to training and

testing cohorts (7:3). For each 3-category survival time, predictions were made by 4 ML algorithms (all-variable and important variable-only datasets), each of which was validated *via* 5-fold cross-validation and bootstrap validation. Important variables were screened with multivariable regression methods. Model performance was evaluated and compared before and after variable screening with the area under the curve (AUC). SHapley Additive exPlanations (SHAP) further demonstrated the impact of important variables on model decision-making. Nomograms were constructed for practical model application.

RESULTS

Our ML models performed well; the model performance before and after important parameter identification was consistent, and variable screening was effective. The highest pre- and postscreening model AUCs 95% confidence intervals in the testing set were 0.87 (0.81-0.92) and 0.89 (0.84-0.93) for overall survival, 0.75 (0.69-0.82) and 0.73 (0.64-0.81) for disease-free survival, 0.95 (0.88-1.00) and 0.88 (0.75-0.97) for recurrence-free survival, and 0.76 (0.47-0.95) and 0.80 (0.53-0.94) for distant metastasis-free survival. Repeated cross-validation and bootstrap validation were performed in both the training and testing datasets. The SHAP values of the important variables were consistent with the clinicopathological characteristics of patients with tumors. The nomograms were created.

CONCLUSION

We constructed a comprehensive, high-accuracy, important variable-based ML architecture for predicting the 3-category survival times. This architecture could serve as a vital reference for managing CRC patients.

Key Words: Colorectal cancer; Machine learning; Prognostic prediction model; Survival times; Important variables

Core Tip: We developed and validated a promising machine learning architecture for predicting the 3-category survival times (cutoff values of 3 years and 5 years) for four survival times (overall, disease-free, recurrence-free, and distant metastasis-free survival) and screened corresponding important variables. Fivefold cross validation and bootstrap validation were conducted. The models were evaluated with the area under the curve (AUC); moreover, the effectiveness of our variable screening methods was evaluated by comparing the models' pre- and post-screening AUCs. SHapley Additive exPlanations were used to explain the decision-making process. Nomograms were drawn for various applications.

Citation: Ji XL, Xu S, Li XY, Xu JH, Han RS, Guo YJ, Duan LP, Tian ZB. Prognostic prediction models for postoperative patients with stage I to III colorectal cancer based on machine learning. *World J Gastrointest Oncol* 2024; 16(12): 4597-4613
URL: https://www.wjgnet.com/1948-5204/full/v16/i12/4597.htm
DOI: https://dx.doi.org/10.4251/wjgo.v16.i12.4597

INTRODUCTION

Colorectal cancer (CRC) is characterized by high heterogeneity and aggressiveness and high morbidity and mortality rates[1] due to disease progression and inadequate treatment strategies[2]. Furthermore, overdiagnosis, overtreatment, false positives, false reassurance, uncertain findings, and complications are common and can lead to unnecessary psychological burdens on the patients[3-6]. Accurate prediction of the outcomes of CRC patients could be a vital reference when making clinical decisions. The American Joint Committee on Cancer (AJCC) classification system for CRC remains the primary tool for predicting these outcomes, especially for making adjuvant chemoradiotherapy decisions[7,8]. However, the survival observations associated with the AJCC classifications for CRC patients have been reported to exhibit certain inconsistencies[9-11]. Researchers have investigated and built prognostic models for CRC patients with traditional statistical methods; some of these models include the tumor node metastasis (TNM) stage, whereas others do not[12-15]. However, the performance of these models is not very satisfactory, likely due to methodological limitations. Therefore, it seems possible that the power of machine learning (ML) could be leveraged for improvements.

ML is a branch of artificial intelligence in which a computer generates rules underlying or based on raw data[16]; it has gradually been found to be useful in various applications in the field of medicine[17-20]. ML can be used to directly compare the accuracy of two or more quantitative tests for the same disease/condition[21], playing a role in formulating diagnosis and treatment rules[22-24]. ML algorithms have also been used to construct risk forecast models that predict the hazard ratio of adverse events[25,26] or predict the classification of double-class/multiclass endpoints at a specific time[27]. Nevertheless, the time interval of occurrence of specific oncological outcomes for CRC patients cannot be vertically predicted in these models, and some of the models' important variables are unknown, casting doubt on their clinical credibility.

In our work, we developed a new ML architecture to predict 3-category occurrence times (cutoff values of 3 years and 5 years) of four oncological outcomes (death, tumor recurrence/distant metastasis, tumor recurrence, and tumor distant metastasis) in patients with stage I, II, and III CRC who underwent curative resection. The longitudinal predictive

mentality is different from that in previous studies. Moreover, the models' important variables and their order of importance were determined. These important parameters were used as clinical references, allowing the identification of hotspot indicators such as the lymph node ratio (LNR) and improving the clinical credibility of our models. The performances of the prediction models with all variables and only the important variables were compared to demonstrate the effectiveness of the variable screening method. SHapley Additive exPlanations (SHAP) was used to provide a more intuitive analysis of the importance of characteristic variables for predicting the net benefits of the model. Nomograms based on different outcomes and classifications were generated for use and reference.

MATERIALS AND METHODS

Patient selection

This study was performed in accordance with the principles of the Declaration of Helsinki. Approval was granted by the Ethics Committee of the Affiliate Hospital of Qingdao University (Grant number QYFYWZLL26957). We retrospectively analyzed the data of patients who underwent curative surgery for primary stage I, II, and III CRC at the Affiliated Hospital of Qingdao University from 2001 to 2020. Patients who received neoadjuvant chemoradiotherapy or who died due to a noncancer-specific cause were excluded. The postoperative adjuvant chemoradiotherapy history of our CRC patients was unclear, and the data were acquired through the hospital information system. A detailed flowchart is shown in Figure 1.

Potential variables for model construction included age, sex, body mass index (BMI), hypertension, diabetes mellitus (DM), chronic heart disease (CHD), smoking history, drinking history, family history of tumors, family history of gastrointestinal tumors, serum carcinoembryonic antigen (CEA) level, serum C-reactive protein (CRP) level, tumor position (ascending colon *vs* transverse colon *vs* descending colon *vs* sigmoid colon *vs* rectum), tumor differentiation grade, histological type, tumor size (diameter, 20 mm cutoff), perineural invasion (PNI), lymphovascular invasion, lesion number (unifocal *vs* multifocal), Ki-67 protein level, operation method (laparotomy *vs* laparoscopy), LNR, and TNM stage. These characteristics mainly consisted of patient demographics and health, tumor and treatment characteristics. Missing values only appeared in the serum CEA, CRP, and Ki-67 protein level data and were processed as a corresponding variable classification.

Outcome selection

The outcomes were the 3-category survival times (cutoff values of 3 years and 5 years). The four survival times were overall survival (OS), disease-free survival (DFS), recurrence-free survival (RFS), and distant metastasis-free survival (DMFS), which were defined as the time from the date of surgery to the date of patient death, tumor recurrence/distant metastasis, tumor recurrence, and distant tumor metastasis, respectively. The three classifications of each outcome were labeled class 1 (cl 1) (< 3 years), class 2 (cl 2) (3-5 years), and class 3 (cl 3) (> 5 years).

ML algorithms and multivariable regression methods

The four ML algorithms used here were linear regression (LR)[28], linear discriminant analysis (LDA), *eXtreme* gradient boosting (XGBoost)[29], and categorical features and gradient boosting (CatBoost)[30]. Best subset selection regression, ridge regression, least absolute shrinkage and selection operator (LASSO) regression, and LASSO cross-validation methods were selected for multivariable regression methods.

SHAPs

SHAP[31] was used to analyze the number of important input variables screened by the prediction model for achieving net benefit. As the SHAP value approached 0, the possibility of further deleting input variables increased (the SHAP value was approximately 0), ultimately improving the net benefits of the prediction model. The Y-axis refers to various characteristic variables, the X-axis refers to variable SHAP values; a point in the graph represents a sample, the color of the point represents the eigenvalue, data jitter (data metastable state) reflects the distribution of SHAP values, and the order of the variables represents their importance.

Nomogram

Nomograms based on the important variables screened for each outcome class for the four ML models were constructed to improve the applicability of our work. The variables in the nomograms are arranged according to the order mentioned in the variable selection.

ML model training and validation

Figure 1 shows the process of dataset division. Preliminary predictions were made with the four algorithms with the data from all variables, yielding corresponding area under the curve (AUC). The outcomes were then classified prior to the important variable screening step. For each ML model, variables were screened with the four multivariate regression methods, and the most appropriate regression method was selected on the basis of the difference between the predicted value and the true values [*e.g.*, the mean-square errors (MSEs); the smaller the MSE was, the greater the fit]. Moreover, commonly used clinical guidelines were used to aid in determining important variables. The selected predictors were subsequently input into the four algorithms, and the AUCs were recalculated. All ML algorithm models were validated with 5-fold cross-validation and bootstrap validation with 300 resamplings. The SHAP values of important variables were

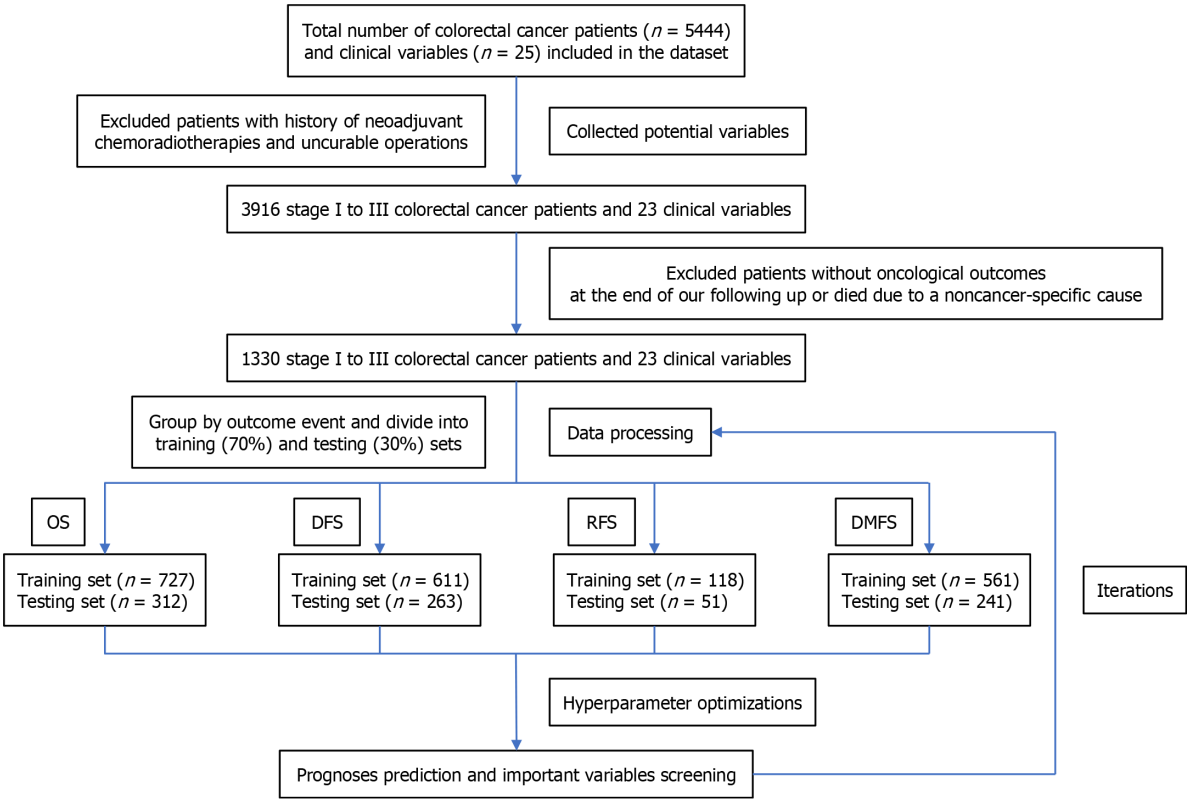

Figure 1 Flowchart showing colorectal cancer patient cohort selection and model training and performance evaluation. A total of 1330 patients were recruited for model development and were grouped by oncological outcomes; then, the data were randomly divided at a 7:3 ratio into a training set and a testing set. The hyperparameters were determined for both the training set and testing set, and model performance was evaluated on the basis of the area under the receiver operating characteristic curve. Finally, we predicted patient outcomes, screened important variables, and processed the bootstrap iterations. DFS: Disease-free survival; DMFS: Distant metastasis-free survival; OS: Overall survival; RFS: Recurrence-free survival.

also categorized, and nomograms were constructed for practical use.

Optimization and hyperparameter configuration for classification models

The optimizer was configured for optimizing the XGBoost- and CatBoost-based models. To improve the predictive stability of our models and reduce the imbalance in the data, three optimization steps were performed. First, the maximum depth of the tree in the XGBoost algorithm was reduced and the penalty coefficients of the L2 and L1 regularization weights were increased to prevent overfitting of the prediction model. Second, the maximum depth in the CatBoost algorithm was reduced, and the corresponding L2 weight was increased. Third, we introduced the kernel density estimation (KDE) algorithm[32] for classifying small sample sizes. The maximum number of iterations was 500. The learning rate was set to 0.1 in the hyperparameter configurations. The other hyperparameters were set to their default optimized values.

Proposed architecture

The technical architecture used in this study was Model-View-View Model: Preprocessing of databases, view: Executing predictions, view model: Implementation of the prediction algorithms). The specific implementation plan involved providing the data processed by R language to the ML model that had been built and finally obtaining the prediction results of the entire architecture. Previous works involved either only processing the data in R to build the models or only performing the prediction tasks with the ML models. Our work combined the advantages of the R language itself with those of mature ML models. Our prediction algorithms were developed in Python 3.11, and our regression methods were based on the R language (version 4.3.2). The AUCs were compared and the SHAP values were implemented after the data iterations. The nomograms were established in R and were used as scoring systems in our work.

Statistical analysis

The clinicopathological characteristics of the patients were compared between the training and testing sets for each model with the χ^2 test or Fisher's exact test.

Biostatistics

The statistical methods used in this study were reviewed by Shu-Cheng Si from Peking University Third Hospital.

RESULTS

Study population characteristics

The clinical and therapeutic characteristics of the study population are detailed in Supplementary Table 1. In addition, we further perform χ^2 tests/Fisher's exact tests to compare the variable distributions between the training sets and testing sets of the four models (OS, DFS, RFS, and DMFS model) and found that there were almost no significant differences. In the OS model, 66.3% (689/1039) of the patients died 3 years after surgery, and 81.9% (716/874), 81.7% (138/169) and 82.7% (663/802) of the patients experienced tumor recurrence/distant metastasis, recurrence, and distant metastasis, respectively, within 3 years after surgery. After the 5-year follow-up, 18.5% (192/1039) of the patients were still alive; additionally, 3.9% (34/874), 4.7% (8/169) and 3.4% (27/802) of the patients did not demonstrate tumor recurrence/distant metastasis, recurrence, and distant metastasis, respectively.

Performance of the all-variable database models

The results for the full-variable models are shown as solid lines. Only the results in the testing sets in terms of the receiver operating characteristic (ROC) curves are shown here; the results in the training sets are shown in detail in Figures 2, 3, 4 and 5. The AUCs [95% confidence intervals (CIs)] of the OS models produced by the four ML algorithms are shown in Figure 2 [LR: cl 1: 0.75 (0.70-0.80), cl 2: 0.65 (0.59-0.72), cl 3: 0.87 (0.81-0.92); LDA: cl 1: 0.76 (0.71-0.81), cl 2: 0.66 (0.60-0.72), cl 3: 0.86 (0.80-0.92); XGBoost: cl 1: 0.71 (0.64-0.76), cl 2: 0.62 (0.55-0.70), cl 3: 0.79 (0.71-0.86); and CatBoost: cl 1: 0.75 (0.70-0.81), cl 2: 0.65 (0.59-0.72), cl 3: 0.83 (0.77-0.89)]. Figure 3 shows the AUCs (95%CI) for the DFS models [LR: cl 1: 0.71 (0.61-0.80), cl 2: 0.70 (0.61-0.80), cl 3: 0.65 (0.35-0.89); LDA: cl 1: 0.71 (0.61-0.80), cl 2: 0.70 (0.61-0.80), cl 3: 0.62 (0.34-0.88); XGBoost: cl 1: 0.69 (0.60-0.78), cl 2: 0.66 (0.57-0.76), cl 3: 0.70 (0.46-0.89); and CatBoost: cl 1: 0.75 (0.69-0.82), cl 2: 0.71 (0.63-0.80), cl 3: 0.68 (0.43-0.90)]. The obtained AUCs (95%CIs) for the RFS models are shown in Figure 4 [LR: cl 1: 0.80 (0.65-0.92), cl 2: 0.76 (0.53-0.92), cl 3: 0.95 (0.88-1.00); LDA: cl 1: 0.83 (0.69-0.93), cl 2: 0.77 (0.57-0.93), cl 3: 0.92 (0.83-0.99); XGBoost: cl 1: 0.81 (0.65-0.93), cl 2: 0.70 (0.47-0.87), cl 3: 0.79 (0.56-0.96); and CatBoost: cl 1: 0.82 (0.67-0.93), cl 2: 0.72 (0.51-0.90), cl 3: 0.83 (0.67-0.96)]. Figure 5 shows the AUCs (95%CI) for the DMFS models [LR: cl 1: 0.65 (0.56-0.73), cl 2: 0.63 (0.54-0.71), cl 3: 0.76 (0.47-0.95); LDA: cl 1: 0.64 (0.56-0.72), cl 2: 0.63 (0.55-0.71), cl 3: 0.74 (0.45-0.93); XGBoost: cl 1: 0.66 (0.57-0.75), cl 2: 0.65 (0.55-0.74), cl 3: 0.76 (0.47-0.93); and CatBoost: cl 1: 0.65 (0.56-0.74), cl 2: 0.62 (0.54-0.71), cl 3: 0.75 (0.50-0.92)].

Model explanatory features

The important variables differed by study outcome. The detailed MSEs are shown in Table 1. We selected ridge regression for the patient OS model, and the most important variable for predicting patient death was tumor differentiation grade, whereas the tumor differentiation grade, Ki-67 protein level, TNM stage, histological type, CHD, PNI, serum CRP level, and tumor size were the leading features for predicting multicategory OS (8 in total, Table 2 and Supplementary Figure 1). Subset regression was used for the DFS model, and the six important indicators were PNI, Ki-67 protein level, tumor differentiation grade, serum CRP level, histological type, and TNM stage; moreover, the most important variable was PNI (Supplementary Figure 2). For RFS, we used LASSO regression, and DM was found to be the most important variable. The nine important indicators were DM, histological type, serum CEA level, Ki-67 protein level, PNI, serum CRP level, drinking history, LNR, and BMI (Table 2 and Supplementary Figure 3). Subset regression was also chosen for the DMFS model, and PNI, Ki-67 protein level, TNM stage, tumor differentiation grade, and histological type were identified as the five important features; of these, PNI was the most important variable (Supplementary Figure 2).

Performance of important variable models

The ROC curves of the models based on datasets containing only important variables identified after variable screening are shown as dashed lines. Only the results in the testing sets are shown here; the results in the training sets are shown in detail in Figures 2, 3, 4 and 5. The AUCs of the OS models obtained by the four ML algorithms are shown in Figure 2 [LR: cl 1: 0.78 (0.73-0.83), cl 2: 0.67 (0.61-0.74), cl 3: 0.88 (0.82-0.93); LDA: cl 1: 0.78 (0.74-0.84), cl 2: 0.67 (0.61-0.74), cl 3: 0.89 (0.84-0.93); XGBoost: cl 1: 0.76 (0.70-0.81), cl 2: 0.64 (0.57-0.71), cl 3: 0.85 (0.77-0.91); and CatBoost: cl 1: 0.77 (0.72-0.82), cl 2: 0.65 (0.58-0.72), cl 3: 0.86 (0.78-0.92)]. Figure 3 shows the AUCs for the DFS models in detail [LR: cl 1: 0.70 (0.60-0.79), cl 2: 0.69 (0.57-0.80), cl 3: 0.68 (0.43-0.87); LDA: cl 1: 0.70 (0.60-0.79), cl 2: 0.69 (0.57-0.79), cl 3: 0.69 (0.43-0.88); XGBoost: cl 1: 0.71 (0.62-0.80), cl 2: 0.72 (0.62-0.81), cl 3: 0.70 (0.48-0.88); and CatBoost: cl 1: 0.73 (0.64-0.81), cl 2: 0.72 (0.63-0.81), cl 3: 0.70 (0.50-0.87)]. The obtained AUCs for the RFS models are shown in Figure 4 [LR: cl 1: 0.68 (0.53-0.82), cl 2: 0.66 (0.44-0.82), cl 3: 0.85 (0.66-0.97); LDA: cl 1: 0.70 (0.56-0.85), cl 2: 0.67 (0.46-0.83), cl 3: 0.85 (0.65-0.98); XGBoost: cl 1: 0.83 (0.68-0.95), cl 2: 0.70 (0.45-0.87), cl 3: 0.88 (0.75-0.97); and CatBoost: cl 1: 0.79 (0.64-0.91), cl 2: 0.68 (0.45-0.85), cl 3: 0.84 (0.68-0.93)]. Figure 5 shows the AUCs for the DMFSs [LR: cl 1: 0.67 (0.58-0.76), cl 2: 0.63 (0.54-0.72), cl 3: 0.79 (0.48-0.95); LDA: cl 1: 0.65 (0.56-0.74), cl 2: 0.62 (0.53-0.71), cl 3: 0.79 (0.48-0.95); XGBoost: cl 1: 0.68 (0.60-0.76), cl 2: 0.64 (0.55-0.73), cl 3: 0.80 (0.53-0.94); and CatBoost: cl 1: 0.67 (0.59-0.75), cl 2: 0.63 (0.54-0.72), cl 3: 0.78 (0.54-0.94)]. The model AUCs did not significantly decrease and, in some cases, even increased after reducing the variables to only those identified as important.

SHAP value

Supplementary Figure 4 shows the plots of the model SHAP values. A higher probability of outcome occurrence is represented by a SHAP value less than zero. Patients with poor tumor differentiation, high Ki-67 protein level, poor histological type, late TNM stage, high tumor size, PNI, high serum CRP level, and CHD tended to have poorer OS. For DFS, PNI, high Ki-67 protein level, poor tumor differentiation, poor histological type, late TNM stage, and high serum CRP level were related to earlier tumor recurrence/distant metastasis. According to the RFS model, tumor recurrence was

Table 1 Comparisons of the mean square error of the four regression methods

Regression methods	MSEs			
	OS	DFS	RFS	DMFS
Subset regression method	0.3451435	0.2798500	0.2982825	0.2473204
Ridge regression method	0.3446552	0.2851649	0.3134211	0.2618467
LASSO regression method	0.3539798	0.2841859	0.3051014	0.2600286
LASSO cross-validation method	0.3594004	0.3240556	0.3087686	0.2833409

DFS: Disease-free survival; DMFS: Distant metastasis-free survival; LASSO: Least absolute shrinkage and selection operator; MSE: Mean square error; OS: Overall survival; RFS: Recurrence-free survival.

Table 2 Regression coefficients for each variable after ridge regression for overall survival, and least absolute shrinkage and selection operator regression for recurrence-free survival

No.	Intercept	s1	s1
1	Sex	-0.018391078	0
2	Age	-0.038454863	0
3	BMI	0.021728968	-0.001371348
4	HP	0.004982681	0
5	DM	0.001375364	0.119909730
6	CHD	0.096041621	0
7	Smoking history	0.028673390	0
8	Drinking history	0.057936668	0.013536804
9	Family history of tumors	-0.006440690	0
10	Family history of gastrointestinal tumors	0.049916084	0
11	Serum CEA level	0.045104522	-0.043589364
12	Serum CRP level	-0.069915886	-0.026111125
13	Tumor position	0.001514524	0
14	Tumor differentiation grade	-0.295140732	0
15	Histological type	-0.109175968	-0.063182813
16	Tumor size	-0.063522898	0
17	PNI	-0.092586921	-0.031648909
18	LVI	-0.026426021	0
19	Lesion number	0.037347444	0
20	Ki-67 protein level	-0.163277916	-0.033951556
21	Operation method	0.055820722	0
22	LNR	0.040875360	-0.009499988
23	TNM stage	-0.150669578	0

BMI: Body mass index, CEA: Carcinoembryonic antigen; CHD: Chronic heart disease; CRP: C-reactive protein; DM: Diabetes mellitus; HP: Hypertension; LNR: Lymph node ratio; LVI: Lymphovascular invasion; PNI: Perineural invasion; TNM: Tumor node metastasis.

more frequent in patients with poor histological type, high BMI, high Ki-67 protein level, drinking history, high serum CEA level, PNI, DM, high LNR, and high serum CRP level. The distant metastasis model suggested that distant metastasis was more likely for a patient with PNI, high Ki-67 protein level, poor tumor differentiation, late TNM stage, and poor histological type.

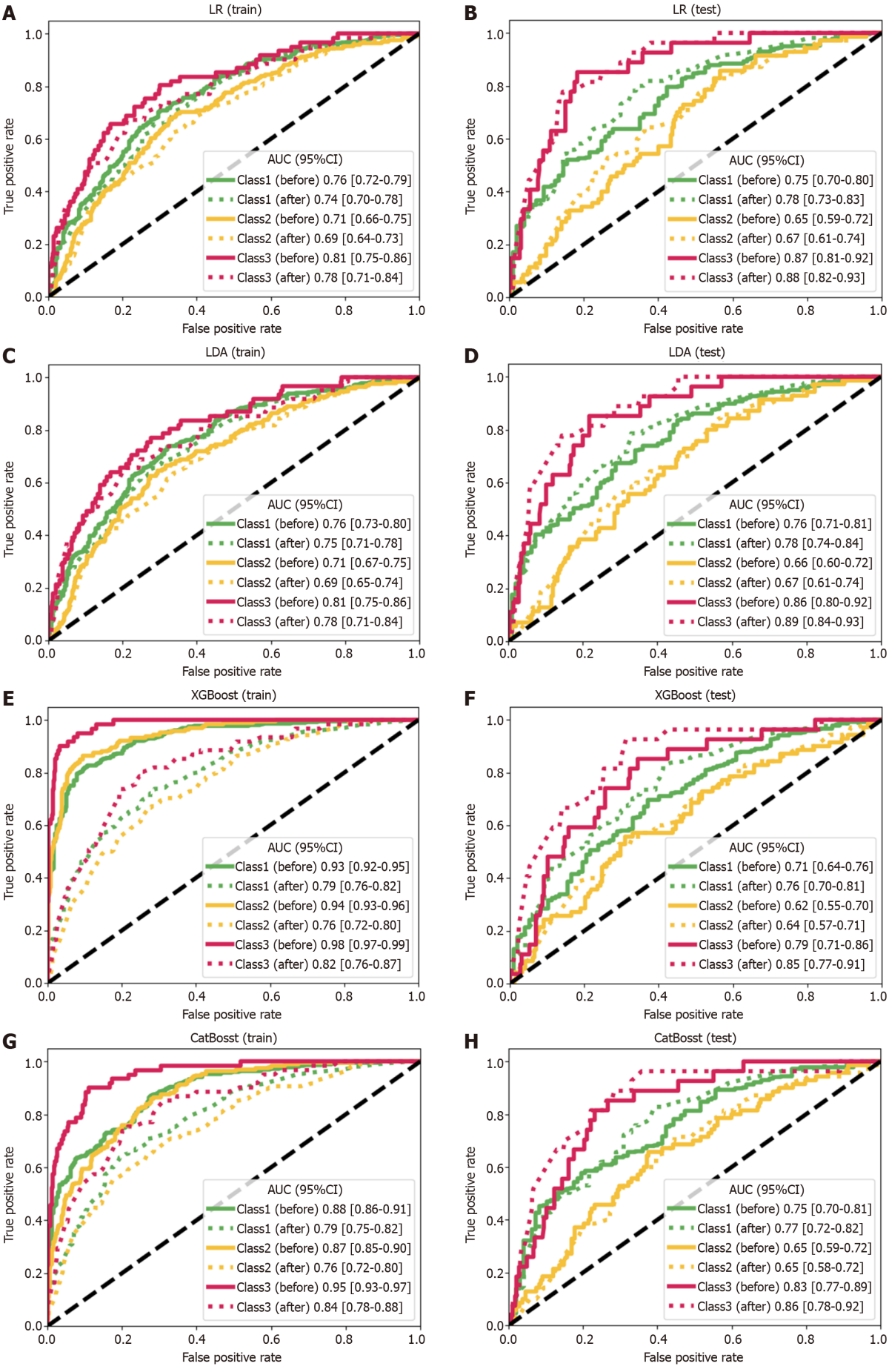

Figure 2 Prediction of overall survival by machine learning models. The plots show the areas under the curve (AUCs) and their 95% confidence interval

(CI). A: The linear regression (LR) in the training set [class 1 (cl 1): Before: 0.76 (0.72-0.79), after: 0.74 (0.70-0.78); class 2 (cl 2): Before: 0.71 (0.66-0.75), after: 0.69 (0.64-0.73); class 3 (cl 3): Before: 0.81 (0.75-0.86), after: 0.78 (0.71-0.84)]; B: The LR model in the testing set [cl 1: Before: 0.75 (0.70-0.80), after: 0.78 (0.73-0.83); cl 2: Before: 0.65 (0.59-0.72), after: 0.67 (0.61-0.74); cl 3: Before: 0.87 (0.81-0.92), after: 0.88 (0.82-0.93)]; C: The linear discriminant analysis (LDA) model in the training set [cl 1: Before: 0.76 (0.73-0.80), after: 0.75 (0.71-0.78); cl 2: Before: 0.71 (0.67-0.75), after: 0.69 (0.65-0.74); cl 3: Before: 0.81 (0.75-0.86), after: 0.78 (0.71-0.84)]; D: The LDA model in the testing set [cl 1: Before: 0.76 (0.71-0.81), after: 0.78 (0.74-0.84); cl 2: Before: 0.66 (0.60-0.72), after: 0.67 (0.61-0.74); cl 3: Before: 0.86 (0.80-0.92), after: 0.89 (0.84-0.93)]; E: The *eXtreme* gradient boosting (XGBoost) model in the training set [cl 1: Before: 0.93 (0.92-0.95), after: 0.79 (0.76-0.82); cl 2: Before: 0.94 (0.93-0.96), after: 0.76 (0.72-0.80); cl 3: Before: 0.98 (0.97-0.99), after: 0.82 (0.76-0.87)]; F: The XGBoost model in the testing set [cl 1: Before: 0.71 (0.64-0.76), after: 0.76 (0.70-0.81); cl 2: Before: 0.62 (0.55-0.70), after: 0.64 (0.57-0.71); cl 3: Before: 0.79 (0.71-0.86), after: 0.85 (0.77-0.91)]; G: The categorical features and gradient boosting (CatBoost) model in the training set [cl 1: Before: 0.88 (0.86-0.91), after: 0.79 (0.75-0.82); cl 2: Before: 0.87 (0.85-0.90), after: 0.76 (0.72-0.80); cl 3: Before: 0.95 (0.93-0.97), after: 0.84 (0.78-0.88)]; H: The CatBoost model in the testing set [cl 1: Before: 0.75 (0.70-0.81), after: 0.77 (0.72-0.82); cl 2: Before: 0.65 (0.59-0.72), after: 0.65 (0.58-0.72); cl 3: Before: 0.83 (0.77-0.89), after: 0.86 (0.78-0.92)]. The curves of the models constructed with the full-variable datasets and the datasets containing only important variables are depicted with solid lines and dashed lines, respectively (abbreviated as "before" and "after" in this annotation).

Nomogram

Supplementary Figures 5-8 show the nomograms of each ML model. The total scores and the probability of outcome occurrence can be obtained from these nomograms.

Model validation

The 5-fold cross-validation and bootstrap validation results of our ML models are detailed in Supplementary Figures 9-12.

DISCUSSION

In this study, we developed and validated a promising ML architecture for predicting the 3-class occurrence time (cutoff values of 3 years and 5 years) for four oncological outcomes (patient death, tumor recurrence/distant metastasis, tumor recurrence, and distant tumor metastasis) and identified corresponding important variables. Moreover, 5-fold cross-validations and bootstrap validations were conducted. The AUC was calculated to evaluate our predictive models, and the effectiveness of our variable screening methods was evaluated by comparing the pre- and post-screening AUCs of the models. SHAP values aided in improving the explanation of the decision-making processes of the models. Moreover, nomograms were produced for ease of application of the models. This architecture represents a comprehensive, practical, and robust tool that clinicians can use when making clinical decisions. Additionally, given the nature of the included patient data, our architecture has good tolerance for heterogeneity and does not require clear patient medical histories, lowering the threshold for use. We cut the survival times, predicted them as multicategory endpoints, and assessed patient outcomes longitudinally through our results, providing a perspective that differs from those of previous studies. Our ML models were designed on the basis of specific oncological outcomes to predict the possible occurrence time category. Some of the important indicators, such as LNR, were newly identified as important predictors of CRC patient outcomes, providing possible insights for researchers and clinicians. Our work demonstrated the feasibility of applying ML models to CRC patients to a certain extent; moreover, the adaptability and interpretability of our architecture can help promote its application in hospitals at different levels.

To improve the practicality of the architecture, we selected clinicopathological indicators that are easily obtained, although several genetic and molecular markers have been proven to be correlated with patient prognoses[25,33]. Eschewing selection biases, we avoided the TNM stage-centric impasse by inputting multipotential variables into the parameter screening step, allowing the ML algorithms to screen important variables that performed best. Missing values were treated as one of the categories of corresponding categorical variables in our study for the sake of applicability and to avoid biases caused by improper filling of missing values to a certain extent. In practice, clinicians can choose the classification that represents missing data when missing values are encountered. We randomly grouped the patients into a training and testing cohort to avoid selection bias, and the differences in baseline characteristics between the two sets were almost not significant. Therefore, we did not further explore potential confounding factors. However, future studies should consider investigating the effects of such confounding factors on model outcomes.

We included patients with a clear medical history before the operation who underwent curative initial treatment; in this way, we excluded stage I, II, and III CRC patients who had received neoadjuvant chemoradiotherapy (which may have led to a vague history). Patients with stage IV CRC who were not eligible for radical surgery were also excluded. However, the history of postoperative adjuvant chemoradiotherapy in our patients was unclear. Consequently, the models might serve as simply rough references when physicians at higher-level hospitals redesign treatment strategies for patients from lower-level hospitals with unclear postoperative radiotherapy and chemotherapy histories. Treatment options for these patients are difficult to determine, and it is difficult for oncologists to obtain references from previous studies that stratify patients by chemotherapy regimen. Moreover, to avoid bias, we excluded patients who did not have endpoint data. When applying our architecture, patients who were predicted to not have outcomes were classified as having an outcome greater than 5 years. We cautiously excluded patients with long follow-up intervals and patients with clear, noncancer-specific deaths to further avoid bias. In addition, the number of patients with tumor recurrence was the smallest; therefore, after strict 7:3 classification into the training and testing cohorts, the sample size for the testing cohort

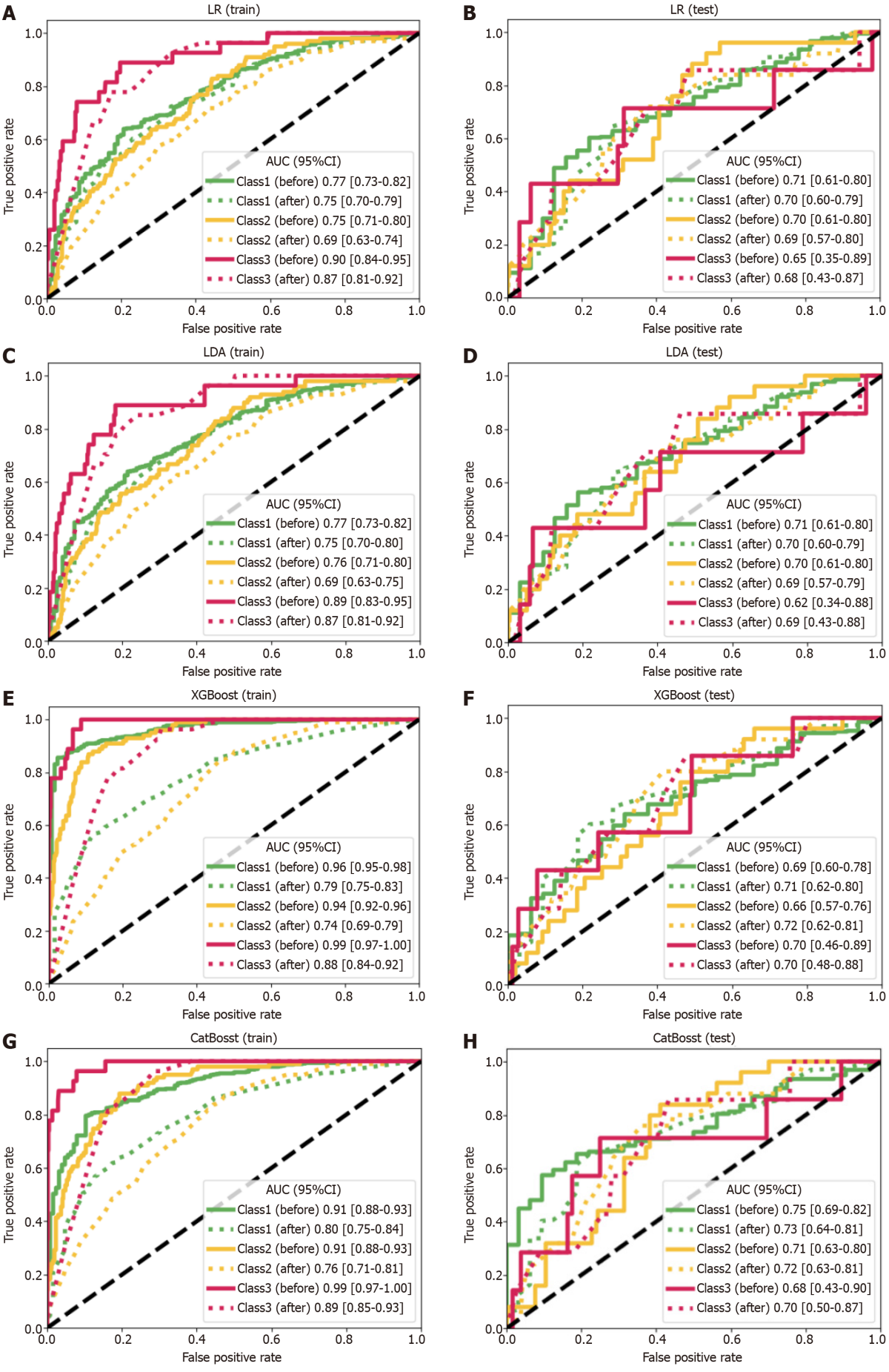

Figure 3 Prediction of disease-free survival by machine learning models. The plots show the areas under the curve (AUCs) and their 95%CI. A: The

linear regression (LR) model in the training set [class 1 (cl 1): Before: 0.77 [0.73-0.82), after: 0.75 (0.70-0.79); class 2 (cl 2): Before: 0.75 (0.71-0.80), after: 0.69 (0.63-0.74); class 3 (cl 3): Before: 0.90 (0.84-0.95), after: 0.87 (0.81-0.92)]; B: The LR model in the testing set [cl 1: Before: 0.71 (0.61-0.80), after: 0.70 (0.60-0.79); cl 2: Before: 0.70 (0.61-0.80), after: 0.69 (0.57-0.80); cl 3: Before: 0.65 (0.35-0.89), after: 0.68 (0.43-0.87)]; C: The linear discriminant analysis (LDA) model in the training set [cl 1: Before: 0.77 (0.73-0.82), after: 0.75 (0.70-0.80); cl 2: Before: 0.76 (0.71-0.80), after: 0.69 (0.63-0.75); cl 3: Before: 0.89 (0.83-0.95), after: 0.87 (0.81-0.92)]; D: The LDA model in the testing set [cl 1: Before: 0.71 (0.61-0.80), after: 0.70 (0.60-0.79); cl 2: Before: 0.70 (0.61-0.80), after: 0.69 (0.57-0.79); cl 3: Before: 0.62 (0.34-0.88), after: 0.69 (0.43-0.88)]; E: The *eXtreme* gradient boosting (XGBoost) model in the training set [cl 1: Before: 0.96 (0.95-0.98), after: 0.79 (0.75-0.83); cl 2: Before: 0.94 (0.92-0.96), after: 0.74 (0.69-0.79); cl 3: Before: 0.99 (0.97-1.00), after: 0.88 (0.84-0.92)]; F: The XGBoost model in the testing set [cl 1: Before: 0.69 (0.60-0.78), after: 0.71 (0.62-0.80); cl 2: Before: 0.66 (0.57-0.76), after: 0.72 (0.62-0.81); cl 3: Before: 0.70 (0.46-0.89), after: 0.70 (0.48-0.88)]; G: The categorical features and gradient boosting (CatBoost) model in the training set [cl 1: Before: 0.91 (0.88-0.93), after: 0.80 (0.75-0.84); cl 2: Before: 0.91 (0.88-0.93), after: 0.76 (0.71-0.81); cl 3: Before: 0.99 (0.97-1.00), after: 0.89 (0.85-0.93)]; H: The CatBoost model in the testing set [cl 1: Before: 0.75 (0.69-0.82), after: 0.73 (0.64-0.81); cl 2: Before: 0.71 (0.63-0.80), after: 0.72 (0.63-0.81); cl 3: Before: 0.68 (0.43-0.90), after: 0.70 (0.50-0.87)]. The curves of the models constructed with the full-variable datasets and the datasets containing only important variables are depicted with solid lines and dashed lines, respectively (abbreviated as "before" and "after" in this annotation).

in the RFS model was still small; therefore, we used the KDE algorithm to address this situation. The similarity between the fitting and original data was evaluated by the bandwidth in KDE, and the fitted data were merged with the original data to form a new RFS dataset. The data introduced here were only used as model training data to assess the performance of the prediction model.

We decomposed the 3-category outcomes into binary outcomes and introduced the data into a LR prediction model, LR; ultimately, 23 original characteristic variables were given outcome labels. As the dataset was multidimensional, the supervised dimensionality reduction algorithm LDA[34,35] was introduced to effectively improve the establishment of the prediction models. We selected XGBoost to optimize the prediction models, although calculating leaf weights is a complex process. The predictive values were obtained by directly summing the leaf weights of all the weak classifiers. We adopted CatBoost because it is based on a tree structure algorithm that can increase the robustness of prediction models. Most importantly, CatBoost can process categorical features into numerical features. The algorithm counts the categorical features, calculates the frequency of appearance of each categorical feature, and subsequently adds hyperparameters to generate new numerical features. CatBoost also uses combined category features, which can leverage the connections between features, greatly enriching the feature dimensions. After analyzing the performance of CatBoost and comparing it with that of LDA, we found that the advantages of the former outweighed those of the latter. To avoid bias in gradient estimation and address prediction bias, we adopted a sorting enhancement method to combat noise in the training dataset. In addition, to better predict the 3-category survival time for patients with different oncological outcomes, we configured and optimized the hyperparameters wherever possible. Furthermore, to reduce bias, the computer experts were blinded to the meaning of each indicator when building the ML models.

Taking survival time as a categorical variable and making more precise predictions to obtain a time interval of oncological outcome occurrence reflects one of the potential applications of our models in clinical practice and provides a different perspective for making predictions from previous studies. A more accurate prediction of possible patient outcomes could translate into more precise formulations of treatment therapies and patient management strategies. Extending survival time is a shared goal among clinicians and oncology patients, and quantifying patient outcomes aids in shared decision making[36]. Because of the heterogeneity of CRC, physicians and patients must seriously consider the trade-offs between adverse effects and benefits[37] when choosing a treatment strategy. It is possible to improve outcomes by administering closer follow-up or additional chemoradiotherapy to patients who are predicted to have poorer outcomes. Consequently, we suggest that patients expected to have a shorter DMFS receive prophylactic chemotherapy or regional radiotherapy at common CRC metastasis sites, as described by Jiang *et al*[38]. Moreover, the identification of patients with better outcomes could reduce medical care costs and improve the level of humanistic care by reducing the psychological burden on patients and their families. Therefore, predictive tools such as those produced with our architecture should be adopted quickly in clinical practice. However, the results output by models with unclear vital parameters for managing patients are not always acceptable to clinicians and patients[39,40]. Model interpretability is important, especially in biomedicine[41,42]. To turn a model with unclear important parameters into a model with clear important parameters model, we screened the corresponding predictors and showed their importance for different patient outcomes. TNM stage, the primary indicator for chemoradiotherapy decisions, was included in the OS, DFS, and DMFS models, which made our models more credible. Moreover, indicators that have been widely found to be correlated with patient outcome, such as PNI[43-45], pathological type[46-49], and tumor differentiation grade[50], were also included in the models, further confirming the credibility of our architecture. One of the potential benefits of using ML models is that important variables can be identified, while less important parameters can be ignored. Several predictors that were not widely used as important predictors for CRC patient outcome were also included in our model, providing new insights into the concept of predicting patient outcomes. The LNR, whose high prognostic value has been previously demonstrated[51,52], was selected for inclusion in our RFS model and could emerge as an important prognostic indicator for CRC patients for clinical decision-making. The levels of serum CRP and tumor Ki-67 protein were also shown to be prognostic factors, which is consistent with studies showing that high serum CRP levels are associated with increased postoperative complication rates[53,54] and that Ki-67 levels reflect the proliferative capacity of cells[55], especially tumor cells[56]. Our models also identified several predictors that were not previously considered to be directly linked to a poor outcome (unifocal *vs* multifocal lesions and laparotomy *vs* laparoscopy)[57-60]. These factors are more likely to be directly related to surgical trauma rather than survival time, however. For the OS and RFS models, chronic diseases, CHD and DM, were selected together with alcohol consumption history and BMI, suggesting that clinicians need to be mindful of

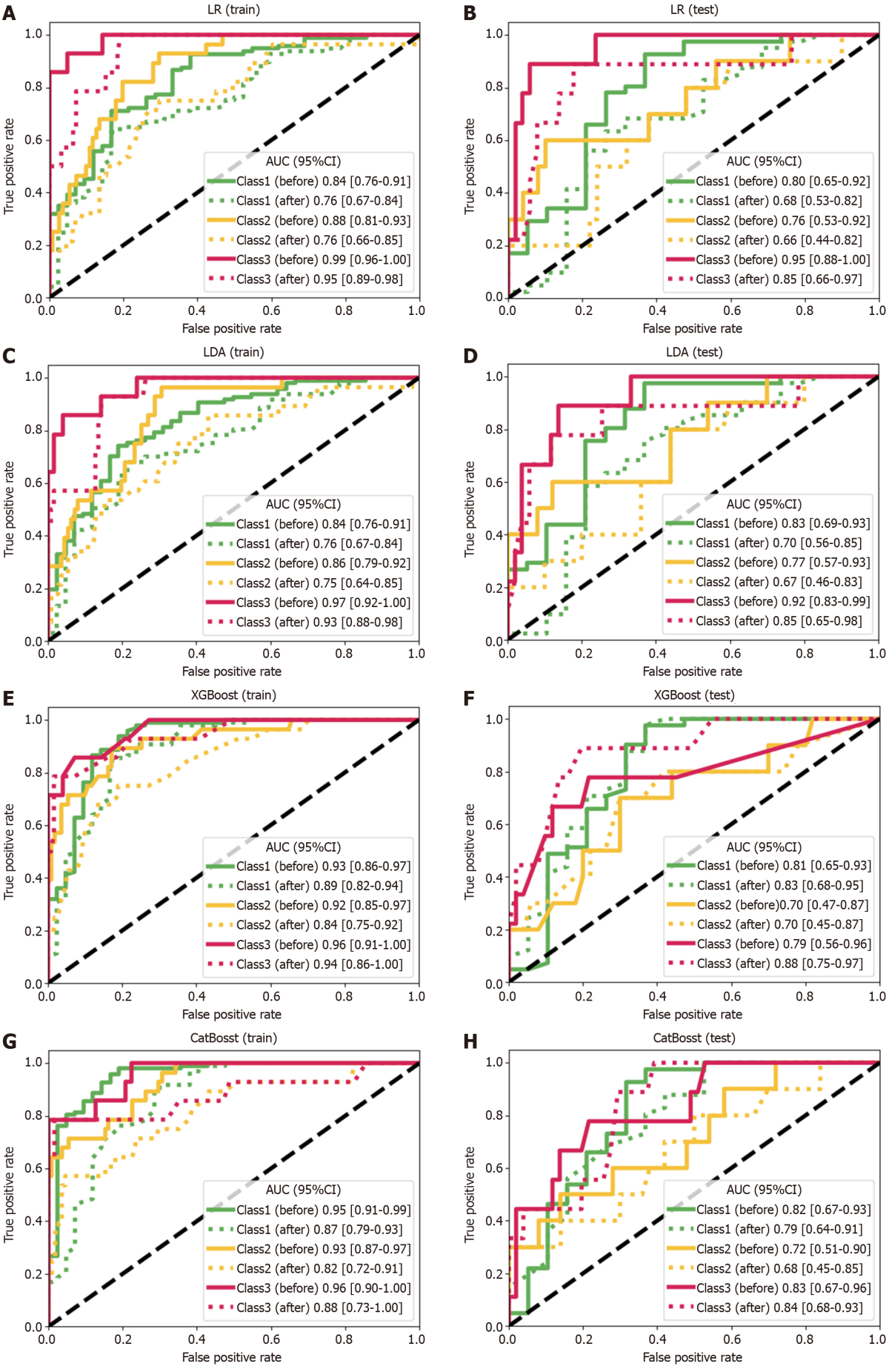

Figure 4 Prediction of recurrence-free survival by machine learning models. The plots show the areas under the curve (AUCs) and their 95%CI. A:

The linear regression (LR) model in the training set [class 1 (cl 1): Before: 0.84 (0.76-0.91), after: 0.76 (0.67-0.84); class 2 (cl 2): Before: 0.88 (0.81-0.93), after: 0.76 (0.66-0.85); class 3 (cl 3): Before: 0.99 (0.96-1.00), after: 0.95 (0.89-0.98)]; B: The LR model in the testing set [cl 1: Before: 0.80 (0.65-0.92), after: 0.68 (0.53-0.82); cl 2: Before: 0.76 (0.53-0.92), after: 0.66 (0.44-0.82); cl 3: Before: 0.95 (0.88-1.00), after: 0.85 (0.66-0.97)]; C: The linear discriminant analysis (LDA) model in the training set [cl 1: Before: 0.84 (0.76-0.91), after: 0.76 (0.67-0.84); cl 2: Before: 0.86 (0.79-0.92), after: 0.75 (0.64-0.85); cl 3: Before: 0.97 (0.92-1.00), after: 0.93 (0.88-0.98)]; D: The LDA model in the testing set [cl 1: Before: 0.83 (0.69-0.93), after: 0.70 (0.56-0.85); cl 2: Before: 0.77 (0.57-0.93), after: 0.67 (0.46-0.83); cl 3: Before: 0.92 (0.83-0.99), after: 0.85 (0.65-0.98)]; E: The *eXtreme* gradient boosting (XGBoost) model in the training set [cl 1: Before: 0.93 (0.86-0.97), after: 0.89 (0.82-0.94); cl 2: Before: 0.92 (0.85-0.97), after: 0.84 (0.75-0.92); cl 3: Before: 0.96 (0.91-1.00), after: 0.94 (0.86-1.00)]; F: The XGBoost model in the testing set [cl 1: Before: 0.81 (0.65-0.93), after: 0.83 (0.68-0.95); cl 2: Before: 0.70 (0.47-0.87), after: 0.70 (0.45-0.87); cl 3: Before: 0.79 (0.56-0.96), after: 0.88 (0.75-0.97)]; G: The categorical features and gradient boosting (CatBoost) model in the training set [cl 1: Before: 0.95 (0.91-0.99), after: 0.87 (0.79-0.93); cl 2: Before: 0.93 (0.87-0.97), after: 0.82 (0.72-0.91); cl 3: Before: 0.96 (0.90-1.00), after: 0.88 (0.73-1.00)]; and H: The CatBoost model in the testing set [cl 1: Before: 0.82 (0.67-0.93), after: 0.79 (0.64-0.91); cl 2: Before: 0.72 (0.51-0.90), after: 0.68 (0.45-0.85); cl 3: Before: 0.83 (0.67-0.96), after: 0.84 (0.68-0.93)]. The curves of the models constructed with the full-variable datasets and the datasets containing only important variables are depicted with solid lines and dashed lines, respectively (abbreviated as "before" and "after" in this annotation).

cancer patients with underlying diseases and poor health conditions. Moreover, we validated the effectiveness of our screening method by comparing the AUCs of the all-variable and important variable-only predictive models. Model performance did not significantly decrease and in some cases even improved when constructed only with the important variables. This finding indicates that our important variables indeed play key roles in our prediction models. After calculating SHAP values, we found that different variables had different degrees of impact on the predictions. Furthermore, clinicians could directly and conveniently reference our results through the nomograms provided in the Results section.

Our findings revealed the formidable predictive power of ML methods, particularly for heterogeneous diseases whose outcome stratifications serve as important clinical references. ML has unique value in clinical applications; when guiding patient management, improving patient outcomes, and tailoring treatment regimens, it could provide important reference values, especially under conditions of resource scarcity (for example, when only clinicopathological and surgical variables are available for analysis). In terms of the computer calculations used, the function parameters were those of the multiple LR model, whereas the optimization parameter b applied in the Cox proportional hazards model is consistent with that of the multiple LR model. Moreover, compared with the Cox proportional hazards model[61], ML has some advantages, although the Cox proportional hazards model and the multivariate linear model in the ML model are similar. When selecting the important parameters, the Cox proportional hazards model commonly shows independent prognostic factors and more indirectly compares their predictive value, whereas ML finds important factors and compares their importance more reliably and directly. When building models and determining their performance, the Cox proportional hazards model typically takes a specific survival time and builds double/multiclass risk stratifications based on this survival time, whereas we predicted the 3-category occurrence time of the oncological outcomes, *i.e.* patient survival times from a longitudinal perspective, with our ML models. Moreover, the number of variables for which the Cox proportional hazards model performed best was less than that of the ML model, which could include multiple variables [62,63]. In addition, the ML and Cox proportional hazards models also differed in terms of the AUC. In our study, the AUC refers to the percentage of correct prediction results in the total sample and specifically refers to the ratio of 3-category survival times (OS, DFS, RFS, and DMFS) to the corresponding sample size of the datasets. In the ML model, we binarized the three categories, and the AUC value was the same as the conventional value. The final AUC was obtained from the last module of the ML model[64] and corresponded to the three outcome classifications. Although we obtained encouragingly high predictive performance, high robustness, and transparently important variables, more progress is needed before ML can be fully relied upon. In addition, in clinical practice, traditional performance measures such as the AUC must be translated into medically relevant measures to elucidate the patient-centric value of the ML model, indicating that ML is still lacking in some ways.

The limitations of our study must be noted. First, the sample size needed to collect the data to be input into the ML models was not large (especially for the RFS model). When the data were input into the ML models for parameter optimization, the sensitivity of parameter adjustment could not be estimated because of the small sample size. To compensate for this limitation, we introduced the KDE algorithm for the RFS model (classes 2 and 3); the algorithm was only applied during the training and testing process of the models and achieved good results. Second, the sample uniformity of the data could not be estimated. This is a common problem in ML[41] that can possibly affect the final results. Furthermore, this was a retrospective study, which implies the presence of certain selection biases. However, the patient data were obtained from a well-conceived and well-characterized cohort, which increases the credibility of our results; thus, this study can serve as the basis for subsequent prospective studies. In addition, postoperative treatment information, such as information regarding specific radiotherapy and chemotherapy treatments as well as details of the surgical methods, was not available in our datasets and should be considered for inclusion in future works.

Prospective research with a larger sample size and a more comprehensive and consummate design is needed in the future. Moreover, information involving omics data and microbial analyses is highly worthy of inclusion in the predictive models. We look forward to carrying out more in-depth work in the future.

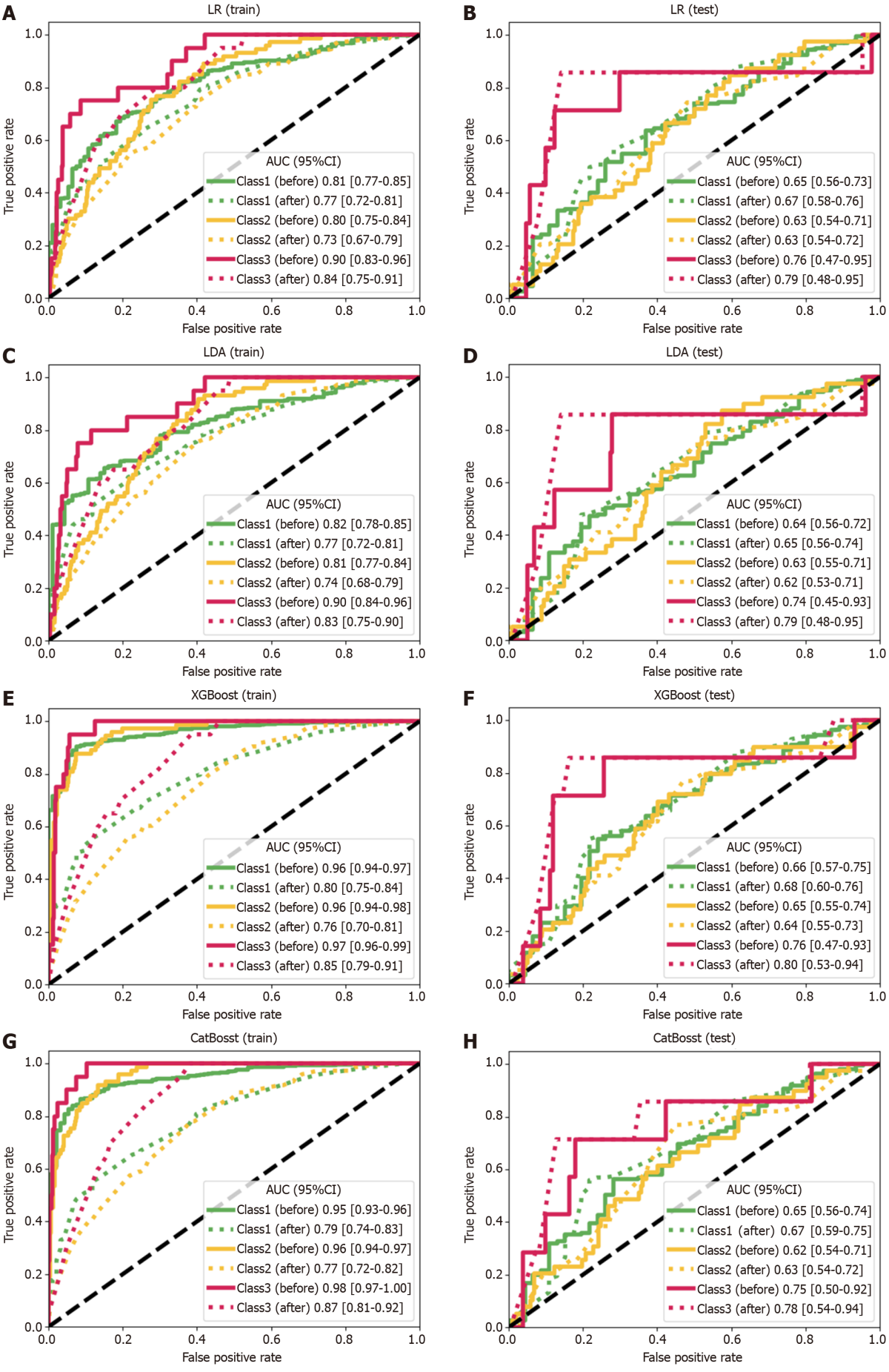

Figure 5 Prediction of distant metastasis-free survival by machine learning models. The plots show the areas under the curve (AUCs) and their

95%CI. A: The linear regression (LR) model in the training set [class 1 (cl 1): Before: 0.81 (0.77-0.85), after: 0.77 (0.72-0.81); class 2 (cl 2): Before: 0.80 (0.75-0.84), after: 0.73 (0.67-0.79); class 3 (cl 3): Before: 0.90 (0.83-0.96), after: 0.84 (0.75-0.91)]; B: The LR model in the testing set [cl 1: Before: 0.65 (0.56-0.73), after: 0.67 (0.58-0.76); cl 2: Before: 0.63 (0.54-0.71), after: 0.63 (0.54-0.72); cl 3: Before: 0.76 (0.47-0.95), after: 0.79 (0.48-0.95)]; C: The linear discriminant analysis (LDA) model in the training set [cl 1: Before: 0.82 (0.78-0.85), after: 0.77 (0.72-0.81); cl 2: Before: 0.81 (0.77-0.84), after: 0.74 (0.68-0.79); cl 3: Before: 0.90 (0.84-0.96), after: 0.83 (0.75-0.90)]; D: The LDA model in the testing set [cl 1: Before: 0.64 (0.56-0.72), after: 0.65 (0.56-0.74); cl 2: Before: 0.63 (0.55-0.71), after: 0.62 (0.53-0.71); cl 3: Before: 0.74 (0.45-0.93), after: 0.79 (0.48-0.95)]; E: The *eXtreme* gradient boosting (XGBoost) model in the training set [cl 1: Before: 0.96 (0.94-0.97), after: 0.80 (0.75-0.84); cl 2: Before: 0.96 (0.94-0.98), after: 0.76 (0.70-0.81); cl 3: Before: 0.97 (0.96-0.99), after: 0.85 (0.79-0.91)]; F: The XGBoost model in the testing set [cl 1: Before: 0.66 (0.57-0.75), after: 0.68 (0.60-0.76); cl 2: Before: 0.65 (0.55-0.74), after: 0.64 (0.55-0.73); cl 3: Before: 0.76 (0.47-0.93), after: 0.80 (0.53-0.94)]; G: The categorical features and gradient boosting (CatBoost) model in the training set [cl 1: Before: 0.95 (0.93-0.96), after: 0.79 (0.74-0.83); cl 2: Before: 0.96 (0.94-0.97), after: 0.77 (0.72-0.82); cl 3: Before: 0.98 (0.97-1.00), after: 0.87 (0.81-0.92)]; H: The CatBoost model in the testing set [cl 1: Before: 0.65 (0.56-0.74), after: 0.67 (0.59-0.75); cl 2: Before: 0.62 (0.54-0.71), after: 0.63 (0.54-0.72); cl 3: Before: 0.75 (0.50-0.92), after: 0.78 (0.54-0.94)]. The curves of the models constructed with the full-variable datasets and the datasets containing only important variables are depicted with solid lines and dashed lines, respectively (abbreviated as "before" and "after" in this annotation).

CONCLUSION

We successfully designed and validated comprehensive, accessible, and robust clinicopathological-based ML prediction models built from clearly identified important variables. Our work could serve as a reference for CRC patient management and outcome improvement. We demonstrated the potential of the proposed ML architecture for clinical application.

ACKNOWLEDGEMENTS

We thank all the authors for their contributions to the manuscript and for their recognition of the data and conclusions; moreover, we thank Shu-Cheng Si, who reviewed the statistical methods of this study.

FOOTNOTES

Author contributions: Ji XL and Xu S designed the study, acquired and analyzed the data, and wrote the manuscript; Ji XL and Xu S contributed equally to this work; Li XY prepared the materials; Xu JH provided methods; Han RS, and Guo YJ participated in the data acquisition and analysis; Tian ZB and Duan LP managed and designed the project, and performed critical revisions of the manuscript; Tian ZB and Duan LP contributed equally to this work; All authors have read and approve the final manuscript. Ji XL and Xu S contributed equally to this work as co-first authors. The designation of Tian ZB and Duan LP as co-corresponding authors of this work is primarily based on the following three reasons. First, this research project spans multiple disciplines. As the main provider of data, Tian ZB ensures the reliability and integrity of the research. His work in data collection, collation and analysis is crucial to the quality of the paper, while Duan LP ensures the comprehensiveness and depth of the research. Second, Duan LP was the main provider of the core ideas of the paper, setting the foundation for the direction and framework of the entire research and promoting the innovation and scientific value of the research. Moreover, Tian ZB put forward suggestions during this process. The two co-corresponding authors have similar contributions to the project and work closely together. Balancing their contributions is crucial for fairness and transparency. Third, Tian ZB and Duan LP jointly undertook the task of revising the manuscript, reducing the burden of a single corresponding author and ensuring timely and efficient responses. In short, designating two corresponding authors helps promote cooperation, enhance academic influence, and improve the quality of research results. The contributions of Tian ZB and Duan LP are equally important at different stages, so being co-corresponding authors more fairly reflects their collaboration and contribution to this research.

Supported by National Natural Science Foundation of China, No. 81802777.

Institutional review board statement: The study was reviewed and approved for publication by the Ethics Committee of the Affiliate Hospital of Qingdao University (Grant No. QYFYWZLL26957).

Informed consent statement: All study participants or their legal guardians provided informed verbal consent for personal and medical data collection prior to study enrollment.

Conflict-of-interest statement: The authors have no conflicts of interest related to the manuscript.

Data sharing statement: The original anonymized dataset is available upon request from the corresponding author at duanlp@bjmu.edu.cn.

STROBE statement: The authors have read the STROBE Statement-checklist of items, and the manuscript was prepared and revised according to the STROBE Statement-checklist of items.

Country of origin: China

ORCID number: Xiao-Lin Ji 0000-0003-3198-7381; Shuo Xu 0000-0002-3953-7425; Xiao-Yu Li 0000-0001-8017-207X; Jin-Huan Xu 0000-0002-5374-4498; Rong-Shuang Han 0009-0007-3915-9595; Ying-Jie Guo 0000-0003-2909-9887; Li-Ping Duan 0000-0001-6886-6888; Zi-Bin Tian 0000-0001-7047-2327.

S-Editor: Qu XL
L-Editor: Filipodia
P-Editor: Wang WB

REFERENCES

1 **Bray F**, Ferlay J, Soerjomataram I, Siegel RL, Torre LA, Jemal A. Global cancer statistics 2018: GLOBOCAN estimates of incidence and mortality worldwide for 36 cancers in 185 countries. *CA Cancer J Clin* 2018; **68**: 394-424 [PMID: 30207593 DOI: 10.3322/caac.21492]
2 **Koncina E**, Haan S, Rauh S, Letellier E. Prognostic and Predictive Molecular Biomarkers for Colorectal Cancer: Updates and Challenges. *Cancers (Basel)* 2020; **12** [PMID: 32019056 DOI: 10.3390/cancers12020319]
3 **Vermeer NC**, Snijders HS, Holman FA, Liefers GJ, Bastiaannet E, van de Velde CJ, Peeters KC. Colorectal cancer screening: Systematic review of screen-related morbidity and mortality. *Cancer Treat Rev* 2017; **54**: 87-98 [PMID: 28236723 DOI: 10.1016/j.ctrv.2017.02.002]
4 **Kalager M**, Wieszczy P, Lansdorp-Vogelaar I, Corley DA, Bretthauer M, Kaminski MF. Overdiagnosis in Colorectal Cancer Screening: Time to Acknowledge a Blind Spot. *Gastroenterology* 2018; **155**: 592-595 [PMID: 30076834 DOI: 10.1053/j.gastro.2018.07.037]
5 **Ma C**, Teriaky A, Sheh S, Forbes N, Heitman SJ, Jue TL, Munroe CA, Jairath V, Corley DA, Lee JK. Morbidity and Mortality After Surgery for Nonmalignant Colorectal Polyps: A 10-Year Nationwide Analysis. *Am J Gastroenterol* 2019; **114**: 1802-1810 [PMID: 31634261 DOI: 10.14309/ajg.0000000000000407]
6 **Peery AF**, Cools KS, Strassle PD, McGill SK, Crockett SD, Barker A, Koruda M, Grimm IS. Increasing Rates of Surgery for Patients With Nonmalignant Colorectal Polyps in the United States. *Gastroenterology* 2018; **154**: 1352-1360.e3 [PMID: 29317277 DOI: 10.1053/j.gastro.2018.01.003]
7 **Nagtegaal ID**, Quirke P, Schmoll HJ. Has the new TNM classification for colorectal cancer improved care? *Nat Rev Clin Oncol* 2011; **9**: 119-123 [PMID: 22009076 DOI: 10.1038/nrclinonc.2011.157]
8 **Dienstmann R**, Mason MJ, Sinicrope FA, Phipps AI, Tejpar S, Nesbakken A, Danielsen SA, Sveen A, Buchanan DD, Clendenning M, Rosty C, Bot B, Alberts SR, Milburn Jessup J, Lothe RA, Delorenzi M, Newcomb PA, Sargent D, Guinney J. Prediction of overall survival in stage II and III colon cancer beyond TNM system: a retrospective, pooled biomarker study. *Ann Oncol* 2017; **28**: 1023-1031 [PMID: 28453697 DOI: 10.1093/annonc/mdx052]
9 **Mo S**, Dai W, Xiang W, Huang B, Li Y, Feng Y, Li Q, Cai G. Survival Contradiction Between Stage IIA and Stage IIIA Rectal Cancer: A Retrospective Study. *J Cancer* 2018; **9**: 1466-1475 [PMID: 29721057 DOI: 10.7150/jca.23311]
10 **Chu QD**, Zhou M, Medeiros KL, Peddi P, Kavanaugh M, Wu XC. Poor survival in stage IIB/C (T4N0) compared to stage IIIA (T1-2 N1, T1N2a) colon cancer persists even after adjusting for adequate lymph nodes retrieved and receipt of adjuvant chemotherapy. *BMC Cancer* 2016; **16**: 460 [PMID: 27412163 DOI: 10.1186/s12885-016-2446-3]
11 **Greene FL**, Stewart AK, Norton HJ. A new TNM staging strategy for node-positive (stage III) colon cancer: an analysis of 50,042 patients. *Ann Surg* 2002; **236**: 416-21; discussion 421 [PMID: 12368669 DOI: 10.1097/00000658-200210000-00003]
12 **Beaton C**, Twine CP, Williams GL, Radcliffe AG. Systematic review and meta-analysis of histopathological factors influencing the risk of lymph node metastasis in early colorectal cancer. *Colorectal Dis* 2013; **15**: 788-797 [PMID: 23331927 DOI: 10.1111/codi.12129]
13 **Rekhraj S**, Aziz O, Prabhudesai S, Zacharakis E, Mohr F, Athanasiou T, Darzi A, Ziprin P. Can intra-operative intraperitoneal free cancer cell detection techniques identify patients at higher recurrence risk following curative colorectal cancer resection: a meta-analysis. *Ann Surg Oncol* 2008; **15**: 60-68 [PMID: 17909914 DOI: 10.1245/s10434-007-9591-5]
14 **Choi JY**, Jung SA, Shim KN, Cho WY, Keum B, Byeon JS, Huh KC, Jang BI, Chang DK, Jung HY, Kong KA; Korean ESD Study Group. Meta-analysis of predictive clinicopathologic factors for lymph node metastasis in patients with early colorectal carcinoma. *J Korean Med Sci* 2015; **30**: 398-406 [PMID: 25829807 DOI: 10.3346/jkms.2015.30.4.398]
15 **Ha GW**, Kim JH, Lee MR. Oncologic Impact of Anastomotic Leakage Following Colorectal Cancer Surgery: A Systematic Review and Meta-Analysis. *Ann Surg Oncol* 2017; **24**: 3289-3299 [PMID: 28608118 DOI: 10.1245/s10434-017-5881-8]
16 **Choi RY**, Coyner AS, Kalpathy-Cramer J, Chiang MF, Campbell JP. Introduction to Machine Learning, Neural Networks, and Deep Learning. *Transl Vis Sci Technol* 2020; **9**: 14 [PMID: 32704420 DOI: 10.1167/tvst.9.2.14]
17 **Grimm LJ**, Plichta JK, Hwang ES. More Than Incremental: Harnessing Machine Learning to Predict Breast Cancer Risk. *J Clin Oncol* 2022; **40**: 1713-1717 [PMID: 35245093 DOI: 10.1200/JCO.21.02733]
18 **Metsky HC**, Welch NL, Pillai PP, Haradhvala NJ, Rumker L, Mantena S, Zhang YB, Yang DK, Ackerman CM, Weller J, Blainey PC, Myhrvold C, Mitzenmacher M, Sabeti PC. Designing sensitive viral diagnostics with machine learning. *Nat Biotechnol* 2022; **40**: 1123-1131 [PMID: 35241837 DOI: 10.1038/s41587-022-01213-5]
19 **Xie C**, Zhuang XX, Niu Z, Ai R, Lautrup S, Zheng S, Jiang Y, Han R, Gupta TS, Cao S, Lagartos-Donate MJ, Cai CZ, Xie LM, Caponio D, Wang WW, Schmauck-Medina T, Zhang J, Wang HL, Lou G, Xiao X, Zheng W, Palikaras K, Yang G, Caldwell KA, Caldwell GA, Shen HM, Nilsen H, Lu JH, Fang EF. Amelioration of Alzheimer's disease pathology by mitophagy inducers identified *via* machine learning and a cross-species workflow. *Nat Biomed Eng* 2022; **6**: 76-93 [PMID: 34992270 DOI: 10.1038/s41551-021-00819-5]
20 **Kim M**, Chen C, Wang P, Mulvey JJ, Yang Y, Wun C, Antman-Passig M, Luo HB, Cho S, Long-Roche K, Ramanathan LV, Jagota A, Zheng M, Wang Y, Heller DA. Detection of ovarian cancer *via* the spectral fingerprinting of quantum-defect-modified carbon nanotubes in serum by machine learning. *Nat Biomed Eng* 2022; **6**: 267-275 [PMID: 35301449 DOI: 10.1038/s41551-022-00860-y]
21 **Tripepi G**, Jager KJ, Dekker FW, Zoccali C. Diagnostic methods 2: receiver operating characteristic (ROC) curves. *Kidney Int* 2009; **76**: 252-

256 [PMID: 19455194 DOI: 10.1038/ki.2009.171]
22 **Liang R**, Xie J, Zhang C, Zhang M, Huang H, Huo H, Cao X, Niu B. Identifying Cancer Targets Based on Machine Learning Methods *via* Chou's 5-steps Rule and General Pseudo Components. *Curr Top Med Chem* 2019; **19**: 2301-2317 [PMID: 31622219 DOI: 10.2174/1568026619666191016155543]
23 **Liu C**, Zhao J, Lu W, Dai Y, Hockings J, Zhou Y, Nussinov R, Eng C, Cheng F. Individualized genetic network analysis reveals new therapeutic vulnerabilities in 6,700 cancer genomes. *PLoS Comput Biol* 2020; **16**: e1007701 [PMID: 32101536 DOI: 10.1371/journal.pcbi.1007701]
24 **Liang H**, Tsui BY, Ni H, Valentim CCS, Baxter SL, Liu G, Cai W, Kermany DS, Sun X, Chen J, He L, Zhu J, Tian P, Shao H, Zheng L, Hou R, Hewett S, Li G, Liang P, Zang X, Zhang Z, Pan L, Cai H, Ling R, Li S, Cui Y, Tang S, Ye H, Huang X, He W, Liang W, Zhang Q, Jiang J, Yu W, Gao J, Ou W, Deng Y, Hou Q, Wang B, Yao C, Liang Y, Zhang S, Duan Y, Zhang R, Gibson S, Zhang CL, Li O, Zhang ED, Karin G, Nguyen N, Wu X, Wen C, Xu J, Xu W, Wang B, Wang W, Li J, Pizzato B, Bao C, Xiang D, He W, He S, Zhou Y, Haw W, Goldbaum M, Tremoulet A, Hsu CN, Carter H, Zhu L, Zhang K, Xia H. Evaluation and accurate diagnoses of pediatric diseases using artificial intelligence. *Nat Med* 2019; **25**: 433-438 [PMID: 30742121 DOI: 10.1038/s41591-018-0335-9]
25 **Liu Z**, Liu L, Weng S, Guo C, Dang Q, Xu H, Wang L, Lu T, Zhang Y, Sun Z, Han X. Machine learning-based integration develops an immune-derived lncRNA signature for improving outcomes in colorectal cancer. *Nat Commun* 2022; **13**: 816 [PMID: 35145098 DOI: 10.1038/s41467-022-28421-6]
26 **D'Ascenzo F**, De Filippo O, Gallone G, Mittone G, Deriu MA, Iannaccone M, Ariza-Solé A, Liebetrau C, Manzano-Fernández S, Quadri G, Kinnaird T, Campo G, Simao Henriques JP, Hughes JM, Dominguez-Rodriguez A, Aldinucci M, Morbiducci U, Patti G, Raposeiras-Roubin S, Abu-Assi E, De Ferrari GM; PRAISE study group. Machine learning-based prediction of adverse events following an acute coronary syndrome (PRAISE): a modelling study of pooled datasets. *Lancet* 2021; **397**: 199-207 [PMID: 33453782 DOI: 10.1016/S0140-6736(20)32519-8]
27 **Yala A**, Mikhael PG, Strand F, Lin G, Smith K, Wan YL, Lamb L, Hughes K, Lehman C, Barzilay R. Toward robust mammography-based models for breast cancer risk. *Sci Transl Med* 2021; **13** [PMID: 33504648 DOI: 10.1126/scitranslmed.aba4373]
28 **Vinga S**. Structured sparsity regularization for analyzing high-dimensional omics data. *Brief Bioinform* 2021; **22**: 77-87 [PMID: 32597465 DOI: 10.1093/bib/bbaa122]
29 **Wang R**, Zhang J, Shan B, He M, Xu J. XGBoost Machine Learning Algorithm for Prediction of Outcome in Aneurysmal Subarachnoid Hemorrhage. *Neuropsychiatr Dis Treat* 2022; **18**: 659-667 [PMID: 35378822 DOI: 10.2147/NDT.S349956]
30 **Hancock JT**, Khoshgoftaar TM. CatBoost for big data: an interdisciplinary review. *J Big Data* 2020; **7**: 94 [PMID: 33169094 DOI: 10.1186/s40537-020-00369-8]
31 **Yi F**, Yang H, Chen D, Qin Y, Han H, Cui J, Bai W, Ma Y, Zhang R, Yu H. XGBoost-SHAP-based interpretable diagnostic framework for alzheimer's disease. *BMC Med Inform Decis Mak* 2023; **23**: 137 [PMID: 37491248 DOI: 10.1186/s12911-023-02238-9]
32 **Mi J**, Wang L, Liu Y, Zhang J. KDE-GAN: A multimodal medical image-fusion model based on knowledge distillation and explainable AI modules. *Comput Biol Med* 2022; **151**: 106273 [PMID: 36368109 DOI: 10.1016/j.compbiomed.2022.106273]
33 **Hossain MJ**, Chowdhury UN, Islam MB, Uddin S, Ahmed MB, Quinn JMW, Moni MA. Machine learning and network-based models to identify genetic risk factors to the progression and survival of colorectal cancer. *Comput Biol Med* 2021; **135**: 104539 [PMID: 34153790 DOI: 10.1016/j.compbiomed.2021.104539]
34 **Gupta A**, Katarya R. PAN-LDA: A latent Dirichlet allocation based novel feature extraction model for COVID-19 data using machine learning. *Comput Biol Med* 2021; **138**: 104920 [PMID: 34655902 DOI: 10.1016/j.compbiomed.2021.104920]
35 **Yoshida T**, Hisano R, Ohnishi T. Gaussian hierarchical latent Dirichlet allocation: Bringing polysemy back. *PLoS One* 2023; **18**: e0288274 [PMID: 37436968 DOI: 10.1371/journal.pone.0288274]
36 **Howard FM**, Kochanny S, Koshy M, Spiotto M, Pearson AT. Machine Learning-Guided Adjuvant Treatment of Head and Neck Cancer. *JAMA Netw Open* 2020; **3**: e2025881 [PMID: 33211108 DOI: 10.1001/jamanetworkopen.2020.25881]
37 **Ganguli R**, Franklin J, Yu X, Lin A, Heffernan DS. Machine learning methods to predict presence of residual cancer following hysterectomy. *Sci Rep* 2022; **12**: 2738 [PMID: 35177700 DOI: 10.1038/s41598-022-06585-x]
38 **Jiang B**, Mu Q, Qiu F, Li X, Xu W, Yu J, Fu W, Cao Y, Wang J. Machine learning of genomic features in organotropic metastases stratifies progression risk of primary tumors. *Nat Commun* 2021; **12**: 6692 [PMID: 34795255 DOI: 10.1038/s41467-021-27017-w]
39 **Parikh RB**, Manz CR, Nelson MN, Evans CN, Regli SH, O'Connor N, Schuchter LM, Shulman LN, Patel MS, Paladino J, Shea JA. Clinician perspectives on machine learning prognostic algorithms in the routine care of patients with cancer: a qualitative study. *Support Care Cancer* 2022; **30**: 4363-4372 [PMID: 35094138 DOI: 10.1007/s00520-021-06774-w]
40 **Watson DS**, Krutzinna J, Bruce IN, Griffiths CE, McInnes IB, Barnes MR, Floridi L. Clinical applications of machine learning algorithms: beyond the black box. *BMJ* 2019; **364**: l886 [PMID: 30862612 DOI: 10.1136/bmj.l886]
41 **Yu MK**, Ma J, Fisher J, Kreisberg JF, Raphael BJ, Ideker T. Visible Machine Learning for Biomedicine. *Cell* 2018; **173**: 1562-1565 [PMID: 29906441 DOI: 10.1016/j.cell.2018.05.056]
42 **Murdoch WJ**, Singh C, Kumbier K, Abbasi-Asl R, Yu B. Definitions, methods, and applications in interpretable machine learning. *Proc Natl Acad Sci U S A* 2019; **116**: 22071-22080 [PMID: 31619572 DOI: 10.1073/pnas.1900654116]
43 **Nikberg M**, Chabok A, Letocha H, Kindler C, Glimelius B, Smedh K. Lymphovascular and perineural invasion in stage II rectal cancer: a report from the Swedish colorectal cancer registry. *Acta Oncol* 2016; **55**: 1418-1424 [PMID: 27732105 DOI: 10.1080/0284186X.2016.1230274]
44 **Song JH**, Yu M, Kang KM, Lee JH, Kim SH, Nam TK, Jeong JU, Jang HS, Lee JW, Jung JH. Significance of perineural and lymphovascular invasion in locally advanced rectal cancer treated by preoperative chemoradiotherapy and radical surgery: Can perineural invasion be an indication of adjuvant chemotherapy? *Radiother Oncol* 2019; **133**: 125-131 [PMID: 30935568 DOI: 10.1016/j.radonc.2019.01.002]
45 **Knijn N**, Mogk SC, Teerenstra S, Simmer F, Nagtegaal ID. Perineural Invasion is a Strong Prognostic Factor in Colorectal Cancer: A Systematic Review. *Am J Surg Pathol* 2016; **40**: 103-112 [PMID: 26426380 DOI: 10.1097/PAS.0000000000000518]
46 **Wu X**, Lin H, Li S. Prognoses of different pathological subtypes of colorectal cancer at different stages: A population-based retrospective cohort study. *BMC Gastroenterol* 2019; **19**: 164 [PMID: 31601167 DOI: 10.1186/s12876-019-1083-0]
47 **Sheng H**, Wei X, Mao M, He J, Luo T, Lu S, Zhou L, Huang Z, Yang A. Adenocarcinoma with mixed subtypes is a rare but aggressive histologic subtype in colorectal cancer. *BMC Cancer* 2019; **19**: 1071 [PMID: 31703713 DOI: 10.1186/s12885-019-6245-5]
48 **Kim SH**, Shin SJ, Lee KY, Kim H, Kim TI, Kang DR, Hur H, Min BS, Kim NK, Chung HC, Roh JK, Ahn JB. Prognostic value of mucinous histology depends on microsatellite instability status in patients with stage III colon cancer treated with adjuvant FOLFOX chemotherapy: a retrospective cohort study. *Ann Surg Oncol* 2013; **20**: 3407-3413 [PMID: 23943026 DOI: 10.1245/s10434-013-3169-1]

49 **Nitsche U**, Zimmermann A, Späth C, Müller T, Maak M, Schuster T, Slotta-Huspenina J, Käser SA, Michalski CW, Janssen KP, Friess H, Rosenberg R, Bader FG. Mucinous and signet-ring cell colorectal cancers differ from classical adenocarcinomas in tumor biology and prognosis. *Ann Surg* 2013; **258**: 775-82; discussion 782 [PMID: 23989057 DOI: 10.1097/SLA.0b013e3182a69f7e]

50 **Garrity MM**, Burgart LJ, Mahoney MR, Windschitl HE, Salim M, Wiesenfeld M, Krook JE, Michalak JC, Goldberg RM, O'Connell MJ, Furth AF, Sargent DJ, Murphy LM, Hill E, Riehle DL, Meyers CH, Witzig TE; North Central Cancer Treatment Group. Prognostic value of proliferation, apoptosis, defective DNA mismatch repair, and p53 overexpression in patients with resected Dukes' B2 or C colon cancer: a North Central Cancer Treatment Group Study. *J Clin Oncol* 2004; **22**: 1572-1582 [PMID: 15117979 DOI: 10.1200/JCO.2004.10.042]

51 **Orive M**, Anton A, Gonzalez N, Aguirre U, Anula R, Lázaro S, Redondo M, Bare M, Briones E, Escobar A, Sarasqueta C, Ferreiro J, Quintana JM; REDISSEC-CARESS/CCR group. Factors associated with colon cancer early, intermediate and late recurrence after surgery for stage I-III: A 5-year prospective study. *Eur J Cancer Care (Engl)* 2020; **29**: e13317 [PMID: 32945024 DOI: 10.1111/ecc.13317]

52 **Yang Y**, Wang Y, Wang Z. Construction of a new clinical staging system for colorectal cancer based on the lymph node ratio: A validation study. *Front Surg* 2022; **9**: 929576 [PMID: 36090338 DOI: 10.3389/fsurg.2022.929576]

53 **Domínguez-Comesaña E**, Estevez-Fernández SM, López-Gómez V, Ballinas-Miranda J, Domínguez-Fernández R. Procalcitonin and C-reactive protein as early markers of postoperative intra-abdominal infection in patients operated on colorectal cancer. *Int J Colorectal Dis* 2017; **32**: 1771-1774 [PMID: 28918433 DOI: 10.1007/s00384-017-2902-9]

54 **Muñoz JL**, Alvarez MO, Cuquerella V, Miranda E, Picó C, Flores R, Resalt-Pereira M, Moya P, Pérez A, Arroyo A. Procalcitonin and C-reactive protein as early markers of anastomotic leak after laparoscopic colorectal surgery within an enhanced recovery after surgery (ERAS) program. *Surg Endosc* 2018; **32**: 4003-4010 [PMID: 29520440 DOI: 10.1007/s00464-018-6144-x]

55 **Schlüter C**, Duchrow M, Wohlenberg C, Becker MH, Key G, Flad HD, Gerdes J. The cell proliferation-associated antigen of antibody Ki-67: a very large, ubiquitous nuclear protein with numerous repeated elements, representing a new kind of cell cycle-maintaining proteins. *J Cell Biol* 1993; **123**: 513-522 [PMID: 8227122 DOI: 10.1083/jcb.123.3.513]

56 **Starborg M**, Gell K, Brundell E, Höög C. The murine Ki-67 cell proliferation antigen accumulates in the nucleolar and heterochromatic regions of interphase cells and at the periphery of the mitotic chromosomes in a process essential for cell cycle progression. *J Cell Sci* 1996; **109** (Pt 1): 143-153 [PMID: 8834799 DOI: 10.1242/jcs.109.1.143]

57 **Barz C**, Stöss C, Neumann PA, Wilhelm D, Janssen KP, Friess H, Nitsche U. Retrospective study of prognosis of patients with multiple colorectal carcinomas: synchronous versus metachronous makes the difference. *Int J Colorectal Dis* 2021; **36**: 1487-1498 [PMID: 33855608 DOI: 10.1007/s00384-021-03926-6]

58 **Chin CC**, Kuo YH, Chiang JM. Synchronous colorectal carcinoma: predisposing factors and characteristics. *Colorectal Dis* 2019; **21**: 432-440 [PMID: 30578740 DOI: 10.1111/codi.14539]

59 **Fleshman J**, Branda ME, Sargent DJ, Boller AM, George VV, Abbas MA, Peters WR Jr, Maun DC, Chang GJ, Herline A, Fichera A, Mutch MG, Wexner SD, Whiteford MH, Marks J, Birnbaum E, Margolin DA, Larson DW, Marcello PW, Posner MC, Read TE, Monson JRT, Wren SM, Pisters PWT, Nelson H. Disease-free Survival and Local Recurrence for Laparoscopic Resection Compared With Open Resection of Stage II to III Rectal Cancer: Follow-up Results of the ACOSOG Z6051 Randomized Controlled Trial. *Ann Surg* 2019; **269**: 589-595 [PMID: 30080730 DOI: 10.1097/SLA.0000000000003002]

60 **Hida K**, Okamura R, Sakai Y, Konishi T, Akagi T, Yamaguchi T, Akiyoshi T, Fukuda M, Yamamoto S, Yamamoto M, Nishigori T, Kawada K, Hasegawa S, Morita S, Watanabe M; Japan Society of Laparoscopic Colorectal Surgery. Open versus Laparoscopic Surgery for Advanced Low Rectal Cancer: A Large, Multicenter, Propensity Score Matched Cohort Study in Japan. *Ann Surg* 2018; **268**: 318-324 [PMID: 28628565 DOI: 10.1097/SLA.0000000000002329]

61 **Poortmans PM**, Collette S, Kirkove C, Van Limbergen E, Budach V, Struikmans H, Collette L, Fourquet A, Maingon P, Valli M, De Winter K, Marnitz S, Barillot I, Scandolaro L, Vonk E, Rodenhuis C, Marsiglia H, Weidner N, van Tienhoven G, Glanzmann C, Kuten A, Arriagada R, Bartelink H, Van den Bogaert W; EORTC Radiation Oncology and Breast Cancer Groups. Internal Mammary and Medial Supraclavicular Irradiation in Breast Cancer. *N Engl J Med* 2015; **373**: 317-327 [PMID: 26200978 DOI: 10.1056/NEJMoa1415369]

62 **Lee S**, Han S, Shim JH, Kim SY, Won HJ, Shin YM, Kim PN, An J, Lee D, Kim KM, Lim YS, Chung YH, Lee YS, Lee HC. A Patient-Based Nomogram for Predicting Overall Survival after Radiofrequency Ablation for Hepatocellular Carcinoma. *J Vasc Interv Radiol* 2015; **26**: 1787-94.e1 [PMID: 26542708 DOI: 10.1016/j.jvir.2015.08.013]

63 **Gunter MJ**, Murphy N, Cross AJ, Dossus L, Dartois L, Fagherazzi G, Kaaks R, Kühn T, Boeing H, Aleksandrova K, Tjønneland A, Olsen A, Overvad K, Larsen SC, Redondo Cornejo ML, Agudo A, Sánchez Pérez MJ, Altzibar JM, Navarro C, Ardanaz E, Khaw KT, Butterworth A, Bradbury KE, Trichopoulou A, Lagiou P, Trichopoulos D, Palli D, Grioni S, Vineis P, Panico S, Tumino R, Bueno-de-Mesquita B, Siersema P, Leenders M, Beulens JWJ, Uiterwaal CU, Wallström P, Nilsson LM, Landberg R, Weiderpass E, Skeie G, Braaten T, Brennan P, Licaj I, Muller DC, Sinha R, Wareham N, Riboli E. Coffee Drinking and Mortality in 10 European Countries: A Multinational Cohort Study. *Ann Intern Med* 2017; **167**: 236-247 [PMID: 28693038 DOI: 10.7326/M16-2945]

64 **Kadan A**, Ryczko K, Wildman A, Wang R, Roitberg A, Yamazaki T. Accelerated Organic Crystal Structure Prediction with Genetic Algorithms and Machine Learning. *J Chem Theory Comput* 2023; **19**: 9388-9402 [PMID: 38059458 DOI: 10.1021/acs.jctc.3c00853]

World Journal of Gastrointestinal Oncology

Submit a Manuscript: https://www.f6publishing.com

World J Gastrointest Oncol 2024 December 15; 16(12): 4614-4624

DOI: 10.4251/wjgo.v16.i12.4614

ISSN 1948-5204 (online)

ORIGINAL ARTICLE

Retrospective Cohort Study

Local excision for middle-low rectal cancer after neoadjuvant chemoradiation: A retrospective study from a single tertiary center

Nan Chen, Chang-Long Li, Lin Wang, Yun-Feng Yao, Yi-Fan Peng, Tian-Cheng Zhan, Jun Zhao, Ai-Wen Wu

Specialty type: Oncology

Provenance and peer review: Unsolicited article; Externally peer reviewed.

Peer-review model: Single blind

Peer-review report's classification

Scientific Quality: Grade B, Grade C

Novelty: Grade B, Grade C

Creativity or Innovation: Grade B, Grade B

Scientific Significance: Grade B, Grade B

P-Reviewer: Chang YH; Olivani A

Received: July 23, 2024

Revised: August 13, 2024

Accepted: September 5, 2024

Published online: December 15, 2024

Processing time: 112 Days and 0.6 Hours

Nan Chen, Chang-Long Li, Lin Wang, Yun-Feng Yao, Yi-Fan Peng, Tian-Cheng Zhan, Jun Zhao, Ai-Wen Wu, Key Laboratory of Carcinogenesis and Translational Research (Ministry of Education/Beijing), Gastrointestinal Center, Unit III, Peking University Cancer Hospital and Institute, Beijing 100142, China

Co-first authors: Nan Chen and Chang-Long Li.

Corresponding author: Ai-Wen Wu, MD, PhD, Professor, Key Laboratory of Carcinogenesis and Translational Research (Ministry of Education/Beijing), Gastrointestinal Center, Unit III, Peking University Cancer Hospital and Institute, No. 52 Fucheng Road, Haidian District, Beijing 100142, China. wuaw@sina.com

Abstract

BACKGROUND

Rectal cancer has become one of the leading malignancies threatening people's health. For locally advanced rectal cancer (LARC), the comprehensive strategy combining neoadjuvant chemoradiotherapy (NCRT), total mesorectal excision (TME), and adjuvant chemotherapy has emerged as a standard treatment regimen, leading to favorable local control and long-term survival. However, in recent years, an increasing attention has been paid on the exploration of organ preservation strategies, aiming to enhance quality of life while maintaining optimal oncological treatment outcomes. Local excision (LE), compared with low anterior resection (LAR) or abdominal-perineal resection (APR) was introduced dating back to 1970's. LE has historically been linked to a heightened risk of recurrence compared to TME, potentially due to occult lymph node metastasis and intraluminal recurrence. Recent evidence has demonstrated that LE might be an alternative approach, instead of LAR or APR, in cases with favorable tumor regression after NCRT with potentially better quality of life. Therefore, a retrospective analysis of clinicopathological data from mid-low LARC patients who underwent LE after NCRT was conducted, aiming to evaluate the treatment's efficacy, safety, and oncologic prognosis.

AIM

To explore the safety, efficacy, and long-term prognosis of LE in patients with mid-low rectal cancer who had a good response to NCRT.

METHODS

Patients with LE between 2012 to 2021 were retrospectively collected from the

rectal cancer database from Gastro-intestinal Ward III in Peking University Cancer Hospital. The clinicopathological features, postoperative complications, and long-term prognosis of these patients were analyzed. The Kaplan-Meier method was used to create cancer-specific survival curve, and the log-rank test was used to compare the differences regarding outcomes.

RESULTS

A total of 33 patients were included in this study. The median interval between NCRT and surgery was 25.4 (range: 8.7-164.4) weeks. The median operation time was 57 (20.0-137.0) minutes. The initial clinical T staging (cT): 9 (27.3%) patients were cT2, 19 (57.6%) patients were cT3, and 5 (15.2%) patients were cT4; The initial N staging (cN): 8 patients (24.2%) were cN negative, 25 patients (75.8%) were cN positive; The initial M stage (cM): 2 patients (6.1%) had distant metastasis (ycM1), 31 (93.9%) patients had no distant metastasis (cM0). The pathological results: 18 (54.5%) patients were pathological T0 stage (ypT0), 6 (18.2%) patients were ypT1, 7 (21.2%) patients were ypT2, and 2 (6.1%) patients were ypT3. For 9 cT2 patients, 5 (5/9, 55.6%) had a postoperative pathological result of ypT0. For 19 cT3 patients, 11 (57.9%) patients were ypT0, and 2 (40%) were ypT0 in 5 cT4 patients. The most common complication was chronic perineal pain (71.4%, 5/7), followed by bleeding (43%, 3/7), stenosis (14.3%, 1/7), and fecal incontinence (14.3%, 1/7). The median follow-up time was 42.0 (4.0-93.5) months. For 31 patients with cM0, the 5-year disease-free survival (DFS) rate, 5-year local recurrence-free survival (LRFS) rate, and 5-year overall survival (OS) rate were 88.4%, 96.7%, and 92.9%, respectively. There were significant differences between the ycT groups concerning either DFS (P = 0.042) or OS (P = 0.002) in the Kaplan-Meier analysis. The LRFS curve of ycT ≤ T1 patients was better than that of ycT ≥ T2 patients, and the P value was very close to 0.05 (P = 0.070). The DFS curve of patients with ypT ≤ T1 was better than that of patients with ypT ≥ T2, but the P value was not statistically significant (P = 0.560). There was a significant difference between the ypT groups concerning OS (P = 0.014) in the Kaplan-Meier analysis. The LRFS curve of ypT ≤ T1 patients was better than that of ypT ≥ T2 patients, and the P value was very close to 0.05 (P = 0.070). Two patients with initial cM1 were alive at the last follow-up.

CONCLUSION

LE for rectal cancer with significant tumor regression after NCRT can obtain better safety, efficiency, and oncological outcome. Minimally invasive or nonsurgical treatment with patient participation in decision-making can be performed for highly selected patients. Further investigation from multiple centers will bring better understanding of potential advantages regarding local resection.

Key Words: Rectal cancer; Neoadjuvant chemoradiotherapy; Local excision; Prognosis

Core Tip: This retrospective study explores the safety, efficacy, and long-term prognosis of local excision (LE) in patients with middle-low rectal cancer who responded well to neoadjuvant chemoradiotherapy. The findings demonstrate that LE can achieve high rates of organ preservation and favorable oncological outcomes, including a 5-year disease-free survival rate of 88.4% and overall survival rate of 92.9%. Complications were manageable and non-severe. This study supports the potential of minimally invasive treatments in selected patients, highlighting the importance of patient participation in treatment decisions.

Citation: Chen N, Li CL, Wang L, Yao YF, Peng YF, Zhan TC, Zhao J, Wu AW. Local excision for middle-low rectal cancer after neoadjuvant chemoradiation: A retrospective study from a single tertiary center. *World J Gastrointest Oncol* 2024; 16(12): 4614-4624
URL: https://www.wjgnet.com/1948-5204/full/v16/i12/4614.htm
DOI: https://dx.doi.org/10.4251/wjgo.v16.i12.4614

INTRODUCTION

Rectal cancer has attracted more and more attention as a tumor worldwide. Neoadjuvant chemoradiotherapy (NCRT) followed by total mesorectal excision (TME) and adjuvant chemotherapy has been widely used as a classic treatment strategy for patients with locally advanced rectal cancer (LARC), which has shown good local control rate and survival results[1,2]. However, for mid-low rectal cancer, the traditional low anterior resection (LAR) or abdominal-perineal resection (APR) treatment has a series of disadvantages, such as LAR syndrome or permanent stoma[3,4]. In recent years, organ preservation strategy has been recognized by more and more surgeons. Morson *et al*[5] introduced their experience of the traditional transanal approach and surgical criteria for local excision (LE) of early rectal cancer in 1977. Since then, the application of LE for early rectal cancer has gradually increased, and patients have high function preservation and prognosis results[6-8]. However, for more advanced tumors, LE has long been associated with a higher risk of recurrence than TME, which is considered to be related to occult lymph node metastasis and intraluminal recurrence[9,10]. For

LARC, strengthening the intensity of preoperative treatment, such as total neoadjuvant therapy treatment strategy or consolidation chemotherapy, brings better tumor treatment response, and some patients may achieve clinical complete response (cCR) or near-cCR status[11,12]. To date, LE, known as the total mesorectal neglect strategy, for these well-responding rectal cancer patients is still in the exploratory stage[13,14]. The ACOSOG Z6041 study showed that for patients with early rectal cancer, NCRT combined with LE can obtain a better oncologic prognosis and a higher quality of life and anal function[15]. However, some studies have also reported that LE after NCRT has a high incidence of complications and a variable recurrence rate[16,17]. A meta-analysis showed no difference in the risk of postoperative complications between radical surgery and transanal endoscopic microsurgery[18]. Based on these inconsistent results, we retrospectively analyzed the clinicopathological data of patients with mid-low LARC who underwent LE after NCRT in our center and explored the efficiency, safety, and oncological prognosis.

MATERIALS AND METHODS

Patients' selection

The study subjects were rectal cancer patients with a follow-up period of more than 3 years, therefore, databased was formed focusing patients with LE between 2012 to 2021 were retrospectively collected from the rectal cancer database at Peking University Cancer Hospital., and local resection was chosen as the surgical treatment. The exclusion criterion was total mesorectal resection. Screening criteria: (1) Patients with mid-low rectal cancer treated with intensity-modulated radiation therapy (IMRT); and (2) Patients who underwent transanal LE or transanal minimally invasive surgery (TAMIS). The study was approved by the medical ethics committee of the Peking University Cancer Hospital, and informed consent was waived (2015KT31/2017KT104).

IMRT

The IMRT regimen consisted of 22 fractions of 2.3 Gy (gross tumor volume, GTV) and 1.9 Gy (clinical target volume, CTV), which has been described in our previous report[19,20]: The total dose of 50.6 Gy (GTV)/41.8 Gy (CTV) was administered 5 times per week over a period of 30 days. IMRT was administered using the Varian Rapid Arc system. The GTV was defined as the primary tumor, including the mesorectum. The CTV was defined as the primary tumor, mesorectal region, presacral region, mesorectal lymph nodes, lateral lymph nodes, internal iliac lymph node chain, or pelvic wall area. Capecitabine treatment was administered concurrently with IMRT at a dose of 825 mg/m^2 orally, twice *per* day.

LE

The patient was given general anesthesia. According to the location of the tumor, the lithotomy position (the tumor was located in the posterior wall of the rectum) or the jackknife position (the tumor was located in the anterior wall of the rectum) was used. Transanal LE or TAMIS surgery was performed by a skilled surgeon. Local full-thickness resection was performed using an ultrasonic scalpel or electric scalpel at a distance of 1cm from the tumor. The surgical wound was closed by continuous suture with barbed suture or intermittent suture with 4-0 absorbable sutures to ensure complete suture and no active bleeding. After flattening, the surgical specimen was fixed on a soft plate with a pin and sent to the pathology department for paraffin pathological examination. Negative margins were defined as microscopically confirmed full-thickness resections with a circumferential resection margin of 1 mm or more.

Follow up

Patients were regularly followed up every 3 months for the first 2 years and every 6 months thereafter for 3 years. After 5 years, follow-up visits were performed once a year until death or loss of follow-up. Follow-up examinations included digital rectal examination, serum tumor markers, thoracoabdominal/pelvic computed tomography or magnetic resonance imaging, and enteroscopy. Local recurrence-free survival (LRFS) was defined as the time from surgery to the local recurrence, final follow-up, or death (without recurrence or metastasis). Disease-free survival (DFS) was defined as the time from surgery to the first recurrence (local or distant), final follow-up, or death (without recurrence or metastasis). Overall survival (OS) was defined as the time from surgery to death from any cause or final follow-up. The follow-up information was obtained through telephone communication or inquiry into outpatient medical records.

Statistical analysis

Statistical analyses were performed using R software (4.0.4, R Foundation for Statistical Computing, Vienna, Austria). The 'survival' and 'survminer' package were used for survival analysis, and the 'ggplot2' package was used for plotting. The clinicopathological characteristics of patients were descriptive. The measurement variables were expressed as means and standard deviations. Count variables were expressed as percentages. The Kaplan-Meier method was used to draw the tumor-specific survival curve. The Log-rank test was used to examine differences in outcomes. Differences with *P*-values < 0.05 were considered statistically significant.

RESULTS

Basic information of patients

A total of 33 patients were included in this study, and the basic information is shown in Table 1. There were 16 (48.5%) males and 17 (51.5%) females, aged 61.0 (28.0-75.0) years; The median distance between the lower edge of the tumor and the anal verge was 3 (1.0-10.0) cm. The median interval time between NCRT and surgery was 25.4 (8.7-164.4) weeks. The median operation time was 57 (20.0-137.0) min. Four patients underwent salvage APR surgery, and organ preservation was achieved in 29/33 (87.9%) patients. The initial clinical T staging (cT): 9 (27.3%) patients were cT2, 19 (57.6%) patients were cT3, and 5 (15.2%) patients were cT4; The initial N staging (cN): 8 patients (24.2%) were cN negative, 25 patients (75.8%) were cN positive; The initial M stage (cM): 2 patients (6.1%) had distant metastasis (cM1), 31 (93.9%) patients had no distant metastasis (cM0).

Treatment response of the patients

The pathological results: 18 (54.5%) patients were pathological T0 stage (ypT0), 6 (18.2%) patients were ypT1, 7 (21.2%) patients were ypT2, and 2 (6.1%) patients were ypT3. Table 2 shows the treatment response of the patients. For 9 cT2 patients, 5 (5/9, 55.6%) had a postoperative pathological result of ypT0. For 19 cT3 patients, 11 (57.9%) patients were ypT0, and 2 (40%) were ypT0 in 5 cT4 patients.

Perioperative complications of patients

Table 3 shows the perioperative complications of patients. The overall postoperative complication rate was 21.2% (7/33). The most common complication was bleeding (43%, 3/7), followed by chronic perineal pain and stenosis.

Long term of follow-up

The median follow-up time was 42.0 (4.0-93.5) months. For 31 patients with cM0, the 5-year DFS rate, 5-year LRFS rate, and 5-year OS rate were 88.4%, 96.7%, and 92.9%, respectively. Three patients (9.7%, 3/31) had disease progression, including 2 cases of distant metastasis (1 case of lung metastasis, 1 case of bone metastasis) and 1 case of local tumor recurrence and distant metastasis (sacrum and lung metastasis). After local recurrence or distant metastasis, patients received systemic combined local treatment, one patient achieved no evidence of disease status, and two patients died (Shown in Table 4). Figure 1, Figure 2, and Figure 3 show the survival of patients with different cT stages, ycT stages, and ypT stages. There were no significant differences between the cT groups concerning DFS, LRFS or OS in the Kaplan-Meier analysis. There were significant differences between the ycT groups (ycT ≤ T1 *vs* ycT ≥ T2) concerning either DFS (P = 0.042) or OS (P = 0.002) in the Kaplan-Meier analysis. The LRFS curve of ycT ≤ T1 patients was better than that of ycT ≥ T2 patients, and the P value was very close to 0.05 (P = 0.070). The DFS curve of patients with ypT ≤ T1 was better than that of patients with ypT ≥ T2, but the P value was not statistically significant (P = 0.560). There was a significant difference between the ypT groups (ypT ≤ T1 *vs* ypT ≥ T2) concerning OS (P = 0.014) in the Kaplan-Meier analysis. The LRFS curve of ypT ≤ T1 patients was better than that of ypT ≥ T2 patients, and the P value was very close to 0.05 (P = 0.070). Two patients with initial cM1 were alive at the last follow-up.

DISCUSSION

There are few studies on LE after NCRT for rectal cancer, and there are significant differences in surgical indications, technical and pathological reports, postoperative complications, and survival[13,21,22]. The efficacy of LE in patients with different stages is inconsistent[23-26]. This study retrospectively collected the data of patients who underwent LE in our center and clarified the good organ preservation rate, oncological outcomes, and the safety and efficacy of LE after NCRT for rectal cancer. In addition, we found that for patients with initial cM1 and significant local tumor regression after preoperative treatment, LE combined with late systemic treatment also seems to have better clinical results. We believe that for highly selected patients, under the guarantee of salvage surgery and complete postoperative follow-up, the treatment strategy of LE with patient participation in decision-making after NCRT can not only obtain organ preservation but also achieve good long-term survival outcomes.

Safety and efficiency

Our results show that LE is feasible and effective for rectal cancer with significant tumor regression after NCRT. LE was successfully performed in all patients with a median postoperative hospital stay of 4 days. The median operation time was 57.0 minutes, the median intraoperative blood loss was about 10 mL, and no intraoperative adverse events occurred. These results are better than those of conventional TME surgery, which is consistent with the results reported in the meta-analysis[18]. Four patients underwent salvage APR surgery, and organ preservation was achieved in all 29 patients. Previous studies have found that the incidence of complications of LE after NCRT is not low, mainly manifested as incision dehiscence, bleeding, and pain[15-17,27]. Gascon *et al*[28] reported the results of local full-thickness excision for 404 patients with rectal adenoma or rectal cancer, with a complication rate of 12.6%, among which postoperative bleeding was the most common early complication, with an incidence rate of 8%, but the patients in this study did not receive radio chemotherapy before surgery. Geubels *et al*[29] reported LE in patients with regeneration after watch and wait (WW) and the authors believed that LE after radiotherapy had higher surgical complications compared with patients who did not receive radiotherapy. In our study, all patients received preoperative IMRT, which caused intestinal edema,

Table 1 Clinicopathological characteristics of 33 patients

Variables	*n* (%) or median (range)
Age (years)	61.0 (28.0-75.0)
Gender	
Male	16 (48.5)
Female	17 (51.5)
Diameter of lesion (cm)	2.0 (1.0-3.0)
Distance from the anal verge (cm)	3.0 (1.0-10.0)
cT baseline	
1	0 (0.0)
2	9 (27.3)
3	19 (57.6)
4	5 (15.2)
cN baseline	
Negative	8 (24.2)
Positive	25 (75.8)
cM baseline	
M0	31 (93.9)
M1	2 (6.1)
ycT	
0	21 (63.6)
1	5 (15.2)
2	6 (18.2)
3	1 (3.0)
4	0 (0.0)
ypT	
0	18 (54.5)
1	6 (18.2)
2	7 (21.2)
3	2 (6.1)
4	0 (0.0)
Differentiation	
G1	3 (9.1)
G2	29 (87.9)
G3	1(3.0)
Baseline CEA	
Normal	32 (97.0)
Abnormal	1 (3.0)
Interval between NCRT and surgery (week)	25.4 (8.7-164.4)
Chemotherapy	
Cap	13 (39.4)
CapeOx	20 (60.6)
Surgical duration (minute)	57.0 (20.0-137.0)

Blood loss (mL)	10.0 (5.0-50.0)
Postoperative hospital stay (days)	4.0 (1.0-11.0)
Complication	
No complication	26 (78.8)
With complication	7 (21.2)
CD grade	
Grade I	1 (3)
Grade II	6 (18.2)
Grade III-IV	0 (0.0)
Recurrence	
No	31 (93.9)
Yes	2 (6.1)
Metastasis (cM0, *n* = 31)	
No	28 (90.3)
Yes	3 (9.7)
Follow-up time (month)	42.0 (4.0-93.5)

CEA: Carcinoembryonic antigen; NCRT: Neoadjuvant chemoradiotherapy; CD: Clavien dindo; Cap: Capecitabine; CapeOx: Capecitabine + oxaliplatin.

Table 2 Clinical-pathological response to neoadjuvant chemoradiation, *n* (%)

Pre-cT	ypT after local excision			
	ypT0	ypT1	ypT2	ypT3
cT2 (*n* = 9)	5 (55.6)	2 (22.2)	2 (22.2)	0 (0.0)
cT3 (*n* = 19)	11 (57.9)	3 (15.8)	4 (21.1)	1 (5.3)
cT4 (*n* = 5)	2 (40.0)	1 (20.0)	1 (20.0)	1 (20.0)

Table 3 Patients with perioperative complications

Gender	Age	Neoadjuvant	Interval from NCRT to local excision (week)	Type of complications	Clavien-Dindo grades
Male	74	NCRT	69	Bleeding	II
Male	68	NCRT	18	Bleeding	I
Female	59	NCRT	11	Perineal pain	II
Female	71	NCRT	11	Perineal pain	II
Male	40	NCRT + CapOx	24	Perineal pain + stricture	II
Male	56	NCRT + CapOx	59	Pain + fecal incontinence	II
Female	66	NCRT + CapOx	32	Bleeding + pain	II

NCRT: Neoadjuvant chemoradiotherapy; CapOx: Capecitabine + oxaliplatin.

fibrosis changes, and relatively poor intestinal quality, which could explain the high overall complication rate of 21.2% (7/33). The most common complication was chronic perineal pain (71.4%, 5/7), followed by bleeding (43%, 3/7), stenosis (14.3%, 1/7), and fecal incontinence (14.3%, 1/7). However, all complications were grade I-II and improved after the drug or conservative treatment, and no serious postoperative adverse events occurred. Therefore, we believe that LE has good safety for rectal cancer with a good response after NCRT. There is no unified standard for LE after chemoradiotherapy. The experience of our center is as follows: For residual tumors or scars after chemoradiotherapy, it is recommended to perform localized scar and full-thickness bowel wall resection followed by full-thickness suture. Because the defect of the intestinal wall after tumor resection, especially the significant retraction of the mucosa, will make the tension of the

Table 4 Patients with disease progression after local excision

Patient (sex/age)	Primary staging				NCRT	Interval time (week)	Response		Disease progression		Prognosis			
	cT	cN	cM	High-risk factor (s)			mrTRG	ypT	Local recurrence	Distant metastasis	Treatment	DFS (month)	OS (month)	Status
Male/74	T4	N1	cM0	cT4	NCRT	8.7	0	ypT0	Negative	Bone	C	9.3	64.6	Dead
Female/57	T3	N2	cM0	EMVI+	NCRT + CapOx2	9	0	ypT0	Negative	Lung	C+ resection	27.5	76.5	Alive (NED)
Female /61	T2	N2	cM0	N2	NCRT	101	3	ypT0	Positive	Sacrum and Lung	Resection	6.1	49.4	Dead
Female /36	T4	N1	cM1	cT4	CRT + CapOx2	19	2	ypT2	Negative	Lung	C+ resection		42.0	Alive (NED)
Female /30	T4	N2	cM1	cT4	CRT+CapOx1	36	1	ypT0	Positive	Liver	Resection		27.5	Alive (NED)

NCRT: Neoadjuvant chemoradiotherapy; EMVI: Extramural venous invasion; DFS: Disease-free survival; OS: Overall survival; NED: No evidence of disease; CapOx: Capecitabine + oxaliplatin.

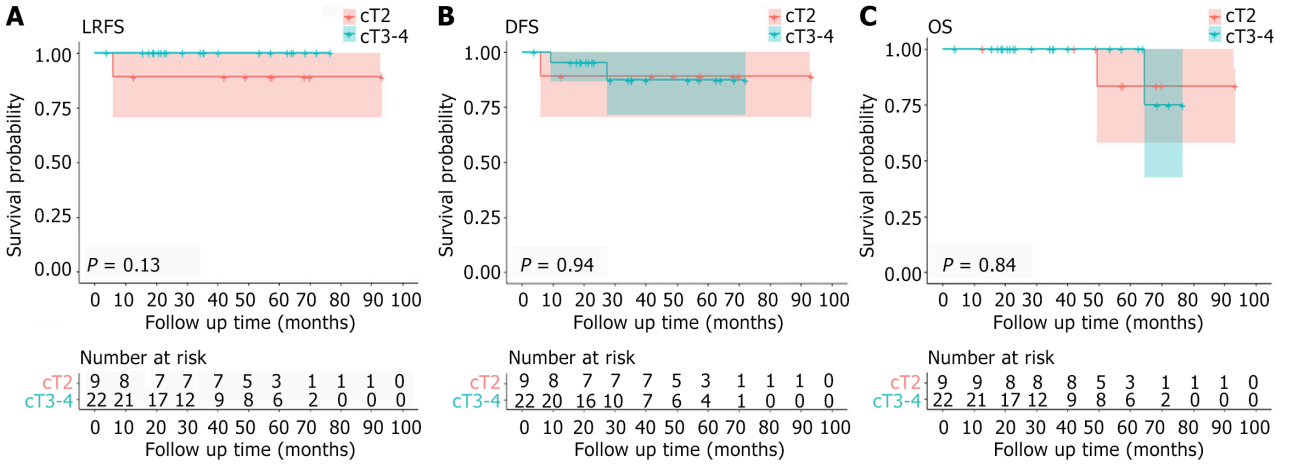

Figure 1 The prognosis analysis of 31 cM0 patients by Kaplan–Meier curves for cT stage groups. A: Local recurrence-free survival curves (P = 0.127); B: Disease-free survival curves (P = 0.945); C: Overall survival curves (P = 0.838). LRFS: Local recurrence-free survival; DFS: Disease-free survival; OS: Overall survival.

primary suture high. So the problems of incision dehiscence, dead space, and infection caused by large-scale mucosal resection and simple mucosal suture should be avoided. For the mass of the anterior wall, attention should be paid to the protection of the prostate or vagina with a rich blood supply during the suture, to avoid intraoperative or postoperative bleeding.

Prognosis

As a surgical treatment method that ignores the whole mesentery, LE breaks the long-standing principle of TME, but local recurrence is its Achilles heel, and patients with different T stages have different recurrence rates[30]. In a multicenter prospective study of LE in T1 patients and LE plus adjuvant chemoradiotherapy in T2 patients, the 7-year local recurrence rate was 8% in T1 patients and 18% in T2 patients[23]. A systematic review including 20 studies and 1068 patients showed that the local recurrence rate of ypT0 patients was 4%, and that of ypT1-3 patients was more than 21.9% [31]. In our study, the local recurrence rate was 0% (0/17) in patients with ypT0 and 7.1% (1/14) in patients with ypT1-3. No recurrence or metastasis events occurred in the 2 patients with ypT3. One of the patients with ypT3 underwent salvage surgery, and the other patient refused salvage surgery and took an observation strategy. Local recurrence occurred in only 1 (ycT2/ypT2) of 31 patients with cM0 rectal cancer and did not result in uncontrolled regional disease. Our study showed a very high local control rate, and the overall 5-year LRFS rate was 96.7%. The 5-year DFS rate was 88.4%, which is similar to CARTS Study[9], but our study had more clinical stage III patients and a better local recurrence rate. Although 3 patients (9.7%, 3/31) had disease progression (recurrence and/or metastasis), the OS of the patients after systemic therapy was up to 76.5 months, and the 5-year OS rate was 92.9%, showing a good survival result. Similar to our findings, ACOSOG Z6041 also showed favorable oncological outcomes. When the authors performed NCRT plus LE

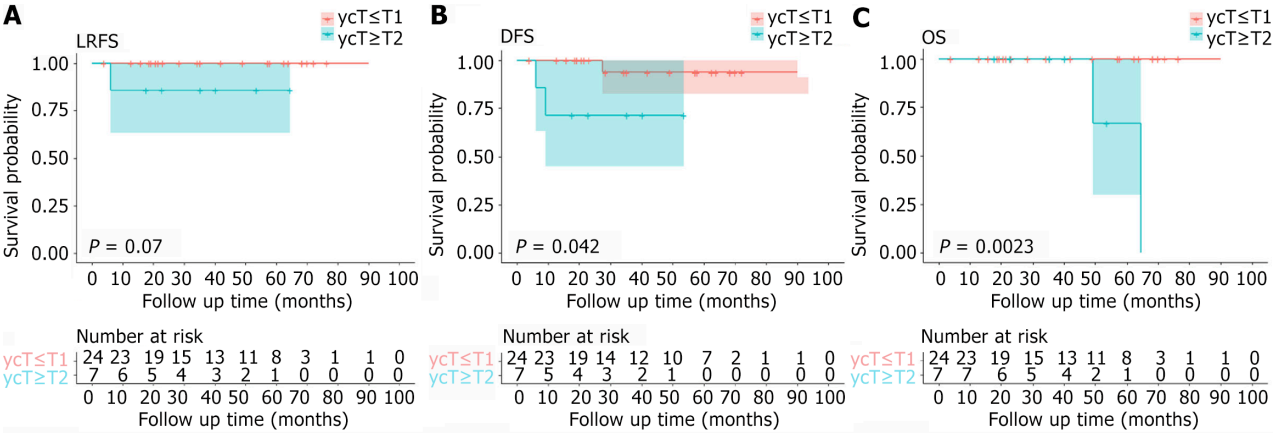

Figure 2 The prognosis analysis of 31 cM0 patients by Kaplan– Meier curves for ycT stage groups. A: Local recurrence-free survival curves (P = 0.070); B: Disease-free survival curves (P = 0.042); C: Overall survival curves (P = 0.002). LRFS: Local recurrence-free survival; DFS: Disease-free survival; OS: Overall survival.

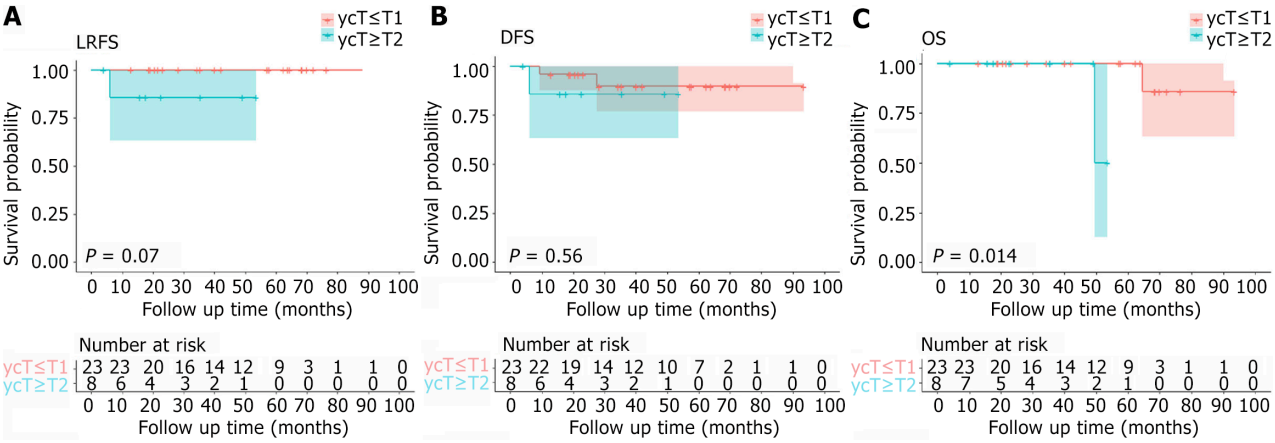

Figure 3 The prognosis analysis of 31 cM0 patients by Kaplan–Meier curves for ypT stage groups. A: Local recurrence-free survival curves (P = 0.070); B: Disease-free survival curves (P = 0.560); C: Overall survival curves (P = 0.014). LRFS: Local recurrence-free survival; DFS: Disease-free survival; OS: Overall survival.

surgery in T2N0 patients, distant recurrence occurred in 6% of patients and local recurrence occurred in 4% of patients, resulting in 3-year disease-free and OS rates of 88% and 95%, respectively[15]. We believe that this better prognosis result was due to patient screening. In our study, after intensive NCRT, most of the patients were the ypT0-2 stage, and only 2 were ypT3 stage. On the other hand, salvage surgery based on postoperative pathology ensures a good prognosis for patients. The 2 initial M1 patients were both alive at the last follow-up, and the OS was 27.5 months and 42.0 months, respectively, which achieved a good prognosis but needed more data support. We believe that for highly selected patients, under the guarantee of salvage surgery and complete postoperative follow-up, the treatment strategy of LE after NCRT can not only obtain organ preservation but also achieve good long-term survival outcomes.

Our study did not involve the analysis of predictive factors for tumor recurrence and metastasis. However, the KM survival curve showed that the LRFS, DFS, and OS curves of patients with earlier ycT and ypT stages (ycT ≤ T1 and ypT ≤ T1) were better than those of other patients. Previous reports have shown that the pT stage, sm stage, tumor grading, histological risk status, and local surgical resection technique are independent risk factors for local recurrence[6,32]. Other studies have also shown a large difference in the recurrence rate of different T stages. It has been reported that the 5-year LRFS after local resection is 28%, which is 18% in T1 patients and 47% in T2 patients[30]. In our study, the 5-year LRFS rates of patients with ycT0-1 and ypT0-1 were both 100%, so we should strengthen the follow-up of patients with ypT2 and more after LE.

Our study had some limitations. First, it was a retrospective study. High-quality prospective randomized controlled studies may be needed to verify our better results. Second, the number of patients is not large, and this limited our statistical analyses, and we may need to expand the sample size for further verification.

Prospect

For rectal cancer patients with near-cCR after NCRT, selective implementation of LE is a safe and effective treatment strategy. For patients judged as cCR or possible pCR, the non-surgical strategy of the WW strategy can be selected[11]. Even in the WW process, early local regeneration followed by LE is a safe and effective treatment strategy. So, we

emphasize the importance of predicting tumor response to NCRT, which is also described in our other article. Minimally invasive or nonsurgical treatment with patient participation in decision-making can be performed for highly selected patients.

CONCLUSION

LE for rectal cancer with significant tumor regression after NCRT can obtain better safety, efficiency, and oncological prognosis. Minimally invasive or nonsurgical treatment with patient participation in decision-making can be performed for highly selected patients. More studies are needed to verify this result.

FOOTNOTES

Author contributions: Chen N and Li CL performed the data collection and analysis, and wrote the paper; Chen N, Wang L, Yao YF, Peng YF, Zhan TC, Zhao J and Wu AW helped the recruitment of patients; Wu AW designed study.

Supported by Beijing Municipal Administration of Hospitals Incubating Program, No. PZ2020027; Beijing Talent Incubating Funding, No. 2019-4; National Natural Science Foundation of China, No. 81773214; Beijing Hospitals Authority Clinical Medicine Development of Special Funding Support, No. ZYLX202116; National Key R and D Program of China, No. 2021YFF1201104; 2019 Major and Difficult Diseases Chinese and Western Medicine Coordination Capacity Colorectal Cancer Project, No. (2018) 275; Science Foundation of Peking University Cancer Hospital-2023, No. JC202310; and Natural Science Project of Chifeng City, No. 2023-114.

Institutional review board statement: The study was approved by the medical ethics committee of the Peking University Cancer Hospital, and informed consent was waived (2015KT31/2017KT104).

Informed consent statement: All study participants, or their legal guardian, provided informed written consent prior to study enrollment.

Conflict-of-interest statement: All authors declare no conflict of interest.

Data sharing statement: No additional data are available.

STROBE statement: The authors have read the STROBE Statement—checklist of items, and the manuscript was prepared and revised according to the STROBE Statement—checklist of items.

Country of origin: China

ORCID number: Nan Chen 0000-0002-0085-7472; Chang-Long Li 0000-0001-6665-2341; Lin Wang 0000-0002-5313-5297; Yun-Feng Yao 0000-0001-8433-0688; Yi-Fan Peng 0000-0002-6159-6088; Tian-Cheng Zhan 0000-0002-4711-5505; Ai-Wen Wu 0000-0002-9650-1962.

S-Editor: Liu H
L-Editor: A
P-Editor: Zhang XD

REFERENCES

1 **National Health Commission of the People's Republic of China**. National guidelines for diagnosis and treatment of colorectal cancer 2020 in China (English version). *Chin J Cancer Res* 2020; **32**: 415-445 [PMID: 32965276 DOI: 10.21147/j.issn.1000-9604.2020.04.01]
2 **Zaborowski A**, Stakelum A, Winter DC. Systematic review of outcomes after total neoadjuvant therapy for locally advanced rectal cancer. *Br J Surg* 2019; **106**: 979-987 [PMID: 31074508 DOI: 10.1002/bjs.11171]
3 **Lindgren R**, Hallböök O, Rutegård J, Sjödahl R, Matthiessen P. What is the risk for a permanent stoma after low anterior resection of the rectum for cancer? A six-year follow-up of a multicenter trial. *Dis Colon Rectum* 2011; **54**: 41-47 [PMID: 21160312 DOI: 10.1007/DCR.0b013e3181fd2948]
4 **Bulens PP**, Smets L, Debucquoy A, Joye I, D'Hoore A, Wolthuis A, Debrun L, Dekervel J, Van Cutsem E, Dresen R, Vandecaveye V, Deroose CM, Sagaert X, Haustermans K. Nonoperative versus operative approach according to the response to neoadjuvant chemoradiotherapy for rectal cancer: A prospective cohort study. *Clin Transl Radiat Oncol* 2022; **36**: 113-120 [PMID: 35993092 DOI: 10.1016/j.ctro.2022.07.009]
5 **Morson BC**, Bussey HJ, Samoorian S. Policy of local excision for early cancer of the colorectum. *Gut* 1977; **18**: 1045-1050 [PMID: 606631 DOI: 10.1136/gut.18.12.1045]

6 **Dekkers N**, Dang H, van der Kraan J, le Cessie S, Oldenburg PP, Schoones JW, Langers AMJ, van Leerdam ME, van Hooft JE, Backes Y, Levic K, Meining A, Saracco GM, Holman FA, Peeters KCMJ, Moons LMG, Doornebosch PG, Hardwick JCH, Boonstra JJ. Risk of recurrence after local resection of T1 rectal cancer: a meta-analysis with meta-regression. *Surg Endosc* 2022; **36**: 9156-9168 [PMID: 35773606 DOI: 10.1007/s00464-022-09396-3]

7 **Lee L**, Kelly J, Nassif GJ, Atallah SB, Albert MR, Shridhar R, Monson JRT. Chemoradiation and Local Excision for T2N0 Rectal Cancer Offers Equivalent Overall Survival Compared to Standard Resection: a National Cancer Database Analysis. *J Gastrointest Surg* 2017; **21**: 1666-1674 [PMID: 28819913 DOI: 10.1007/s11605-017-3536-5]

8 **Halverson AL**, Morris AM, Cleary RK, Chang GJ. For Patients with Early Rectal Cancer, Does Local Excision Have an Impact on Recurrence, Survival, and Quality of Life Relative to Radical Resection? *Ann Surg Oncol* 2019; **26**: 2497-2506 [PMID: 31025228 DOI: 10.1245/s10434-019-07328-5]

9 **Stijns RCH**, de Graaf EJR, Punt CJA, Nagtegaal ID, Nuyttens JJME, van Meerten E, Tanis PJ, de Hingh IHJT, van der Schelling GP, Acherman Y, Leijtens JWA, Bremers AJA, Beets GL, Hoff C, Verhoef C, Marijnen CAM, de Wilt JHW; CARTS Study Group. Long-term Oncological and Functional Outcomes of Chemoradiotherapy Followed by Organ-Sparing Transanal Endoscopic Microsurgery for Distal Rectal Cancer: The CARTS Study. *JAMA Surg* 2019; **154**: 47-54 [PMID: 30304338 DOI: 10.1001/jamasurg.2018.3752]

10 **Landmann RG**, Wong WD, Hoepfl J, Shia J, Guillem JG, Temple LK, Paty PB, Weiser MR. Limitations of early rectal cancer nodal staging may explain failure after local excision. *Dis Colon Rectum* 2007; **50**: 1520-1525 [PMID: 17674104 DOI: 10.1007/s10350-007-9019-0]

11 **Wang L**, Zhang XY, Zhao YM, Li SJ, Li ZW, Sun YS, Wang WH, Wu AW; Rectal Cancer Cooperative Group of Peking University Cancer Hospital. Intentional Watch and Wait or Organ Preservation Surgery Following Neoadjuvant Chemoradiotherapy Plus Consolidation CAPEOX for MRI-defined Low-risk Rectal Cancer: Findings From a Prospective Phase 2 Trial (PKUCH-R01 Trial, NCT02860234). *Ann Surg* 2023; **277**: 647-654 [PMID: 35766394 DOI: 10.1097/SLA.0000000000005507]

12 **Cerdán-Santacruz C**, Vailati BB, São Julião GP, Habr-Gama A, Perez RO. Watch and wait: Why, to whom and how. *Surg Oncol* 2022; **43**: 101774 [PMID: 35491334 DOI: 10.1016/j.suronc.2022.101774]

13 **Smith FM**, Ahad A, Perez RO, Marks J, Bujko K, Heald RJ. Local Excision Techniques for Rectal Cancer After Neoadjuvant Chemoradiotherapy: What Are We Doing? *Dis Colon Rectum* 2017; **60**: 228-239 [PMID: 28059920 DOI: 10.1097/DCR.0000000000000749]

14 **Madoff RD**. Total mesorectal neglect in the age of total mesorectal excision. *J Clin Oncol* 2013; **31**: 4273-4275 [PMID: 24166519 DOI: 10.1200/JCO.2013.52.6434]

15 **Garcia-Aguilar J**, Renfro LA, Chow OS, Shi Q, Carrero XW, Lynn PB, Thomas CR Jr, Chan E, Cataldo PA, Marcet JE, Medich DS, Johnson CS, Oommen SC, Wolff BG, Pigazzi A, McNevin SM, Pons RK, Bleday R. Organ preservation for clinical T2N0 distal rectal cancer using neoadjuvant chemoradiotherapy and local excision (ACOSOG Z6041): results of an open-label, single-arm, multi-institutional, phase 2 trial. *Lancet Oncol* 2015; **16**: 1537-1546 [PMID: 26474521 DOI: 10.1016/S1470-2045(15)00215-6]

16 **Perez RO**, Habr-Gama A, Lynn PB, São Julião GP, Bianchi R, Proscurshim I, Gama-Rodrigues J. Transanal endoscopic microsurgery for residual rectal cancer (ypT0-2) following neoadjuvant chemoradiation therapy: another word of caution. *Dis Colon Rectum* 2013; **56**: 6-13 [PMID: 23222274 DOI: 10.1097/DCR.0b013e318273f56f]

17 **Rullier E**, Rouanet P, Tuech JJ, Valverde A, Lelong B, Rivoire M, Faucheron JL, Jafari M, Portier G, Meunier B, Sileznieff I, Prudhomme M, Marchal F, Pocard M, Pezet D, Rullier A, Vendrely V, Denost Q, Asselineau J, Doussau A. Organ preservation for rectal cancer (GRECCAR 2): a prospective, randomised, open-label, multicentre, phase 3 trial. *Lancet* 2017; **390**: 469-479 [PMID: 28601342 DOI: 10.1016/S0140-6736(17)31056-5]

18 **Ahmad NZ**, Abbas MH, Abunada MH, Parvaiz A. A Meta-analysis of Transanal Endoscopic Microsurgery versus Total Mesorectal Excision in the Treatment of Rectal Cancer. *Surg J (N Y)* 2021; **7**: e241-e250 [PMID: 34541316 DOI: 10.1055/s-0041-1735587]

19 **Wang L**, Li ZY, Li ZW, Li YH, Sun YS, Ji JF, Gu J, Cai Y. Efficacy and safety of neoadjuvant intensity-modulated radiotherapy with concurrent capecitabine for locally advanced rectal cancer. *Dis Colon Rectum* 2015; **58**: 186-192 [PMID: 25585076 DOI: 10.1097/DCR.0000000000000294]

20 **Li C**, Guan Z, Zhao Y, Sun T, Li Z, Wang W, Li Z, Wang L, Wu A. Predictors of pathologic complete response in patients with residual flat mucosal lesions after neoadjuvant chemoradiotherapy for locally advanced rectal cancer. *Chin J Cancer Res* 2022; **34**: 383-394 [PMID: 36199540 DOI: 10.21147/j.issn.1000-9604.2022.04.06]

21 **Leijtens JWA**, Smits LJH, Koedam TWA, Orsini RG, van Aalten SM, Verseveld M, Doornebosch PG, de Graaf EJR, Tuynman JB. Long-term oncological outcomes after local excision of T1 rectal cancer. *Tech Coloproctol* 2023; **27**: 23-33 [PMID: 36028782 DOI: 10.1007/s10151-022-02661-6]

22 **Ung L**, Chua TC, Engel AF. A systematic review of local excision combined with chemoradiotherapy for early rectal cancer. *Colorectal Dis* 2014; **16**: 502-515 [PMID: 24605870 DOI: 10.1111/codi.12611]

23 **Greenberg JA**, Shibata D, Herndon JE 2nd, Steele GD Jr, Mayer R, Bleday R. Local excision of distal rectal cancer: an update of cancer and leukemia group B 8984. *Dis Colon Rectum* 2008; **51**: 1185-91; discussion 1191 [PMID: 18536973 DOI: 10.1007/s10350-008-9231-6]

24 **Guerrieri M**, Gesuita R, Ghiselli R, Lezoche G, Budassi A, Baldarelli M. Treatment of rectal cancer by transanal endoscopic microsurgery: experience with 425 patients. *World J Gastroenterol* 2014; **20**: 9556-9563 [PMID: 25071352 DOI: 10.3748/wjg.v20.i28.9556]

25 **Peltrini R**, Imperatore N, Di Nuzzo MM, Pellino G. Towards personalized treatment of T2N0 rectal cancer: A systematic review of long-term oncological outcomes of neoadjuvant therapy followed by local excision. *J Gastroenterol Hepatol* 2022; **37**: 1426-1433 [PMID: 35614027 DOI: 10.1111/jgh.15898]

26 **Peltrini R**, Sacco M, Luglio G, Bucci L. Local excision following chemoradiotherapy in T2-T3 rectal cancer: current status and critical appraisal. *Updates Surg* 2020; **72**: 29-37 [PMID: 31621033 DOI: 10.1007/s13304-019-00689-2]

27 **Arezzo A**, Arolfo S, Allaix ME, Munoz F, Cassoni P, Monagheddu C, Ricardi U, Ciccone G, Morino M. Results of neoadjuvant short-course radiation therapy followed by transanal endoscopic microsurgery for t1-t2 n0 extraperitoneal rectal cancer. *Int J Radiat Oncol Biol Phys* 2015; **92**: 299-306 [PMID: 25772184 DOI: 10.1016/j.ijrobp.2015.01.024]

28 **Gascon MA**, Aguilella V, Martinez T, Antinolfi L, Valencia J, Ramírez JM. Local full-thickness excision for sessile adenoma and cT1-2 rectal cancer: long-term oncological outcome. *Langenbecks Arch Surg* 2022; **407**: 2431-2439 [PMID: 35732844 DOI: 10.1007/s00423-022-02593-7]

29 **Geubels BM**, Meyer VM, van Westreenen HL, Beets GL, Grotenhuis BA; On Behalf Of The Dutch Watch And Wait Consortium. Role of Local Excision for Suspected Regrowth in a Watch and Wait Strategy for Rectal Cancer. *Cancers (Basel)* 2022; **14** [PMID: 35804843 DOI: 10.3390/cancers14133071]

30 **Mellgren A**, Sirivongs P, Rothenberger DA, Madoff RD, García-Aguilar J. Is local excision adequate therapy for early rectal cancer? *Dis Colon Rectum* 2000; **43**: 1064-71; discussion 1071 [PMID: 10950004 DOI: 10.1007/BF02236551]

31 **Hallam S**, Messenger DE, Thomas MG. A Systematic Review of Local Excision After Neoadjuvant Therapy for Rectal Cancer: Are ypT0 Tumors the Limit? *Dis Colon Rectum* 2016; **59**: 984-997 [PMID: 27602930 DOI: 10.1097/DCR.0000000000000613]

32 **Morino M**, Allaix ME, Caldart M, Scozzari G, Arezzo A. Risk factors for recurrence after transanal endoscopic microsurgery for rectal malignant neoplasm. *Surg Endosc* 2011; **25**: 3683-3690 [PMID: 21647814 DOI: 10.1007/s00464-011-1777-z]

World Journal of Gastrointestinal Oncology

Submit a Manuscript: https://www.f6publishing.com

World J Gastrointest Oncol 2024 December 15; 16(12): 4625-4635

DOI: 10.4251/wjgo.v16.i12.4625

ISSN 1948-5204 (online)

ORIGINAL ARTICLE

Retrospective Study

Risk factors for hepatocellular carcinoma in cirrhosis: A comprehensive analysis from a decade-long study

Da-Qiong Zhou, Jiang-Yu Liu, Feng Zhao, Jing Zhang, Li-Li Liu, Jian-Ru Jia, Zhen-Huan Cao

Specialty type: Oncology

Provenance and peer review: Unsolicited article; Externally peer reviewed.

Peer-review model: Single blind

Peer-review report's classification

Scientific Quality: Grade C, Grade D

Novelty: Grade C, Grade C

Creativity or Innovation: Grade C, Grade C

Scientific Significance: Grade B, Grade D

P-Reviewer: Cai SS; Jayakumar S

Received: May 9, 2024

Revised: August 28, 2024

Accepted: October 9, 2024

Published online: December 15, 2024

Processing time: 187 Days and 8.4 Hours

Da-Qiong Zhou, Jiang-Yu Liu, Jing Zhang, Li-Li Liu, Zhen-Huan Cao, Department of Hepatology, Beijing Youan Hospital, Capital Medical University, Beijing 100069, China

Feng Zhao, Jian-Ru Jia, Hepatology Center, Baoding People's Hospital, Baoding 071000, Hebei Province, China

Co-first authors: Da-Qiong Zhou and Jiang-Yu Liu.

Co-corresponding authors: Jian-Ru Jia and Zhen-Huan Cao.

Corresponding author: Zhen-Huan Cao, Doctor, Professor, Department of Hepatology, Beijing Youan Hospital, Capital Medical University, No. 8 Xitoutiao, You'anmen Wai, Fengtai District, Beijing 100069, China. caozhenhuanyu@mail.ccmu.edu.cn

Abstract

BACKGROUND

Cirrhosis is a significant risk factor for the development of hepatocellular carcinoma (HCC). Variability in HCC risk among patients with cirrhosis is notable, particularly when considering the diverse etiologies of cirrhosis.

AIM

To identify specific risk factors contributing to HCC development in patients with cirrhosis.

METHODS

This retrospective study analyzed data from cirrhotic patients at Beijing Youan Hospital from January 1, 2012 to September 30, 2022 with at least 6 mo of follow-up. Patient demographics, medical histories, etiologies, and clinical characteristics were examined. Cox regression analysis was used to analyze correlations of the above parameters with hepatocarcinogenesis, while competing risk regression was used to estimate their adjusted hazard ratios accounting for death. The cumulative incidence was plotted over time.

RESULTS

Overall, 5417 patients with cirrhosis (median age: 54 years; 65.8% males) were analyzed. Hepatitis B virus (HBV) was the most common etiology (23.3%), with 25% (n = 1352) developing HCC over a 2.9-year follow-up period. Patients with multiple etiologies had the HCC highest incidence (30.3%), followed by those with HBV-related cirrhosis (29.5%). Significant risk factors included male sex,

advanced age, hepatitis C virus (HCV) infection, elevated blood ammonia, and low platelet count. Men had a higher 5-year HCC risk than women (37.0% *vs* 31.5%). HBV, HCV, and HBV/HCV co-infected patients had 5-year risks of HCC of 45.8%, 42.9%, and 48.1%, respectively, compared to 29.5% in nonviral hepatitis cases, highlighting the significant HCC risk from viral hepatitis, especially HBV, and underscores the importance of monitoring these high-risk groups.

CONCLUSION

In conclusion, HBV-related cirrhosis strongly correlates with HCC, with male sex, older age, viral hepatitis, elevated blood ammonia, and lower albumin and platelet levels increasing the risk of HCC.

Key Words: Cirrhosis; Hepatocellular carcinoma; Risk factors; Hepatitis B virus; Competing risk analysis

Core Tip: Our retrospective analysis spanned a decade (January 1, 2012 to September 30, 2022) and included 5417 patients from Beijing Youan Hospital, Capital Medical University. Using Cox regression and competing risk regression models, we identified several key factors that significantly contributed to the risk of hepatocellular carcinoma in patients with cirrhosis. Specifically, this study underscores the increased association of hepatitis B cirrhosis with hepatocellular carcinoma incidence and highlights other significant risk factors, including male sex, advanced age, viral hepatitis-related cirrhosis, elevated blood ammonia, and lower albumin and platelet levels.

Citation: Zhou DQ, Liu JY, Zhao F, Zhang J, Liu LL, Jia JR, Cao ZH. Risk factors for hepatocellular carcinoma in cirrhosis: A comprehensive analysis from a decade-long study. *World J Gastrointest Oncol* 2024; 16(12): 4625-4635
URL: https://www.wjgnet.com/1948-5204/full/v16/i12/4625.htm
DOI: https://dx.doi.org/10.4251/wjgo.v16.i12.4625

INTRODUCTION

Cirrhosis is a major cause of morbidity and mortality in patients with chronic liver disease[1]. In 2019, 2.4% of the global deaths were related to cirrhosis. It is among the top 20 causes of death worldwide[2]. Abnormalities in liver function of patients with cirrhosis include varices, gastrointestinal bleeding, ascites, and hepatic encephalopathy. Hepatocellular carcinoma (HCC) is a serious complication. The prognosis of HCC is usually poor[3]. According to global burden statistics, there were approximately 534000 liver cancer cases and 485000 deaths in 2019[4]. With over 290000 people diagnosed with liver cancer and approximately 188000 deaths from liver cancer in 2019[5], China has the highest burden of liver cancer worldwide.

Major causes of cirrhosis include chronic viral hepatitis, such as hepatitis B virus (HBV) and hepatitis C virus (HCV), chronic alcohol abuse, metabolic disorders, and autoimmune liver diseases. Specifically, HBV infection is the leading cause of liver cancer-related mortality and the third leading cause of cirrhosis[6]. While antiviral therapies for chronic hepatitis B have shown efficacy in reducing the risk of cirrhosis, decompensation, and HCC, their ability to significantly affect HBV-related mortality trends remains limited[7]. As of 2019, only 10.3% of chronic HBV infections have been diagnosed, of which only 22.7% are eligible for antiviral treatment[8]. Despite a notable decline in HBV and HCV incidences, China continues to bear the highest global disease burden for HBV (74 million) and HCV (9.48 million) infections, attributed to its vast patient population[9]. Concurrently, the rise in alcohol-associated cirrhosis (AC) and metabolic dysfunction-associated liver disease (MASLD) parallels lifestyle shifts and economic progression, increasing the annual prevalence of advanced liver diseases and the overall disease burden[10].

Cirrhosis is a major risk factor for HCC, with autopsy studies showing cirrhosis in 80%-90% of cases worldwide. In areas with high HBV prevalence, cirrhotic individuals have triple the risk of developing HCC compared to non-cirrhotic individuals and 16 times that of inactive HBV carriers[11]. Beyond progression to HCC, patients with cirrhosis also face an increased risk of liver complications and mortality, particularly as the disease progresses from the compensated to the decompensated stages[12]. The survival rates at 1 and 5 years for patients with compensated cirrhosis were 87% and 67%, in contrast to 75% and 45%, respectively, for patients with decompensated cirrhosis. Compared to the general population, mortality increases five-fold in patients with compensated cirrhosis and ten-fold in decompensated cirrhosis[13]. Notably, chronic comorbidities such as chronic kidney and cardiovascular diseases are often associated with death due to compensatory cirrhosis[14].

To gain a deeper understanding of the prognosis of cirrhosis with different etiologies and liver function states, this retrospective observational study retrieved data from patients with cirrhosis hospitalized at Beijing Youan Hospital over the past 10 years. This study aimed to better understand and guide the clinical management of cirrhosis, as well as to improve the prognosis and personalized treatment planning for patients with cirrhosis.

MATERIALS AND METHODS

Research population

Patients with cirrhosis who were admitted to our hospital from January 1, 2012 to September 30, 2022 were identified from our inpatient system based on the diagnosis code K74 (cirrhosis). The main inclusion criteria were: (1) Diagnosis of cirrhosis based on histology (liver biopsy), imaging (evidence of esophagogastric fundal varices, portal hypertension, splenomegaly, and ascites), or noninvasive examination (FibroScan); (2) Two or more hospitalizations; (3) No diagnosis of HCC at the initial hospitalization and within 6 mo of initial admission; and (4) A minimum of 6 mo of follow-up. Patients with other combined malignancies or those who underwent liver transplantation were excluded.

The time of first admission was defined as the baseline, and clinical characteristics at baseline were collected, including demographics (sex, age, and place of origin), comorbidities (diabetes mellitus, hypertension, and coronary artery disease), liver disease-related complications (esophagogastric fundal varices, gastrointestinal bleeding, ascites, abdominal infections, hepatic encephalopathy, and hepatorenal syndrome), etiology [HBV, HCV, AC, MASLD, primary biliary cirrhosis (PBC), drug-induced cirrhosis, cryptogenic cirrhosis, and mixed cirrhosis], laboratory findings, and liver function scores (model for end-stage liver disease score and Child-Pugh classification).

Endpoint events

The primary endpoint was HCC. Observational endpoint was the time to first document HCC. For patients who did not develop HCC, the observational endpoint was death or time to the last follow-up. Death was a competing risk event for hepatocarcinogenesis because patients with cirrhosis who died were no longer at risk of developing HCC.

Statistical analysis

Pearson χ^2 test and Wilcoxon signed-rank test were used to evaluate correlations of categorical and continuous variables with HCC occurrence for clinical characteristics and laboratory values, respectively. The results are expressed as percentages and interquartile ranges. Only patients with cirrhosis for at least 6 mo from baseline to endpoint events were included in the analysis of all HCC-associated risk factors.

Multiple imputations were used to adjust for missing values of all variables. Cox proportional hazards regression analysis was performed on the imputed data set. Clinical and demographic variables that differed significantly between the groups ($P < 0.05$) were included in the first statistical step of the model by univariate analysis using both forward and backward stepwise Cox regressions. The same set of seven significant risk factors were selected: Age, sex, history of HBV/HCV infection, albumin level, globulin level, platelet count, and blood ammonia level.

The decompensation rate in patients with cirrhosis was 76.6%. Death was considered a competing risk event when assessing the incidence of HCC in patients with decompensated cirrhosis to obtain a reliable risk estimate because the potential risk of death is high[15]. Cox regression analyses were performed for selected multivariate risk factors from the Cox analysis. We then calculated adjusted hazard ratios (aHRs). A fine and gray regression model was used to estimate the cumulative incidence function (CIF) for HCC development in cirrhotic patients of different sexes, ages, and etiologies.

All statistical analyses in this study were performed using R version 4.2.0 and IBM Statistical Product and Service Solutions 27.0.

RESULTS

Patient characteristics at first admission

Overall, 5417 patients were included (Figure 1). The median age was 54 years, 3567 (65.8%) patients were male, and 4149 (76.6%) had decompensated cirrhosis. Etiological distribution of cirrhosis is shown in Figure 2: 1261 cases (23.3%) of HBV; 354 cases (6.5%) of HCV; 1274 cases (23.5%) of AC; 51 cases (0.9%) of MASLD; 470 cases (8.7%) of PBC; 66 cases (1.2%) of drug-induced cirrhosis; 1459 cases (26.9%) of cryptogenic cirrhosis; and 482 cases (8.9%) of mixed cirrhosis (two or more etiologies).

HCC occurred in 1352 patients (25%) and 4065 patients did not develop HCC during the in-hospital follow-up period. There were 262 deaths (4.84%) due to complications or other comorbidities among the patients who did not develop HCC.

Based on the occurrence of HCC during follow-up, the observational cohort was divided into HCC and non-HCC groups. The demographic characteristics of the cohort at baseline are presented in Table 1. Patients in the HCC group were more likely to be male (71.7% *vs* 63.9%, $P < 0.001$). The median age of the patients was slightly higher (56 *vs* 54 years, $P < 0.001$). Decompensated cirrhosis was more common in patients with HCC than in those without (77.5% *vs* 73.9%), and a greater proportion of patients with HCC had Child-Pugh grades A and B (32.6% *vs* 29.5% and 49.1% *vs* 48.0%, respectively, $P = 0.003$). Gastrointestinal bleeding was more common in patients without HCC (24.1% *vs* 18.0%).

Risk assessment of HCC in patients with cirrhosis

There was a significant difference in the risk of HCC among patients with cirrhosis of different etiologies ($P < 0.001$). Cirrhotic patients with two or more etiologies had the highest incidence of HCC among all patients with cirrhosis during the entire follow-up period, at 30.3% (Figure 3A), and their mean time to the development of HCC was also the shortest at 5.3 years [95% confidence interval (CI): 4.9-5.7] (Figure 3B). In contrast, patients with HBV cirrhosis had the highest incidence of HCC among single etiologies, at 29.5%, with a median time to HCC was 5.4 years (95%CI: 5.1-5.6 years).

Table 1 Demographic and clinical characteristics

Parameter	HCC cases (*n* = 1352)	Non-HCC controls (*n* = 4065)	*P* value
Sex (Male), *n* (%)	969 (71.7)	2598 (63.9)	< 0.001
Age	56 (50, 62)	54 (46, 62)	< 0.001
Hypertension, *n* (%)	255 (18.9)	727 (17.9)	0.419
Diabetes, *n* (%)	321 (23.7)	860 (21.2)	0.046
Coronary disease, *n* (%)	35 (2.6)	154 (3.8)	0.037
Gastrointestinal bleeding, *n* (%)	243 (18.0)	978 (24.1)	< 0.001
Hepatic encephalopathy, *n* (%)	219 (16.2)	633 (15.6)	0.584
Decompensated cirrhosis, *n* (%)	999 (73.9)	3150 (77.5)	0.007
Child-Pugh grade A, *n* (%)	430 (32.6)	1162 (29.5)	0.003
Child-Pugh grade B, *n* (%)	648 (49.1)	1893 (48.0)	
Child-Push grade C, *n* (%)	241 (18.3)	890 (22.6)	
HBV, *n* (%)	372 (27.5)	889 (21.9)	< 0.001
HCV, *n* (%)	93 (6.9)	261 (6.4)	
AC, *n* (%)	261 (19.3)	1013 (24.9)	
MASLD, *n* (%)	9 (0.7)	42 (1.0)	
PBC, *n* (%)	72 (5.3)	398 (9.8)	
Drug-induced cirrhosis, *n* (%)	12 (0.9)	54 (1.3)	
Cryptogenic cirrhosis, *n* (%)	387 (28.6)	1072 (26.4)	
Mixed cirrhosis, *n* (%)	146 (10.8)	336 (8.3)	
ALT (U/L)	31.1 (21.2, 53.1)	27.0 (18.2, 47.5)	< 0.001
AST (U/L)	47.7 (31.7, 77.4)	44 (29.1, 79.9)	< 0.001
Albumin (g/L)	31.2 (27.4, 34.6)	30.7 (26.8, 34.8)	0.106
Globin (g/L)	31.6 (26.5, 37.1)	31.3 (25.7, 38.0)	0.268
INR	1.27 (1.12, 1.45)	1.32 (1.16, 1.54)	0.002
Prothrombin time (S)	14.2 (12.6, 16.3)	14.8 (13.0, 17.4)	0.017
Direct bilirubin (μmol/L)	11.0 (6.3, 19.2)	12.7 (6.6, 33.6)	0.001
Triglycerides (mmol/L)	0.81 (0.62, 1.11)	0.89 (0.67, 1.26)	< 0.001
Platelets ($\times 10^9$/L)	78 (54, 109)	80 (54, 118)	0.096
γ-GT (U/L)	50.1 (26.0, 119.8)	53.7 (25.4, 143.8)	0.157
AFP (ng/mL)	4.64 (2.60, 10.35)	3.36 (2.02, 6.26)	< 0.001
CA19-9 (U/mL)	26.72 (13.76, 48.40)	25.00 (11.93, 52.82)	0.070
Neutrophils ($\times 10^9$/L)	2.30 (1.59, 3.44)	2.43 (1.59, 3.76)	0.024
Serum ammonia (μg/dL)	73 (51, 95)	67 (46, 95)	< 0.001
MELD	8 (4, 12)	10 (5, 15)	< 0.001

HBV: Hepatitis B virus; HCV: Hepatitis C virus; AC: Alcohol-associated cirrhosis; MASLD: Metabolic dysfunction-associated liver disease; PBC: Primary biliary cirrhosis; Mixed cirrhosis: Cirrhosis caused by two or more etiologies; MELD: Model for end-stage liver disease; ALT: Alanine aminotransferase; AST: Aspartate transaminase; INR: International normalized ratio; γ-GT: Gamma-glutamyltransferase; AFP: Alpha fetoprotein; CA: Carbohydrate antigen; HCC: Hepatocellular carcinoma.

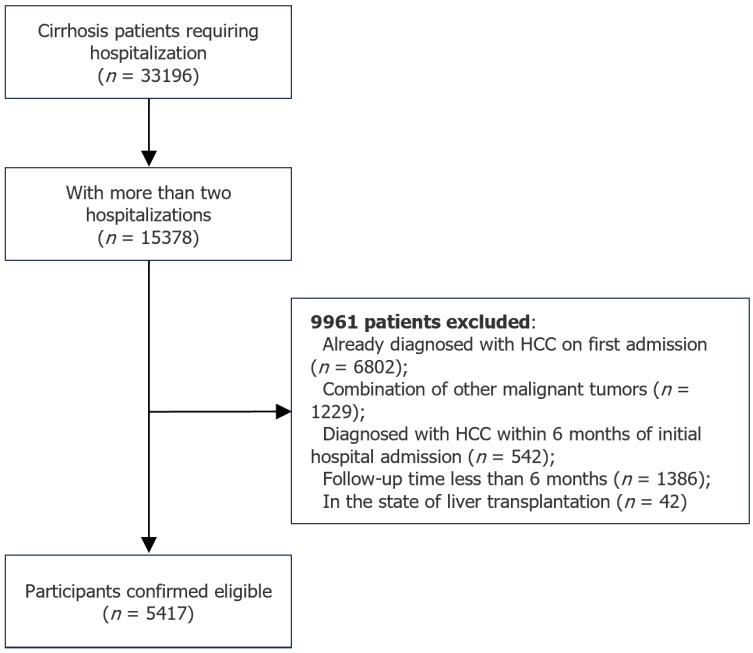

Figure 1 Flowchart of the cohort included in the analysis. HCC: Hepatocellular carcinoma.

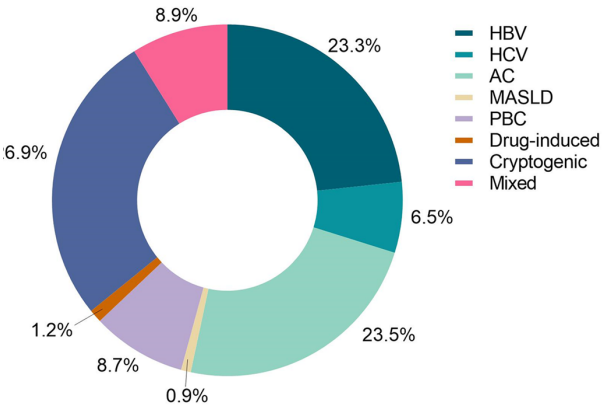

Figure 2 Distribution of etiology. HBV: Hepatitis B virus; HCV: Hepatitis C virus; AC: Alcohol-associated cirrhosis; MASLD: Metabolic dysfunction-associated liver disease; PBC: Primary biliary cirrhosis.

Among cirrhotic patients in this study cohort, higher Child-Pugh grades were associated with a lower risk of HCC and shorter survival: The incidence of HCC was 21.3% in patients with Child-Pugh grade C (Figure 3C), and the mean survival was 6.1 years (95%CI: 5.8-6.5 years) (Figure 3D). Compared to compensated cirrhosis, decompensated cirrhosis had a shorter mean time to HCC [6.4 years (95%CI: 6.3-6.6 years) *vs* 6.8 years (95%CI: 6.5-7.1 years)].

Risk factors associated with the development of HCC

To investigate the risk factors associated with the development of HCC, one-way Cox regression analysis of possible influencing factors was performed, and the following 15 clinical characteristics and laboratory markers were associated with HCC ($P < 0.05$): Age, sex, HBV/HCV history, compensation status, diabetes history, albumin, globulin, international normalized ratio, prothrombin time, triglycerides, platelets, serum ammonia, and child classification. From these candidate risk factors, the same set of seven significant risk factors (age, sex, HBV/HCV history, albumin, globulin, platelet count, and serum ammonia) was selected using forward and backward stepwise Cox regression, as shown in Table 2.

Considering death as a competing risk event for hepatocarcinogenesis, competing risk regression analysis was performed on the risk factors examined in the Cox regression analysis, and the aHRs of these risk factors were estimated. The results of this analysis are presented in Table 2. In the competing risk regression analysis, a higher risk of liver cancer was associated with male sex (aHR = 1.482; 95%CI: 1.313-1.673), advanced age (aHR = 1.025; 95%CI: 1.020-1.030), HBV infection (aHR = 1.950; 95%CI: 1.734-2.193), HCV infection (aHR = 1.533; 95%CI: 1.274-1.846), and co-infection of HBV and HCV (aHR = 2.074; 95%CI: 1.038-4.143), and higher blood ammonia levels (aHR = 1.002; 95%CI: 1.001-1.003), globulin levels (aHR = 1.012; 95%CI: 1.005-1.019), and lower platelet count (aHR = 0.998; 95%CI: 0.998-1.000) at baseline also

Table 2 Hepatocarcinogenesis hazard ratio in Cox and competing risk regression analysis

Parameter	Univariate Cox regression analysis		Multivariable Cox regression analysis		Multivariable competitive risk regression analysis	
	aHR (95%CI)	*P* value	aHR (95%CI)	*P* value	aHR (95%CI)	*P* value
Age	1.023 (1.018-1.027)	< 0.001	1.029 (1.024-1.034)	< 0.001	1.025 (1.020-1.030)	< 0.001
Sex (male)	1.321 (1.174-1.487)	< 0.001	1.537 (1.359-1.738)	< 0.001	1.482 (1.313-1.673)	< 0.001
Diabetes	1.155 (1.019-1.309)	0.025				
Hypertension	1.128 (0.984-1.292)	0.084				
Coronary disease	0.951 (0.680-1.330)	0.769				
HBV	1.801 (1.602-2.025)	< 0.001	1.963 (1.742-2.211)	< 0.001	1.950 (1.734-2.193)	< 0.001
HCV	1.837 (1.352-1.981)	< 0.001	1.567 (1.293-1.900)	< 0.001	1.533 (1.274-1.846)	< 0.001
HBV and HCV	2.062 (1.068-3.980)	0.031	2.456 (1.270-4.747)	0.008	2.074 (1.038-4.143)	0.039
Decompensation	1.146 (1.015-1.295)	0.028				
ALT	1.000 (1.000-1.000)	0.974				
AST	1.000 (1.000-1.000)	0.815				
Albumin	0.976 (0.967-0.985)	< 0.001	0.986 (0.977-0.995)	0.002	0.995 (0.987-1.005)	0.381
Globulin	1.017 (1.010-1.023)	< 0.001	1.016 (1.009-1.023)	< 0.001	1.012 (1.005-1.019)	< 0.001
INR	1.271 (1.084-1.490)	0.003				
Prothrombin time	1.016 (1.002-1.031)	0.024				
Direct bilirubin	1.000 (0.999-1.001)	0.943				
Triglycerides	0.854 (0.776-0.939)	0.001				
Hemoglobin	1.004 (1.002-1.006)	< 0.001				
γ-GT	1.000 (0.999-1.000)	0.075				
AFP	1.000 (1.000-1.001)	0.543				
CA19-9	1.000 (0.999-1.001)	0.713				
Platelets	0.999 (0.998-1.000)	0.017	0.999 (0.998-1.000)	0.015	0.998 (0.998-1.000)	0.011
Neutrophils	0.998 (0.976-1.020)	0.829				
Serum ammonia	1.002 (1.001-1.003)	0.004	1.002 (1.001-1.003)	0.003	1.002 (1.001-1.003)	< 0.001
MELD	0.999 (0.990-1.008)	0.843				

HBV: Hepatitis B virus; HCV: Hepatitis C virus; MELD: Model for end-stage liver disease; ALT: Alanine aminotransferase; AST: Aspartate transaminase; INR: International normalized ratio; γ-GT: Gamma-glutamyltransferase; AFP: Alpha fetoprotein; CA: Carbohydrate antigen; aHR: Adjusted hazard ratio; CI: Confidence interval.

showed a significant association with liver cancer risk.

Based on the CIF curves from the competing risk regression analyses (Figure 4A), the risk of HCC in these hospitalized cirrhotic patients was 19.2% (95%CI: 17.9%-20.5%) at 3 years, and 35.2% (95%CI: 33.4%-37.0%) at 5 years. In these patients with cirrhosis, the risk of total mortality was 1.49% (95%CI: 1.15%-1.83%) at 1 year, 4.83% (95%CI: 4.17%-5.50%) at 3 years, and 6.66% (95%CI: 5.81%-7.51%) at 5 years. Men had a higher risk of HCC than women, with a 5-year risk of 37.0% (95%CI: 34.8%-39.3%) *vs* 31.5% (95%CI: 28.4%-34.7%) (Figure 4B). The risk of HCC increased with age, and the 5-year risk of HCC for decreasing age by 10 years (44) *vs* increasing age by 10 years (64), based on a median age of 54 years, was 23.6% (95%CI: 12.9%-34.3%) *vs* 42.4% (95%CI: 29.2%-55.7%) (Figure 4C). The 5-year risk of HCC in cirrhotic patients with HBV, HCV, and HBV/HCV coinfection was 45.8% (95%CI: 42.1%-49.4%), 42.9% (95%CI: 35.9%-49.9%), and 48.1% (95%CI: 20.2%-75.9%), respectively, whereas the 5-year risk of HCC in cirrhotic patients with nonviral hepatitis was only 29.5% (95%CI: 27.3%-31.7%) (Figure 4D).

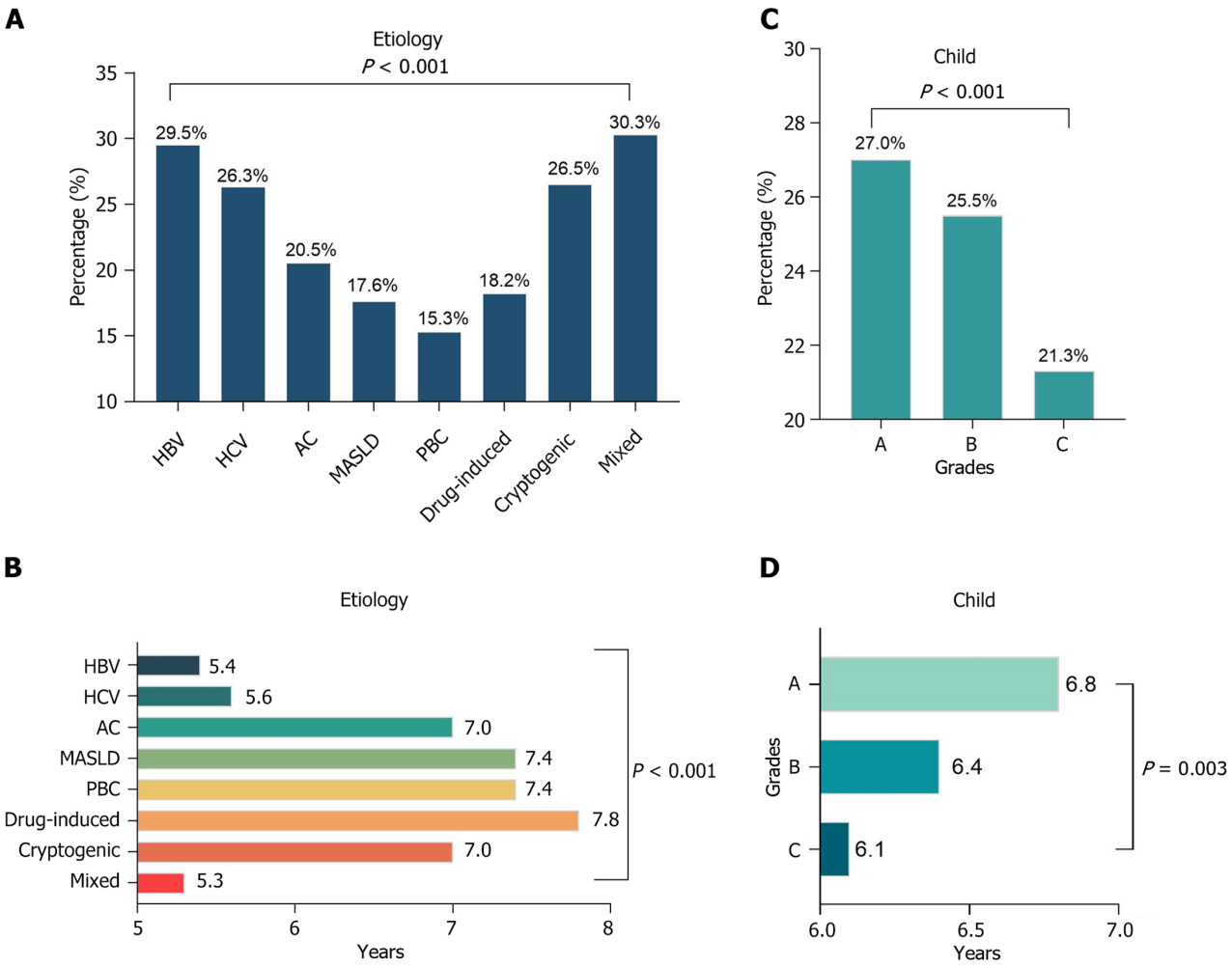

Figure 3 Incidence of hepatocellular carcinoma in cirrhotic patients with different etiologies. A and C: Child-Pugh grades; B and D: Mean time to occurrence. HBV: Hepatitis B virus; HCV: Hepatitis C virus; AC: Alcohol-associated cirrhosis; MASLD: Metabolic dysfunction-associated liver disease; PBC: Primary biliary cirrhosis.

DISCUSSION

In this study, we found that patients with hepatitis B cirrhosis had the highest incidence of HCC and the shortest median survival among all causative factors in this retrospective cohort study of hospitalized patients with cirrhosis. The risk of HCC at 5 years was 45.8% (95%CI: 42.0%-49.4%). Among patients with cirrhosis, male sex, older age, and a history of chronic HBV and HCV infections were risk factors for the development of HCC after adjusting for death as a competing risk. Compared with non-viral cirrhosis, viral cirrhosis had a higher cumulative risk of developing HCC within 5 years: 45.3% (95%CI: 42.0%-48.5%) *vs* 29.5% (95%CI: 27.3%-31.7%).

The Western Pacific Region, including China, has the highest prevalence of HBV infection among patients with cirrhosis (59%), according to the World Health Organization regional classification[16]. These statistics were based on the leading causes of cirrhosis reported between 1993 and 2021. The burden of alcohol-related liver disease, cirrhosis, and HCC is expected to increase with an increase in global alcohol consumption *per* capita[17]. In our study, 1261 cases (23.3%) of HBV, 1274 cases (23.5%) of AC, and 1459 cases (26.9%) of cryptogenic cirrhosis were the three main etiologies. The proportion of AC almost reached the level of HBV-associated cirrhosis, and even exceeded that of cirrhotic patients with chronic hepatitis B. Screening for alcohol use disorders is urgent. In addition, the prevalence of MASLD by imaging has been estimated to be 25.24% (95%CI: 22.10%-28.65%) worldwide and 27.37% (95%CI: 23.29%-31.88%) in Asia[10]. This study found a significant number of patients with cryptogenic cirrhosis. We speculate that most patients with cryptogenic cirrhosis would develop MASLD. The likely reason is that most hospitalized patients with cirrhosis have a long history of cirrhosis and the initial steatosis has progressed to significant liver fibrosis, making the specific etiology difficult to trace.

Among patients with compensated viral cirrhosis, the cumulative risk of HCC varies according to etiology. The cumulative incidences of HCC in hepatitis B surface antigen (HBsAg), HCV, and HBsAg/HCV positive patients were 10%, 21%, and 23%, respectively, at 5 years, and 16%, 28%, and 45%, respectively, at 10 years[18]. Without HBV and HCV infection, patients with compensated alcoholic cirrhosis have a lower incidence of HCC, with cumulative 1 and 2-year incidence rates of 1% and 5%, respectively[19,20], but a significantly higher risk of death[21]. A prospective study reported that the estimated risk of developing HCC was lower than the observed incidence (2.4% at 1 year and 7.3% at 3 years) in the majority (77.6%) of patients with decompensated cirrhosis. However, only 11.6% of the patients have a 3-

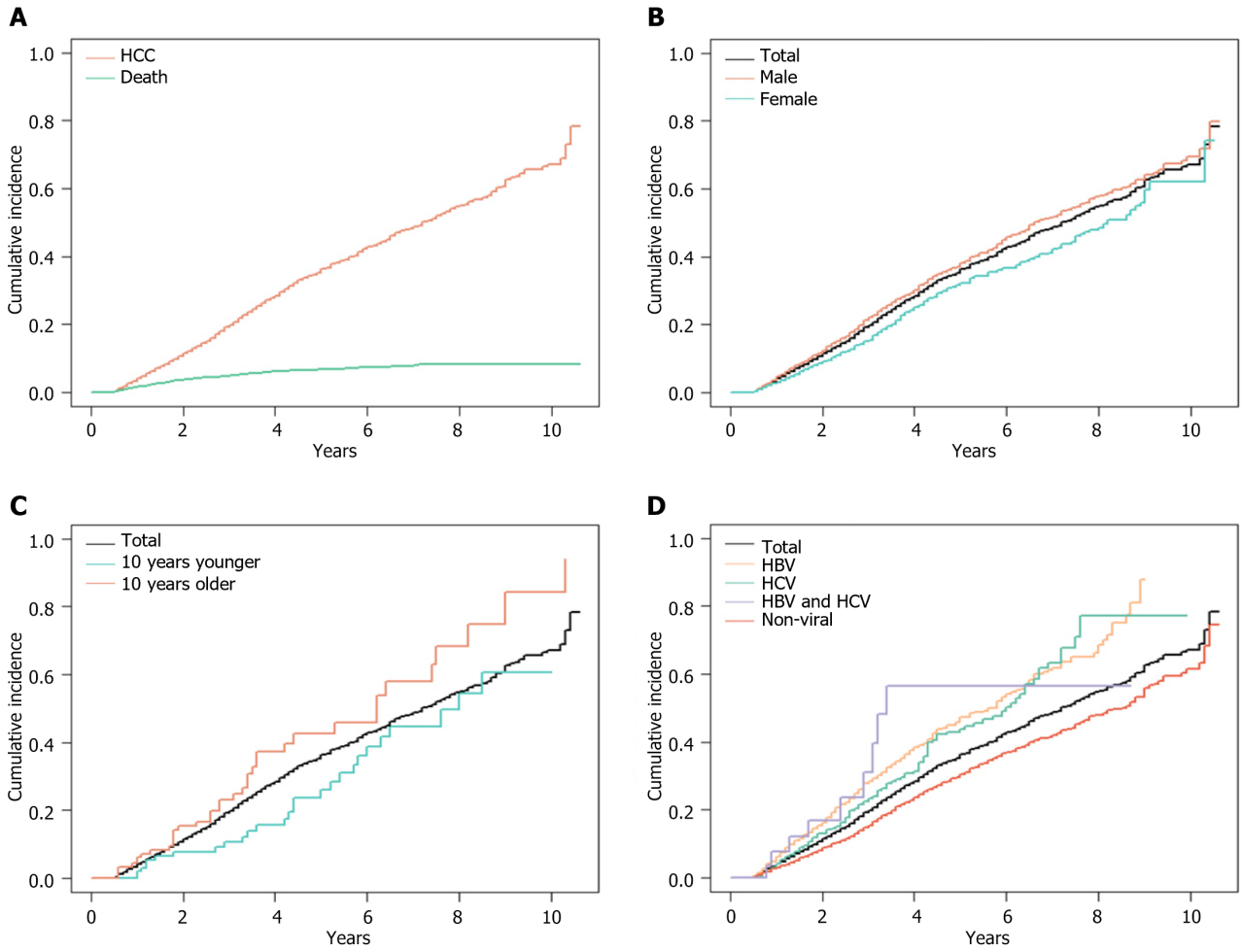

Figure 4 Cumulative incidence curves for overall hepatocellular carcinoma. A: Mortality; B: Sex; C: Age; D: Etiology. HBV: Hepatitis B virus; HCV: Hepatitis C virus; HCC: Hepatocellular carcinoma.

year risk, ranging from 10% to 47%[22]. Our study yielded similar results, showing that HBV and HCV infections were associated with a higher risk of HCC after considering death as a competing risk factor for hepatocarcinogenesis. Among cirrhotic patients with HBV, HCV, and HBV/HCV coinfection, the 5-year risk of HCC was 45.8%, 42.9%, and 48.1%, respectively, whereas the 5-year risk of HCC was only 29.5% in patients with cirrhosis who had never had hepatitis.

Male sex and advanced age are risk factors for developing HCC in patients with cirrhosis[5,23], and our study reported similar results. Furthermore, predictors of HCC in patients with cirrhosis include baseline objective and conventional risk indicators, including alpha-fetoprotein, albumin, alanine aminotransferase, and platelet levels[24]. In patients with AC, baseline bilirubin and prothrombin levels were associated with the risk of HCC in a prospective analysis[19]. Our study showed that in addition to sex, age, and hepatitis virus infection, baseline albumin and globulin levels, as well as platelet and blood ammonia levels, were equally significant risk factors for HCC. The differences in the roles of these conventional risk indicators in different studies may be related to the varying etiologic distributions and hepatic function compensation statuses in the corresponding study populations.

Over 10 years of follow-up, large sample size, and detailed objective baseline biochemical data are the strengths of our study. However, there are several limitations to this study: (1) There is no data on the effect of therapeutic interventions in reducing HCC risk; and (2) Our data were collected retrospectively and may be subject to biases associated with retrospective studies. Additionally, there may have been unmeasured confounders, such as family history of cirrhosis, which were not included in the multivariate analysis.

In conclusion, our study showed that viral hepatitis cirrhosis increased the risk of HCC. Male sex and older age are consistently associated with a higher risk of developing HCC in patients with cirrhosis. Furthermore, high blood ammonia levels, and low albumin and platelet levels may predict a higher risk of HCC. These findings emphasize the need to strengthen the management of objective biochemical parameters in patients with cirrhosis.

CONCLUSION

Of the 5417 patients included, 1352 developed HCC and 262 died. The risk of developing HCC was 19.2% (95%CI: 17.9%-20.5%) at 3 years and 35.2% (95%CI: 33.4%-37.0%) at 5 years. Male sex, older age, and viral hepatitis and cirrhosis were

associated with a higher risk of HCC. Increased risk of HCC may also be associated with lower albumin and platelet levels, higher globulin levels, and higher baseline blood ammonia levels.

ACKNOWLEDGEMENTS

The authors highly appreciate all the patients who were involved in the present study and our team from Beijing Youan Hospital.

FOOTNOTES

Author contributions: Zhou DQ, Liu JY, and Zhao F analyzed the data and wrote the manuscript; Zhang J and Liu LL collected the data and contributed analytic tools; Jia JR and Cao ZH designed the research study and revised the manuscript.

Institutional review board statement: The protocol and consent form for the study were approved by the research ethics committee of Beijing Youan Hospital, Capital Medical University, Notification of Ethical Review Opinions (No. 2024051).

Informed consent statement: All study participants, or their legal guardian, provided informed written consent prior to study enrollment.

Conflict-of-interest statement: The authors declare that they have no conflict of interest to disclose.

Data sharing statement: The data used to support the findings are available from the corresponding author upon request.

Country of origin: China

ORCID number: Da-Qiong Zhou 0009-0008-4266-8152; Jing Zhang 0000-0002-3082-8330; Zhen-Huan Cao 0000-0003-4204-1049.

S-Editor: Fan M
L-Editor: Wang TQ
P-Editor: Chen YX

REFERENCES

1 **Ginès P**, Krag A, Abraldes JG, Solà E, Fabrellas N, Kamath PS. Liver cirrhosis. *Lancet* 2021; **398**: 1359-1376 [PMID: 34543610 DOI: 10.1016/S0140-6736(21)01374-X]

2 **Asrani SK**, Devarbhavi H, Eaton J, Kamath PS. Burden of liver diseases in the world. *J Hepatol* 2019; **70**: 151-171 [PMID: 30266282 DOI: 10.1016/j.jhep.2018.09.014]

3 **Brar G**, Greten TF, Graubard BI, McNeel TS, Petrick JL, McGlynn KA, Altekruse SF. Hepatocellular Carcinoma Survival by Etiology: A SEER-Medicare Database Analysis. *Hepatol Commun* 2020; **4**: 1541-1551 [PMID: 33024922 DOI: 10.1002/hep4.1564]

4 **Global Burden of Disease 2019 Cancer Collaboration**, Kocarnik JM, Compton K, Dean FE, Fu W, Gaw BL, Harvey JD, Henrikson HJ, Lu D, Pennini A, Xu R, Ababneh E, Abbasi-Kangevari M, Abbastabar H, Abd-Elsalam SM, Abdoli A, Abedi A, Abidi H, Abolhassani H, Adedeji IA, Adnani QES, Advani SM, Afzal MS, Aghaali M, Ahinkorah BO, Ahmad S, Ahmad T, Ahmadi A, Ahmadi S, Ahmed Rashid T, Ahmed Salih Y, Akalu GT, Aklilu A, Akram T, Akunna CJ, Al Hamad H, Alahdab F, Al-Aly Z, Ali S, Alimohamadi Y, Alipour V, Aljunid SM, Alkhayyat M, Almasi-Hashiani A, Almasri NA, Al-Maweri SAA, Almustanyir S, Alonso N, Alvis-Guzman N, Amu H, Anbesu EW, Ancuceanu R, Ansari F, Ansari-Moghaddam A, Antwi MH, Anvari D, Anyasodor AE, Aqeel M, Arabloo J, Arab-Zozani M, Aremu O, Ariffin H, Aripov T, Arshad M, Artaman A, Arulappan J, Asemi Z, Asghari Jafarabadi M, Ashraf T, Atorkey P, Aujayeb A, Ausloos M, Awedew AF, Ayala Quintanilla BP, Ayenew T, Azab MA, Azadnajafabad S, Azari Jafari A, Azarian G, Azzam AY, Badiye AD, Bahadory S, Baig AA, Baker JL, Balakrishnan S, Banach M, Bärnighausen TW, Barone-Adesi F, Barra F, Barrow A, Behzadifar M, Belgaumi UI, Bezabhe WMM, Bezabih YM, Bhagat DS, Bhagavathula AS, Bhardwaj N, Bhardwaj P, Bhaskar S, Bhattacharyya K, Bhojaraja VS, Bibi S, Bijani A, Biondi A, Bisignano C, Bjørge T, Bleyer A, Blyuss O, Bolarinwa OA, Bolla SR, Braithwaite D, Brar A, Brenner H, Bustamante-Teixeira MT, Butt NS, Butt ZA, Caetano Dos Santos FL, Cao Y, Carreras G, Catalá-López F, Cembranel F, Cerin E, Cernigliaro A, Chakinala RC, Chattu SK, Chattu VK, Chaturvedi P, Chimed-Ochir O, Cho DY, Christopher DJ, Chu DT, Chung MT, Conde J, Cortés S, Cortesi PA, Costa VM, Cunha AR, Dadras O, Dagnew AB, Dahlawi SMA, Dai X, Dandona L, Dandona R, Darwesh AM, das Neves J, De la Hoz FP, Demis AB, Denova-Gutiérrez E, Dhamnetiya D, Dhimal ML, Dhimal M, Dianatinasab M, Diaz D, Djalalinia S, Do HP, Doaei S, Dorostkar F, Dos Santos Figueiredo FW, Driscoll TR, Ebrahimi H, Eftekharzadeh S, El Tantawi M, El-Abid H, Elbarazi I, Elhabashy HR, Elhadi M, El-Jaafary SI, Eshrati B, Eskandarieh S, Esmaeilzadeh F, Etemadi A, Ezzikouri S, Faisaluddin M, Faraon EJA, Fares J, Farzadfar F, Feroze AH, Ferrero S, Ferro Desideri L, Filip I, Fischer F, Fisher JL, Foroutan M, Fukumoto T, Gaal PA, Gad MM, Gadanya MA, Gallus S, Gaspar Fonseca M, Getachew Obsa A, Ghafourifard M, Ghashghaee A, Ghith N, Gholamalizadeh M, Gilani SA, Ginindza TG, Gizaw ATT, Glasbey JC, Golechha

M, Goleij P, Gomez RS, Gopalani SV, Gorini G, Goudarzi H, Grosso G, Gubari MIM, Guerra MR, Guha A, Gunasekera DS, Gupta B, Gupta VB, Gupta VK, Gutiérrez RA, Hafezi-Nejad N, Haider MR, Haj-Mirzaian A, Halwani R, Hamadeh RR, Hameed S, Hamidi S, Hanif A, Haque S, Harlianto NI, Haro JM, Hasaballah AI, Hassanipour S, Hay RJ, Hay SI, Hayat K, Heidari G, Heidari M, Herrera-Serna BY, Herteliu C, Hezam K, Holla R, Hossain MM, Hossain MBH, Hosseini MS, Hosseini M, Hosseinzadeh M, Hostiuc M, Hostiuc S, Househ M, Hsairi M, Huang J, Hugo FN, Hussain R, Hussein NR, Hwang BF, Iavicoli I, Ibitoye SE, Ida F, Ikuta KS, Ilesanmi OS, Ilic IM, Ilic MD, Irham LM, Islam JY, Islam RM, Islam SMS, Ismail NE, Isola G, Iwagami M, Jacob L, Jain V, Jakovljevic MB, Javaheri T, Jayaram S, Jazayeri SB, Jha RP, Jonas JB, Joo T, Joseph N, Joukar F, Jürisson M, Kabir A, Kahrizi D, Kalankesh LR, Kalhor R, Kaliyadan F, Kalkonde Y, Kamath A, Kameran Al-Salihi N, Kandel H, Kapoor N, Karch A, Kasa AS, Katikireddi SV, Kauppila JH, Kavetskyy T, Kebede SA, Keshavarz P, Keykhaei M, Khader YS, Khalilov R, Khan G, Khan M, Khan MN, Khan MAB, Khang YH, Khater AM, Khayamzadeh M, Kim GR, Kim YJ, Kisa A, Kisa S, Kissimova-Skarbek K, Kopec JA, Koteeswaran R, Koul PA, Koulmane Laxminarayana SL, Koyanagi A, Kucuk Bicer B, Kugbey N, Kumar GA, Kumar N, Kumar N, Kurmi OP, Kutluk T, La Vecchia C, Lami FH, Landires I, Lauriola P, Lee SW, Lee SWH, Lee WC, Lee YH, Leigh J, Leong E, Li J, Li MC, Liu X, Loureiro JA, Lunevicius R, Magdy Abd El Razek M, Majeed A, Makki A, Male S, Malik AA, Mansournia MA, Martini S, Masoumi SZ, Mathur P, McKee M, Mehrotra R, Mendoza W, Menezes RG, Mengesha EW, Mesregah MK, Mestrovic T, Miao Jonasson J, Miazgowski B, Miazgowski T, Michalek IM, Miller TR, Mirzaei H, Mirzaei HR, Misra S, Mithra P, Moghadaszadeh M, Mohammad KA, Mohammad Y, Mohammadi M, Mohammadi SM, Mohammadian-Hafshejani A, Mohammed S, Moka N, Mokdad AH, Molokhia M, Monasta L, Moni MA, Moosavi MA, Moradi Y, Moraga P, Morgado-da-Costa J, Morrison SD, Mosapour A, Mubarik S, Mwanri L, Nagarajan AJ, Nagaraju SP, Nagata C, Naimzada MD, Nangia V, Naqvi AA, Narasimha Swamy S, Ndejjo R, Nduaguba SO, Negoi I, Negru SM, Neupane Kandel S, Nguyen CT, Nguyen HLT, Niazi RK, Nnaji CA, Noor NM, Nuñez-Samudio V, Nzoputam CI, Oancea B, Ochir C, Odukoya OO, Ogbo FA, Olagunju AT, Olakunde BO, Omar E, Omar Bali A, Omonisi AEE, Ong S, Onwujekwe OE, Orru H, Ortega-Altamirano DV, Otstavnov N, Otstavnov SS, Owolabi MO, P A M, Padubidri JR, Pakshir K, Pana A, Panagiotakos D, Panda-Jonas S, Pardhan S, Park EC, Park EK, Pashazadeh Kan F, Patel HK, Patel JR, Pati S, Pattanshetty SM, Paudel U, Pereira DM, Pereira RB, Perianayagam A, Pillay JD, Pirouzpanah S, Pishgar F, Podder I, Postma MJ, Pourjafar H, Prashant A, Preotescu L, Rabiee M, Rabiee N, Radfar A, Radhakrishnan RA, Radhakrishnan V, Rafiee A, Rahim F, Rahimzadeh S, Rahman M, Rahman MA, Rahmani AM, Rajai N, Rajesh A, Rakovac I, Ram P, Ramezanzadeh K, Ranabhat K, Ranasinghe P, Rao CR, Rao SJ, Rawassizadeh R, Razeghinia MS, Renzaho AMN, Rezaei N, Rezaei N, Rezapour A, Roberts TJ, Rodriguez JAB, Rohloff P, Romoli M, Ronfani L, Roshandel G, Rwegerera GM, S M, Sabour S, Saddik B, Saeed U, Sahebkar A, Sahoo H, Salehi S, Salem MR, Salimzadeh H, Samaei M, Samy AM, Sanabria J, Sankararaman S, Santric-Milicevic MM, Sardiwalla Y, Sarveazad A, Sathian B, Sawhney M, Saylan M, Schneider IJC, Sekerija M, Seylani A, Shafaat O, Shaghaghi Z, Shaikh MA, Shamsoddin E, Shannawaz M, Sharma R, Sheikh A, Sheikhbahaei S, Shetty A, Shetty JK, Shetty PH, Shibuya K, Shirkoohi R, Shivakumar KM, Shivarov V, Siabani S, Siddappa Malleshappa SK, Silva DAS, Singh JA, Sintayehu Y, Skryabin VY, Skryabina AA, Soeberg MJ, Sofi-Mahmudi A, Sotoudeh H, Steiropoulos P, Straif K, Subedi R, Sufiyan MB, Sultan I, Sultana S, Sur D, Szerencsés V, Szócska M, Tabarés-Seisdedos R, Tabuchi T, Tadbiri H, Taherkhani A, Takahashi K, Talaat IM, Tan KK, Tat VY, Tedla BAA, Tefera YG, Tehrani-Banihashemi A, Temsah MH, Tesfay FH, Tessema GA, Thapar R, Thavamani A, Thoguluva Chandrasekar V, Thomas N, Tohidinik HR, Touvier M, Tovani-Palone MR, Traini E, Tran BX, Tran KB, Tran MTN, Tripathy JP, Tusa BS, Ullah I, Ullah S, Umapathi KK, Unnikrishnan B, Upadhyay E, Vacante M, Vaezi M, Valadan Tahbaz S, Velazquez DZ, Veroux M, Violante FS, Vlassov V, Vo B, Volovici V, Vu GT, Waheed Y, Wamai RG, Ward P, Wen YF, Westerman R, Winkler AS, Yadav L, Yahyazadeh Jabbari SH, Yang L, Yaya S, Yazie TSY, Yeshaw Y, Yonemoto N, Younis MZ, Yousefi Z, Yu C, Yuce D, Yunusa I, Zadnik V, Zare F, Zastrozhin MS, Zastrozhina A, Zhang J, Zhong C, Zhou L, Zhu C, Ziapour A, Zimmermann IR, Fitzmaurice C, Murray CJL, Force LM. Cancer Incidence, Mortality, Years of Life Lost, Years Lived With Disability, and Disability-Adjusted Life Years for 29 Cancer Groups From 2010 to 2019: A Systematic Analysis for the Global Burden of Disease Study 2019. *JAMA Oncol* 2022; **8**: 420-444 [PMID: 34967848 DOI: 10.1001/jamaoncol.2021.6987]

5 **Huang DQ**, Mathurin P, Cortez-Pinto H, Loomba R. Global epidemiology of alcohol-associated cirrhosis and HCC: trends, projections and risk factors. *Nat Rev Gastroenterol Hepatol* 2023; **20**: 37-49 [PMID: 36258033 DOI: 10.1038/s41575-022-00688-6]

6 **GBD 2019 Hepatitis B Collaborators**. Global, regional, and national burden of hepatitis B, 1990-2019: a systematic analysis for the Global Burden of Disease Study 2019. *Lancet Gastroenterol Hepatol* 2022; **7**: 796-829 [PMID: 35738290 DOI: 10.1016/S2468-1253(22)00124-8]

7 **Lok AS**, McMahon BJ, Brown RS Jr, Wong JB, Ahmed AT, Farah W, Almasri J, Alahdab F, Benkhadra K, Mouchli MA, Singh S, Mohamed EA, Abu Dabrh AM, Prokop LJ, Wang Z, Murad MH, Mohammed K. Antiviral therapy for chronic hepatitis B viral infection in adults: A systematic review and meta-analysis. *Hepatology* 2016; **63**: 284-306 [PMID: 26566246 DOI: 10.1002/hep.28280]

8 **Cui F**, Blach S, Manzengo Mingiedi C, Gonzalez MA, Sabry Alaama A, Mozalevskis A, Séguy N, Rewari BB, Chan PL, Le LV, Doherty M, Luhmann N, Easterbrook P, Dirac M, de Martel C, Nayagam S, Hallett TB, Vickerman P, Razavi H, Lesi O, Low-Beer D. Global reporting of progress towards elimination of hepatitis B and hepatitis C. *Lancet Gastroenterol Hepatol* 2023; **8**: 332-342 [PMID: 36764320 DOI: 10.1016/S2468-1253(22)00386-7]

9 **Polaris Observatory HCV Collaborators**. Global change in hepatitis C virus prevalence and cascade of care between 2015 and 2020: a modelling study. *Lancet Gastroenterol Hepatol* 2022; **7**: 396-415 [PMID: 35180382 DOI: 10.1016/S2468-1253(21)00472-6]

10 **Younossi ZM**, Koenig AB, Abdelatif D, Fazel Y, Henry L, Wymer M. Global epidemiology of nonalcoholic fatty liver disease-Meta-analytic assessment of prevalence, incidence, and outcomes. *Hepatology* 2016; **64**: 73-84 [PMID: 26707365 DOI: 10.1002/hep.28431]

11 **Fattovich G**, Stroffolini T, Zagni I, Donato F. Hepatocellular carcinoma in cirrhosis: incidence and risk factors. *Gastroenterology* 2004; **127**: S35-S50 [PMID: 15508101 DOI: 10.1053/j.gastro.2004.09.014]

12 **Jepsen P**, Vilstrup H, Andersen PK, Lash TL, Sørensen HT. Comorbidity and survival of Danish cirrhosis patients: a nationwide population-based cohort study. *Hepatology* 2008; **48**: 214-220 [PMID: 18537190 DOI: 10.1002/hep.22341]

13 **Fleming KM**, Aithal GP, Card TR, West J. All-cause mortality in people with cirrhosis compared with the general population: a population-based cohort study. *Liver Int* 2012; **32**: 79-84 [PMID: 21745279 DOI: 10.1111/j.1478-3231.2011.02517.x]

14 **Asrani SK**, Hall L, Reddy V, Ogola G, Izzy M. Comorbid Chronic Diseases and Survival in Compensated and Decompensated Cirrhosis: A Population-Based Study. *Am J Gastroenterol* 2022; **117**: 2009-2016 [PMID: 35849622 DOI: 10.14309/ajg.0000000000001909]

15 **D'Amico G**, Morabito A, D'Amico M, Pasta L, Malizia G, Rebora P, Valsecchi MG. Clinical states of cirrhosis and competing risks. *J Hepatol* 2018; **68**: 563-576 [PMID: 29111320 DOI: 10.1016/j.jhep.2017.10.020]

16 **Huang DQ**, Terrault NA, Tacke F, Gluud LL, Arrese M, Bugianesi E, Loomba R. Global epidemiology of cirrhosis - aetiology, trends and predictions. *Nat Rev Gastroenterol Hepatol* 2023; **20**: 388-398 [PMID: 36977794 DOI: 10.1038/s41575-023-00759-2]

17 **Manthey J**, Shield KD, Rylett M, Hasan OSM, Probst C, Rehm J. Global alcohol exposure between 1990 and 2017 and forecasts until 2030: a modelling study. *Lancet* 2019; **393**: 2493-2502 [PMID: 31076174 DOI: 10.1016/S0140-6736(18)32744-2]

18 **Chiaramonte M**, Stroffolini T, Vian A, Stazi MA, Floreani A, Lorenzoni U, Lobello S, Farinati F, Naccarato R. Rate of incidence of

hepatocellular carcinoma in patients with compensated viral cirrhosis. *Cancer* 1999; **85**: 2132-2137 [PMID: 10326690]

19 **Ganne-Carrié N**, Chaffaut C, Bourcier V, Archambeaud I, Perarnau JM, Oberti F, Roulot D, Moreno C, Louvet A, Dao T, Moirand R, Goria O, Nguyen-Khac E, Carbonell N, Antonini T, Pol S, de Ledinghen V, Ozenne V, Henrion J, Péron JM, Tran A, Perlemuter G, Amiot X, Zarski JP, Beaugrand M, Chevret S; for CIRRAL Group. Estimate of hepatocellular carcinoma incidence in patients with alcoholic cirrhosis. *J Hepatol* 2018; **69**: 1274-1283 [PMID: 30092234 DOI: 10.1016/j.jhep.2018.07.022]

20 **Huang DQ**, Tan DJH, Ng CH, Amangurbanova M, Sutter N, Lin Tay PW, Lim WH, Yong JN, Tang A, Syn N, Muthiah MD, Tan EXX, Dave S, Tay B, Majzoub AM, Gerberi D, Kim BK, Loomba R. Hepatocellular Carcinoma Incidence in Alcohol-Associated Cirrhosis: Systematic Review and Meta-analysis. *Clin Gastroenterol Hepatol* 2023; **21**: 1169-1177 [PMID: 35940513 DOI: 10.1016/j.cgh.2022.06.032]

21 **Jepsen P**, Kraglund F, West J, Villadsen GE, Sørensen HT, Vilstrup H. Risk of hepatocellular carcinoma in Danish outpatients with alcohol-related cirrhosis. *J Hepatol* 2020; **73**: 1030-1036 [PMID: 32512015 DOI: 10.1016/j.jhep.2020.05.043]

22 **Reddy KR**, McLerran D, Marsh T, Parikh N, Roberts LR, Schwartz M, Nguyen MH, Befeler A, Page-Lester S, Tang R, Srivastava S, Rinaudo JA, Feng Z, Marrero JA. Incidence and Risk Factors for Hepatocellular Carcinoma in Cirrhosis: The Multicenter Hepatocellular Carcinoma Early Detection Strategy (HEDS) Study. *Gastroenterology* 2023; **165**: 1053-1063.e6 [PMID: 37429366 DOI: 10.1053/j.gastro.2023.06.027]

23 **Rong G**, Wang H, Bowlus CL, Wang C, Lu Y, Zeng Z, Qu J, Lou M, Chen Y, An L, Yang Y, Gershwin ME. Incidence and risk factors for hepatocellular carcinoma in primary biliary cirrhosis. *Clin Rev Allergy Immunol* 2015; **48**: 132-141 [PMID: 25762349 DOI: 10.1007/s12016-015-8483-x]

24 **Kanwal F**, Khaderi S, Singal AG, Marrero JA, Asrani SK, Amos CI, Thrift AP, Kramer JR, Yu X, Cao Y, Luster M, Al-Sarraj A, Ning J, El-Serag HB. Risk Stratification Model for Hepatocellular Cancer in Patients With Cirrhosis. *Clin Gastroenterol Hepatol* 2023; **21**: 3296-3304.e3 [PMID: 37390101 DOI: 10.1016/j.cgh.2023.04.019]

World Journal of Gastrointestinal Oncology

Submit a Manuscript: https://www.f6publishing.com

World J Gastrointest Oncol 2024 December 15; 16(12): 4636-4649

DOI: 10.4251/wjgo.v16.i12.4636

ISSN 1948-5204 (online)

ORIGINAL ARTICLE

Retrospective Study

Prognosis of radiotherapy for esophageal cancer in elderly patients exceeding seventy-five years old

Li-Li Hu, Feng Rong, Lei Liu, Ling Zhang, Lei-Lei Zhang, Qun Yang, Zhao-Long Xia, Hui Wang

Specialty type: Oncology

Provenance and peer review: Unsolicited article; Externally peer reviewed.

Peer-review model: Single blind

Peer-review report's classification

Scientific Quality: Grade C
Novelty: Grade B
Creativity or Innovation: Grade B
Scientific Significance: Grade B

P-Reviewer: Beeraka NM

Received: May 30, 2024
Revised: September 22, 2024
Accepted: October 8, 2024
Published online: December 15, 2024
Processing time: 165 Days and 22.8 Hours

Li-Li Hu, Feng Rong, Ling Zhang, Lei-Lei Zhang, Qun Yang, Zhao-Long Xia, Department of Cancer Center, Lu'an Hospital of Anhui Medical University, Lu'an 237002, Anhui Province, China

Lei Liu, College of Health and Elderly Care, Anhui Vocational College of City Management, Hefei 230012, Anhui Province, China

Hui Wang, Department of Oncology, The Second Affiliated Hospital of Anhui Medical University, Hefei 230601, Anhui Province, China

Corresponding author: Hui Wang, MD, PhD, Doctor, Department of Oncology, The Second Affiliated Hospital of Anhui Medical University, No. 678 Furong Road, Hefei Economic Development Zone, Hefei 230601, Anhui Province, China. 1223556508@qq.com

Abstract

BACKGROUND

Esophageal cancer (EC) often occurs in the elderly, with approximately 33% of patients aged ≥ 75 years at the time of diagnosis.

AIM

To evaluate the prognostic factors for radiotherapy (RT) in elderly patients with unresectable EC.

METHODS

We retrospectively analyzed the clinical characteristics, toxic reactions, and survival information of EC patients aged ≥ 75 years who underwent intensity-modulated RT at Lu'an Hospital of Anhui Medical University between January 2016 and September 2023. Kaplan-Meier analysis was used to draw the overall survival (OS) curves, and Cox regression analysis was employed to evaluate the influence of various clinical factors on the prognosis.

RESULTS

A total of 139 patients were enrolled. The median follow-up time was 52.0 months. The median OS was 20.0 months. The 1-year, 2-year, 3-year, and 5-year OS rates were 69.8%, 38.7%, 28.2%, and 17.5%, respectively. Univariate analysis showed that age, radiation dose, and chemotherapy had no significant impact on prognosis. Multivariate analysis indicated that clinical stage [III-IVa *vs* I-II, hazard ratio (HR) = 2.421, 95% confidence interval (CI): 1.242-4.718, $P = 0.009$; IVb *vs* I-II, HR = 4.222, 95%CI: 1.888-9.438, $P < 0.001$), Charlson comorbidity index (CCI) (0 *vs*

≥ 1, HR = 1.539, 95%CI: 1.015-2.332, P = 0.042), and nutritional risk screening 2002 (NRS2002) (< 3 *vs* ≥ 3, HR = 2.491, 95%CI: 1.601-3.875, P < 0.001) were independent prognostic factors for OS.

CONCLUSION

Our results suggest that CCI and NRS2002 were independent prognostic factors of OS for unresectable elderly EC patients undergoing RT. For elderly patients with EC, full attention should be given to biological age-related indicators, such as comorbidities and nutrition, when formulating treatment protocols. These factors should be considered in future clinical practice.

Key Words: Elderly patient; Esophageal cancer; Radiotherapy; Prognosis; Comorbidity; Nutritional risk

Core Tip: Esophageal cancer (EC) often occurs in the elderly, with approximately 33% of patients aged ≥ 75 years at the time of diagnosis. Since patients aged 75 years and above are often excluded from many clinical trials of EC, there is a lack of agreement regarding the prognosis and treatment of this population. We retrospectively analyzed the clinical characteristics, toxic reactions, and survival information of elderly patients with EC aged ≥ 75 years who received intensity-modulated radiotherapy. Our analysis aimed to evaluate the prognostic factors affecting overall survival. We found that the Charlson comorbidity index and nutritional risk screening 2002 were independent prognostic factors for overall survival. Our results suggest that when formulating treatment plans for elderly patients with EC, full attention should be given to age-related biological indicators such as comorbidities and nutrition.

Citation: Hu LL, Rong F, Liu L, Zhang L, Zhang LL, Yang Q, Xia ZL, Wang H. Prognosis of radiotherapy for esophageal cancer in elderly patients exceeding seventy-five years old. *World J Gastrointest Oncol* 2024; 16(12): 4636-4649
URL: https://www.wjgnet.com/1948-5204/full/v16/i12/4636.htm
DOI: https://dx.doi.org/10.4251/wjgo.v16.i12.4636

INTRODUCTION

Esophageal cancer (EC), a common malignant tumor of the digestive tract, poses a significant threat to human health. The Global Cancer Observatory's 2022 online platform, Cancer Today, 2022 (GLOBOCAN 2022), reported that the global incidence and mortality rates of EC are approximately 2.6% and 4.6%, respectively, ranking 11th and 7th, respectively among all malignant tumors[1]. With the extension of life expectancy, the aging of the population, and the improvement of diagnosis methods, the proportion of elderly EC patients has gradually increased, with 33% of patients being over 75 years old at the time of diagnosis[2,3]. Elderly patients often have degraded physiological functions, multiple comorbidities, and poor treatment tolerance, necessitating particularly cautious treatment approaches for this group.

Endoscopic resection and surgery (preferred for early-stage patients) and neoadjuvant chemoradiotherapy followed by surgery (trimodality therapy) are common treatment modalities for EC[4-6]. While advancements in survival have been noted, age significantly impacts the treatment of EC. Lester *et al*[7] indicated that older patients with trimodality therapy encountered increased postoperative cardiopulmonary toxicity and mortality, with cardiotoxicity exhibiting a linear correlation with age and a 61% rise in relative risk for every 10-year increase in age. Given the elevated postoperative complications, heightened in-hospital mortality, and reduced overall survival (OS) among elderly patients, non-surgical treatment is typically advised[8].

For patients with locally advanced EC who refuse surgery and are medically considered inoperable or have unresectable tumors, the efficacy of radical chemoradiotherapy (CRT) has been confirmed in numerous randomized clinical trials, whether using conventional two-dimensional radiotherapy (RT) or three-dimensional intensity-modulated RT (IMRT) technology. The earliest data were obtained from the Radiation Therapy Oncology Group (RTOG) 8501 and RTOG9405 studies[9-12]. For patients with metastatic EC, systemic therapy is effective, and RT to the primary tumor can relieve patients' dysphagia and pain and improve patients' survival[13,14]. However, the clinical trials that back these treatments excluded individuals aged over 75, with older patients showing lower tolerance to CRT and experiencing a higher incidence of side effects compared to their younger counterparts[15]. Therefore, these clinical data are underrepresented in elderly patients. There are limited data on the efficacy and safety of RT in EC patients aged 75 years and older, and there is no consensus on prognosis and treatment in this population.

Studies have revealed that elderly patients with EC often receive inadequate treatment due to concerns about side effects, comorbidities, and poor outcome, even when the disease is at a curable stage. Notably, the decision to forgo treatment was attributed to physicians in 46% of cases and to patients in 46% of cases[16]. However, the actual age of the patient does not truly reflect their biological aging level. Studies have shown that carefully selected elderly patients can tolerate the treatment and have a survival benefit[17]. More attention should be given to physiological age in medicine, which includes factors such as comorbidities, nutrition, and physical condition.

Based on the clinical information of elderly patients with unresectable EC who received IMRT at Lu'an Hospital of Anhui Medical University, this study explored prognostic factors associated with aging and provided a reference for individualized diagnosis and treatment of elderly EC patients.

MATERIALS AND METHODS

Patients

Retrospective analysis was conducted on elderly (≥ 75 years) EC patients who received IMRT with or without chemotherapy at Lu'an Hospital of Anhui Medical University from January 2016 to September 2023. All patients were pathologically diagnosed with esophageal squamous cell carcinoma (ESCC) or adenocarcinoma, had no prior history of thoracic RT, and had not undergone previous EC surgery. They were receiving RT for the first time and had complete follow-up data. Exclusion criteria included patients with severe cardiopulmonary dysfunction or other critical diseases affecting important systems. Clinical stages were classified according to the eighth edition of the American Joint Committee on Cancer (AJCC) staging system. This study was conducted in accordance with the ethical guidelines set forth in the World Medical Association Declaration of Helsinki and received approval from the Ethics Committee of Lu'an Hospital, Anhui Medical University.

Treatment

All patients received IMRT. Each patient was immobilized in the supine position, and a spiral computed tomography (CT) scan was performed with a slice thickness of 0.5 cm, covering the range from the lower edge of the mandible to the lower edge of the liver. The gross tumor volume (GTV) was defined as any visible primary tumor and included metastatic lymph nodes, determined by comprehensive esophagogram, esophagoscopy, contrast-enhanced thoracic CT or positron emission tomography. The clinical target volume (CTV) was defined as the GTV plus 3 cm cranial-caudal and 0.5 cm radial margin. For lymph nodes, the CTV was generated by extending the nodal GTV by 0.5 cm. The planning target volume (PTV) was generated by additional 0.5 cm radial margin for CTV. The prescription dose to 95% of PTV ranged from 44 Gray (Gy) to 66 Gy in 22-33 fractions. The use of chemotherapy and the choice of regimen were determined by the clinician based on the patient's specific circumstances.

Follow-up and treatment evaluation

All patients were followed up every 3 months during the first 2 years and every 6 months thereafter. Follow-up assessments included blood tests, esophagogram, esophagoscopy, and CT scans of the neck, chest, and abdomen. Follow-ups were conducted *via* telephone and outpatient visits, with a final deadline of January 23, 2024. Treatment-related toxicities were evaluated according to the RTOG radiation injury grading criteria.

Statistical analysis

Continuous variables were expressed as means ± SD or medians depending on whether they were normally distributed. The median follow-up time was estimated using the reverse Kaplan-Meier method. The Kaplan-Meier function was utilized to draw the OS curves, and the log-rank test was employed to compare OS among different groups. Univariate and multivariate Cox proportional hazards regression models were used to evaluate the relationship between various clinical variables and prognosis. Potential prognostic factors with $P < 0.05$ in univariate analysis were included in the multivariate analysis. The hazard ratio (HR) and the corresponding 95% confidence interval (CI) were used to predict the effect of each variable on OS. The OS time was defined as the period from the date of diagnosis until death from any cause. Receiver operating characteristic (ROC) curves were drawn to verify the accuracy of the Charlson comorbidity index (CCI), nutritional risk screening 2002 (NRS2002) and clinical stage for survival prediction. The OS and ROC curves were calculated using statistical product and service solutions 24.0, while the remaining statistical analyses were performed using R software (version 4.3.0, http://www.r-project.org/).

RESULTS

Patients' characteristics

During the study period, a total of 158 elderly (≥ 75 years) EC patients were treated with IMRT. After exclusions, 139 cases remained for analysis. The exclusions were due to the following reasons: 4 cases had concurrent malignant tumors, 1 case had small cell pathology, 8 cases had incomplete clinical data, and 6 cases were lost to follow-up. The median age was 79 years (range from 75 years to 92 years). According to the eighth edition of the AJCC staging system, 93 patients (66.9%) were distributed in stages III to IVa. Chemotherapy was administered to 103 patients (74.1%) at different phases of treatment, including 84 patients (60.4%) who received concurrent chemotherapy. 129 patients (92%) completed the planned RT, with a median radiation dose of 60 Gy (range from 20 to 66 Gy). The clinical characteristics are summarized in Table 1.

Survival and prognostic analysis

The median follow-up time was 52.0 months. The median OS was 20.0 months. The 1-year, 2-year, 3-year, and 5-year OS

Table 1 Demographics and clinical characteristics of patients, *n* (%)

Variables	Number of patients
Age	
≥ 75 and < 80	70 (50.4)
≥ 80	69 (49.6)
Sex	
Female	39 (28.1)
Male	100 (72.9)
Marital status	
Married	133 (95.7)
Unmarried	6 (4.3)
Smoke	
No	84 (60.4)
Yes	55 (39.6)
Drink	
No	102 (73.4)
Yes	37 (26.6)
C stage	
I-II	24 (17.3)
III-IVa	93 (66.9)
IVb	22 (15.8)
T stage	
T1-T2	22 (15.8)
T3-T4	117 (84.2)
N stage	
Negative	22 (15.8)
Positive	117 (84.2)
M stage	
M0	117 (84.2)
M1	22 (15.8)
Tumor length	
< 6	90 (64.7)
≥ 6	49 (35.3)
Tumor location	
Upper thoracic	34 (24.5)
Middle thoracic	62 (44.6)
Lower thoracic	43 (30.9)
ECOG	
0-1	133 (95.7)
2	6 (4.3)
CCI	
0	62 (44.6)
≥ 1	77 (55.4)

NRS2002	
< 3	66 (47.5)
≥ 3	73 (52.5)
BMI	
< 18.5	32 (23.0)
≥ 18.5	107 (77.0)
Weight loss	
< 10%	128 (92.1)
≥ 10%	11 (7.9)
Radiation dose	
< 60	57 (41.0)
≥ 60	82 (59.0)
Chemotherapy	
No	36 (25.9)
Yes	103 (74.1)

BMI: Body mass index; ECOG: Eastern Cooperative Oncology Group; CCI: Charlson comorbidity index; NRS2002: Nutritional risk screening 2002.

rates were 69.8%, 38.7%, 28.2%, and 17.5%, respectively.

Univariate analysis showed that patients with a CCI score of ≥ 1 had worse OS compared to those with a score of 0 (HR = 1.620; 95%CI: 1.080-2.429; P = 0.019). Patients with an NRS2002 score of < 3 before RT had better OS than those with a score of ≥ 3 (HR = 2.215; 95%CI: 1.466-3.348; P < 0.001). Patients with weight loss (WL) of < 10% before RT had better OS compared to those with WL of ≥ 10% (HR = 2.947; 95%CI: 1.473-5.898; P = 0.002). Other statistically significant prognostic factors included clinical stage, lymph node metastasis, and distant metastasis. Conversely, factors such as age, radiation dose, and chemotherapy did not have a significant impact on prognosis. The survival curves of elderly patients with EC in different groups are depicted in Figure 1.

The subsequent multivariate analysis was conducted based on clinical stage, CCI, NRS2002, and WL. The results indicated that the clinical stage (III-IVa *vs* I-II, HR = 2.421, 95%CI: 1.242-4.718, P = 0.009; IVb *vs* I-II, HR = 4.222, 95%CI: 1.888-9.438, P < 0.001), CCI (HR = 1.539; 95%CI: 1.015-2.332; P = 0.042) and NRS2002 (HR = 2.491; 95%CI: 1.601-3.875; P < 0.001) were independent prognostic factors for elderly patients with EC. The results of both univariate and multivariate analyses are presented in Table 2.

ROC curve for survival prediction

ROC curves for OS were plotted. As shown in Figure 2, the area under the curve (AUC) for NRS2002 was 0.665, the AUC for CCI was 0.530, and the AUC for clinical stage was 0.608. When all three indicators were combined for prediction, the AUC increased to 0.726 (95%CI: 0.635-0.817), demonstrating superior predictive accuracy compared to any single indicator alone.

Toxicity

Toxicity primarily occurred in grade 1 or 2, with a low incidence of grade 3 and higher adverse reactions. Table 3 demonstrated treatment-related acute toxic reactions, including leukopenia, anemia, thrombocytopenia, esophagitis, pneumonitis, and dermatitis. Specifically, the incidence of grade 3 hematological toxicity was 8.6%, grade 3 esophagitis was 5.5%, and grade 3 pneumonitis was 1.4%. Additionally, one patient experienced grade 4 hematological toxicity, while no grade 4 or higher non-hematological toxicity was observed.

DISCUSSION

In this study, we conducted a retrospective analysis of the clinical characteristics, toxic reactions, and survival information of elderly EC patients aged ≥ 75 years who underwent IMRT and aimed to evaluate the prognostic factors for OS. Our analysis revealed that CCI and NRS2002 are independent prognostic factors for OS. These findings underscore the significance of comorbidities and nutrition in influencing the prognosis of elderly EC patients. Therefore, when formulating treatment protocols for elderly EC patients, it is crucial to consider aging-related prognostic factors, specifically comorbidities and nutrition, as indicated by CCI and NRS2002.

Table 2 Univariate and multivariate Cox analysis of the determinants of overall survival of patients

Variables	Univariate analysis				Multivariate analysis			
	HR	Lower 95%CI	Upper 95%CI	*P* value	HR	Lower 95%CI	Upper 95%CI	*P* value
Age								
≥ 75 and < 80	1							
≥ 80	1.147	0.769	1.710	0.502				
Sex								
Female	1							
Male	0.656	0.427	1.009	0.055				
Marital status								
Married	1							
Unmarried	0.538	0.132	2.188	0.387				
Smoke								
No	1							
Yes	0.821	0.544	1.239	0.348				
Drink								
No	1							
Yes	0.869	0.545	1.387	0.557				
C stage								
I-II	1				1			
III-IVa	2.261	1.189	4.298	0.013	2.421	1.242	4.718	0.009
IVb	3.444	1.593	7.446	0.002	4.222	1.888	9.438	< 0.001
T stage								
T1-T2	1							
T3-T4	1.575	0.876	2.831	0.129				
N stage								
Negative	1							
Positive	2.030	1.104	3.732	0.023				
M stage								
M0	1							
M1	1.761	1.038	2.986	0.036				
Tumor length								
< 6	1							
≥ 6	1.261	0.836	1.904	0.269				
Tumor location								
Upper thoracic	1							
Middle thoracic	1.054	0.632	1.759	0.840				
Lower thoracic	1.146	0.665	1.976	0.623				
ECOG								
0-1	1							
2	2.023	0.820	4.995	0.126				
CCI								
0	1				1			

≥ 1	1.620	1.080	2.429	0.020	1.539	1.015	2.332	0.042
NRS2002								
< 3	1				1			
≥ 3	2.215	1.466	3.348	< 0.001	2.491	1.601	3.875	< 0.001
BMI								
< 18.5	1							
≥ 18.5	0.756	0.482	1.183	0.221				
Weight loss								
< 10%	1				1			
≥ 10%	2.947	1.473	5.898	0.002	1.798	0.870	3.715	0.113
Radiation dose								
< 60	1							
≥ 60	0.771	0.511	1.164	0.217				
Chemotherapy								
No	1							
Yes	0.847	0.543	1.320	0.463				

HR: Hazard ratio; CI: Confidence interval; BMI: Body mass index; ECOG: Eastern Cooperative Oncology Group; CCI: Charlson comorbidity index; NRS2002: Nutritional risk screening 2002.

Table 3 Treatment-related acute toxicities in patients, *n* (%)

Toxicity	Grade 1	Grade 2	Grade 3	Grade 4
Leukocytopenia	31 (22.3)	43 (30.9)	6 (4.3)	1 (0.7)
Anemia	29 (20.8)	21 (15.1)	8 (5.7)	1 (0.7)
Thrombopenia	3 (2.1)	2 (1.4)	2 (1.4)	1 (0.7)
Esophagitis	19 (13.6)	40 (28.7)	7 (5.5)	0 (0.0)
Pneumonitis	1 (0.7)	2 (1.4)	2 (1.4)	0 (0.0)
Dermatitis	2 (1.4)	0 (0.0)	0 (0.0)	0 (0.0)

With the advancement of medical technology and the improvement of medical security levels, human life expectancy continues to increase, leading to a growing proportion of elderly individuals in the population. China, which accounts for about one-fifth of the world's population, sees more than half of the global EC cases. Elderly EC patients represent a heterogeneous group that warrants significant attention. Although there are limited avenues of treatment for elderly EC patients, any treatment modality can provide substantial survival benefits compared to best supportive care[18]. Currently, many clinical studies on elderly EC have focused on patients over 70 years of age. A multi-center retrospective study from China revealed that the survival time of patients over 75 years is significantly lower than that of patients under 75 years. Therefore, the optimal treatment strategy for elderly EC patients over 75 years is still under exploration [19-21].

Due to demographic shifts, the number of elderly patients with EC is increasing, and many patients have unhealthy lifestyle habits such as smoking and alcohol consumption, leading to a higher prevalence of comorbidities among this group. Observational studies have consistently indicated that cancer patients with comorbidities experience lower survival rates compared to those without comorbidities[22-24]. The most commonly used model for quantifying comorbidities is the CCI. Currently, several studies have investigated the relationship between comorbidities and prognosis in patients with different stages of EC. For instance, Ishido *et al*[25] found that a CCI ≥ 2 was a prognostic factor for endoscopic treatment in elderly patients with superficial EC. Similarly, Yamashita *et al*[26] reported that a high CCI was associated with poor prognosis in stage II and above staged EC. Bernardi *et al*[27] highlighted that age alone could not directly indicate a patient's ability to tolerate treatment, instead, comorbidities played a central role in the decision-making process, with the routine use of CCI aiding in prognostic risk stratification. While the value of CCI has been extensively studied in surgery, it has been less explored in RT for elderly EC. Our results align with these findings, showing that more than half of elderly EC patients had comorbidities, with CCI ≥ 1 accounting for 55.4% (77/139). Univariate and multivariate analyses indicated that the OS of the "CCI = 0" group was better than that of the "CCI ≥ 1"

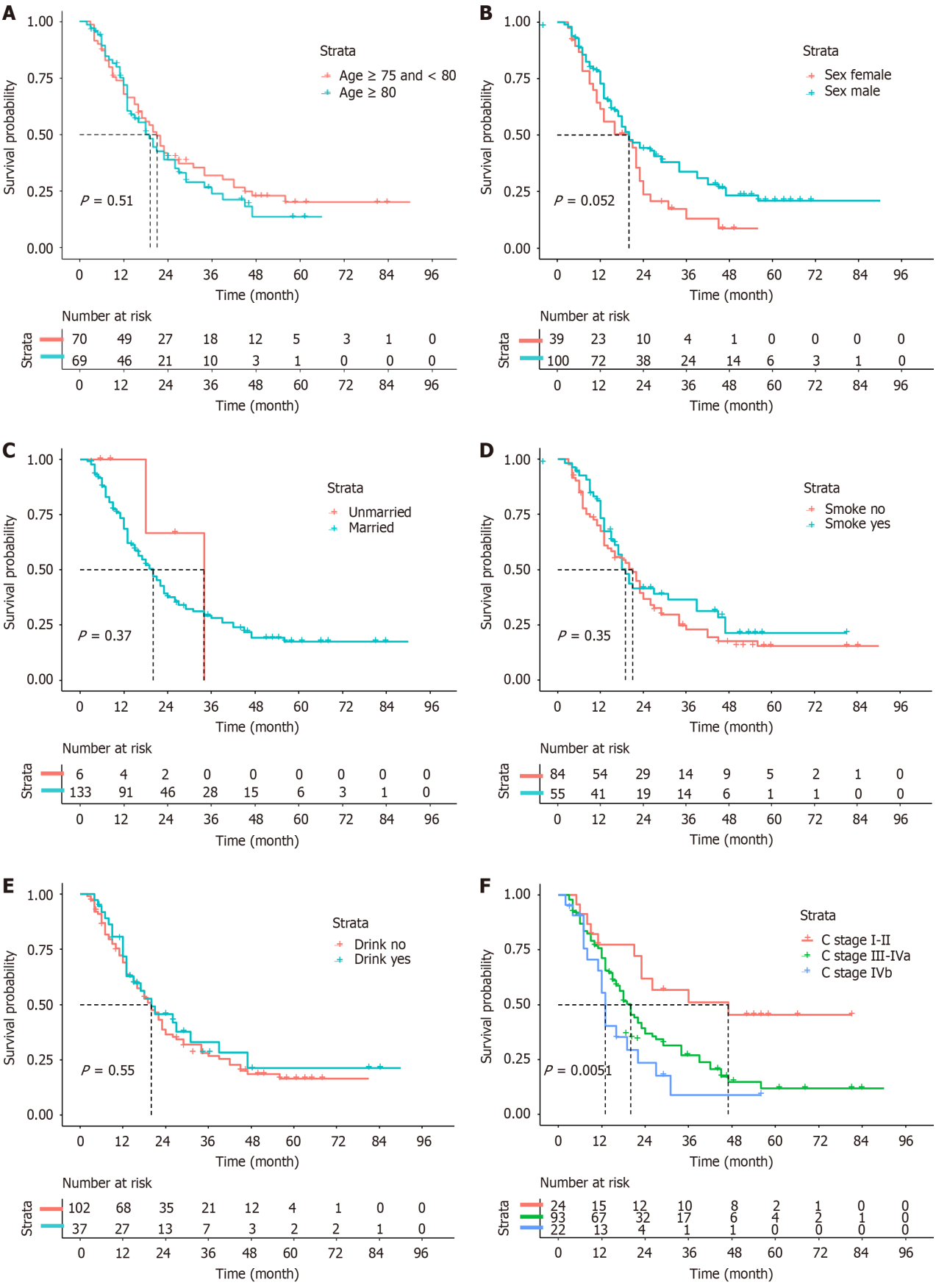
A
Survival probability
1.00
0.75
0.50
0.25
0.00
Strata
Age ≥ 75 and < 80
Age ≥ 80
P = 0.51
0 12 24 36 48 60 72 84 96
Time (month)
Number at risk
Strata
70 49 27 18 12 5 3 1 0
69 46 21 10 3 1 0 0 0
0 12 24 36 48 60 72 84 96
Time (month)
B
Survival probability
1.00
0.75
0.50
0.25
0.00
Strata
Sex female
Sex male
P = 0.052
0 12 24 36 48 60 72 84 96
Time (month)
Number at risk
Strata
39 23 10 4 1 0 0 0 0
100 72 38 24 14 6 3 1 0
0 12 24 36 48 60 72 84 96
Time (month)
C
Survival probability
1.00
0.75
0.50
0.25
0.00
Strata
Unmarried
Married
P = 0.37
0 12 24 36 48 60 72 84 96
Time (month)
Number at risk
Strata
6 4 2 0 0 0 0 0 0
133 91 46 28 15 6 3 1 0
0 12 24 36 48 60 72 84 96
Time (month)
D
Survival probability
1.00
0.75
0.50
0.25
0.00
Strata
Smoke no
Smoke yes
P = 0.35
0 12 24 36 48 60 72 84 96
Time (month)
Number at risk
Strata
84 54 29 14 9 5 2 1 0
55 41 19 14 6 1 1 0 0
0 12 24 36 48 60 72 84 96
Time (month)
E
Survival probability
1.00
0.75
0.50
0.25
0.00
Strata
Drink no
Drink yes
P = 0.55
0 12 24 36 48 60 72 84 96
Time (month)
Number at risk
Strata
102 68 35 21 12 4 1 0 0
37 27 13 7 3 2 2 1 0
0 12 24 36 48 60 72 84 96
Time (month)
F
Survival probability
1.00
0.75
0.50
0.25
0.00
Strata
C stage I-II
C stage III-IVa
C stage IVb
P = 0.0051
0 12 24 36 48 60 72 84 96
Time (month)
Number at risk
Strata
24 15 12 10 8 2 1 0 0
93 67 32 17 6 4 2 1 0
22 13 4 1 1 0 0 0 0
0 12 24 36 48 60 72 84 96
Time (month)

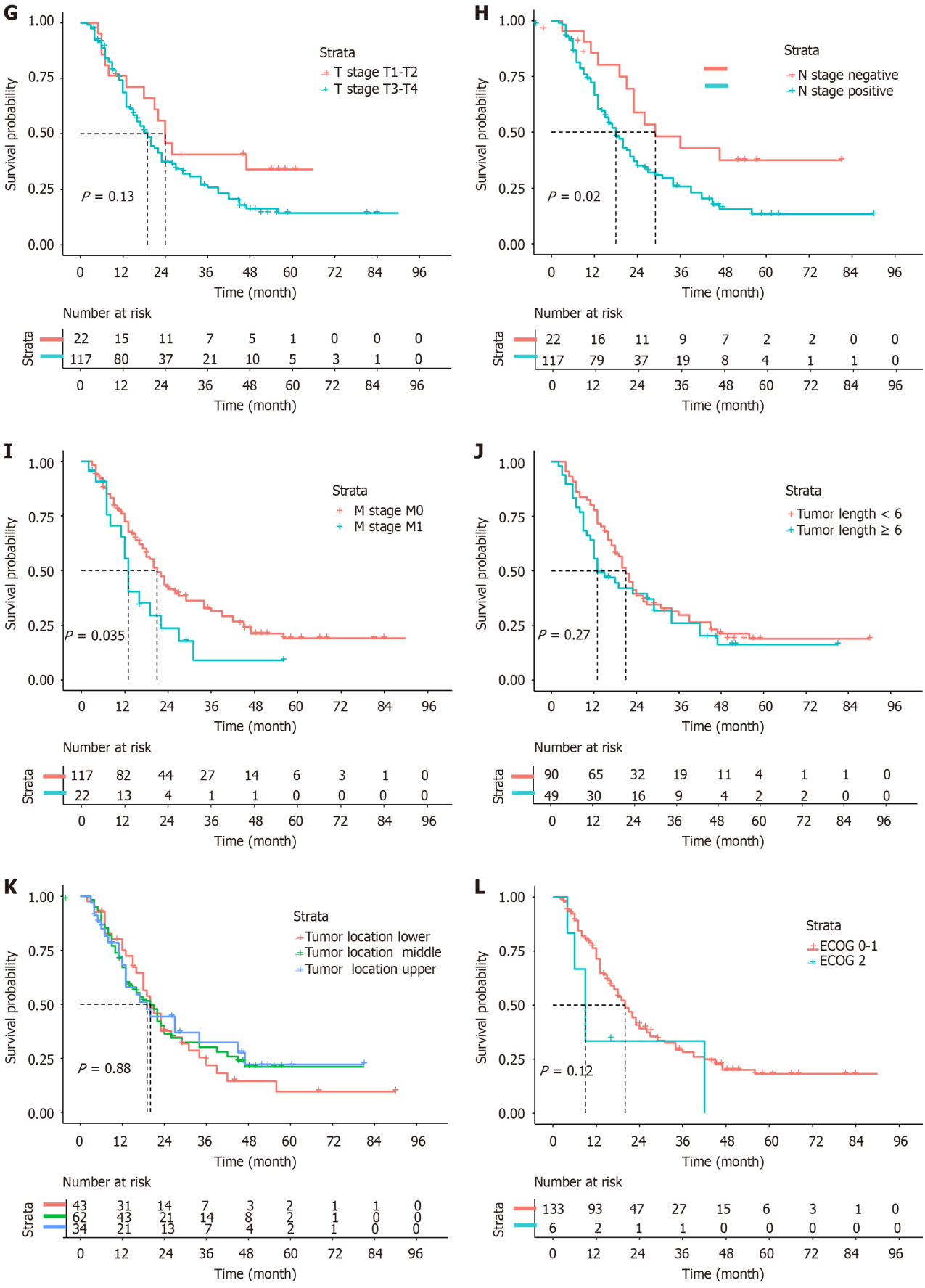
G
Survival probability
1.00
0.75
0.50
0.25
0.00
Strata
T stage T1-T2
T stage T3-T4
P = 0.13
0 12 24 36 48 60 72 84 96
Time (month)
Number at risk
Strata
22 15 11 7 5 1 0 0 0
117 80 37 21 10 5 3 1 0
0 12 24 36 48 60 72 84 96
Time (month)
H
Survival probability
1.00
0.75
0.50
0.25
0.00
Strata
N stage negative
N stage positive
P = 0.02
0 12 24 36 48 60 72 84 96
Time (month)
Number at risk
Strata
22 16 11 9 7 2 2 0 0
117 79 37 19 8 4 1 1 0
0 12 24 36 48 60 72 84 96
Time (month)
I
Survival probability
1.00
0.75
0.50
0.25
0.00
Strata
M stage M0
M stage M1
P = 0.035
0 12 24 36 48 60 72 84 96
Time (month)
Number at risk
Strata
117 82 44 27 14 6 3 1 0
22 13 4 1 1 0 0 0 0
0 12 24 36 48 60 72 84 96
Time (month)
J
Survival probability
1.00
0.75
0.50
0.25
0.00
Strata
Tumor length < 6
Tumor length ≥ 6
P = 0.27
0 12 24 36 48 60 72 84 96
Time (month)
Number at risk
Strata
90 65 32 19 11 4 1 1 0
49 30 16 9 4 2 2 0 0
0 12 24 36 48 60 72 84 96
Time (month)
K
Survival probability
1.00
0.75
0.50
0.25
0.00
Strata
Tumor location lower
Tumor location middle
Tumor location upper
P = 0.88
0 12 24 36 48 60 72 84 96
Time (month)
Number at risk
Strata
43 31 14 7 3 2 1 1 0
62 43 21 14 8 2 1 0 0
34 21 13 7 4 2 1 0 0
0 12 24 36 48 60 72 84 96
Time (month)
L
Survival probability
1.00
0.75
0.50
0.25
0.00
Strata
ECOG 0-1
ECOG 2
P = 0.12
0 12 24 36 48 60 72 84 96
Time (month)
Number at risk
Strata
133 93 47 27 15 6 3 1 0
6 2 1 1 0 0 0 0 0
0 12 24 36 48 60 72 84 96
Time (month)

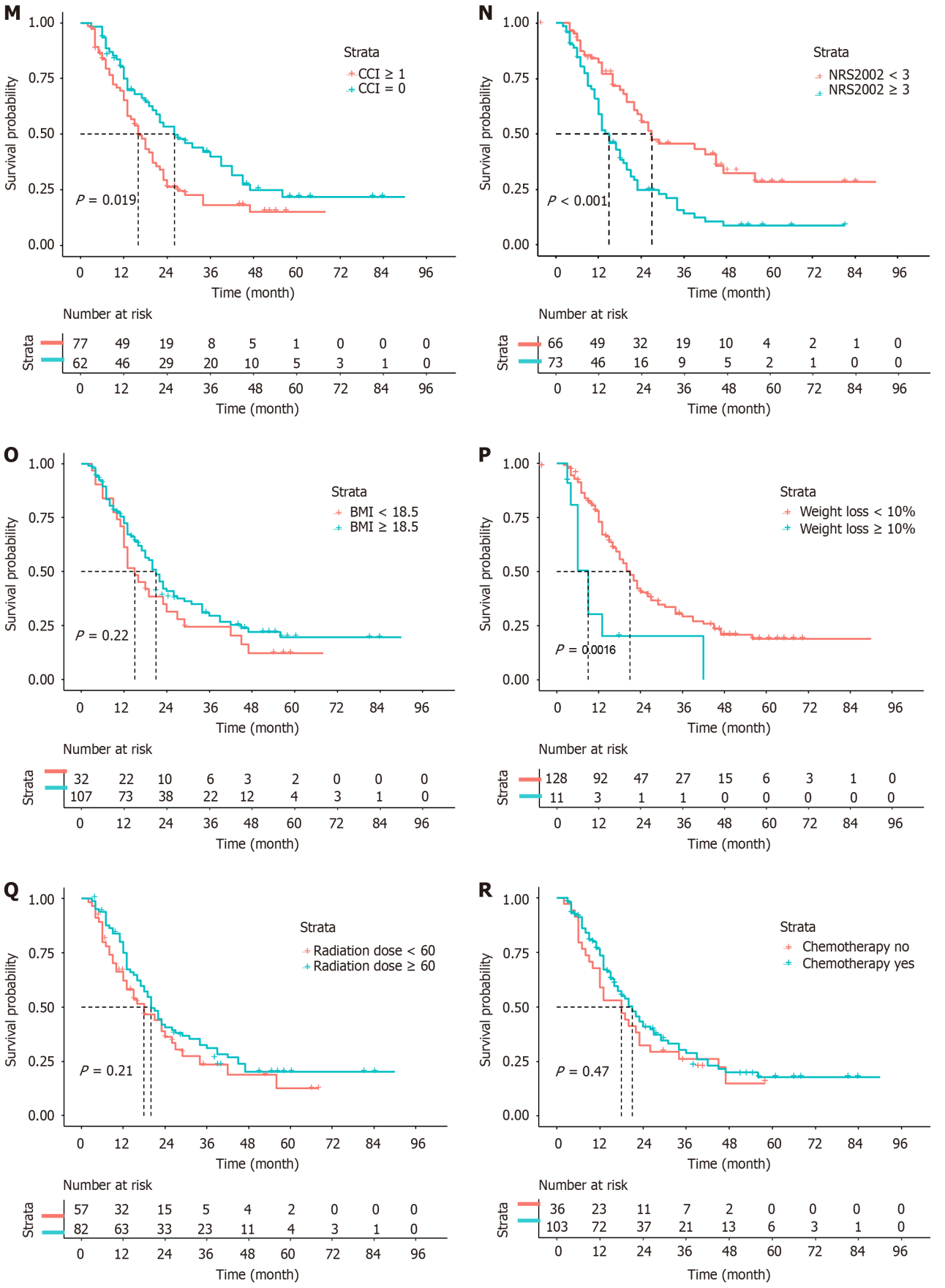

Figure 1 The survival curves of elderly patients with esophageal cancer in different groups. A: Age; B: Sex; C: Marital status; D: Smoke; E: Drink; F: C stage; G: T stage; H: N stage; I: M stage; J: Tumor length; K: Tumor location; L: Eastern Cooperative Oncology Group; M: Charlson comorbidity index; N: Nutritional risk screening 2002; O: Body mass index; P: Weight loss; Q: Radiation dose; R: Chemotherapy. BMI: Body mass index; ECOG: Eastern Cooperative Oncology Group; CCI: Charlson comorbidity index; NRS2002: Nutritional risk screening 2002.

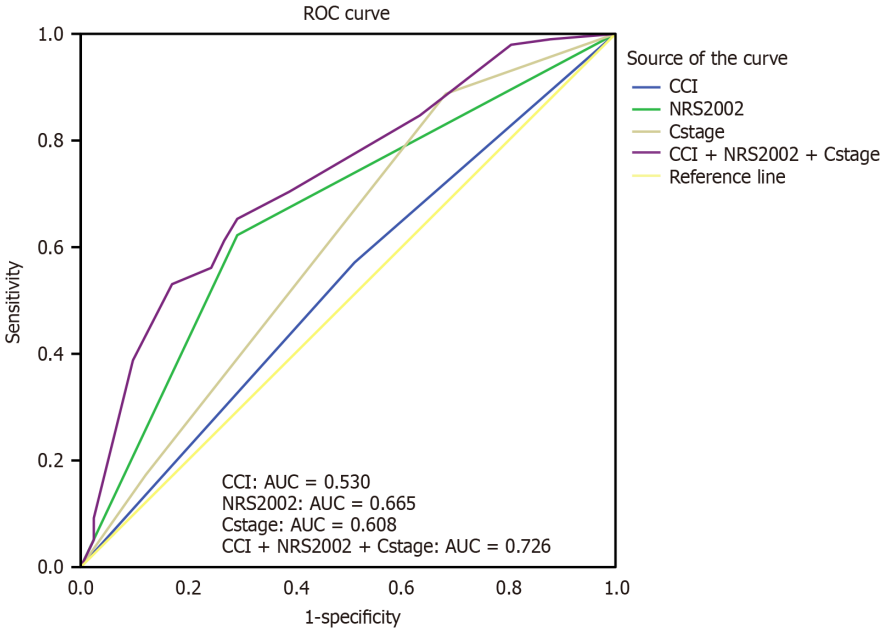

Figure 2 Receiver operating characteristic curves of Charlson comorbidity index, nutritional risk screening 2002, and clinical stage for predicting odds ratio in elderly patients with esophageal cancer after radiotherapy. ROC: Receiver operating characteristic; AUC: Area under curve; CCI: Charlson comorbidity index; NRS2002: Nutritional risk screening 2002.

group. Therefore, our study suggests that comorbidities could affect the survival of elderly EC patients receiving RT.

Some studies have reported that approximately 60% to 85% of EC patients suffer from malnutrition, ranking first among malignant tumors[28]. Malnutrition can cause various harms to patients undergoing RT for EC, such as increasing positioning errors, side effects, and reducing efficacy. It can even lead to treatment interruptions, prolonged hospitalization, increased medical expenses, and decreased survival rates. Studies have indicated that malnutrition is a prognostic factor in elderly EC patients receiving RT[21,29]. Currently, there are many nutritional assessment tools for the prognosis assessment of EC, such as the controlling nutritional status (CONUT), the prognostic nutritional index (PNI), the patient-generated subjective global assessment, and the NRS2002[30-33]. Compared with the invasive and complex inconveniences of the first three assessment methods, the NRS2002 screening tool is non-invasive, inexpensive, time-saving, and easy to use[34]. Noh *et al*[35] analyzed 274 patients undergoing surgery for ESCC, using PNI, NRS2002, and CONUT to assess preoperative nutritional status. The results indicated that during a median follow-up of 55 months, a high NRS2002 was associated with poor OS and a high incidence of postoperative complications. Thus, NRS2002 was considered the most appropriate scoring system for assessing patients' nutritional status. Song *et al*[36] retrospectively investigated 202 patients with locally advanced unresectable EC who received CRT to explore their prognostic factors. The results revealed that NRS ≥ 3 points was a poor prognostic factor. Similarly, the study by Wang *et al*[33] demonstrated that the baseline NRS2002 score serves as a simple and effective biomarker for predicting the long-term prognosis of patients with EC undergoing CRT. Consistent with previous studies, our study showed that NRS2002 was an independent prognostic factor for OS in elderly EC patients receiving RT. Therefore, pretreatment nutritional assessment and correction of malnutrition may improve survival outcomes in elderly EC patients undergoing RT.

Currently, CRT with 5-fluorouracil and cisplatin is the standard care for non-surgical EC treatment[9]. However, due to the serious toxic and side effects of double-drug concurrent chemoradiation (CCRT), most elderly EC patients often cannot tolerate it and thus cannot complete standard CCRT treatment. Ji *et al*[37] enrolled 298 elderly EC patients aged 70 and above to investigate the efficacy and toxicities of CCRT with S-1. The results indicated that the survival outcomes were superior in the CCRT group compared to the RT group alone, and the toxicities were manageable, suggesting that elderly patients could benefit from a treatment regimen involving combined RT and single-agent chemotherapy. Regarding EC patients 75 years and older, there are no large-scale prospective randomized clinical trials comparing the efficacy of CCRT with RT alone. Some retrospective studies have revealed that CCRT has no statistically significant survival benefit[21,38]. The findings of our study are consistent with these reports. Therefore, caution should be exercised when using CCRT in elderly EC patients aged 75 years and older, and omitting or using milder chemotherapy regimens may be more appropriate.

To further analyze the prognostic value of CCI, NRS2002, and clinical stage in elderly patients with unresectable EC, we plotted ROC curves. The combined prediction of these three factors for the survival of elderly EC patients yielded an AUC of 0.726, which outperformed the predictive ability of any individual factor. This finding suggests that treatment strategies for elderly EC patients should be tailored based on factors such as disease stage, nutritional status, and comorbidity. Individualized treatment plans should be carefully designed for elderly patients through meticulous selection, aiming to provide the best possible treatment while ensuring safety.

In the study of Yin *et al*[19], the median OS of elderly EC patients who received RT, including patients with metastatic lesions, was 20.68 months. The 1-year, 2-year, 3-year, and 5-year OS rates were 62.6%, 41.8%, 11.1%, and 0%, respectively. Our study showed that the median OS of elderly EC patients receiving RT was 20.0 months, and the 1-year, 2-year, 3-year, and 5-year OS rates were 69.8%, 38.7%, 28.2%, and 17.5%, respectively. Since their study enrolled patients over 70 years, and ours included patients over 75 years, it showed that we had a greater advantage in survival of elderly EC patients. In the study of Suzuki *et al*[38], the median OS of older patients aged ≥ 75 years with localized EC who received RT was 30.0 months, and the 2-year OS rate was 53%. Zhou *et al*[21] retrospectively analyzed 149 patients over the age of 75 with localized EC and reported that the 2-year OS rate was 51.6%. The survival time of patients in our study was slightly worse than that of the above two studies, which may be due to the inclusion of 15.8% of patients with metastatic EC. Therefore, RT is an effective treatment for patients with unresectable EC over the age of 75, and advanced age alone should not be a reason to exclude patients from RT.

There were some limitations to this study. Firstly, it was a single-center retrospective study with a relatively small sample size, introducing selection bias. Secondly, variables such as smoking, drinking, and comorbidity were all self-reported by elderly patients, who were elderly, leading to recall bias. Finally, some potential prognostic factors, such as elective nodal irradiation and involved-field irradiation, were not included in the study. Therefore, prospective research is still needed to provide a basis for the treatment of elderly EC patients.

CONCLUSION

This study identified prognostic factors for RT in elderly patients with unresectable EC. "CCI ≥ 1" and "NRS2002 ≥ 3" were independent prognostic factors associated with worse OS. Increasing the dose of RT and combining chemotherapy did not significantly improve survival. For elderly patients with EC, the focus should be on biological age rather than physiologic age. Future clinical practice should consider indicators associated with aging, such as comorbidities and nutritional status.

FOOTNOTES

Author contributions: Hu LL and Wang H conceived and designed the study and performed the data analysis and interpretation, as well as the initial drafting of the manuscript; Zhang L, Yang Q and Xia ZL helped collect the data; and Rong F, Liu L, and Zhang LL provided critical revisions to the manuscript; All authors reviewed the results and approved the final version of the manuscript.

Supported by the Science and Technology Program of Lu'an, No. 2022 Lakj042.

Institutional review board statement: This study was approved by the Ethics Committee of Lu'an Hospital of Anhui Medical University, No. 2023 LLKS035.

Informed consent statement: In this study, informed consent was obtained from the patients and their families.

Conflict-of-interest statement: The authors declare that they have no conflict of interest.

Data sharing statement: The datasets generated and/or analyzed in the current study can be obtained from the corresponding author upon a reasonable request.

Country of origin: China

ORCID number: Li-Li Hu 0009-0002-3920-5057; Feng Rong 0000-0001-7827-6347; Lei Liu 0009-0009-3348-4965; Ling Zhang 0009-0008-8937-2578; Lei-Lei Zhang 0009-0000-7662-7924; Zhao-Long Xia 0009-0006-7820-1365; Hui Wang 0000-0001-5503-0547.

S-Editor: Fan M
L-Editor: A
P-Editor: Wang WB

REFERENCES

1 **Bray F**, Laversanne M, Sung H, Ferlay J, Siegel RL, Soerjomataram I, Jemal A. Global cancer statistics 2022: GLOBOCAN estimates of incidence and mortality worldwide for 36 cancers in 185 countries. *CA Cancer J Clin* 2024; **74**: 229-263 [PMID: 38572751 DOI: 10.3322/caac.21834]

2 **Rustgi AK**, El-Serag HB. Esophageal carcinoma. *N Engl J Med* 2014; **371**: 2499-2509 [PMID: 25539106 DOI: 10.1056/NEJMra1314530]

3 **van Blankenstein M**, Looman CW, Siersema PD, Kuipers EJ, Coebergh JW. Trends in the incidence of adenocarcinoma of the oesophagus and cardia in the Netherlands 1989-2003. *Br J Cancer* 2007; **96**: 1767-1771 [PMID: 17505507 DOI: 10.1038/sj.bjc.6603798]

4 **Lu W**, Li P, Wen W, Jian Y. Comparison of Long-Term Survival Between cT1N0 Stage Esophageal Cancer Patients Receiving Endoscopic Dissection and Esophagectomy: A Meta-Analysis. *Front Surg* 2022; **9**: 917689 [PMID: 36017523 DOI: 10.3389/fsurg.2022.917689]

5 **van Hagen P**, Hulshof MC, van Lanschot JJ, Steyerberg EW, van Berge Henegouwen MI, Wijnhoven BP, Richel DJ, Nieuwenhuijzen GA, Hospers GA, Bonenkamp JJ, Cuesta MA, Blaisse RJ, Busch OR, ten Kate FJ, Creemers GJ, Punt CJ, Plukker JT, Verheul HM, Spillenaar Bilgen EJ, van Dekken H, van der Sangen MJ, Rozema T, Biermann K, Beukema JC, Piet AH, van Rij CM, Reinders JG, Tilanus HW, van der Gaast A; CROSS Group. Preoperative chemoradiotherapy for esophageal or junctional cancer. *N Engl J Med* 2012; **366**: 2074-2084 [PMID: 22646630 DOI: 10.1056/NEJMoa1112088]

6 **Yang H**, Liu H, Chen Y, Zhu C, Fang W, Yu Z, Mao W, Xiang J, Han Y, Chen Z, Yang H, Wang J, Pang Q, Zheng X, Yang H, Li T, Lordick F, D'Journo XB, Cerfolio RJ, Korst RJ, Novoa NM, Swanson SJ, Brunelli A, Ismail M, Fernando HC, Zhang X, Li Q, Wang G, Chen B, Mao T, Kong M, Guo X, Lin T, Liu M, Fu J; AME Thoracic Surgery Collaborative Group. Neoadjuvant Chemoradiotherapy Followed by Surgery Versus Surgery Alone for Locally Advanced Squamous Cell Carcinoma of the Esophagus (NEOCRTEC5010): A Phase III Multicenter, Randomized, Open-Label Clinical Trial. *J Clin Oncol* 2018; **36**: 2796-2803 [PMID: 30089078 DOI: 10.1200/JCO.2018.79.1483]

7 **Lester SC**, Lin SH, Chuong M, Bhooshan N, Liao Z, Arnett AL, James SE, Evans JD, Spears GM, Komaki R, Haddock MG, Mehta MP, Hallemeier CL, Merrell KW. A Multi-institutional Analysis of Trimodality Therapy for Esophageal Cancer in Elderly Patients. *Int J Radiat Oncol Biol Phys* 2017; **98**: 820-828 [PMID: 28476435 DOI: 10.1016/j.ijrobp.2017.02.021]

8 **Markar SR**, Karthikesalingam A, Thrumurthy S, Ho A, Muallem G, Low DE. Systematic review and pooled analysis assessing the association between elderly age and outcome following surgical resection of esophageal malignancy. *Dis Esophagus* 2013; **26**: 250-262 [PMID: 22591068 DOI: 10.1111/j.1442-2050.2012.01353.x]

9 **Cooper JS**, Guo MD, Herskovic A, Macdonald JS, Martenson JA Jr, Al-Sarraf M, Byhardt R, Russell AH, Beitler JJ, Spencer S, Asbell SO, Graham MV, Leichman LL. Chemoradiotherapy of locally advanced esophageal cancer: long-term follow-up of a prospective randomized trial (RTOG 85-01). Radiation Therapy Oncology Group. *JAMA* 1999; **281**: 1623-1627 [PMID: 10235156 DOI: 10.1001/jama.281.17.1623]

10 **Minsky BD**, Pajak TF, Ginsberg RJ, Pisansky TM, Martenson J, Komaki R, Okawara G, Rosenthal SA, Kelsen DP. INT 0123 (Radiation Therapy Oncology Group 94-05) phase III trial of combined-modality therapy for esophageal cancer: high-dose versus standard-dose radiation therapy. *J Clin Oncol* 2002; **20**: 1167-1174 [PMID: 11870157 DOI: 10.1200/JCO.2002.20.5.1167]

11 **Hulshof MCCM**, Geijsen ED, Rozema T, Oppedijk V, Buijsen J, Neelis KJ, Nuyttens JJME, van der Sangen MJC, Jeene PM, Reinders JG, van Berge Henegouwen MI, Thano A, van Hooft JE, van Laarhoven HWM, van der Gaast A. Randomized Study on Dose Escalation in Definitive Chemoradiation for Patients With Locally Advanced Esophageal Cancer (ARTDECO Study). *J Clin Oncol* 2021; **39**: 2816-2824 [PMID: 34101496 DOI: 10.1200/JCO.20.03697]

12 **Xu Y**, Dong B, Zhu W, Li J, Huang R, Sun Z, Yang X, Liu L, He H, Liao Z, Guan N, Kong Y, Wang W, Chen J, He H, Qiu G, Zeng M, Pu J, Hu W, Bao Y, Liu Z, Ma J, Jiang H, Du X, Hu J, Zhuang T, Cai J, Huang J, Tao H, Liu Y, Liang X, Zhou J, Tao G, Zheng X, Chen M. A Phase III Multicenter Randomized Clinical Trial of 60 Gy versus 50 Gy Radiation Dose in Concurrent Chemoradiotherapy for Inoperable Esophageal Squamous Cell Carcinoma. *Clin Cancer Res* 2022; **28**: 1792-1799 [PMID: 35190815 DOI: 10.1158/1078-0432.CCR-21-3843]

13 **Li LQ**, Fu QG, Zhao WD, Wang YD, Meng WW, Su TS. Chemoradiotherapy Versus Chemotherapy Alone for Advanced Esophageal Squamous Cell Carcinoma: The Role of Definitive Radiotherapy for Primary Tumor in the Metastatic Setting. *Front Oncol* 2022; **12**: 824206 [PMID: 35433478 DOI: 10.3389/fonc.2022.824206]

14 **Guttmann DM**, Mitra N, Bekelman J, Metz JM, Plastaras J, Feng W, Swisher-McClure S. Improved Overall Survival with Aggressive Primary Tumor Radiotherapy for Patients with Metastatic Esophageal Cancer. *J Thorac Oncol* 2017; **12**: 1131-1142 [PMID: 28461255 DOI: 10.1016/j.jtho.2017.03.026]

15 **Takeuchi S**, Ohtsu A, Doi T, Kojima T, Minashi K, Mera K, Yano T, Tahara M, Muto M, Nihei K. A retrospective study of definitive chemoradiotherapy for elderly patients with esophageal cancer. *Am J Clin Oncol* 2007; **30**: 607-611 [PMID: 18091055 DOI: 10.1097/COC.0b013e3180ca7c84]

16 **Qu X**, Biagi J, Banashkevich A, Mercer CD, Tremblay L, Mahmud A. Management and outcomes of localized esophageal and gastroesophageal junction cancer in older patients. *Curr Oncol* 2015; **22**: e435-e442 [PMID: 26715880 DOI: 10.3747/co.22.2661]

17 **Bracken-Clarke D**, Farooq AR, Horgan AM. Management of Locally Advanced and Metastatic Esophageal Cancer in the Older Population. *Curr Oncol Rep* 2018; **20**: 99 [PMID: 30426245 DOI: 10.1007/s11912-018-0745-3]

18 **Mantziari S**, Teixeira Farinha H, Bouygues V, Vignal JC, Deswysen Y, Demartines N, Schäfer M, Piessen G. Esophageal Cancer in Elderly Patients, Current Treatment Options and Outcomes; A Systematic Review and Pooled Analysis. *Cancers (Basel)* 2021; **13** [PMID: 33925512 DOI: 10.3390/cancers13092104]

19 **Yin H**, E M, Zhang H, Wang C. The outcomes of radiotherapy and factors that predict overall survival in elderly patients with esophageal squamous cell carcinoma. *Clin Transl Oncol* 2017; **19**: 742-749 [PMID: 28091898 DOI: 10.1007/s12094-016-1603-0]

20 **Li R**, He Y, Sun X, Wang N, Zhang M, Wei K, Li H, Dong P, Du L, Chen W. The long-term survival of esophageal cancer in elderly patients: A multi-center, retrospective study from China. *Cancer Med* 2023; **12**: 4852-4863 [PMID: 36210795 DOI: 10.1002/cam4.5307]

21 **Zhou YC**, Chen LL, Xu HB, Sun Q, Zhang Q, Cai HF, Jiang H. Aging-related prognosis analysis of definitive radiotherapy for very elderly esophageal cancer. *Cancer Med* 2018; **7**: 1837-1844 [PMID: 29608256 DOI: 10.1002/cam4.1456]

22 **Søgaard M**, Thomsen RW, Bossen KS, Sørensen HT, Nørgaard M. The impact of comorbidity on cancer survival: a review. *Clin Epidemiol* 2013; **5**: 3-29 [PMID: 24227920 DOI: 10.2147/CLEP.S47150]

23 **Morishima T**, Matsumoto Y, Koeda N, Shimada H, Maruhama T, Matsuki D, Nakata K, Ito Y, Tabuchi T, Miyashiro I. Impact of Comorbidities on Survival in Gastric, Colorectal, and Lung Cancer Patients. *J Epidemiol* 2019; **29**: 110-115 [PMID: 30012908 DOI: 10.2188/jea.JE20170241]

24 **Jørgensen TL**, Hallas J, Friis S, Herrstedt J. Comorbidity in elderly cancer patients in relation to overall and cancer-specific mortality. *Br J Cancer* 2012; **106**: 1353-1360 [PMID: 22353805 DOI: 10.1038/bjc.2012.46]

25 **Ishido K**, Tanabe S, Katada C, Kubota Y, Furue Y, Wada T, Watanabe A, Koizumi W. Usefulness of endoscopic submucosal dissection for superficial esophageal squamous cell carcinoma in elderly patients: a single-center retrospective cohort study. *Jpn J Clin Oncol* 2021; **51**: 895-904 [PMID: 33738500 DOI: 10.1093/jjco/hyab030]

26 **Yamashita K**, Watanabe M, Mine S, Fukudome I, Okamura A, Yuda M, Hayami M, Imamura Y. The impact of the Charlson comorbidity

index on the prognosis of esophageal cancer patients who underwent esophagectomy with curative intent. *Surg Today* 2018; **48**: 632-639 [PMID: 29383595 DOI: 10.1007/s00595-018-1630-2]

27 **Bernardi D**, Asti E, Aiolfi A, Bonitta G, Luporini A, Bonavina L. Outcome of Trimodal Therapy in Elderly Patients with Esophageal Cancer: Prognostic Value of the Charlson Comorbidity Index. *Anticancer Res* 2018; **38**: 1815-1820 [PMID: 29491121 DOI: 10.21873/anticanres.12420]

28 **Chen MF**, Hsieh CC, Chen PT, Lu MS. Role of Nutritional Status in the Treatment Outcome for Esophageal Squamous Cell Carcinoma. *Nutrients* 2021; **13** [PMID: 34578883 DOI: 10.3390/nu13092997]

29 **Wang Y**, Wang L, Fang M, Li J, Song T, Zhan W, Xu H. Prognostic Value of the Geriatric Nutritional Risk Index in Patients Exceeding 70 Years Old with Esophageal Squamous Cell Carcinoma. *Nutr Cancer* 2020; **72**: 620-626 [PMID: 31390885 DOI: 10.1080/01635581.2019.1650189]

30 **Takagi K**, Buettner S, Ijzermans JNM, Wijnhoven BPL. Systematic Review on the Controlling Nutritional Status (CONUT) Score in Patients Undergoing Esophagectomy for Esophageal Cancer. *Anticancer Res* 2020; **40**: 5343-5349 [PMID: 32988852 DOI: 10.21873/anticanres.14541]

31 **Qi Q**, Song Q, Cheng Y, Wang N. Prognostic Significance of Preoperative Prognostic Nutritional Index for Overall Survival and Postoperative Complications in Esophageal Cancer Patients. *Cancer Manag Res* 2021; **13**: 8585-8597 [PMID: 34815713 DOI: 10.2147/CMAR.S333190]

32 **Chen SB**, Liu DT, Chen YP. The Impact of Preoperative Nutritional Status on the Survival of Patients With Esophageal Squamous Cell Carcinoma. *Front Surg* 2021; **8**: 752792 [PMID: 34988110 DOI: 10.3389/fsurg.2021.752792]

33 **Wang J**, Yu B, Ye Y, Shen J, Ding N, Tang H, Xu Y, Song L, Zhu Z, Chen Y, Xie S, Chen M. Predictive Value of Nutritional Risk Screening 2002 and Prognostic Nutritional Index for Esophageal Cancer Patients Undergoing Definitive Radiochemotherapy. *Nutr Cancer* 2018; **70**: 879-885 [PMID: 30273001 DOI: 10.1080/01635581.2018.1470656]

34 **Kondrup J**, Rasmussen HH, Hamberg O, Stanga Z; Ad Hoc ESPEN Working Group. Nutritional risk screening (NRS 2002): a new method based on an analysis of controlled clinical trials. *Clin Nutr* 2003; **22**: 321-336 [PMID: 12765673 DOI: 10.1016/s0261-5614(02)00214-5]

35 **Noh JH**, Na HK, Kim YH, Song HJ, Kim HR, Choi KD, Lee GH, Jung HY. Influence of Preoperative Nutritional Status on Patients Who Undergo Upfront Surgery for Esophageal Squamous Cell Carcinoma. *Nutr Cancer* 2022; **74**: 2910-2919 [PMID: 35234093 DOI: 10.1080/01635581.2022.2042573]

36 **Song T**, Wan Q, Yu W, Li J, Lu S, Xie C, Wang H, Fang M. Pretreatment nutritional risk scores and performance status are prognostic factors in esophageal cancer patients treated with definitive chemoradiotherapy. *Oncotarget* 2017; **8**: 98974-98984 [PMID: 29228742 DOI: 10.18632/oncotarget.21940]

37 **Ji Y**, Du X, Zhu W, Yang Y, Ma J, Zhang L, Li J, Tao H, Xia J, Yang H, Huang J, Bao Y, Du D, Liu D, Wang X, Li C, Yang X, Zeng M, Liu Z, Zheng W, Pu J, Chen J, Hu W, Li P, Wang J, Xu Y, Zheng X, Chen J, Wang W, Tao G, Cai J, Zhao J, Zhu J, Jiang M, Yan Y, Xu G, Bu S, Song B, Xie K, Huang S, Zheng Y, Sheng L, Lai X, Chen Y, Cheng L, Hu X, Ji W, Fang M, Kong Y, Yu X, Li H, Li R, Shi L, Shen W, Zhu C, Lv J, Huang R, He H, Chen M. Efficacy of Concurrent Chemoradiotherapy With S-1 vs Radiotherapy Alone for Older Patients With Esophageal Cancer: A Multicenter Randomized Phase 3 Clinical Trial. *JAMA Oncol* 2021; **7**: 1459-1466 [PMID: 34351356 DOI: 10.1001/jamaoncol.2021.2705]

38 **Suzuki G**, Yamazaki H, Aibe N, Masui K, Kimoto T, Shimizu D, Nishimura T, Nakashima A, Machida K, Kawabata K, Ota Y, Fujiwara H, Ishikawa T, Yamada K. Definitive Radiotherapy for Older Patients Aged ≥75 Years With Localized Esophageal Cancer. *In Vivo* 2019; **33**: 925-932 [PMID: 31028218 DOI: 10.21873/invivo.11560]

World Journal of Gastrointestinal Oncology

Submit a Manuscript: https://www.f6publishing.com

World J Gastrointest Oncol 2024 December 15; 16(12): 4650-4662

DOI: 10.4251/wjgo.v16.i12.4650

ISSN 1948-5204 (online)

ORIGINAL ARTICLE

Retrospective Study

Nomogram model based on γ-glutamyl transferase to albumin ratio predicts survival in hepatocellular carcinoma patients with transarterial chemoembolization treatment

Zhen-Ying Wu, Han Li, Jia-Li Chen, Ke Su, Mei-Ling Weng, Yun-Wei Han

Specialty type: Oncology

Provenance and peer review: Unsolicited article; Externally peer reviewed.

Peer-review model: Single blind

Peer-review report's classification
Scientific Quality: Grade C
Novelty: Grade C
Creativity or Innovation: Grade C
Scientific Significance: Grade B

P-Reviewer: Mirminachi S

Received: June 13, 2024
Revised: September 16, 2024
Accepted: October 11, 2024
Published online: December 15, 2024
Processing time: 152 Days and 4.3 Hours

Zhen-Ying Wu, Han Li, Jia-Li Chen, Mei-Ling Weng, Yun-Wei Han, Department of Oncology, The Affiliated Hospital of Southwest Medical University, Luzhou 646000, Sichuan Province, China

Zhen-Ying Wu, Department of Oncology, Pangang Group General Hospital, Panzhihua 617000, Sichuan Province, China

Ke Su, Department of Oncology, National Cancer Center, Beijing 100000, China

Ke Su, Department of Oncology, National Clinical Research Center for Cancer, Beijing 100000, China

Ke Su, Department of Oncology, Cancer Hospital, Chinese Academy of Medical Sciences and Peking Union Medical College, Beijing 100000, China

Co-first authors: Zhen-Ying Wu and Han Li.

Corresponding author: Yun-Wei Han, MD, PhD, Academic Research, Full Professor, Department of Oncology, The Affiliated Hospital of Southwest Medical University, No. 25 Taiping Street, Jiangyang District, Luzhou 646000, Sichuan Province, China.
lanpaoxiansheng@126.com

Abstract

BACKGROUND

The development of tumor is closely linked to inflammation. Therefore, targeting molecules involved in inflammation may be effective in predicting cancer prognosis. Transarterial chemoembolization (TACE) holds significant therapeutic significance in addressing hepatocellular carcinoma (HCC). At present, no studies have evaluated the predictive value of γ-glutamyl transferase to albumin ratio (GAR) on the prognosis of HCC undergoing TACE.

AIM

To explore the potential prognostic significance of the GAR in individuals undergoing TACE for HCC.

METHODS

A total of 1231 patients from seven hospitals in China were randomized into a training cohort (n = 862) and a validation cohort (n = 369). To establish inde-

pendent prognostic factors for overall survival (OS), we utilized multivariate and univariate Cox regression models. The best cut-off value of the GAR was determined with the X-tile software, with OS as the basis. Validations were performed using dual therapy cohort and triple therapy cohort.

RESULTS

X-tile software revealed a GAR threshold of 4.75 as optimal. Both pre- and post-propensity score matching analyses demonstrated that the median OS in the low-GAR group (< 4.75) was notably longer compared to the high-GAR group (≥ 4.75), showing results of 26.9 *vs* 9.8 months ($P < 0.001$) initially, and 18.1 *vs* 11.3 months ($P < 0.001$) after match. Furthermore, multivariate analysis identified GAR ≥ 4.75 as an independent prognostic factor ($P < 0.001$). The receiver operating characteristic curves for the nomogram showed area under receiver operating characteristic curves of 0.741, 0.747, and 0.708 for predicting 1-, 2-, and 3-year survival, respectively. Consistent findings were reiterated in the two cohorts involving TACE in combination with targeted therapy and TACE in combination with targeted therapy and immunotherapy. Calibration curve and decision curve analyses substantiated the model's relatively robust predictive capabilities.

CONCLUSION

Our study validates the effective prognostic capacity of the GAR-based nomogram for HCC patients undergoing TACE or TACE in combination with systemic therapy.

Key Words: Transarterial chemoembolization; Immunotherapy; Targeted therapy; Hepatocellular carcinoma; Prognosis

Core Tip: γ-glutamyl transferase to albumin ratio has been confirmed for the first time to be predictive in hepatocellular carcinoma undergoing transarterial chemoembolization and transarterial chemoembolization combined with systemic therapy in this large-sample multicenter study. A nomogram model for predicting postoperative survival was also established based on γ-glutamyl transferase to albumin ratio, which was empirically demonstrated to have strong predictive ability.

Citation: Wu ZY, Li H, Chen JL, Su K, Weng ML, Han YW. Nomogram model based on γ-glutamyl transferase to albumin ratio predicts survival in hepatocellular carcinoma patients with transarterial chemoembolization treatment. *World J Gastrointest Oncol* 2024; 16(12): 4650-4662

URL: https://www.wjgnet.com/1948-5204/full/v16/i12/4650.htm

DOI: https://dx.doi.org/10.4251/wjgo.v16.i12.4650

INTRODUCTION

Hepatocellular carcinoma (HCC) is prevalent worldwide and is a life-threatening malignancy, witnessing an escalating incidence that represents a large proportion of deaths related to cancer. Projections indicate that the annual HCC incidence will exceed one million individuals by the year 2025[1]. Sadly, patients devoid of effective therapeutic interventions succumb to an abysmal median overall survival (mOS) of merely four months[2].

The latest guidelines released by the National Comprehensive Cancer Network advocate for the combined employment of atezolizumab and bevacizumab as the prime systemic therapy option for individuals affected by advanced HCC. Additionally, in cases of unresectable or inoperable HCC exceeding 5 centimeters, transarterial chemoembolization (TACE) may merit consideration to extend patient survival. Following the established staging system of Barcelona Clinical Liver Cancer (BCLC), TACE has become the mainstay of therapy for intermediate-stage HCC. Specifically, this encompasses patients boasting asymptomatic, multi-nodular tumors devoid of vascular invasion or extrahepatic spread [3]. Indeed, TACE has also yielded surprising results for some early patients who were not suitable for surgery or ablation[4-6]. In some series of studies, the majority of patients treated with TACE were in the early stages of disease, with more than 40% being solitary nodules[7,8]. Importantly, TACE has also garnered favorable treatment responses in advanced-stage HCC cases. An extensive longitudinal cohort study across 14 countries discovered that TACE served as the primary treatment for nearly 50% of individuals afflicted with BCLC-C-stage HCC[9]. This assertion is further supported by the findings of two prospective non-randomized trials[10,11], which confirmed the superiority of conventional TACE over basic supportive care.

Scientific investigations have illuminated the intricate relationship between long-standing inflammatory factors and the malignant transformation of tumors, highlighting the fundamental role of chronic inflammation and its associated factors in the emergence of tumorigenesis[12]. Inflammatory factors are important players in the regulation of the tumor microenvironment. They possess the capacity to instigate tumor epithelial-mesenchymal transition, generate reactive oxygen species, and thereby facilitate tumor cell proliferation, angiogenesis, invasion, and metastasis[12,13]. γ-glutamyl transferase (GGT) is a kind of glycoprotein secreted by Kupffer cells and bile duct endothelial cells. Elevated GGT levels are a marker of liver dysfunction and alcohol intake, and can be used to measure the severity of liver inflammation and

cellular damage[14]. GGT's main role is to mediate the hydrolysis of extracellular glutathione, which produces large amounts of hydrogen peroxide and reactive oxygen species and other free radicals, leading to oxidative stress in tissues [15]. Many experimental studies have also shown that the expression of GGT makes cancer cells more invasive and even leads to the emergence of anticancer drug resistance[16].

Albumin (ALB) is the most important protein in humans, synthesized by liver cells. It has a wide range of important physiological functions, such as regulating immunity, stabilizing endothelium, and binding to various drugs and toxins [17]. In addition, ALB binds to a series of inflammatory mediators and interacts with nitric oxide, playing anti-inflammatory and antioxidant roles[18]. Serum ALB levels reflect liver reserve function and nutritional status of the body. In cases of malnutrition, hepatitis, and cirrhosis, the concentration of ALB in the human body will significantly decrease [19]. Therefore, ALB is frequently utilized in the assessment of liver function prior to hepatic resection[20]. Recent research has confirmed that ALB can also exert a protective influence after a variety of radical surgeries[21]. Although some studies have shown that GAR can predict the outcome of HCC[22,23], these studies only focused on hepatectomy, and their sample sizes were small. In this study, we developed a predictive model for HCC based on a convenient and inexpensive liquid biopsy technique, which can effectively predict not only survival after TACE alone, but also outcomes of dual therapy or triple therapy.

MATERIALS AND METHODS

Study design

TACE alone cohort: During the period spanning from January 2019 to June 2023, 1231 patients with HCC, who received either drug-eluting beads TACE or conventional TACE, were gathered from seven hospitals in China. The diagnosis of HCC was confirmed by histology, at least two typical radiological features, or one typical imaging manifestation with a serum alpha-fetoprotein (AFP) level > 400 ng/mL. The inclusion criteria consisted of the following prerequisites: (1) Patients who had not previously received any form of antitumour therapy prior to TACE; (2) Patients exhibiting measurable lesions that aligned with the response assessment criteria specifically tailored for solid tumours (RECIST 1.1); and (3) GGT and ALB were measured within 7 days before TACE. The exclusion criteria were: (1) Presence of other malignant tumors other than HCC; (2) Patients with a history of other anti-tumor therapies; and (3) Lack of follow-up data.

Dual therapy cohort: Patients with HCC who received TACE in combination with targeted therapy at the above hospitals were included in the two-combination therapy cohort. The clinical data including demographic characteristics, hematological parameters, imaging data and tumor staging were collected retrospectively. At the same time, GGT and ALB values at baseline were obtained.

Triple therapy cohort: Patients with HCC who received TACE in conjunction with immunotherapy and targeted therapy at the same hospitals were enrolled in this cohort. Complete baseline clinical and laboratory data were recorded for subsequent analysis. The study intentionally excluded those patients who had incomplete follow-up information.

Data assessment

The laboratory parameters included AFP, GGT, alanine aminotransferase, ALB, total bilirubin, red blood cells, lactate dehydrogenase, alkaline phosphatase, hemoglobin, white blood cells, lymphocyte count, hepatitis B virus infection, and hepatitis C virus infection. Tumor burden was assessed by magnetic resonance imaging. Enhanced computer tomography or single-organ contrast-enhanced ultrasound, including tumor diameter and number, portal vein invasion, lymph node metastases and extrahepatic metastases. Additional data encompassed variables such as sex, age, presence of alcohol consumption, hepatitis B virus, hepatitis C virus infection, hypertension and diabetes mellitus. Both the training and validation cohorts underwent bi-monthly computer tomography or magnetic resonance imaging examinations following the initial treatment. All patients were evaluated according to RECIST 1.1.

Statistical analysis

All of the statistical analyses were implemented with R 4.1.3 software and SPSS 26.0 software. A bilateral P value of < 0.05 was viewed as statistically significant. Tumor response data and baseline features were summed up with descriptive statistics. Comparisons of categorical variables were done with χ^2 test. The best threshold value for serum GAR was identified from OS utilizing X-tile software. To ensure balanced baseline characteristics, propensity score matching (PSM) scale was exploited for determining the low and high GAR groups. All patients were randomized into a validation group (n = 369) and a training group (n = 862). With the Kaplan-Meier statistical approach, the log-rank test was employed to estimate and compare mOS between groups. Subsequently, all covariates exhibiting an impact on survival in univariate analysis with P < 0.05 were included in the multivariate Cox proportional hazards model. Multivariate cox analysis was carried out to identify independent influencing factors, which were utilized to establish a nomogram. The nomogram's prognostic effect was evaluated using receiver operating characteristic, calibration curve and decision curve analysis.

Ethical statements

The study protocol was authorized by the Ethics Committee of the Affiliated Hospital of Southwest Medical University (No. KY2021063) and complied with the guidelines of the Helsinki Declaration. Written informed consent was waived because of the retrospective study.

RESULTS

Patients and tumor characteristics

This retrospective study enrolled a total of 1231 HCC patients. There were 1044 (85%) males and 187 (15%) females. There were 501 (41%) patients aged ≥ 60 years. There were 749 patients (61%) who were positive for hepatitis B. AFP ≥ 500 ng/mL was detected in 528 patients (43%). Multiple tumor masses were present in 890 patients (72%). Tumor diameter ≥ 10 cm was found in 352 patients (29%). Portal vein tumor thrombus (PVTT) was found in 484 patients (39%). According to BCLC tumor staging, 177 (14%) were stage A, 188 (15%) were stage B, 853 (69%) were stage C, and 13 (1%) were stage D. The remaining baseline characteristics are shown in Table 1.

GAR levels and OS before and after PSM

Both multivariate and univariate Cox analyses displayed that GAR value ≥ 4.75 was an independent prognostic risk factor for OS (Table 2). Based on X-tile software analysis, the best cut-off of GAR is 4.75. Based on the cutoff value, all 1231 patients were further divided into two groups, GAR ≥ 4.75 (n = 525) and GAR < 4.75 (n = 706). The high GAR group tended to exhibit higher tumor load before PSM (P < 0.05, Table 1). All patients in high and low GAR groups had a mOS of 9.8 months [95% confidence interval (CI): 8.9-11.5] and 26.9 months (95%CI: 24.0-30.2), respectively. Statistically significant differences existed between the two groups in mOS [hazard ratio (HR) = 2.079, 95%CI: 1.807-2.392, P < 0.001, Figure 1A]. There were no statistically significant differences between the two groups after PSM (Table 3). In the high GAR group, the mOS was 11.3 months (95%CI: 9.1-15.3), while in the low group, it was 18.1 months (95%CI: 13.4-23.3). The former was noticeably shorter as compared to the latter (HR = 1.461, 95%CI: 1.185-1.802, P < 0.001, Figure 1B).

Prognostic factors influencing OS

Before PSM, we performed univariate and multivariate Cox analyses and identified six independent factors affecting OS prognosis, including number of tumors ≥ 2 (P = 0.001), GAR value ≥ 4.75 (P < 0.001), PVTT (P < 0.001), Child-Pugh B/C (P < 0.001), larger tumor diameter (P < 0.001), and extra-hepatic metastasis (P = 0.003) respectively (Table 2).

After PSM, each GAR group had 256 patients enrolled in the study cohort. Univariate and multivariate Cox regression analyses pinpointed several independent prognostic factors impacting OS: GAR value ≥ 4.75 (P < 0.001), PVTT (P = 0.001), higher Child-Pugh classification (P = 0.004), multiple tumors (P < 0.001), and larger tumor diameter (P < 0.001). Notably, the prognostic significance of high-GAR remained robust even after PSM (Supplementary Table 1).

GAR can predict OS in validation set and training set (TACE alone cohort)

A total of 1231 patients were grouped into the validation and training groups in a 3:7 ratio. There were no evident statistical differences in the baseline features of the patients in both groups (Supplementary Table 2). The mOS for patients in the low group in the training set was 27.1 months (95%CI: 24.2-32.2) *vs* 9.9 months (95%CI: 8.6-11.8) for patients in the high group (P < 0.001). Significantly shorter mOS was observed in the high GAR group, demonstrating statistical significance (HR = 2.061, 95%CI: 1.74-2.442, P < 0.001, Figure 1C). There were comparable results observed in the validation set, with the mOS for high GAR and low GAR groups being 25.4 (95%CI: 21.0-30.3) and 9.5 (95%CI: 7.6-12.5) months, respectively. The high group presented remarkably shorter mOS in contrast to the low group (HR = 2.119, 95%CI: 1.648-2.723, P < 0.001, Figure 1D).

Nomogram construction and validation

In the training cohort, we found six independent factors affecting OS prognosis, including GAR, number of tumors, PVTT, Child-Pugh classification, tumor diameter, and extra-hepatic metastasis respectively (Table 4). The nomogram was constructed based on independent factors that significantly affected OS (Figure 2). Time-varying receiver operating characteristic curves in the validation set displayed that the area under receiver operating characteristic curve values of this model in predicting 1-, 2-, and 3-year survival were 0.741, 0.747, and 0.708, respectively (Figure 3). Additionally, the calibration curves and decision curve analysis curves demonstrated good predictive potential of the model (Figures 4 and 5).

GAR can predict OS of cohort for dual therapy

In total, 90 patients who received the combination therapy of TACE along with targeted therapy were encompassed within the dual therapy cohort. The mOS was found to be 36.1 months (95%CI: 24.5 to not applicable) in the low group, whereas it reduced significantly to 13.6 months (95%CI: 9.2-26.8) in the high group. Comparative analysis revealed a noteworthy disparity in mOS between both GAR groups, and the survival time was obviously shorter in high GAR group (HR = 2.079, 95%CI: 1.807-2.392, P < 0.001; Figure 1E). Additionally, in this particular cohort, GAR demonstrated a substantial association with patient survival.

GAR can predict the OS of triple therapy cohort

There were 63 patients who received a combination therapy of TACE, targeted therapy, and immunotherapy were included in this analysis. The mOS for the low GAR group was not reached, while it amounted to 9.8 months (95%CI: 8.27 to not applicable) for the high GAR group. Upon comparing the two groups, it was evident that the high GAR group exhibited a significantly shorter mOS (HR = 4.615, 95%CI: 1.844-11.55, P < 0.001; Figure 1F). These findings strongly indicate a pronounced correlation between GAR and the survival rate of patients.

Table 1 Baseline characteristics of low and high γ-glutamyl transferase to albumin ratio groups before propensity score matching

Variables	Total	GAR-low	GAR-high	*P* value
Patients	1231	706	525	
Gender				< 0.001
Female, *n* (%)	187 (0.15)	129 (0.18)	58 (0.11)	
Male, *n* (%)	1044 (0.85)	577 (0.82)	467 (0.89)	
Age ≥ 60 years, *n* (%)	501 (0.41)	305 (0.43)	196 (0.37)	0.044
HBV, *n* (%)	749 (0.61)	432 (0.61)	317 (0.60)	0.819
HCV, *n* (%)	38 (0.03)	27 (0.04)	11 (0.02)	0.117
Alcohol, *n* (%)	482 (0.39)	243 (0.34)	239 (0.46)	< 0.001
Diabetes, *n* (%)	122 (0.10)	69 (0.10)	53 (0.10)	0.928
Hypertension, *n* (%)	178 (0.14)	106 (0.15)	72 (0.14)	0.576
ALT levels ≥ 40, U/L, *n* (%)	639 (0.52)	274 (0.39)	365 (0.70)	< 0.001
ALP levels ≥ 125, U/L, *n* (%)	714 (0.58)	249 (0.35)	465 (0.89)	< 0.001
Serum AFP ≥ 500, ng/mL, *n* (%)	528 (0.43)	254 (0.36)	274 (0.52)	< 0.001
Child-Pugh class, *n* (%)				< 0.001
A	920 (0.75)	585 (0.83)	335 (0.64)	
B	297 (0.24)	114 (0.16)	183 (0.35)	
C	14 (0.01)	7 (0.01)	7 (0.01)	
Lymph node metastasis, *n* (%)	617 (0.50)	312 (0.44)	305 (0.58)	< 0.001
Extrahepatic metastasis, *n* (%)	238 (0.19)	116 (0.16)	122 (0.23)	0.004
PVTT, *n* (%)	484 (0.39)	196 (0.28)	288 (0.55)	< 0.001
BCLC stage, *n* (%)				< 0.001
A	177 (0.14)	137 (0.19)	40 (0.08)	
B	188 (0.15)	129 (0.18)	59 (0.11)	
C	853 (0.69)	433 (0.61)	420 (0.80)	
D	13 (0.01)	7 (0.01)	6 (0.01)	
Number of tumors ≥ 2, *n* (%)	890 (0.72)	469 (0.66)	421 (0.80)	< 0.001
Tumor diameter, cm, *n* (%)				< 0.001
< 3	172 (0.14)	133 (0.19)	39 (0.07)	
≥ 3, < 5	216 (0.18)	155 (0.22)	61 (0.12)	
≥ 5, < 10	491 (0.40)	302 (0.43)	189 (0.36)	
≥ 10	352 (0.29)	116 (0.16)	236 (0.45)	

GAR-low: γ-glutamyl transferase to albumin ratio < 4.75; GAR-high: γ-glutamyl transferase to albumin ratio ≥ 4.75; HBV: Hepatitis B virus; HCV: Hepatitis C virus; ALT: Alanine aminotransferase; ALP: Alkaline phosphatase; AFP: Alpha-fetoprotein; PVTT: Portal vein tumor thrombus; BCLC: Barcelona Clinic Liver Cancer.

DISCUSSION

TACE has become an important treatment method in the era of tumor precision therapy[24]. Although some studies have shown that GAR can be applied for the prediction of HCC prognosis, the study sample is generally small, and the study objects are all surgical resection. At present, no study has confirmed the predictive value of GAR in TACE. Therefore, we initiated a large-sample, multicenter TACE cohort study and established a nomogram model of HCC patient survival based on GAR. In this study, the patients with GAR ≥ 4.75 had lower mOS than those with GAR < 4.75(P < 0.001). High predictive accuracy of GAR was also found in both the dual and triple therapy cohorts for the first time.

Table 2 Univariate and multivariate Cox regression analyses of overall survival before propensity score matching

Variables	HR (95%CI)	*P* value	HR (95%CI)	*P* value
Gender (male/female)	1.094 (0.898-1.334)	0.372		
Age (≥ 60/< 60 years)	0.888 (0.770-1.024)	0.102		
HBV (positive/negative)	1.087 (0.941-1.255)	0.257		
HCV (positive/negative)	0.657 (0.406-1.062)	0.086		
Alcohol (yes/no)	1.069 (0.927-1.233)	0.360		
Diabetes (yes/no)	0.913 (0.718-1.162)	0.460		
Hypertension (yes/no)	0.899 (0.732-1.104)	0.310		
GAR-high	2.075 (1.804-2.388)	< 0.001	1.533 (1.285-1.828)	< 0.001
ALT levels ≥ 40, U/L	1.313 (1.141-1.511)	< 0.001	1.003 (0.862-1.166)	0.973
ALP levels ≥ 125, U/L	1.730 (1.495-2.001)	< 0.001	1.008 (0.840-1.209)	0.932
Serum AFP ≥ 500, ng/mL	1.326 (1.152-1.525)	< 0.001	0.982 (0.846-1.140)	0.814
Child-Pugh A *vs* B/C	1.812 (1.553-2.113)	< 0.001	1.389 (1.176-1.640)	< 0.001
Lymph node metastasis	1.435 (1.246-1.652)	< 0.001	0.940 (0.779-1.133)	0.514
Extrahepatic metastasis	1.679 (1.424-1.979)	< 0.001	1.301 (1.091-1.550)	0.003
PVTT	1.958 (1.701-2.253)	< 0.001	1.372 (1.150-1.637)	< 0.001
BCLC stage A *vs* B *vs* C *vs* D				
A	1	< 0.001	1	0.106
B	1.409 (1.036-1.916)	0.029	0.865 (0.603-1.241)	0.432
C	2.447 (1.911-3.135)	< 0.001	1.142 (0.810-1.611)	0.447
D	3.538 (1.823-6.868)	< 0.001	1.867 (0.929-3.752)	0.079
Number of tumors ≥ 2	1.614 (1.365-1.909)	< 0.001	1.381 (1.132-1.685)	0.001
Tumor diameter, cm				
< 3	1	< 0.001	1	< 0.001
≥ 3, < 5	1.692 (1.262-2.270)	< 0.001	1.684 (1.245-2.278)	0.001
≥ 5, < 10	2.114 (1.633-2.737)	< 0.001	1.756 (1.337-2.306)	< 0.001
≥ 10	2.930 (2.250-3.816)	< 0.001	1.822 (1.364-2.435)	< 0.001

GAR-high: γ-glutamyl transferase to albumin ratio ≥ 4.75; HR: Hazard ratio; CI: Confidence interval; HBV: Hepatitis B virus; HCV: Hepatitis C virus; ALT: Alanine aminotransferase; ALP: Alkaline phosphatase; AFP: Alpha-fetoprotein; PVTT: Portal vein tumor thrombus; BCLC: Barcelona Clinic Liver Cancer.

At present, TACE-based prognostic models have been gradually established. The neutrophil-lymphocyte ratio model and platelet-to-lymphocyte ratio have been demonstrated to predict survival prognosis and metastasis in HCC patients treated with TACE[25,26]. However, there is no prognostic marker for patients suffering from HCC after TACE in conjugation with immunotherapy or targeted therapy. TACE was once the first-line therapy for stage B BCLC patients, and recent prospective clinical studies have shown that TACE is also a novel ideal treatment option for patients with early-stage (solitary nodules) and some advanced-stage HCC[27]. More and more HCC patients are expected to benefit from TACE treatment, so it is of great clinical significance to search for an effective prognostic marker for TACE treatment.

The role of inflammation in cancer has long been the focus of researchers. Inflammation promotes tumor development through a multi-faceted process, including angiogenesis, extracellular matrix remodeling, immunosuppression, invasion, and distant infiltration[28,29]. Various inflammatory cells create a favorable environment for tumor growth, thus exacerbating the development of this pathological process[30]. High levels of serum GGT are often a marker of severe hepatitis, cirrhosis, and advanced cancer. There is evidence that it mediates the hydrolysis of glutathione, which can lead to the formation of free radicals, lipid peroxidation and induce malignant transformation of cells. GGT is also thought to promote rapid growth and turnover of tumor cells[16]. A number of published prospective studies have shown a positive correlation between the levels of GGT and a number of cancers, including liver, breast, and prostate cancer[31,32].

In contrast, ALB plays a vital role in counteracting oxidative stress, enhancing microcirculation, and inhibiting inflammatory responses. It has been demonstrated that ALB exerts DNA replication stabilization and immune response

Table 3 Baseline characteristics of high and low γ-glutamyl transferase to albumin ratio groups after propensity score matching, *n* (%)

Variables	Total	GAR-low	GAR-high	*P* value
Patients	512	256	256	
Gender				0.798
Female	71 (0.14)	34 (0.13)	37 (0.14)	
Male	441 (0.86)	222 (0.87)	219 (0.86)	
Age ≥ 60 years	215 (0.42)	107 (0.42)	108 (0.42)	1
HBV	293 (0.57)	148 (0.58)	145 (0.57)	0.858
HCV	17 (0.03)	8 (0.03)	9 (0.04)	1
Alcohol	203 (0.40)	99 (0.39)	104 (0.41)	0.718
Diabetes	47 (0.09)	25 (0.1)	22 (0.09)	0.76
Hypertension	65 (0.13)	29 (0.11)	36 (0.14)	0.426
ALT levels ≥ 40, U/L	304 (0.59)	147 (0.57)	157 (0.61)	0.418
ALP levels ≥ 125, U/L	395 (0.77)	196 (0.77)	199 (0.78)	0.833
Serum AFP ≥ 500, ng/mL	221 (0.43)	108 (0.42)	113 (0.44)	0.721
Child-Pugh class				0.93
A	371 (0.72)	186 (0.73)	185 (0.72)	
B	134 (0.26)	67 (0.26)	67 (0.26)	
C	7 (0.01)	3 (0.01)	4 (0.02)	
Lymph node metastasis	269 (0.53)	139 (0.54)	130 (0.51)	0.479
Extrahepatic metastasis	99 (0.19)	49 (0.19)	50 (0.20)	1
PVTT	232 (0.45)	125 (0.49)	107 (0.42)	0.131
BCLC stage				0.347
A	58 (0.11)	25 (0.10)	33 (0.13)	
B	67 (0.13)	29 (0.11)	38 (0.15)	
C	380 (0.74)	199 (0.78)	181 (0.71)	
D	7 (0.01)	3 (0.01)	4 (0.02)	
Number of tumors ≥ 2	385 (0.75)	192 (0.75)	193 (0.75)	1
Tumor diameter, cm				0.797
< 3	50 (0.10)	22 (0.09)	28 (0.11)	0.797
≥ 3, < 5	79 (0.15)	41 (0.16)	38 (0.15)	
≥ 5, < 10	234 (0.46)	116 (0.45)	118 (0.46)	
≥ 10	149 (0.29)	77 (0.30)	72 (0.28)	

GAR-low: γ-glutamyl transferase to albumin ratio < 4.75; GAR-high: γ-glutamyl transferase to albumin ratio ≥ 4.75; HBV: Hepatitis B virus; HCV: Hepatitis C virus; ALT: Alanine aminotransferase; ALP: Alkaline phosphatase; AFP: Alpha-fetoprotein; PVTT: Portal vein tumor thrombus; BCLC: Barcelona Clinic Liver Cancer.

potentiation, thus impeding tumor progression[33]. Furthermore, hypoalbuminemia has been consistently linked to unfavorable prognoses in cancer patients[34,35]. McMillan *et al*[35] found that individuals with advanced lung or gastrointestinal malignancies exhibit a persistent systemic inflammatory response, which results in a continuous reduction in ALB concentration. To some extent, serum GGT levels can reflect tumor load, whereas liver metabolic ability and immune function are determined by ALB levels. Consequently, in comparison with other biomarkers, the GAR value more accurately reflects the relative tumor burden and liver function, thus affording a more effective prognostic tool for predicting the survival outcomes of patients diagnosed with HCC.

In preceding investigations, the prognostic outcome of HCC has been linked to factors such as GAR, PVTT, tumor number, tumor size, and Child grade[23,36]. The present study further corroborates this finding. Furthermore, we extended the nomogram model, demonstrating its commendable performance for prediction in the validation set. This

Table 4 Univariate and multivariate Cox analyses for identifying clinical characteristics influencing overall survival in the training cohort

Variables	HR (95%CI)	*P* value	HR (95%CI)	*P* value
Gender (male/female)	1.129 (0.888-1.435)	0.321		
Age (≥ 60/< 60 years)	0.895 (0.754-1.063)	0.206		
HBV (positive/negative)	1.145 (0.962-1.362)	0.128		
HCV (positive/negative)	0.691 (0.406-1.175)	0.172		
Alcohol (yes/no)	1.017 (0.856-1.208)	0.851		
Diabetes (yes/no)	0.883 (0.662-1.179)	0.399		
Hypertension (yes/no)	0.856 (0.673-1.090)	0.208		
GAR-high	2.058 (1.737-2.438)	< 0.001	1.516 (1.218-1.885)	< 0.001
ALT levels ≥ 40, U/L	1.278 (1.079-1.514)	0.005	0.904 (0.749-1.090)	0.291
ALP levels ≥ 125, U/L	1.756 (1.475-2.091)	< 0.001	1.106 (0.882-1.388)	0.382
Serum AFP ≥ 500, ng/mL	1.252 (1.057-1.484)	0.009	0.904 (0.752-1.086)	0.281
Child-Pugh A *vs* B/C	1.858 (1.544-2.234)	< 0.001	1.389 (1.133-1.703)	0.002
Lymph node metastasis	1.354 (1.143-1.603)	< 0.001	0.951 (0.756-1.197)	0.669
Extrahepatic metastasis	1.608 (1.311-1.973)	< 0.001	1.263 (1.013-1.575)	0.038
PVTT	2.009 (1.696-2.380)	< 0.001	1.510 (1.214-1.879)	< 0.001
BCLC stage A *vs* B *vs* C *vs* D				
A	1	< 0.001	1	0.146
B	1.363 (0.957-1.942)	0.086	0.865 (0.571-1.311)	0.494
C	2.183 (1.639-2.907)	< 0.001	0.999 (0.667-1.498)	0.998
D	4.106 (1.949-8.648)	< 0.001	2.174 (0.989-4.775)	0.053
Number of tumors ≥ 2	1.511 (1.241-1.838)	< 0.001	1.335 (1.057-1.685)	0.015
Tumor diameter, cm				
< 3	1	< 0.001	1	0.002
≥ 3, < 5	1.755 (1.226-2.513)	0.002	1.752 (1.211-2.534)	0.003
≥ 5, < 10	2.312 (1.691-3.162)	< 0.001	1.912 (1.372-2.665)	< 0.001
≥ 10	2.924 (2.117-4.039)	< 0.001	1.793 (1.256-2.559)	0.001

GAR-high: γ-glutamyl transferase to albumin ratio ≥ 4.75; HR: Hazard ratio; CI: Confidence interval; HBV: Hepatitis B virus; HCV: Hepatitis C virus; ALT: Alanine aminotransferase; ALP: Alkaline phosphatase; AFP: Alpha-fetoprotein; PVTT: Portal vein tumor thrombus; BCLC: Barcelona Clinic Liver Cancer.

has enhanced the GAR's practical application in clinical settings. Particularly for patients with elevated GAR, vigilance and proactive management should be emphasized.

The strength of the current research is the large sample size, which improves the reliability of results. We performed a PSM analysis, which reduced the effect of bias and confounding variables in the study and could more truthfully reflect the association of GAR with OS. Post-PSM survival analysis reaffirmed the prognostic value of GAR, with the low-GAR group demonstrating superior mOS. Further statistical scrutiny of the matched cohort, including both univariate and multivariate models, consistently highlighted GAR as a pivotal, independent determinant of OS outcomes. GAR was not only internally validated by the test data set, but also validated TACE in conjunction with targeted cohorts and TACE in conjunction with immunotherapy and targeted therapy. Therefore, it further improves the clinical applicability in the future treatment of HCC.

This study does, however, have some limitations. In the first place, this was a retrospective study, so selection bias was inevitable. Second, GGT and ALB levels can be influenced by different laboratory hematologic techniques, which may lead to some deviations. Third, although the predictive performance of GAR in dual and triple therapy cohorts has been verified, the number of patients was small, which may compromise the reliability of the conclusion. Therefore, multicenter, a large population, and prospective studies are expected to confirm and update the findings of this study in the future.

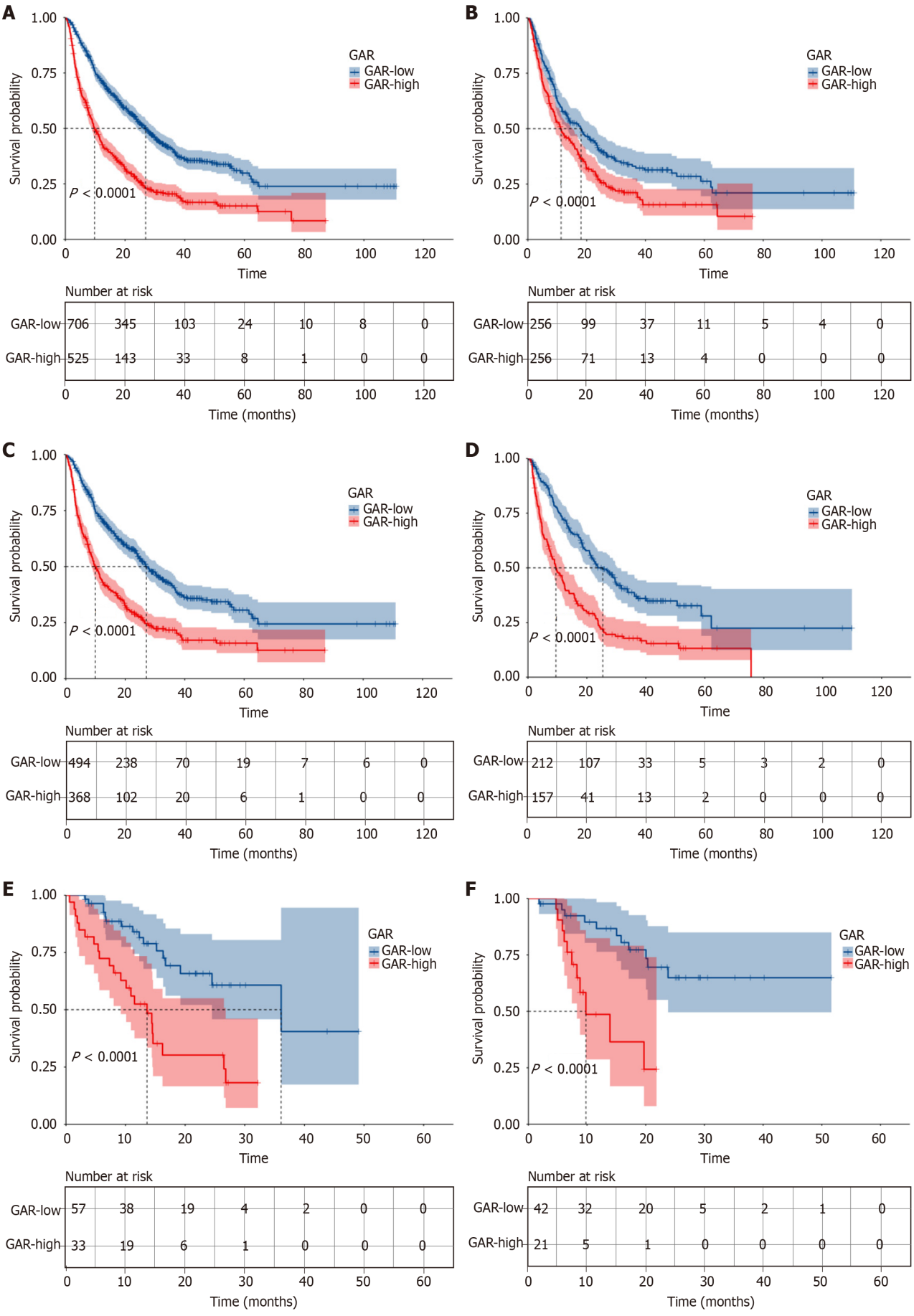

Figure 1 Kaplan-Meier survival curves stratified by γ-glutamyl transferase to albumin ratio. A: Overall survival of the transarterial

chemoembolization alone cohort; B: The cohort after propensity score matching; C: Training set; D: Validation set; E: Dual therapy cohort; F: Triple therapy cohort. GAR: γ-glutamyl transferase to albumin ratio.

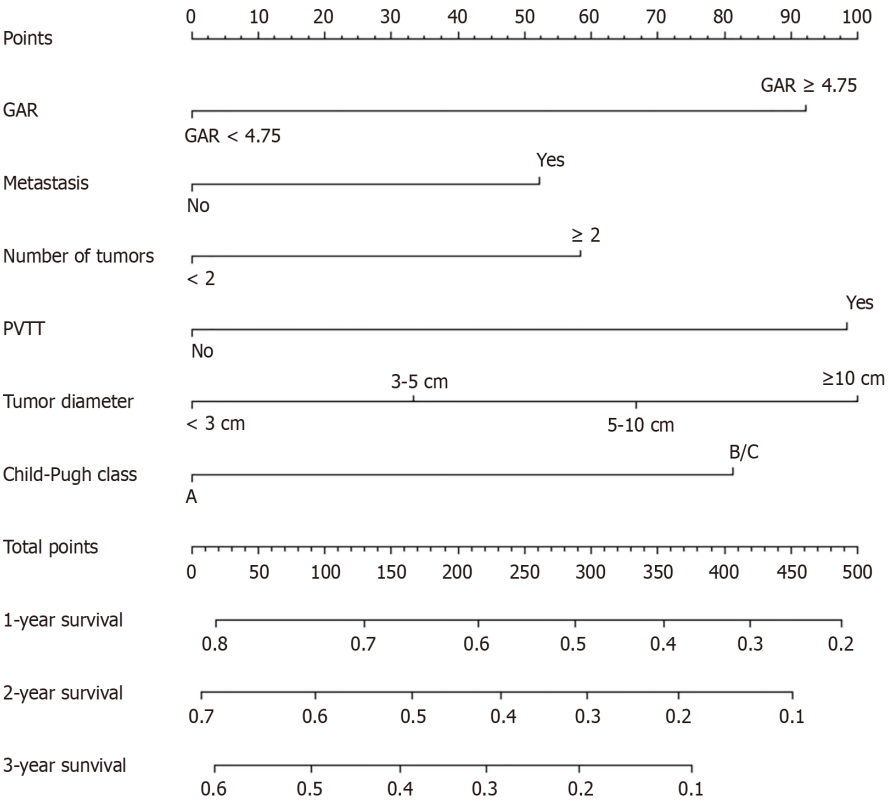

Figure 2 Nomogram constructed based on independent risk factors for predicting 1-, 2-, and 3-year overall survival in patients with hepatocellular carcinoma. GAR: γ-glutamyl transferase to albumin ratio; PVTT: Portal vein tumor thrombus.

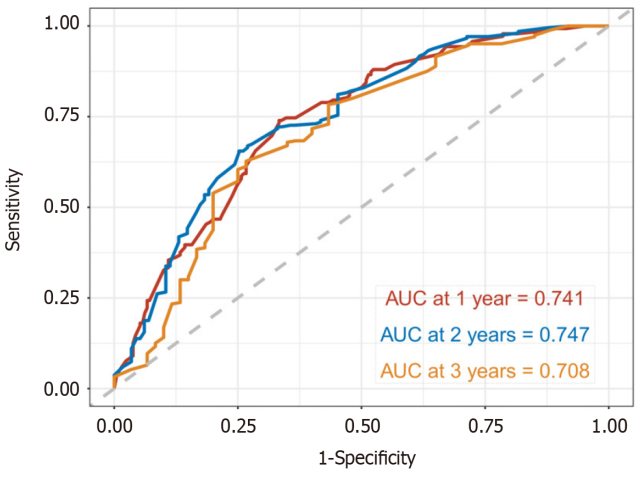

Figure 3 Time-dependent receiver operating characteristic curves of this predictive model. AUC: Area under receiver operating characteristic curve.

CONCLUSION

Our study validates the effective prognostic capacity of the GAR-based nomogram for HCC patients undergoing TACE or TACE in combination with systemic therapy.

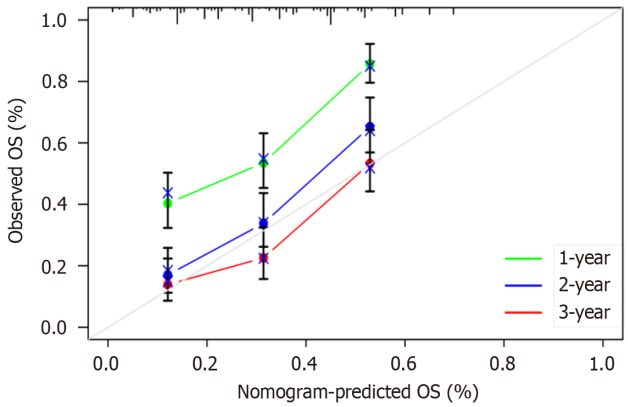

Figure 4 Calibration curve of validation cohort. OS: Overall survival.

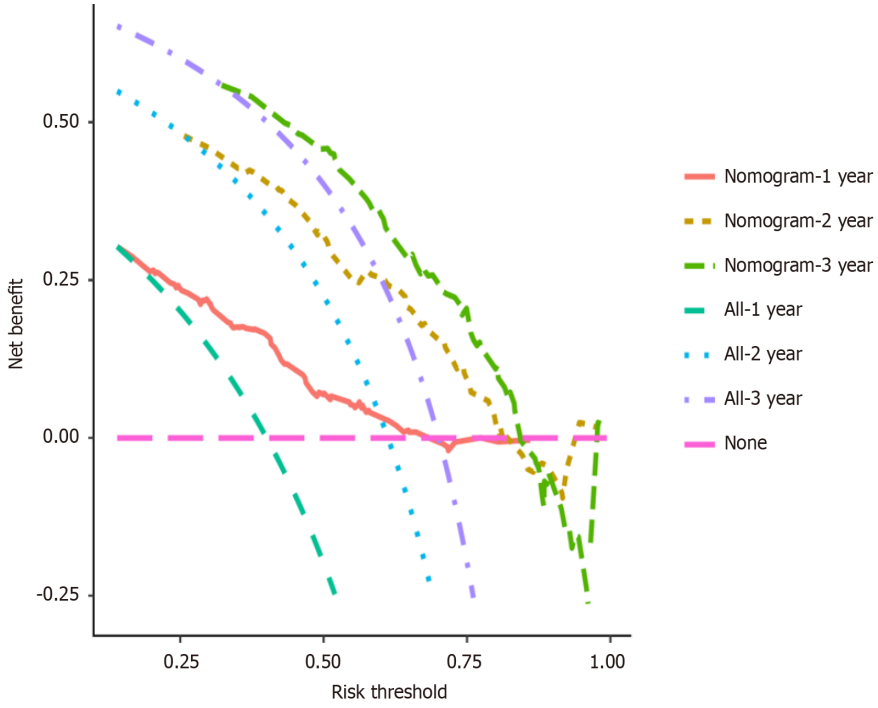

Figure 5 Decision curve analyses curve of validation cohort.

ACKNOWLEDGEMENTS

The authors would like to thank all the reviewers who participated in the review.

FOOTNOTES

Author contributions: Wu ZY, Li H, and Han YW conceived, designed and refined the study protocol; Chen JL, Su K, and Weng ML were involved in the data collection and formulation of research objectives; Wu ZY and Li H drafted the manuscript; and all authors were involved in the critical review of the results and approved the final manuscript. Wu ZY and Li H contributed equally to this work. The reasons for designating Wu ZY and Li H as co-first authors are threefold. First, the research was performed as a collaborative effort, and the designation of co-first authorship accurately reflects the distribution of responsibilities and burdens associated with the time and effort required to complete the study and the resultant paper. This also ensures effective communication and management of post-submission matters, ultimately enhancing the paper's quality and reliability. Second, the overall research team encompassed authors with a variety of expertise and skills from different fields, and the designation of co-first authors best reflect this diversity. This also promotes the most comprehensive and in-depth examination of the research topic, ultimately enriching readers' understanding by offering various expert perspectives. Third, Wu ZY and Li H contributed efforts of equal substance throughout the research process. They equally made a significant contribution to the work reported, in the design of methodology, creation of models, testing of code, statistical analysis, validation of results, writing the initial draft, and revision of articles. The choice of these researchers as co-first authors acknowledge and respects this equal contribution, while recognizing the spirit of teamwork and collaboration of this study. In

summary, we believe that designating Wu ZY and Li H as co-first authors of are fitting for our manuscript as it accurately reflects our team's collaborative spirit, equal contributions, and diversity.

Institutional review board statement: The study protocol was authorized by the Ethics Committee of the Affiliated Hospital of Southwest Medical University (No. KY2021063) and complied with the Code of Ethics of the World Medical Association.

Informed consent statement: Written informed consent was waived because of the retrospective study.

Conflict-of-interest statement: All the authors report no relevant conflicts of interest for this article.

Data sharing statement: All data generated or analyzed during this study are included in this article and its Supplementary material files. Further inquiries can be directed to the corresponding author (lanpaoxiansheng@126.com).

Country of origin: China

ORCID number: Zhen-Ying Wu 0000-0002-2269-8804; Han Li 0000-0003-0846-3846; Jia-Li Chen 0000-0002-2692-8179; Ke Su 0000-0002-7948-6335; Mei-Ling Weng 0009-0001-8850-8858; Yun-Wei Han 0000-0002-0942-9095.

S-Editor: Wang JJ
L-Editor: A
P-Editor: Wang WB

REFERENCES

1 **Villanueva A**. Hepatocellular Carcinoma. *N Engl J Med* 2019; **380**: 1450-1462 [PMID: 30970190 DOI: 10.1056/NEJMra1713263]
2 **Schöniger-Hekele M**, Müller C, Kutilek M, Oesterreicher C, Ferenci P, Gangl A. Hepatocellular carcinoma in Central Europe: prognostic features and survival. *Gut* 2001; **48**: 103-109 [PMID: 11115830 DOI: 10.1136/gut.48.1.103]
3 **European Association for the Study of the Liver**. EASL Clinical Practice Guidelines: Management of hepatocellular carcinoma. *J Hepatol* 2018; **69**: 182-236 [PMID: 29628281 DOI: 10.1016/j.jhep.2018.03.019]
4 **Burrel M**, Reig M, Forner A, Barrufet M, de Lope CR, Tremosini S, Ayuso C, Llovet JM, Real MI, Bruix J. Survival of patients with hepatocellular carcinoma treated by transarterial chemoembolisation (TACE) using Drug Eluting Beads. Implications for clinical practice and trial design. *J Hepatol* 2012; **56**: 1330-1335 [PMID: 22314428 DOI: 10.1016/j.jhep.2012.01.008]
5 **Malagari K**, Pomoni M, Moschouris H, Bouma E, Koskinas J, Stefaniotou A, Marinis A, Kelekis A, Alexopoulou E, Chatziioannou A, Chatzimichael K, Dourakis S, Kelekis N, Rizos S, Kelekis D. Chemoembolization with doxorubicin-eluting beads for unresectable hepatocellular carcinoma: five-year survival analysis. *Cardiovasc Intervent Radiol* 2012; **35**: 1119-1128 [PMID: 22614031 DOI: 10.1007/s00270-012-0394-0]
6 **Golfieri R**, Cappelli A, Cucchetti A, Piscaglia F, Carpenzano M, Peri E, Ravaioli M, D'Errico-Grigioni A, Pinna AD, Bolondi L. Efficacy of selective transarterial chemoembolization in inducing tumor necrosis in small (<5 cm) hepatocellular carcinomas. *Hepatology* 2011; **53**: 1580-1589 [PMID: 21351114 DOI: 10.1002/hep.24246]
7 **Terzi E**, Golfieri R, Piscaglia F, Galassi M, Dazzi A, Leoni S, Giampalma E, Renzulli M, Bolondi L. Response rate and clinical outcome of HCC after first and repeated cTACE performed "on demand". *J Hepatol* 2012; **57**: 1258-1267 [PMID: 22871502 DOI: 10.1016/j.jhep.2012.07.025]
8 **Takayasu K**, Arii S, Kudo M, Ichida T, Matsui O, Izumi N, Matsuyama Y, Sakamoto M, Nakashima O, Ku Y, Kokudo N, Makuuchi M. Superselective transarterial chemoembolization for hepatocellular carcinoma. Validation of treatment algorithm proposed by Japanese guidelines. *J Hepatol* 2012; **56**: 886-892 [PMID: 22173160 DOI: 10.1016/j.jhep.2011.10.021]
9 **Park JW**, Chen M, Colombo M, Roberts LR, Schwartz M, Chen PJ, Kudo M, Johnson P, Wagner S, Orsini LS, Sherman M. Global patterns of hepatocellular carcinoma management from diagnosis to death: the BRIDGE Study. *Liver Int* 2015; **35**: 2155-2166 [PMID: 25752327 DOI: 10.1111/liv.12818]
10 **Niu ZJ**, Ma YL, Kang P, Ou SQ, Meng ZB, Li ZK, Qi F, Zhao C. Transarterial chemoembolization compared with conservative treatment for advanced hepatocellular carcinoma with portal vein tumor thrombus: using a new classification. *Med Oncol* 2012; **29**: 2992-2997 [PMID: 22200992 DOI: 10.1007/s12032-011-0145-0]
11 **Luo J**, Guo RP, Lai EC, Zhang YJ, Lau WY, Chen MS, Shi M. Transarterial chemoembolization for unresectable hepatocellular carcinoma with portal vein tumor thrombosis: a prospective comparative study. *Ann Surg Oncol* 2011; **18**: 413-420 [PMID: 20839057 DOI: 10.1245/s10434-010-1321-8]
12 **Coussens LM**, Werb Z. Inflammation and cancer. *Nature* 2002; **420**: 860-867 [PMID: 12490959 DOI: 10.1038/nature01322]
13 **Comen EA**, Bowman RL, Kleppe M. Underlying Causes and Therapeutic Targeting of the Inflammatory Tumor Microenvironment. *Front Cell Dev Biol* 2018; **6**: 56 [PMID: 29946544 DOI: 10.3389/fcell.2018.00056]
14 **Whitfield JB**. Gamma glutamyl transferase. *Crit Rev Clin Lab Sci* 2001; **38**: 263-355 [PMID: 11563810 DOI: 10.1080/20014091084227]
15 **Tate SS**, Meister A. gamma-Glutamyl transpeptidase: catalytic, structural and functional aspects. *Mol Cell Biochem* 1981; **39**: 357-368 [PMID: 6118826 DOI: 10.1007/BF00232585]
16 **Hanigan MH**, Gallagher BC, Townsend DM, Gabarra V. Gamma-glutamyl transpeptidase accelerates tumor growth and increases the

resistance of tumors to cisplatin in vivo. *Carcinogenesis* 1999; **20**: 553-559 [PMID: 10223181 DOI: 10.1093/carcin/20.4.553]

17 **Spinella R**, Sawhney R, Jalan R. Albumin in chronic liver disease: structure, functions and therapeutic implications. *Hepatol Int* 2016; **10**: 124-132 [PMID: 26420218 DOI: 10.1007/s12072-015-9665-6]

18 **Arroyo V**, García-Martinez R, Salvatella X. Human serum albumin, systemic inflammation, and cirrhosis. *J Hepatol* 2014; **61**: 396-407 [PMID: 24751830 DOI: 10.1016/j.jhep.2014.04.012]

19 **Domenicali M**, Baldassarre M, Giannone FA, Naldi M, Mastroroberto M, Biselli M, Laggetta M, Patrono D, Bertucci C, Bernardi M, Caraceni P. Posttranscriptional changes of serum albumin: clinical and prognostic significance in hospitalized patients with cirrhosis. *Hepatology* 2014; **60**: 1851-1860 [PMID: 25048618 DOI: 10.1002/hep.27322]

20 **Johnson PJ**, Berhane S, Kagebayashi C, Satomura S, Teng M, Reeves HL, O'Beirne J, Fox R, Skowronska A, Palmer D, Yeo W, Mo F, Lai P, Iñarrairaegui M, Chan SL, Sangro B, Miksad R, Tada T, Kumada T, Toyoda H. Assessment of liver function in patients with hepatocellular carcinoma: a new evidence-based approach-the ALBI grade. *J Clin Oncol* 2015; **33**: 550-558 [PMID: 25512453 DOI: 10.1200/JCO.2014.57.9151]

21 **Gupta D**, Lis CG. Pretreatment serum albumin as a predictor of cancer survival: a systematic review of the epidemiological literature. *Nutr J* 2010; **9**: 69 [PMID: 21176210 DOI: 10.1186/1475-2891-9-69]

22 **Liu KJ**, Lv YX, Niu YM, Bu Y. Prognostic value of γ-glutamyl transpeptidase to albumin ratio combined with aspartate aminotransferase to lymphocyte ratio in patients with hepatocellular carcinoma after hepatectomy. *Medicine (Baltimore)* 2020; **99**: e23339 [PMID: 33235099 DOI: 10.1097/MD.0000000000023339]

23 **Pang S**, Shi Y, Xu D, Sun Z, Chen Y, Yang Y, Zhao X, Si-Ma H, Yang N. Screening of Hepatocellular Carcinoma Patients with High Risk of Early Recurrence After Radical Hepatectomy Using a Nomogram Model Based on the γ-Glutamyl Transpeptidase-to-Albumin Ratio. *J Gastrointest Surg* 2022; **26**: 1-9 [PMID: 35508683 DOI: 10.1007/s11605-022-05326-9]

24 **Pinato DJ**, Howell J, Ramaswami R, Sharma R. Review article: delivering precision oncology in intermediate-stage liver cancer. *Aliment Pharmacol Ther* 2017; **45**: 1514-1523 [PMID: 28440552 DOI: 10.1111/apt.14066]

25 **Liu C**, Li L, Lu WS, Du H, Yan LN, Yang JY, Wen TF, Zeng GJ, Jiang L, Yang J. Neutrophil-lymphocyte Ratio Plus Prognostic Nutritional Index Predicts the Outcomes of Patients with Unresectable Hepatocellular Carcinoma After Transarterial Chemoembolization. *Sci Rep* 2017; **7**: 13873 [PMID: 29066730 DOI: 10.1038/s41598-017-13239-w]

26 **Fan W**, Zhang Y, Wang Y, Yao X, Yang J, Li J. Neutrophil-to-lymphocyte and platelet-to-lymphocyte ratios as predictors of survival and metastasis for recurrent hepatocellular carcinoma after transarterial chemoembolization. *PLoS One* 2015; **10**: e0119312 [PMID: 25742141 DOI: 10.1371/journal.pone.0119312]

27 **Raoul JL**, Forner A, Bolondi L, Cheung TT, Kloeckner R, de Baere T. Updated use of TACE for hepatocellular carcinoma treatment: How and when to use it based on clinical evidence. *Cancer Treat Rev* 2019; **72**: 28-36 [PMID: 30447470 DOI: 10.1016/j.ctrv.2018.11.002]

28 **Qian BZ**. Inflammation fires up cancer metastasis. *Semin Cancer Biol* 2017; **47**: 170-176 [PMID: 28838845 DOI: 10.1016/j.semcancer.2017.08.006]

29 **Chiba T**, Marusawa H, Ushijima T. Inflammation-associated cancer development in digestive organs: mechanisms and roles for genetic and epigenetic modulation. *Gastroenterology* 2012; **143**: 550-563 [PMID: 22796521 DOI: 10.1053/j.gastro.2012.07.009]

30 **Coffelt SB**, de Visser KE. Cancer: Inflammation lights the way to metastasis. *Nature* 2014; **507**: 48-49 [PMID: 24572360 DOI: 10.1038/nature13062]

31 **Van Hemelrijck M**, Jassem W, Walldius G, Fentiman IS, Hammar N, Lambe M, Garmo H, Jungner I, Holmberg L. Gamma-glutamyltransferase and risk of cancer in a cohort of 545,460 persons - the Swedish AMORIS study. *Eur J Cancer* 2011; **47**: 2033-2041 [PMID: 21486691 DOI: 10.1016/j.ejca.2011.03.010]

32 **Breitling LP**, Claessen H, Drath C, Arndt V, Brenner H. Gamma-glutamyltransferase, general and cause-specific mortality in 19,000 construction workers followed over 20 years. *J Hepatol* 2011; **55**: 594-601 [PMID: 21256904 DOI: 10.1016/j.jhep.2010.12.029]

33 **Bağırsakçı E**, Şahin E, Atabey N, Erdal E, Guerra V, Carr BI. Role of Albumin in Growth Inhibition in Hepatocellular Carcinoma. *Oncology* 2017; **93**: 136-142 [PMID: 28486226 DOI: 10.1159/000471807]

34 **McMillan DC**. Systemic inflammation, nutritional status and survival in patients with cancer. *Curr Opin Clin Nutr Metab Care* 2009; **12**: 223-226 [PMID: 19318937 DOI: 10.1097/MCO.0b013e32832a7902]

35 **McMillan DC**, Watson WS, O'Gorman P, Preston T, Scott HR, McArdle CS. Albumin concentrations are primarily determined by the body cell mass and the systemic inflammatory response in cancer patients with weight loss. *Nutr Cancer* 2001; **39**: 210-213 [PMID: 11759282 DOI: 10.1207/S15327914nc392_8]

36 **Fulgenzi CAM**, Cheon J, D'Alessio A, Nishida N, Ang C, Marron TU, Wu L, Saeed A, Wietharn B, Cammarota A, Pressiani T, Personeni N, Pinter M, Scheiner B, Balcar L, Napolitano A, Huang YH, Phen S, Naqash AR, Vivaldi C, Salani F, Masi G, Bettinger D, Vogel A, Schönlein M, von Felden J, Schulze K, Wege H, Galle PR, Kudo M, Rimassa L, Singal AG, Sharma R, Cortellini A, Gaillard VE, Chon HJ, Pinato DJ. Reproducible safety and efficacy of atezolizumab plus bevacizumab for HCC in clinical practice: Results of the AB-real study. *Eur J Cancer* 2022; **175**: 204-213 [PMID: 36148739 DOI: 10.1016/j.ejca.2022.08.024]

World Journal of Gastrointestinal Oncology

Submit a Manuscript: https://www.f6publishing.com

World J Gastrointest Oncol 2024 December 15; 16(12): 4663-4674

DOI: 10.4251/wjgo.v16.i12.4663

ISSN 1948-5204 (online)

ORIGINAL ARTICLE

Retrospective Study

Deep learning model combined with computed tomography features to preoperatively predicting the risk stratification of gastrointestinal stromal tumors

Yi Li, Yan-Bei Liu, Xu-Bin Li, Xiao-Nan Cui, Dong-Hua Meng, Cong-Cong Yuan, Zhao-Xiang Ye

Specialty type: Oncology

Provenance and peer review: Unsolicited article; Externally peer reviewed.

Peer-review model: Single blind

Peer-review report's classification
Scientific Quality: Grade C
Novelty: Grade B
Creativity or Innovation: Grade A
Scientific Significance: Grade B

P-Reviewer: Zheng S

Received: June 25, 2024
Revised: October 2, 2024
Accepted: October 22, 2024
Published online: December 15, 2024
Processing time: 140 Days and 7.4 Hours

Yi Li, Xu-Bin Li, Xiao-Nan Cui, Dong-Hua Meng, Zhao-Xiang Ye, Department of Radiology, Tianjin Medical University Cancer Institute and Hospital, National Clinical Research Center for Cancer, Tianjin's Clinical Research Center for Cancer, State Key Laboratory of Druggability Evaluation and Systematic Translational Medicine, Tianjin Key Laboratory of Digestive Cancer, Tianjin 300060, China

Yan-Bei Liu, School of Life Sciences, Tiangong University, Tianjin 300387, China

Cong-Cong Yuan, Department of Radiology, Tianjin First Central Hospital, Tianjin 300190, China

Co-corresponding authors: Zhao-Xiang Ye and Xu-Bin Li.

Corresponding author: Zhao-Xiang Ye, PhD, Chief, Chief Doctor, Professor, Department of radiology, Tianjin Medical University Cancer Institute and Hospital, National Clinical Research Center for Cancer, Tianjin's Clinical Research Center for Cancer, State Key Laboratory of Druggability Evaluation and Systematic Translational Medicine, Tianjin Key Laboratory of Digestive Cancer, Huanhuxi Road, Hexi District, Tianjin 300060, China.
yezhaoxiang@163.com

Abstract

BACKGROUND

Gastrointestinal stromal tumors (GIST) are prevalent neoplasm originating from the gastrointestinal mesenchyme. Approximately 50% of GIST patients experience tumor recurrence within 5 years. Thus, there is a pressing need to accurately evaluate risk stratification preoperatively.

AIM

To assess the application of a deep learning model (DLM) combined with computed tomography features for predicting risk stratification of GISTs.

METHODS

Preoperative contrast-enhanced computed tomography (CECT) images of 551 GIST patients were retrospectively analyzed. All image features were independently analyzed by two radiologists. Quantitative parameters were statistically analyzed to identify significant predictors of high-risk malignancy. Patients were

randomly assigned to the training (n = 386) and validation cohorts (n = 165). A DLM and a combined DLM were established for predicting the GIST risk stratification using convolutional neural network and subsequently evaluated in the validation cohort.

RESULTS

Among the analyzed CECT image features, tumor size, ulceration, and enlarged feeding vessels were identified as significant risk predictors (P < 0.05). In DLM, the overall area under the receiver operating characteristic curve (AUROC) was 0.88, with the accuracy (ACC) and AUROCs for each stratification being 87% and 0.96 for low-risk, 79% and 0.74 for intermediate-risk, and 84% and 0.90 for high-risk, respectively. The overall ACC and AUROC were 84% and 0.94 in the combined model. The ACC and AUROCs for each risk stratification were 92% and 0.97 for low-risk, 87% and 0.83 for intermediate-risk, and 90% and 0.96 for high-risk, respectively. Differences in AUROCs for each risk stratification between the two models were significant (P < 0.05).

CONCLUSION

A combined DLM with satisfactory performance for preoperatively predicting GIST stratifications was developed using routine computed tomography data, demonstrating superiority compared to DLM.

Key Words: Gastrointestinal stromal tumors; Deep learning; Risk stratification; Tomography, X-ray computed; Prognosis

Core Tip: The deep learning model (DLM) was validated to accurately predict the risk classification of gastrointestinal stromal tumors. The combined DLM outperformed DLM in predicting risk stratification. The combined model has potential to guide and facilitate clinical decision-making.

Citation: Li Y, Liu YB, Li XB, Cui XN, Meng DH, Yuan CC, Ye ZX. Deep learning model combined with computed tomography features to preoperatively predicting the risk stratification of gastrointestinal stromal tumors. *World J Gastrointest Oncol* 2024; 16(12): 4663-4674

URL: https://www.wjgnet.com/1948-5204/full/v16/i12/4663.htm

DOI: https://dx.doi.org/10.4251/wjgo.v16.i12.4663

INTRODUCTION

As is well documented, gastrointestinal stromal tumors (GIST) are prevalent tumors originating from the gastrointestinal mesenchyme. Approximately 50% of GIST patients experience tumor recurrence within 5 years, and surgical intervention alone is inadequate for achieving an optimal prognosis[1,2]. Earlier studies established that 85% of GISTs are associated with receptor tyrosine kinase (c-kit) mutations, and 3%–5% are linked to platelet derived growth factor receptor alpha gene mutation[1,3-5]. The mutation type determines response to imatinib[6-8]. Considering the lack of effective conventional chemotherapy drugs, and the activity of Imatinib, adjuvant Imatinib may be a potential treatment option for patients with GIST[1,5,9]. A study assessing the efficacy of long-term imatinib treatment in advanced GIST patients documented a median overall survival exceeding four years[10]. Moreover, considering the recurrence and metastasis rate of intermediate- and high-risk GISTs after surgery, targeted drug therapy can improve the prognosis of GISTs[11,12]. Therefore, there is an urgent need to accurately evaluate risk stratification prior to surgery to obtain valuable information for evaluating the necessity of surgery and adjuvant treatment.

At present, the risk stratification of GISTs is based on histologic (mitotic index) and imaging characteristics (including tumor size and site) of the lesion as outlined in the National Institutes of Health (NIH) consensus classification system [13]. However, it is challenging to determine the mitotic index without histological examination. Indeed, the malignancy risk of most tumors is confirmed histologically after surgery. Although, endoscopic biopsy has also been widely used preoperatively, its utility may be limited if the tumor sample contains large areas of necrosis or hemorrhage, yielding inconclusive results[14-16].

Recently, the deep learning model (DLM), composed of multi-types of self-learning units, has emerged as a promising technique for analyzing medical imaging data[17-20]. Notably, DLM has demonstrated efficacy in clinical applications such as the assessment of differentiation grades in meningioma and renal cell carcinoma, as well as in predicting the molecular subtypes and grades of glioma[17-19,21]. Overall, deep learning transforms medical images into high-dimensional mineable data, offering rapid insights with high repeatability and providing a novel approach for GIST risk assessment[22-24]. This study aimed to establish and validate DLMs for predicting preoperative GIST risk stratification based on routine post-contrast computed tomography (CT) and clinical data.

MATERIALS AND METHODS

Characteristics of patients

This study was approved by our institutional ethics committee. All the patients signed the informed consent form before examinations. From January 2012 to December 2022, 606 patients with GISTs were initially enrolled in this retrospective study. A total of 55 patients were subsequently excluded for the following reasons: (1) Lack of preoperative contrast-enhanced CT images (n = 19); (2) Suboptimal CT image quality (n = 9); (3) Preoperative therapy or experienced metastasis to other sites (n = 25); and (4) Absence of required pathologic data (n = 2). Finally, a total of 551 patients were included in this study (256 men and 295 women; mean age 60.3 ± 9.8 years). The study population flow chart is illustrated in Figure 1.

All patients underwent complete surgical resection. GIST risk classification was based on National Comprehensive Cancer Network (NCCN) guidelines[15]. According to risk categories, patients in this study were classified into the high-risk (high risk), intermediate-risk (intermediate risk), and low-risk (very low and low risk) groups.

CT image acquisition

All patients underwent abdominal contrast-enhanced CT examination covering the whole tumor. After a non-contrast CT scan (Scanner: Philips Iqon, GE Healthcare Discovery CT750 HD or SIEMENS 64-MDCT) with a thickness of 1.0-1.5 mm, three-phase contrast-enhanced scans were performed, with 90 to 100 mL iodine contrast medium (Ultravist 370, Bayer Schering Pharma, Germany) intravenously injected at a rate of 2.5 to 3.0 mL/s.

Clinical and CT image feature analysis

All CT images were independently analyzed by two radiologists with 3 and 13 years of experience in abdominal radiology. In cases of disagreement, the radiologist with 13 years of experience reviewed the images to reach a consensus. Clinical information, image features and pathologic characteristics, including gender, age, tumor location, growth pattern (exophytic, endoluminal, mixed), tumor size (measured as the maximum diameter of the largest tumor section), tumor morphology (round or oval shape was considered regular, and lobulated or other irregular shapes were categorized as irregular), necrosis, ulceration, internal hemorrhagic foci, calcification, lymph node status, presence of enlarged feeding vessels, tumor boundary (clear or blurred), the pattern and degree of tumor enhancement during the venous phase and the range of tumor enhancement across the three phases, were derived from CT images and medical records. For CT value measurements of each tumor, regions of interest (ROIs) were delineated to cover tumor parenchyma while avoiding areas with evidence of cystic, necrotic or hemorrhagic changes at the level of the largest solid tumor regions and their adjacent upper and lower levels during the plain phase, arterial phase, venous phase and delay phase, respectively. The ROIs for CT value measurements were consistently sized using the copy and paste function across the different phases of images. Next, the average of three measurements was calculated. According to the difference between the venous phase and plain CT, the enhancement degree was defined as mild (CT value difference ≤ 20 HU), moderate (CT value difference between 20 HU and 40 HU), and obvious enhancement (CT value difference > 40 Hu). According to differences between the CT values of the venous and arterial phases, the enhancement pattern was defined as continuous (CT value difference ≥ 0) and attenuation (CT value difference < 0). The enhancement tumor range was calculated during the arterial phase (ER1 = arterial phase CT value-precontrast CT value), venous phase (ER2 = venous phase CT value-precontrast phase CT value), and delay phase (ER3 = delay phase CT value - precontrast scan CT value).

Image segmentation

All the CT images were exported in Joint Photographic Experts Group format. Then, two radiologists with extensive experience in abdominal imaging diagnosis (3 years and 13 years, respectively) participated in the segmentation of the entire tumor. One radiologist manually delineated the ROIs of the entire tumor layer by layer on venous phase CT images. The segmented images were subsequently confirmed by the other radiologist. Both radiologists were blinded to the pathological reports for risk stratification. Based on recommendations from previous literature[21], ImageJ (NIH, Bethesda, MD) was employed to apply an adaptive contrast filter to images. Besides, CT- segmented images were randomly selected from 20 patients, and the Dice similarity coefficient (DSC) was used to evaluate the inter-reader consistency in image segmentation. Detailed information of image preprocessing can be found in the Supplementary material 1.

The DLM construction

The DLM was constructed in two steps: Tumor features and tumor classification were initially extracted from CT images to generate the DLM, followed by the establishment of the combined model for tumor classification by integrating subject clinical-imaging features after statistical analysis. Figure 2 displays the detailed framework of this process. In the current study, a stratified random split was utilized at the patient level to randomly divide all patients into a training cohort and a validation cohort in a 7:3 ratio.

The 3D residual network (ResNet) was used to train our image dataset and establish the DLM. The 3D-ResNet is a three-dimensional convolutional neural network model based on the ResNet architecture. It is an extension of ResNet in two-dimensional image classification tasks used to process three-dimensional volume data. Besides, it accepts 3D volumetric data as input, positioning it as a powerful model for learning volume datasets. Furthermore, it can be adjusted according to the task complexity and dataset characteristics with variable depth. It can enhance the network depth by increasing the number of stacked layers of residual blocks, thereby optimizing the model's expressive ability. During the training phase, 3D-Resnet was used to extract and learn deep tumor features related to GIST risk stratification from each patient's CT images.

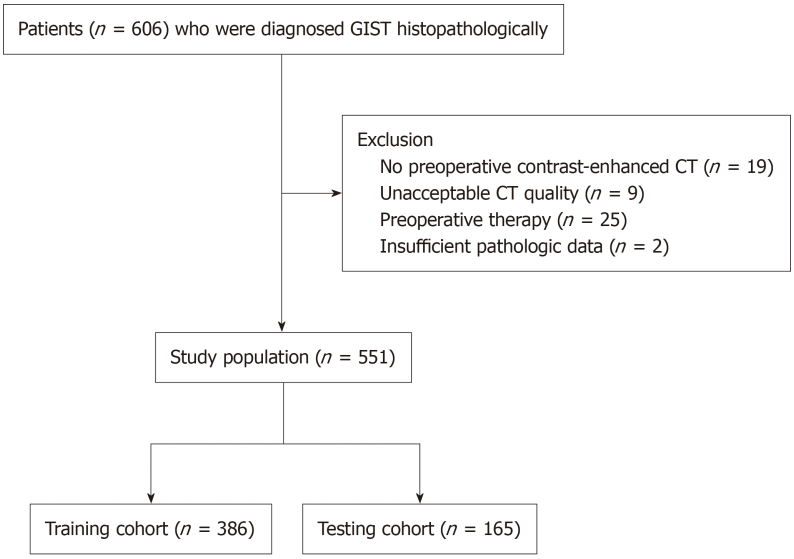

Figure 1 Study population flowchart. CT: Computed tomography; GIST: Gastrointestinal stromal tumors.

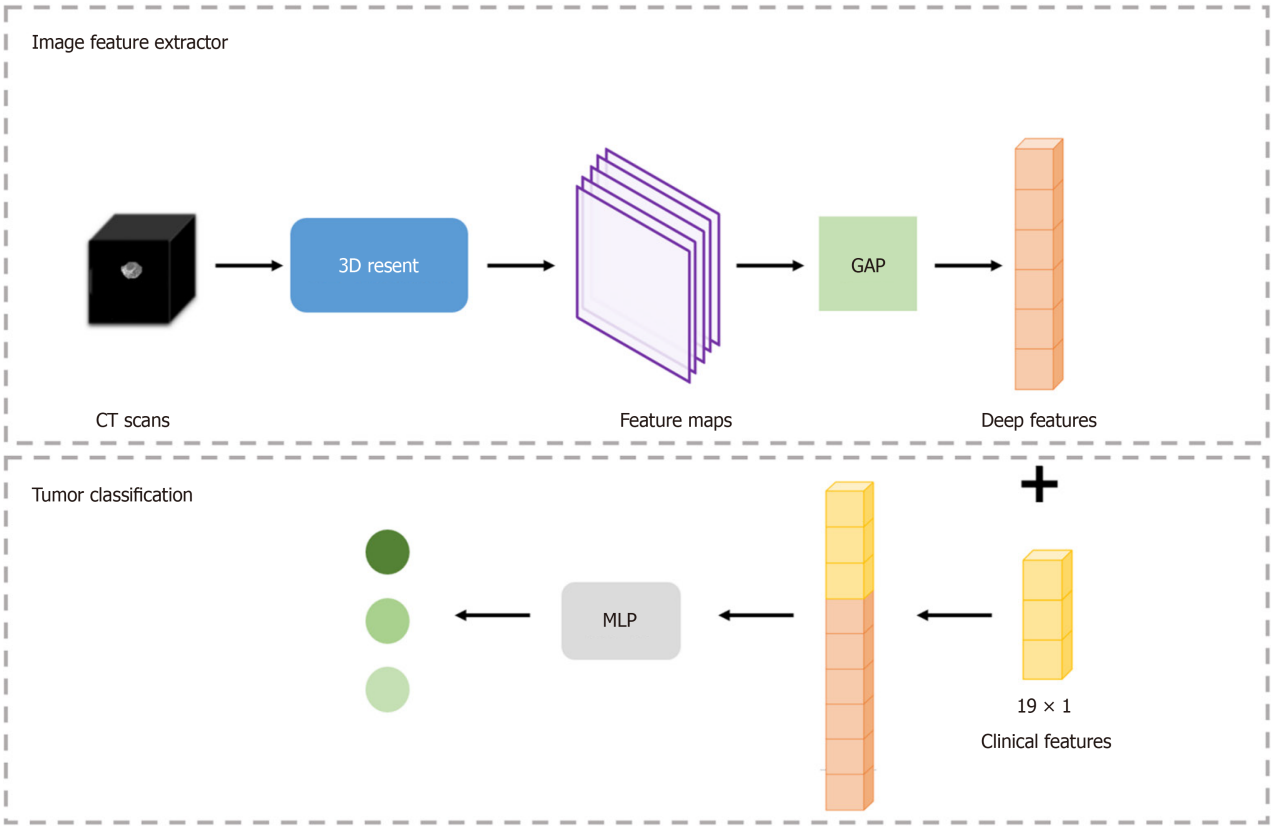

Figure 2 Overall gastrointestinal stromal tumor risk stratification framework. CT: Computed tomography; MLP: Multilayer perceptron; GAP: Global average pooling.

Multilayer perceptron (MLP) was employed for tumor risk stratification by combining imaging features and clinical data. It is a universal function approximator based on feedforward artificial neural networks that can learn and represent nonlinear relationships through multiple fully connected hidden layers and an output layer, making it suitable for various machine learning tasks. In the current model, a batch normalization (BN) layer was introduced following each linear layer in MLP to accelerate the convergence rate of the neural network, reduce the dependence of the model on the initial parameters, and improve the robustness of the model. The BN layer normalized each mini-batch data to stabilize the input of the neural network, thus improving the convergence rate and generalizability of the model. Figure 3 shows the feature extraction process. In the present study, the subject clinical-image data features of patients were concatenated with imaging features extracted by the 3D ResNet, and their feature vectors were inputted into the MLP to establish the

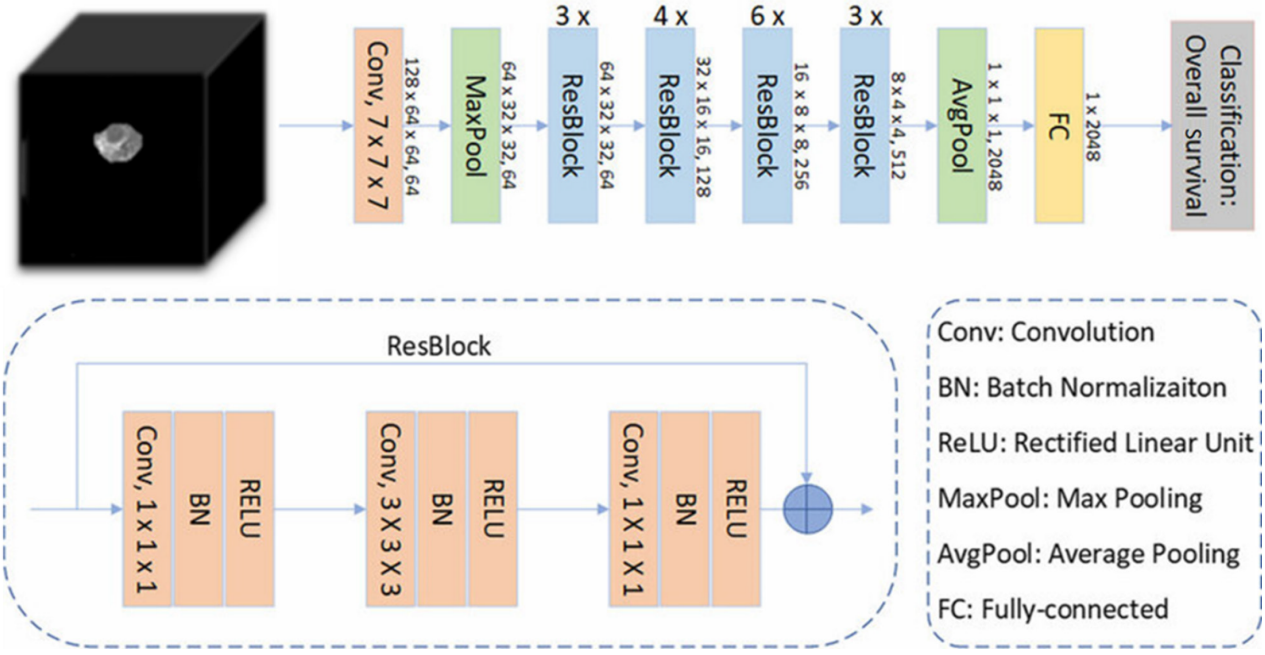

Figure 3 Schematic diagram of feature extraction process. BN: Batch normalization; RELU: Rectified linear unit.

combined DLM for tumor risk stratification.

Training details

In this study, the network architecture was implemented using the Pytorch framework and trained on NVIDIA GPU to accelerate training speed. Additionally, the transfer learning method was adopted, leveraging pre-training weights to improve model performance. Detailed information of model training process can be found in the Supplementary materials 2.

Statistical analysis

Statistical analysis was performed using the software SPSS version 22.0 (SPSS Inc., Chicago, IL, United States) and MedCalc version 22.002 (MedCalc Software Ltd, Ostend, Belgium). A P value of < 0.05 was considered statistically significant.

The interobserver agreement of measurements between the two radiologists was evaluated using the interclass correlation coefficient (ICC). The χ^2 test, independent two-sample t-test, one-way analysis of variance and Bonferroni tests were used to evaluate the significance of correlations between various clinical- imaging features and pathological GIST risk classifications from surgical resection specimens. Ordinary logistic regression was performed to identify significant predictive factors for relapse[25,26].

To assess the performance of DLM and combined DLM, five different indicators, namely area under the receiver operating characteristic curve (AUROC), F1 score (F1), accuracy (ACC), sensitivity (SEN), and specificity (SPE), were used. AUROC was calculated along with its 95%CI.

RESULTS

Clinical-imaging characteristics

ICC analysis showed a good concordance of measurements between the two radiologists (tumor size, ICC = 0.985; CT value in the plain phase, ICC = 0.812; CT value in the arterial phase, ICC = 0.906; CT value in the venous phase, ICC = 0.921; CT value in the delay phase, ICC = 0.848). Among the analyzed CECT image features, tumor size, tumor morphology, tumor location, growth pattern, necrosis, ulceration, calcification, lymph node status, presence of enlarged feeding vessels, tumor enhancement pattern during the venous phase, and the range of tumor enhancement across the three phases were found to be significantly associated with GIST risk categories ($P < 0.05$). The distribution of these features in the risk categories and the results of the χ^2 test are listed in Table 1. Meanwhile, ordinary logistic regression analysis identified tumor size, ulceration, and the presence of enlarged feeding vessels as statistically significant predictors ($P < 0.05$, Table 2).

Diagnostic performance of the DLM

All patients were randomly associated into two independent cohorts, namely a training cohort (386 patients: 176 males, mean age, 60.2 ± 9.8 years; 210 females, mean age, 59.9 ± 10.2 years) and a validation cohort (165 patients: 80 males, mean

Table 1 Distribution of the analyzed clinical-imaging features across pathologic risk categories, mean ± SD

CECT features		Pathologic risk categories			*P* value
		High (*n* = 213)	Moderated (*n* = 143)	Low (*n* = 195)	
Gender	Male	107	60	89	0.296
	Female	106	83	106	
Location	Gastric	139	136	171	0.000
	Non-gastric	74	7	24	
Morphology	Regular	54	94	170	0.000
	Irregular	159	49	25	
Growth pattern	Endoluminal	35	54	93	0.000
	Mixed	51	22	28	
	Exophytic	127	67	74	
Degree of contrast enhancement in the venous phase	Mild (≤ 20 HU)	30	20	20	0.424
	Moderate (20-40 HU)	101	74	90	
	Obvious (≥ 40 HU)	82	49	85	
Contrast enhancement pattern during the venous phase	Continuous	198	142	193	0.000
	Attenuation	15	1	2	
Calcification	Present	22	16	21	0.967
	Absent	191	127	174	
Necrosis	Present	155	65	33	0.000
	Absent	58	78	162	
Ulceration	Present	53	23	8	0.000
	Absent	160	120	187	
Enlarged feeding vessels	Present	183	60	14	0.000
	Absent	30	83	181	
Lymph nodes	Present	19	1	1	0.000
	Absent	194	142	194	
Age		59.44 ± 10.41	61.39 ± 9.83	60.37 ± 9.13	0.183
Size		9.03 ± 4.42	4.90 ± 1.89	2.77 ± 1.20	0.000
Range of tumor enhancement during the arterial phase		18.83 ± 17.81	14.24 ± 11.53	18.45 ± 17.47	0.004
Range of tumor enhancement during the venous phase		41.59 ± 25.73	38.97 ± 18.96	45.22 ± 25.70	0.038
Range of tumor enhancement during the delay phase		42.73 ± 18.89	43.72 ± 17.97	47.97 ± 20.27	0.016

CECT: Contrast-enhanced computed tomography.

age, 59.8 ± 9.9 years; 85 females, mean age, 60.0 ± 10.1 years). There were 136 (35.2%) cases of low-risk GISTs, 101 (26.2%) cases of intermediate-risk GISTs, and 149 (38.6%) cases of high-risk GISTs in the training cohort. In contrast, the validation cohort comprised 59 (35.8%) cases of low-risk GISTs, 42 (25.5%) cases of intermediate-risk GISTs, and 64 (38.8%) cases of high-risk GISTs.

The DSC value showed a good concordance of image segmentation between the two radiologists (DSC = 99.96%). The results for the different algorithms are detailed in Table 3. The model constructed using 3D-ResNet with 34 Layers demonstrated the optimal performance, with an ACC of 75%, a SEN of 72%, a SPE of 87%, and a F1 score of 72%. The overall AUROC for DLM was 0.88 (0.83, 0.93). The ROCs are depicted in Figure 4A. In DLM, the ACC and AUROCs for each stratification were 87% (144/165) and 0.96 (0.94, 0.98) for low-risk GISTs, 79% (131/165) and 0.74 (0.67, 0.81) for intermediate-risk GISTs, and 84% (138/165) and 0.90 (0.85, 0.95) for high-risk GISTs, respectively. The results for the validation cohorts were visualized as confusion matrices to compare the GIST risk stratification predicted by DLM against the pathological risk stratification (Figure 5A).

Table 2 Logistic regression analysis of risk classification based on clinical-imaging feature

	P value	95%CI	
		Lower bound	Upper bound
Size	0.000	-0.763	-0.473
Range of tumor enhancement during the arterial phase	0.131	-0.035	0.005
Range of tumor enhancement during the venous phase	0.220	-0.007	0.032
Range of tumor enhancement during the delay phase	0.858	-0.021	0.017
Morphology	0.602	-0.387	0.608
Location	0.074	-0.063	1.386
Ulceration	0.004	-1.622	-0.300
Enlarged feeding vessels	0.000	-2.134	-1.094
Growth pattern	0.224	-0.833	0.328
Contrast enhancement during the venous phase	0.428	-2.266	1.384
Necrosis	0.236	-0.195	0,793
Lymph nodes	0.890	-1.934	1.678

Table 3 Different algorithms for predicting gastrointestinal stromal tumor risk classification

Different method	Accuracy (%)	Sensitivity (%)	Specificity (%)	F1 score (%)
3DCNN	60	51	68	52
3DResnet_50	66	58	71	59
3DResnet_18	71	66	76	67
3DResnet_34	75	72	87	72
Combined model (3DResnet + MLP)	84	83	92	83

3DCNN: Three-dimensional convolutional neural network; 3DResnet: Three-dimensional residual network; MLP: Multilayer perceptron.

The combined DLM achieved satisfactory performance in assessing GIST risk stratification. The overall ACC and AUROC were 84% (139/165) and 0.94 (0.93, 0.95) for the combined model. The ROCs are delineated in Figure 4B. The ACC and AUROCs for each tumor risk stratification were 92% (152/165) and 0.97 (0.96, 0.98) for low-risk GISTs, 87% (143/165) and 0.83 (0.78, 0.88) for intermediate-risk GISTs, and 90% (148/165) and 0.96 (0.94, 0.98) for high-risk GISTs, respectively. The results for the validation cohorts were visualized as confusion matrices to compare the GIST risk stratification predicted by the combined model against pathological risk stratification (Figure 5B).

The ACC, SEN, SPE, F1 score and AUROCs for each tumor risk stratification across different models are summarized in Table 4. Importantly, differences in AUROCs between DLM and the combined model were significant ($P < 0.001$).

DISCUSSION

In this retrospective research, a DLM and a combined DLM were constructed. Notably, the latter (AUROC = 0.94) outperformed the former (AUROC = 0.88) in assessing GIST grading.

According to the modified NIH criteria and NCCN guidelines, the need of adjuvant treatment for GIST patients and the duration of treatment are associated with the risk stratification of GISTs[8,15,27,28]. Combining adjuvant treatment such as Imatinib before and after surgery may extend the recurrence free survival and overall survival of intermediate and high-risk GIST patients[1,5,29]. Therefore, an accurate preoperative categorization of risk classification, especially in high-risk GISTs, can provide valuable information for evaluating the necessity of surgical resection and adjuvant treatments[30-32]. In this study, two models were developed to predict preoperative GIST risk stratification: DLM and combined DLM. To the best of our knowledge, studies that combined clinical-imaging features and convolutional neural

Table 4 Accuracy, sensitivity, specificity, F1 score and areas under the receiver operating characteristic curves for each tumor risk stratification, *n* (%)/95%CI

		Accuracy (*n* = 165)	Sensitivity	Specificity	F1 score (%)	AUROC
DLM	High	138 (84); (78-90)	81 (52/64); (76-86)	85 (86/101); (78-91)	79	0.90 (85-95)
	Moderate	131 (79); (71-87)	50 (21/42); (25-74)	89 (110/123); (82-96)	55	0.74 (67-81)
	Low	144 (87); (81-93)	86 (51/59); (81-91)	88 (93/106); (83-94)	83	0.96 (94-98)
	Overall	75	72	87	72	0.88 (83-93)
Combined model	High	148 (90); (86-94)	88 (56/64); (83-93)	91 (92/101); (83-98)	87	0.96 (94-98)
	Moderate	143 (87); (83-92)	69 (29/42); (66-71)	93 (114/123); (86-98)	72	0.83 (78-88)
	Low	152 (92); (85-96)	92 (54/59); (89-93)	92 (98/106); (86-97)	89	0.97 (96-98)
	Overall	84	83	92	83	0.94 (93-95)

DLM: Deep learning model; AUROC: Areas under the receiver operating characteristic curve.

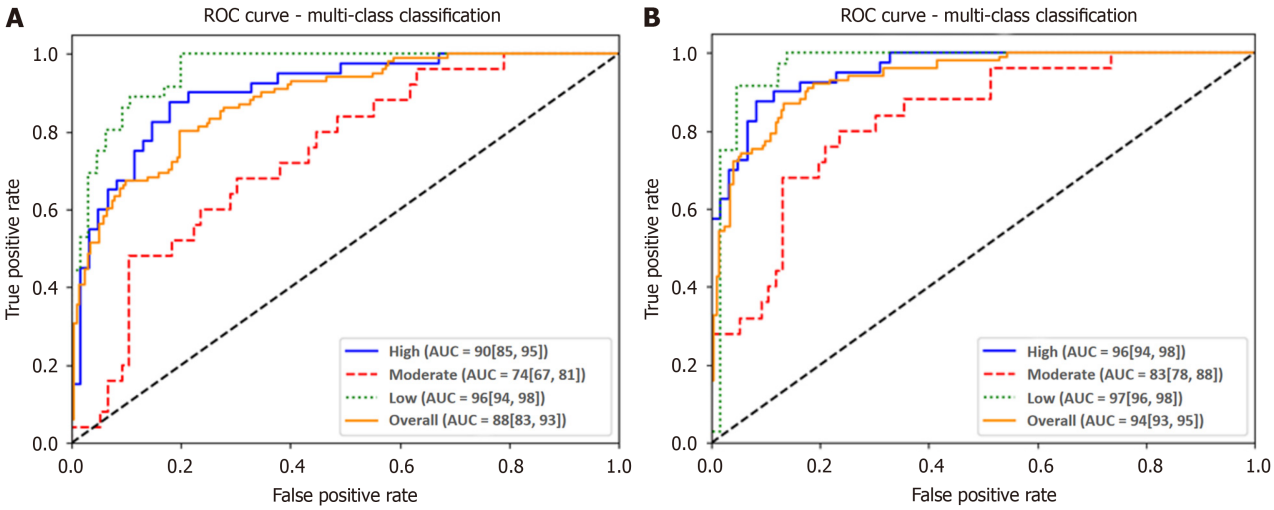

Figure 4 Receiver operating characteristic curves for the deep learning model and combined model. A: Receiver operating characteristic curve (ROC) for the deep learning model in the validation cohort; B: ROC curve for the combined model in the validation cohort. ROC: Receiver operating characteristic; AUC: Area under the curve.

network models to establish a combined model for predicting GIST risk stratification and distinguishing between different categorizations of risk classification (high-risk, intermediate-risk and low-risk GISTs) are scarce.

Analysis of clinical-imaging features revealed that tumor size, morphology, location, growth pattern, the presence of necrosis, ulceration, calcification, lymph nodes, and enlarged feeding vessels, as well as the tumor enhancement pattern during the venous phase and the range of tumor enhancement, were significantly associated with pathologic GIST risk categories. Logistic regression analysis subsequently identified tumor size, the presence of ulcers, and enlarged feeding vessels as predictors of pathologic risk categories, consistent with the results of previous studies[25,26,33]. Zhou *et al*[34] reported that tumors with large sizes (> 10 cm) and enlarged feeding vessels were more likely to be a high -risk GISTs [34]. Moreover, mucosal destruction promotes the formation of ulcers due to the influence of gastric acid[35]. The NCCN guideline recommend patients with GISTs larger than 2 cm to undergo surgical resection[28], while according to Nishida's[36] report, small GIST tumors may also be invasive and linked to a poor prognosis. Therefore, evaluating the risk stratification of GISTs exclusively based on tumor size could be insufficient. Other imaging features were also subjectively assessed and heavily relied on the experience of observers. While the degree of contrast enhancement is typically considered a characteristic of tumor biological activity, it showed no significant association with pathologic risk stratification as a predictive factor in our study, in line with the results of previous articles[26,33].

The results of our study unveiled that the DLM could accurately predict GIST risk classifications, with an AUROC of 0.88 in the validation cohort. However, the performance of the combined DLM was relatively higher (AUROC = 0.94), attributable to the combination of DLM with clinical-imaging features increasing the ability to assess the GIST risk classification. Overall, our study offers a novel method for optimizing the preoperative assessment of GIST risk stratification based on CT images, moving beyond dependence on postoperative specimens. Zhou *et al*[34] documented that the AUROC of the multinomial logistic regression model with subjective CT image features for GIST risk stratification was 0.806. At the same time, Wang *et al*[22] divided patients with GISTs into the high malignant potential group (intermediate

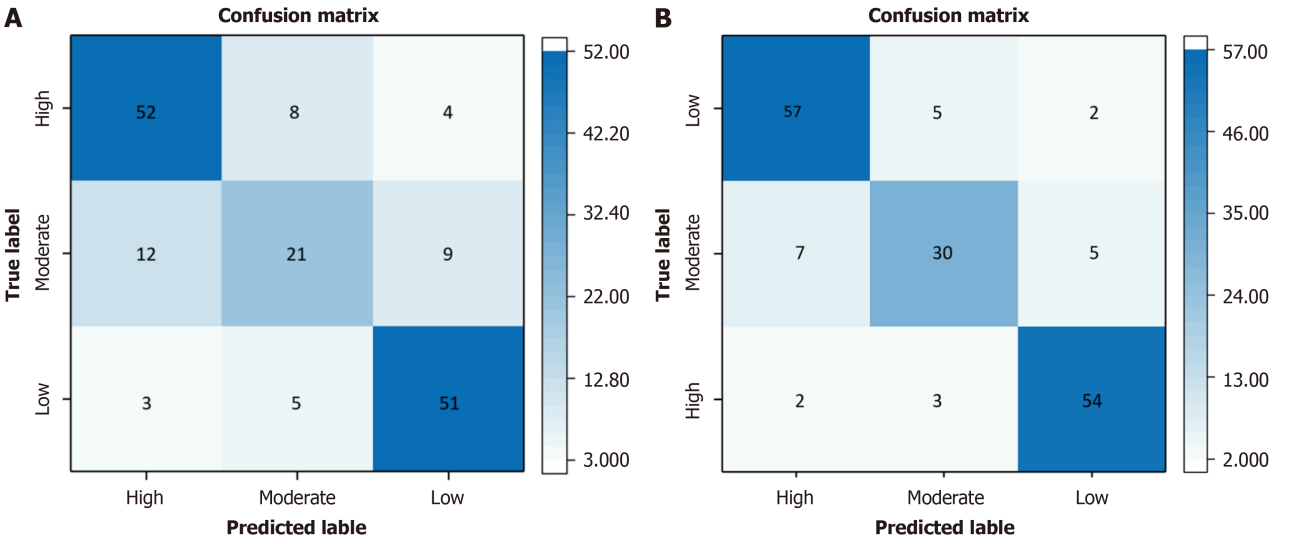

Figure 5 Confusion matrix for the deep learning model and combined model for gastrointestinal stromal tumors risk stratification. A: Confusion matrix for the deep learning model; B: Confusion matrix for the combined model.

risk and high risk) and the low malignancy potential group (very low risk and low risk) and described that the area under the curve (AUC) of the combined model (clinical features and the radiomics) was significantly higher in the validation group (0.913 *vs* 0.792, P = 0.019) compared to the clinical model. Importantly, Kang *et al*[37] concluded that the DLM (AUROCs; testing, 0.89; external validation, 0.85) outperformed the radiomics model in terms of GIST risk classification. In this study, the DLM and the combined DLM had an AUROC of 0.88 and 0.94 for distinguishing between the three types of GIST risk classifications (high-risk, intermediate-risk and low-risk) in the validation cohort. Indeed, the combined model outperformed DLM, with ACCs and AUROCs of 92% and 0.97 for low-risk GISTs, 87% and 0.83 for intermediate-risk GISTs, and 90% and 0.96 for high-risk GISTs, respectively. Notably, the AUROCs for different risk stratifications in the combined model were significantly superior to those of the DLM. These results collectively indicated that the combined DLM had superior predictive capabilities, especially for low- and high-risk GISTs.

However, the results for the intermediate-risk class were relatively unsatisfactory, with an accuracy of 87% and an AUROC of 0.83. This may be ascribed to imbalanced sample sizes. Specifically, there were only 143 cases of intermediate-risk GISTs in this study, which was lower than those of non-intermediate-risk GISTs (408 cases). This may result in relatively fewer features being extracted from intermediate-risk GISTs compared to machine learning algorithms, thereby introducing model bias. Nevertheless, compared to DLM (AUC = 0.74), the combined model (AUC = 0.83) demonstrated advantages in predicting intermediate-risk GISTs.

Of note, deep learning is a subfield of artificial intelligence that performs tasks by analyzing relationships between existing data points[38-40]. In recent years, image analysis based on deep learning algorithm has been increasingly applied to tumor diagnosis, grading, staging, prediction, and treatment evaluation. Zhu *et al*[41] concluded that the DLM outperformed in assessing the risk of screening-detected breast cancer. Similarly, Doppalapudi *et al*[42] pointed out that the accuracy of lung cancer classification predicted by DLM was 71.18%, while that of traditional machine learning models was merely 61.12%, indicating that DLM displayed superior performance for predicting lung cancer subtypes. A study investigating glioma showed that DLM achieved high performance in predicting molecular subtypes and grades, with an isocitrate dehydrogenase-AUC of 0.90, an 1p/19q co-deletion AUC of 0.85, and a grade AUC of 0.81 (grade II/III/IV)[17]. Wang *et al*[43] developed the convolutional neural network models with varying layers, achieving AUROCs above 0.8 for differentiating high-risk gastric GISTs from intermediate-risk and very low/low-risk gastric GISTs in the validation dataset. In the present study, the DLM based on the 3D-ResNet method increased the network depth by increasing the number of stacked layers of residual blocks, thereby improving the model's expressive ability. In addition, the clinical data of patients were concatenated with the imaging features extracted by the 3D- ResNet and then incorporated their feature vectors into the MLP for risk classification. As anticipated, the results uncovered that the DLM based on the 3D-ResNet method combined with clinical-imaging features could accurately predict GIST risk classifications.

Nevertheless, this study has several limitations that cannot be overlooked. Firstly, this was a retrospective study based on a limited sample size, resulting in an imbalance in the data for risk stratification. Therefore, an ideal DLM should be constructed with a larger training set containing datasets from multiple-centers to balance the data for different risk stratifications. Further prospective studies with external validation cohorts are warranted to validate our results. Secondly, the DLM developed in our study required manual segmentation of tumors on CT images remains a semi-automatic model. Thirdly, radiomics features were used for the risk stratification of GISTs in previous studies[22,32,39,44,45]. Therefore, future studies can compare the performance of radiomics models with DLM.

CONCLUSION

In summary, a high-performance combined DLM for preoperative prediction of the GIST risk stratification was developed and validated in this study. Noteworthily, this model has the potential to guide and facilitate clinical decision-making for GIST patients.

ACKNOWLEDGEMENTS

We are grateful to Yan-Bei Liu and Cong-Cong Yuan for their supports. We would also like to thank Yan-Bei Liu for his scientific advice and intellectual discussions.

FOOTNOTES

Author contributions: Li Y completed the research design and data analysis, and was a major contributor in writing the manuscript; Liu YB completed data analysis and model establishment; Cui XN, Yuan CC, and Meng DH participated in data collection and preliminary reports; Li XB and Ye ZX provided guidance on the paper and objectively reviewed it; Li Y and Cui XN were responsible for the processing of inspection analysis and statistical data to ensure the quality of the data. All authors read and approved the final manuscript.

Supported by The Chinese National Key Research and Development Project, No. 2021YFC2500400 and No. 2021YFC2500402; and Tianjin Key Medical Discipline (Specialty) Construction Project, No. TJYXZDXK-009A.

Institutional review board statement: The study was reviewed and approved by Tianjin Medical University Cancer Institute and Hospital (EK20240015).

Informed consent statement: All study participants, or their legal guardian, provided informed written consent prior to study enrollment.

Conflict-of-interest statement: The authors declare that they have no known competing financial interests or personal relationships that could have appeared to influence the work reported in this paper.

Data sharing statement: Technical appendix, statistical code, and dataset available from the corresponding author at yezhaoxiang@163.com.

Country of origin: China

ORCID number: Xu-Bin Li 0000-0002-9888-4267; Zhao-Xiang Ye 0000-0003-3157-8393.

S-Editor: Liu H
L-Editor: A
P-Editor: Xu ZH

REFERENCES

1 **Dematteo RP**, Ballman KV, Antonescu CR, Maki RG, Pisters PW, Demetri GD, Blackstein ME, Blanke CD, von Mehren M, Brennan MF, Patel S, McCarter MD, Polikoff JA, Tan BR, Owzar K; American College of Surgeons Oncology Group (ACOSOG) Intergroup Adjuvant GIST Study Team. Adjuvant imatinib mesylate after resection of localised, primary gastrointestinal stromal tumour: a randomised, double-blind, placebo-controlled trial. *Lancet* 2009; **373**: 1097-1104 [PMID: 19303137 DOI: 10.1016/S0140-6736(09)60500-6]

2 **DeMatteo RP**, Lewis JJ, Leung D, Mudan SS, Woodruff JM, Brennan MF. Two hundred gastrointestinal stromal tumors: recurrence patterns and prognostic factors for survival. *Ann Surg* 2000; **231**: 51-58 [PMID: 10636102 DOI: 10.1097/00000658-200001000-00008]

3 **Yang J**, Chen Z, Liu W, Wang X, Ma S, Jin F, Wang X. Development of a Malignancy Potential Binary Prediction Model Based on Deep Learning for the Mitotic Count of Local Primary Gastrointestinal Stromal Tumors. *Korean J Radiol* 2021; **22**: 344-353 [PMID: 33169545 DOI: 10.3348/kjr.2019.0851]

4 **Wang Y**, Call J. Mutational Testing in Gastrointestinal Stromal Tumor. *Curr Cancer Drug Targets* 2019; **19**: 688-697 [PMID: 30914028 DOI: 10.2174/1568009619666190326123945]

5 **Wozniak A**, Gebreyohannes YK, Debiec-Rychter M, Schöffski P. New targets and therapies for gastrointestinal stromal tumors. *Expert Rev Anticancer Ther* 2017; **17**: 1117-1129 [PMID: 29110548 DOI: 10.1080/14737140.2017.1400386]

6 **Gastrointestinal Stromal Tumor Meta-Analysis Group (MetaGIST)**. Comparison of two doses of imatinib for the treatment of unresectable

or metastatic gastrointestinal stromal tumors: a meta-analysis of 1,640 patients. *J Clin Oncol* 2010; **28**: 1247-1253 [PMID: 20124181 DOI: 10.1200/JCO.2009.24.2099]

7 **Patrikidou A**, Domont J, Chabaud S, Ray-Coquard I, Coindre JM, Bui-Nguyen B, Adenis A, Rios M, Bertucci F, Duffaud F, Chevreau C, Cupissol D, Pérol D, Emile JF, Blay JY, Le Cesne A; French Sarcoma Group. Long-term outcome of molecular subgroups of GIST patients treated with standard-dose imatinib in the BFR14 trial of the French Sarcoma Group. *Eur J Cancer* 2016; **52**: 173-180 [PMID: 26687836 DOI: 10.1016/j.ejca.2015.10.069]

8 **Tirumani SH**, Baheti AD, Tirumani H, O'Neill A, Jagannathan JP. Update on Gastrointestinal Stromal Tumors for Radiologists. *Korean J Radiol* 2017; **18**: 84-93 [PMID: 28096720 DOI: 10.3348/kjr.2017.18.1.84]

9 **Druker BJ**, Talpaz M, Resta DJ, Peng B, Buchdunger E, Ford JM, Lydon NB, Kantarjian H, Capdeville R, Ohno-Jones S, Sawyers CL. Efficacy and safety of a specific inhibitor of the BCR-ABL tyrosine kinase in chronic myeloid leukemia. *N Engl J Med* 2001; **344**: 1031-1037 [PMID: 11287972 DOI: 10.1056/NEJM200104053441401]

10 **Li GZ**, Raut CP. Targeted therapy and personalized medicine in gastrointestinal stromal tumors: drug resistance, mechanisms, and treatment strategies. *Onco Targets Ther* 2019; **12**: 5123-5133 [PMID: 31308690 DOI: 10.2147/OTT.S180763]

11 **Park SH**, Lee HJ, Kim MC, Yook JH, Sohn TS, Hyung WJ, Ryu SW, Kurokawa Y, Kim YW, Han SU, Kim HH, Park DJ, Kim W, Lee SI, Cho H, Cho GS, Kim JJ, Kim KH, Yoo MW, Yang HK. Early experience of laparoscopic resection and comparison with open surgery for gastric gastrointestinal stromal tumor: a multicenter retrospective study. *Sci Rep* 2022; **12**: 2290 [PMID: 35145127 DOI: 10.1038/s41598-022-05044-x]

12 **Takahashi R**, Toyokawa T, Yoshii M, Tamura T, Tanaka H, Lee S, Muguruma K, Yashiro M, Ohira M. A Giant Gastric Gastrointestinal Stromal Tumor Successfully Resected Following Neoadjuvant Treatment With Imatinib Mesylate. *Anticancer Res* 2020; **40**: 1147-1152 [PMID: 32014967 DOI: 10.21873/anticanres.14056]

13 **Fletcher CD**, Berman JJ, Corless C, Gorstein F, Lasota J, Longley BJ, Miettinen M, O'Leary TJ, Remotti H, Rubin BP, Shmookler B, Sobin LH, Weiss SW. Diagnosis of gastrointestinal stromal tumors: a consensus approach. *Int J Surg Pathol* 2002; **10**: 81-89 [PMID: 12075401 DOI: 10.1177/106689690201000201]

14 **Eckardt AJ**, Adler A, Gomes EM, Jenssen C, Siebert C, Gottschalk U, Koch M, Röcken C, Rösch T. Endosonographic large-bore biopsy of gastric subepithelial tumors: a prospective multicenter study. *Eur J Gastroenterol Hepatol* 2012; **24**: 1135-1144 [PMID: 22797706 DOI: 10.1097/MEG.0b013e328356eae2]

15 **Demetri GD**, von Mehren M, Antonescu CR, DeMatteo RP, Ganjoo KN, Maki RG, Pisters PW, Raut CP, Riedel RF, Schuetze S, Sundar HM, Trent JC, Wayne JD. NCCN Task Force report: update on the management of patients with gastrointestinal stromal tumors. *J Natl Compr Canc Netw* 2010; **8** Suppl 2: S1-41; quiz S42 [PMID: 20457867 DOI: 10.6004/jnccn.2010.0116]

16 **Park CH**, Kim GH, Lee BE, Song GA, Park DY, Choi KU, Kim DH, Jeon TY. Two staging systems for gastrointestinal stromal tumors in the stomach: which is better? *BMC Gastroenterol* 2017; **17**: 141 [PMID: 29207963 DOI: 10.1186/s12876-017-0705-7]

17 **van der Voort SR**, Incekara F, Wijnenga MMJ, Kapsas G, Gahrmann R, Schouten JW, Nandoe Tewarie R, Lycklama GJ, De Witt Hamer PC, Eijgelaar RS, French PJ, Dubbink HJ, Vincent AJPE, Niessen WJ, van den Bent MJ, Smits M, Klein S. Combined molecular subtyping, grading, and segmentation of glioma using multi-task deep learning. *Neuro Oncol* 2023; **25**: 279-289 [PMID: 35788352 DOI: 10.1093/neuonc/noac166]

18 **Zhao Y**, Chang M, Wang R, Xi IL, Chang K, Huang RY, Vallières M, Habibollahi P, Dagli MS, Palmer M, Zhang PJ, Silva AC, Yang L, Soulen MC, Zhang Z, Bai HX, Stavropoulos SW. Deep Learning Based on MRI for Differentiation of Low- and High-Grade in Low-Stage Renal Cell Carcinoma. *J Magn Reson Imaging* 2020; **52**: 1542-1549 [PMID: 32222054 DOI: 10.1002/jmri.27153]

19 **Zhu Y**, Man C, Gong L, Dong D, Yu X, Wang S, Fang M, Wang S, Fang X, Chen X, Tian J. A deep learning radiomics model for preoperative grading in meningioma. *Eur J Radiol* 2019; **116**: 128-134 [PMID: 31153553 DOI: 10.1016/j.ejrad.2019.04.022]

20 **Jiang Y**, Yang M, Wang S, Li X, Sun Y. Emerging role of deep learning-based artificial intelligence in tumor pathology. *Cancer Commun (Lond)* 2020; **40**: 154-166 [PMID: 32277744 DOI: 10.1002/cac2.12012]

21 **Banzato T**, Causin F, Della Puppa A, Cester G, Mazzai L, Zotti A. Accuracy of deep learning to differentiate the histopathological grading of meningiomas on MR images: A preliminary study. *J Magn Reson Imaging* 2019; **50**: 1152-1159 [PMID: 30896065 DOI: 10.1002/jmri.26723]

22 **Wang P**, Yan J, Qiu H, Huang J, Yang Z, Shi Q, Yan C. A radiomics-clinical combined nomogram-based on non-enhanced CT for discriminating the risk stratification in GISTs. *J Cancer Res Clin Oncol* 2023; **149**: 12993-13003 [PMID: 37464150 DOI: 10.1007/s00432-023-05170-7]

23 **Vernuccio F**, Cannella R, Comelli A, Salvaggio G, Lagalla R, Midiri M. [Radiomics and artificial intelligence: new frontiers in medicine.]. *Recenti Prog Med* 2020; **111**: 130-135 [PMID: 32157259 DOI: 10.1701/3315.32853]

24 **Esteva A**, Kuprel B, Novoa RA, Ko J, Swetter SM, Blau HM, Thrun S. Dermatologist-level classification of skin cancer with deep neural networks. *Nature* 2017; **542**: 115-118 [PMID: 28117445 DOI: 10.1038/nature21056]

25 **Yang TH**, Hwang JI, Yang MS, Hung SW, Chan SW, Wang J, Tyan YS. Gastrointestinal stromal tumors: computed tomographic features and prediction of malignant risk from computed tomographic imaging. *J Chin Med Assoc* 2007; **70**: 367-373 [PMID: 17908650 DOI: 10.1016/S1726-4901(08)70022-4]

26 **Grazzini G**, Guerri S, Cozzi D, Danti G, Gasperoni S, Pradella S, Miele V. Gastrointestinal stromal tumors: relationship between preoperative CT features and pathologic risk stratification. *Tumori* 2021; **107**: 556-563 [PMID: 33620027 DOI: 10.1177/0300891621996447]

27 **Joensuu H**, Hohenberger P, Corless CL. Gastrointestinal stromal tumour. *Lancet* 2013; **382**: 973-983 [PMID: 23623056 DOI: 10.1016/S0140-6736(13)60106-3]

28 **von Mehren M**, Randall RL, Benjamin RS, Boles S, Bui MM, Conrad EU 3rd, Ganjoo KN, George S, Gonzalez RJ, Heslin MJ, Kane JM 3rd, Koon H, Mayerson J, McCarter M, McGarry SV, Meyer C, O'Donnell RJ, Pappo AS, Paz IB, Petersen IA, Pfeifer JD, Riedel RF, Schuetze S, Schupak KD, Schwartz HS, Tap WD, Wayne JD, Bergman MA, Scavone J. Soft Tissue Sarcoma, Version 2.2016, NCCN Clinical Practice Guidelines in Oncology. *J Natl Compr Canc Netw* 2016; **14**: 758-786 [PMID: 27283169 DOI: 10.6004/jnccn.2016.0078]

29 **Wang FH**, Zheng HL, Li JT, Li P, Zheng CH, Chen QY, Huang CM, Xie JW. Prediction of recurrence-free survival and adjuvant therapy benefit in patients with gastrointestinal stromal tumors based on radiomics features. *Radiol Med* 2022; **127**: 1085-1097 [PMID: 36057930 DOI: 10.1007/s11547-022-01549-7]

30 **Lin JX**, Chen QF, Zheng CH, Li P, Xie JW, Wang JB, Lu J, Chen QY, Cao LL, Lin M, Tu RH, Huang CM. Is 3-years duration of adjuvant imatinib mesylate treatment sufficient for patients with high-risk gastrointestinal stromal tumor? A study based on long-term follow-up. *J Cancer Res Clin Oncol* 2017; **143**: 727-734 [PMID: 28083710 DOI: 10.1007/s00432-016-2334-x]

31 **Liu S**, Pan X, Liu R, Zheng H, Chen L, Guan W, Wang H, Sun Y, Tang L, Guan Y, Ge Y, He J, Zhou Z. Texture analysis of CT images in

predicting malignancy risk of gastrointestinal stromal tumours. *Clin Radiol* 2018; **73**: 266-274 [PMID: 28969853 DOI: 10.1016/j.crad.2017.09.003]

32 **Choi IY**, Yeom SK, Cha J, Cha SH, Lee SH, Chung HH, Lee CM, Choi J. Feasibility of using computed tomography texture analysis parameters as imaging biomarkers for predicting risk grade of gastrointestinal stromal tumors: comparison with visual inspection. *Abdom Radiol (NY)* 2019; **44**: 2346-2356 [PMID: 30923842 DOI: 10.1007/s00261-019-01995-4]

33 **Iannicelli E**, Carbonetti F, Federici GF, Martini I, Caterino S, Pilozzi E, Panzuto F, Briani C, David V. Evaluation of the Relationships Between Computed Tomography Features, Pathological Findings, and Prognostic Risk Assessment in Gastrointestinal Stromal Tumors. *J Comput Assist Tomogr* 2017; **41**: 271-278 [PMID: 27753723 DOI: 10.1097/RCT.0000000000000499]

34 **Zhou C**, Duan X, Zhang X, Hu H, Wang D, Shen J. Predictive features of CT for risk stratifications in patients with primary gastrointestinal stromal tumour. *Eur Radiol* 2016; **26**: 3086-3093 [PMID: 26699371 DOI: 10.1007/s00330-015-4172-7]

35 **Meng X**, Liu J, Kang J, Wang M, Guan Z, Tian D, Chen X. Lamivudine protects mice from gastric ulcer by activating PGK1 to suppress ferroptosis. *Biochem Pharmacol* 2024; **227**: 116440 [PMID: 39029631 DOI: 10.1016/j.bcp.2024.116440]

36 **Nishida T**, Goto O, Raut CP, Yahagi N. Diagnostic and treatment strategy for small gastrointestinal stromal tumors. *Cancer* 2016; **122**: 3110-3118 [PMID: 27478963 DOI: 10.1002/cncr.30239]

37 **Kang B**, Yuan X, Wang H, Qin S, Song X, Yu X, Zhang S, Sun C, Zhou Q, Wei Y, Shi F, Yang S, Wang X. Preoperative CT-Based Deep Learning Model for Predicting Risk Stratification in Patients With Gastrointestinal Stromal Tumors. *Front Oncol* 2021; **11**: 750875 [PMID: 34631589 DOI: 10.3389/fonc.2021.750875]

38 **LeCun Y**, Bengio Y, Hinton G. Deep learning. *Nature* 2015; **521**: 436-444 [PMID: 26017442 DOI: 10.1038/nature14539]

39 **Ning Z**, Luo J, Li Y, Han S, Feng Q, Xu Y, Chen W, Chen T, Zhang Y. Pattern Classification for Gastrointestinal Stromal Tumors by Integration of Radiomics and Deep Convolutional Features. *IEEE J Biomed Health Inform* 2019; **23**: 1181-1191 [PMID: 29993591 DOI: 10.1109/JBHI.2018.2841992]

40 **Tran KA**, Kondrashova O, Bradley A, Williams ED, Pearson JV, Waddell N. Deep learning in cancer diagnosis, prognosis and treatment selection. *Genome Med* 2021; **13**: 152 [PMID: 34579788 DOI: 10.1186/s13073-021-00968-x]

41 **Zhu X**, Wolfgruber TK, Leong L, Jensen M, Scott C, Winham S, Sadowski P, Vachon C, Kerlikowske K, Shepherd JA. Deep Learning Predicts Interval and Screening-detected Cancer from Screening Mammograms: A Case-Case-Control Study in 6369 Women. *Radiology* 2021; **301**: 550-558 [PMID: 34491131 DOI: 10.1148/radiol.2021203758]

42 **Doppalapudi S**, Qiu RG, Badr Y. Lung cancer survival period prediction and understanding: Deep learning approaches. *Int J Med Inform* 2021; **148**: 104371 [PMID: 33461009 DOI: 10.1016/j.ijmedinf.2020.104371]

43 **Wang J**, Shao M, Hu H, Xiao W, Cheng G, Yang G, Ji H, Yu S, Wan J, Xie Z, Xu M. Convolutional neural network applied to preoperative venous-phase CT images predicts risk category in patients with gastric gastrointestinal stromal tumors. *BMC Cancer* 2024; **24**: 280 [PMID: 38429653 DOI: 10.1186/s12885-024-11962-y]

44 **Chen T**, Ning Z, Xu L, Feng X, Han S, Roth HR, Xiong W, Zhao X, Hu Y, Liu H, Yu J, Zhang Y, Li Y, Xu Y, Mori K, Li G. Radiomics nomogram for predicting the malignant potential of gastrointestinal stromal tumours preoperatively. *Eur Radiol* 2019; **29**: 1074-1082 [PMID: 30116959 DOI: 10.1007/s00330-018-5629-2]

45 **Ren C**, Wang S, Zhang S. Development and validation of a nomogram based on CT images and 3D texture analysis for preoperative prediction of the malignant potential in gastrointestinal stromal tumors. *Cancer Imaging* 2020; **20**: 5 [PMID: 31931874 DOI: 10.1186/s40644-019-0284-7]

World Journal of Gastrointestinal Oncology

Submit a Manuscript: https://www.f6publishing.com

World J Gastrointest Oncol 2024 December 15; 16(12): 4675-4684

DOI: 10.4251/wjgo.v16.i12.4675

ISSN 1948-5204 (online)

ORIGINAL ARTICLE

Retrospective Study

Temozolomide and capecitabine regimen as first-line treatment in advanced gastroenteropancreatic neuroendocrine tumors at a Latin American reference center

Wagner Eduardo Cruz-Diaz, Victor Paitan, Jersinho Medina, Raymundo Flores, Juan Haro-Varas, Raul Mantilla, Victor Castro-Oliden

Specialty type: Oncology

Provenance and peer review: Unsolicited article; Externally peer reviewed.

Peer-review model: Single blind

Peer-review report's classification

Scientific Quality: Grade B

Novelty: Grade B

Creativity or Innovation: Grade C

Scientific Significance: Grade C

P-Reviewer: Agidew MM

Received: July 22, 2024

Revised: August 31, 2024

Accepted: September 19, 2024

Published online: December 15, 2024

Processing time: 113 Days and 11.9 Hours

Wagner Eduardo Cruz-Diaz, Victor Paitan, Juan Haro-Varas, Raul Mantilla, Victor Castro-Oliden, Department of Oncology, Instituto Nacional de Enfermedades Neoplásicas, Lima 15038, Perú

Jersinho Medina, Department of Pathology, Instituto Nacional de Enfermedades Neoplásicas, Lima 15038, Perú

Raymundo Flores, Department of Radiology, Instituto Nacional de Enfermedades Neoplásicas, Lima 15038, Perú

Corresponding author: Wagner Eduardo Cruz-Diaz, MD, Staff Physician, Department of Oncology, Instituto Nacional de Enfermedades Neoplásicas, Avenue Angamos Este 2520, Surquillo, Lima 15038, Peru. wagner.cruz@upch.pe

Abstract

BACKGROUND

Numerous studies have indicated that the temozolomide and capecitabine regimen (TEMCAP) exhibits a certain level of efficacy in treating advanced, well-differentiated gastroenteropancreatic neuroendocrine tumors (GEP-NET). However, published data from Peru are limited. We hypothesize that this regimen could be a viable therapeutic option for advanced GEP-NET in the Peruvian population.

AIM

To evaluate overall survival (OS) in patients diagnosed with advanced GEP-NET treated with TEMCAP at the Instituto Nacional de Enfermedades Neoplásicas (INEN) in Lima-Perú.

METHODS

A retrospective review was conducted to identify patients with GEP-NEN treated with the TEMCAP regimen between 2011 and 2021 at the INEN. A total of thirty-eight patients were included in the final analysis: Thirty-five received TEMCAP as a first-line treatment, and three as a second-line treatment. The primary objective was to evaluate OS. The efficacy and safety of TEMCAP were assessed until the occurrence of unacceptable toxicity or disease progression. Survival outcomes were estimated using the Kaplan-Meier method.

RESULTS
The median age of the patients was 52 years (range 24-77 years), and 53.3% were female. The most common symptoms at diagnosis were abdominal pain in 31 patients (81.6%). Primary tumors included 12 in the rectum (31.6%), 11 in the pancreas (28.9%), 3 in the ileum (7.9%), 2 in the mesentery (5.3%), 2 in the small intestine (5.3%), 1 in the appendix (2.6%), 1 in the stomach (2.6%) and 6 cases of liver metastasis of unknown primary (15.8%). Five were neuroendocrine tumors (NET) G1 (13.2%), 33 were NET G2 (86.8%), five had Ki67 < 3% (13.2%), and 33 had Ki67 between 3% and 20% (86.8%). TEMCAP was administered to 35 (92.1%) patients as first-line treatment. OS at 12, 36, and 60 months was estimated in 80%, 66%, and 42%, respectively, with a median OS of 49 months.

CONCLUSION
TEMCAP therapy is a viable first-line option regarding efficacy and tolerability in areas where standard therapy is inaccessible.

Key Words: Well-differentiated; Gastroenteropancreatic neuroendocrine tumors; Capecitabine; Temozolomide; Retrospective study; Treatment; Chemotherapy

Core Tip: In this study, patients diagnosed with advanced gastroenteropancreatic neuroendocrine tumors who were treated with the temozolomide and capecitabine regimen exhibited a median overall survival of 49 months, with 42% surviving at 60 months. The regimen was well-tolerated, and most patients experienced stable disease. These findings suggest that this treatment could be viable in settings where standard therapies are unavailable or inaccessible, although further prospective studies are needed for confirmation.

Citation: Cruz-Diaz WE, Paitan V, Medina J, Flores R, Haro-Varas J, Mantilla R, Castro-Oliden V. Temozolomide and capecitabine regimen as first-line treatment in advanced gastroenteropancreatic neuroendocrine tumors at a Latin American reference center. *World J Gastrointest Oncol* 2024; 16(12): 4675-4684
URL: https://www.wjgnet.com/1948-5204/full/v16/i12/4675.htm
DOI: https://dx.doi.org/10.4251/wjgo.v16.i12.4675

INTRODUCTION

Neuroendocrine tumors (NEN) represent a diverse array of neoplasms arising from cells within the endocrine and nervous systems, and exhibit a broad spectrum of behaviors. While historically considered rare diseases, their prevalence has been increasing. In England, NEN are the 10th most prevalent cancer and the second most common gastrointestinal cancer, only preceded by colorectal cancer[1]. NEN have witnessed a notable surge over the past two decades; the age-adjusted incidence per 100000 persons increased from 4.90 in 2000 to 8.19 in 2018[2]. With regard to gastroenteropancreatic neuroendocrine tumors (GEP-NET) in the United States, the incidence is reported to be 3.56 cases per 100000 individuals[3].

The information published regarding NET in Latin American countries remains largely unreported, and clinical literature is highly scarce. An observational study in Argentina documented 532 NET cases, including 461 GEP-NET and 71 bronchial NET[4]. A NET registry from Brazil has compiled baseline data on the initial 1000 patients enrolled across 32 centers spanning all country regions. It categorized GEP-NET as the second most prevalent type, constituting 20.2% of cases, trailing only thoracic NEN[5]. In a retrospective review at the Instituto Nacional de Enfermedades Neoplásicas (INEN), 367 NEN were reported between 2010 and 2014. Gastroenteropancreatic NEN were the most prevalent, with 152 cases (44.84%), followed by thoracic NEN, with 75 cases (22.12%)[6].

The clinical practice guideline for medical management of GEP-NET at the INEN reported 650 cases of NEN between 2009 and 2018, with an average age of 55 years. The most frequent sites were the rectum (15%), lung (9.84%), stomach (8.3%), neuroendocrine Merkel cells (9.07%), and unknown primary (9.07%)[7]. According to the WHO classification for NEN, they are categorized into well-differentiated low-grade G1 (Ki67 < 3%), intermediate-grade well-differentiated G2 (Ki67 3%-20%), and high-grade well-differentiated G3 (Ki67 > 20%), based on the Ki67 proliferation index. G3 tumors are divided into well-differentiated high-grade or poorly differentiated high-grade neuroendocrine carcinomas (GEP-NEC) [8]. Of all NEN, approximately 80%-90% are well-differentiated[9]. GEP-NET can be classified according to their origin into two main groups: Pancreatic NET (pan-NET) and non-pan-NET. Furthermore, they can be classified based on hormone production in functioning and non-functioning tumors. Most GEP-NET are non-functioning; 20% of intestinal NET are functioning tumors, while pan-NET are functioning in 10%-30% of cases[9]. For non-functioning NET, early detection can be challenging unless the tumor has grown sufficiently large to cause symptoms.

Medical treatment options for advanced GEP-NET with antiproliferative effects include targeted drugs and systemic chemotherapy. Regarding somatostatin analogs (SSA), the CLARINET trial, which compared lanreotide to placebo,

estimated progression-free survival (PFS) rates at 24 months of 65.1% in the experimental arm and 33% in the placebo group[10]. These results were confirmed in the open-label extension study[11]. In the phase III PROMID trial, the median time to progression in the octreotide long-acting release (LAR) and placebo groups was 14.3 and 6 months, respectively [12]. However, the updated trial did not show a difference in OS[13]. Everolimus was shown to prolong PFS compared to placebo in previously treated GEP-NET patients[14,15]. Despite these findings, its efficacy in patients with GEP-NET associated with carcinoid syndrome remains unclear[16]. Sunitinib, a multitargeted tyrosine kinase inhibitor, demonstrated a median PFS of 11.4 months compared to 5.5 months in the placebo group in patients with advanced pan-NET. A 59% reduction in the risk of death was observed in favor of the experimental group[17]. More recently, the Netter 2 trial evaluated 177 Lu-dotatate as a first-line treatment in combination with octreotide LAR. It demonstrated a significant improvement in PFS in patients with newly diagnosed somatostatin receptor positive, G2 and G3, advanced GEP-NET compared to high-dose octreotide LAR alone[18].

Due to their high cost, these new agents are only available to some patients, especially in resource-limited countries. The restriction on access to first-line treatments at our institution creates an urgent need to investigate other effective alternatives. This study aims to assess the efficacy of the TEMCAP regimen as first-line therapy in patients with advanced GEP-NET in a Latin American population.

MATERIALS AND METHODS

Study population and data collection

A retrospective review was conducted to identify patients with GEP-NEN who were treated with the TEMCAP regimen at any point during their disease between 2011 and 2021. The registry data were provided by the Epidemiology and Statistics Department of the INEN. A total of forty-five GEP-NEN patients were identified, of which nine were excluded due to a diagnosis of NEC. Consequently, thirty-eight patients were included in the final analysis: Thirty-five received TEMCAP as a first-line treatment, and three received TEMCAP as a second-line treatment.

Inclusion criteria: Patients with a diagnosis of unresectable, metastatic, or recurrent GEP-NET; histologic grade 1 or 2; Ki67 index less than 20%.

Exclusion criteria: Patients with GEP-NEC, GEP-NET histologic grade 3, a Ki67 index greater than or equal to 20%, and incomplete medical records.

Primary and secondary objectives

The primary objective was to evaluate OS in the entire population. Secondary objectives included assessing PFS, evaluating OS and PFS in specific subgroups, including pan-NET and non-pan-NET; evaluating the objective response rate (ORR) and disease control rate (DCR), and assessing the regimen's toxicity by documenting treatment-related adverse effects.

Treatment and response criteria

The TEMCAP regimen consisted of capecitabine 750 mg/m² twice daily on days 1–14, followed by Temozolomide 200 mg/m² on days 10 to 14 in 28-day cycles until unacceptable toxicity or disease progression. The response was assessed by computed tomography (CT) according to RECIST 1.1 criteria. Toxicity was evaluated according to Common Terminology Criteria for Adverse Events version 5.0 in all 38 patients.

Statistical analysis

A descriptive analysis was performed on qualitative variables using frequencies and percentages. Quantitative variables were summarized using measures of central tendency (mean, minimum, and maximum for normally distributed variables) and measures of dispersion (median, interquartile range, quartiles 1 and 3 for skewed distributions). OS was estimated from the start of chemotherapy to the date of death documentation or the last follow-up date. Patients who did not experience the event of interest were considered censored. PFS was estimated from the start of chemotherapy to the date of documented progression *via* CT following RECIST 1.1 criteria or the last follow-up date, with patients not experiencing the event also considered censored. Both OS and PFS estimates were calculated using the Kaplan-Meier method. Differences in survival according to study variables were evaluated using the log-rank test. A multivariate Cox proportional hazards model was fitted with variables showing significant differences in OS and PFS to assess their effect on the risk of death or progression, respectively. The proportional hazards assumption was tested in the adjusted model. A P value of < 0.05 was considered significant for differences in OS and PFS and for assessing the risk of death. All analyses were performed using R software.

RESULTS

Patient's characteristics

The median age was 52 years (24-77 years); 55.3% were females, and 44.7% were males. Lima was the most common region of origin (36.8%), followed by Huánuco (13.2%). The majority (92.1%) had an Eastern Cooperative Oncology Group

Table 1 Demographic and clinical features, *n* (%)

Feature	*n* = 38
Age at diagnosis (years)	
Median (min-max)	52 (24-77)
Sex	
Female	21 (55.3)
Male	17 (44.7)
Region of birth	
Lima	14 (36.8)
Huánuco	5 (13.2)
Ancash	3 (7.9)
Ica	3 (7.9)
Junín	3 (7.9)
Lambayeque	2 (5.3)
Ayacucho	2 (5.3)
Cajamarca	2 (5.3)
Amazonas	1 (2.6)
Cusco	1 (2.6)
Puno	1 (2.6)
Tacna	1 (2.6)
BMI, kg/m^2	
Median (IQR)	23.438 (20.65-26.279)
ECOG scale	
0	1 (2.6)
1	35 (92.1)
2	2 (5.3)
Symptoms	
Abdominal pain	31 (81.6)
Rectal bleeding	12 (31.6)
Weight loss	9 (23.7)
Diarrhea	5 (13.2)
Emesis	4 (10.5)
Flushing	2 (5.3)

IQR: Interquartile range; BMI: Body mass index; ECOG: Eastern Cooperative Oncology Group.

(ECOG) performance status of 1. The median body mass index (BMI) was 23.438 kg/m^2. The most common symptom was abdominal pain (81.6%), followed by rectal bleeding (31.6%), weight loss (23.7%), diarrhea (13.2%), emesis (10.5%), and flushing (5.3%). Demographic and clinical features are shown in Table 1. According to clinical staging, 15.8% were in stage III, 81.6% in stage IV, and one patient was in an unspecified stage. Two (5.3%) patients had unresectable tumors, 5 (13.2%) had recurrent disease, and 31 (81.6%) had metastatic disease at presentation. Among the 38 patients, the primary tumor locations were distributed as follows: Twelve (31.6%) were rectal tumors, eleven (28.9%) were pancreatic tumors (28.9%), three (7.9%) were ileum tumors, two (5.3%) were mesenteric tumors, two (5.3%) were small intestine tumors, one (2.6%) was an appendix tumor, one (2.6%) was a stomach tumor and six (15.8%) were liver metastases from an unknown primary.

Table 2 Systemic therapy, *n* (%)

Feature	*n* = 38
First-line treatment	
Temozolomide/capecitabine	35 (92.1)
CAPOX	1 (2.6)
Cisplatin/etoposide	1 (2.6)
Interferon alpha	1 (2.6)
First-line cycles	
Median (IQR)	9 (6-22.75)
Duration of first-line treatment, days	
Median (IQR)	331 (133.25-606)
Second-line treatment	
Yes	14 (36.8)
No	24 (63.2)
Second-line regimen, *n* = 14	
Capecitabine	4 (28.6)
CAPOX	3 (21.4)
TEMCAP	3 (21.4)
Cisplatin/etoposide	1 (7.1)
Dacarbazine (DTIC)	1 (7.1)
GEMOX	1 (7.1)
Temozolomide	1 (7.1)

IQR: Interquartile range; TEMCAP: Temozolomide and capecitabine regimen; CAPOX: capecitabine/oxaliplatin; GEMOX: gemcitabine/oxaliplatin.

Chemotherapy treatment

TEMCAP was administered to 35 patients (92.1%). The median number of chemotherapy cycles at first-line was nine. Fourteen patients (36.8%) received a second-line treatment. Among these patients, the most commonly used regimen was capecitabine in four patients (28.6%), followed by capecitabine/oxaliplatin and TEMCAP in three patients (21.4%) each, cisplatin/etoposide in one patient (7.1%), dacarbazine in one patient (7.1%), gemcitabine/oxaliplatin in one patient (7.1%), and temozolomide in one patient (7.1%). Characteristics of systemic therapy are shown in Table 2.

Efficacy

The responses of the 38 patients according to RECIST 1.1 were as follows: One (2.6%) patient had a complete response (CR), two (5.3%) had a partial response (PR), sixteen (42.1%) had stable disease (SD), fifteen (39.5%) had progressive disease (PD), and four (10.5%) were without RECIST evaluation. The ORR was 7.9%, and the DCR was 50%. Regarding the pan-NET subgroup, there was one CR, two PR, three SD, four PD, and one case without response evaluation; the ORR was 27.2%, and the DCR was 54.5%.

OS

With a median follow-up of 33.5 months (range 1–81 months), the estimated OS rates at 12, 36, and 60 months were 80%, 66%, and 42%, respectively, with a median OS of 49 months for the entire population (Figure 1A). The median OS in the pan-NET group was 64 months, compared to 44 months in the non-pan-NET group, with a *P*-value of 0.056, which was not statistically significant (Figure 1B).

PFS

Among the total population (*n* = 34; RECIST criteria not evaluated in 4 patients), 15 (44.1%) patients experienced PD, with a median follow-up time for PFS of 20 months (range 5-81 months). The estimated PFS at 12, 36, and 60 months was 84.2%, 49.9%, and 49.9%, respectively, with a median PFS of 34 months. In the pan-NET group, the median PFS was 78 months, compared to 27 months in the non-pan-NET group (Figure 1C).

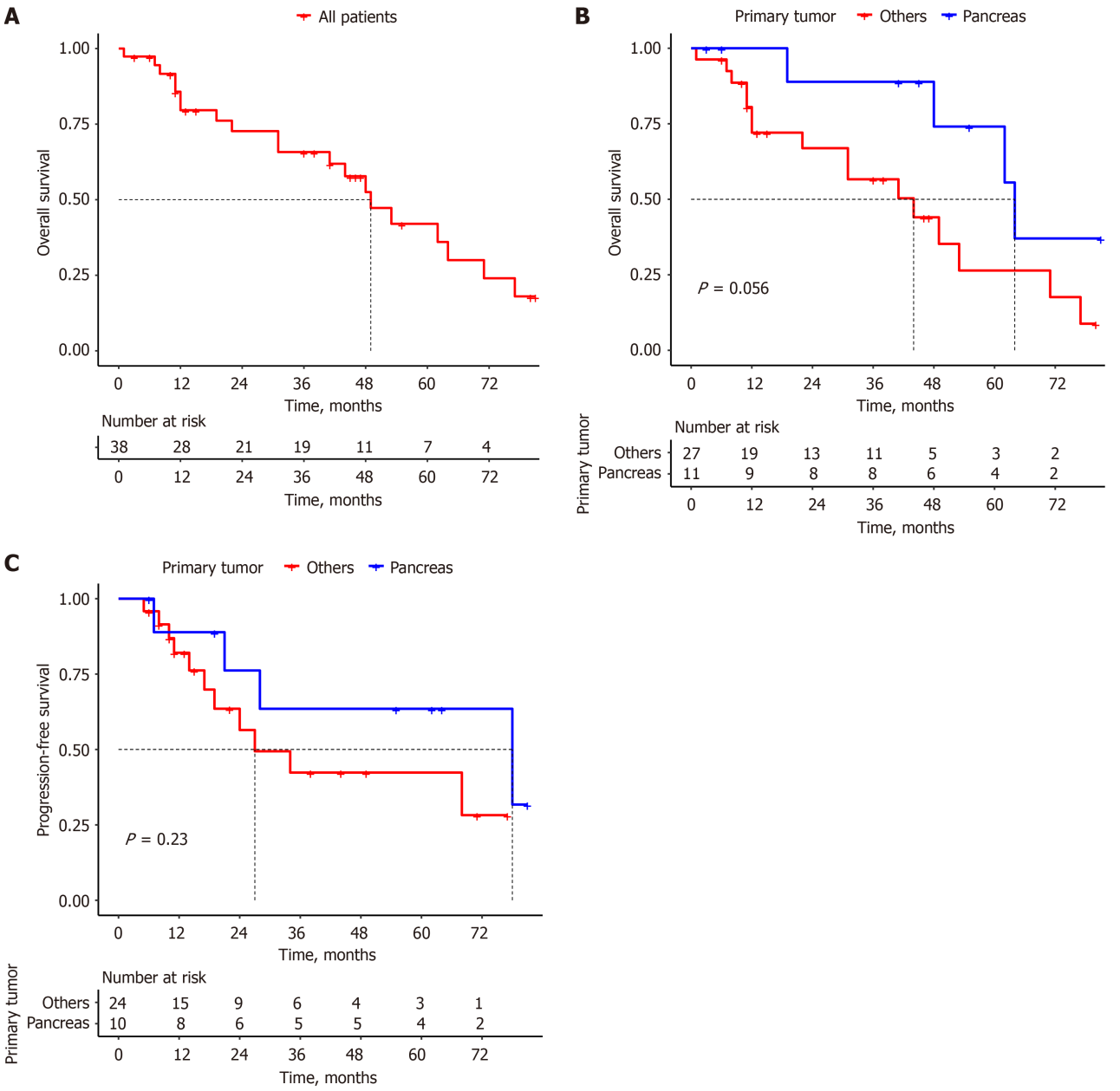

Figure 1 Overall survival. A: Overall survival (OS) in patients with gastroenteropancreatic neuroendocrine tumors; B: OS according to primary tumor; C: Progression-free survival based on primary tumor.

Safety profile

The most common adverse event of any grade was neutropenia, with 7 (18.4%) recorded events, followed by hand-foot syndrome with 6 (15.8%) events, and hypertransaminasemia and nausea with 5 (13.2%) events each. The total number of adverse events is shown in Table 3. Regarding adverse events grade 3 and 4, neutropenia occurred in three patients (7.9%), two (5.3%) experiencing grade 3 and one (2.6%) grade 4; Thrombocytopenia was observed in four patients (10.6%), two (5.3%) experiencing grade 3 and two (5.3%) grade 4; anemia was reported in two patients (5.3%), one (2.6%) experiencing grade 3 and one (2.6%) grade 4. Additionally, nausea of grade 3 was documented in one patient (2.6%).

DISCUSSION

We observed a median OS of 49 months in our study, similar to the findings of other studies that retrospectively evaluated OS with the TEMCAP regimen in GEP-NET[19-25].

Prospective data evaluating TEMCAP are scarce. The first prospective trial was phase II ECOG-ACRIN E2211, which compared TEMCAP *vs* temozolomide in advanced pan-NET. This trial met its primary endpoint with a PFS of 22.7 months in the TEMCAP arm *vs* 14.4 months in the temozolomide arm. Although the median OS was 4.9 months superior in the TEMCAP arm, it did not achieve statistical significance[26].

Table 3 Adverse events during chemotherapy by grade, *n* (%)

	Grade			
	1	2	3	4
Neutropenia	3 (7.9)	1 (2.6)	2 (5.3)	1 (2.6)
Hand-foot syndrome	5 (13.2)	1 (2.6)		
Hypertransaminasemia	3 (7.9)	2 (5.3)		
Nausea	4 (10.5)		1 (2.6)	
Peripheral neuropathy	4 (10.5)	1 (2.6)		
Vomiting	4 (10.5)	1 (2.6)		
Anemia	2 (5.3)		1 (2.6)	1 (2.6)
Asthenia	4 (10.5)			
Constipation	4 (10.5)			
Thrombocytopenia			2 (5.3)	2 (5.3)
Anorexia	3 (7.9)			
Diarrhea	2 (5.3)			
Sialorrhea	2 (5.3)			
Hyperbilirubinemia	1 (2.6)			

In our study, we observed an ORR of 7.9% with one (2.6%) CR and two (5.3%) PR; the DCR was 50%, including 16 patients (42.1%) with SD. Our DCR results are very similar to those in other retrospective studies. Crespo *et al*[22] evaluated TEMCAP in 65 patients with GEP-NET (70.8% had pan-NET) and the DCR was 47.7%, with two CR (3.1%), 29 PR (44.6%), and 27 (41.5%) SD. Fine *et al*[19] evaluated 18 patients with well-differentiated NET metastatic to the liver who had failed front-line therapy. The ORR was 61%, and the DCR was 83.2%. Abbasi *et al*[27] evaluated 21 patients (14 with pan-NET and 7 with carcinoid tumors) who failed treatment with SSA and platinum-based chemotherapy combined with etoposide and reported a DCR of 80%. The systematic review by Arrivi *et al*[25] evaluated 1,818 patients from 42 articles with advanced NEN of gastroenteropancreatic, lung, and unknown origin. The ORR was 77%, with a median OS ranging from 8 to 103 months. ORR and DCR appear more critical as surrogates of the PFS and OS for the TEMCAP regimen in GEP-NET.

Our results for pan-NET showed an ORR of 27.2% and a DCR of 54.5%, consistent with what has been described in the literature. Pan-NET have historically better chemotherapy responses than non-pan-NET. Our study also showed this trend, with OS in pan-NET being 20 months longer than non-pan-NET. The PSF for pan-NET in our series was 78 months compared to 27 months in non-pan-NET. Notably, of the 11 patients with pan-NET, 10 were evaluated according to RECIST 1.1, of which 4 showed disease progression; the remaining patients are still alive and continue to be followed up.

A meta-analysis revealed a lower ORR in non-pan-NET than in pan-NET patients; however, this difference was not statistically significant when high-risk bias studies were excluded[28]. In a cohort of 101 patients, which included 53 with pan-NEN and 44 with carcinoid tumors treated with temozolomide-based chemotherapy, an ORR of 34% was observed in pan-NEN compared to 2% in carcinoid tumors[29]. Patients with pan-NET who require clinically meaningful tumor shrinkage may benefit more from chemotherapeutic regimens.

Anemia, neutropenia, and thrombocytopenia were the most common grade 3-4 adverse events observed in our study, consistent with findings from other trials. Crespo *et al*[22] reported neutropenia in 7.7% of patients, while in the systematic review by Arrivi *et al*[25], the safety analysis of TEMCAP showed that 16.4% of the population experienced grade 3-4 toxicities, with hematological toxicities being the most common (27.2%). The prospective ECOG-ACRIN E2211 study reported grade 3-4 neutropenia in 13% of cases and thrombocytopenia in 10%[26]. Temozolomide-based regimens using a dose-dense schedule of 150 mg/m² daily every other week resulted in more hematological toxicities compared to the TEMCAP regimen. Grade 3-4 lymphopenia was reported in more than 50% of patients. Chan *et al*[30] reported grade 3 thrombocytopenia in 18% of patients. Opportunistic infectious complications were also reported during treatment with dose-dense temozolomide-based regimens[30,31]. This contrasts with our study, where no opportunistic infections were observed at a dose of 200 mg/m² for 5 days.

We must consider some limitations in our study inherent to all retrospective analyses, particularly the potential for selection bias. Additionally, the small sample size of 38 patients may have contributed to the lack of statistical significance in some outcomes. Despite these limitations, our data support the effectiveness of the TEMCAP regimen in patients with advanced GEP-NET.

CONCLUSION

This is the first retrospective study in Peru to evaluate the use of TEMCAP for advanced GEP-NET. The findings suggest that TEMCAP could be a viable first-line treatment in regions where standard therapies are not readily accessible, particularly for grade 2 tumors. A notable 42% OS rate at 60 months was observed. Prospective studies are needed to determine its value as a treatment option in this setting.

FOOTNOTES

Author contributions: Cruz-Diaz WE collected the data at the Instituto Nacional de Enfermedades Neoplásicas and wrote the initial manuscript; Paitan V and Haro-Varas J supervised the initial manuscript; Medina J reviewed the pathology slides, and Flores R reviewed the computed tomography and magnetic resonance imaging images; Mantilla R was responsible for conducting the statistical analysis, and Castro-Oliden V provided expert guidance and supervision throughout the study and critically reviewed the final manuscript; All authors read and approved the final manuscript.

Institutional review board statement: Approved by the Research Protocol Review Committee of Instituto Nacional de Enfermedades Neoplásicas, No. INEN 24-61.

Informed consent statement: The need for patient consent was waived due to the retrospective nature of the study.

Conflict-of-interest statement: All the authors report no relevant conflicts of interest for this article.

Data sharing statement: No additional data are available.

Country of origin: Peru

ORCID number: Wagner Eduardo Cruz-Diaz 0009-0006-8138-4430; Victor Paitan 0000-0003-1120-4335; Juan Haro-Varas 0000-0003-0678-585X; Raul Mantilla 0000-0001-6010-1741; Victor Castro-Oliden 0000-0003-2828-7325.

S-Editor: Li L
L-Editor: Webster JR
P-Editor: Zhao YQ

REFERENCES

1 **White BE**, Rous B, Chandrakumaran K, Wong K, Bouvier C, Van Hemelrijck M, George G, Russell B, Srirajaskanthan R, Ramage JK. Incidence and survival of neuroendocrine neoplasia in England 1995-2018: A retrospective, population-based study. *Lancet Reg Health Eur* 2022; **23**: 100510 [PMID: 36176500 DOI: 10.1016/j.lanepe.2022.100510]

2 **Wu P**, He D, Chang H, Zhang X. Epidemiologic trends of and factors associated with overall survival in patients with neuroendocrine tumors over the last two decades in the USA. *Endocr Connect* 2023; **12** [PMID: 37924638 DOI: 10.1530/EC-23-0331]

3 **Dasari A**, Shen C, Halperin D, Zhao B, Zhou S, Xu Y, Shih T, Yao JC. Trends in the Incidence, Prevalence, and Survival Outcomes in Patients With Neuroendocrine Tumors in the United States. *JAMA Oncol* 2017; **3**: 1335-1342 [PMID: 28448665 DOI: 10.1001/jamaoncol.2017.0589]

4 **O'Connor JM**, Marmissolle F, Bestani C, Pesce V, Belli S, Dominichini E, Mendez G, Price P, Giacomi N, Pairola A, Loria FS, Huertas E, Martin C, Patane K, Poleri C, Rosenberg M, Cabanne A, Kujaruk M, Caino A, Zamora V, Mariani J, Dioca M, Parma P, Podesta G, Andriani O, Gondolesi G, Roca E. Observational study of patients with gastroenteropancreatic and bronchial neuroendocrine tumors in Argentina: Results from the large database of a multidisciplinary group clinical multicenter study. *Mol Clin Oncol* 2014; **2**: 673-684 [PMID: 25054030 DOI: 10.3892/mco.2014.332]

5 **Younes RN**; GETNE (Grupo de Estudo de Tumores Neuroendócrinos). Neuroendocrine tumors: a registry of 1,000 patients. *Rev Assoc Med Bras (1992)* 2008; **54**: 305-307 [PMID: 18719787 DOI: 10.1590/s0104-42302008000400014]

6 19th Annual ENETS Conference for the Diagnosis and Treatment of Neuroendocrine Tumor Disease, 10 - 11 March 2022. *J Neuroendocrinol* 2022; **34**: e13108 [PMID: 35253281 DOI: 10.1111/jne.13108]

7 **Instituto Nacional de Enfermedades Neoplásicas (INEN)**. Resolución Jefatural N° 026-2021-J-INEN. 2021. [cited 3 September 2024]. Available from: https://portal.inen.sld.pe/wp-content/uploads/2021/02/RJ-026-2021-J-INEN.pdf

8 **Rindi G**, Mete O, Uccella S, Basturk O, La Rosa S, Brosens LAA, Ezzat S, de Herder WW, Klimstra DS, Papotti M, Asa SL. Overview of the 2022 WHO Classification of Neuroendocrine Neoplasms. *Endocr Pathol* 2022; **33**: 115-154 [PMID: 35294740 DOI: 10.1007/s12022-022-09708-2]

9 **Pavel M**, Öberg K, Falconi M, Krenning EP, Sundin A, Perren A, Berruti A; ESMO Guidelines Committee. Gastroenteropancreatic neuroendocrine neoplasms: ESMO Clinical Practice Guidelines for diagnosis, treatment and follow-up. *Ann Oncol* 2020; **31**: 844-860 [PMID: 32272208 DOI: 10.1016/j.annonc.2020.03.304]

10 **Caplin ME**, Pavel M, Ćwikła JB, Phan AT, Raderer M, Sedláčková E, Cadiot G, Wolin EM, Capdevila J, Wall L, Rindi G, Langley A,

Martinez S, Blumberg J, Ruszniewski P; CLARINET Investigators. Lanreotide in metastatic enteropancreatic neuroendocrine tumors. *N Engl J Med* 2014; **371**: 224-233 [PMID: 25014687 DOI: 10.1056/NEJMoa1316158]

11 **Caplin ME**, Pavel M, Phan AT, Ćwikła JB, Sedláčková E, Thanh XT, Wolin EM, Ruszniewski P; CLARINET Investigators. Lanreotide autogel/depot in advanced enteropancreatic neuroendocrine tumours: final results of the CLARINET open-label extension study. *Endocrine* 2021; **71**: 502-513 [PMID: 33052555 DOI: 10.1007/s12020-020-02475-2]

12 **Rinke A**, Müller HH, Schade-Brittinger C, Klose KJ, Barth P, Wied M, Mayer C, Aminossadati B, Pape UF, Bläker M, Harder J, Arnold C, Gress T, Arnold R; PROMID Study Group. Placebo-controlled, double-blind, prospective, randomized study on the effect of octreotide LAR in the control of tumor growth in patients with metastatic neuroendocrine midgut tumors: a report from the PROMID Study Group. *J Clin Oncol* 2009; **27**: 4656-4663 [PMID: 19704057 DOI: 10.1200/JCO.2009.22.8510]

13 **Rinke A**, Wittenberg M, Schade-Brittinger C, Aminossadati B, Ronicke E, Gress TM, Müller HH, Arnold R; PROMID Study Group. Placebo-Controlled, Double-Blind, Prospective, Randomized Study on the Effect of Octreotide LAR in the Control of Tumor Growth in Patients with Metastatic Neuroendocrine Midgut Tumors (PROMID): Results of Long-Term Survival. *Neuroendocrinology* 2017; **104**: 26-32 [PMID: 26731483 DOI: 10.1159/000443612]

14 **Yao JC**, Shah MH, Ito T, Bohas CL, Wolin EM, Van Cutsem E, Hobday TJ, Okusaka T, Capdevila J, de Vries EG, Tomassetti P, Pavel ME, Hoosen S, Haas T, Lincy J, Lebwohl D, Öberg K; RAD001 in Advanced Neuroendocrine Tumors, Third Trial (RADIANT-3) Study Group. Everolimus for advanced pancreatic neuroendocrine tumors. *N Engl J Med* 2011; **364**: 514-523 [PMID: 21306238 DOI: 10.1056/NEJMoa1009290]

15 **Yao JC**, Fazio N, Singh S, Buzzoni R, Carnaghi C, Wolin E, Tomasek J, Raderer M, Lahner H, Voi M, Pacaud LB, Rouyrre N, Sachs C, Valle JW, Fave GD, Van Cutsem E, Tesselaar M, Shimada Y, Oh DY, Strosberg J, Kulke MH, Pavel ME; RAD001 in Advanced Neuroendocrine Tumours, Fourth Trial (RADIANT-4) Study Group. Everolimus for the treatment of advanced, non-functional neuroendocrine tumours of the lung or gastrointestinal tract (RADIANT-4): a randomised, placebo-controlled, phase 3 study. *Lancet* 2016; **387**: 968-977 [PMID: 26703889 DOI: 10.1016/S0140-6736(15)00817-X]

16 **Pavel ME**, Hainsworth JD, Baudin E, Peeters M, Hörsch D, Winkler RE, Klimovsky J, Lebwohl D, Jehl V, Wolin EM, Öberg K, Van Cutsem E, Yao JC; RADIANT-2 Study Group. Everolimus plus octreotide long-acting repeatable for the treatment of advanced neuroendocrine tumours associated with carcinoid syndrome (RADIANT-2): a randomised, placebo-controlled, phase 3 study. *Lancet* 2011; **378**: 2005-2012 [PMID: 22119496 DOI: 10.1016/S0140-6736(11)61742-X]

17 **Raymond E**, Dahan L, Raoul JL, Bang YJ, Borbath I, Lombard-Bohas C, Valle J, Metrakos P, Smith D, Vinik A, Chen JS, Hörsch D, Hammel P, Wiedenmann B, Van Cutsem E, Patyna S, Lu DR, Blanckmeister C, Chao R, Ruszniewski P. Sunitinib malate for the treatment of pancreatic neuroendocrine tumors. *N Engl J Med* 2011; **364**: 501-513 [PMID: 21306237 DOI: 10.1056/NEJMoa1003825]

18 **Singh S**, Halperin DM, Myrehaug S, Herrmann K, Pavel M, Kunz PL, Chasen B, Capdevila J, Tafuto S, Oh D, Yoo C, Falk S, Halfdanarson TR, Folitar I, Zhang Y, Santoro P, Aimone P, de Herder WW, Ferone D. [^{177}Lu]Lu-DOTA-TATE in newly diagnosed patients with advanced grade 2 and grade 3, well-differentiated gastroenteropancreatic neuroendocrine tumors: Primary analysis of the phase 3 randomized NETTER-2 study. *J Clin Oncol* 2024; **42**: LBA588-LBA588 [DOI: 10.1200/jco.2024.42.3_suppl.lba588]

19 **Fine RL**, Gulati AP, Krantz BA, Moss RA, Schreibman S, Tsushima DA, Mowatt KB, Dinnen RD, Mao Y, Stevens PD, Schrope B, Allendorf J, Lee JA, Sherman WH, Chabot JA. Capecitabine and temozolomide (CAPTEM) for metastatic, well-differentiated neuroendocrine cancers: The Pancreas Center at Columbia University experience. *Cancer Chemother Pharmacol* 2013; **71**: 663-670 [PMID: 23370660 DOI: 10.1007/s00280-012-2055-z]

20 **Strosberg JR**, Fine RL, Choi J, Nasir A, Coppola D, Chen DT, Helm J, Kvols L. First-line chemotherapy with capecitabine and temozolomide in patients with metastatic pancreatic endocrine carcinomas. *Cancer* 2011; **117**: 268-275 [PMID: 20824724 DOI: 10.1002/cncr.25425]

21 **Cives M**, Ghayouri M, Morse B, Brelsford M, Black M, Rizzo A, Meeker A, Strosberg J. Analysis of potential response predictors to capecitabine/temozolomide in metastatic pancreatic neuroendocrine tumors. *Endocr Relat Cancer* 2016; **23**: 759-767 [PMID: 27552969 DOI: 10.1530/ERC-16-0147]

22 **Crespo G**, Jiménez-Fonseca P, Custodio A, López C, Carmona-Bayonas A, Alonso V, Navarro M, Aller J, Sevilla I, Grande E, Gajate P, Alonso-Gordoa T, Matos I, Capdevila J, Nieto B, Barriuso J. Capecitabine and temozolomide in grade 1/2 neuroendocrine tumors: a Spanish multicenter experience. *Future Oncol* 2017; **13**: 615-624 [PMID: 27802780 DOI: 10.2217/fon-2016-0434]

23 **de Mestier L**, Walter T, Brixi H, Evrard C, Legoux JL, de Boissieu P, Hentic O, Cros J, Hammel P, Tougeron D, Lombard-Bohas C, Rebours V, Ruszniewski P, Cadiot G. Comparison of Temozolomide-Capecitabine to 5-Fluorouracile-Dacarbazine in 247 Patients with Advanced Digestive Neuroendocrine Tumors Using Propensity Score Analyses. *Neuroendocrinology* 2019; **108**: 343-353 [PMID: 30759445 DOI: 10.1159/000498887]

24 **Lamarca A**, Barriuso J, Mccallum L, Papaxoinis G, Nasralla M, Nuttall C, Frizziero M, Kordatou Z, Mcnamara M, Hubner R, Manoharan P, Mansoor W, Valle J. Temozolomide-capecitabine (TemCap) chemotherapy for neuroendocrine neoplasms (NENs): Time to maximum response and optimal treatment duration. *Ann Oncol* 2017; **28**: v151 [DOI: 10.1093/annonc/mdx368.024]

25 **Arrivi G**, Verrico M, Roberto M, Barchiesi G, Faggiano A, Marchetti P, Mazzuca F, Tomao S. Capecitabine and Temozolomide (CAPTEM) in Advanced Neuroendocrine Neoplasms (NENs): A Systematic Review and Pooled Analysis. *Cancer Manag Res* 2022; **14**: 3507-3523 [PMID: 36575665 DOI: 10.2147/CMAR.S372776]

26 **Kunz PL**, Graham NT, Catalano PJ, Nimeiri HS, Fisher GA, Longacre TA, Suarez CJ, Martin BA, Yao JC, Kulke MH, Hendifar AE, Shanks JC, Shah MH, Zalupski MM, Schmulbach EL, Reidy-Lagunes DL, Strosberg JR, O'Dwyer PJ, Benson AB 3rd. Randomized Study of Temozolomide or Temozolomide and Capecitabine in Patients With Advanced Pancreatic Neuroendocrine Tumors (ECOG-ACRIN E2211). *J Clin Oncol* 2023; **41**: 1359-1369 [PMID: 36260828 DOI: 10.1200/JCO.22.01013]

27 **Abbasi S**, Kashashna A, Albaba H. Efficacy of capecitabine and temozolomide combination in well-differentiated neuroendocrine tumors: Jordan experience. *Pancreas* 2014; **43**: 1303-1305 [PMID: 25036906 DOI: 10.1097/MPA.0000000000000174]

28 **Lamarca A**, Elliott E, Barriuso J, Backen A, McNamara MG, Hubner R, Valle JW. Chemotherapy for advanced non-pancreatic well-differentiated neuroendocrine tumours of the gastrointestinal tract, a systematic review and meta-analysis: A lost cause? *Cancer Treat Rev* 2016; **44**: 26-41 [PMID: 26855376 DOI: 10.1016/j.ctrv.2016.01.005]

29 **Kulke MH**, Hornick JL, Frauenhoffer C, Hooshmand S, Ryan DP, Enzinger PC, Meyerhardt JA, Clark JW, Stuart K, Fuchs CS, Redston MS. O6-methylguanine DNA methyltransferase deficiency and response to temozolomide-based therapy in patients with neuroendocrine tumors. *Clin Cancer Res* 2009; **15**: 338-345 [PMID: 19118063 DOI: 10.1158/1078-0432.CCR-08-1476]

30 **Chan JA**, Stuart K, Earle CC, Clark JW, Bhargava P, Miksad R, Blaszkowsky L, Enzinger PC, Meyerhardt JA, Zheng H, Fuchs CS, Kulke MH. Prospective study of bevacizumab plus temozolomide in patients with advanced neuroendocrine tumors. *J Clin Oncol* 2012; **30**: 2963-

2968 [PMID: 22778320 DOI: 10.1200/JCO.2011.40.3147]

31 **Kulke MH**, Stuart K, Enzinger PC, Ryan DP, Clark JW, Muzikansky A, Vincitore M, Michelini A, Fuchs CS. Phase II study of temozolomide and thalidomide in patients with metastatic neuroendocrine tumors. *J Clin Oncol* 2006; **24**: 401-406 [PMID: 16421420 DOI: 10.1200/JCO.2005.03.6046]

World Journal of Gastrointestinal Oncology

Submit a Manuscript: https://www.f6publishing.com

World J Gastrointest Oncol 2024 December 15; 16(12): 4685-4699

DOI: 10.4251/wjgo.v16.i12.4685

ISSN 1948-5204 (online)

ORIGINAL ARTICLE

Basic Study

Vitamin D 1,25-Dihydroxyvitamin D_3 reduces lipid accumulation in hepatocytes by inhibiting M1 macrophage polarization

Wen-Jing Luo, Xian-Wen Dong, Hua Ye, Qiao-Su Zhao, Qiu-Bo Zhang, Wen-Ying Guo, Hui-Wei Liu, Feng Xu

Specialty type: Oncology

Provenance and peer review: Unsolicited article; Externally peer reviewed.

Peer-review model: Single blind

Peer-review report's classification

Scientific Quality: Grade B, Grade B, Grade B, Grade C

Novelty: Grade B, Grade B, Grade B, Grade B

Creativity or Innovation: Grade B, Grade B, Grade B, Grade B

Scientific Significance: Grade B, Grade B, Grade B, Grade C

P-Reviewer: Chen H; Wu JZ; Zongo E

Received: April 16, 2024

Revised: September 9, 2024

Accepted: October 8, 2024

Published online: December 15, 2024

Processing time: 210 Days and 2.8 Hours

Wen-Jing Luo, Xian-Wen Dong, Hua Ye, Qiao-Su Zhao, Qiu-Bo Zhang, Wen-Ying Guo, Hui-Wei Liu, Feng Xu, Department of Gastroenterology, Ningbo Medical Center Lihuili Hospital, Ningbo 315000, Zhejiang Province, China

Corresponding author: Feng Xu, MAMS, Chief Physician, Department of Gastroenterology, Ningbo Medical Center Lihuili Hospital, No. 57 Xingning Road, Ningbo 315000, Zhejiang Province, China. xufeng200468@126.com

Abstract

BACKGROUND

Non-alcoholic fatty liver disease (NAFLD), which is a significant liver condition associated with metabolic syndrome, is the leading cause of liver diseases globally and its prevalence is on the rise in most nations. The protective impact of vitamin D on NAFLD and its specific mechanism remains unclear.

AIM

To examine the role of vitamin D in NAFLD and how vitamin D affects the polarization of hepatic macrophages in NAFLD through the vitamin D receptor (VDR)-peroxisome proliferator activated receptor (PPAR)γ pathway.

METHODS

Wild-type C57BL/6 mice were provided with a high-fat diet to trigger NAFLD model and administered 1,25-dihydroxy-vitamin D [1,25$(OH)_2D_3$] supplementation. 1,25$(OH)_2D_3$ was given to RAW264.7 macrophages that had been treated with lipid, and a co-culture with AML12 hepatocytes was set up. Lipid accumulation, lipid metabolism enzymes, M1/M2 phenotype markers, proinflammatory cytokines and VDR-PPARγ pathway were determined.

RESULTS

Supplementation with 1,25$(OH)_2D_3$ relieved hepatic steatosis and decreased the proinflammatory M1 polarization of hepatic macrophages in NAFLD. Administration of 1,25$(OH)_2D_3$ suppressed the proinflammatory M1 polarization of macrophages induced by fatty acids, thereby directly relieving lipid accumulation and metabolism in hepatocytes. The VDR-PPARγ pathway had a notable impact on reversing lipid-induced proinflammatory M1 polarization of macrophages regulated by the administration of 1,25$(OH)_2D_3$.

CONCLUSION

Supplementation with 1,25$(OH)_2D_3$ improved hepatic steatosis and lipid metabolism in NAFLD, linked to its capacity to reverse the proinflammatory M1 polarization of hepatic macrophages, partially by regulating the VDR-PPARγ pathway. The involvement of 1,25$(OH)_2D_3$ in inhibiting fatty-acid-induced proinflammatory M1 polarization of macrophages played a direct role in relieving lipid accumulation and metabolism in hepatocytes.

Key Words: Non-alcoholic fatty liver disease; Hepatocytes; Macrophages; Polarization; Vitamin D receptor; Peroxisome proliferator activated receptor γ

Core Tip: Supplementation with 1,25-dihydroxy-vitamin D [1,25$(OH)_2D_3$] improved hepatic steatosis and lipid metabolism in nonalcoholic fatty liver disease, linked to its capacity to reverse the proinflammatory M1 polarization of hepatic macrophages, partially by regulating the vitamin D receptor-peroxisome proliferator activated receptor γ pathway. The involvement of 1,25$(OH)_2D_3$ in inhibiting fatty-acid-induced proinflammatory M1 polarization of macrophages played a direct role in relieving lipid accumulation and metabolism in hepatocytes.

Citation: Luo WJ, Dong XW, Ye H, Zhao QS, Zhang QB, Guo WY, Liu HW, Xu F. Vitamin D 1,25-Dihydroxyvitamin D_3 reduces lipid accumulation in hepatocytes by inhibiting M1 macrophage polarization. *World J Gastrointest Oncol* 2024; 16(12): 4685-4699
URL: https://www.wjgnet.com/1948-5204/full/v16/i12/4685.htm
DOI: https://dx.doi.org/10.4251/wjgo.v16.i12.4685

INTRODUCTION

Nonalcoholic fatty liver disease (NAFLD) is a common chronic liver condition, affecting 25%-45% of the population worldwide[1,2]. It is a key manifestation of metabolic syndrome and progresses through stages, beginning with simple fat accumulation (steatosis), advancing to nonalcoholic steatohepatitis (NASH), fibrosis, and potentially leading to cirrhosis and liver cancer (hepatocellular carcinoma)[3]. The accumulation of excess fatty acids, driven by insulin resistance and increased fat production in the liver, is the primary trigger for NAFLD. This predisposes the liver to further damage, known as multiple-hit injuries. These include mitochondrial dysfunction, stress in the endoplasmic reticulum, inflammation from endotoxins, activation of inflammasomes, iron overload, and vitamin D deficiency[3-5].

Vitamin D, a steroid hormone, has various functions beyond regulating calcium, phosphate metabolism, and bone health. It also influences immune, inflammatory, and metabolic processes. The connection between its active form, 1,25-dihydroxy-vitamin D [1,25$(OH)_2D_3$], and the vitamin D receptor (VDR) has been widely recognized in relation to insulin resistance and related conditions[6-9]. Recent observational studies show a strong link between low vitamin D levels and NAFLD. Vitamin D deficiency has been associated with liver fat accumulation, inflammation, fibrosis, and disease progression. Another study found that healthy men with higher vitamin D levels had a reduced risk of developing NAFLD[10-12].

However, most clinical trials examining the effects of vitamin D supplementation on NAFLD patients, involving different stages of liver damage, have been underpowered. More research is needed to understand the underlying mechanisms between vitamin D and NAFLD development[13,14]. Kupffer cells, located in the liver's sinusoids and comprising 20%-25% of non-parenchymal liver cells, respond to various stimuli from the bloodstream. Macrophages, including Kupffer cells, are highly adaptable, changing their function and behavior based on environmental signals[15,16].

Macrophages typically undergo M1 activation when exposed to molecules like Toll-like receptor ligands, lipopolysaccharide (LPS), and interferon-γ, releasing proinflammatory substances. Alternatively, when stimulated by interleukins (IL-4/IL-13), they shift to the M2 state, producing anti-inflammatory factors, supporting tissue repair, and regulating immune responses[17,18]. Extensive evidence confirms the critical role of liver macrophages, particularly Kupffer cells, in the progression of NAFLD and NASH. Our previous research demonstrated that in mice with high-fat (HF) diet-induced NAFLD, Kupffer cells are predominantly polarized towards the M1 state[19]. Similarly, Maina and colleagues found that M1 macrophage activation correlates with the severity of NASH[20]. Modulating the M1/M2 balance may offer a new therapeutic approach for NAFLD.

The nuclear receptor peroxisome proliferator activated receptor (PPAR)γ, when activated by specific ligands, is known to drive macrophage polarization, encouraging the development of anti-inflammatory M2 macrophages. Disruption of PPARγ in myeloid cells impairs this alternative activation and increases vulnerability to obesity and insulin resistance caused by a HF diet[21-23]. In our earlier research, PPARγ activation reversed M1 polarization of Kupffer cells induced by a HF diet and improved liver fat accumulation in NAFLD[19]. Similarly, VDR, activated by 1,25$(OH)_2D_3$, is a transcription factor that, like PPARγ, plays a key role in regulating macrophage function[24,25].

The VDR and PPARγ pathways are interconnected and influence various cell functions, including growth, differentiation, and immune response. However, the exact mechanisms behind their interaction are unclear. A recent study found that active vitamin D promotes the conversion of M1 macrophages, induced by high glucose, into the M2 state *via* the VDR-PPARγ pathway[25-27]. This indicates that VDR-PPARγ signaling could be a target for vitamin D to shift macrophage polarization from the M1 to the M2 phenotype, potentially leading to new therapeutic approaches for NAFLD.

MATERIALS AND METHODS

Animal experiments

Male adult (aged 6-8 weeks) wild-type C57BL/6 mice were acquired from the Vital River Laboratory (China). Mice were fed either a regular normal control (NC) diet (15% kilocalories from fat) or a HF diet (60% kilocalories from fat) for a period of 16 weeks. For $1,25(OH)_2D_3$ supplementation, HF diet-fed mice received $1,25(OH)_2D_3$ (20 μg/kg, MedChemExpress, United States) or phosphate-buffered saline (PBS; Gibco, United States) by oral gavage every alternate day for 16 weeks. The dose of $1,25(OH)_2D_3$ (20 μg/kg) used in this study was selected based on previous research demonstrating its efficacy in reducing liver fibrosis and inflammation in murine models of NASH. A study by Ma *et al*[28] utilized a similar dose of $1,25(OH)_2D_3$ to reveal its antifibrotic properties in female mice fed a HF diet. This concentration has been shown to exert beneficial effects in liver pathology models, making it a suitable choice for our investigation. While we recognize the importance of assessing a range of concentrations, this dose was chosen for its established efficacy. Future studies could explore different dose gradients to further refine the therapeutic potential of $1,25(OH)_2D_3$. All mice were kept in a temperature- and light-controlled facility and permitted to consume water and pellet chow ad libitum. After being fed diets for 16 weeks, the mice were either anesthetized for *in situ* perfusion or sacrificed to collect liver tissues through intraperitoneal injection of 0.3% pentobarbital sodium. The humane treatment of laboratory animals was ensured in all animal experiments, which were approved by the Ningbo University Animal Care and Use Committee according to the criteria set by Ningbo University.

Kupffer cell isolation

Hepatic macrophages, also known as Kupffer cells, were obtained by *in situ* liver perfusion as previously described. Following perfusion, cells were isolated *via* centrifugation using a Percoll density gradient (25% and 50% Percoll; GE Healthcare, United States) at 800 *g* for 15 minutes. The isolated cells were cultured in Dulbecco's modified Eagle's medium (DMEM; Gibco), supplemented with 12% fetal bovine serum (FBS; Gibco), 100 U/mL penicillin G (Gibco), and 100 U/mL streptomycin sulfate (Gibco) at 37 °C with 5% CO_2. After a 2-hour incubation period, non-adherent cells were removed, and Kupffer cells were collected. Cell viability was assessed using the trypan blue exclusion method, with viability exceeding 95%.

Identification of Kupffer cells

To verify that the isolated cells were Kupffer cells, immunohistochemical (IHC) staining was performed. Kupffer cells were identified by the expression of F4/80, a macrophage-specific marker. The isolated cells were fixed, blocked with normal serum, and incubated with anti-mouse F4/80 antibody (1:100; GeneTex, United States) overnight at 4 °C. After washing, secondary antibodies conjugated to horseradish peroxidase were applied. The detection was carried out using diaminobenzidine (DAB), followed by counterstaining with hematoxylin. Kupffer cells positive for F4/80 were observed in liver sections under an Olympus light microscope at a magnification of 200 ×. This staining confirms the identity of the Kupffer cells, reflecting the efficiency of the isolation process.

RAW264.7 macrophage culture and treatment

RAW264.7 murine macrophages (Cell Bank of the Chinese Academic of Sciences, China) were cultured in DMEM supplemented with 10% FBS, 100 U/mL penicillin G, and 100 U/mL streptomycin sulfate at a temperature of 37 °C in the presence of 5% CO_2. All the treatments were performed on the third passage of cells. Palmitic acid (PA, 0.5 mmol/L; Sigma Aldrich, United States) was administered to RAW264.7 macrophages for a duration of 24 hours. To assess macrophage M1 or M2 polarization, LPS (100 ng/mL; Sigma-Aldrich) or IL-4 (5 ng/mL; PeproTech, United States) treatment was used as a positive control, respectively. DMEM was employed as the NC. To carry out the impact of $1,25(OH)_2D_3$, RAW264.7 macrophages were incubated with $1,25(OH)_2D_3$ (20 ng/mL) for an additional 24 hours in a sequential manner.

AML12 hepatocyte culture

AML12 murine hepatocytes (Cell Bank of the Chinese Academic of Sciences, China) were cultured in DMEM supplemented with 10% FBS, 100 U/mL penicillin G, and 100 U/mL streptomycin sulfate at a temperature of 37 °C in the presence of 5% CO_2. All the treatments were performed on the third passage of cells.

RAW264.7 macrophage and AML12 hepatocyte coculture system

Impurities were removed from the collected culture supernatants of RAW264.7 macrophages through centrifugation and filtration. The AML12 hepatocytes were exposed to the prepared conditioned media (CMs) for 24 hours in order to establish the coculture system. The initial cell density for RAW264.7 macrophages was 1×10^6 cells/mL, and AML12 hepatocytes were seeded at a density of 5×10^5 cells/mL. The coculture duration was 24 hours for all experiments to

Table 1 Murine primers

Primer	Forward (5'-3')	Reverse (5'-3')
iNOS2	GTGTTCCACCAGGAGATGTTG	CTCCTGCCCACTGAGTTCGTC
TNFα	TCTTCTCATTCCTGCTTGTGG	GGTCTGGGCCATAGAACTGA
IL-6	GTTCTCTGGGAAATCGTGGA	GGAAATTGGGGTAGGAAGGA
Arg1	CTCCAAGCCAAAGTCCTTAGAG	AGGAGCTGTCATTAGGGACATC
Mrc2	TACAGCTCCACGCTATGGATT	CACTCTCCCAGTTGAGGTACT
IL-10	GTTACTTGGGTTGCCAAG	TTGATCATCATGTATGCTTC
VDR	GCTTCCACTTCAACGCTAT	ACTCCTTCATCATGCCAAT
PPARγ	GCCCTTTACCACAGTTGATTTCT	GTGATTTGTCCGTTGTCTTTCCT
IL-1β	CCCAAGCAATACCCAAAGAA	TTGTGAGGTGCTGATGTACCA
SREBP1C	ACAGCAACCAGAAGCTCAAG	TGCCCTCCATAGACACATCT
FASN	TTGGGTGCTGACTACAACCT	TGGATGATGTTGATGATGGA
ACOX1	ACCAGCCCAACTGTGACTTC	ACAAAGGCATGTAACCCGTA
CPT1A	CTTCCCATTTGACACCTTTG	ATACGTGAGGCAGAACTTGC
GAPDH	CCTTCCGTGTTCCTACCC	CAACCTGGTCCTCAGTGTAG

iNOS2: Nitric oxide synthase; TNFα: Tumor necrosis factor α; IL: Interleukin; Arg1 Arginine 1; Mrc2: Macrophage mannose receptor 2; VDR: Vitamin D receptor; PPARγ: Peroxisome proliferator activated receptor γ; SREBP1C: Sterol-regulatory element binding protein 1C; FASN: Fatty acid synthase; CPT1A: Carnitine palmitoyl transferase 1A.

allow sufficient time for interactions between the cells while maintaining cellular viability.

Liver histology, oil red o staining and immunohistochemistry analysis

To perform histological analysis, liver tissues were fixed in 10% formalin, then embedded in paraffin, and finally stained using hematoxylin and eosin (HE). To perform cytohistologic analysis, the AML12 hepatocytes were first fixed in 4% paraformaldehyde, and then stained with Oil Red O and subsequently counterstained with HE. To perform immunohistochemistry analysis, the liver sections were first blocked in normal serum, then incubated with anti-mouse F4/80 antibody (1:100; GeneTex, United States), anti-mouse CD11c antibody (1:50; OriGene, United States), and anti-mouse CD206 antibody (1:100; Abcam, United Kingdom) at a temperature of 4 °C overnight. Afterward, the sections were incubated with secondary antibodies conjugated with horseradish-peroxidase. Finally, the detection process involved the use of DAB and hematoxylin as the counter stain. Cells positive for F4/80, CD11c, and CD206 were quantified in three randomly selected fields under an Olympus light microscope at a magnification of 200 ×.

Total RNA isolation and real-time PCR

Total RNA was extracted from murine liver tissue, isolated Kupffer cells, RAW264.7 macrophages and AML12 hepatocytes using TRIzol reagent (Invitrogen, United States). cDNA was synthesized from 2 μg total RNA using Primescript RT Reagent kit (TaKaRa, Japan). In the real-time PCR assay, a 10 μL reaction mixture consisting of 10 ng template, each murine primer (shown in Table 1, provided by Sangong Biotech, China) and SYBR Green PCR Master Mix (TaKaRa, Japan) was used. The PCR thermocycling condition consisted of an initial denaturation step at 95 °C for 30 seconds, followed by 40 cycles of denaturation at 95 °C for 5 seconds and annealing at 60 °C for 30 seconds using the ABI Prism 7300 system (Applied Biosystems, United States). Each reaction was conducted three times. Quantification of the target genes' expression levels was performed using the double-delta method ($2^{-\Delta\Delta Ct}$).

Western blotting

Protein from the murine liver tissues, RAW264.7 macrophages, and AML12 hepatocytes were resolved using 8% SDS-PAGE. The samples were transferred to polyvinylidene difluoride membranes (Bio-Rad, United States) and left to incubate overnight at 4 °C with antibodies against VDR (1:2000; Abcam), PPARγ (1:2000; Abcam), sterol-regulatory element binding protein (SREBP)1C (1:1000; Abcam), fatty acid synthase (FASN) (1:1000; Abcam), acyl-CoA oxidase (ACOX)1 (1:500; Abcam), carnitine palmitoyl transferase (CPT)1A (1:1000; Abcam), and the endogenous control GAPDH (1:3000; Bioworld, United States). The blots were then incubated with secondary antibodies conjugated with horseradish peroxidase at room temperature for 1 hour. The bands showing immunoreactivity were detected using the ECL Western Blotting Kit (Thermo Scientific Pierce, United States) and then exposed to films and developed. Image J software (National Institutes of Health, United States) was used to measure the density of the immunoblots, which was normalized using GAPDH.

ELISA

Tumor necrosis factor (TNF) α, IL-6, and IL-1β production were assessed by ELISA kit (eBioscience, United States) according to the manufacturer's protocol with collecting and analyzing the cell culture supernatants from isolated Kupffer cells and RAW264.7 macrophages.

Statistical analysis

All statistical analyses were conducted using GraphPad Prism 9. The data were presented as mean ± SEM. Statistical differences were determined using Student's *t* test. $^{a}P < 0.05$ was considered statistically significant.

RESULTS

$1,25(OH)_2D_3$ supplementation improves hepatic steatosis and lipid metabolism in NAFLD

The link between vitamin D deficiency and the progression of NAFLD has become increasingly evident through observational studies. However, few studies have examined the effects and mechanisms of vitamin D supplementation on NAFLD. In a murine model of NAFLD, we found that supplementation with $1,25(OH)_2D_3$ significantly improved hepatic steatosis induced by a HF diet, resulting in reduced liver and body weight. This treatment also markedly decreased the expression of proinflammatory cytokines in the liver (Figure 1A-D). Additionally, the mRNA and protein levels of enzymes involved in lipid synthesis (SREBP1C and FASN) and lipid breakdown (ACOX1 and CPT1A) were elevated in HF-fed mice, but these levels were significantly reduced in the $1,25(OH)_2D_3$-treated group (Figure 1E and F). Overall, $1,25(OH)_2D_3$ supplementation alleviated hepatic steatosis, reduced local inflammation, and improved hepatic lipid metabolism in NAFLD.

$1,25(OH)_2D_3$ decreases proinflammatory M1 polarization of hepatic macrophages in NAFLD

Our previous work showed that hepatic macrophages in NAFLD mice on an HF diet predominantly exhibited an M1 proinflammatory phenotype[19]. In this study, we used a similar HF diet-induced NAFLD model supplemented with $1,25(OH)_2D_3$. IHC analysis revealed a decrease in M1-polarized (F4/80+CD11c+) hepatic macrophages after $1,25(OH)_2D_3$ supplementation (Figure 2A). Moreover, the expression of M1 markers, including inducible nitric oxide synthase (iNOS2), TNFα, and IL-6, was significantly reduced, while the M2 marker IL-10 also showed a moderate decrease (Figure 2B). In parallel, $1,25(OH)_2D_3$ treatment significantly reduced the secretion of proinflammatory cytokines, such as TNFα, IL-6, and IL-1β, which were elevated in the HF-fed group (Figure 2C). These findings suggest that $1,25(OH)_2D_3$ decreases the proinflammatory M1 polarization of hepatic macrophages in NAFLD.

$1,25(OH)_2D_3$ inhibits fatty-acid-induced proinflammatory M1 polarization of macrophages

Lipid accumulation in NAFLD is largely driven by increased free fatty acids, a hallmark of disease progression[28,29]. In our previous research, we found that PA, a common saturated fatty acid, induces M1 polarization in Kupffer cells/macrophages[19]. Here, we showed that $1,25(OH)_2D_3$ administration significantly reduced the expression of M1 markers (iNOS2, TNFα, and IL-6) and M2 marker IL-10, which were elevated in PA-treated macrophages (Figure 3A). Additionally, $1,25(OH)_2D_3$ significantly decreased the secretion of proinflammatory cytokines (TNFα, IL-6, and IL-1β) that were induced by PA (Figure 3B). These results demonstrate that $1,25(OH)_2D_3$ effectively inhibits fatty-acid-induced M1 polarization of macrophages *in vitro*.

The role of the VDR-PPARγ pathway in $1,25(OH)_2D_3$-mediated modulation of macrophage polarization

Our study further explored the molecular mechanisms through which $1,25(OH)_2D_3$ modulates macrophage polarization in the context of a HF diet or fatty-acid stimulation. We focused on the VDR and peroxisome proliferator-activated receptor gamma (PPARγ), both of which are nuclear receptors that influence macrophage polarization but with opposing effects[24-27]. *In vivo*, hepatic macrophages from HF-fed NAFLD mice showed increased expression of VDR and PPARγ at both mRNA and protein levels. In contrast, $1,25(OH)_2D_3$ supplementation significantly decreased VDR expression but did not alter PPARγ expression (Figure 4A and B). *In vitro*, $1,25(OH)_2D_3$ treatment reduced the expression of both VDR and PPARγ in PA-stimulated macrophages (Figure 4C and D). Thus, $1,25(OH)_2D_3$ attenuated HF diet- and fatty-acid-induced proinflammatory M1 polarization of macrophages by inhibiting VDR and PPARγ. These findings suggest that the VDR-PPARγ pathway plays a crucial role in $1,25(OH)_2D_3$-mediated regulation of macrophage polarization.

$1,25(OH)_2D_3$ inhibits proinflammatory macrophage polarization, improving hepatocyte lipid metabolism

Our *in vivo* data showed that $1,25(OH)_2D_3$ reduced proinflammatory M1 polarization of hepatic macrophages and improved hepatic lipid metabolism in NAFLD. To determine whether $1,25(OH)_2D_3$ directly affects hepatocyte lipid metabolism by inhibiting macrophage polarization, we used a co-culture system with RAW264.7 macrophages and AML12 hepatocytes. Oil Red O staining revealed increased lipid accumulation in hepatocytes incubated with CM from LPS- and PA-treated macrophages, which was significantly reduced following $1,25(OH)_2D_3$ administration (Figure 5A). Additionally, $1,25(OH)_2D_3$ treatment reduced the expression of proinflammatory cytokines in hepatocytes treated with CM from LPS- and PA-stimulated macrophages (Figure 5B). M1-polarized macrophage CM also increased the expression of lipid synthesis genes (FASN and SREBP1C), which were reduced after $1,25(OH)_2D_3$ treatment (Figure 5C and D). Conversely, lipid breakdown genes (ACOX1 and CPT1A) were elevated in hepatocytes treated with CM from PA-stimulated macrophages but declined with $1,25(OH)_2D_3$ treatment (Figure 5C and D). These findings indicate that

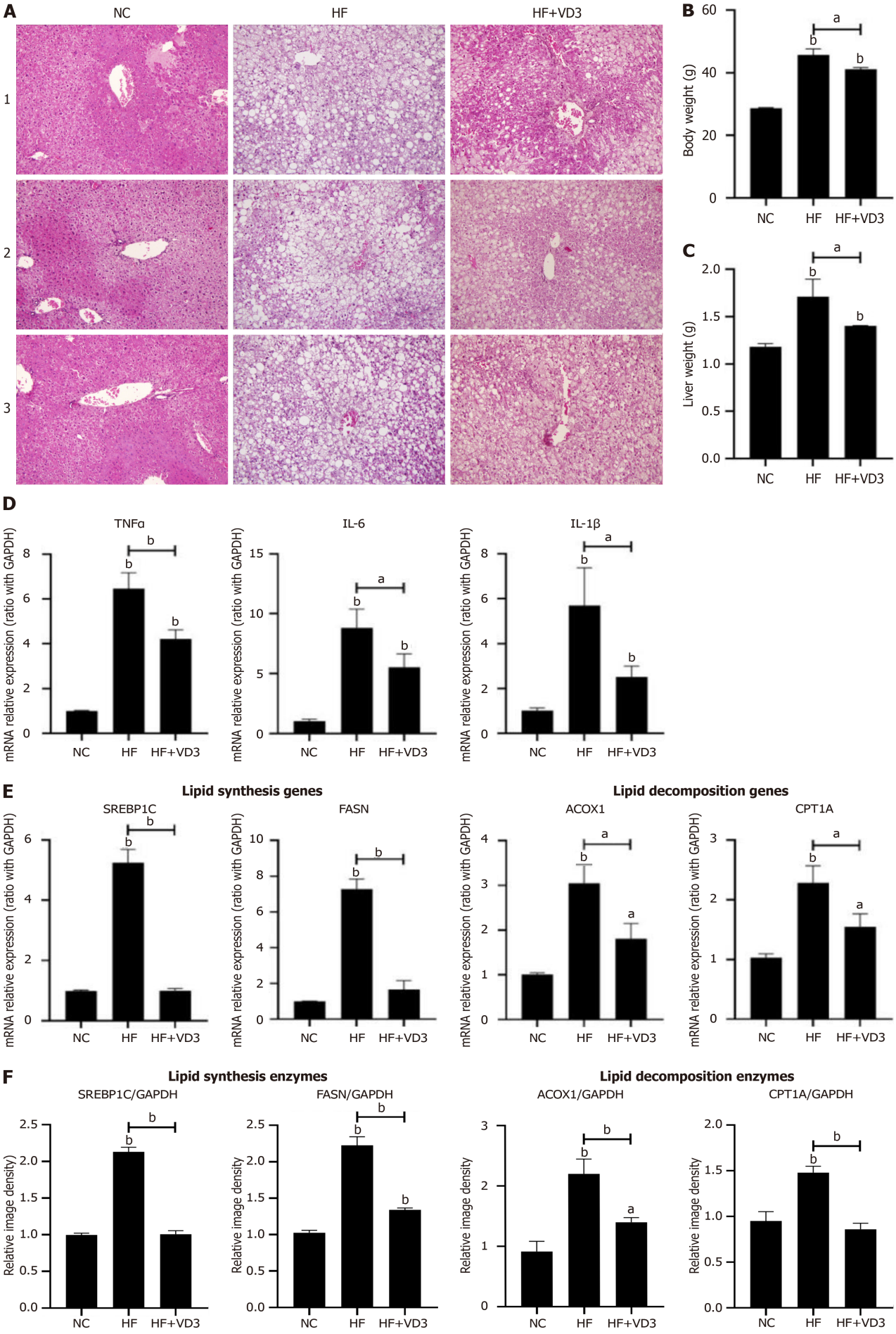
A
NC
HF
HF+VD3
1
2
3
B
Body weight (g)
C
Liver weight (g)
D
TNFα
IL-6
IL-1β
mRNA relative expression (ratio with GAPDH)
E
Lipid synthesis genes
Lipid decomposition genes
SREBP1C
FASN
ACOX1
CPT1A
F
Lipid synthesis enzymes
Lipid decomposition enzymes
SREBP1C/GAPDH
FASN/GAPDH
ACOX1/GAPDH
CPT1A/GAPDH
Relative image density
NC
HF
HF+VD3

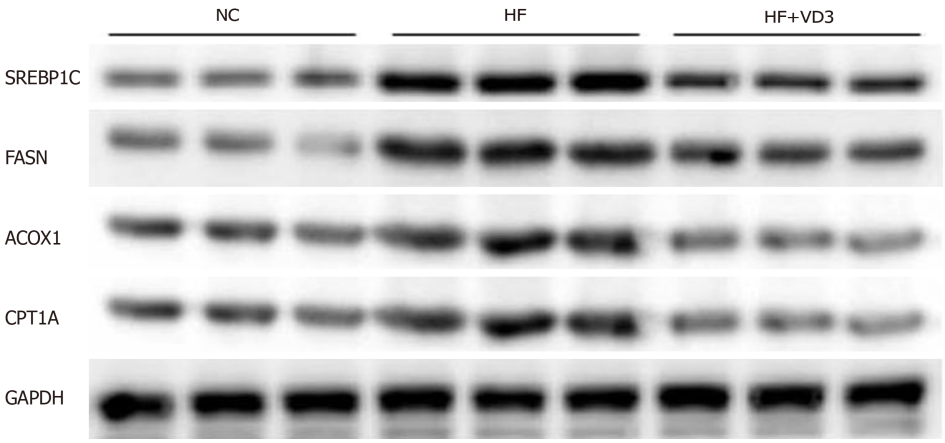

Figure 1 Supplementation with 1,25-dihydroxy-vitamin D improves hepatic steatosis and lipid metabolism in non-alcoholic fatty liver disease. Wild-type C57BL/6 mice were fed normal control diet or high-fat (HF) diet for 16 weeks, or HF diet plus 1,25-dihydroxy-vitamin D (20 μg/kg) by oral gavage every alternate day for 16 weeks. Phosphate-buffered saline by oral gavage served as a control (n = 10/group). A: Hepatic steatosis determined by hematoxylin & eosin staining (200 ×); B: Body weight of mice; C: Liver weight of mice; D: Hepatic proinflammatory cytokines expression; E: Hepatic lipid metabolism genes mRNA expression; F: Hepatic lipid metabolism enzymes protein expression. Values are mean ± SEM, $^{a}P < 0.05$, $^{b}P < 0.01$, n = 10 animals per group; NC: Normal control; HF: High-fat; VD3: 1,25-dihydroxy-vitamin D; TNFα: Tumor necrosis factor α; IL: Interleukin; SREBP1C: Sterol-regulatory element binding protein 1C; FASN: Fatty acid synthetase; ACOX1: Acyl-CoA oxidase 1; CPT1A: Carnitine palmitoyltransferase 1A.

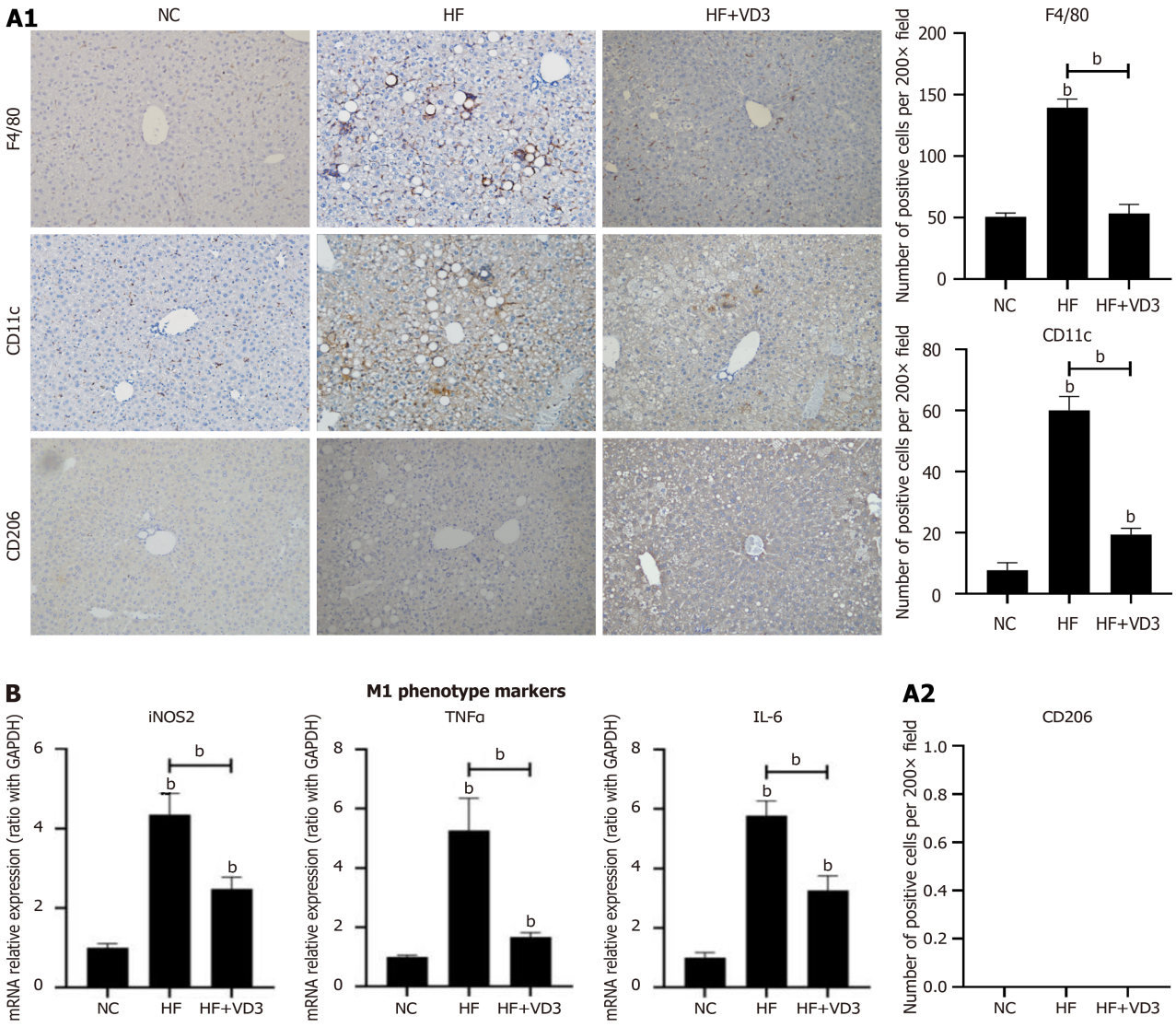

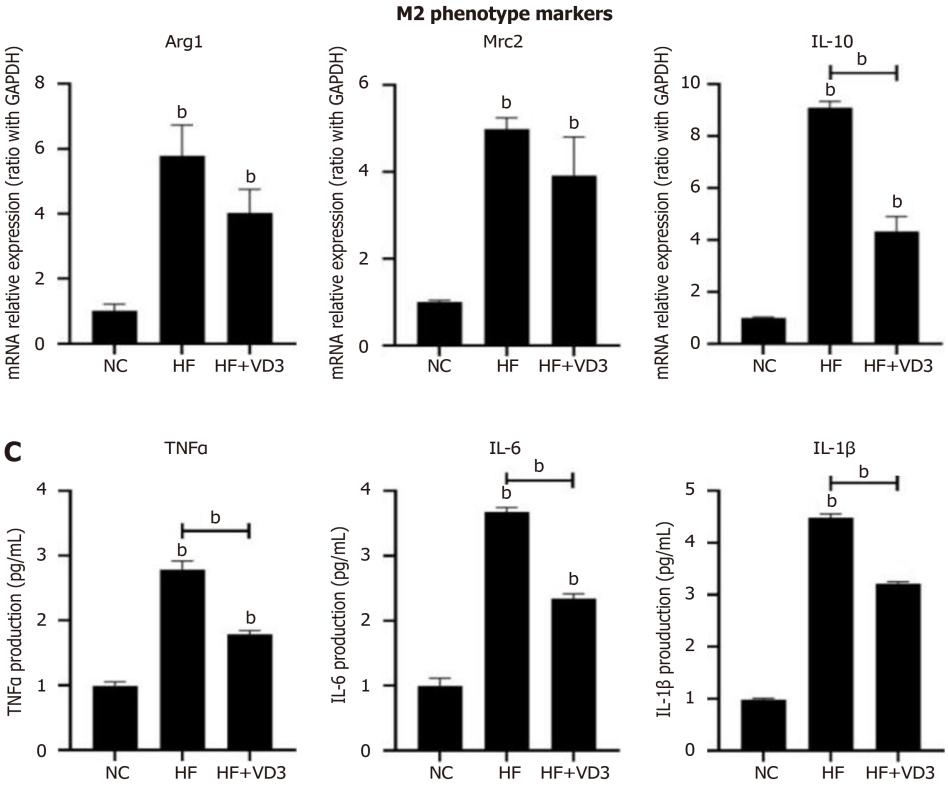

Figure 2 Supplementation with 1,25-dihydroxy-vitamin D decreases the proinflammatory M1 polarization of hepatic macrophages in non-alcoholic fatty liver disease. Wild-type C57BL/6 mice were fed either normal control (NC) diet or high-fat (HF) diet for 16 weeks, or HF diet plus 1,25-dihydroxy-vitamin D [1,25(OH)2D3] (20 μg/kg) by oral gavage every alternate day for 16 weeks. Phosphate-buffered saline by oral gavage served as a control (n = 10/group). Hepatic macrophages were isolated from mice administered NC diet, HF diet alone or plus 1,25(OH)2D3. A: M1/M2 phenotype of hepatic macrophages determined by immunohistochemical staining (200 ×); B: M1/M2 gene marker expression on hepatic macrophages; C: Proinflammatory cytokine secretion from hepatic macrophages. Values are mean ± SEM, $^{a}P < 0.05$, $^{b}P < 0.01$, n = 10 animals per group; NC: Normal control; HF: High-fat; VD3: 1,25-dihydroxy-vitamin D; iNOS: Inducible NO synthase; TNFα: Tumor necrosis factor α; IL: Interleukin; Arg1 Arginine 1; Mrc2: Macrophage mannose receptor 2.

$1,25(OH)_2D_3$ improves hepatocyte lipid metabolism by inhibiting proinflammatory macrophage polarization.

DISCUSSION

Insulin resistance significantly elevates the risk of NAFLD due to systemic low-grade inflammation[30]. Vitamin D is recognized for its anti-inflammatory, anti-proliferative, and anti-fibrotic effects, which may influence the development of NAFLD[31]. However, the precise role of vitamin D in NAFLD remains incompletely understood. Emerging evidence suggests that the proinflammatory activation of hepatic macrophages, particularly Kupffer cells, plays a pivotal role in the pathogenesis of NAFLD[32]. In this study, a murine model of NAFLD induced by a HF diet showed that supplementation with $1,25(OH)_2D_3$ alleviated hepatic steatosis, likely by reducing proinflammatory M1 polarization of hepatic macrophages. Furthermore, our cell culture experiments demonstrated that $1,25(OH)_2D_3$ suppressed fatty-acid-induced M1 polarization, which improved lipid metabolism and reduced lipid accumulation in hepatocytes. The ability of $1,25(OH)_2D_3$ to shift macrophage polarization was linked to the VDR-PPARγ signaling pathway in both *in vivo* and *in vitro* settings.

Clinical studies increasingly indicate that vitamin D deficiency correlates with metabolic syndrome features, including NAFLD[11,33]. Approximately 55% of NAFLD patients exhibit vitamin D deficiency[34]. Despite this association, results from clinical trials evaluating the impact of vitamin D supplementation on NAFLD have been mixed[35-37]. In our study, $1,25(OH)_2D_3$ supplementation *in vivo* was found to improve hepatic steatosis and reduce local inflammation. Since altered lipid homeostasis is a key characteristic of NAFLD[38], we investigated how $1,25(OH)_2D_3$ affects enzymes involved in lipid synthesis and breakdown in the liver. Our findings indicate that $1,25(OH)_2D_3$ improves both lipid anabolic and catabolic processes, potentially explaining the divergent results seen in previous clinical studies. These results highlight the potential of $1,25(OH)_2D_3$ as a treatment option for NAFLD by simultaneously addressing hepatic steatosis and inflammation.

Macrophages exhibit two main phenotypes: The proinflammatory M1 and anti-inflammatory M2 states[17,18]. Prior research suggests that obesity, induced by HF diets, shifts macrophages in adipose tissue towards the M1 phenotype, promoting insulin resistance[39]. Our earlier work showed that HF diets increase M1 polarization of hepatic macrophages in NAFLD[19]. In this study, we demonstrated that $1,25(OH)_2D_3$ significantly reduces M1 polarization in hepatic macrophages *in vivo*. This was further supported by our *in vitro* experiments, where $1,25(OH)_2D_3$ inhibited fatty-acid-induced

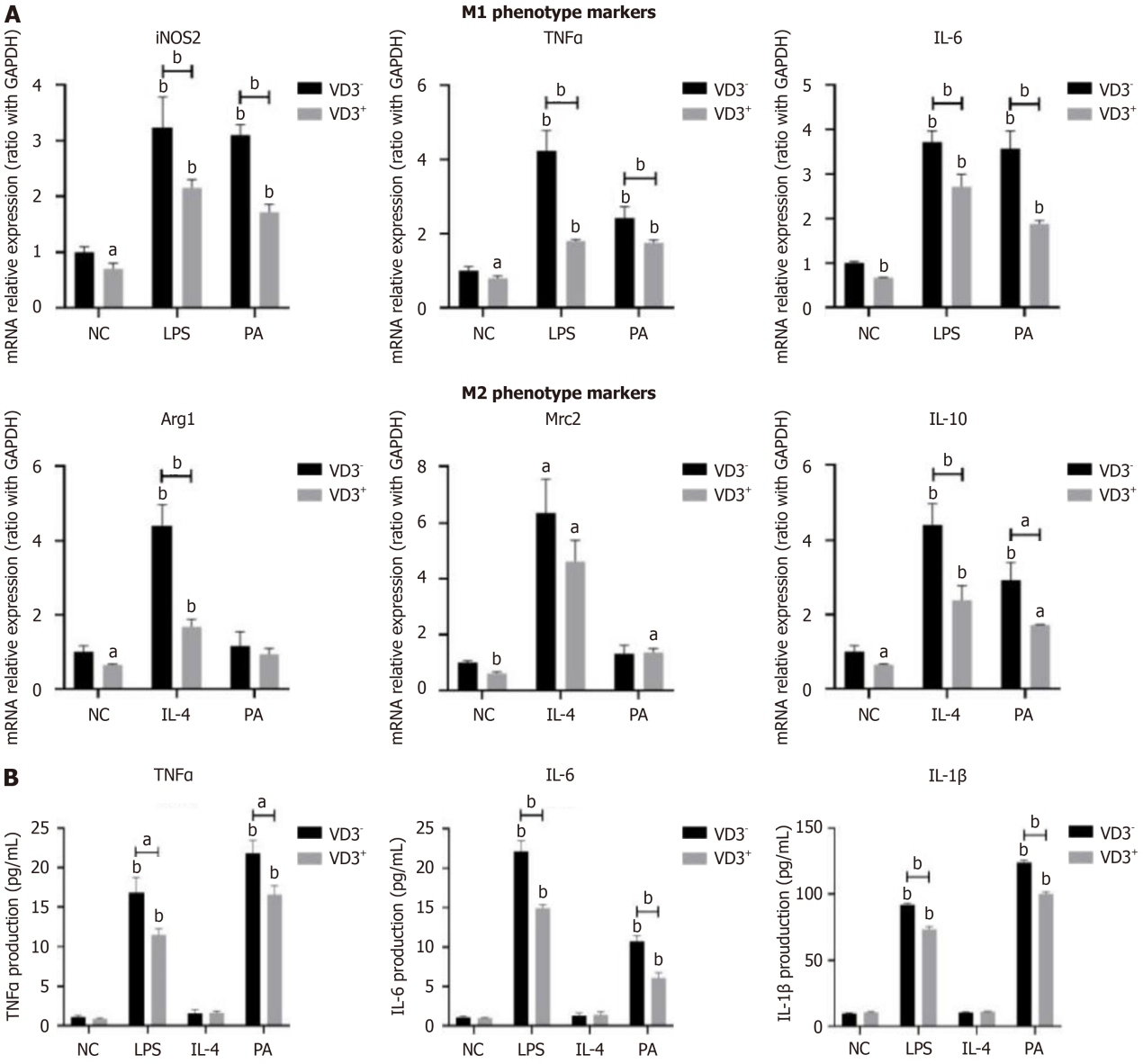

Figure 3 Administration of 1,25-dihydroxy-vitamin D inhibits fatty-acid-induced proinflammatory M1 polarization of macrophages. RAW264.7 macrophages were incubated with palmitic acid (0.5 mmol/L) for 24 hours or Dulbecco's modified Eagle's medium as a normal control. Lipopolysaccharide (100 ng/mL) or interleukin-4 (5 ng/mL) treatment served as positive controls for macrophage M1 or M2 polarization. For administration of 1,25-dihydroxy-vitamin D (1,25(OH)2D3), RAW264.7 macrophages were incubated with 1,25(OH)2D3 (VD3, 20 ng/mL) for a further 24 hours. A: M1/M2 gene marker expression on RAW264.7 macrophages; B: Proinflammatory cytokine secretion from RAW264.7 macrophages. Values are mean ± SEM, $^{a}P < 0.05$, $^{b}P < 0.01$, $n = 3$ experiments; NC: Normal control; PA; Palmitic acid; VD3: 1,25-dihydroxy-vitamin D; LPS: Lipopolysaccharide; IL: Interleukin; iNOS: Inducible NO synthase; TNFα: Tumor necrosis factor α; Arg1 Arginine 1; Mrc2: Macrophage mannose receptor 2.

M1 polarization of macrophages. Lipid accumulation in the liver is recognized as an early and essential step in NAFLD [40], with free fatty acids accounting for a major portion of hepatic lipid buildup[28]. In previous studies, we found that saturated fatty acids promote M1 polarization in Kupffer cells[19]. In this study, we found that $1,25(OH)_2D_3$ effectively suppressed this fatty-acid-induced M1 polarization, linking its effect on reducing hepatic steatosis to the inhibition of proinflammatory macrophage activity.

Both VDR and PPARγ, members of the nuclear receptor superfamily, are known to regulate lipid metabolism and macrophage polarization[24-27]. Studies have shown that VDR overexpression in adipose tissue leads to increased fat mass and elevated serum lipid levels, while VDR-knockout mice exhibit improved lipid profiles[41]. Consistent with these findings, our study revealed that VDR expression was upregulated in macrophages in response to an HF diet and fatty acids, but this upregulation was reversed by $1,25(OH)_2D_3$ supplementation. Interestingly, although $1,25(OH)_2D_3$ is the natural ligand for VDR, its supplementation led to a decrease in VDR expression, likely due to a feedback mechanism [42,43]. Deletion of macrophage VDR in mice has been shown to result in insulin resistance, partly by shifting macrophage polarization from M1 to M2[44]. Our data suggest that $1,25(OH)_2D_3$ alleviates hepatic steatosis in NAFLD by inhibiting the proinflammatory M1 polarization of hepatic macrophages through the downregulation of VDR.

In addition, the HF diet increased PPARγ expression in hepatic macrophages, consistent with our previous findings [19]. However, supplementation with $1,25(OH)_2D_3$ did not significantly alter PPARγ expression *in vivo*, potentially due to

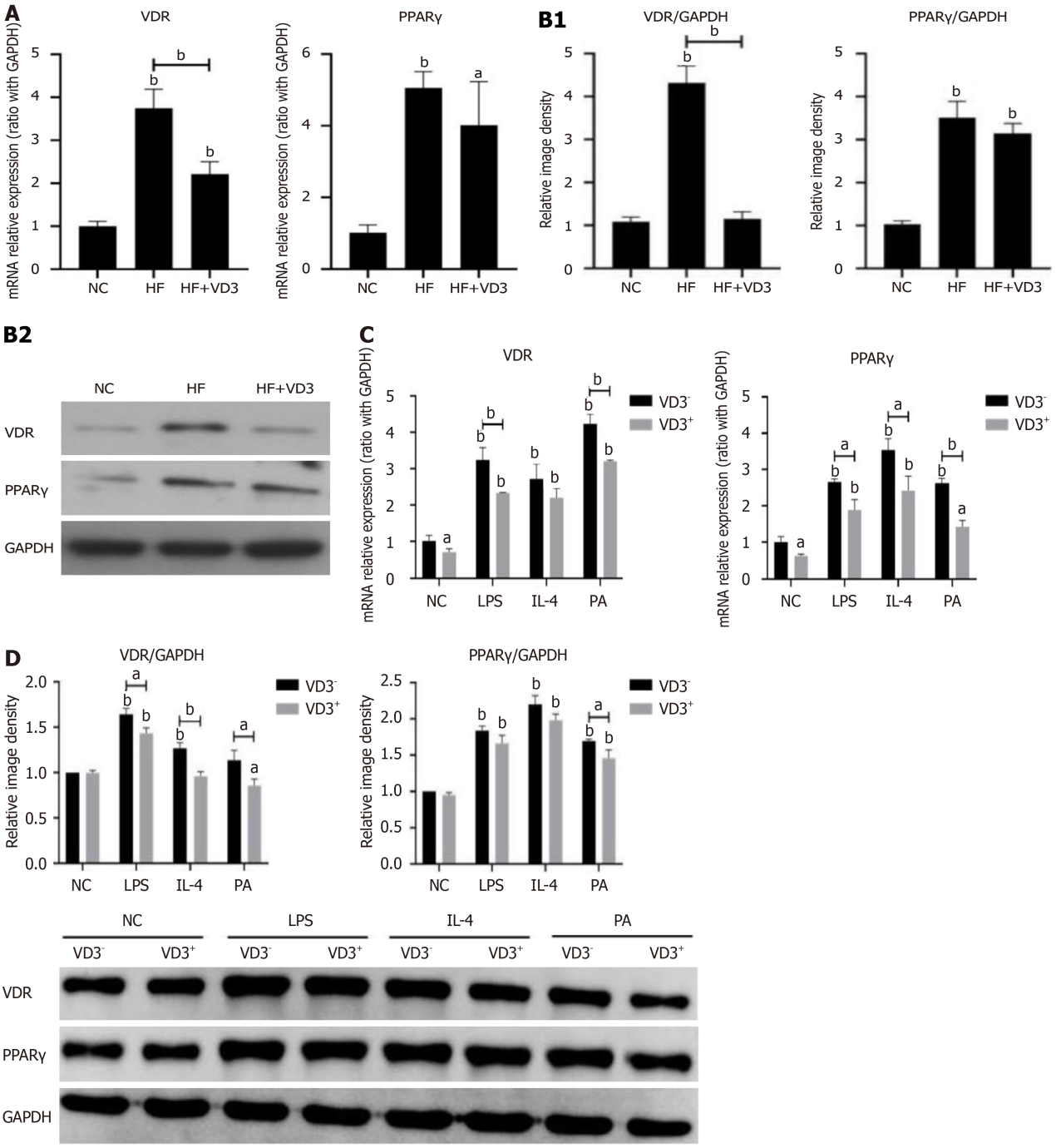

Figure 4 Effect of vitamin D receptor-peroxisome proliferator activated receptor γ pathway modulating 1,25-dihydroxy-vitamin D administration on high-fat diet/fatty acid-induced hepatic macrophage polarization. Wild-type C57BL/6 mice were fed either normal control (NC) diet or high-fat (HF) diet for 16 week, or HF diet plus 1,25-dihydroxy-vitamin D [1,25(OH)2D3] (20 μg/kg) by oral gavage every alternate day for 16 weeks. Phosphate-buffered saline by oral gavage served as a control (n = 10/group). Hepatic macrophages were isolated from mice administered NC diet, HF diet alone or plus 1,25(OH)2D3. RAW264.7 macrophages were incubated with palmitic acid (0.5 mmol/L) for 24 hours or Dulbecco's modified Eagle's medium as a normal control. Lipopolysaccharide (100 ng/mL) or interleukin-4 (5 ng/mL) treatment served as positive controls for macrophage M1 or M2 polarization. For administration of 1,25(OH)2D3, RAW264.7 macrophages were incubated with 1,25(OH)2D3 (20 ng/mL) for a further 24 hours. A: MRNA expression of vitamin D receptor (VDR)-peroxisome proliferator activated receptor γ on hepatic macrophages; B: Protein expression of VDR and PPARγ on hepatic macrophages; C: MRNA expression of VDR and PPARγ on RAW264.7 macrophages; D: Protein expression of VDR and PPARγ on RAW264.7 macrophages. Values are mean ± SEM, $^{a}P < 0.05$, $^{b}P < 0.01$, n = 10 animals per group, n = 3 experiments; VDR: Vitamin D receptor; PPARγ: Peroxisome proliferator activated receptor γ; NC: Normal control; HF: High-fat; VD3: 1,25-dihydroxy-vitamin D; PA: Palmitic acid; LPS: Lipopolysaccharide; IL: Interleukin.

complex interactions between VDR and PPARγ[25,26]. In contrast, *in vitro* experiments demonstrated that $1,25(OH)_2D_3$ suppressed PPARγ expression in macrophages in response to fatty acid stimulation. This suggests that VDR and PPARγ may operate in tandem during macrophage polarization under these conditions. Mechanistically, $1,25(OH)_2D_3$ likely modulates PPARγ by directly interacting with VDR, which, in turn, influences macrophage polarization and lipid metabolism. This dual regulation of VDR and PPARγ may be critical for reducing inflammation and improving lipid

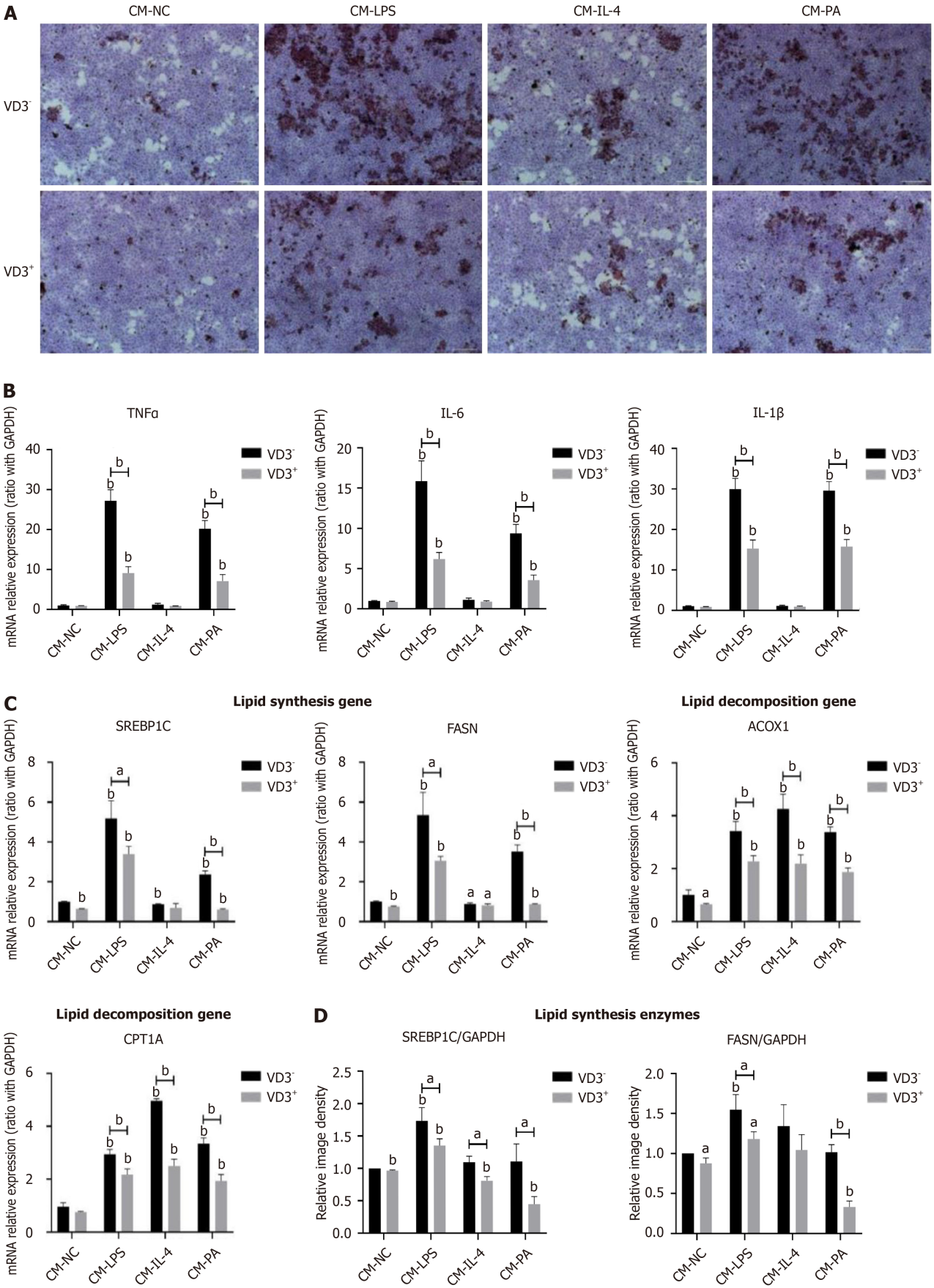
A
CM-NC
CM-LPS
CM-IL-4
CM-PA
VD3-
VD3+
B
TNFα
IL-6
IL-1β
mRNA relative expression (ratio with GAPDH)
VD3-
VD3+
C
Lipid synthesis gene
Lipid decomposition gene
SREBP1C
FASN
ACOX1
CPT1A
D
Lipid synthesis enzymes
SREBP1C/GAPDH
FASN/GAPDH
Relative image density

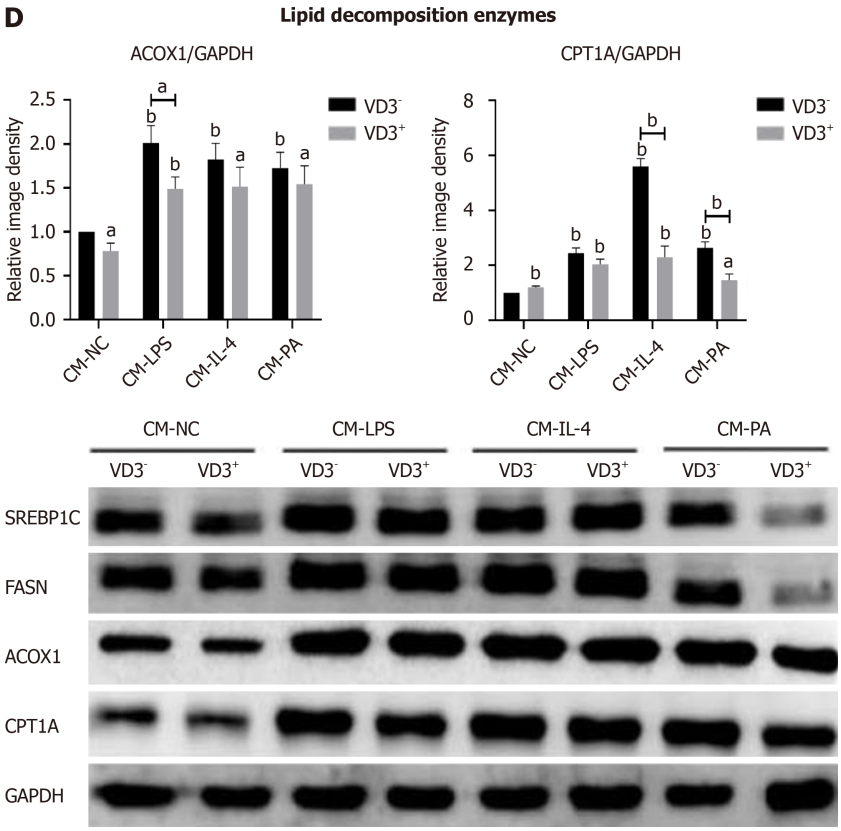

Figure 5 Administration of 1,25-dihydroxy-vitamin D inhibiting fatty-acid-induced proinflammatory M1 polarization of macrophages directly relieves lipid accumulation and metabolism in hepatocytes. RAW264.7 macrophages were incubated with palmitic acid (0.5 mmol/L) for 24 hours or Dulbecco's modified Eagle's medium as a normal control. Lipopolysaccharide (100 ng/mL) or interleukin-4 (5 ng/mL) treatment served as positive controls for macrophage M1 or M2 polarization. For administration of 1,25-dihydroxy-vitamin D [1,25(OH)2D3], RAW264.7 macrophages were incubated with 1,25(OH)2D3 (20 ng/mL) for a further 24 hours. The cell culture supernatants were collected and prepared for conditioned media (CMs). AML12 hepatocytes were treated with different CMs from RAW264.7 macrophages for 24 hours. A: Lipid accumulation in AML12 hepatocytes determined by Oil Red O staining (200 ×); B: Proinflammatory cytokines mRNA expression on AML12 hepatocytes; C: Lipid metabolism genes mRNA expression on AML12 hepatocytes; D: Lipid metabolism enzymes protein expression on AML12 hepatocytes. Values are mean ± SEM, $^{a}P < 0.05$, $^{b}P < 0.01$, $n = 3$ experiments; CM: Conditioned media; NC: Normal control; LPS: Lipopolysaccharide; IL: Interleukin; PA: Palmitic acid; VD3: 1,25-dihydroxy-vitamin D; TNFα: Tumor necrosis factor α; SREBP1C: Sterol-regulatory element binding protein 1C; FASN: Fatty acid synthetase; ACOX1: Acyl-CoA oxidase 1; CPT1A: Carnitine palmitoyltransferase 1A.

homeostasis in NAFLD.

Earlier studies have shown that hepatic lipid accumulation in NAFLD is initiated by the production of proinflammatory cytokines from Kupffer cells[45-47]. Depletion of Kupffer cells in animal models reduced hepatic steatosis, suggesting that the inflammatory activation of Kupffer cells is key to disrupting hepatic lipid homeostasis. A critical question is whether polarized macrophages directly influence lipid metabolism in hepatocytes. Recent research indicates that lipid-induced M1 macrophages can promote lipid synthesis in hepatocytes[48,49]. In our study, we demonstrated that supplementation with $1,25(OH)_2D_3$ improved hepatic steatosis and lipid metabolism *in vivo*, likely due to its ability to reverse M1 polarization in hepatic macrophages. Our *in vitro* co-culture experiments further supported these findings by showing that suppression of M1 polarization in macrophages, induced by fatty acids, directly reduced lipid accumulation and improved lipid metabolism in hepatocytes. This suggests that $1,25(OH)_2D_3$ not only reduces hepatic inflammation but also exerts a beneficial effect on lipid metabolism, potentially making it a valuable therapeutic option for NAFLD.

Limitations and future perspectives

Conditioned medium limitation: While the use of conditioned medium from RAW264.7 macrophages in this study provided valuable insights into paracrine signaling mechanisms, it may not fully capture the complex *in vivo* interactions between macrophages and hepatocytes. Future studies should consider employing a direct co-culture system, with macrophages in the upper compartment and liver cells in the lower compartment, to better understand how fatty acids and inflammatory signals concurrently affect both cell types. This would provide a more complete picture of the metabolic changes occurring in hepatocytes.

Mechanistic studies: Future research should focus on delineating the precise molecular mechanisms by which $1,25(OH)_2D_3$ regulates macrophage polarization through VDR-PPARγ signaling and its downstream effects on lipid metabolism. Dose-Response Exploration: Investigating the effects of different doses of $1,25(OH)_2D_3$ on NAFLD will help determine the optimal therapeutic dosage while minimizing potential side effects, such as hypercalcemia.

Long-term effects: Longitudinal studies are needed to assess the long-term safety and efficacy of $1,25(OH)_2D_3$, particularly with respect to chronic supplementation and the potential risk of hypercalcemia. Combination Therapies: Evaluating the potential of $1,25(OH)_2D_3$ in combination with other pharmacological agents could enhance its therapeutic efficacy and offer novel treatment strategies for NAFLD.

CONCLUSION

This study demonstrates that $1,25(OH)_2D_3$ supplementation can effectively reduce lipid accumulation in hepatocytes by inhibiting fatty-acid-induced proinflammatory M1 polarization of macrophages. These findings offer a promising theoretical basis for the therapeutic potential of vitamin D in managing NAFLD. However, further research is necessary to advance our understanding and application of $1,25(OH)_2D_3$ in clinical settings.

FOOTNOTES

Author contributions: Luo WJ, Dong XW and Ye H designed the research study; Zhao QS, Zhang QB and Guo WY performed the research; Liu HW and Xu F conducted experiments, analyzed the data; All authors contributed to editorial changes in the manuscript; All authors read and approved the final manuscript.

Supported by the Natural Science Foundation of Ningbo, No. 202003N4234; and Medical and Health Research Project of Zhejiang Province, No. 2024KY1477.

Institutional animal care and use committee statement: This study was approved by the Ningbo University Animal Care and Use Committee according to the criteria set by Ningbo Medical Center Lihuili Hospital, No. IACUC202013.

Conflict-of-interest statement: The authors declare that they have no competing interests

Data sharing statement: The datasets used and analysed during the current study are available from the corresponding author on reasonable request at xufeng200468@126.com.

ARRIVE guidelines statement: The authors have read the ARRIVE Guidelines, and the manuscript was prepared and revised according to the ARRIVE Guidelines.

Country of origin: China

ORCID number: Feng Xu 0000-0003-3962-2918.

S-Editor: Li L
L-Editor: A
P-Editor: Xu ZH

REFERENCES

1 **Rinella ME**. Nonalcoholic fatty liver disease: a systematic review. *JAMA* 2015; **313**: 2263-2273 [PMID: 26057287 DOI: 10.1001/jama.2015.5370]
2 **Neuschwander-Tetri BA**. Non-alcoholic fatty liver disease. *BMC Med* 2017; **15**: 45 [PMID: 28241825 DOI: 10.1186/s12916-017-0806-8]
3 **Powell EE**, Wong VW, Rinella M. Non-alcoholic fatty liver disease. *Lancet* 2021; **397**: 2212-2224 [PMID: 33894145 DOI: 10.1016/S0140-6736(20)32511-3]
4 **Bessone F**, Razori MV, Roma MG. Molecular pathways of nonalcoholic fatty liver disease development and progression. *Cell Mol Life Sci* 2019; **76**: 99-128 [PMID: 30343320 DOI: 10.1007/s00018-018-2947-0]
5 **Buzzetti E**, Pinzani M, Tsochatzis EA. The multiple-hit pathogenesis of non-alcoholic fatty liver disease (NAFLD). *Metabolism* 2016; **65**: 1038-1048 [PMID: 26823198 DOI: 10.1016/j.metabol.2015.12.012]
6 **Charoenngam N**, Holick MF. Immunologic Effects of Vitamin D on Human Health and Disease. *Nutrients* 2020; **12**: 2097 [PMID: 32679784 DOI: 10.3390/nu12072097]
7 **Szymczak-Pajor I**, Drzewoski J, Śliwińska A. The Molecular Mechanisms by Which Vitamin D Prevents Insulin Resistance and Associated Disorders. *Int J Mol Sci* 2020; **21**: 6644 [PMID: 32932777 DOI: 10.3390/ijms21186644]
8 **Barchetta I**, Cimini FA, Cavallo MG. Vitamin D and Metabolic Dysfunction-Associated Fatty Liver Disease (MAFLD): An Update. *Nutrients* 2020; **12**: 3302 [PMID: 33126575 DOI: 10.3390/nu12113302]

9 **Zhang H**, Shen Z, Lin Y, Zhang J, Zhang Y, Liu P, Zeng H, Yu M, Chen X, Ning L, Mao X, Cen L, Yu C, Xu C. Vitamin D receptor targets hepatocyte nuclear factor 4α and mediates protective effects of vitamin D in nonalcoholic fatty liver disease. *J Biol Chem* 2020; **295**: 3891-3905 [PMID: 32051143 DOI: 10.1074/jbc.RA119.011487]

10 **Cimini FA**, Barchetta I, Carotti S, Bertoccini L, Baroni MG, Vespasiani-Gentilucci U, Cavallo MG, Morini S. Relationship between adipose tissue dysfunction, vitamin D deficiency and the pathogenesis of non-alcoholic fatty liver disease. *World J Gastroenterol* 2017; **23**: 3407-3417 [PMID: 28596677 DOI: 10.3748/wjg.v23.i19.3407]

11 **Wang X**, Li W, Zhang Y, Yang Y, Qin G. Association between vitamin D and non-alcoholic fatty liver disease/non-alcoholic steatohepatitis: results from a meta-analysis. *Int J Clin Exp Med* 2015; **8**: 17221-17234 [PMID: 26770315]

12 **Rhee EJ**, Kim MK, Park SE, Park CY, Baek KH, Lee WY, Kang MI, Park SW, Kim SW, Oh KW. High serum vitamin D levels reduce the risk for nonalcoholic fatty liver disease in healthy men independent of metabolic syndrome. *Endocr J* 2013; **60**: 743-752 [PMID: 23411507 DOI: 10.1507/endocrj.ej12-0387]

13 **Sakpal M**, Satsangi S, Mehta M, Duseja A, Bhadada S, Das A, Dhiman RK, Chawla YK. Vitamin D supplementation in patients with nonalcoholic fatty liver disease: A randomized controlled trial. *JGH Open* 2017; **1**: 62-67 [PMID: 30483536 DOI: 10.1002/jgh3.12010]

14 **Kitson MT**, Pham A, Gordon A, Kemp W, Roberts SK. High-dose vitamin D supplementation and liver histology in NASH. *Gut* 2016; **65**: 717-718 [PMID: 26294696 DOI: 10.1136/gutjnl-2015-310417]

15 **Gao B**, Jeong WI, Tian Z. Liver: An organ with predominant innate immunity. *Hepatology* 2008; **47**: 729-736 [PMID: 18167066 DOI: 10.1002/hep.22034]

16 **Dixon LJ**, Barnes M, Tang H, Pritchard MT, Nagy LE. Kupffer cells in the liver. *Compr Physiol* 2013; **3**: 785-797 [PMID: 23720329 DOI: 10.1002/cphy.c120026]

17 **Sica A**, Mantovani A. Macrophage plasticity and polarization: in vivo veritas. *J Clin Invest* 2012; **122**: 787-795 [PMID: 22378047 DOI: 10.1172/JCI59643]

18 **Murray PJ**, Allen JE, Biswas SK, Fisher EA, Gilroy DW, Goerdt S, Gordon S, Hamilton JA, Ivashkiv LB, Lawrence T, Locati M, Mantovani A, Martinez FO, Mege JL, Mosser DM, Natoli G, Saeij JP, Schultze JL, Shirey KA, Sica A, Suttles J, Udalova I, van Ginderachter JA, Vogel SN, Wynn TA. Macrophage activation and polarization: nomenclature and experimental guidelines. *Immunity* 2014; **41**: 14-20 [PMID: 25035950 DOI: 10.1016/j.immuni.2014.06.008]

19 **Luo W**, Xu Q, Wang Q, Wu H, Hua J. Effect of modulation of PPAR-γ activity on Kupffer cells M1/M2 polarization in the development of non-alcoholic fatty liver disease. *Sci Rep* 2017; **7**: 44612 [PMID: 28300213 DOI: 10.1038/srep44612]

20 **Maina V**, Sutti S, Locatelli I, Vidali M, Mombello C, Bozzola C, Albano E. Bias in macrophage activation pattern influences non-alcoholic steatohepatitis (NASH) in mice. *Clin Sci (Lond)* 2012; **122**: 545-553 [PMID: 22142284 DOI: 10.1042/CS20110366]

21 **Chinetti G**, Fruchart JC, Staels B. Peroxisome proliferator-activated receptors: new targets for the pharmacological modulation of macrophage gene expression and function. *Curr Opin Lipidol* 2003; **14**: 459-468 [PMID: 14501584 DOI: 10.1097/00041433-200310000-00006]

22 **Bouhlel MA**, Derudas B, Rigamonti E, Dièvart R, Brozek J, Haulon S, Zawadzki C, Jude B, Torpier G, Marx N, Staels B, Chinetti-Gbaguidi G. PPARgamma activation primes human monocytes into alternative M2 macrophages with anti-inflammatory properties. *Cell Metab* 2007; **6**: 137-143 [PMID: 17681149 DOI: 10.1016/j.cmet.2007.06.010]

23 **Odegaard JI**, Ricardo-Gonzalez RR, Goforth MH, Morel CR, Subramanian V, Mukundan L, Red Eagle A, Vats D, Brombacher F, Ferrante AW, Chawla A. Macrophage-specific PPARgamma controls alternative activation and improves insulin resistance. *Nature* 2007; **447**: 1116-1120 [PMID: 17515919 DOI: 10.1038/nature05894]

24 **Di Rosa M**, Malaguarnera G, De Gregorio C, Palumbo M, Nunnari G, Malaguarnera L. Immuno-modulatory effects of vitamin D3 in human monocyte and macrophages. *Cell Immunol* 2012; **280**: 36-43 [PMID: 23261827 DOI: 10.1016/j.cellimm.2012.10.009]

25 **Alimirah F**, Peng X, Yuan L, Mehta RR, von Knethen A, Choubey D, Mehta RG. Crosstalk between the peroxisome proliferator-activated receptor γ (PPARγ) and the vitamin D receptor (VDR) in human breast cancer cells: PPARγ binds to VDR and inhibits 1α,25-dihydroxyvitamin D3 mediated transactivation. *Exp Cell Res* 2012; **318**: 2490-2497 [PMID: 22884583 DOI: 10.1016/j.yexcr.2012.07.020]

26 **Sertznig P**, Seifert M, Tilgen W, Reichrath J. Peroxisome proliferator-activated receptor (PPAR) and vitamin D receptor (VDR) signaling pathways in melanoma cells: promising new therapeutic targets? *J Steroid Biochem Mol Biol* 2010; **121**: 383-386 [PMID: 20214982 DOI: 10.1016/j.jsbmb.2010.03.003]

27 **Zhang X**, Zhou M, Guo Y, Song Z, Liu B. 1,25-Dihydroxyvitamin D_3 Promotes High Glucose-Induced M1 Macrophage Switching to M2 *via* the VDR-PPARγ Signaling Pathway. *Biomed Res Int* 2015; **2015**: 157834 [PMID: 25961000 DOI: 10.1155/2015/157834]

28 **Ma L**, Ishigami M, Honda T, Yokoyama S, Yamamoto K, Ishizu Y, Kuzuya T, Hayashi K, Hirooka Y, Goto H. Antifibrotic Effects of 1,25(OH)2D3 on Nonalcoholic Steatohepatitis in Female Mice. *Dig Dis Sci* 2019; **64**: 2581-2590 [PMID: 30825110 DOI: 10.1007/s10620-019-05560-3]

29 **Cusi K**. Role of obesity and lipotoxicity in the development of nonalcoholic steatohepatitis: pathophysiology and clinical implications. *Gastroenterology* 2012; **142**: 711-725.e6 [PMID: 22326434 DOI: 10.1053/j.gastro.2012.02.003]

30 **Machado MV**, Diehl AM. Pathogenesis of Nonalcoholic Steatohepatitis. *Gastroenterology* 2016; **150**: 1769-1777 [PMID: 26928243 DOI: 10.1053/j.gastro.2016.02.066]

31 **Pacifico L**, Osborn JF, Bonci E, Pierimarchi P, Chiesa C. Association between Vitamin D Levels and Nonalcoholic Fatty Liver Disease: Potential Confounding Variables. *Mini Rev Med Chem* 2019; **19**: 310-332 [PMID: 30360708 DOI: 10.2174/1389557518666181025153712]

32 **Friedman SL**, Neuschwander-Tetri BA, Rinella M, Sanyal AJ. Mechanisms of NAFLD development and therapeutic strategies. *Nat Med* 2018; **24**: 908-922 [PMID: 29967350 DOI: 10.1038/s41591-018-0104-9]

33 **Kim HS**, Rotundo L, Kothari N, Kim SH, Pyrsopoulos N. Vitamin D Is Associated with Severity and Mortality of Non-alcoholic Fatty Liver Disease: A US Population-based Study. *J Clin Transl Hepatol* 2017; **5**: 185-192 [PMID: 28936398 DOI: 10.14218/JCTH.2017.00025]

34 **Barchetta I**, Angelico F, Del Ben M, Baroni MG, Pozzilli P, Morini S, Cavallo MG. Strong association between non alcoholic fatty liver disease (NAFLD) and low 25(OH) vitamin D levels in an adult population with normal serum liver enzymes. *BMC Med* 2011; **9**: 85 [PMID: 21749681 DOI: 10.1186/1741-7015-9-85]

35 **Wu C**, Qiu S, Zhu X, Li L. Vitamin D supplementation and glycemic control in type 2 diabetes patients: A systematic review and meta-analysis. *Metabolism* 2017; **73**: 67-76 [PMID: 28732572 DOI: 10.1016/j.metabol.2017.05.006]

36 **Mousa A**, Naderpoor N, de Courten MP, Teede H, Kellow N, Walker K, Scragg R, de Courten B. Vitamin D supplementation has no effect on insulin sensitivity or secretion in vitamin D-deficient, overweight or obese adults: a randomized placebo-controlled trial. *Am J Clin Nutr* 2017; **105**: 1372-1381 [PMID: 28490514 DOI: 10.3945/ajcn.117.152736]

37 **Li X**, Liu Y, Zheng Y, Wang P, Zhang Y. The Effect of Vitamin D Supplementation on Glycemic Control in Type 2 Diabetes Patients: A

Systematic Review and Meta-Analysis. *Nutrients* 2018; **10**: 375 [PMID: 29562681 DOI: 10.3390/nu10030375]

38 **Katsiki N**, Mikhailidis DP, Mantzoros CS. Non-alcoholic fatty liver disease and dyslipidemia: An update. *Metabolism* 2016; **65**: 1109-1123 [PMID: 27237577 DOI: 10.1016/j.metabol.2016.05.003]

39 **Morris DL**, Singer K, Lumeng CN. Adipose tissue macrophages: phenotypic plasticity and diversity in lean and obese states. *Curr Opin Clin Nutr Metab Care* 2011; **14**: 341-346 [PMID: 21587064 DOI: 10.1097/MCO.0b013e328347970b]

40 **Tilg H**, Moschen AR. Insulin resistance, inflammation, and non-alcoholic fatty liver disease. *Trends Endocrinol Metab* 2008; **19**: 371-379 [PMID: 18929493 DOI: 10.1016/j.tem.2008.08.005]

41 **Xu Y**, Lou Y, Kong J. VDR regulates energy metabolism by modulating remodeling in adipose tissue. *Eur J Pharmacol* 2019; **865**: 172761 [PMID: 31669589 DOI: 10.1016/j.ejphar.2019.172761]

42 **Panda DK**, Miao D, Bolivar I, Li J, Huo R, Hendy GN, Goltzman D. Inactivation of the 25-hydroxyvitamin D 1alpha-hydroxylase and vitamin D receptor demonstrates independent and interdependent effects of calcium and vitamin D on skeletal and mineral homeostasis. *J Biol Chem* 2004; **279**: 16754-16766 [PMID: 14739296 DOI: 10.1074/jbc.M310271200]

43 **Yuzbashian E**, Asghari G, Hedayati M, Zarkesh M, Mirmiran P, Khalaj A. Determinants of vitamin D receptor gene expression in visceral and subcutaneous adipose tissue in non-obese, obese, and morbidly obese subjects. *J Steroid Biochem Mol Biol* 2019; **187**: 82-87 [PMID: 30412764 DOI: 10.1016/j.jsbmb.2018.11.004]

44 **Oh J**, Riek AE, Darwech I, Funai K, Shao J, Chin K, Sierra OL, Carmeliet G, Ostlund RE Jr, Bernal-Mizrachi C. Deletion of macrophage Vitamin D receptor promotes insulin resistance and monocyte cholesterol transport to accelerate atherosclerosis in mice. *Cell Rep* 2015; **10**: 1872-1886 [PMID: 25801026 DOI: 10.1016/j.celrep.2015.02.043]

45 **Lanthier N**, Molendi-Coste O, Horsmans Y, van Rooijen N, Cani PD, Leclercq IA. Kupffer cell activation is a causal factor for hepatic insulin resistance. *Am J Physiol Gastrointest Liver Physiol* 2010; **298**: G107-G116 [PMID: 19875703 DOI: 10.1152/ajpgi.00391.2009]

46 **Li P**, He K, Li J, Liu Z, Gong J. The role of Kupffer cells in hepatic diseases. *Mol Immunol* 2017; **85**: 222-229 [PMID: 28314211 DOI: 10.1016/j.molimm.2017.02.018]

47 **Huang W**, Metlakunta A, Dedousis N, Zhang P, Sipula I, Dube JJ, Scott DK, O'Doherty RM. Depletion of liver Kupffer cells prevents the development of diet-induced hepatic steatosis and insulin resistance. *Diabetes* 2010; **59**: 347-357 [PMID: 19934001 DOI: 10.2337/db09-0016]

48 **Wu HM**, Ni XX, Xu QY, Wang Q, Li XY, Hua J. Regulation of lipid-induced macrophage polarization through modulating peroxisome proliferator-activated receptor-gamma activity affects hepatic lipid metabolism *via* a Toll-like receptor 4/NF-κB signaling pathway. *J Gastroenterol Hepatol* 2020; **35**: 1998-2008 [PMID: 32128893 DOI: 10.1111/jgh.15025]

49 **Nakashima M**, Suga N, Ikeda Y, Yoshikawa S, Matsuda S. Relevant MicroRNAs of MMPs and TIMPs with Certain Gut Microbiota Could Be Involved in the Invasiveness and Metastasis of Malignant Tumors. *Innov Discov* 2024; **1**: 10 [DOI: 10.53964/id.2024010]

World Journal of Gastrointestinal Oncology

Submit a Manuscript: https://www.f6publishing.com

World J Gastrointest Oncol 2024 December 15; 16(12): 4700-4715

DOI: 10.4251/wjgo.v16.i12.4700

ISSN 1948-5204 (online)

ORIGINAL ARTICLE

Basic Study

Matrine promotes colorectal cancer apoptosis by downregulating shank-associated RH domain interactor expression

Yuan-Chen Zhou, Qian-Qian Wang, Ge-Yu-Jia Zhou, Teng-Fei Yin, Dong-Yan Zhao, Xi-Zhen Sun, Chang Tan, Lei Zhou, Shu-Kun Yao

Specialty type: Oncology

Provenance and peer review: Unsolicited article; Externally peer reviewed.

Peer-review model: Single blind

Peer-review report's classification
Scientific Quality: Grade C
Novelty: Grade C
Creativity or Innovation: Grade B
Scientific Significance: Grade B

P-Reviewer: Kong MW

Received: June 16, 2024
Revised: September 17, 2024
Accepted: October 16, 2024
Published online: December 15, 2024
Processing time: 148 Days and 22.5 Hours

Yuan-Chen Zhou, Qian-Qian Wang, Chang Tan, Shu-Kun Yao, Graduate School, Peking University China-Japan Friendship School of Clinical Medicine, Beijing 100029, China

Ge-Yu-Jia Zhou, Department of Gastroenterology, China-Japan Friendship Hospital (Institute of Clinical Medical Sciences), Beijing 100029, China

Teng-Fei Yin, Department of Gastroenterology, Qilu Hospital, Shandong University, Jinan 250012, Shandong Province, China

Dong-Yan Zhao, Department of Gastroenterology, The First Affiliated Hospital of Soochow University, Suzhou 215006, Jiangsu Province, China

Xi-Zhen Sun, Department of Gastroenterology, Beijing Jishuitan Hospital, Beijing 100035, China

Lei Zhou, Department of General Surgery, China-Japan Friendship Hospital, Beijing 100029, China

Shu-Kun Yao, Department of Gastroenterology, China-Japan Friendship Hospital, Beijing 100029, China

Co-corresponding authors: Lei Zhou and Shu-Kun Yao.

Corresponding author: Shu-Kun Yao, MD, PhD, Chief Physician, Doctor, Professor, Graduate School, Peking University China-Japan Friendship School of Clinical Medicine, No. 2 Yinghua East Road, Chaoyang District, Beijing 100029, China. shukunyao@126.com

Abstract

BACKGROUND

The 5-year survival rate of patients with colorectal cancer (CRC) in China is only 56.9%, highlighting the need for new therapeutic drugs. Previous studies have shown that matrine exhibits antitumor effects by inducing apoptosis. However, the mechanism by which matrine regulates antiapoptotic proteins in CRC remains unclear.

AIM

To identify apoptotic proteins from proteomics and investigate the role of matrine in impeding CRC apoptosis by regulating these proteins.

METHODS
Tumor and adjacent normal tissues were collected from 52 patients with CRC who underwent surgery between January and December 2021. Data-independent acquisition quantitative proteomic analysis was performed to identify differentially expressed apoptotic proteins. The selected apoptotic proteins were identified through their association with tumor-node-metastasis (TNM) stage and prognosis, then confirmed by immunohistochemical (IHC) staining in validation cohort. *In vitro*, the role of matrine or apoptotic proteins on cancer cells were analyzed.

RESULTS
Compared to normal tissues, 88 anti-apoptotic proteins from proteomic results were selected. Among them, Shank-associated RH domain interactor (SHARPIN) was identified because of its relationship with TNM stage and overall survival in TCGA database. In the IHC-confirmed cohort, SHARPIN was highly expressed in CRC tissues and localized in the cytoplasm. Higher SHARPIN expression was associated with TNM stage, carbohydrate antigen 153 levels, and gross type compared to low expression. SHARPIN knockdown promoted apoptosis, significantly upregulated the expression of Bcl-2 associated agonist of cell death, Bcl-2 associated X protein, caspase 3, and caspase 8, and downregulated B-cell lymphoma-2 ($P < 0.05$). Importantly, matrine treatment promoted apoptosis and reversed the proliferation, invasion, and migration of CRC cells by repressing SHARPIN.

CONCLUSION
SHARPIN was identified as an upregulated anti-apoptotic protein in CRC, and matrine exhibited anticancer effects by downregulating its expression. Thus, matrine appears to be a promising drug for CRC.

Key Words: Colorectal cancer; Proteomics; Shank-associated RH domain interactor; Matrine; Apoptosis

Core Tip: Despite advances in therapy for colorectal cancer (CRC), the 5-year survival rate for CRC patients in China remains only 56.9%. This study explored the effects of matrine on CRC by targeting a newly identified anti-apoptotic protein, Shank-associated RH domain interactor (SHARPIN). SHARPIN was discovered through proteomic analysis and its expression was validated in both the TCGA database and our patient cohort using immunohistochemistry. Inhibiting SHARPIN expression led to increased apoptosis and reduced proliferation, invasion, and migration of CRC cells *in vitro*. Matrine's ability to inhibit SHARPIN and induce apoptosis highlights its potential as a promising therapeutic agent for CRC.

Citation: Zhou YC, Wang QQ, Zhou GYJ, Yin TF, Zhao DY, Sun XZ, Tan C, Zhou L, Yao SK. Matrine promotes colorectal cancer apoptosis by downregulating shank-associated RH domain interactor expression. *World J Gastrointest Oncol* 2024; 16(12): 4700-4715
URL: https://www.wjgnet.com/1948-5204/full/v16/i12/4700.htm
DOI: https://dx.doi.org/10.4251/wjgo.v16.i12.4700

INTRODUCTION

Colorectal cancer (CRC) is the third most common cancer type worldwide and ranks second in China[1]. It imposes a significant burden on both individuals and the healthcare system because of its high incidence and mortality rate. Despite notable advancements in systemic therapy, CRC prognosis remains poor. In China, although 5-year survival rate increased from 47.2% to 56.9% between 2003 and 2015, it still lagged that of a developed country[2]. The poor prognosis of CRC can be attributed to factors, such as advanced TNM stage, genetic dysregulation or mutation, and drug resistance. Hence, it is imperative to explore novel targets and corresponding drugs to enhance the treatment efficacy.

Cell death resistance is a crucial hallmark of cancer[3]. The dysregulation of apoptotic proteins promotes CRC progression, especially at early-stage, and identified as promising targets for improving therapeutic outcomes. Proteomics offers a means of characterizing protein profiles, including those involved in anti-apoptosis, in CRC tissues. However, there is a paucity of drugs designed to induce apoptosis in the treatment of CRC. Matrine, a natural alkaloid derived from plants such as Sophora flavescens (kushen), has shown anticancer effects without obvious adverse effects. Notably, few studies have explored the effect of matrine on the induction of apoptosis in CRC cells. This study aimed to select anti-apoptotic proteins from CRC proteomic profiles and investigate the ability of matrine to induce apoptosis in CRC cells by inhibiting these anti-apoptotic proteins.

MATERIALS AND METHODS

Patient recruitment and sample collection

From January 2021 to December 2021, we recruited patients diagnosed with CRC (n = 158) and health control subjects (n = 35) at our hospital. First, 52 paired tumor and adjacent tissues (5 cm away from the tumor) were collected from patients with CRC for proteomic analysis. Four CRC samples were missing, and 9 samples did not contain tumor tissue. Finally, 93 tumor tissues from patients with CRC (Figure 1) and 35 normal tissues from healthy subjects were used as a validation cohort to examine protein expression using immunohistochemistry (IHC). Clean Tissues were transferred by liquid nitrogen and stored in a -80 °C freezer. Other tissues were fixed and processed into sections.

Surgical resection samples diagnosed with CRC were included. Inflammatory bowel disease–associated, hereditary, and neuroendocrine CRC were excluded. Additionally, patients who had received chemoradiotherapy, targeted therapy, immunotherapy, or participated in clinical trials within the past 6 months were also excluded. All enrolled patients provided written informed consent. This study was conducted in accordance with the Declaration of Helsinki and approved by the Clinical Research Ethics Committee of the China-Japan Friendship Hospital (2018-116-K85).

Data independent acquisition analysis

The 52 pairs of CRC tissue samples were analyzed using high-performance liquid chromatography–mass spectrometry/mass spectrometry to identify differentially expressed proteins (DEPs). Samples were prepared through various processes, including protein denaturation, reduction, alkylation, tryptic digestion, and peptide clean-up, using an iST Sample Preparation Kit (PreOmics, Germany). The eluted peptides were lyophilized using SpeedVac. The peptides were then redissolved in solvent A (0.1% formic acid in water) and analyzed using an Orbitrap Fusion Lumos Tribrid coupled to an EASY-nano LC 1200 system (Thermo Fisher Scientific, MA, United States). The mass spectrometer was run in data independent acquisition (DIA) mode with a hybrid data strategy[4].

Raw DIA data were processed and analyzed using Spectronaut 15.0 (Biognosys AG, Switzerland) with default settings. The spectra were configured to search the UniProt-Homo sapiens database (version201907, 20428 entries), assuming trypsin as the digestion enzyme. The Q value false discovery rate (FDR) cutoff was set to 1% at both the precursor and protein levels. Decoy generation was set to mutated, which is similar to scrambled generation but only applies a random number of amino acid position swamps (min = 2, max = length/2). A normalization strategy was set for local normalization. The average of the top three filtered peptides that passed the 1% Q value cutoff was used to calculate the major group quantities. DEPs were selected if their P_{adj} value was < 0.05, and absolute fold change (FC) > 2 after the t-test.

Bioinformatic analysis

Quality control showed a low coefficient of variation and good reliability of the proteomic results: (1) DEPs were analyzed using R packages such as BiocManager, org.Hs.eg.db, colorspace, stringi, and ggplot2, and pairwise comparisons between two groups. The differential protein screening criteria were a t-test with Benjamini & Hochberg-corrected P value < 0.05 and an absolute FC > 2. Principal component analysis (PCA) was performed to determine the differences between tumor and normal samples. The upregulated and downregulated DEPs are displayed as volcano plots, and hierarchical clustering analysis was performed for expressed proteins and samples simultaneously, with the results displayed as heatmaps; and (2) Functional annotation and enrichment analyses were performed on all identified DEPs, and their functions were marked using Gene Ontology (GO) and Kyoto Encyclopedia of Genes and Genomes (KEGG).

RNA sequencing quantification and relevant clinical and survival data[5] of CRC tissues (n = 647) and normal colorectal tissues (n = 51) were obtained from TCGA database. (https://portal.gdc.cancer.gov). The ggplot2 and survminer packages were used to visualize the analyzed data.

IHC

Methanal-Fixed and Paraffin-Embedded tumors were stained for the Shank-associated RH domain interactor (SHARPIN) protein. Antigen retrieval was performed using an automatic antigen repair instrument (LBP-5196-II; Guangzhou LBP Medicine Science & Technology Co., Ltd) for 15 minutes in Tris-EDTA buffer (pH 9.0), followed by treatment with an enhanced endogenous peroxidase-blocking buffer (P0100B, Beyotime, Shanghai, China) for 10 minutes. Specimens were incubated overnight at 4 °C with polyclonal antibodies against human SHARPIN (1:100; 14626-1-AP, Proteintech, Wuhan, China). After rinsing three times with phosphate buffered saline (PBS), the slides were incubated with goat anti-rabbit IgG (1:2000, ab6721; Abcam) for 1 hour at room temperature. A coloring reaction was performed using a 3,3N-Diaminobenzidine Tertrahydrochloride chromogenic kit (ZLI-9017; Zhongshan Golden Bridge, Beijing, China). Nuclei were stained with Harris hematoxylin and mounted with neutral gum. Finally, the slides were photographed using a BX53 upright bright-field microscope (Olympus).

Evaluation of IHC staining

The ImageJ software was used for image quantification. SHARPIN expression was quantified using the H-score method in ImageJ; weak immunostaining was assigned a score of 1, moderate immunoreactivity was assigned a score of 2, and strong immunostaining was assigned a score of 3. The percentage of tumor cells stained at each intensity level was multiplied by the respective numeric score of the staining intensity, and the results were summed to quantify the total H-score.

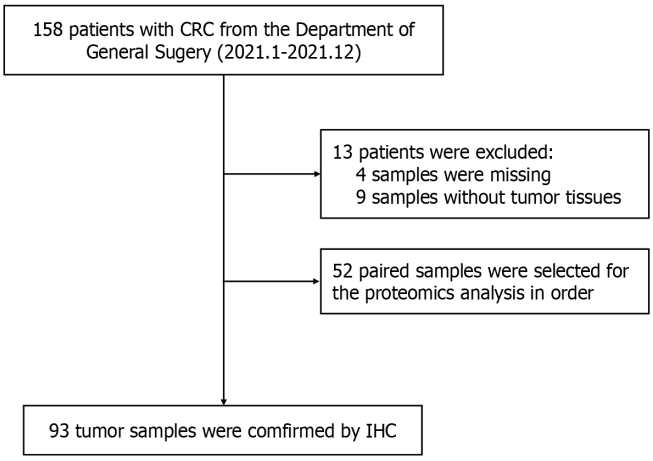

Figure 1 Flow chart. CRC: Colorectal cancer; IHC: Immunohistochemistry.

Data collection

Demographic data, clinicopathological features, and tumor markers, including age, sex, gross type, differentiation, tumor size, tumor location, histopathological type and manifestation, microsatellite instability, TNM stage, carcinoembryonic antigen, carbohydrate antigen 199 (CA199), CA125, CA153, and CA724 were collected from the medical record system.

Cell culture

Two CRC cells, HCT116 and SW480, obtained from the Procell Life Science & Technology Co., Ltd (Wuhan, China), were cultured in McCoy's 5A or DMEM supplemented 10% fetal bovine serum (FBS) (Gibco), 1% penicillin/streptomycin solution (C125C5, NCM Biotech) at 37.7 °C in a humidified atmosphere with 5% CO_2.

Cell transfection and matrine intervention

CRC cells were transfected with SHARPIN small interfering RNA (GenePharma) or negative control siRNA (GenePharma). The sequence pairs of the SHARPIN were as followed: Sense, 5′-CCUGAGGCAGAUCUUCCUATT-3′, antisense, 5′-UAGGAAGAUCUGCCUCAGGTT-3′. Lipofectamine 3000 Transfection Reagent (Invitrogen) was used to transfect CRC cells with the above siRNAs, according to the manufacturer's instructions. After 24 hours, the CRC cells were collected for subsequent experiments.

Matrine (MCE) stock solution was diluted with dimethyl sulfoxide and stored in -20 °C in the dark. CRC cells were treated with matrine at concentration of 2.5 mg/mL for 48 hours, which refer to previously described[6].

Quantitative reverse transcription-PCR

Total RNA was extracted from the cells using TRIzol reagent (Vazyme, Nanjing, China). The following primers were used for SHARPIN: Forward 5′- TGTTCTCAGAGCTCGGTTT -3′ and reverse 5′- AAGTTCCCCGTCCATCTT -3′. Fluorescence was detected using a CFX Connect instrument (Bio-Rad). Each sample was run in triplicate and compared using GAPDH as the reference gene. Results were analyzed using the $2^{-\Delta\Delta CT}$ method for the relative quantification of mRNA expression.

Western blotting

Cell lysis buffer for western blotting, IP (P0013, Beyotime), and a protease and phosphatase inhibitor cocktail (P1045, Beyotime) were used for protein extraction. The BCA Protein Assay Kit (P0012S, Beyotime) was used to measure the amount of protein.

Total proteins were subjected to sodium dodecyl sulfate/polyacrylamide gel electrophoresis and electrotransferred to PVDF membranes (Merck Millipore, China). Nonspecific binding sites were blocked using 5% nonfat milk for 2 hours and the membranes were incubated at 4 °C overnight with SHARPIN Monoclonal antibody (1:1000, Immunoway, United States), Caspase 3/p17/p19 Polyclonal antibody (1:1000, Proteintech), Caspase 8/p43/p18 Polyclonal antibody (1:1000, Proteintech), B-cell lymphoma-2 (Bcl-2) Polyclonal antibody (1:1000, Proteintech), Bcl-2 associated agonist of cell death (BAD) Polyclonal antibody (1:1000, Proteintech), Bcl-2 associated X protein (BAX) Polyclonal antibody (1:1000, Proteintech), GAPDH antibody (1:4000; Abcam), β-actin (1:1000, Proteintech). The PVDF membranes were then treated for 1 hour with a goat anti-rabbit secondary antibody (1:10000; D21109-35, IRDye® 800CW, LI-COR, United States). Fluorescence imaging was performed using an LI-COR Odyssey CLx imaging system. ImageJ software was used to quantify the chemiluminescent signals of the protein bands, using GAPDH, β-actin or tubulin as an internal control.

Flow cytometry analysis

An Annexin V-fluorescein isothiocyanate/propidium iodide apoptosis kit (556547, BD, United States) was used to detect the proportion of apoptotic cells after transfection. All procedures were performed according to manufacturer's instructions. Flow cytometry (FACSCanto II, BD, United States) and FlowJo (V_10.8.1) software were used to determine cell apoptosis rates.

Cell counting kit-8 proliferation assay

The collected CRC cells were seeded in each well of a 96-well plate at a density of 1 × 10^4 cells/well. Then, at 0 hour, 24 hours, 48 hours and 72 hours, 10 μL of cell counting kit-8 (CCK-8) reagent (C0037, Beyotome) and 90 μL of medium were added after the previous medium was removed. Then, the cells were incubated for 1 hours at 37 °C with 5% CO_2, and the optical density was detected at 450 nm using a microplate reader (Tecan infinite M200, Switzerland).

Transwell invasion assay

CRC cells were suspended in 200 μL of serum-free medium and seeded in the upper chambers coated with matrigel (Corning, United States). The bottom 24-well plates were filled with 600 μL of medium containing 10% FBS as a chemoattractant. After incubation for 72 hours, the cells remaining in the upper chamber were gently removed using cotton swabs, and the cells on the lower surface were photographed and counted after fixing with 4% paraformaldehyde and staining with 0.1% crystal violet.

Wound healing assay

CRC cells were cultured in 6-well plates for 24 hours, and cell transfection was performed as described above. After incubation for 48 hours, a wound was scratched with a 200 μL sterile pipette tip. The cells were then washed with PBS 3 times and incubated in a serum-free medium. Representative images were captured 0 and 24 hours after scratching. The total wound area was measured using the ImageJ software, and the relative migration rate was calculated.

Statistical analysis

Statistical programs for R software (version 4.0.3) and GraphPad Prism (version 9) were used to perform statistical analyses. Quantitative data with a normal distribution are presented as the mean ± SD and were analyzed using Student's *t*-test or one-way analysis of variance, while variables with a non-normal distribution are presented as the median and interquartile range and were compared using a Mann-Whitney *U* test or Kruskal-Wallis's test. Categorical variables were analyzed using the χ^2 test or a nonparametric test. Receiver operating characteristic curves were constructed to examine the diagnostic efficiency of RNA molecules by assessing the area under the curve. Statistical significance was set at $P < 0.05$.

RESULTS

Proteomics profiling of CRC patients

52 pairs of cancerous and matched adjacent normal tissues were collected from patients with CRC after surgical treatment for quantitative proteomic detection. 46.2% CRC patients were male, with a mean age of 64.6 ± 15.1 yeas old (Supplementary Table 1). A total of 7666 proteins were identified, and PCA demonstrated a clear separation between the CRC and normal groups (Figure 2A and B). Among these, 1960 DPEs with an FDR of < 1% were identified between the two groups (Figure 2C).

GO and KEGG enrichment analyses were performed for 1960 DEPs. GO enrichment analysis (Figure 2D) revealed the significant enrichment of various biological processes, molecular functions, and cellular components. In the biological processes, enrichment was observed in response to stimuli (oxygen-containing compounds, oxidative stress, and corticosteroids), RNA metabolic processes (ncRNA metabolic processes, rRNA metabolic processes, *etc.*), and other processes. In terms of molecular functions, enrichment was noted for binding (proteins, ions, *etc.*) and catalytic activity (acting on RNA). Among the cellular components, enrichment was found in organelles (chromosomal part, nucleolus, *etc.*), extracellular regions (extracellular space, extracellular matrix, *etc.*), and cell junctions (anchoring junction, adheres junction, *etc.*). KEGG pathway enrichment analysis (Figure 2E) indicated the activation of several pathways, including the PI3K-Akt signaling pathway, focal adhesion, cell cycle, and extracellular matrix-receptor interaction.

The enrichment of responses to stimuli in biological processes is often associated with cell death. Resistance to cell death is a crucial hallmark of cancer and the upregulation of anti-apoptotic proteins is known to promote tumor progression.

Selecting anti-apoptotic proteins in tissue proteomics profiling and TCGA database of CRC patients

To identify these anti-apoptotic proteins, 88 proteins were selected by negative regulation of apoptotic proteins based on GO enrichment analysis and were upregulated in tumor tissue (Supplementary Table 2). SHARPIN, metalloproteinase inhibitor 1 (TIMP1), nucleolar complex protein 2 homolog (NOC2 L), and DNA ligase 4 (LIG4) were significantly different among the TNM stages (Supplementary Table 3). As shown in Figure 3A, the expression of SHARPIN was significantly higher in stage III than in stage I. TIMP1 and NOC2 L expression levels were significantly higher in stage III than in stage II. With the advancement of TNM staging, the expression of SHARPIN was gradually increased, but not that of the others.

SHARPIN, TIMP1, NOC2 L, and LIG4 were further confirmed using TCGA database. As shown in Figure 3B, expect for LIG4, the expression of SHARPIN, TIMP1, NOC2 L was higher in tumor tissues than in normal tissues. As shown in Figure 3C, only SHARPIN was associated with the TNM stage. In the survival analysis, higher expression of SHARPIN and TIMP1 significantly decreased the overall survival (Figure 3D). Thus, upregulation SHARPIN was associated with the pathological stage and prognosis of CRC.

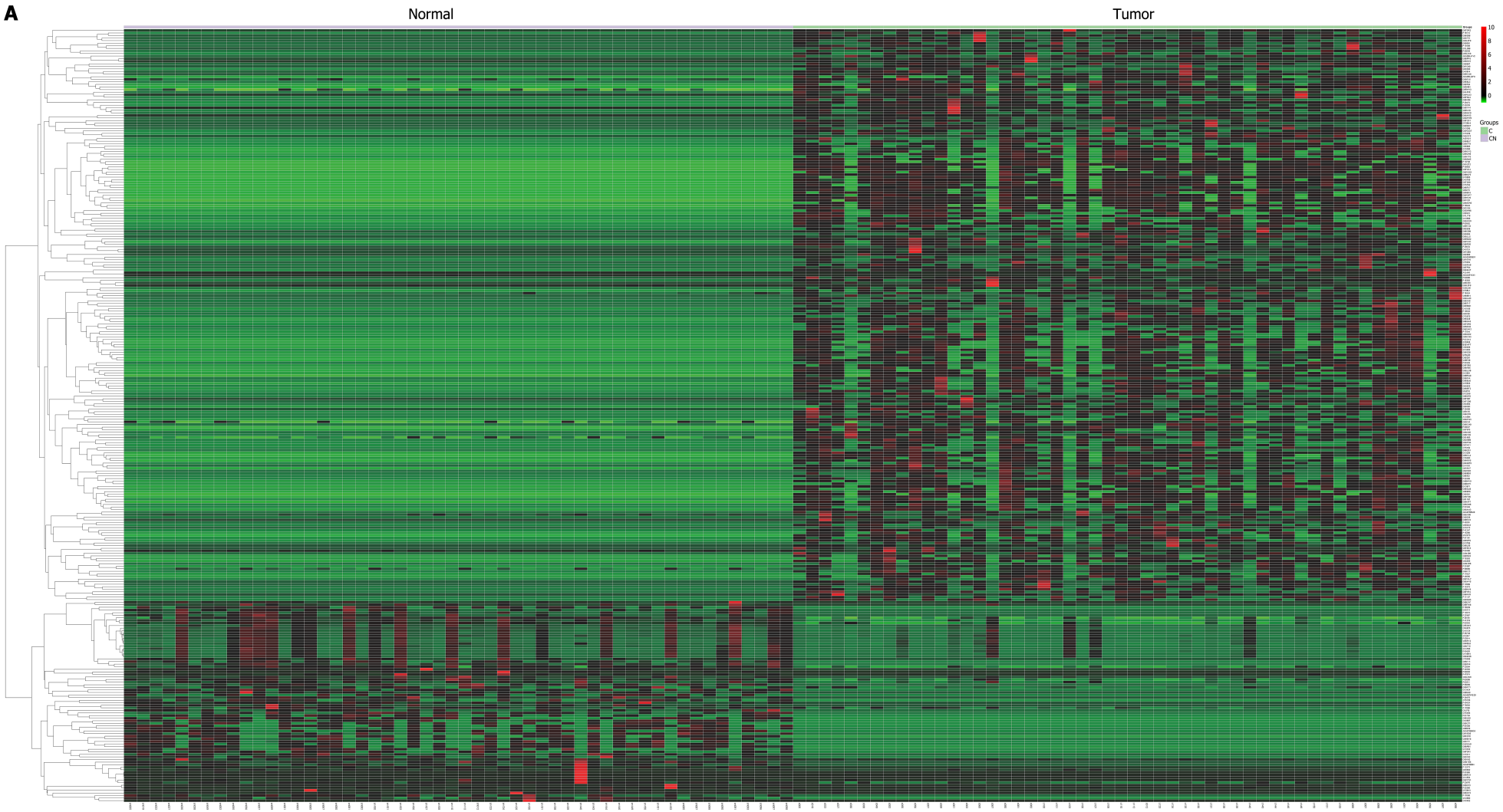
A
Normal
Tumor
10
8
6
4
2
0
Groups
C
CN

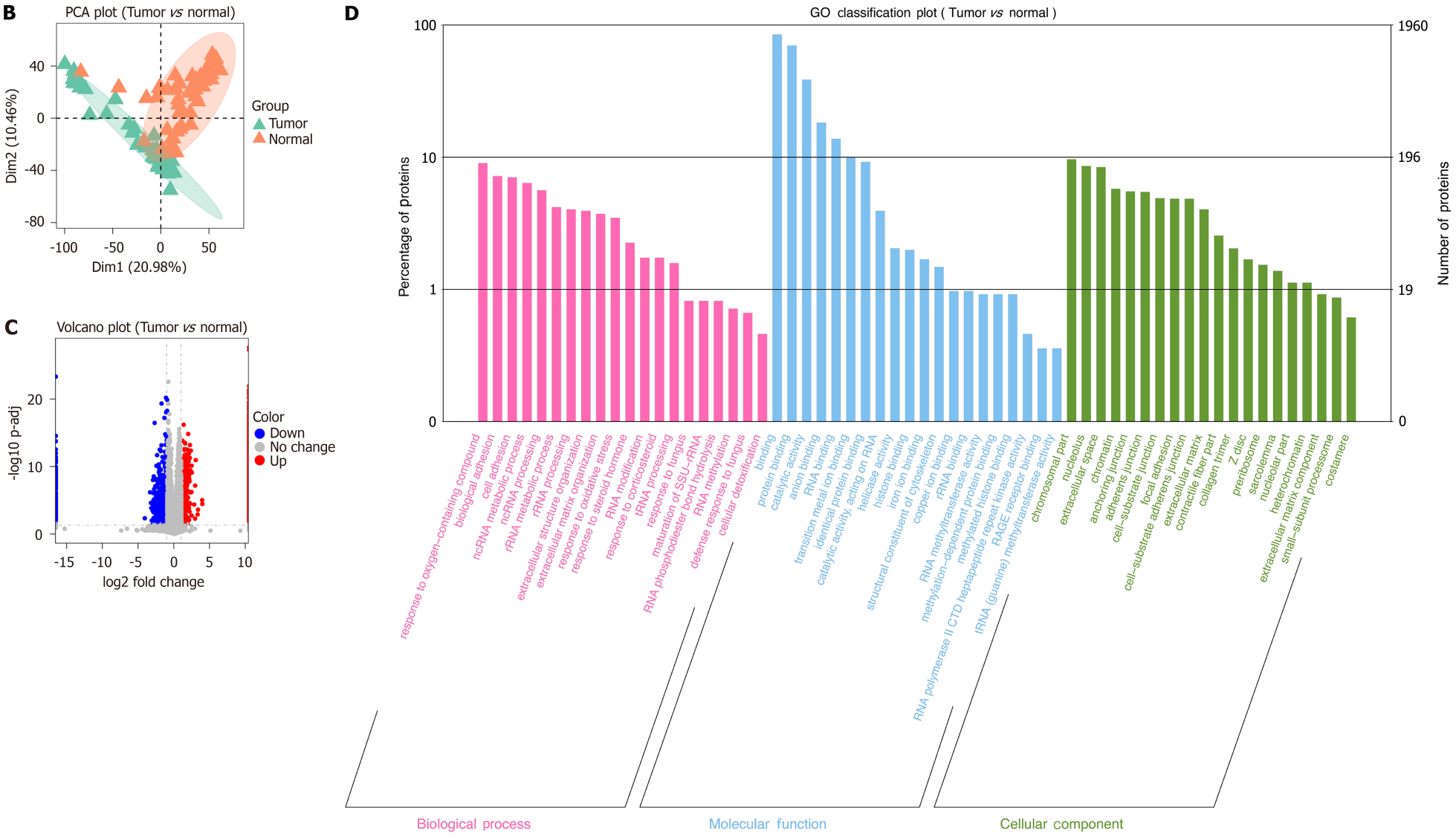
B
PCA plot (Tumor vs normal)
Dim2 (10.46%)
Dim1 (20.98%)
Group
Tumor
Normal
C
Volcano plot (Tumor vs normal)
-log10 p-adj
log2 fold change
Color
Down
No change
Up
D
GO classification plot (Tumor vs normal)
Percentage of proteins
Number of proteins
Biological process
Molecular function
Cellular component

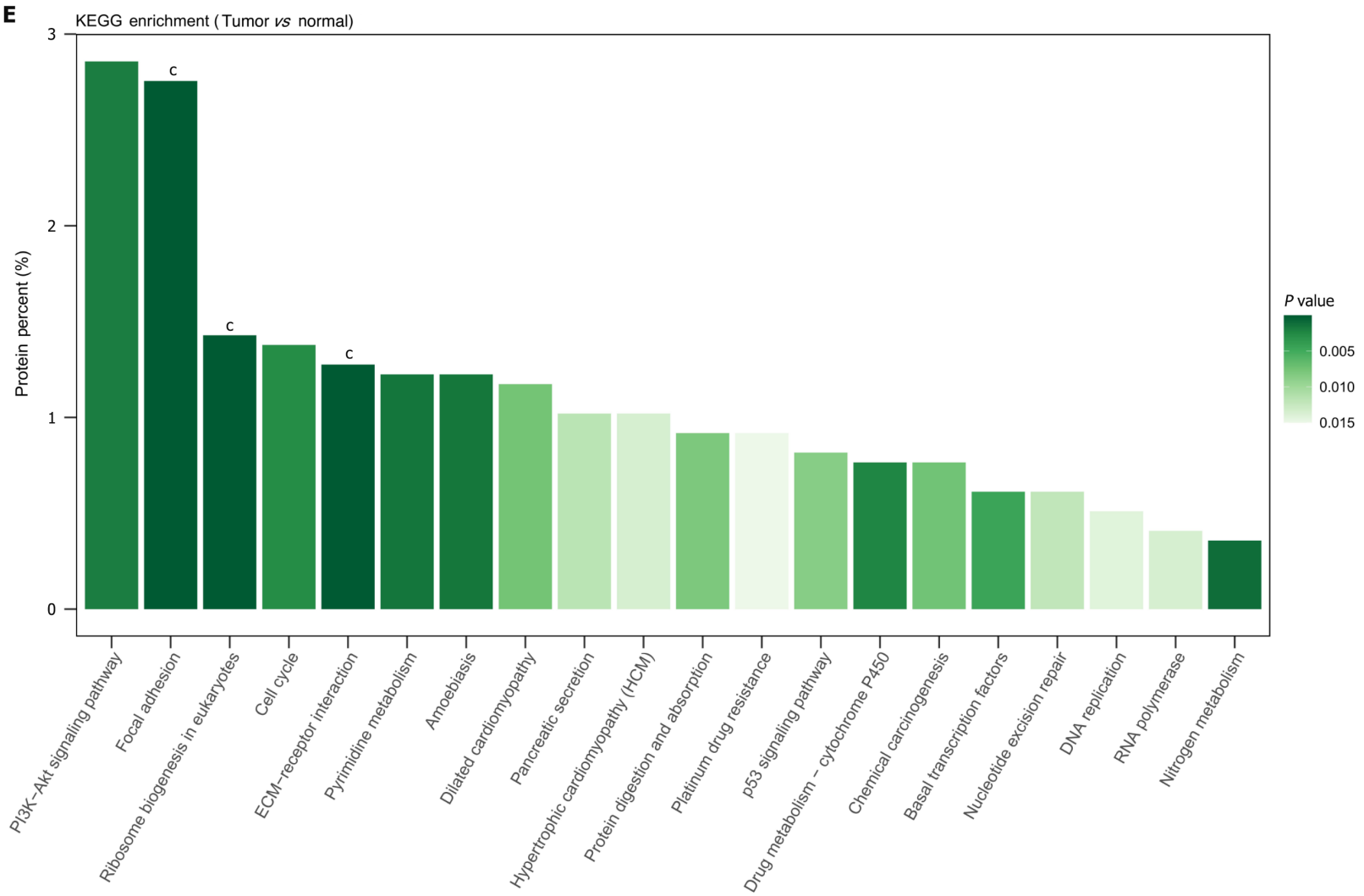

Figure 2 Proteomic profiles and bioinformatic analysis of colorectal cancer patients. A: Hierarchical cluster analysis shows the global differentially expressed proteins. Upregulated (red) and downregulated (green) differentially expressed proteins in the CRC group compared to the normal group; B: Principal component analysis shows the protein expression in the cancer tissues (green) and normal tissues (orange) of colorectal cancer (CRC) patients; C: Volcano plot shows the fold changes of identified proteins. Significantly upregulated or downregulated proteins are represented in red and blue, respectively, while proteins without significant changes are shown in gray; D: Gene Ontology analysis shows the enrichment results for differentially expressed proteins; E: Kyoto encyclopedia of genes and genomes analysis shows that differentially expressed proteins are significantly enriched in multiple pathways, °P < 0.001. CRC: Colorectal cancer; PCA: Principal component analysis; HCA: Hierarchical cluster analysis; GO: Gene ontology; KEGG: Kyoto encyclopedia of genes and genomes; PI3K-Akt: Phosphatidylinositol 3-kinase serine/threonine kinase; ECM: Extracellular matrix.

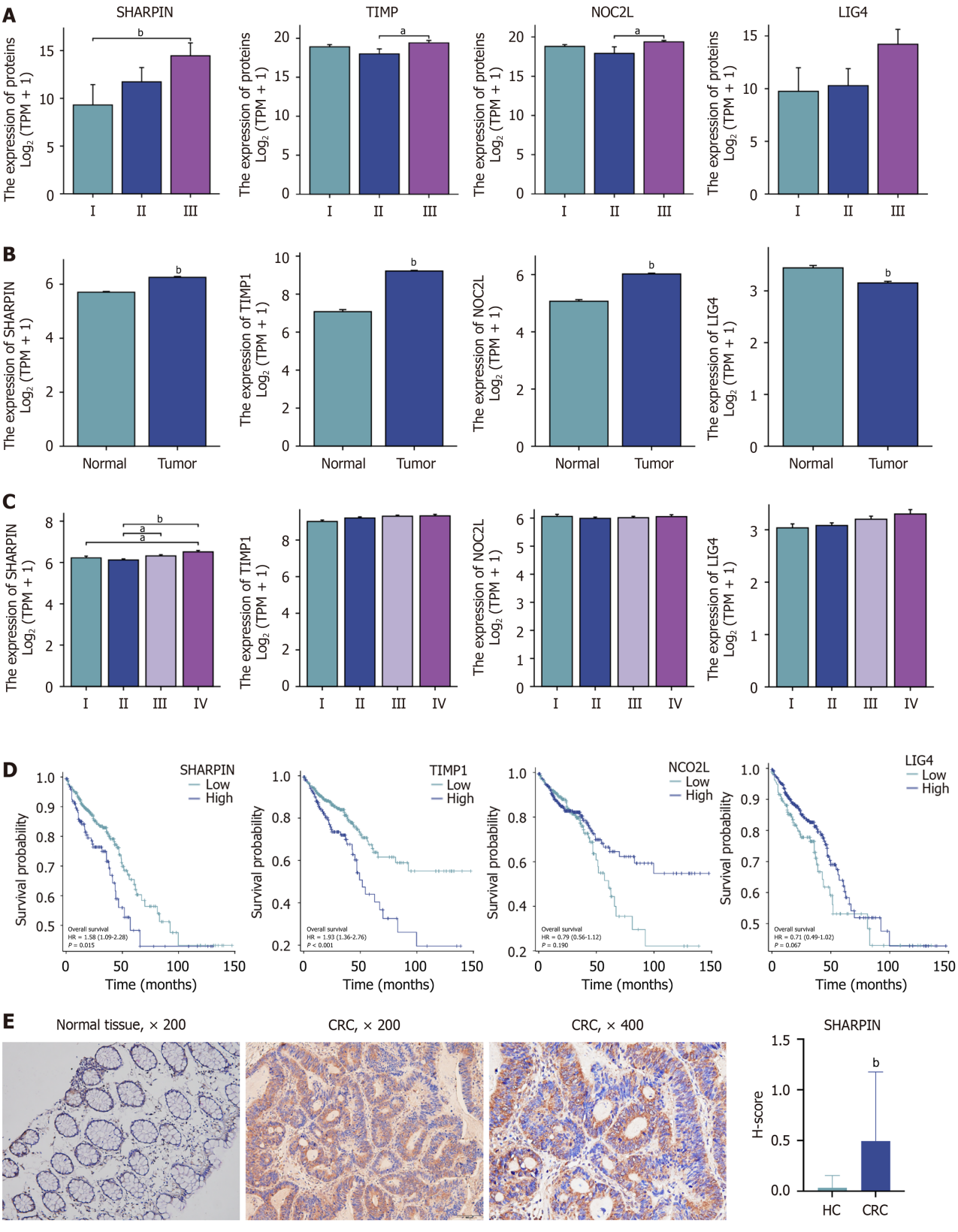

Figure 3 The expression of shank-associated RH domain interactor, metalloproteinase inhibitor 1, nucleolar complex protein 2 homolog, and DNA ligase 4 proteins and its association with tumor-node-metastasis and overall survival in colorectal cancer. A: The expression of 4 proteins among tumor-node-metastasis (TNM) stages in 52 colorectal cancer (CRC) patients; B: The expression of 4 proteins in TCGA; C: The expression of 4 proteins among TNM stages in TCGA; D: The association between expression of 4 proteins and overall survival in TCGA; E: The immunohistochemistry of shank-associated RH domain interactor in 93 CRC tissues and 35 normal tissues. $^{a}P < 0.05$; $^{b}P < 0.01$; CRC: Colorectal cancer; HC: Health control; SHARPIN: Shank-associated RH domain interactor; TIMP1: Metalloproteinase inhibitor 1; NOC2 L: Nucleolar complex protein 2 homolog; LIG4: DNA ligase 4.

High expression of SHARPIN and its association with clinicopathological characteristics in CRC

IHC was conducted to investigate the expression of SHARPIN between CRC tumor tissues (n = 93) and normal tissues (n = 35). Compared with normal tissues (Figure 3E), CRC tissues showed significantly higher SHARPIN expression (P < 0.01). SHARPIN was hardly stained in normal tissues but was highly expressed in the cytoplasm of CRC cells.

93 CRC patients were divided into two groups according to their mean H-score. As indicated in Table 1, the average age was 67.5 ± 10.9 years, and 49 participants (52.7%) were male. SHARPIN expression correlated with serum CA153 Levels, gross type, T stage, N stage, and TNM stage (all P < 0.05; Table 1).

Downregulated SHARPIN induced CRC cells apoptosis

To further investigate the effects of SHARPIN on the apoptosis of two CRC cell lines (HCT116 and SW480), siRNA was used to knockdown the expression of SHARPIN. The efficiency of SHARPIN knockdown was confirmed by Quantitative reverse transcription-PCR and western blot analysis (Supplementary Figure 1). Apoptotic cells were assessed by flow cytometry, and the expression of apoptotic proteins (Caspase 3, caspase 8, BAD, BAX, and Bcl-2) was determined by western blotting. The results showed that SHARPIN knockdown promoted apoptosis in CRC cells, as indicated by the increased proportion of apoptotic cells in the siSHARPIN group compared to that in the control group (Figure 4A; P < 0.05). Additionally, the expression levels of Caspase 3, Caspase 8, BAD, and BAX were significantly upregulated in the siSHARPIN group, whereas the expression level of Bcl-2 was downregulated in siSHARPIN + Matrine group (Figure 4B).

Matrine induced apoptosis of CRC cells by downregulating SHARPIN

Subsequently, we explored the role of SHARPIN in suppressing matrine-induced apoptosis in CRC cells. We observed the apoptosis-promoting effects of matrine in CRC cells. In CRC cell lines treated with matrine, there was a significant downregulation of SHARPIN expression (Figure 4C) and significant increase in the number of apoptotic cells (Figure 4A). The siSHARPIN + matrine group enhanced this effect. As shown in Figure 4, caspase 3 was significantly upregulated and Bcl-2 was significantly downregulated in the matrine group. Furthermore, in the siSHARPIN + matrine group, the expression of caspase 3, caspase 8, BAD, and BAX was significantly upregulated, whereas that of Bcl-2 was significantly downregulated.

Matrine inhibited progression of CRC cells by downregulating SHARPIN

Next, we examined the effects of matrine and SHARPIN knockdown on the proliferation, invasion, and migration of CRC cells. The viability of CRC cells was assessed using the CCK-8 assay, whereas cell invasion and migration were evaluated using transwell invasion and wound-healing assays, respectively.

The viability of CRC cells was significantly inhibited in the siSHARPIN, matrine, and siSHARPIN + matrine groups compared to that in the control group (P < 0.01; Figure 5A). In the transwell invasion assay, the number of invasive cells markedly decreased in the siSHARPIN, matrine, and siSHARPIN + matrine groups (Figure 5B). Furthermore, the wound healing rates of CRC cells were significantly reduced in the siSHARPIN, matrine, and siSHARPIN + matrine groups, indicating a decreased migratory capacity (Figure 5C).

DISCUSSION

The incidence and mortality rates of CRC are on the rise, and despite advances in treatment strategies, improvements in prognosis have been modest. Resistance to cell death is a critical hallmark of cancer, and there are relatively few drugs specifically designed to induce apoptosis in cancer cells. Apoptotic drugs hold promise for tumor treatment, and further exploration of molecules involved in regulating the apoptotic pathway is essential for advancing CRC therapies. In the present study, SHARPIN was both found to be upregulated in CRC tissues based on our proteomic and TCGA database and validated by IHC staining in our CRC cohort. Additionally, the expression of SHARPIN was associated with different TNM stages and a poor prognosis. *In vitro* experiments, this study demonstrated that the downregulation of SHARPIN induces apoptosis in CRC cells. Matrine treatment also induced apoptosis and inhibited the proliferation, invasion, and migration of CRC cells by downregulating SHARPIN expression. Therefore, the role of SHARPIN in CRC was initially validated in our study, providing further evidence supporting the potential of matrine in preventing CRC and colorectal adenoma. Our study identifies SHARPIN as a potential anti-apoptotic molecule, shedding light on the mechanisms of matrine's impact on CRC. Moreover, matrine has a favorable safety profile with minimal side effects. In the future, it is interesting to explore the effect of matrine in preventing tumor progression in high-risk patients.

SHARPIN is enriched at synaptic sites in mature neurons[7]. Located in the cytoplasm, SHARPIN is an approximately 40 kDa conserved protein that is ubiquitously expressed in various human tissues[8]. Furthermore, SHARPIN is amplified in some cancers, such as prostate, breast, and ovarian cancers. Zhang *et al*[9] demonstrated that upregulated SHARPIN activated the NF-κB pathway and suppressed cell apoptosis, potentially contributing to prostate cancer progression[9]. Overexpression of SHARPIN has been shown to increase the breast cancer risk[10] and promote the breast cancer progression by regulating *p53* and *ERα*[11]. Knockdown of SHARPIN expression leads to apoptosis and inhibits the proliferation, invasion, and migration of ovarian cancer cells[12]. However, the role of SHAPRIN in CRC has not yet been reported. In the present study, SHARPIN expression was significantly higher in tumor tissues than in normal tissues in our proteomic data (n = 52), TCGA database (n = 698), and IHC-confirmed cohort (n = 93). Additionally, higher SHARPIN expression was associated with poor overall survival in CRC patients compared to that in the low expression group.

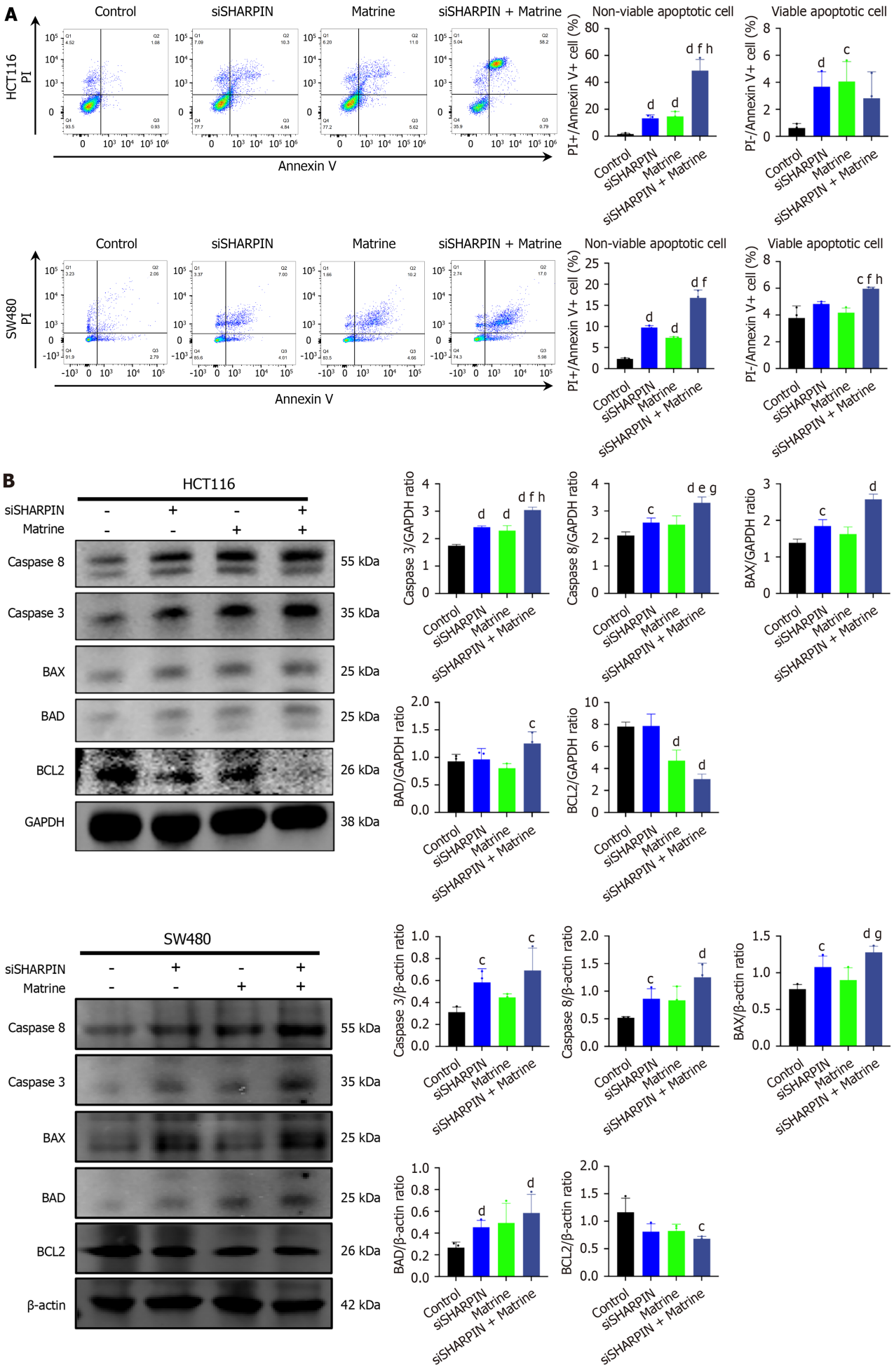
A
Control
siSHARPIN
Matrine
siSHARPIN + Matrine
HCT116
PI
Annexin V
Non-viable apoptotic cell
Viable apoptotic cell
PI+/Annexin V+ cell (%)
PI-/Annexin V+ cell (%)
SW480
B
HCT116
siSHARPIN
Matrine
Caspase 8
Caspase 3
BAX
BAD
BCL2
GAPDH
55 kDa
35 kDa
25 kDa
25 kDa
26 kDa
38 kDa
Caspase 3/GAPDH ratio
Caspase 8/GAPDH ratio
BAX/GAPDH ratio
BAD/GAPDH ratio
BCL2/GAPDH ratio
SW480
β-actin
42 kDa
Caspase 3/β-actin ratio
Caspase 8/β-actin ratio
BAX/β-actin ratio
BAD/β-actin ratio
BCL2/β-actin ratio

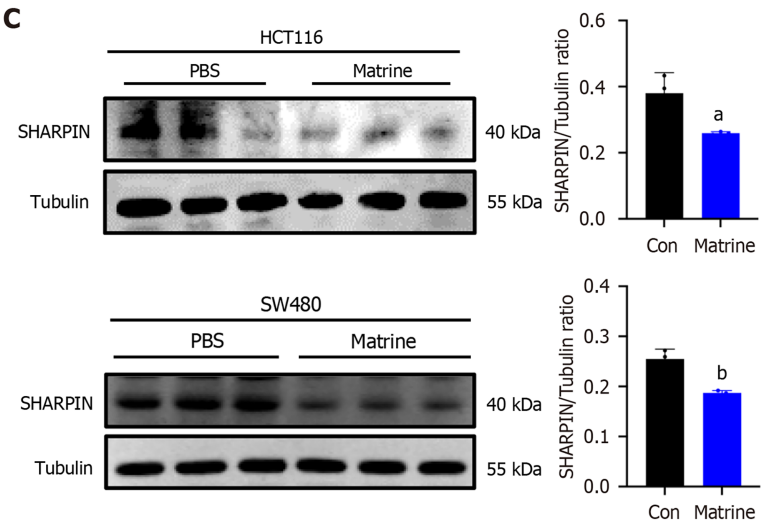

Figure 4 Matrine induces apoptosis and regulates apoptotic proteins by downregulating shank-associated RH domain interactor. A: The apoptosis rate of colorectal cancer (CRC) cells in 4 groups [control group (con group), SHARPIN knockdown group (siSHARPIN group), matrine, siSHARPIN + matrine]; B: The expression of caspase 3, caspase 8, B-cell lymphoma-2 (Bcl-2) associated X protein, Bcl-2 associated agonist of cell death, Bcl-2 proteins in CRC cells in 4 groups; C: The suppressing effect of matrine on shank-associated RH domain interactor (SHARPIN) in CRC cells. $^{a}P < 0.05$; $^{b}P < 0.01$; $^{c}P < 0.05$ *vs* con, $^{d}P < 0.01$ *vs* con; $^{e}P < 0.05$ *vs* siSHARPIN, $^{f}P < 0.01$ *vs* siSHARPIN; $^{g}P < 0.05$ *vs* matrine, $^{h}P < 0.01$ *vs* matrine; Con: Control group; siSHARPIN: SHARPIN knockdown group; matrine: Matrine group; siSHARPIN + matrine: Matrine and SHARPIN knockdown group; CRC: Colorectal cancer; SHARPIN: Shank-associated RH domain interactor; Bcl-2: B-cell lymphoma-2; BAD: Bcl-2 associated agonist of cell death; BAX: Bcl-2 associated X protein.

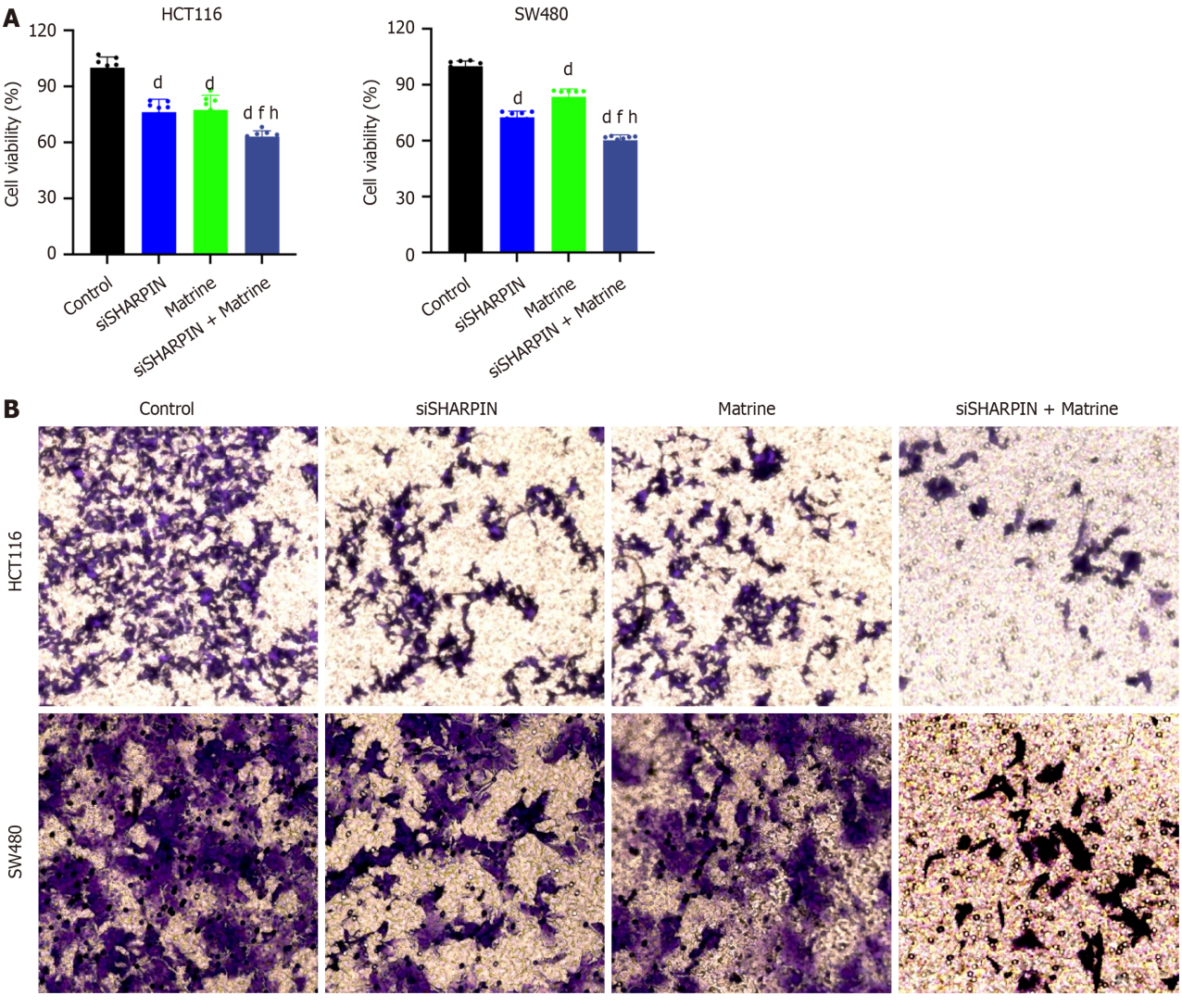

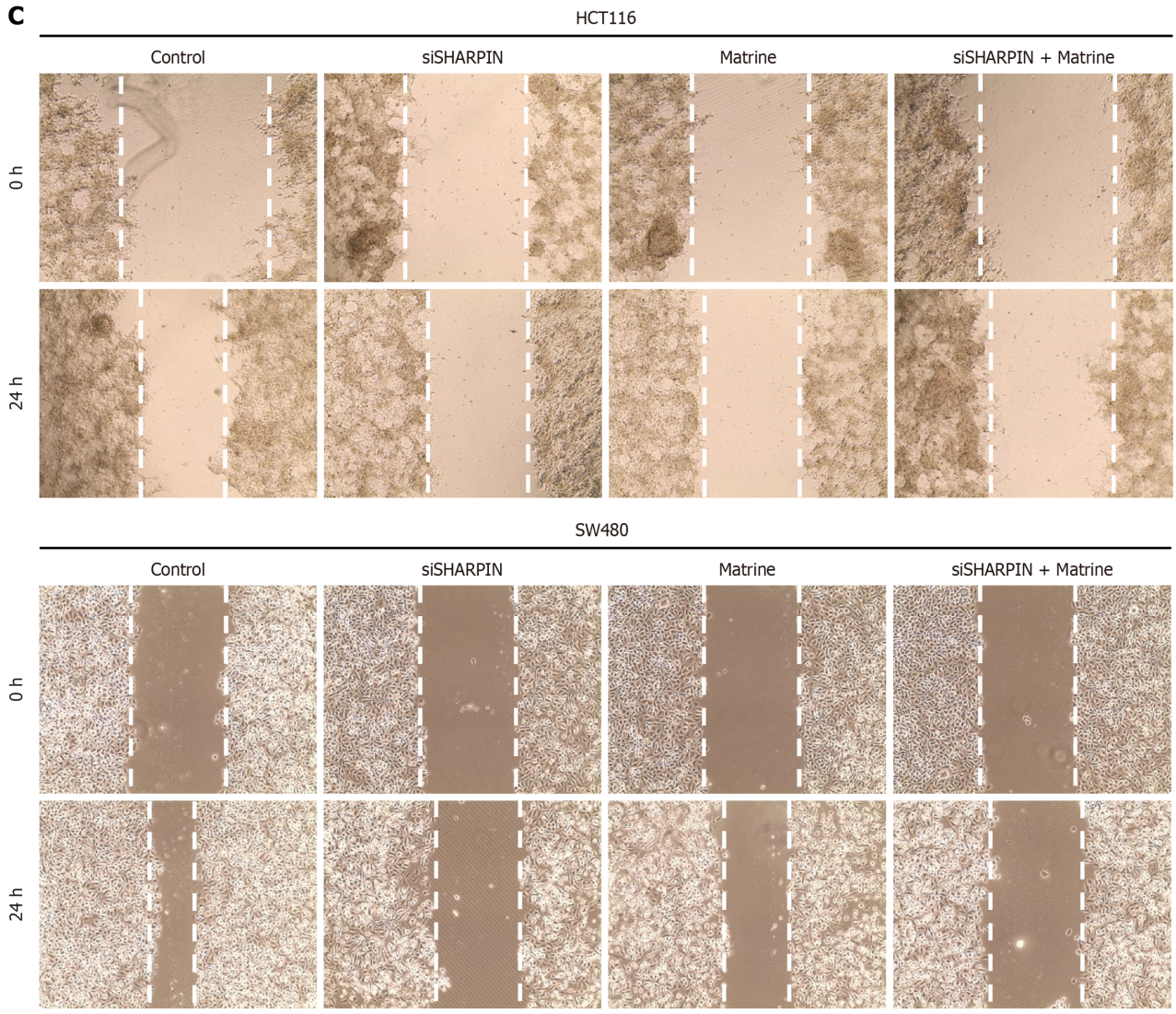

Figure 5 Matrine impedes proliferation, invasion and migration in colorectal cancer by downregulating shank-associated RH domain interactor. A: The viability of colorectal cancer (CRC) cells using the cell counting kit-8 assay in 4 groups [control (con), si-Shank-associated RH domain interactor (SHARPIN), matrine, siSHARPIN + matrine]; B: The invasion cells of CRC in 4 groups; C: The wound healing of CRC cells in 4 groups. $^{c}P < 0.05$ *vs* con, $^{d}P < 0.01$ *vs* con; $^{e}P < 0.05$ *vs* siSHARPIN, $^{f}P < 0.01$ *vs* siSHARPIN; $^{g}P < 0.05$ *vs* matrine, $^{h}P < 0.01$ *vs* matrine; Con: Control group; SHARPIN: Shank-associated RH domain interactor; siSHARPIN: SHARPIN knockdown group; matrine: Matrine group; siSHARPIN + matrine: Matrine and SHARPIN knockdown group; CRC: Colorectal cancer.

In a 14-year-old boy, a homozygous deficiency of SHARPIN led to a shift in signaling from pro-survival to cell death in immune cells, contributing to an observed discrepancy in immune function[13]. Because of the effect of SHARPIN deficiency on cell death, knockdown expression of SHARPIN may induce apoptosis in cancer. As the component of the linear ubiquitin chain activation complex, SHARPIN plays an important role in inflammatory response and apoptosis by regulating canonical NF-κB signaling[8,14,15]. For anti-tumor effect, NF-kB pathway was activated by SHARPIN overexpression with upregulated anti-apoptosis proteins in prostate cancer[9,16]. As a *p53* mediator, SHARPIN may facilitate its degradation or ubiquitination in a mouse double minute 2 homolog-dependent manner[17], which is an inhibitor of *p53* transcriptional activation[18]. SHARPIN is a negative regulator of PTEN in human tumor cell lines and primary cervical cancer cells both *in vitro* and *in vivo*. SHARPIN activates the PI3K/AKT pathway and induces tumorigenesis by interacting with PTEN.

Matrine is an alkaloid isolated from the traditional Chinese medicine, Sophora flavescens Aiton. In China, matrine injections are used to treat hepatitis. Owing to its anti-inflammatory effects, matrine also exhibits antitumor properties, especially apoptosis. Previous studies have shown that matrine inducs autophagy and apoptosis by downregulating β-catenin and mediating the JNK-Bcl-2/Bcl-xL-Bax/Bak pathway in hepatocellular carcinoma cells[19,20]. In CRC cells, matrine induces apoptosis by regulating associated proteins. Zhang *et al*[21] demonstrated matrine reduce the ratio of Bcl-2/Bax and increase caspase-9 *in vitro*. Gu *et al*[22] explored effects of matrine on Bcl-2, Bax and caspase-3 in several cell lines. And Chang *et al*[23] showed that matrine activated apoptosis by regulating BAX,Bcl-2 and Cyto C. However, the precise mechanism underlying the matrine-induced apoptosis in CRC cells remains unclear. In the current study, we found that matrine induced cell apoptosis by inhibiting SHARPIN expression, while also repressing the proliferation, invasion, and migration of CRC cells. Targeted SHARPIN drugs might lead to various adverse effects, while matrine

Table 1 Clinicalpathological charateristics of colorectal cancer according to Shank-associated RH domain interactor expression, *n* (%)

Variables	Total (*n* = 93)	Low (*n* = 50)	High (*n* = 43)	*P* value
Sex, male	49 (52.7)	28 (56)	21 (48.8)	0.49
Age, years	67.5 ± 10.9	67.4 ± 10.6	67.7 ± 11.4	0.89
Location				0.38
Left	75 (80.6)	42 (84)	33 (76.7)	
Right	18 (19.4)	8 (16)	10 (23.3)	
Gross type				0.03
Fungating	32 (34.4)	21 (42)	11 (25.6)	
Ulceroinfiltrative	54 (58.1)	23 (46)	31 (72.1)	
Ulcerofungating	7 (7.5)	6 (12)	1 (2.3)	
Differentiation				0.443
Poor	10 (11.1)	3 (10.3)	4 (12.5)	
Moderate	70 (77.8)	21 (72.4)	26 (81.2)	
Well	10 (11.1)	5 (17.2)	2 (6.2)	
Tumor size, ≥ 5 cm	48 (51.6)	24 (48)	24 (55.8)	0.45
Histopathologic type				0.76
AC	79 (84.9)	43 (86)	36 (83.7)	
MAC	14 (15.1)	7 (14)	7 (16.3)	
Venous invasion	21 (22.6)	10 (20)	11 (25.6)	0.52
Perineural invasion	48 (51.6)	24 (48)	24 (55.8)	0.45
MSI	7 (7.5)	3 (6)	4 (9.3)	0.70
T stage				0.02
1	4 (4.3)	4 (8)	0 (0)	
2	17 (18.3)	13 (26)	4 (9.3)	
3	60 (64.5)	29 (58)	31 (72.1)	
4	12 (12.9)	4 (8)	8 (18.6)	
N stage				0.02
0	63 (67.7)	40 (80)	23 (53.5)	
1	18 (19.4)	7 (14)	11 (25.6)	
2	12 (12.9)	3 (6)	9 (20.9)	
M stage				0.09
0	87 (93.5)	49 (98)	38 (88.4)	
1	6 (6.5)	1 (2)	5 (11.6)	
TNM stage				0.01
I	20 (21.5)	16 (32)	4 (9.3)	
II	41 (44.1)	22 (44)	19 (44.2)	
III	26 (28.0)	11 (22)	15 (34.9)	
IV	6 (6.5)	1 (2)	5 (11.6)	
CA125, ng/mL	9.0 (7.0, 14.5)	9.0 (7.0, 14.5)	9.0 (7.1, 13.7)	0.96
CA199, U/mL	14.1 (9.2, 24.0)	14.5 (8.0, 23.0)	13.6 (10.0, 26.0)	0.97
CA724, U/mL	1.7 (1.5, 4.7)	1.9 (1.5, 4.9)	1.6 (1.5, 2.8)	0.61
CEA, ng/mL	4.8 (2.5, 11.1)	5.5 (2.6, 11.5)	3.5 (2.5, 8.8)	0.26

CA153, U/mL	8.1 (6.0, 12.4)	7.2 (5.3, 10.6)	9.2 (6.9, 13.3)	0.04

Two groups were divided the mean of the H-score. AC: Adenocarcinoma; MAC: Mucinous adenocarcinoma; MSI: Microsatellite instability; CEA Carcinoembryonic antigen; CA199: Carbohydrate antigen 19-9; CA724: Carbohydrate antigen 724; TNM: Tumor-node-metastasis.

shows potential in multiple therapeutic roles, making it a promising candidate for treatment.

Our study has some limitations. First, the follow-up time of the enrolled 52 patients was not available, and the association between SHARPIN expression and CRC survival needs to be investigated in Chinese population. Second, the therapeutic effects of matrine on CRC need to be validated *in vivo* and in clinical trials. Matrine injection has been used to improve hepatitis; however, the dosage of matrine that inhibits tumor progression remains to be explored. Third, the mechanism of matrine repressing SHARPIN expression remains to be conducted in the further study.

CONCLUSION

In conclusion, this study identified overexpressed SHARPIN in CRC tissues. High expression SHARPIN is associated with TNM stage and poor prognosis. Matrine promotes cell apoptosis and inhibits proliferation, invasion, and migration by repressing SHARPIN expression in CRC. Thus, matrine could be considered as a novel therapeutic agent for CRC.

ACKNOWLEDGEMENTS

The authors thank Wei-Liang Sun (China-Japan Friendship Hospital, Beijing, PhD) and Tian-Hui Zhou (Graduate School of Beijing University of Chinese Medicine, Beijing University of Chinese Medicine, MD) for their technical assistance.

FOOTNOTES

Author contributions: Zhou YC conceived and designed the study, performed sample collection, experiments, acquired and analyzed data, and prepared the original draft; Wang QQ, Zhou GY, Zhao DY, Yin TF, Tan C, and Sun XZ participated in sample acquisition, data analysis, and manuscript revision; All authors read and approved the final manuscript. Both Yao SK and Zhou L have played important and indispensable roles in the experimental design, data interpretation and manuscript preparation as the co-corresponding authors. Yao SK applied for and obtained the funds for this research project.

Supported by National Key Development Plan for Precision Medicine Research, No. 2017YFC0910002.

Institutional review board statement: The study was reviewed and approved by the Clinical Research Ethics Committee of the China-Japan Friendship Hospital (No. 2018-116-K85).

Conflict-of-interest statement: The authors declare that the research was conducted in the absence of any commercial or financial relationships that could be construed as potential conflicts of interest.

Data sharing statement: Technical appendix, statistical code, and dataset available from the corresponding author at shukunyao@126.com.

Country of origin: China

ORCID number: Yuan-Chen Zhou 0000-0001-6024-6246; Qian-Qian Wang 0000-0002-7709-2121; Ge-Yu-Jia Zhou 0000-0002-4196-1436; Teng-Fei Yin 0000-0003-1140-8637; Dong-Yan Zhao 0000-0002-7026-068X; Xi-Zhen Sun 0000-0001-9967-5726; Chang Tan 0000-0002-0969-1851; Shu-Kun Yao 0000-0002-8512-2589.

S-Editor: Li L
L-Editor: A
P-Editor: Zhao S

REFERENCES

1 **Sung H**, Ferlay J, Siegel RL, Laversanne M, Soerjomataram I, Jemal A, Bray F. Global Cancer Statistics 2020: GLOBOCAN Estimates of Incidence and Mortality Worldwide for 36 Cancers in 185 Countries. *CA Cancer J Clin* 2021; **71**: 209-249 [PMID: 33538338 DOI: 10.3322/caac.21660]

2 **Zeng H**, Chen W, Zheng R, Zhang S, Ji JS, Zou X, Xia C, Sun K, Yang Z, Li H, Wang N, Han R, Liu S, Li H, Mu H, He Y, Xu Y, Fu Z, Zhou Y, Jiang J, Yang Y, Chen J, Wei K, Fan D, Wang J, Fu F, Zhao D, Song G, Chen J, Jiang C, Zhou X, Gu X, Jin F, Li Q, Li Y, Wu T, Yan C, Dong J, Hua Z, Baade P, Bray F, Jemal A, Yu XQ, He J. Changing cancer survival in China during 2003-15: a pooled analysis of 17 population-based cancer registries. *Lancet Glob Health* 2018; **6**: e555-e567 [PMID: 29653628 DOI: 10.1016/S2214-109X(18)30127-X]

3 **Hanahan D**. Hallmarks of Cancer: New Dimensions. *Cancer Discov* 2022; **12**: 31-46 [PMID: 35022204 DOI: 10.1158/2159-8290.CD-21-1059]

4 **Prakash A**, Peterman S, Ahmad S, Sarracino D, Frewen B, Vogelsang M, Byram G, Krastins B, Vadali G, Lopez M. Hybrid data acquisition and processing strategies with increased throughput and selectivity: pSMART analysis for global qualitative and quantitative analysis. *J Proteome Res* 2014; **13**: 5415-5430 [PMID: 25244318 DOI: 10.1021/pr5003017]

5 **Liu J**, Lichtenberg T, Hoadley KA, Poisson LM, Lazar AJ, Cherniack AD, Kovatich AJ, Benz CC, Levine DA, Lee AV, Omberg L, Wolf DM, Shriver CD, Thorsson V; Cancer Genome Atlas Research Network, Hu H. An Integrated TCGA Pan-Cancer Clinical Data Resource to Drive High-Quality Survival Outcome Analytics. *Cell* 2018; **173**: 400-416.e11 [PMID: 29625055 DOI: 10.1016/j.cell.2018.02.052]

6 **Zhang X**, Xu H, Bi X, Hou G, Liu A, Zhao Y, Wang G, Cao X. Src acts as the target of matrine to inhibit the proliferation of cancer cells by regulating phosphorylation signaling pathways. *Cell Death Dis* 2021; **12**: 931 [PMID: 34642304 DOI: 10.1038/s41419-021-04221-6]

7 **Seymour RE**, Hasham MG, Cox GA, Shultz LD, Hogenesch H, Roopenian DC, Sundberg JP. Spontaneous mutations in the mouse Sharpin gene result in multiorgan inflammation, immune system dysregulation and dermatitis. *Genes Immun* 2007; **8**: 416-421 [PMID: 17538631 DOI: 10.1038/sj.gene.6364403]

8 **Wang Z**, Potter CS, Sundberg JP, Hogenesch H. SHARPIN is a key regulator of immune and inflammatory responses. *J Cell Mol Med* 2012; **16**: 2271-2279 [PMID: 22452937 DOI: 10.1111/j.1582-4934.2012.01574.x]

9 **Zhang Y**, Huang H, Zhou H, Du T, Zeng L, Cao Y, Chen J, Lai Y, Li J, Wang G, Guo Z. Activation of nuclear factor κB pathway and downstream targets survivin and livin by SHARPIN contributes to the progression and metastasis of prostate cancer. *Cancer* 2014; **120**: 3208-3218 [PMID: 24925528 DOI: 10.1002/cncr.28796]

10 **De Melo J**, Tang D. Elevation of SIPL1 (SHARPIN) Increases Breast Cancer Risk. *PLoS One* 2015; **10**: e0127546 [PMID: 25992689 DOI: 10.1371/journal.pone.0127546]

11 **Tian Z**, Tang J, Yang Q, Li X, Zhu J, Wu G. Atypical ubiquitin-binding protein SHARPIN promotes breast cancer progression. *Biomed Pharmacother* 2019; **119**: 109414 [PMID: 31518875 DOI: 10.1016/j.biopha.2019.109414]

12 **Wang G**, Zhuang Z, Cheng J, Yang F, Zhu D, Jiang Z, Du W, Shen S, Huang J, Hua L, Chen Y. Overexpression of SHARPIN promotes tumor progression in ovarian cancer. *Exp Mol Pathol* 2022; 104806 [PMID: 35798064 DOI: 10.1016/j.yexmp.2022.104806]

13 **Oda H**, Manthiram K, Chavan PP, Rieser E, Veli Ö, Kaya Ö, Rauch C, Nakabo S, Kuehn HS, Swart M, Wang Y, Çelik NI, Molitor A, Ziaee V, Movahedi N, Shahrooei M, Parvaneh N, Alipour-Olyei N, Carapito R, Xu Q, Preite S, Beck DB, Chae JJ, Nehrebecky M, Ombrello AK, Hoffmann P, Romeo T, Deuitch NT, Matthíasardóttir B, Mullikin J, Komarow H, Stoddard J, Niemela J, Dobbs K, Sweeney CL, Anderton H, Lawlor KE, Yoshitomi H, Yang D, Boehm M, Davis J, Mudd P, Randazzo D, Tsai WL, Gadina M, Kaplan MJ, Toguchida J, Mayer CT, Rosenzweig SD, Notarangelo LD, Iwai K, Silke J, Schwartzberg PL, Boisson B, Casanova JL, Bahram S, Rao AP, Peltzer N, Walczak H, Lalaoui N, Aksentijevich I, Kastner DL. Biallelic human SHARPIN loss of function induces autoinflammation and immunodeficiency. *Nat Immunol* 2024; **25**: 764-777 [PMID: 38609546 DOI: 10.1038/s41590-024-01817-w]

14 **Tokunaga F**, Nakagawa T, Nakahara M, Saeki Y, Taniguchi M, Sakata S, Tanaka K, Nakano H, Iwai K. SHARPIN is a component of the NF-κB-activating linear ubiquitin chain assembly complex. *Nature* 2011; **471**: 633-636 [PMID: 21455180 DOI: 10.1038/nature09815]

15 **Ikeda F**, Deribe YL, Skånland SS, Stieglitz B, Grabbe C, Franz-Wachtel M, van Wijk SJ, Goswami P, Nagy V, Terzic J, Tokunaga F, Androulidaki A, Nakagawa T, Pasparakis M, Iwai K, Sundberg JP, Schaefer L, Rittinger K, Macek B, Dikic I. SHARPIN forms a linear ubiquitin ligase complex regulating NF-κB activity and apoptosis. *Nature* 2011; **471**: 637-641 [PMID: 21455181 DOI: 10.1038/nature09814]

16 **Li J**, Lai Y, Cao Y, Du T, Zeng L, Wang G, Chen X, Chen J, Yu Y, Zhang S, Zhang Y, Huang H, Guo Z. SHARPIN overexpression induces tumorigenesis in human prostate cancer LNCaP, DU145 and PC-3 cells *via* NF-κB/ERK/Akt signaling pathway. *Med Oncol* 2015; **32**: 444 [PMID: 25550157 DOI: 10.1007/s12032-014-0444-3]

17 **Yang H**, Yu S, Wang W, Li X, Hou Y, Liu Z, Shi Y, Mu K, Niu G, Xu J, Wang H, Zhu J, Zhuang T. SHARPIN Facilitates p53 Degradation in Breast Cancer Cells. *Neoplasia* 2017; **19**: 84-92 [PMID: 28063307 DOI: 10.1016/j.neo.2016.12.002]

18 **Lessel D**, Wu D, Trujillo C, Ramezani T, Lessel I, Alwasiyah MK, Saha B, Hisama FM, Rading K, Goebel I, Schütz P, Speit G, Högel J, Thiele H, Nürnberg G, Nürnberg P, Hammerschmidt M, Zhu Y, Tong DR, Katz C, Martin GM, Oshima J, Prives C, Kubisch C. Dysfunction of the MDM2/p53 axis is linked to premature aging. *J Clin Invest* 2017; **127**: 3598-3608 [PMID: 28846075 DOI: 10.1172/JCI92171]

19 **Xie BS**, He XX, Ai ZL, Yao SK. Involvement of β-catenin in matrine-induced autophagy and apoptosis in WB-F344 cells. *Mol Med Rep* 2014; **9**: 2547-2553 [PMID: 24718323 DOI: 10.3892/mmr.2014.2107]

20 **Yang J**, Yao S. JNK-Bcl-2/Bcl-xL-Bax/Bak Pathway Mediates the Crosstalk between Matrine-Induced Autophagy and Apoptosis *via* Interplay with Beclin 1. *Int J Mol Sci* 2015; **16**: 25744-25758 [PMID: 26516844 DOI: 10.3390/ijms161025744]

21 **Zhang S**, Cheng B, Li H, Xu W, Zhai B, Pan S, Wang L, Liu M, Sun X. Matrine inhibits proliferation and induces apoptosis of human colon cancer LoVo cells by inactivating Akt pathway. *Mol Biol Rep* 2014; **41**: 2101-2108 [PMID: 24452711 DOI: 10.1007/s11033-014-3059-z]

22 **Gu YY**, Chen MH, May BH, Liao XZ, Liu JH, Tao LT, Man-Yuen Sze D, Zhang AL, Mo SL. Matrine induces apoptosis in multiple colorectal cancer cell lines in vitro and inhibits tumour growth with minimum side effects *in vivo via* Bcl-2 and caspase-3. *Phytomedicine* 2018; **51**: 214-225 [PMID: 30466620 DOI: 10.1016/j.phymed.2018.10.004]

23 **Chang C**, Liu SP, Fang CH, He RS, Wang Z, Zhu YQ, Jiang SW. Effects of matrine on the proliferation of HT29 human colon cancer cells and its antitumor mechanism. *Oncol Lett* 2013; **6**: 699-704 [PMID: 24137393 DOI: 10.3892/ol.2013.1449]

World Journal of Gastrointestinal Oncology

Submit a Manuscript: https://www.f6publishing.com

World J Gastrointest Oncol 2024 December 15; 16(12): 4716-4727

DOI: 10.4251/wjgo.v16.i12.4716

ISSN 1948-5204 (online)

ORIGINAL ARTICLE

Basic Study

Enhancing the radiosensitivity of colorectal cancer cells by reducing spermine synthase through promoting autophagy and DNA damage

Yu-Bin Guo, Yue-Ming Wu, Zhi-Zhao Lin

Specialty type: Oncology

Provenance and peer review: Unsolicited article; Externally peer reviewed.

Peer-review model: Single blind

Peer-review report's classification

Scientific Quality: Grade C
Novelty: Grade C
Creativity or Innovation: Grade B
Scientific Significance: Grade B

P-Reviewer: Lane M

Received: June 17, 2024
Revised: September 3, 2024
Accepted: October 18, 2024
Published online: December 15, 2024
Processing time: 148 Days and 4.4 Hours

Yu-Bin Guo, Yue-Ming Wu, Zhi-Zhao Lin, Guangdong Provincial Key Laboratory of Gastroenterology, Department of Gastroenterology, Nanfang Hospital, Southern Medical University, Guangzhou 510515, Guangdong Province, China

Corresponding author: Yu-Bin Guo, PhD, Attending Doctor, Guangdong Provincial Key Laboratory of Gastroenterology, Department of Gastroenterology, Nanfang Hospital, Southern Medical University, No. 1838 Guangzhou Avenue North, Guangzhou 510515, Guangdong Province, China. 928526639@qq.com

Abstract

BACKGROUND

Colorectal cancer (CRC), the third most common cancer worldwide, has increasingly detrimental effects on human health. Radiotherapy resistance diminishes treatment efficacy. Studies suggest that spermine synthase (SMS) may serve as a potential target to enhance the radiosensitivity.

AIM

To investigate the association between SMS and radiosensitivity in CRC cells, along with a detailed elucidation of the underlying mechanisms.

METHODS

Western blot was adopted to assess SMS expression in normal colonic epithelial cells and CRC cell lines. HCT116 cells were transfected with control/SMS-specific shRNA or control/pcDNA3.1-SMS plasmids. Assessments included cell viability, colony formation, and apoptosis *via* MTT assays, colony formation assays, and flow cytometry. Radiosensitivity was studied in SMS-specific shRNA-transfected HCT116 cells post-4 Gy radiation, evaluating cell viability, colony formation, apoptosis, DNA damage (comet assays), autophagy (immunofluorescence), and mammalian target of rapamycin (mTOR) pathway protein expression (western blot).

RESULTS

Significant up-regulation of SMS expression levels was observed in the CRC cell lines. Upon down-regulation of SMS expression, cellular viability and colony-forming ability were markedly suppressed, concomitant with a notable increase in apoptotic indices. Furthermore, attenuation of SMS expression significantly augmented the sensitivity of HCT116 cells to radiation therapy, evidenced by a pronounced elevation in levels of cellular DNA damage and autophagy. Impor-

tantly, down-regulation of SMS corresponded with a marked reduction in the expression levels of proteins associated with the mTOR signaling pathway.

CONCLUSION

Knocking down SMS attenuates the mTOR signaling pathway, thereby promoting cellular autophagy and DNA damage to enhance the radiosensitivity of CRC cells.

Key Words: Spermine synthase; Colorectal cancer; Radiosensitivity; Autophagy; DNA damage

Core Tip: This study highlighted spermine synthase (SMS) as a pivotal molecule regulating DNA damage and autophagy in cancer cells. SMS promoted DNA repair and activated the mammalian target of rapamycin signaling pathway, resulting in the inhibition of cellular autophagy. Collectively, SMS emerges as a promising therapeutic target to enhance colorectal cancer radiosensitivity, providing novel insights into the development of colorectal cancer treatment strategies.

Citation: Guo YB, Wu YM, Lin ZZ. Enhancing the radiosensitivity of colorectal cancer cells by reducing spermine synthase through promoting autophagy and DNA damage. *World J Gastrointest Oncol* 2024; 16(12): 4716-4727
URL: https://www.wjgnet.com/1948-5204/full/v16/i12/4716.htm
DOI: https://dx.doi.org/10.4251/wjgo.v16.i12.4716

INTRODUCTION

Globally, colorectal cancer (CRC) ranks third in prevalence among cancers, constituting about 10% of all newly diagnosed cancer cases. In 2022, the global incidence of CRC was estimated at 1.9 million new cases, with mortality rates reaching as high as 900000[1]. As age advances, the risk of developing CRC grows, with individuals aged 65 and older exhibiting substantially higher incidence rates compared to other age groups. However, in recent years, there has also been an observed rise in CRC incidence among younger populations[2]. Known risk factors for CRC include genetics, dietary habits (such as high-fat, low-fiber diets), obesity, smoking, alcohol consumption, and lack of physical activity[3]. Currently, the foremost therapy for early-stage CRC is surgical resection. It is worth noting that, in addition to surgery, chemotherapy and radiotherapy are often necessary for advanced CRC. Nevertheless, early-stage CRC typically presents with few noticeable symptoms, making it easily overlooked. Hence, the majority of CRC patients also require radiotherapy[4]. More terribly, a portion of CRC patients exhibit resistance to radiation therapy, leading to poor treatment outcomes. Approximately 20% of patients with locally advanced rectal cancer are inherently insensitive to radiotherapy. As for patients with metastatic CRC, the proportion of insensitivity may be even higher[5]. Studies indicate that the reasons for CRC's resistance to radiation therapy include genetic mutations and enhanced DNA repair capabilities. Mutations in genes such as KRAS and BRAF may render tumor cells insensitive to radiation[6]. Furthermore, some tumor cells possess highly efficient DNA damage repair capabilities, which can diminish the cytotoxic effects of radiation[7]. To overcome the challenge of radiation insensitivity, researchers have proposed various strategies, including the use of combined chemotherapy and screening for radiosensitizers, *etc.*[8]. Among these strategies, the screening of radiosensitizers has shown tremendous potential.

Evidence from research shows that spermine synthase (SMS) has a pivotal role in polyamine metabolism. Polyamine compounds such as spermine not only participate in the regulation of growth and development in organisms but also correlate with physiological processes like cell apoptosis and proliferation[9]. Spermine can also protect DNA from damage and plays a role in antioxidant stress and ion channel regulation[10]. It is known that SMS is a group of key enzymes associated with the synthesis of polyamines such as spermine, spermidine, and putrescine in organisms[11,12]. Polyamines and spermine are essential for maintaining cell growth and proliferation. Additionally, polyamines act as important scavengers of intracellular free radicals, alleviating oxidative stress in tumor cells[13]. In various tumor cells, the expression levels of SMS are significantly elevated, thereby promoting spermine synthesis. Elevated levels of spermine can accelerate the tumor cell proliferation, and increased expression of SMS can promote the proliferation of CRC[14]. Recent studies have revealed a correlation between the expression levels of SMS and cancer development. Fahrmann *et al*[15] discovered a correlation between plasma spermidine levels and distant metastasis risk in patients with triple-negative breast cancer. Velenosi *et al*[16] proposed that diacetylspermine could serve as a biomarker for predicting the development and progression of triple-negative breast cancer. Additionally, research indicates a down-regulation in spermine levels in prostate cancer tissue, and such a down-regulation is considered an indicator of the transition from normal prostate tissue to malignant tissue[17]. Other studies have found that SMS is upregulated in pancreatic cancer, promoting cancer cell proliferation and migration, and is associated with poorer overall survival[18]. Snezhkina *et al*[19] identified dysregulated spermine metabolism in CRC. Some studies propose that during the development of CRC, SMS collaborates with the MYC protein (an oncogene associated with cell proliferation) to suppress the expression of the *Bim* gene[14]. This collaboration is believed to sustain the survival of CRC cells and enhance their malignant behavior. Other

studies have found that SMS is overexpressed in CRC, and targeting SMS inhibition induces lipid metabolism reprogramming and ferroptosis, significantly inhibiting the growth of CRC cells[20]. Notably, some research has demonstrated that inhibiting spermine biosynthesis can render cells more sensitive to radiation damage[21]. Mivechi *et al*[22] in 1986 claimed that inhibitors of ornithine decarboxylase such as alpha-difluoromethylornithine could increase radiation-induced inter-strand DNA crosslink damage, thereby enhancing the radiosensitivity of cancer cells. The aforementioned findings emphasize the importance of SMS in the occurrence and progression of CRC, suggesting its potential role as a key regulator of cellular sensitivity to radiotherapy. Therefore, this study aimed to clarify the link between SMS and the radiosensitivity of CRC cells, elucidating its mechanisms and providing insights for improving the treatment of CRC.

MATERIALS AND METHODS

Cell culture and grouping

Normal colonic epithelial cells FHC (CRL-1831), CRC cell line HCT116 (CRL-247), SW62, SW480, HT-29 and LoVo cells were both purchased from WHELAB. The culture of FHC cells was performed in a DMEM/F12 medium comprising 10% fetal bovine serum, 100 μg/mL streptomycin, and 100 U/mL penicillin; HCT116, SW62, SW480, HT-29 and LoVo cells culture were finished in a RPMI1640 medium under the same conditions. Cells were maintained in a humidified environment at 37 °C with 50 mL/L CO_2. When cells reached 80%-90% confluence, they were rinsed twice *via* phosphate-buffered saline (PBS), detached through 2.5 g/L trypsin-EDTA solution, and passaged. Cell grouping was initiated at the third passage. HCT116 cells were transfected with SMS shRNA (sh-SMS) and negative control shRNA (shNC) using Lipofectamine 3000 (L3000001, ThermoFisher, USA). Over-expression of SMS was achieved by transfecting HCT116 cells with SMS over-expression vector (OE-SMS) or negative control vector (OE-NC). HCT116 cells transfected with sh-SMS and shNC were subjected to a 4 Gy X-ray dose. Subsequent biological assays were performed after completion of the radiation treatment. The sequence for sh-SMS was 5′-CCGGCGCTTTAAAGAACAGCCTTTACTCGAGTAAAGGCTGT TCTTTAAAGC GTTTTT-3′, and the sequence for shNC was 5′-CCGGCAACAAGATGAAGAGCACCAACTC GAGTTG-GTGCTCTTCATCTTGTTG-3′.

MTT assay

In 96-well plates, HCT116 cells were plated at a density of 5000 cells per well, with three replicate wells per condition. The plates were then incubated in a humidified incubator at 37 °C with 50 mL/L CO_2 until the cells adhered completely. Subsequently, the cells were transfected or subjected to radiation treatment. Following that, the plates were returned to the incubator. At 24, 48, and 72 hours post-treatment, each well received 20 μL of MTT solution (5 mg/mL, ml057897, mlbio, China), and the cells underwent another four hours of incubation. Following the removal of the culture medium, 150 μL of dimethyl sulfoxide was provided for dissolving the MTT crystals. Ultimately, the absorbance (OD) of each well was measured using a microplate reader (Varioskan LUX, ThermoFisher, United States) at a wavelength of 490 nm.

Colony formation assay

HCT116 cells in the logarithmic growth phase were collected for transfection or radiation treatment. Following two washes utilizing PBS, cells were digested *via* 2.5 g/L trypsin-EDTA solution and subsequently cleaned twice with PBS to terminate digestion. Later, the cell samples were suspended in a complete medium containing 3-4 g/L agarose to create single-cell suspensions. Next, 2 mL of the cell suspension, with a density of 1000 cells per well, was supplemented into each well of a 6-well plate. The plate was then cultured in a humidified atmosphere at 37 °C with 50 mL/L CO_2 for 2-3 weeks. Following culture, the cells were gently washed *via* PBS, stained utilizing 5 g/L crystal violet for 30 minutes, and then washed again with PBS. Lastly, cell colonies with a diameter ≥ 50 μm were observed and computed under an inverted microscope (BDS400, OPTEC, China).

Flow cytometry

HCT116 cells were cultured in a humidified atmosphere at 37 °C with 50 mL/L CO_2, followed by transfection or radiation treatment. After treatment, cells were detached using trypsin and collected into centrifuge tubes. They were then stained using fluorescein isothiocyanate (FITC)-conjugated Annexin V (Annexin V-FITC) and propidium iodide (PI) from the Annexin V Apoptosis Detection Kit (E606336, Sangon, China). Annexin V-FITC bound to exposed phosphatidylserine on the outer membrane of early apoptotic cells, while PI entered late apoptotic/necrotic cells with compromised membranes. Finally, a flow cytometer (CytoFLEX, Beckman, Germany) was utilized to analyze the cells stained to detect and analyze apoptotic cells.

Comet assay

The comet assay, utilizing a Comet Assay Kit (C2041M, Beyotime, China), was employed to assess the level of DNA damage in HCT116 cells following transfection or radiation treatment. Cells were detached using trypsin and collected into centrifuge tubes. Low-melting agarose was added, and the mixture was spread onto slides to form a gel. A high-salt solution was applied to remove cell membranes and most proteins, followed by alkaline buffer to unwind DNA strands. Under an electric field (voltage 25 V), damaged DNA fragments migrated towards the anode, forming a "comet" shape. Subsequently, DNA was stained using PI (Ex/Em = 535/617 nm), and comet tail DNA level and comet tail length were observed under a fluorescence microscope (BX43, Olympus, Japan).

Immunofluorescence

The treated HCT116 cells were washed twice through PBS and fixed *via* 40 g/L paraformaldehyde for 30 minutes to preserve cell structure and antigenicity. Upon two PBS washes, the cells were permeabilized *via* 4 g/L Triton X-100 for 30 minutes, given two times of washes *via* PBS again, and then incubated with 50 g/L bovine serum albumin to block non-specific binding sites. Afterwards, the cells were incubated overnight at a low temperature with Alexa Fluor® 488 Rabbit monoclonal anti-LC3 antibody (1:500, Ex/Em = 495 nm/519 nm, ab225382, Abcam, United Kingdom). After washing twice by virtue of PBS, cell samples were stained with a nuclear dye (DAPI, Ex/Em = 364 nm/454 nm, C1005, Beyotime, China) for 5 minutes and washed twice with PBS. Eventually, LC3 puncta were observed under a fluorescence microscope (BX43, Olympus, Japan), and the proportion of LC3-positive cells was analyzed.

Western blot

FHC, HCT116, SW62, SW480, HT-29 and LoVo cells, along with HCT116 cells transfected or treated with radiation, were lysed using RIPA buffer. The protein concentration was determined utilizing a bicinchoninic acid assay kit. Upon mixing with SDS-PAGE loading buffer, the samples were denatured at 95 °C for 5 minutes. Denatured protein samples were loaded onto SDS-PAGE gels and isolated by electrophoresis. Following this, the samples were shifted from the gel to the polyvinylidene fluoride membrane by electroblotting. Then, 50 g/L bovine serum albumin solution was offered to block the membrane for 1 hour. Later, the membrane was subject to an overnight incubation with primary antibodies specific to the target proteins, including SMS (1:1000, ab151547, Abcam, United Kingdom), γH2AX (1:1000, ab124781, Abcam, United Kingdom), p-γH2AX (1:1000, ab81299, Abcam, United Kingdom), ATR (1:1000, ab2905, Abcam, United Kingdom), p-ATR (1:1000, ab289363, Abcam, United Kingdom), P53 (1:1000, ab26, Abcam, United Kingdom), LC3-I (1:1000, ab52628, Abcam, United Kingdom), LC3-II (1:1000, ab63817, Abcam, United Kingdom), p62 (1:1000, ab109012, Abcam, United Kingdom), Beclin 1 (1:1000, ab207612, Abcam, United Kingdom), mammalian target of rapamycin (mTOR, 1:1000, ab134903, Abcam, United Kingdom), p-mTOR (1:1000, ab109268, Abcam, United Kingdom), S6K1 (1:1000, ab32359, Abcam, United Kingdom), p-S6K1 (1:1000, ab59208, Abcam, United Kingdom), S6 (1:1000, ab250753, Abcam, United Kingdom), p-S6 (1:1000, ab2571, Abcam, United Kingdom), β-actin (1:1000, ab8227, Abcam, United Kingdom). Subsequently, the membrane was provided an incubation with HRP-conjugated secondary antibodies, including HRP Anti-Rabbit IgG antibody (1:5000, ab288151, Abcam, United Kingdom) and HRP Goat Anti-Mouse IgG (1:5000, ab6708, Abcam, United Kingdom). Further, a chemiluminescent substrate solution (P0211, Beyotime, China) was offered to initiate enzyme-linked secondary antibody reaction. The luminescence of the proteins was scanned using a ChemiDoc™ MP Imaging System (BioRed, United States).

Statistical analysis

The experiments were conducted with three independent replicates. Independent sample *t*-tests (between two groups) or one-way analysis of variance (among multiple groups) were performed using SPSS version 25. Data were displayed as mean ± SEM, with a significance threshold of $P < 0.05$. In addition, graphs were generated using GraphPad Prism 8.

RESULTS

Elevated SMS expression promotes proliferation and reduces apoptosis in CRC cells

Initially, a detection was performed on the expression of SMS in normal colonic epithelial cells (FHC) and the CRC cell line HCT116, SW62, SW480, HT-29 and LoVo. The detection results disclosed that the protein expression levels of SMS were notable elevated in HCT116, SW62, SW480, HT-29 and LoVo cells in contrast to FHC cells. Additionally, SMS expression in HCT116 cells was higher than in SW62, SW480, HT-29, and LoVo cells (Figure 1A). For observing the impact of SMS expression levels on cell radiosensitivity, we established HCT116 cell groups with SMS knockdown or over-expression (Figure 1B). Subsequently, we observed the influence of diverse SMS expression levels on cell viability, colony formation ability, and apoptosis levels. The observational outcomes showed that relative to the shNC group, the viability and colony formation ability of HCT116 cells in the sh-SMS group were remarkably cut down, but the apoptosis level was increased. In contrast, compared to the OE-NC group, the viability and colony formation ability of HCT116 cells in the OE-SMS group were increased, while the apoptosis level was significantly decreased (Figure 1C-E). These results indicated that increased expression of SMS in HCT116 promoted cell proliferation and inhibited apoptosis.

Down-regulation of SMS enhances the radiosensitivity of HCT116 cells, inhibits cell proliferation, and promotes apoptosis

Although it is known that the activity of SMS can affect the sensitivity of CRC cells to radiotherapy, increased activity of SMS can lead to increased resistance of CRC cells to radiation. Additionally, SMS is involved in various reactions, but the mechanism of action of SMS on radiotherapy sensitivity is not yet clear. Therefore, we observed the effect of down-regulating SMS expression on cellular radiosensitivity. After altering the expression levels of SMS, cells were treated utilizing a dose of 4 Gy X-rays, and cell colony formation ability, viability, and apoptosis levels were assessed. The assessment outcomes exhibited that X-rays reduced cell viability and colony formation ability but encouraged apoptosis. Briefly, compared to the shNC + Ionizing radiation (IR) group, the viability and colony formation ability of HCT116 cells in the sh-SMS + IR group were significantly reduced, while the apoptosis levels were increased (Figure 2). Thus, down-regulation of SMS enhanced the radiosensitivity of HCT116 cells, inhibited cell proliferation, and promoted apoptosis.

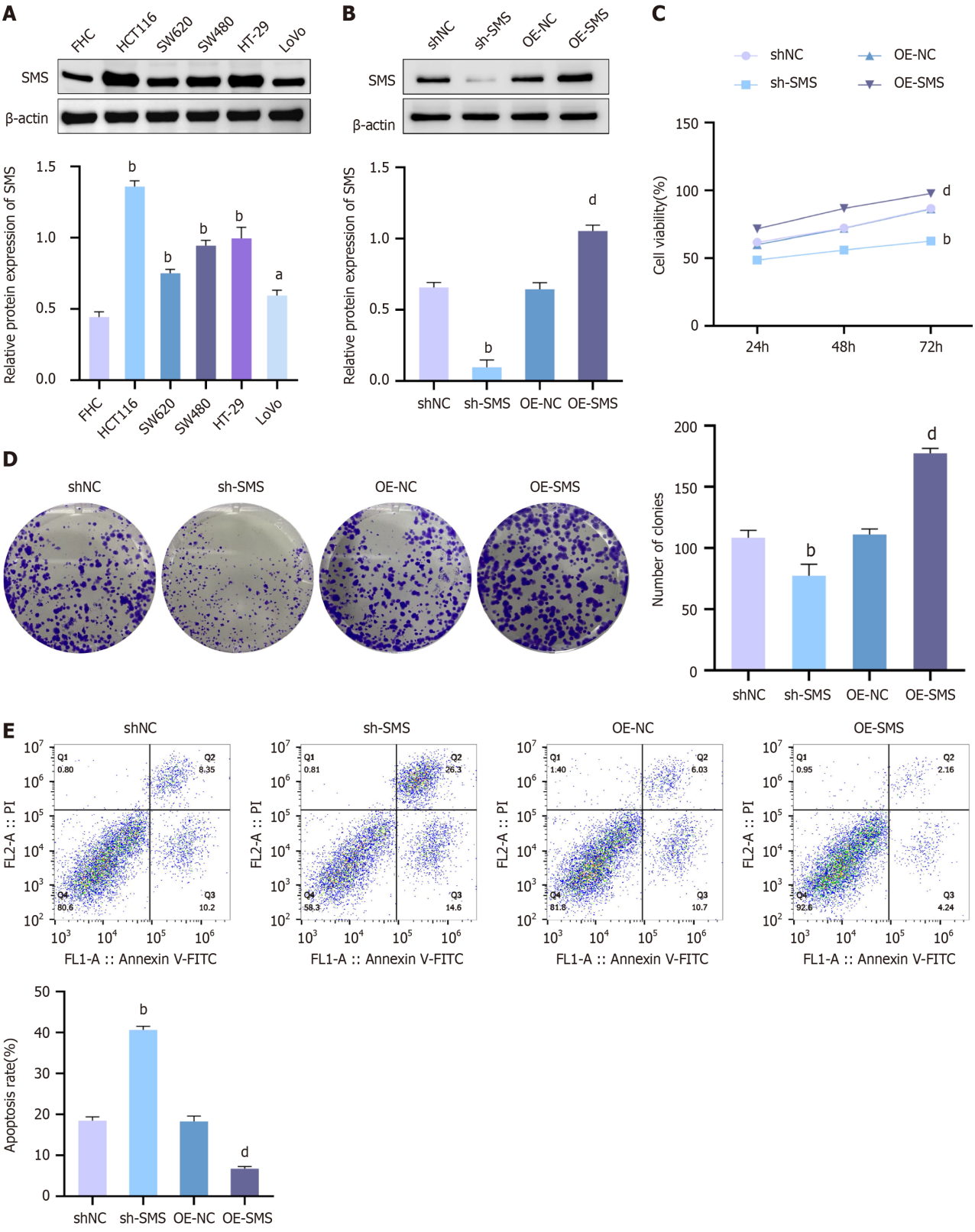

Figure 1 Up-regulation of spermine synthase in colorectal cancer cells HCT116 promotes cell proliferation and inhibits apoptosis. A and B: Western blot analysis for spermine synthase (SMS) protein expression levels in FHC, HCT116, SW62, SW480, HT-29 and LoVo cells groups (A), as well as in negative control shRNA (shNC), SMS shRNA (sh-SMS), negative control over-expression vector (OE-NC), and OE-SMS HCT116 cell groups (B); C: MTT assay to detect the viability of cells in shNC, sh-SMS, OE-NC, and OE-SMS HCT116 groups; D: Colony formation assay to assess the colony formation ability of cells in shNC, sh-SMS, OE-NC, and OE-SMS HCT116 groups; E: Flow cytometry analysis of cell apoptosis levels in shNC, sh-SMS, OE-NC, and OE-SMS HCT116 groups. $^{a}P<0.05$, $^{b}P<0.01$ *vs* FHC, shNC; $^{d}P<0.01$ *vs* OE-NC; SMS: Spermine synthase; sh-SMS: Spermine synthase shRNA; shNC: Negative control shRNA; OE-SMS: Spermine synthase over-expression vector; OE-NC: Negative control over-expression vector.

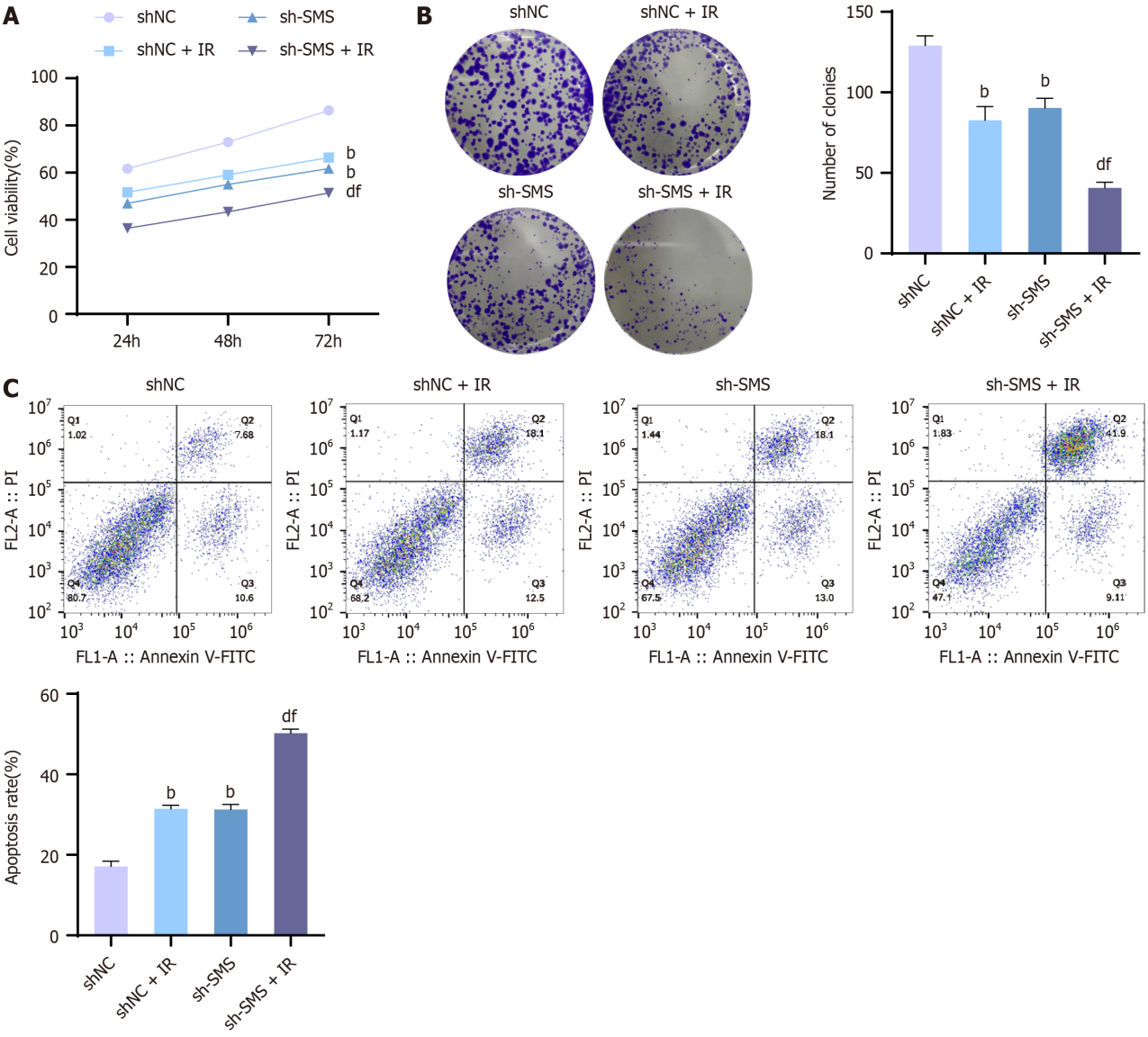

Figure 2 Down-regulation of spermine synthase enhances the radiosensitivity of HCT116 cells, inhibits cell proliferation, and promotes apoptosis. A: MTT assay to detect the viability of HCT116 cells in the negative control shRNA (shNC) group, shNC + IR group, spermine synthase shRNA (sh-SMS) group, and sh-SMS + IR group; B: Colony formation assay to assess the colony formation ability of HCT116 cells in the shNC group, shNC + IR group, sh-SMS group, and sh-SMS + IR group; C: Flow cytometry analysis to measure the apoptosis levels of HCT116 cells in the shNC group, shNC + IR group, sh-SMS group, and sh-SMS + IR group. ^{b}P < 0,01 *vs* shNC, ^{d}P < 0.01 *vs* shNC + IR, ^{f}P < 0.01 *vs* sh-SMS; SMS: Spermine synthase; sh-SMS: Spermine synthase shRNA; shNC: Negative control shRNA; OE-SMS: Spermine synthase over-expression vector; OE-NC: Negative control over-expression vector.

Knocking down SMS enhances the radiosensitivity of HCT116 cells by promoting DNA damage

Research has already indicated that knocking down SMS leads to DNA damage and impedes DNA repair processes[23,24]. To examine the relationship between SMS and radiation-induced DNA damage in cancer cells, HCT116 cells were treated *via* a dose of 4 Gy X-rays following SMS knockdown. The comet assay was employed to determine the extent of DNA damage in HCT116 cells, and the western blot assay was recruited to analyze the expression of DNA damage-related proteins (γH2AX, p-γH2AX, ATR, p-ATR, P53). Our comet assay results revealed an increase in DNA damage levels in HCT116 cells following down-regulation of SMS expression, including notable elevations in comet tail DNA levels and comet tail moments. Compared to the shNC + IR or sh-SMS groups, the sh-SMS + IR group exhibited markedly elevated DNA damage levels in HCT116 cells, along with increased comet tail DNA levels and comet tail moments (Figure 3A-C). Moreover, knocking down SMS expression resulted in significant up-regulation of p-γH2AX, p-ATR, and P53 protein levels in HCT116 cells. Importantly, when compared to the shNC + IR or sh-SMS groups, the sh-SMS + IR group displayed substantially raised γH2AX, p-γH2AX, p-ATR, and P53 protein levels in HCT116 cells (Figure 3D and E). In a nutshell, knocking down SMS enhanced the radiosensitivity of HCT116 cells through supporting DNA damage.

Knocking down SMS enhances the radiosensitivity of HCT116 cells by promoting autophagy

While the correlation between SMS and DNA damage has been established, autophagy also serves as a mechanism of cell death induced by radiation therapy[25,26]. It is worth noting that the relationship between SMS and cellular autophagy

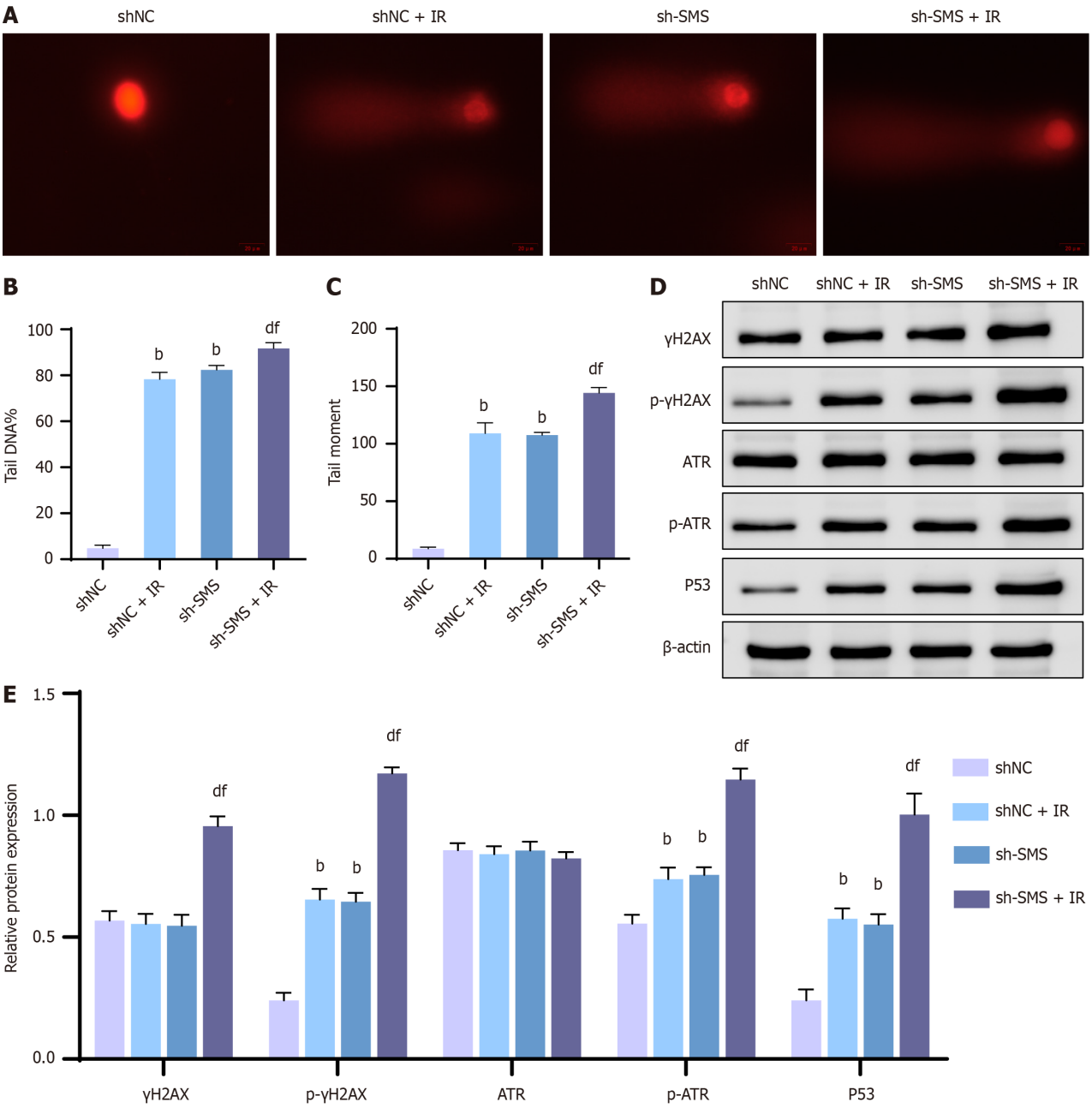

Figure 3 Knockdown of spermine synthase enhances the radiosensitivity of HCT116 cells by advancing DNA damage. A-C: Comet assay for assessing DNA damage levels in HCT116 cells of the negative control shRNA (shNC), shNC + IR, spermine synthase shRNA (sh-SMS), and sh-SMS + IR groups (A), and analysis of comet tail DNA levels (B) and comet tail moments (C); D and E: Western blot analysis of γH2AX, p-γH2AX, ATR, p-ATR, and P53 protein levels in HCT116 cells of the shNC group, shNC + IR group, sh-SMS group, and sh-SMS + IR group. $^{b}P < 0,01$ *vs* shNC, $^{d}P < 0.01$ *vs* shNC + IR, $^{f}P < 0.01$ *vs* sh-SMS; SMS: Spermine synthase; sh-SMS: Spermine synthase shRNA; shNC: Negative control shRNA; OE-SMS: Spermine synthase over-expression vector; OE-NC: Negative control over-expression vector.

remains controversial[27,28]. Therefore, immunofluorescence and western blot analysis of autophagy-related protein expression were performed to observe the level of cellular autophagy after knocking down SMS expression. Immunofluorescence results revealed an increase in the number of LC3 puncta and the proportion of LC3-positive cells following SMS knockdown. Moreover, compared to the shNC + IR or sh-SMS groups, the sh-SMS + IR group displayed a marked increase in the number of LC3 puncta and the proportion of LC3-positive cells (Figure 4A and B). Additionally, western blot analysis revealed an escalation in the protein levels of LC3-I, LC3-II, and Beclin 1, along with a down-regulation in p62 protein levels, and an up-regulation in the LC3-II/LC3-I ratio following SMS knockdown. Importantly, compared to the shNC + IR or sh-SMS groups, the sh-SMS + IR group exhibited significantly elevated protein levels of LC3-I, LC3-II, and Beclin 1, decreased p62 protein levels, and down-regulated ratio of LC3-II/LC3-I (Figure 4C and D). These results indicated that knocking down SMS enhanced the radiosensitivity of HCT116 cells by promoting autophagy.

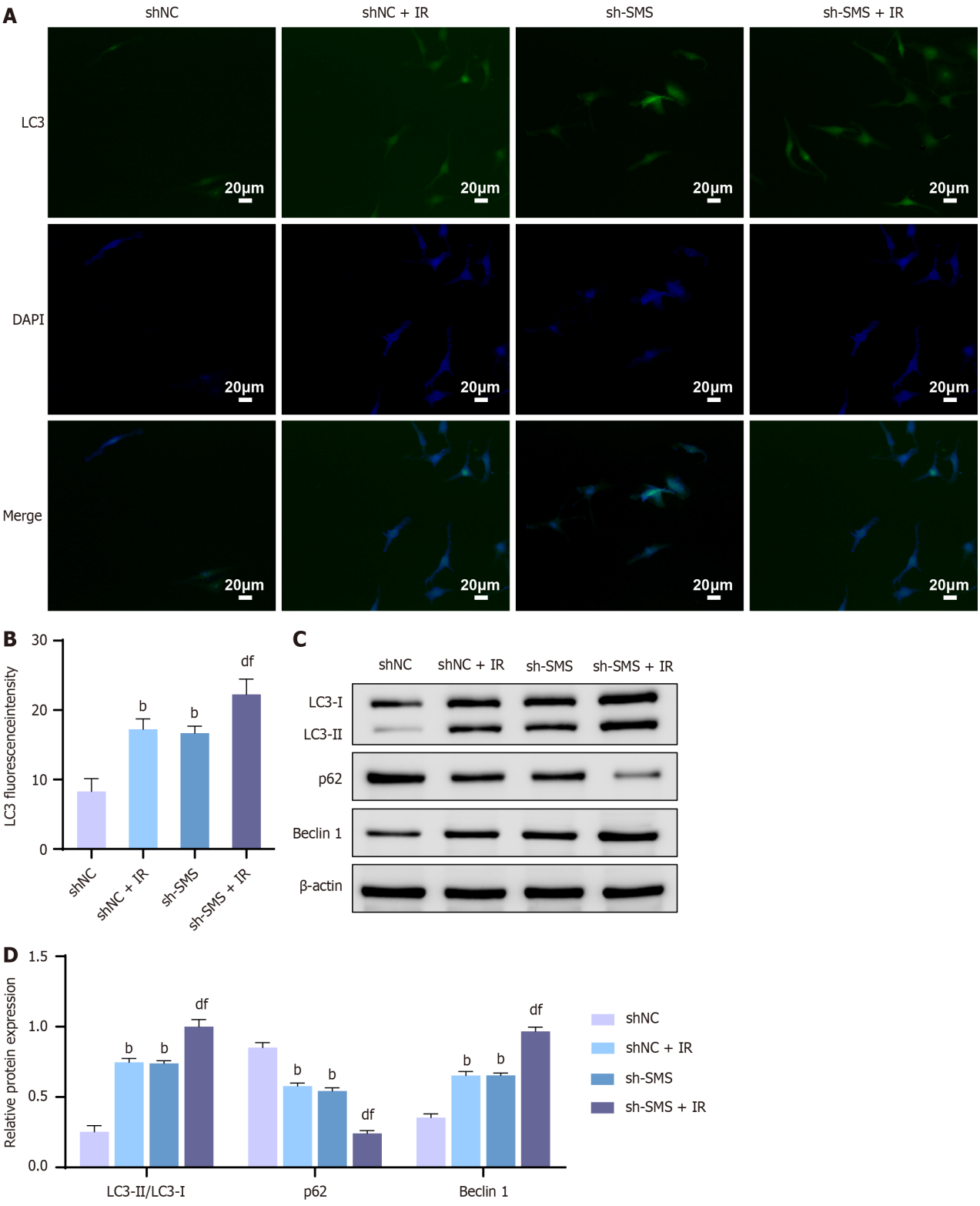

Figure 4 Knockdown of spermine synthase enhances the radiosensitivity of HCT116 cells by promoting autophagy. A and B: Immunofluorescence detection for LC3 puncta in HCT116 cells of the negative control shRNA (shNC) group, shNC + IR group, spermine synthase shRNA (sh-SMS) group, and sh-SMS + IR group; C and D: Western blot analysis for protein levels of LC3-I, LC3-II, p62, and Beclin 1 in HCT116 cells of the shNC group, shNC + IR group, sh-SMS group, and sh-SMS + IR group. $^{b}P < 0.01$ *vs* shNC, $^{d}P < 0.01$ *vs* shNC + IR, $^{f}P < 0.01$ *vs* sh-SMS; SMS: Spermine synthase; sh-SMS: Spermine synthase shRNA; shNC: Negative control shRNA; OE-SMS: Spermine synthase over-expression vector; OE-NC: Negative control over-expression vector.

Knocking down SMS enhances the radiosensitivity of HCT116 cells by suppressing the mTOR pathway

The aforementioned research suggests that spermine negatively regulates cellular autophagy. Studies have shown that SMS can modulate autophagy-related signaling through the mTOR pathway[29,30]. Therefore, we hypothesized that the mTOR pathway may be a key regulator of SMS-mediated cellular autophagy. According to western blot results, knocking down SMS expression lowered the p-mTOR, p-S6K1, and p-S6 protein expression levels in HCT116 cells, resulting in

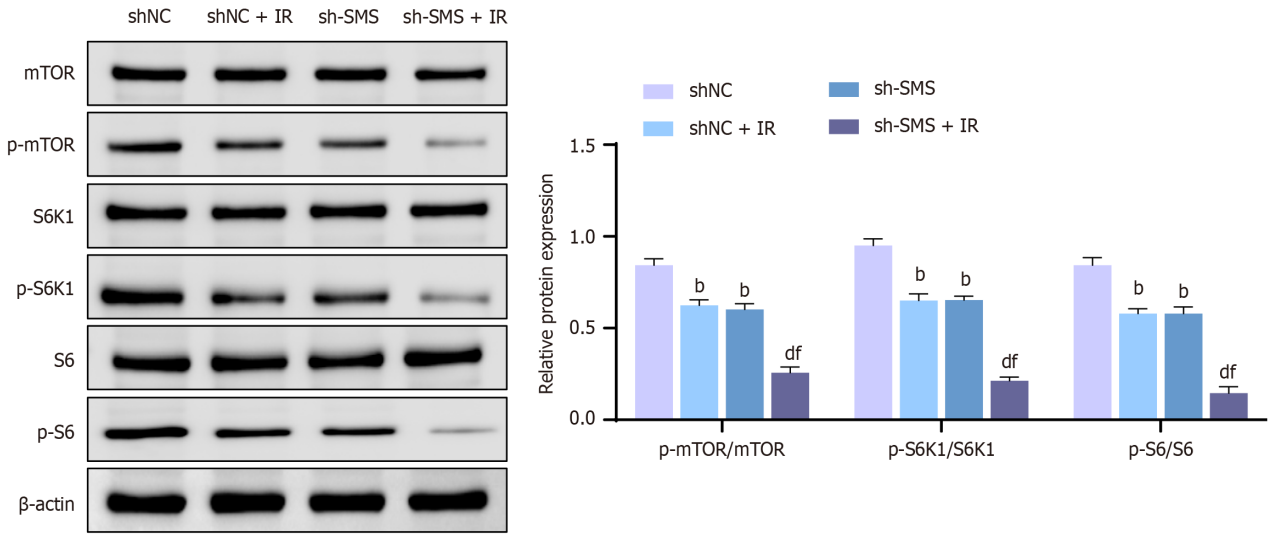

Figure 5 Knocking down spermine synthase enhances radiosensitivity of HCT116 cells by suppressing the mammalian target of rapamycin pathway. Western blot analysis for detecting the protein expression levels of mammalian target of rapamycin (mTOR), p-mTOR, S6K1, p-S6K1, S6, and p-S6 in HCT116 cells under the following conditions: Negative control shRNA (ShNC), shNC + IR, spermine synthase shRNA (sh-SMS), and sh-SMS + IR. $^{b}P < 0.01$ *vs* shNC, $^{d}P < 0.01$ *vs* shNC + IR, $^{f}P < 0.01$ *vs* sh-SMS; SMS: Spermine synthase; sh-SMS: Spermine synthase shRNA; shNC: Negative control shRNA; OE-SMS: Spermine synthase over-expression vector; OE-NC: Negative control over-expression vector; mTOR: Mammalian target of rapamycin.

lessened ratios of p-mTOR/mTOR, p-S6K1/S6K1, and p-S6/S6. Furthermore, compared to the shNC + IR or sh-SMS groups, the sh-SMS + IR group exhibited lower protein expression levels of p-mTOR, p-S6K1, and p-S6, along with down-regulated ratios of p-mTOR/mTOR, p-S6K1/S6K1, and p-S6/S6 (Figure 5). These findings indicated that knocking down SMS enhanced the radiosensitivity of HCT116 cells by suppressing the mTOR pathway.

DISCUSSION

As a pivotal part of comprehensive CRC management, radiotherapy effectively shrinks tumors and prepares patients for further surgical interventions[31,32]. Postoperatively, radiotherapy can effectively eliminate residual cancer cells and reduce the risk of recurrence. Moreover, as for patients with advanced CRC who are unable to undergo surgery, radiotherapy can improve their quality of life and prognosis by alleviating symptoms[33]. However, the current radiotherapy outcomes for patients with CRC are not satisfactory, and adjuvant therapies are needed to improve the efficacy of radiotherapy[34]. In this study, the SMS expression level significantly impacted the radiosensitivity of CRC cells, suggesting its potential as a potential therapeutic target to enhance radiosensitivity.

SMS, an enzyme that converts spermidine to spermine, is involved in diverse physiological processes such as cell proliferation, differentiation, and apoptosis[11]. Recent research has displayed that *SMS* over-expression is associated with tumorigenesis, progression, invasion, and metastasis in various cancers[12]. SMS expression is highest in the prostate, being approximately 10-20 times higher than in other tissues[35]. Prostate cancer tissues exhibit significantly higher SMS expression compared to adjacent normal tissues, and SMS levels correlate with tumor stage and poor prognosis[36]. Additionally, SMS over-expression has been observed in lung, gastric, liver, bladder, and ovarian cancers [37,38]. Notably, research has demonstrated elevated SMS expression in CRC tissues as opposed to adjacent normal tissues, with a positive correlation to tumor malignancy[14]. These findings indicate that SMS can serve as a potential therapeutic target for CRC. In line with previous findings, our study demonstrated a significant up-regulation of SMS expression in the CRC cell line HCT116 compared to normal colonic epithelial cells (FHC). Notably, reducing SMS expression remarkably suppressed HCT116 cell viability and induced apoptosis. These outcomes strongly support the oncogenic role of SMS in CRC. While reducing SMS expression has been shown to induce chemoresistance in CRC cells [39], our study unveiled a novel role for SMS in regulating radiosensitivity. Furthermore, our research demonstrated that silencing SMS expression significantly enhanced the radiosensitivity of HCT116 cells. Consequently, SMS can be a critical determinant of cancer cell responsiveness to both radiotherapy and chemotherapy.

SMS catalyzes the conversion of spermidine to spermine, a polyamine with potent antioxidant properties that can alleviate oxidative DNA damage[40]. Spermine also plays a crucial role in DNA repair, particularly in double-strand break and base excision repair pathways. Upon DNA damage, SMS is activated and rapidly mobilized to the lesion site, facilitating DNA repair. Additionally, SMS maintains chromosomal structure and function, preventing DNA breaks and aberrations[41]. Given these pro-survival functions, SMS inhibitors have been extensively investigated to enhance radiotherapy efficacy[42]. For instance, eflornithine and difluoromethylornithine, SMS inhibitors, have demonstrated radiosensitizing effects in glioma and CRC cells. These inhibitors augment radiosensitivity by impairing the ability of cancer cells to repair radiation-induced DNA damage[43-46]. In line with these observations, our study provided compelling evidence that SMS knockdown sensitized HCT116 cells to radiotherapy by exacerbating DNA damage.

Autophagy, a programmed cell death pathway, plays a crucial role in influencing radiotherapy sensitivity[47]. However, the relationship between SMS and autophagy remains controversial. Some studies suggest that SMS promotes autophagy through lipid metabolism, facilitating autophagosome formation[48]. Moreover, in neurodegenerative disease models, decreased SMS activity is often associated with autophagy impairment. Conversely, other studies propose an inverse correlation between SMS and autophagy. SMS may suppress autophagy by regulating the NAD+/NADH ratio, inhibiting AMPK activity, and activating the mTOR signaling pathway[49,50]. Additionally, SMS can induce the activation of transcription factors such as NF-κB and HIF-1α, which can repress the expression of autophagy-related genes [51,52]. In our study, upon silencing SMS, the protein levels of LC3-I, LC3-II, and Beclin 1 rose, whereas p62 Levels fell, indicating that SMS suppressed cellular autophagy. Notably, SMS silencing markedly inhibited the phosphorylation of mTOR, S6K1, and S6 (p-mTOR, p-S6K1, p-S6), suggesting a positive regulatory relationship between SMS and mTOR. This implied that SMS may enhance chemotherapy resistance by suppressing autophagy through activating the mTOR signaling pathway.

It is important to note that this study did not include *in vivo* experiments to examine the effects of SMS inhibition on CRC chemosensitivity. Moreover, the specific molecular mechanisms connecting SMS to DNA damage and the mTOR signaling pathway are not yet fully understood. Besides, our research did not investigate whether SMS knockdown might increase radiotherapy resistance. These gaps necessitate further investigation through well-designed experiments. In addition, our research was limited to a single CRC cell line, which somewhat restricts the generalizability of our findings.

CONCLUSION

This study highlighted SMS as a pivotal molecule regulating DNA damage and autophagy in cancer cells. SMS promotes DNA repair and activates the mTOR signaling pathway to suppress cellular autophagy. All in all, SMS emerges as a promising therapeutic target to enhance CRC radiosensitivity, providing novel insights for the development of CRC treatment strategies.

FOOTNOTES

Author contributions: Guo YB, Wu YM and Lin ZZ contributed to study concept and design; Wu YM and Lin ZZ contributed to analysis and interpretation of data; Guo YB contributed to drafting of the manuscript; Lin ZZ contributed to critical revision of the manuscript for important intellectual content; Wu YM contributed to statistical analysis; All authors contributed to study supervision and have read and approved the manuscript.

Supported by National Natural Science Foundation of China, No. 82102996; Guangdong Provincial Natural Science Foundation, No. 2022A1515010517; Guangzhou Science and Technology Plan Project, No. 202201011016; and President Foundation of Nanfang Hospital, Southern Medical University, No. 2020C038.

Institutional animal care and use committee statement: This study did not involve animal or clinical trials and did not require ethics. Normal colonic epithelial cells FHC (CRL-1831), CRC cell line HCT116 (CRL-247), SW62, SW480, HT-29, and LoVo cells were all purchased from WHELAB.

Conflict-of-interest statement: The authors declare that they have no competing interests.

Data sharing statement: The data used to support the findings of this study are available from the corresponding author upon request at 928526639@qq.com.

Country of origin: China

ORCID number: Yu-Bin Guo 0000-0002-7748-1805.

S-Editor: Li L
L-Editor: A
P-Editor: Wang WB

REFERENCES

1 **Bray F**, Laversanne M, Sung H, Ferlay J, Siegel RL, Soerjomataram I, Jemal A. Global cancer statistics 2022: GLOBOCAN estimates of incidence and mortality worldwide for 36 cancers in 185 countries. *CA Cancer J Clin* 2024; **74**: 229-263 [PMID: 38572751 DOI:

10.3322/caac.21834]
2 **Siegel RL**, Wagle NS, Cercek A, Smith RA, Jemal A. Colorectal cancer statistics, 2023. *CA Cancer J Clin* 2023; **73**: 233-254 [PMID: 36856579 DOI: 10.3322/caac.21772]
3 **Kędzia-Berut R**, Berut M, Włodarczyk M, Włodarczyk J, Dziki Ł, Dziki A, Mik M. Colorectal Cancer: Is it Still a Disease of the Elderly? *Pol Przegl Chir* 2023; **96**: 41-45 [PMID: 38348978 DOI: 10.5604/01.3001.0054.0956]
4 **Tessmann JW**, Rocha MR, Morgado-Díaz JA. Mechanisms of radioresistance and the underlying signaling pathways in colorectal cancer cells. *J Cell Biochem* 2023; **124**: 31-45 [PMID: 36565460 DOI: 10.1002/jcb.30361]
5 **Wang C**, Yuan M, Gao Y, Hou R, Song D, Feng Y. Changes in Tumor Immune Microenvironment after Radiotherapy Resistance in Colorectal Cancer: A Narrative Review. *Oncol Res Treat* 2023; **46**: 177-191 [PMID: 36948165 DOI: 10.1159/000530161]
6 **Liu YP**, Zheng CC, Huang YN, He ML, Xu WW, Li B. Molecular mechanisms of chemo- and radiotherapy resistance and the potential implications for cancer treatment. *MedComm (2020)* 2021; **2**: 315-340 [PMID: 34766149 DOI: 10.1002/mco2.55]
7 **Matsuoka K**, Kobunai T, Nukatsuka M, Takechi T. Improved chemoradiation treatment using trifluridine in human colorectal cancer cells in vitro. *Biochem Biophys Res Commun* 2017; **494**: 249-255 [PMID: 29024630 DOI: 10.1016/j.bbrc.2017.10.044]
8 **Xie X**, Fan C, Luo B, Zhang J, Jensen LD, Burman J, Jönsson C, Ljusberg A, Larsson P, Zhao Z, Sun XF. APR-246 Enhances Colorectal Cancer Sensitivity to Radiotherapy. *Mol Cancer Ther* 2023; **22**: 947-961 [PMID: 37216282 DOI: 10.1158/1535-7163.MCT-22-0275]
9 **Caldwell RB**, Toque HA, Narayanan SP, Caldwell RW. Arginase: an old enzyme with new tricks. *Trends Pharmacol Sci* 2015; **36**: 395-405 [PMID: 25930708 DOI: 10.1016/j.tips.2015.03.006]
10 **S Clemente G**, van Waarde A, F Antunes I, Dömling A, H Elsinga P. Arginase as a Potential Biomarker of Disease Progression: A Molecular Imaging Perspective. *Int J Mol Sci* 2020; **21**: 5291 [PMID: 32722521 DOI: 10.3390/ijms21155291]
11 **Pegg AE**, Michael AJ. Spermine synthase. *Cell Mol Life Sci* 2010; **67**: 113-121 [PMID: 19859664 DOI: 10.1007/s00018-009-0165-5]
12 **Pan X**, Xue L, Sun Y. Spermine synthase (SMS) serves as a prognostic biomarker in head and neck squamous cell carcinoma: a bioinformatics analysis. *Ann Transl Med* 2022; **10**: 1213 [PMID: 36544695 DOI: 10.21037/atm-22-5014]
13 **Gobert AP**, Wilson KT. Polyamine- and NADPH-dependent generation of ROS during Helicobacter pylori infection: A blessing in disguise. *Free Radic Biol Med* 2017; **105**: 16-27 [PMID: 27682363 DOI: 10.1016/j.freeradbiomed.2016.09.024]
14 **Guo Y**, Ye Q, Deng P, Cao Y, He D, Zhou Z, Wang C, Zaytseva YY, Schwartz CE, Lee EY, Evers BM, Morris AJ, Liu S, She QB. Spermine synthase and MYC cooperate to maintain colorectal cancer cell survival by repressing Bim expression. *Nat Commun* 2020; **11**: 3243 [PMID: 32591507 DOI: 10.1038/s41467-020-17067-x]
15 **Fahrmann JF**, Vykoukal J, Fleury A, Tripathi S, Dennison JB, Murage E, Wang P, Yu CY, Capello M, Creighton CJ, Do KA, Long JP, Irajizad E, Peterson C, Katayama H, Disis ML, Arun B, Hanash S. Association Between Plasma Diacetylspermine and Tumor Spermine Synthase With Outcome in Triple-Negative Breast Cancer. *J Natl Cancer Inst* 2020; **112**: 607-616 [PMID: 31503278 DOI: 10.1093/jnci/djz182]
16 **Velenosi TJ**, Krausz KW, Hamada K, Dorsey TH, Ambs S, Takahashi S, Gonzalez FJ. Pharmacometabolomics reveals urinary diacetylspermine as a biomarker of doxorubicin effectiveness in triple negative breast cancer. *NPJ Precis Oncol* 2022; **6**: 70 [PMID: 36207498 DOI: 10.1038/s41698-022-00313-4]
17 **Peng Q**, Wong CY, Cheuk IW, Teoh JY, Chiu PK, Ng CF. The Emerging Clinical Role of Spermine in Prostate Cancer. *Int J Mol Sci* 2021; **22**: 4382 [PMID: 33922247 DOI: 10.3390/ijms22094382]
18 **Guo Z**, Zhang X, Lin C, Huang Y, Zhong Y, Guo H, Zheng Z, Weng S. METTL3-IGF2BP3-axis mediates the proliferation and migration of pancreatic cancer by regulating spermine synthase m6A modification. *Front Oncol* 2022; **12**: 962204 [PMID: 36276112 DOI: 10.3389/fonc.2022.962204]
19 **Snezhkina AV**, Krasnov GS, Lipatova AV, Sadritdinova AF, Kardymon OL, Fedorova MS, Melnikova NV, Stepanov OA, Zaretsky AR, Kaprin AD, Alekseev BY, Dmitriev AA, Kudryavtseva AV. The Dysregulation of Polyamine Metabolism in Colorectal Cancer Is Associated with Overexpression of c-Myc and C/EBPβ rather than Enterotoxigenic Bacteroides fragilis Infection. *Oxid Med Cell Longev* 2016; **2016**: 2353560 [PMID: 27433286 DOI: 10.1155/2016/2353560]
20 **Ma MR**, YB Guo, Ye Q, Deng P, He DH, Wang C, She QB. Targeting spermine synthase triggers lipid metabolism reprogramming as a new therapeutic option to combat colorectal cancer [abstract]. *Cancer Res* 2023; **83** (7_Suppl): Abstract nr 295 [DOI: 10.1158/1538-7445.AM2023-295]
21 **Zhou Y**, Ren D, Bi H, Yi B, Zhang C, Wang H, Sun J. [Tumor-associated Macrophage: Emerging Targets for Modulating the Tumor Microenvironment]. *Zhongguo Fei Ai Za Zhi* 2024; **27**: 231-240 [PMID: 38590197 DOI: 10.3779/j.issn.1009-3419.2024.102.13]
22 **Mivechi NF**, Dewey WC, Feuerstein BG, Deen DF, Marton LJ. Relationship between heat sensitivity and polyamine levels after treatment with alpha-difluoromethylornithine (DFMO). *Radiat Res* 1986; **108**: 269-281 [PMID: 3099327]
23 **Perrone C**, Pomella S, Cassandri M, Pezzella M, Giuliani S, Gasperi T, Porrazzo A, Alisi A, Pastore A, Codenotti S, Fanzani A, Barillari G, Conti LA, De Angelis B, Quintarelli C, Mariottini P, Locatelli F, Marampon F, Rota R, Cervelli M. Spermine oxidase induces DNA damage and sensitizes fusion negative rhabdomyosarcoma cells to irradiation. *Front Cell Dev Biol* 2023; **11**: 1061570 [PMID: 36755974 DOI: 10.3389/fcell.2023.1061570]
24 **Sierra JC**, Piazuelo MB, Luis PB, Barry DP, Allaman MM, Asim M, Sebrell TA, Finley JL, Rose KL, Hill S, Holshouser SL, Casero RA, Cleveland JL, Woster PM, Schey KL, Bimczok D, Schneider C, Gobert AP, Wilson KT. Spermine oxidase mediates Helicobacter pylori-induced gastric inflammation, DNA damage, and carcinogenic signaling. *Oncogene* 2020; **39**: 4465-4474 [PMID: 32350444 DOI: 10.1038/s41388-020-1304-6]
25 **Galluzzi L**, Bravo-San Pedro JM, Demaria S, Formenti SC, Kroemer G. Activating autophagy to potentiate immunogenic chemotherapy and radiation therapy. *Nat Rev Clin Oncol* 2017; **14**: 247-258 [PMID: 27845767 DOI: 10.1038/nrclinonc.2016.183]
26 **Patel NH**, Bloukh S, Alwohosh E, Alhesa A, Saleh T, Gewirtz DA. Autophagy and senescence in cancer therapy. *Adv Cancer Res* 2021; **150**: 1-74 [PMID: 33858594 DOI: 10.1016/bs.acr.2021.01.002]
27 **Xu TT**, Li H, Dai Z, Lau GK, Li BY, Zhu WL, Liu XQ, Liu HF, Cai WW, Huang SQ, Wang Q, Zhang SJ. Spermidine and spermine delay brain aging by inducing autophagy in SAMP8 mice. *Aging (Albany NY)* 2020; **12**: 6401-6414 [PMID: 32268299 DOI: 10.18632/aging.103035]
28 **Luo D**, Lu X, Li H, Li Y, Wang Y, Jiang S, Li G, Xu Y, Wu K, Dou X, Liu Q, Chen W, Zhou Y, Mao H. The Spermine Oxidase/Spermine Axis Coordinates ATG5-Mediated Autophagy to Orchestrate Renal Senescence and Fibrosis. *Adv Sci (Weinh)* 2024; **11**: e2306912 [PMID: 38775007 DOI: 10.1002/advs.202306912]
29 **Zhang X**, Zhang L, Chen Z, Li S, Che B, Wang N, Chen J, Xu C, Wei C. Exogenous spermine attenuates diabetic kidney injury in rats by inhibiting AMPK/mTOR signaling pathway. *Int J Mol Med* 2021; **47**: 27 [PMID: 33537831 DOI: 10.3892/ijmm.2021.4860]

30 **Yan B**, Min SJ, Xu B, Zhang C, Pei J, Zhang W, Luo GH. The protective effects of exogenous spermine on renal ischemia-reperfusion injury in rats. *Transl Androl Urol* 2021; **10**: 2051-2066 [PMID: 34159086 DOI: 10.21037/tau-21-280]

31 **Song Y**, Deng Z, Sun H, Zhao Y, Zhao R, Cheng J, Huang Q. Predicting tumor repopulation through the gene panel derived from radiation resistant colorectal cancer cells. *J Transl Med* 2023; **21**: 390 [PMID: 37328854 DOI: 10.1186/s12967-023-04260-x]

32 **Mohamad I**, Barry A, Dawson L, Hosni A. Stereotactic body radiation therapy for colorectal liver metastases. *Int J Hyperthermia* 2022; **39**: 611-619 [PMID: 35465818 DOI: 10.1080/02656736.2021.1923836]

33 **Flamarique S**, Campo M, Asín G, Pellejero S, Viúdez A, Arias F. Stereotactic body radiation therapy for liver metastasis from colorectal cancer: size matters. *Clin Transl Oncol* 2020; **22**: 2350-2356 [PMID: 32488803 DOI: 10.1007/s12094-020-02375-x]

34 **Hitchcock KE**, Romesser PB, Miller ED. Local Therapies in Advanced Colorectal Cancer. *Hematol Oncol Clin North Am* 2022; **36**: 553-567 [PMID: 35562258 DOI: 10.1016/j.hoc.2022.02.007]

35 **Hibasami H**, Borchardt RT, Chen SY, Coward JK, Pegg AE. Studies of inhibition of rat spermidine synthase and spermine synthase. *Biochem J* 1980; **187**: 419-428 [PMID: 7396856 DOI: 10.1042/bj1870419]

36 **Shukla-Dave A**, Castillo-Martin M, Chen M, Lobo J, Gladoun N, Collazo-Lorduy A, Khan FM, Ponomarev V, Yi Z, Zhang W, Pandolfi PP, Hricak H, Cordon-Cardo C. Ornithine Decarboxylase Is Sufficient for Prostate Tumorigenesis *via* Androgen Receptor Signaling. *Am J Pathol* 2016; **186**: 3131-3145 [PMID: 27770613 DOI: 10.1016/j.ajpath.2016.08.021]

37 **Xie L**, Yang Y, Meng J, Wen T, Liu J, Xu H. Cationic polysaccharide spermine-pullulan drives tumor associated macrophage towards M1 phenotype to inhibit tumor progression. *Int J Biol Macromol* 2019; **123**: 1012-1019 [PMID: 30439425 DOI: 10.1016/j.ijbiomac.2018.11.089]

38 **Chaturvedi R**, de Sablet T, Coburn LA, Gobert AP, Wilson KT. Arginine and polyamines in Helicobacter pylori-induced immune dysregulation and gastric carcinogenesis. *Amino Acids* 2012; **42**: 627-640 [PMID: 21874531 DOI: 10.1007/s00726-011-1038-4]

39 **Huang X**, Zhou H, Jiao R, Liu H, Qin C, Xu L, Chen Y. Supramolecular Chemotherapy: Host-Guest Complexes of Heptaplatin-Cucurbit[7]uril toward Colorectal Normal and Tumor Cells. *Langmuir* 2021; **37**: 5475-5482 [PMID: 33913723 DOI: 10.1021/acs.langmuir.0c03603]

40 **Korhonen VP**, Niiranen K, Halmekytö M, Pietilä M, Diegelman P, Parkkinen JJ, Eloranta T, Porter CW, Alhonen L, Jänne J. Spermine deficiency resulting from targeted disruption of the spermine synthase gene in embryonic stem cells leads to enhanced sensitivity to antiproliferative drugs. *Mol Pharmacol* 2001; **59**: 231-238 [PMID: 11160858 DOI: 10.1124/mol.59.2.231]

41 **Nilsson J**, Gritli-Linde A, Heby O. Skin fibroblasts from spermine synthase-deficient hemizygous gyro male (Gy/Y) mice overproduce spermidine and exhibit increased resistance to oxidative stress but decreased resistance to UV irradiation. *Biochem J* 2000; **352** Pt 2: 381-387 [PMID: 11085931]

42 **Setyawan EMN**, Kim MJ, Oh HJ, Kim GA, Jo YK, Lee SH, Choi YB, Lee BC. Spermine reduces reactive oxygen species levels and decreases cryocapacitation in canine sperm cryopreservation. *Biochem Biophys Res Commun* 2016; **479**: 927-932 [PMID: 27586272 DOI: 10.1016/j.bbrc.2016.08.091]

43 **Levin VA**, Ictech SE, Hess KR. Clinical importance of eflornithine (α-difluoromethylornithine) for the treatment of malignant gliomas. *CNS Oncol* 2018; **7**: CNS16 [PMID: 29378419 DOI: 10.2217/cns-2017-0031]

44 **Alexiou GA**, Vartholomatos E, I Tsamis K, Peponi E, Markopoulos G, A Papathanasopoulou V, Tasiou I, Ragos V, Tsekeris P, Kyritsis AP, Galani V. Combination treatment for glioblastoma with temozolomide, DFMO and radiation. *J BUON* 2019; **24**: 397-404 [PMID: 30941997]

45 **Benrezzak O**, Nigam VN, Madarnas P. Increased survival of CD1 mice bearing dimethylhydrazine induced primary colon and anal cancers by difluoromethylornithine with concomitant increase in angiosarcoma incidence. *Anticancer Res* 1987; **7**: 251-257 [PMID: 3109315]

46 **Courdi A**, Milano G, Bouclier M, Lalanne CM. Radiosensitization of human tumor cells by alpha-difluoromethylornithine. *Int J Cancer* 1986; **38**: 103-107 [PMID: 3087889 DOI: 10.1002/ijc.2910380117]

47 **Gao L**, Zheng H, Cai Q, Wei L. Autophagy and Tumour Radiotherapy. *Adv Exp Med Biol* 2020; **1207**: 375-387 [PMID: 32671760 DOI: 10.1007/978-981-15-4272-5_25]

48 **Li Z**, Wang L, Ren Y, Huang Y, Liu W, Lv Z, Qian L, Yu Y, Xiong Y. Arginase: shedding light on the mechanisms and opportunities in cardiovascular diseases. *Cell Death Discov* 2022; **8**: 413 [PMID: 36209203 DOI: 10.1038/s41420-022-01200-4]

49 **Elustondo PA**, Negoda A, Kane CL, Kane DA, Pavlov EV. Spermine selectively inhibits high-conductance, but not low-conductance calcium-induced permeability transition pore. *Biochim Biophys Acta* 2015; **1847**: 231-240 [PMID: 25448536 DOI: 10.1016/j.bbabio.2014.10.007]

50 **Chen X**, Lu Y, Zhang Z, Wang J, Yang H, Liu G. Intercellular interplay between Sirt1 signalling and cell metabolism in immune cell biology. *Immunology* 2015; **145**: 455-467 [PMID: 25890999 DOI: 10.1111/imm.12473]

51 **Park SK**, Lin HL, Murphy S. Nitric oxide regulates nitric oxide synthase-2 gene expression by inhibiting NF-kappaB binding to DNA. *Biochem J* 1997; **322** (Pt 2): 609-613 [PMID: 9065784 DOI: 10.1042/bj3220609]

52 **Sandau KB**, Fandrey J, Brüne B. Accumulation of HIF-1alpha under the influence of nitric oxide. *Blood* 2001; **97**: 1009-1015 [PMID: 11159530 DOI: 10.1182/blood.v97.4.1009]

World Journal of Gastrointestinal Oncology

Submit a Manuscript: https://www.f6publishing.com

World J Gastrointest Oncol 2024 December 15; 16(12): 4728-4737

DOI: 10.4251/wjgo.v16.i12.4728

ISSN 1948-5204 (online)

META-ANALYSIS

Efficacy and safety of transhepatic arterial chemoembolization with drug-loaded microspheres in unresectable primary liver cancer

Jun Deng, Yan-Hong Mi, Le Xie, Xiong-Xing Sun, Dan-Hong Liu, Hua-Jun Long, Li-Yong He, Da-Hua Wu, Hong-Cai Shang

Specialty type: Oncology

Provenance and peer review: Unsolicited article; Externally peer reviewed.

Peer-review model: Single blind

Peer-review report's classification

Scientific Quality: Grade B
Novelty: Grade B
Creativity or Innovation: Grade B
Scientific Significance: Grade B

P-Reviewer: Pontrelli A

Received: May 5, 2024
Revised: August 11, 2024
Accepted: August 20, 2024
Published online: December 15, 2024
Processing time: 191 Days and 4.8 Hours

Jun Deng, Da-Hua Wu, Department of Integrated Traditional Chinese and Western Medicine, Hunan University of Traditional Chinese Medicine, Changsha 410208, Hunan Province, China

Jun Deng, Le Xie, Xiong-Xing Sun, Da-Hua Wu, Department of Neurology, Hunan Provincial Hospital of Integrated Traditional Chinese and Western Medicine, Changsha 410208, Hunan Province, China

Yan-Hong Mi, Department of Prevention Diseases, Hunan Provincial Hospital of Integrated Traditional Chinese and Western Medicine, Changsha 410006, Hunan Province, China

Dan-Hong Liu, Institute of Clinical Pharmacology of Traditional Chinese Medicine, Hunan Provincial Hospital of Integrated Traditional Chinese and Western Medicine, Changsha 410006, Hunan Province, China

Hua-Jun Long, Department of Emergency, Hunan Provincial Hospital of Integrated Traditional Chinese and Western Medicine, Changsha 410006, Hunan Province, China

Li-Yong He, Department of Hepatobiliary Surgery, The First Affiliated Hospital of Sun Yat-sen University, Guangzhou 510062, Guangdong Province, China

Hong-Cai Shang, State Key Laboratory of Internal Medicine of Traditional Chinese Medicine, Beijing University of Chinese Medicine, Beijing 100700, China

Co-first authors: Jun Deng and Yan-Hong Mi.

Co-corresponding authors: Da-Hua Wu and Hong-Cai Shang.

Corresponding author: Hong-Cai Shang, PhD, Professor, State Key Laboratory of Internal Medicine of Traditional Chinese Medicine, Beijing University of Chinese Medicine, No. 5 Sea Warehouse, Dongcheng District, Beijing 100700, China. shanghongcai@126.com

Abstract

BACKGROUND

Transhepatic arterial chemoembolization (TACE), as a local treatment, has been widely used in the treatment of unresectable liver cancer. The introduction of drug carrier microspheres has brought new hope for the therapeutic effect of TACE. Microspheres can realize the slow release and directional delivery of drugs, reduce systemic toxicity and improve local curative effect.

AIM
To compare the effectiveness of traditional transcatheter arterial chemoembolization against microsphere-assisted transcatheter arterial chemoembolization in the treatment of hepatocellular carcinoma that is incurable.

METHODS
We searched the PubMed, Embase, Cochrane Library, and CNKI databases for clinical trials of drug-luting beads TACE (DEB-TACE) *vs* conventional TACE (cTACE) for the treatment of unresectable liver cancer. We screened references based on inclusion and exclusion criteria and then selected valid data for meta-analysis using RevMan 53 software. The complete response (CR) rate, partial response (PR) rate, postoperative stable disease (SD) rate, and 6-month and 12-month survival rates were compared.

RESULTS
A total of 12 articles were included, including 1177 patients, 519 of whom received DEB-TACE and 658 of whom received cTACE. The CR rate in the DEB-TACE group was much greater than that in the cTACE group [relative risk (RR) = 1.42, 95%CI: 1.18–1.72, P = 0.0002]. The 12-month survival rate significantly increased (RR = 1.09; 95%CI: 1.01- 1.17, P = 0.03); the PR rate (RR = 1.13; 95%CI: 0.97-1.30, P = 0.12); the SD rate (RR = 0.82; 95%CI: 0.64-1.05, P = 0.12); and the 6-month survival rate (RR = 1.05; 95%CI: 1.00-1.10, P = 0.07). There was no significant difference (P < 0.05).

CONCLUSION
Compared with those of iodized oil TACE, the drug-loaded microspheres tended to have therapeutic advantages.

Key Words: Transhepatic arterial chemoembolization; Drug-loaded microspheres; Unresectable primary liver cancer; Meta-analysis

Core Tip: This study systematically evaluated the efficacy and safety of transhepatic arterial chemoembolization with drug-loaded microspheres in the treatment of unresectable primary liver cancer. Through a meta-analysis of relevant literature, the effect of this treatment in prolonging survival, relieving symptoms and improving quality of life of patients was discussed, and the incidence of adverse reactions and complications was evaluated, so as to provide more scientific treatment recommendations for clinicians.

Citation: Deng J, Mi YH, Xie L, Sun XX, Liu DH, Long HJ, He LY, Wu DH, Shang HC. Efficacy and safety of transhepatic arterial chemoembolization with drug-loaded microspheres in unresectable primary liver cancer. *World J Gastrointest Oncol* 2024; 16(12): 4728-4737
URL: https://www.wjgnet.com/1948-5204/full/v16/i12/4728.htm
DOI: https://dx.doi.org/10.4251/wjgo.v16.i12.4728

INTRODUCTION

Each year, nearly 500000 hepatocelluar carcinoma (HCC) patients receive a diagnosis, accounting for more than 5% of all cancer cases. The recurrence rate of HCC is as high as 50% within 3 years and 70% at 5 years after hepatectomy[1-4]. Despite recent advances in surgical techniques and preoperative medical treatment, the incidence of postoperative complications in patients with cirrhosis is still as high as 42%[5]. Transhepatic arterial chemoembolization (TACE) is widely used as a treatment for patients with clinically unresectable HCC. It is composed of conventional TACE (cTACE) and the drug-luting beads TACE (DEB-TACE), which use iodide and DEB, respectively, as chemotherapy drug carriers [6]. DEB-TACE, a novel drug delivery and embolization system, delivers local, controlled, and sustained doses of chemotherapeutic agents to the tumor site through the blood vessels of highly vascularized malignancies. Numerous studies[7-9] have shown that DEB-TACE has a significant advantage in terms of overall survival or tumor response and can reduce the occurrence of adverse events. Despite the extensive studies conducted on cTACE and DEB-TACE, the role of DEB-TACE in comparison to that of cTACE remains relatively inconsistent.

MATERIALS AND METHODS

Retrieval strategy

Our search time was July 2023, and we searched the PubMed, Embase, Cochrane Library, and CNKI databases for controlled clinical studies on DEB-TACE and TACE for comparative treatment of unresectable liver cancer. Using a

combination of subject words and free words, we ended the sentence with "DEB" OR "drug eluting" OR "drug eluting microsphere" OR "doxorubicin eluting". The search terms used were "TACE "OR "transcatheterarterial chemoembolization" AND "hepatocellular carcinoma" OR "adenocarcinoma" OR "carcinoma" OR "cancer" OR "neoplasm" OR " tumor".

Inclusion and exclusion criteria

Inclusion criteria: (1) Clinically controlled studies comparing DEB-TACE with cTACE for the treatment of unresectable liver cancer, regardless of age, sex, or nationality; (2) Had confirmed unresectable liver cancer for which a radiological or histopathological diagnosis was made in addition to alpha-fetoprotein levels; and (3) Had complete primary outcomes, including a complete response (CR) rate, a partial response (PR) rate, a stable disease (SD) rate, and 6- and 12-month survival.

Exclusion criteria: (1) Were conference papers, case reports, editorials, and nonhuman studies; and (2) Had repeated publications of the same data or incomplete data in the literature.

Data extraction and quality assessment

Two researchers independently screened the literature, extracted the data and cross-checked the data. Disagreements were resolved through discussion or by discussion with a third party. The following data were extracted: (1) Basic information of the trial, author name, nationality, publication time, sample size, patient sex, age, tumor diameter, and Child-Pugh grade; (2) Main results, namely, the CR rate, PR rate, SD rate, 6-month survival rate, and 12-month survival rate; and (3) The Newcastle-Ottawa Scale (NOS) score, which was used to assess the risk of bias.

Statistical analysis

RevMan 5.3 was used to determine the relative risk in each study [relative risk (RR), 95%CI]. A $P > 0.05$ indicated that there was no significant difference between the DEB-TACE and cTACE groups. Each study used the value of I2, which represents the percentage of total variation, to assess statistical heterogeneity. Generally, we used the fixed-effects model for analysis when I2 was less than 50%, assuming no significant difference in heterogeneity. A random effects model was used to analyze the heterogeneity when the I^2 was greater than 50%. We used a forest plot to graphically represent and evaluate the treatment effect and the symmetry of the funnel plot to visually assess the presence of bias risk.

RESULTS

Literature search results

A total of 1220 pieces of literature were initially retrieved, 865 duplicated pieces were excluded, 105 reviews were excluded, only 32 abstracts were excluded, 12 animal experiments were excluded, 10 case reports were reviewed, 10 reviews were reviewed, and 3 brief investigations were conducted. Upon reviewing the titles and abstracts, we excluded 171 irrelevant studies, resulting in a total of 1208 excluded studies. The final meta-analysis included 12 studies[10-21]. Table 1 displays the characteristics of the included studies (Figure 1). There were 1177 patients (519 patients who received DEB-TACE and 658 patients who received cTACE), and all studies showed no statistically significant differences in age, sex ratio, Child-Pugh grade, tumor stage, or tumor characteristics between the two groups. Of the 12 studies, 7 were prospective, and the remaining 5 were retrospective. Three studies used epirubicin as a drug-carrying microsphere, and four studies used doxubicin.

Meta-analysis results

Postoperative CR rate: We conducted a comparative study on the CR rate based on mRECIST criteria one month after surgery. Eleven studies[10-20] reported the number of CR patients, and there was no significant heterogeneity among the studies. A fixed-effects model was used for analysis. The results of the meta-analysis showed that, compared with that in the cTACE group, the postoperative CR rate in the DEB-TACE group was significantly greater (RR = 1.42, 95%CI: 1.18-1.72, $Z = 3.73$, $P = 0.0002$) (Figure 2A).

PR rate after surgery: One month after surgery, the PR rate was compared according to the mRECIST standard. Eleven studies[10-20] reported the number of PR patients, and there was no substantial heterogeneity among the investigations. The analysis was conducted using a fixed-effects model. There was no significant difference in the PR rate between the cTACE group and the DEB-TACE group (RR = 1.13, 95%CI: 0.97-1.30, $Z = 1.58$, $P = 0.12$) (Figure 2B).

Comparison of the SD rate after surgery: Based on the mRECIST standard eight studies[10-16,18] reported the number of SD patients, and there was no significant heterogeneity among the studies. An analysis was conducted using a fixed-effects model. The meta-analysis results indicated that there was no statistically significant disparity in the SD rate between the cTACE group and the DEB-TACE group (RR = 0.02, 95%CI: 0.64-1). The values for Z and P are 1.57 and 0.12, respectively, as shown in Figure 2C.

Comparison of the 6-month survival rate after surgery: Seven studies[12,13,16-18,20,21] reported 6-month postoperative survival rates, with no significant heterogeneity among the studies. Fixed-effect response model analysis was used. The results of the meta-analysis showed that there was no significant difference in the 6-month survival rate between the

Table 1 Basic features included in the study, mean ± SD

Ref.	Cases		Average age (years)		Gender (male/female)		Tumor size (mm)		Child-Pugh grading (A/B)		Newcastle-Ottawa Scale
	DEB-TACE	cTACE	DEB-TACE	cTACE	DEB-TACE	cTACE	DEB-TACE	cTACE	DEB-TACE	cTACE	
Chen *et al*[10]	22	20	N/A	N/A	19/3	17/3	N/A	N/A	15/7	17/3	6
Chi *et al*[11]	50	50	60.3 ± 12.3		35/15	40/10	42.5 ± 12.3	43.2 ± 11.8	35/15	40/10	8
Ferrer Puchol *et al*[12]	47	25	59.84 ± 11.216	60.01 ± 12.79	34/13	18/7	61.5 ± 38.4	60.4 ± 39.6	30/17	17/8	7
Huang *et al*[13]	30	30	59.2 ± 6.3	58.3 ± 6.4	18/12	20/10					6
Lammer *et al*[14]	93	108	67.3 ± 9.1	67.4 ± 8.8	79/14	95/13	88.9 ± 52.1	89.2 ± 59.3	77/16	89/19	9
Lencioni *et al*[15]	32	188	67.1 ± 10.56		18/14	100/88	67.2 ± 34.2	65.7 ± 33.6	17/15	100/88	8
Malagari *et al*[16]	41	43	70.7 ± 6.9	70.0 ± 7.9	31/10	34/9	83.5 ± 27.5	81.0 ± 28.0	23/18	26/17	7
Sacco *et al*[17]	33	34	70.0 ± 7.7		20/13	21/13	63.1 ± 32.5	60.8 ± 31.1	20/13	22/12	9
Song *et al*[18]	60	69	61.7 ± 9.8	59.4 ± 11.2	42/18	51/18	42.0 ± 28.0	50.0 ± 31.0	56/4	62/6	7
Wiggermann *et al*[19]	22	22	69.02+8.1		18/4	19/3	74.4 ± 33.7	69.8 ± 38.1	22/0	22/0	8
You *et al*[20]	44	43	65	63	30/14	26/17	N/A	N/A	24/20	24/19	8
Dhanasekaran *et al*[21]	45	26	59.96 ± 11.45	58.96 ± 13.30	35/10	19/7	60.7 ± 45.2	54.9 ± 42.9	28/17	15/11	8

DEB-TACE: Drug-luting beads-transhepatic arterial chemoembolization; cTACE: Conventional transhepatic arterial chemoembolization.

cTACE group and the DEB-TACE group (RR = 1.05, 95%CI: 1.00-1.10, Z = 1.81, P = 0.07) (Figure 2D).

Comparison of the 12-month survival rate after surgery: Eight studies[12,13,16-21] reported the survival rate at 12 months after surgery, and there was no significant heterogeneity among the studies. A fixed-effects model was used for analysis. The meta-analysis revealed that the 12-month survival rate was significantly greater in the DEB-TACE group than in the cTACE group (RR = 1.99, 95%CI: 1.01-1.17; Z = 2.11; P = 0.03) (Figure 2E).

Subgroup analysis was performed based on Barcelona clinic liver cancer (BCLC) stage, Child-Pugh grade, and drug delivery status to further evaluate 12-month survival. First, subgroup meta-analyses were performed for the DEB-TACE group and the cTACE group according to BCLC stage, and the results are shown in the table. For HCC patients with BCLC stage A and BCLC stage B disease, the 12-month survival rate was significantly greater in the DEB-TACE group than in the cTACE group (RR = 1.29, 1.42, 95%CI = 1.03-1.61, 1.07-1. Overall, the 12-month survival rate of patients in the DEB-TACE group was significantly greater than that of patients in the cTACE group (RR = 1.18, 95%CI: 1.08-1.29, P = 0.02). Second, a subgroup meta-analysis was conducted between the DEB-TACE group and the cTACE group according to the Child-Pugh classification. For people with Child-Pugh grade A or B liver cancer, there was no significant difference in the 12-month survival rate between the DEB-TACE group and the cTACE group (RR = 1.42). 1.25, 95%CI = 0.79-2.54. The 12-month survival rate of the DEB-TACE group was, however, considerably higher than that of the cTACE group when the two groups were merged (RR = 1.16, 95%CI: 1.06-1.27). Patients in the DEB-TACE group had a significantly higher 12-month survival rate than those in the cTACE group when doxorubicin was administered (RR = 1.15, 95%CI: 1.03–1.28, P = 0.03). Patient in the cTACE group and those in the DEB-TACE group who received epirubicin had different 12-month survival rates. The storage rate did not differ significantly (RR = 1.07, 95%CI: 0.94-1.22, P = 0.06). Overall, the DEB-TACE group's 12-month survival rate was much higher than the cTACE group's (RR = 1.13, 95%CI: 1.01-1.25; P = 0.03). Based on the above subgroup analysis results, the 12-month survival rate of the DEB-TACE group was greater than that of the cTACE group.

Bias risk assessment: A funnel plot was used to observe the bias risk of the five included studies, and the results showed that the risk of bias on the left and right sides of the five groups of images was basically symmetrical (Figure 3). The NOS scores of 12 studies ranged from 6 to 9, indicating that the results of the meta-analysis had good authenticity, so the conclusions were relatively reliable.

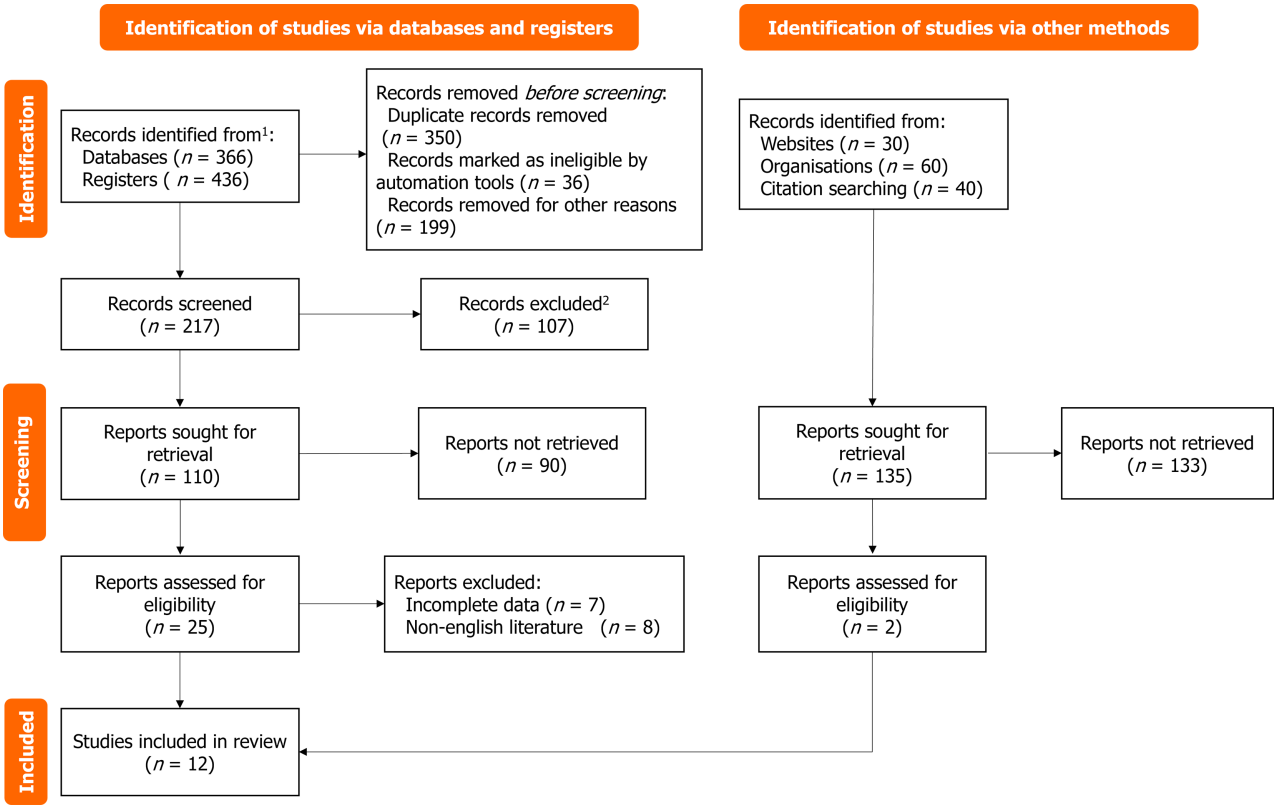

Figure 1 Document screening flow chart. [1]Consider, if feasible to do so, reporting the number of records identified from each database or register searched (rather than the total number across all databases/registers). [2]If automation tools were used, indicate how many records were excluded by a human and how many were excluded by automation tools.

DISCUSSION

TACE has been used as a standard treatment for patients with unresectable liver cancer. The fundamental idea behind TACE is that the combination of intra-arterial chemotherapy with iodide and chemotherapy drugs, along with selective vascular embolization, produces a potent cytotoxic effect and ischemia, leading to a favorable therapeutic outcome and a high survival rate[22-24]. In recent years, developers have developed DEB-TACE to deliver higher doses of chemotherapeutic agents and extend the contact time with tumors, ensuring controlled and sustained release[25]. Compared with those of regular cTACE, the amount of drug needed to reach the systemic circulation of doxorubicin-loaded microspheres treated with DEB-TACE greatly decreased[26]. They also greatly decreased adverse events related to the drug[27-29]. There was no significant difference in the PR rate, SD rate, or 6-month survival rate between the two groups.

In this meta-analysis, the postoperative CR rate in the DEB-TACE group was significantly greater than that in the cTACE group, which was consistent with the results of one meta-analysis and four retrospective studies. Therefore, DEB-TACE may be an effective treatment for HCC[30]. The pharmacokinetic properties of DEB-TACE, which permits higher doses of chemotherapeutic agents and extended contact time with cancer cells, may account for this difference[31-33]. Malagari *et al*[16] reported that there was more tumor necrosis 7–14 days after DEB-TACE treatment, and during this period, the proportion of damaged and necrotic cells was close to 100%, and the plasma amycin concentration was the lowest. These findings suggest that DEB-TACE is a more effective surgical procedure than cTACE.

In addition, DEB-TACE was superior to cTACE in terms of treatment response and tumor progression[34]. Recently, a meta-analysis revealed three previous studies comparing the efficacy of DEB-TACE and cTACE for the treatment of HCC. In terms of the number of included studies[35-37], the meta-analysis of Gao *et al*[3] included 7 studies, including 693 patients. In contrast, this meta-analysis included a larger number of studies and patients (12 studies, 1177 patients). Previous meta-analyses, based on the quality of the included studies, used the NOS, Egger, and Beger tests for risk assessment, whereas this meta-analysis employed the NOS scale for the same purpose. Previous meta-analyses revealed that patients who underwent DEB-TACE had better 1-year and 2-year survival rates than those who underwent cTACE, while the 6-month and 3-year survival rates were similar. In contrast, this meta-analysis revealed that 12-month survival was significantly greater in the DEB-TACE group than in the cTACE group. A meta-subgroup analysis of the 12-month survival rate after a randomized controlled trial. The results showed that the 1- and 2-year survival rates of the DEB-TTACE group were significantly greater than those of the cTACE group in the randomized controlled trial, but there was no significant difference in the 3-year survival rate after surgery[38]. Several studies[39,40] have shown that the Child-Pugh grade, BCLC stage, Eastern Cooperative Oncology Group score, and serum bilirubin level are associated with survival. Song *et al*'s study showed that in patients with mid-stage HCC, the 1-year survival rate in the DEB-TACE group was significantly greater than that in the cTACE group, while in patients with early-stage HCC, there was no significant

A

Study or subgroup	DEB-TACE Events	DEB-TACE Total	cTACE Events	cTACE Total	Weight	Risk ratio M-H, fixed, 95%CI
Chen 2017	3	17	2	16	1.7%	1.41 [0.27, 7.38]
Chi 2018	12	50	9	50	7.4%	1.33 [0.62, 2.88]
Ferrer 2011	10	47	4	25	4.3%	1.33 [0.46, 3.81]
Huang 2018	1	30	0	30	0.4%	3.00 [0.13, 70.83]
Lammer 2010	25	93	24	108	18.4%	1.21 [0.74, 1.97]
Lencioni 2009	29	52	77	160	31.3%	1.16 [0.87, 1.55]
Malagari 2010	11	41	6	43	4.8%	1.92 [0.78, 4.72]
Sacco 2011	17	33	16	34	13.0%	1.09 [0.67, 1.78]
Song 2012	33	60	16	69	12.3%	2.37 [1.46, 3.86]
Wiggermann 2011	3	22	0	22	0.4%	7.00 [0.38, 128.02]
You 2017	11	44	7	43	5.9%	1.54 [0.66, 3.59]
Total (95% CI)		**489**		**600**	**100.0%**	**1.42 [1.18, 1.72]**
Total events	155		161			

Heterogeneity: Chi² = 9.59, df = 10 (P = 0.48); I² = 0%
Test for overall effect: Z = 3.73 (P = 0.0002)

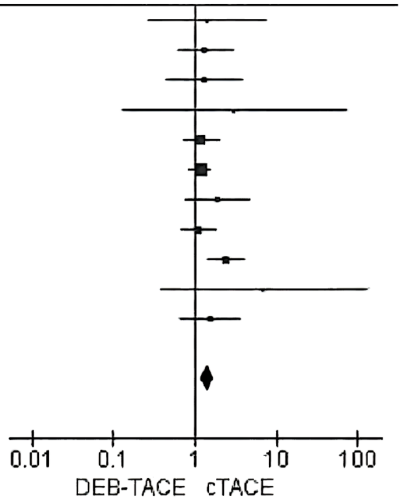

B

Study or subgroup	DEB-TACE Events	DEB-TACE Total	cTACE Events	cTACE Total	Weight	Risk ratio M-H, fixed, 95%CI
Chen 2017	9	17	7	16	3.9%	1.21 [0.59, 2.47]
Chi 2018	15	50	12	50	6.5%	1.25 [0.65, 2.39]
Ferrer 2011	16	47	7	25	5.0%	1.22 [0.58, 2.56]
Huang 2018	25	30	20	30	10.9%	1.25 [0.93, 1.69]
Lammer 2010	23	93	23	108	11.6%	1.16 [0.70, 1.93]
Lencioni 2009	28	50	80	162	20.5%	1.13 [0.85, 1.52]
Malagari 2010	19	41	18	43	9.6%	1.11 [0.68, 1.79]
Sacco 2011	16	33	14	34	7.5%	1.18 [0.69, 2.01]
Song 2012	16	60	18	69	9.1%	1.02 [0.57, 1.82]
Wiggermann 2011	2	22	5	22	2.7%	0.40 [0.09, 1.85]
You 2017	25	44	23	43	12.7%	1.06 [0.73, 1.55]
Total (95% CI)		**487**		**602**	**100.0%**	**1.13 [0.97, 1.30]**
Total events	194		227			

Heterogeneity: Chi² = 2.65, df = 10 (P = 0.99); I² = 0%
Test for overall effect: Z = 1.58 (P = 0.12)

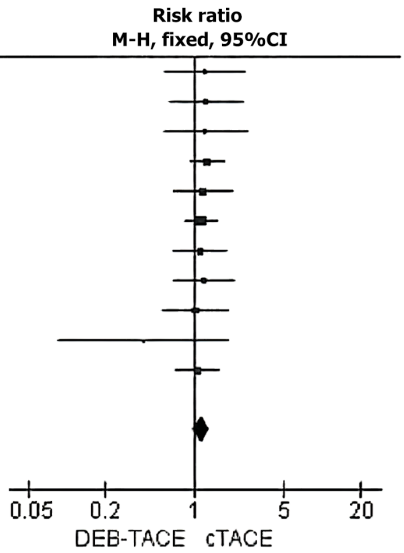

C

Study or subgroup	DEB-TACE Events	DEB-TACE Total	cTACE Events	cTACE Total	Weight	Risk ratio M-H, fixed, 95%CI
Chen 2017	4	17	4	16	4.3%	0.94 [0.28, 3.14]
Chi 2018	20	50	17	50	17.9%	1.18 [0.70, 1.97]
Ferrer 2011	4	47	6	25	8.3%	0.35 [0.11, 1.14]
Huang 2018	2	30	7	30	7.4%	0.29 [0.06, 1.26]
Lammer 2010	11	93	9	108	8.8%	1.42 [0.62, 3.28]
Lencioni 2009	12	24	94	188	22.4%	1.00 [0.65, 1.53]
Malagari 2010	6	41	10	43	10.3%	0.63 [0.25, 1.57]
Song 2012	9	60	21	69	20.6%	0.49 [0.24, 0.99]
Total (95% CI)		**362**		**529**	**100.0%**	**0.82 [0.64, 1.05]**
Total events	68		168			

Heterogeneity: Chi² = 10.72, df = 7 (P = 0.15); I² = 35%
Test for overall effect: Z = 1.57 (P = 0.12)

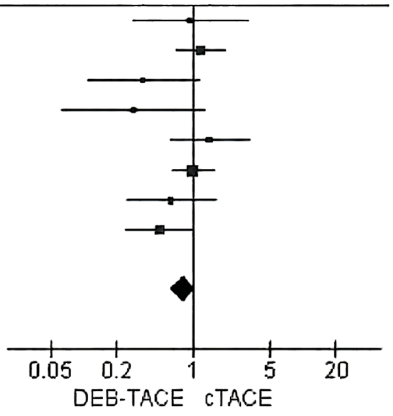

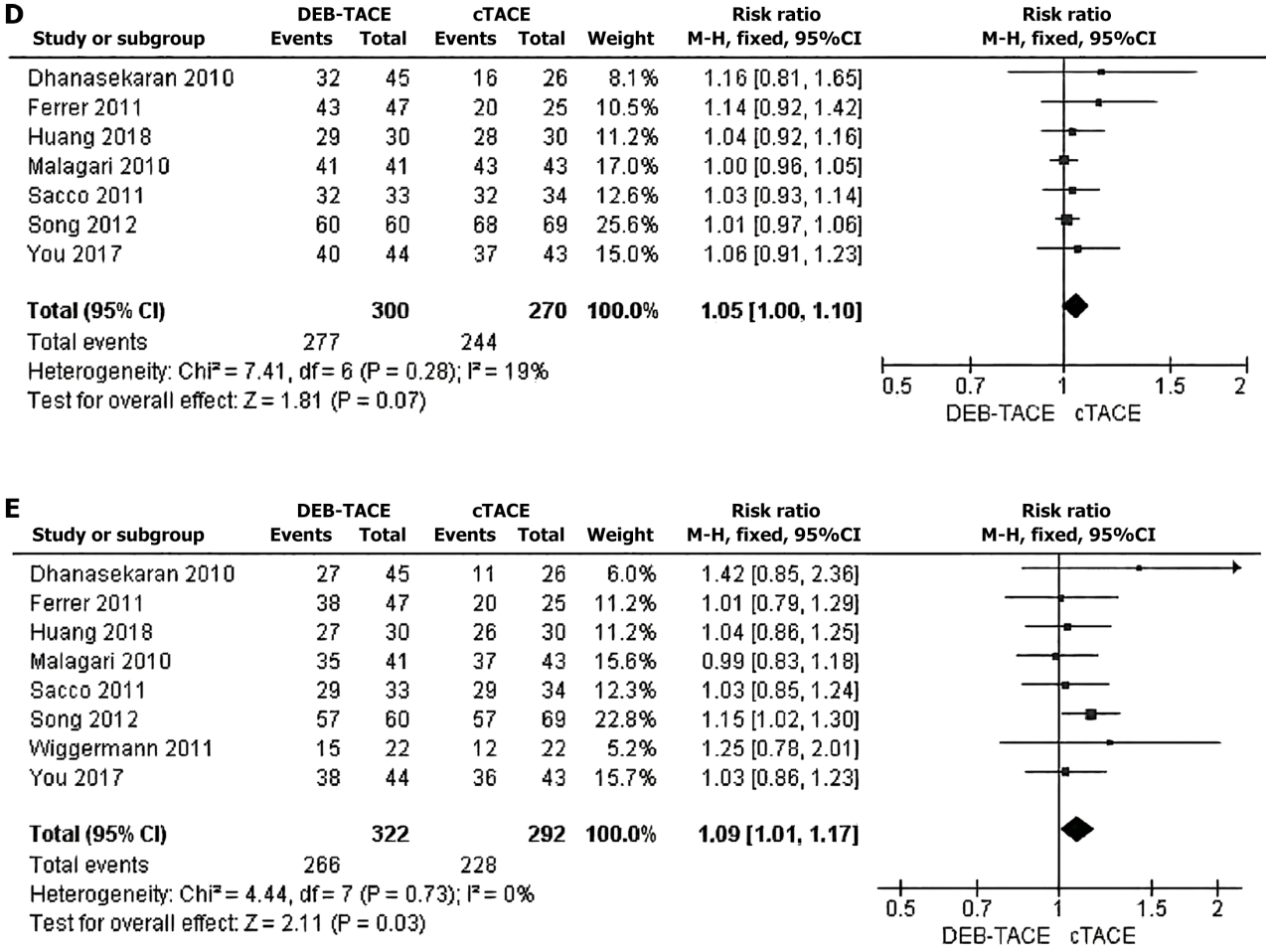

Figure 2 Meta-analysis. A-C: Meta-analysis of postoperative complete response between drug-luting beads-transhepatic arterial chemoembolization (DEB-TACE) and conventional transhepatic arterial chemoembolization (cTACE); D: A meta-analysis of 6-month survival rates between DEB-TACE and cTACE; E: A meta-analysis of 12-month survival after DEB-TACE and cTACE. DEB-TACE: Drug-luting beads-transhepatic arterial chemoembolization; cTACE: Conventional transhepatic arterial chemoembolization.

difference in the survival rate between the two groups[18]. Similarly, Dhanasekaran *et al*[21] reported that among HCC patients with BCLC stage A and BCLC stage B disease, the 1-year survival rate was significantly greater in the DEB-TACE group than in the cTACE group. The results of these two studies were similar to those of this meta-subgroup analysis. Compared with that of patients with early-stage liver cancer, overall survival between the DEB-TACE group and the cTACE group was significantly different only for patients with early-stage liver cancer. Therefore, this paper conducted a subgroup analysis of the 12-month postoperative survival rate according to BCLC stage, Child-Pugh grade, and drugs in drug-loaded microcapsules, resulting in a more substantial and reliable meta-analysis. It is concluded that DEB-TACE is more advantageous for the treatment of HCC.

The limitations of this study include the following: (1) There were fewer studies than DEB-TACE and cTACE, and most of the clinical studies were retrospective studies, suggesting that unmeasured confounding factors and selection bias may have affected the results of these studies; (2) The number of participants is limited, and a large number of samples will increase the accuracy of the results; (3) Heterogeneity of baseline characteristics, such as age, Child-Pugh grade, and tumor diameter, may cause potential bias; (4) Inclusion criteria vary from study to study and may lead to different results; (5) In the selected studies, there were no comprehensive criteria for type, dose, and drug-carrying microsphere size, which may affect the accuracy of the results; and (6) Some studies used the European Society of Hepatology criteria or computed tomography to assess tumor response, which may not take into account the microstructure of necrosis.

CONCLUSION

This meta-analysis compared the efficacy of drug-loaded microspheres and traditional iodized oil in treating unresectable liver cancer *via* hepatic arterial chemoembolization. The results showed that the drug-loaded microsphere treatment had a significant advantage in terms of efficacy, and compared with those in the traditional iodized oil group, the tumor shrinkage rate was greater, survival was significantly longer, and side effects were fewer. Further analysis showed that drug-loaded microspheres had a better local tumor control effect, could release drugs more effectively, reduced damage

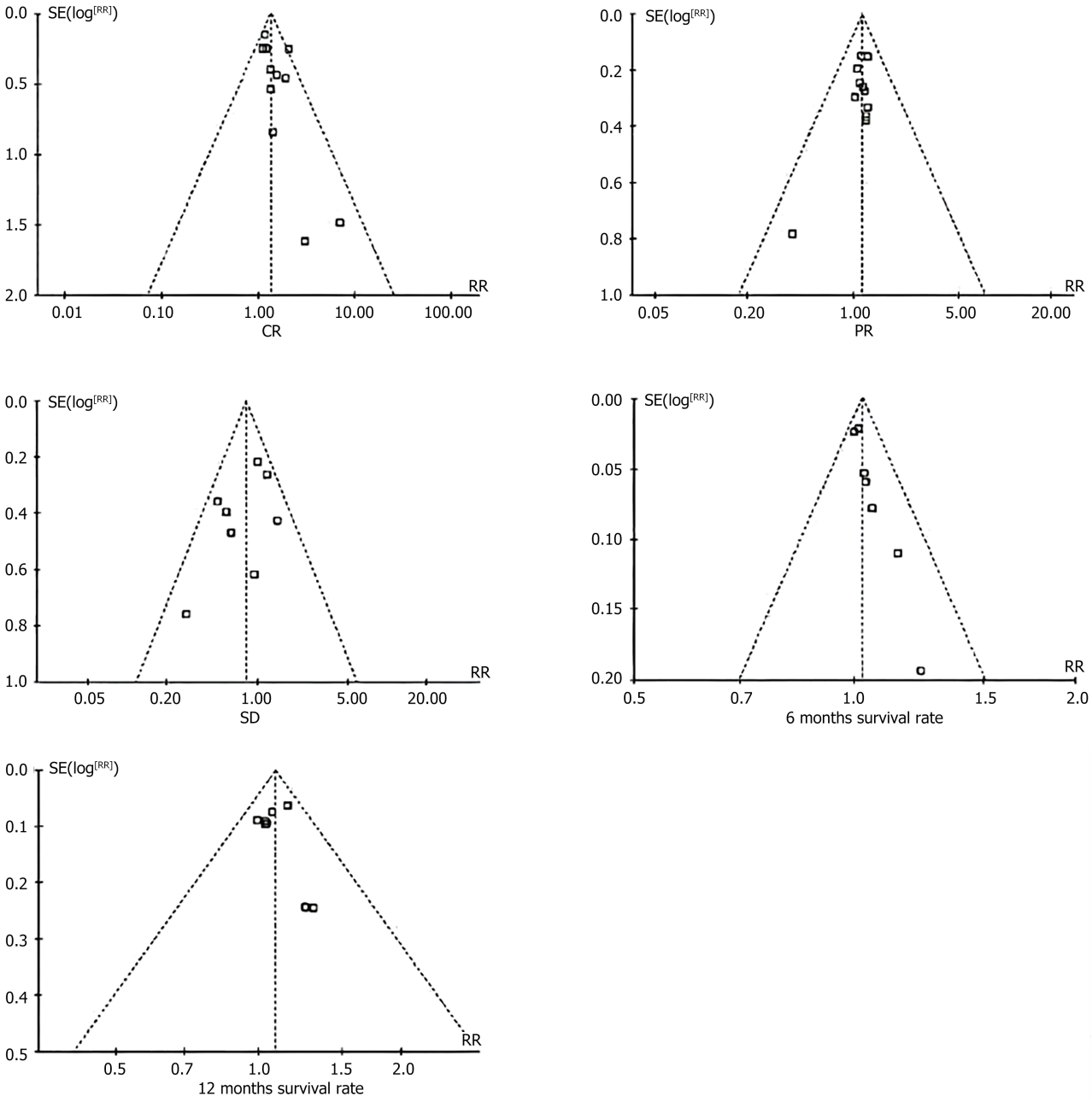

Figure 3 Funnel plot incorporating the results of the study. CR: Complete response rate; PR: Partial response rate; SD: Stable disease.

to normal liver tissue, and improved the safety and tolerability of treatment. Therefore, our results support the idea of using drug-loaded microspheres for hepatic arterial chemoembolization in people with liver cancer that cannot be removed. This should be a better and safer way to treat cancer and provide doctors with important information for their work.

FOOTNOTES

Author contributions: Deng J wrote the manuscript; Mi YH, Xie L, Sun XX, Liu DH, Long HJ and He LY collected the data; Wu DH and Shang HC guided the study; All authors reviewed, edited, and approved the final manuscript and revised it critically for important intellectual content, gave final approval of the version to be published, and agreed to be accountable for all aspects of the work.

Supported by Scientific Research project of Hunan Provincial Health Commission, No. B202303077689; and Hunan Natural Science Foundation Project, No. 2023JJ40397.

Conflict-of-interest statement: The authors declare no conflicts of interest.

PRISMA 2009 Checklist statement: The authors have read the PRISMA 2009 Checklist, and the manuscript was prepared and revised

according to the PRISMA 2009 Checklist.

Country of origin: China

ORCID number: Da-Hua Wu 0000-0002-0943-0037; Hong-Cai Shang 0009-0008-1576-5790.

S-Editor: Liu H
L-Editor: A
P-Editor: Chen YX

REFERENCES

1 **Wang Y**, Benzina A, Molin DG, Akker Nv, Gagliardi M, Koole LH. Preparation and structure of drug-carrying biodegradable microspheres designed for transarterial chemoembolization therapy. *J Biomater Sci Polym Ed* 2015; **26**: 77-91 [PMID: 25425276 DOI: 10.1080/09205063.2014.982242]
2 **Wu L**, Zheng Y, Liu J, Luo R, Wu D, Xu P, Wu D, Li X. Comprehensive evaluation of the efficacy and safety of LPV/r drugs in the treatment of SARS and MERS to provide potential treatment options for COVID-19. *Aging (Albany NY)* 2021; **13**: 10833-10852 [PMID: 33879634 DOI: 10.18632/aging.202860]
3 **Gao F**, Rafiq M, Cong H, Yu B, Shen Y. Current research status and development prospects of embolic microspheres containing biological macromolecules and others. *Int J Biol Macromol* 2024; **267**: 131494 [PMID: 38608974 DOI: 10.1016/j.ijbiomac.2024.131494]
4 **Sun J**, Li WG, Wang Q, He WP, Wang HB, Han P, Zhang T, Zhang AM, Fan YZ, Sun YZ, Duan XZ. Hepatic Resection Versus Stereotactic Body Radiation Therapy Plus Transhepatic Arterial Chemoembolization for Large Hepatocellular Carcinoma: A Propensity Score Analysis. *J Clin Transl Hepatol* 2021; **9**: 672-681 [PMID: 34722182 DOI: 10.14218/JCTH.2020.00188]
5 **Cheng KL**, Cheng YM, Chan CY, Wang CC. Predictors of Liver Dysfunction After Transhepatic Arterial Chemo-embolization in Hepatocellular Carcinoma Patients. *Dig Dis Sci* 2023; **68**: 3467-3472 [PMID: 37266712 DOI: 10.1007/s10620-023-07984-4]
6 **Wu L**, Zhong Y, Wu D, Xu P, Ruan X, Yan J, Liu J, Li X. Immunomodulatory Factor TIM3 of Cytolytic Active Genes Affected the Survival and Prognosis of Lung Adenocarcinoma Patients by Multi-Omics Analysis. *Biomedicines* 2022; **10** [PMID: 36140350 DOI: 10.3390/biomedicines10092248]
7 **Chen NY**, Chen KH, Wang YW, Tsai HH, Lee WC, Weng LC. The impact of symptom distress on health-related quality of life in liver cancer patients receiving arterial chemoembolization: the mediating role of hope. *BMC Gastroenterol* 2022; **22**: 456 [PMID: 36380273 DOI: 10.1186/s12876-022-02529-x]
8 **Liu S**, Yu G, Wang Q, Li L, Liu Y, Du K, Zhang F, Zhao B, Zhao G. CalliSpheres(®) microspheres drug-eluting bead transhepatic artery chemoembolization with or without sorafenib for the treatment of large liver cancer: a multi-center retrospective study. *Am J Transl Res* 2021; **13**: 13931-13940 [PMID: 35035734]
9 **Wang W**, Li F, Gan P, Li B, Li S. Callispheres drug-eluting bead transhepatic artery chemoembolization with oral delivery of sorafenib for the treatment of unresectable liver cancer. *Front Surg* 2022; **9**: 981116 [PMID: 36117819 DOI: 10.3389/fsurg.2022.981116]
10 **Chen G**, Zhang D, Ying YC, Wang ZF, Tao W, Zhu H, Zhang JF, Peng ZY. [Clinical study on the treatment of unresectable primary liver cancer by transarterial chemoembolization with Chinese drug-carrying microspheres]. *hejiang Daxue Xuebao; Yixue Kexueban* 2017; **46**: 44-51
11 **Chi Q**, Zhang L, Liu B, Zhang GA. [Efficacy of Epirubicin combined with iodide and Hepas phere drug-loaded microspheres in the treatment of TACE in patients with liver cancer]. *Xiandai Zhongliu Yixue* 2018; **26**: 2090-2093
12 **Ferrer Puchol MD**, la Parra C, Esteban E, Vaño M, Forment M, Vera A, Cosín O. [Comparison of doxorubicin-eluting bead transarterial chemoembolization (DEB-TACE) with conventional transarterial chemoembolization (TACE) for the treatment of hepatocellular carcinoma]. *Radiologia* 2011; **53**: 246-253 [PMID: 21295802 DOI: 10.1016/j.rx.2010.07.010]
13 **Huang YJ**, Ling YZ, Qin ZL. [Efficacy of HepaSphere drug-loaded microspheres in the treatment of primary liver cancer]. *Linchuang Yixue Zazhi* 2018; **38**: 35-36
14 **Lammer J**, Malagari K, Vogl T, Pilleul F, Denys A, Watkinson A, Pitton M, Sergent G, Pfammatter T, Terraz S, Benhamou Y, Avajon Y, Gruenberger T, Pomoni M, Langenberger H, Schuchmann M, Dumortier J, Mueller C, Chevallier P, Lencioni R; PRECISION V Investigators. Prospective randomized study of doxorubicin-eluting-bead embolization in the treatment of hepatocellular carcinoma: results of the PRECISION V study. *Cardiovasc Intervent Radiol* 2010; **33**: 41-52 [PMID: 19908093 DOI: 10.1007/s00270-009-9711-7]
15 **Lencioni R**, Malagari K, Vogl T, Pilleul F, Denys A, Watkinson A, Lammer J. A randomized phase II trial of a drug eluting bead in the treatment of hepatocellular carcinoma by transcatheter arterial chemoembolization. *J Clin Oncol* 2009; **27**: 4523 [DOI: 10.1200/jco.2009.27.15_suppl.4523]
16 **Malagari K**, Pomoni M, Kelekis A, Pomoni A, Dourakis S, Spyridopoulos T, Moschouris H, Emmanouil E, Rizos S, Kelekis D. Prospective randomized comparison of chemoembolization with doxorubicin-eluting beads and bland embolization with BeadBlock for hepatocellular carcinoma. *Cardiovasc Intervent Radiol* 2010; **33**: 541-551 [PMID: 19937027 DOI: 10.1007/s00270-009-9750-0]
17 **Sacco R**, Bargellini I, Bertini M, Bozzi E, Romano A, Petruzzi P, Tumino E, Ginanni B, Federici G, Cioni R, Metrangolo S, Bertoni M, Bresci G, Parisi G, Altomare E, Capria A, Bartolozzi C. Conventional versus doxorubicin-eluting bead transarterial chemoembolization for hepatocellular carcinoma. *J Vasc Interv Radiol* 2011; **22**: 1545-1552 [PMID: 21849247 DOI: 10.1016/j.jvir.2011.07.002]
18 **Song MJ**, Chun HJ, Song DS, Kim HY, Yoo SH, Park CH, Bae SH, Choi JY, Chang UI, Yang JM, Lee HG, Yoon SK. Comparative study between doxorubicin-eluting beads and conventional transarterial chemoembolization for treatment of hepatocellular carcinoma. *J Hepatol* 2012; **57**: 1244-1250 [PMID: 22824821 DOI: 10.1016/j.jhep.2012.07.017]

19 **Wiggermann P**, Sieron D, Brosche C, Brauer T, Scheer F, Platzek I, Wawrzynek W, Stroszczynski C. Transarterial Chemoembolization of Child-A hepatocellular carcinoma: drug-eluting bead TACE (DEB TACE) vs. TACE with cisplatin/lipiodol (cTACE). *Med Sci Monit* 2011; **17**: CR189-CR195 [PMID: 21455104 DOI: 10.12659/msm.881714]

20 **You JX**, Wang JB, Ai ST, Fan XD, Zheng LZ, Su LX, Wen MZ, Yang XT. [Effect of microspheres combined with liodoembolization in the treatment of hepatocellular carcinoma]. *Jieru Fangshexue Zazhi* 2017; **26**: 531-534

21 **Dhanasekaran R**, Kooby DA, Staley CA, Kauh JS, Khanna V, Kim HS. Comparison of conventional transarterial chemoembolization (TACE) and chemoembolization with doxorubicin drug eluting beads (DEB) for unresectable hepatocelluar carcinoma (HCC). *J Surg Oncol* 2010; **101**: 476-480 [PMID: 20213741 DOI: 10.1002/jso.21522]

22 **Wu L**, Liu Q, Ruan X, Luan X, Zhong Y, Liu J, Yan J, Li X. Multiple Omics Analysis of the Role of RBM10 Gene Instability in Immune Regulation and Drug Sensitivity in Patients with Lung Adenocarcinoma (LUAD). *Biomedicines* 2023; **11** [PMID: 37509501 DOI: 10.3390/biomedicines11071861]

23 **Yuan Y**, He W, Yang Z, Qiu J, Huang Z, Shi Y, Lin Z, Zheng Y, Chen M, Lau WY, Li B, Yuan Y. TACE-HAIC combined with targeted therapy and immunotherapy versus TACE alone for hepatocellular carcinoma with portal vein tumour thrombus: a propensity score matching study. *Int J Surg* 2023; **109**: 1222-1230 [PMID: 37026861 DOI: 10.1097/JS9.0000000000000256]

24 **Brown AM**, Kassab I, Massani M, Townsend W, Singal AG, Soydal C, Moreno-Luna L, Roberts LR, Chen VL, Parikh ND. TACE versus TARE for patients with hepatocellular carcinoma: Overall and individual patient level meta analysis. *Cancer Med* 2023; **12**: 2590-2599 [PMID: 35943116 DOI: 10.1002/cam4.5125]

25 **Liu YM**, Ren YQ, Song SL, Zheng CS. Pyogenic liver abscess in non-liver cancer patients and liver cancer patients treated with TACE: Etiological characteristics, treatment, and outcome analysis. *Kaohsiung J Med Sci* 2023; **39**: 87-94 [PMID: 36354204 DOI: 10.1002/kjm2.12613]

26 **Wu L**, Zheng Y, Ruan X, Wu D, Xu P, Liu J, Wu D, Li X. Long-chain noncoding ribonucleic acids affect the survival and prognosis of patients with esophageal adenocarcinoma through the autophagy pathway: construction of a prognostic model. *Anticancer Drugs* 2022; **33**: e590-e603 [PMID: 34338240 DOI: 10.1097/CAD.0000000000001189]

27 **Aarts BM**, Muñoz FMG, Wildiers H, Dezentjé VO, Baetens TR, Schats W, Lopez-Yurda M, Dresen RC, Wit-van der Veen BJ, Deroose CM, Maleux G, Beets-Tan RGH, Klompenhouwer EG. Intra-Arterial Therapies for Liver Metastatic Breast Cancer: A Systematic Review and Meta-Analysis. *Cardiovasc Intervent Radiol* 2021; **44**: 1868-1882 [PMID: 34322751 DOI: 10.1007/s00270-021-02906-1]

28 **Wu L**, Zhong Y, Yu X, Wu D, Xu P, Lv L, Ruan X, Liu Q, Feng Y, Liu J, Li X. Selective poly adenylation predicts the efficacy of immunotherapy in patients with lung adenocarcinoma by multiple omics research. *Anticancer Drugs* 2022; **33**: 943-959 [PMID: 35946526 DOI: 10.1097/CAD.0000000000001319]

29 **Wang J**, Xu H, Wang Y, Feng L, Yi F. Efficacy and Safety of Drug-Eluting Bead TACE in the Treatment of Primary or Secondary Liver Cancer. *Can J Gastroenterol Hepatol* 2023; **2023**: 5492931 [PMID: 37153689 DOI: 10.1155/2023/5492931]

30 **Wu L**, Li H, Liu Y, Fan Z, Xu J, Li N, Qian X, Lin Z, Li X, Yan J. Research progress of 3D-bioprinted functional pancreas and in vitro tumor models. *IJB* 2024; **10**: 1256 [DOI: 10.36922/ijb.1256]

31 **Kim D**, Lee JH, Moon H, Seo M, Han H, Yoo H, Seo H, Lee J, Hong S, Kim P, Lee HJ, Chung JW, Kim H. Development and evaluation of an ultrasound-triggered microbubble combined transarterial chemoembolization (TACE) formulation on rabbit VX2 liver cancer model. *Theranostics* 2021; **11**: 79-92 [PMID: 33391462 DOI: 10.7150/thno.45348]

32 **Wang Y**, Lin W, Huang G, Nie S, Yu Q, Hou F, Zong S. The therapeutic principle of combined clearing heat and resolving toxin plus TACE on primary liver cancer: A systematic review and meta-analysis. *J Ethnopharmacol* 2024; **319**: 117072 [PMID: 37625603 DOI: 10.1016/j.jep.2023.117072]

33 **Bosi C**, Rimini M, Casadei-Gardini A, Giorgio Ercolani. Understanding the causes of recurrent HCC after liver resection and radiofrequency ablation. *Expert Rev Anticancer Ther* 2023; **23**: 503-515 [PMID: 37060290 DOI: 10.1080/14737140.2023.2203387]

34 **Cao KK**, Ding N, Li XW, Zhong JM, Zhai J, Qu ZQ, Zhang XL. Incidence And Risk Factors Of Contrast Nephropathy After Tace In Patients With Liver Cancer And Chronic Kidney Disease. *Clin Invest Med* 2021; **44**: E19-E24 [PMID: 34600459 DOI: 10.25011/cim.v44i3.36961]

35 **Wu L**, Li X, Qian X, Wang S, Liu J, Yan J. Lipid Nanoparticle (LNP) Delivery Carrier-Assisted Targeted Controlled Release mRNA Vaccines in Tumor Immunity. *Vaccines (Basel)* 2024; **12** [PMID: 38400169 DOI: 10.3390/vaccines12020186]

36 **Wang J**, Huang A, Fu P, Chen X, Zhang X, Yin Y, Zhou J. Effects of TACE combined with microwave ablation on T lymphocyte subsets and prognosis in patients with liver cancer and analysis of safety. *J BUON* 2020; **25**: 1883-1889 [PMID: 33099928]

37 **Liu B**, Zhang Y, Chen H, Li W, Tsochatzis E. The combination of transcatheter arterial chemoembolisation (TACE) and thermal ablation versus TACE alone for hepatocellular carcinoma. *Cochrane Database Syst Rev* 2022; **1**: CD013345 [PMID: 34981511 DOI: 10.1002/14651858.CD013345.pub2]

38 **Wu L**, Chen X, Zeng Q, Lai Z, Fan Z, Ruan X, Li X, Yan J. NR5A2 gene affects the overall survival of LUAD patients by regulating the activity of CSCs through SNP pathway by OCLR algorithm and immune score. *Heliyon* 2024; **10**: e28282 [PMID: 38601554 DOI: 10.1016/j.heliyon.2024.e28282]

39 **Chan KS**, Tay WX, Cheo FY, Shelat VG. Preoperative transarterial chemoembolization (TACE) + liver resection versus upfront liver resection for large hepatocellular carcinoma (≥5 cm): a systematic review and meta-analysis. *Acta Chir Belg* 2023; **123**: 601-617 [PMID: 37681991 DOI: 10.1080/00015458.2023.2256539]

40 **Yin L**, Liu KC, Lv WF, Lu D, Tan YL, Wang GX, Dai JY, Zhu XH, Jiang B. Comparing the effectiveness and safety of Sorafenib plus TACE with Apatinib plus TACE for treating patients with unresectable hepatocellular carcinoma: a multicentre propensity score matching study. *Cancer Imaging* 2023; **23**: 52 [PMID: 37254146 DOI: 10.1186/s40644-023-00574-7]

World Journal of Gastrointestinal Oncology

Submit a Manuscript: https://www.f6publishing.com

World J Gastrointest Oncol 2024 December 15; 16(12): 4738-4745

DOI: 10.4251/wjgo.v16.i12.4738

ISSN 1948-5204 (online)

CASE REPORT

Mixed pancreatic ductal adenocarcinoma and well-differentiated neuroendocrine tumor: A case report

Xiaofeng Zhao, Tina Bocker Edmonston, Ronald Miick, Upasana Joneja

Specialty type: Pathology

Provenance and peer review: Unsolicited article; Externally peer reviewed.

Peer-review model: Single blind

Peer-review report's classification

Scientific Quality: Grade A, Grade B

Novelty: Grade A, Grade B

Creativity or Innovation: Grade A, Grade C

Scientific Significance: Grade A, Grade B

P-Reviewer: Han MZ; Quiñonero F

Received: July 31, 2024

Revised: October 5, 2024

Accepted: October 22, 2024

Published online: December 15, 2024

Processing time: 104 Days and 11.8 Hours

Xiaofeng Zhao, Tina Bocker Edmonston, Ronald Miick, Upasana Joneja, Department of Pathology, Cooper University Hospital, Camden, NJ 08103, United States

Corresponding author: Xiaofeng Zhao, MD, PhD, Assistant Professor, Department of Pathology, Cooper University Hospital, 1 Cooper Plz, Camden, NJ 08103, United States. zhao-xiaofeng@cooperhealth.edu

Abstract

BACKGROUND

Pancreatic mixed neuroendocrine-non-neuroendocrine neoplasms (MiNENs) are rare malignancies affecting the pancreas. The World Health Organization defines MiNENs as neoplasms composed of morphologically recognizable neuroendocrine and non-neuroendocrine components, each constituting 30% or more of the tumor volume. Adenocarcinoma-neuroendocrine carcinoma is the most frequent MiNEN combination. A well-differentiated neuroendocrine tumor (NET) component is rarely reported in MiNENs.

CASE SUMMARY

Here we report a rare case with intermingled components of ductal adenocarcinoma and grade 1 well-differentiated NET in the pancreas. The two tumors show distinct histology and significant differentiation discrepancy (poorly differentiated high grade adenocarcinoma and well-differentiated low grade NET), and also present as metastases in separate lymph nodes. Next generation sequencing of the two components demonstrates *KRAS* and *TP53* mutations in the ductal adenocarcinoma, but no genetic alterations in the NET, suggesting divergent origins for these two components. Although tumors like this meet the diagnostic criteria for MiNEN, clinicians often find the diagnosis and staging confusing and impractical for clinical management.

CONCLUSION

Mixed NET/non-NET tumors with distinct histology and molecular profiles might be better classified as collision tumors rather than MiNENs.

Key Words: Pancreatic mixed neuroendocrine-non-neuroendocrine neoplasms; Pancreatic adenocarcinoma; Grade 1 well-differentiated neuroendocrine tumor; Molecular profile; Collision tumor; Case report

Core Tip: Pancreatic mixed neuroendocrine-non-neuroendocrine neoplasms (MiNENs) are rare malignancies affecting the pancreas, recognized by the World Health Organization as neoplasms composed of morphologically recognizable neuroendocrine and non-neuroendocrine components, each constituting ≥ 30% of the tumor volume. However, whether the tumor should be classified as a MiNEN or collision tumor when there is clear divergence in histology and molecular profiles for each component is still debatable. This paper reports a rare case with high grade adenocarcinoma admixed with low grade neuroendocrine tumor in pancreas, which are demonstrated to have distinct molecular profiles. We discuss the potential impacts of tumor classification on staging and clinical management, hoping to encourage more discussions and studies on this rare entity.

Citation: Zhao X, Bocker Edmonston T, Miick R, Joneja U. Mixed pancreatic ductal adenocarcinoma and well-differentiated neuroendocrine tumor: A case report. *World J Gastrointest Oncol* 2024; 16(12): 4738-4745
URL: https://www.wjgnet.com/1948-5204/full/v16/i12/4738.htm
DOI: https://dx.doi.org/10.4251/wjgo.v16.i12.4738

INTRODUCTION

Pancreatic mixed neuroendocrine-non-neuroendocrine neoplasms (MiNENs) are rare malignancies affecting the pancreas. They are defined as neoplasms composed of morphologically recognizable neuroendocrine and non-neuroendocrine components, each constituting ≥ 30% of the tumor volume[1]. Though the adenocarcinoma-neuroendocrine carcinoma (NEC) association is the most frequent, previously termed as mixed adeno-NEC (MANEC) in 2010[1], the spectrum of this entity is wide, and encompasses variable combinations between neuroendocrine tumors (NETs) and NECs, and other epithelial tumors of the pancreas (acinar cell carcinoma, intraductal papillary mucinous neoplasm, and serous cystic neoplasm)[1]. Among these, a high grade neuroendocrine component, either small or large cell type, is present in the majority of cases[2], and low grade NET is rarer. Limited molecular studies suggest a clonal relationship between the non-neuroendocrine and neuroendocrine components in these cases[1]. We present a case of mixed ductal adenocarcinoma intermingled with grade 1 well-differentiated NET with discussion of histologic and staging difficulties, molecular profiles, and origins.

CASE PRESENTATION

Chief complaints

A 64-year-old female presented to the emergency department with a three-day history of intermittent abdominal pain.

History of present illness

The patient endorsed stinging left-sided flank pain rated at 10/10 on the pain scale. The patient also reported nausea, vomiting, fevers, and chills. Fever was recorded as high as 40.6 C (105 F) at home. Patient denied chest pain or shortness of breath.

History of past illness

The patient has a past medical history of uncontrolled type 2 diabetes mellitus, with long-term current use of insulin.

Personal and family history

Other personal history includes fatty liver disease, tobacco use of 1-2 packs a day for about 50 years. No significant family history is noted.

Physical examination

Physical examination revealed a female with normal appearance, not in acute distress, with stable vital signs. There was abdominal tenderness, without guarding or rebound.

Laboratory examinations

Laboratory tests revealed an elevated serum glucose (up to 377 mg/dL, reference range: 70-110 mg/dL), elevated hemoglobin A1c (11.2%, reference range: 4.8%-5.6%), and elevated carbohydrate antigen 19-9 (CA19-9) of 1474 U/mL (reference range: 0-35 U/mL). Pancreatic amylase was within normal limits (40 U/L, 28-100 U/L).

Imaging examinations

Computed tomography (CT) of the abdomen revealed a 4.0 cm × 2.0 cm ill-defined, infiltrating mass involving the distal pancreatic body and tail (Figure 1). The mass was diffusely hypoenhancing and demonstrated mild T2 hyperintensity, likely representing central necrosis. The mass encased and occluded the splenic artery and abutted and narrowed the

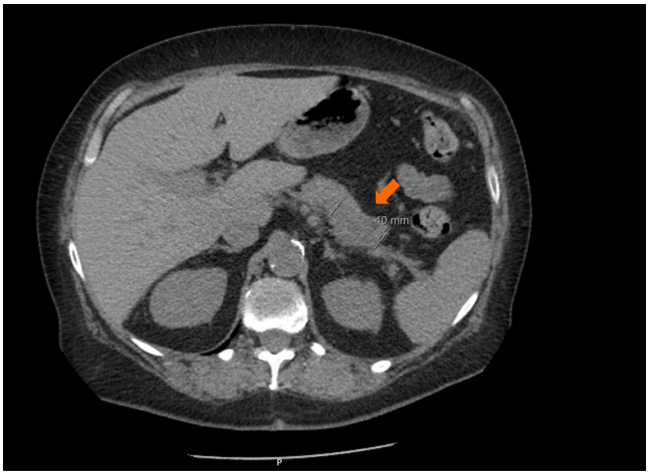

Figure 1 Computed tomography imaging of abdomen showing a 4.0 cm pancreatic tail mass (arrow).

splenic vein which appeared grossly patent. The hepatic arteries, portal vein, and gastroduodenal artery were patent. The findings were highly suspicious for pancreatic adenocarcinoma, and there was no evidence of mesenteric vascular involvement.

FINAL DIAGNOSIS

On distal pancreatectomy, a pale-tan ill-defined mass was identified in the pancreatic tail grossly, measuring 3.5 cm × 2.0 cm × 1.5 cm. Histopathologic examination showed a tumor composed of two morphologically distinct yet intermingled components: A moderately to poorly differentiated ductal adenocarcinoma and a low grade well-differentiated NET, grade 1. The ductal adenocarcinoma consisted of cells with high nuclear/cytoplasm ratio, marked nuclear pleomorphism, and vesicular chromatin with prominent nucleoli (Figure 2A and B). Mitotic figures were brisk. Perineural and intravascular invasions were evident. The adenocarcinoma constituted approximately 60% of the tumor mass volume. The neuroendocrine component was comprised of monotonous bland tumor cells with round nuclei, salt-and-pepper chromatin, and abundant cytoplasm arranged in tubules and nests, constituting approximately 40% of the tumor volume (Figure 3A). No mitotic figures were evident in this component. The neuroendocrine component was positive for pan-cytokeratin AE1/AE3, INSM1, and synaptophysin, and Ki67 was < 3% (Figure 3B-E). The overall findings were consistent with a grade 1 well-differentiated NET component (WDNET). In contrast, the adenocarcinoma component was positive for CK7 and negative for CK20, INSM1, and synaptophysin (Figure 3F-J). Regions of intermingled neuroendocrine and ductal components were present (Figure 2C and D; Figure 3F-J). Examination of the lymph nodes revealed adenocarcinoma involving three lymph nodes and metastatic well- differentiated NET in one of a total of twenty-two lymph nodes (Figure 2E and F).

Next generation sequencing of the two different histologic components was performed after microdissection to determine and compare their molecular profiles. The TruSight Tumor 170 panel (Illumina, San Diego, CA, United States) analyzes tumor DNA for Single Nucleotide Variants and insertion/deletions in 151 genes and for amplifications of 59 genes and analyzes tumor RNA for fusions and splice variants of 55 genes using the NextSeq 550 system (Illumina, San Diego, CA, United States). *KRAS* exon 2 p.G12D (variant frequency 4.9%) and *TP53* exon 5 p.A161T (variant frequency 6.2%) were identified in the adenocarcinoma component. No variants of clinical significance, including *KRAS* and *TP53*, were identified for the WDNET (Figure 4). The DNA mismatch repair status by immunohistochemistry in the adenocarcinoma component was intact.

TREATMENT

The patient underwent distal pancreatectomy, splenectomy and celiac lymph node dissection, as well adjuvant chemotherapy.

OUTCOME AND FOLLOW-UP

The patient's postoperative course was remarkable for uncontrolled diabetes, but otherwise uneventful. CA19-9 was trending down from preop level of 1474 U/mL but remained high above 600 U/mL one-month post-surgery and remained persistently elevated. The patient underwent adjuvant chemotherapy for two months.

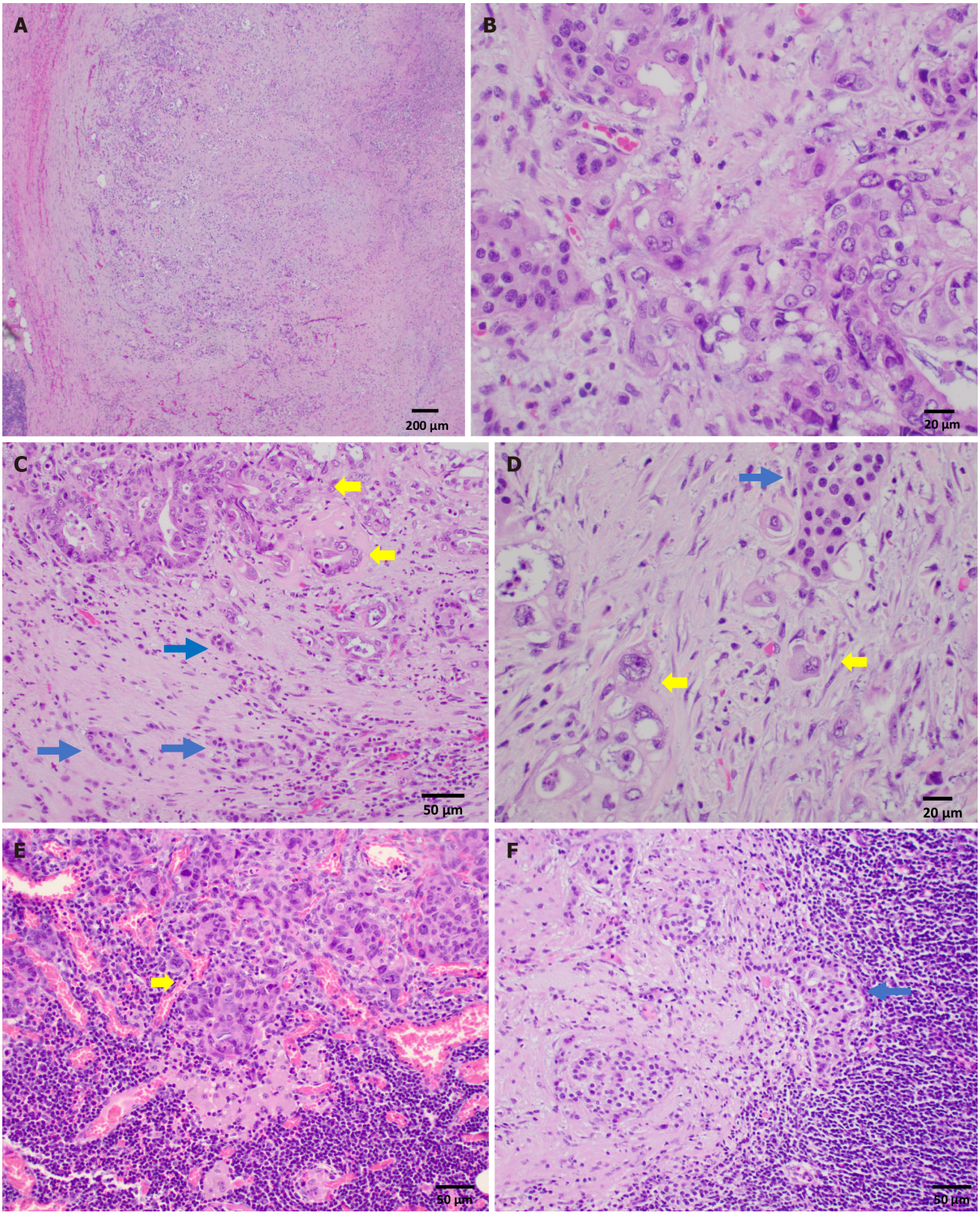

Figure 2 Pancreatic ductal adenocarcinoma and low grade neuroendocrine tumor components. A: Pancreatic ductal adenocarcinoma component in low power (40 ×); B: Pancreatic ductal adenocarcinoma component in high power (400 ×); C and D: Intermingled pancreatic ductal adenocarcinoma (yellow arrow) and well-differentiated neuroendocrine tumor (blue arrow), hematoxylin and eosin (H&E, 200 × and 400 ×); E: Lymph node with metastatic ductal adenocarcinoma (H&E, 200 ×, yellow arrow); F: Lymph node with well-differentiated neuroendocrine tumor (H&E, 200 ×, blue arrow).

CT of the chest before surgery demonstrated three small right lung nodules and bilateral groundglass opacities, which have been closely followed. No definitive distant disease was identified on positron emission tomography/CT. After one month into chemotherapy, CT of chest and abdomen revealed enlargement of lung nodules, as well as a new 22 mm hypoechoic intense lesion and two smaller ring-enhancing hypodense lesions in liver. CT-guided fine needle aspiration of one of the liver lesions was consistent with metastatic adenocarcinoma of pancreatic origin.

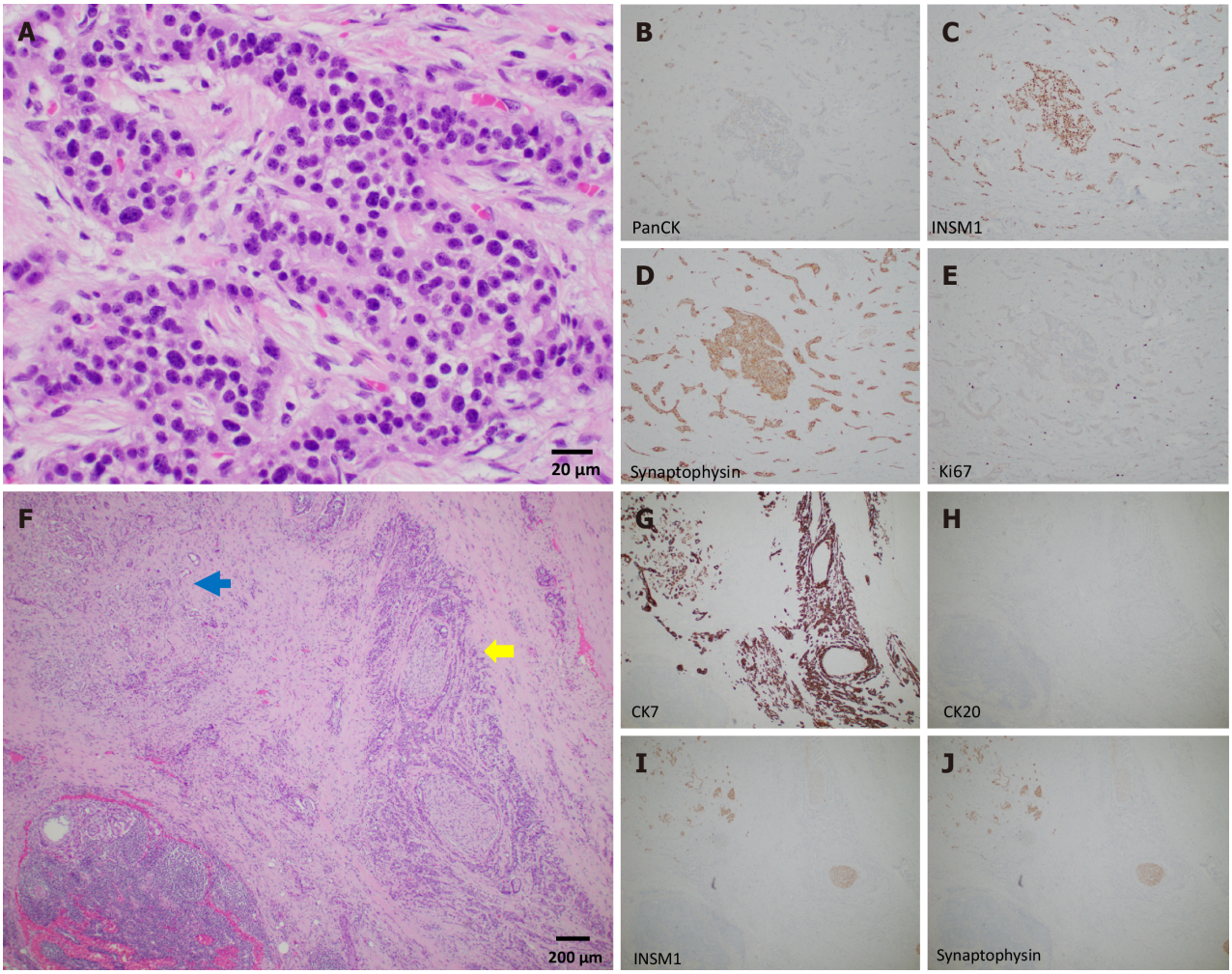

Figure 3 Neuroendocrine tumor component. A-E: Well-differentiated neuroendocrine tumor component. Hematoxylin and eosin (H&E), 400 ×. The tumor is weakly positive for PanCK AE1/AE3 (B), strongly positive for INSM1 and synaptophysin (C and D), proliferative index Ki67 is very low (< 3%, E); F-J: Intermingled pancreatic ductal adenocarcinoma (yellow arrow) and well-differentiated neuroendocrine tumor (blue arrow). Hematoxylin and eosin, 40 ×. Perineural invasion is evident (F); Immunohistochemical stain for CK7 is positive for both component (G); CK20 is negative in both (H); INSM1 and synaptophysin are positive in well-differentiated neuroendocrine tumor (and neurons) (I and J).

DISCUSSION

The diagnosis of MiNEN, especially a mixed ductal adenocarcinoma and well-differentiated NET, can be difficult to assess histologically. The infiltrative ductal adenocarcinoma glands can cause distortion and isolation of native islet cells that can mimic NET. In our case, the distinguishing feature that lent support to the diagnosis of a superimposed low grade NET component was growth of nests and tubules of monotonous neuroendocrine cells that showed a different morphology than native islets cells. Additionally, the neuroendocrine component was also present in lymph node further confirming their neoplastic nature and metastatic potential. Both tumor components comprised ≥ 30% of the tumor volume and were easily identifiable on routine hematoxylin and eosin (H&E)-stained sections, meeting the World Health Organization definitional criteria of MiNEN[1].

The pathogenesis of MiNENs represents a matter of open debate amongst pathologists and clinicians. Three main theories have been proposed for MiNENs of the gastrointestinal tract[3,4]: (1) The neuroendocrine and non-neuroendocrine components originate from separate precursor cells independently, either in a synchronous or metachronous manner, and then merge; (2) The two components derive from a common pluripotent stem cell progenitor, then acquires biphenotypic differentiation during carcinogenesis[5-7], supported by findings that common genetic alterations are exhibited in both components; and (3) The two components share a common monoclonal origin but hypothesizes that the neuroendocrine differentiation develops from an initially non-neuroendocrine cell phenotype[4]. Of note, most of these theories were proposed based on studies of mixed neoplasms composed of adenocarcinoma and NEC from gastrointestinal tract. When the endocrine and exocrine tumor components show significant differentiation discrepancies, as poorly differentiated adenocarcinoma intermingled with well-differentiated grade 1 NET as in our case, it is of interest to determine whether these two components share the same pluripotent stem cell origin.

In our case, the adenocarcinoma component showed *KRAS* exon 2 p.G12D and *TP53* exon 5 p.A161T mutations, which are well known mutations associated with pancreatic adenocarcinoma carcinogenesis and progression[8,9]. *KRAS* mutation is believed to be an early event as it is also present in pancreatic intraepithelial neoplasia (PanIN), and

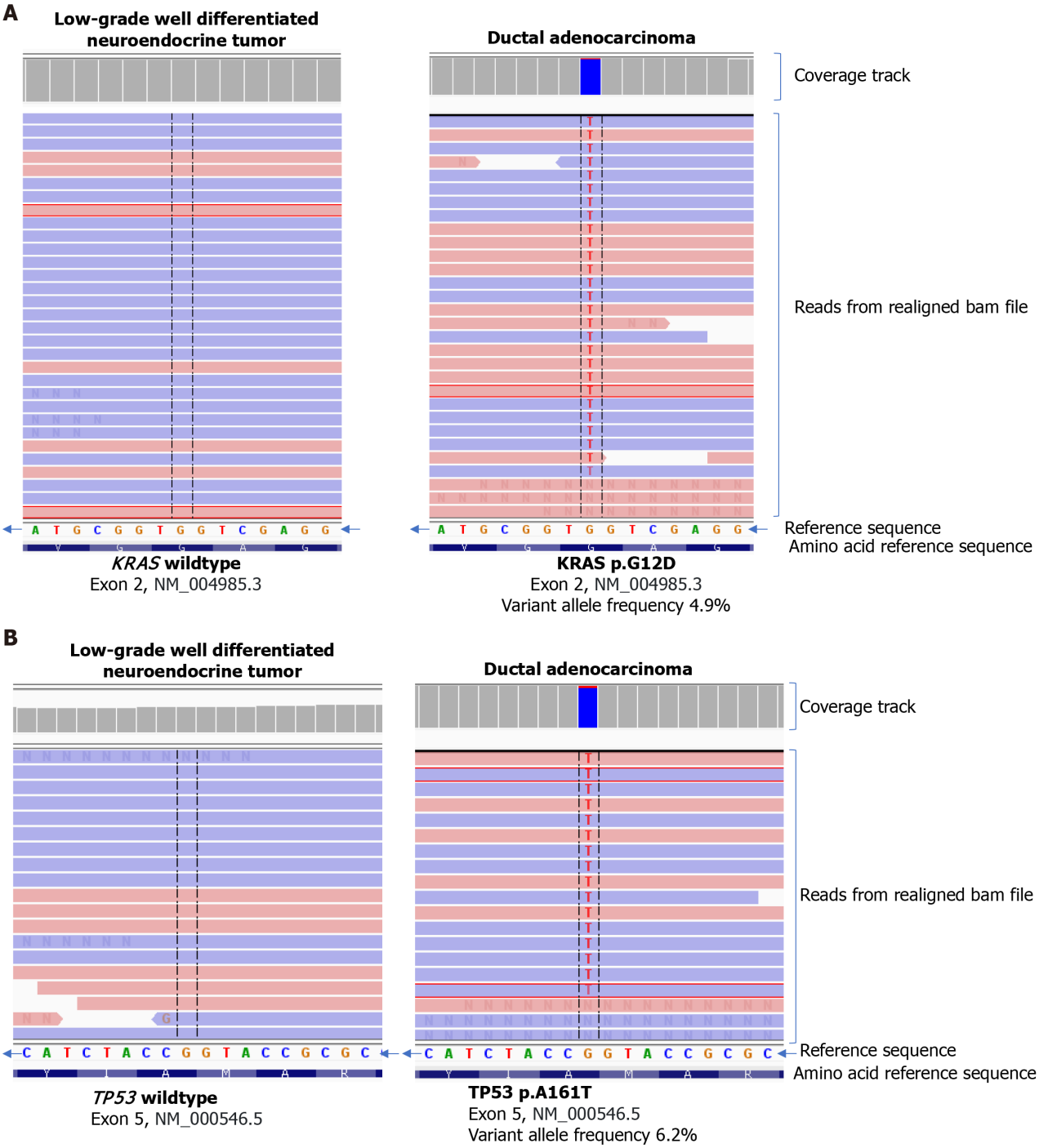

Figure 4 Next generation sequencing. A and B: Next generation sequencing of the two different histologic components. *KRAS* exon 2 p.G12D (variant frequency 4.9%) (A) and *TP53* exon 5 p.A161T (variant frequency 6.2%) (B) were identified in the adenocarcinoma component, but not in the well-differentiated neuroendocrine tumor component.

acquisition of mutation in *TP53* is associated with PanIN progression and development into invasive adenocarcinoma [10]. The absence of these alterations in the well-differentiated NET in our case suggests that the ductal adenocarcinoma and well-differentiated NET more likely developed from separate origins. Perhaps they are just incidental collision tumors. Few other studies have reported cases of mixed adenocarcinoma and well-differentiated NETs[11-13]; however, most of these studies lack molecular profiling data and no studies have been able to prove any clonal relationship between the two components thus far. Of note, one study showed a case of mixed intraductal papillary mucinous neoplasm and NET that showed similar molecular alterations in both components (*KRAS*, *GNAS*, and *CDKN2A* mutations, and amplification of *CCND1* gene)[14].

The terminology of MiNEN *vs* collision tumors is very confusing as it is utilized in the current literature. Given that both have overlapping histologic features, it is worth studying whether the difference between MiNENs and collision tumors is that shared molecular profiles are present in MiNENs while not in the latter. This can also create issues during pathologic staging of these tumors. Currently, MiNENs are staged as one tumor type, but it is imperative to mention in

the report the individual components present as the spectrum of disease, treatment and prognosis can be wide. Providing percent composition of individual components may also be helpful. While pathologic staging of MiNENs with combined adenocarcinoma and NECs as one T stage based on the size of the whole composite tumor may work just fine, such a system might not be always ideal. For cases like ours, since the more aggressive adenocarcinoma component would be the focus of treatment regimen, perhaps two different tumor templates (pancreas exocrine and endocrine) should be utilized with separate T and N staging for the adenocarcinoma and the low grade NET components. Size determination of these tumors tends to be a challenge because of overlapping morphologic areas and size determination is an important criterion in T-stage determination in both tumor types. Cohort studies with more cases and clinical correlations may provide further information in this arena.

The ductal adenocarcinoma component of our case had several histological features associated with aggressive clinical outcomes, including lymphovascular and perineural invasion, and metastasis to lymph nodes. Although the patient underwent aggressive adjuvant chemotherapy, disease progression with distant metastases occurred sooner than expected for typical pancreatic ductal adenocarcinoma cases. Whether the presence of the well-differentiated NET played a role in the process of disease progression and/or treatment resistance, either through modifying the tumor microenvironment or crosstalk between tumors, is unknown, and warrants further investigation.

CONCLUSION

Our case of mixed ductal adenocarcinoma and well-differentiated NET adds to the repertoire of published cases of this entity; however, our case is one of the few that try to address the question of clonal relatedness of the two different histologic components. In contrast to another case report[14], the molecular data shows that the two components in our case have varying molecular profiles based on a 170 gene panel suggesting that these tumors are perhaps best classified as collision tumors rather than MiNENs even though they meet definitional criteria for both. Data from additional cases will benefit the studies of clinical behavior, proper pathologic reporting, as well as optimal therapy of such cases.

FOOTNOTES

Author contributions: Zhao X designed the study and collected the clinical data; Edmonston TB performed the molecular analysis; Zhao X, Miick R, and Joneja U performed the histology analysis; Zhao X, Edmonston TB, Miick R, and Joneja U wrote the manuscript; and all authors have read and approved the final manuscript.

Informed consent statement: Informed written consent was obtained from the patients for the publication of this report and any accompanying images.

Conflict-of-interest statement: The authors declare that they have no conflict of interest to disclose.

CARE Checklist (2016) statement: The authors have read the CARE Checklist (2016), and the manuscript was prepared and revised according to the CARE Checklist (2016).

Country of origin: United States

ORCID number: Xiaofeng Zhao 0000-0003-2932-3324.

S-Editor: Chen YL
L-Editor: A
P-Editor: Guo X

REFERENCES

1 **La Rosa S**, Klimstra DS. Pancreatic MiNENs. WHO Classification of Tumours Editorial Board. Digestive system tumours. 5th ed. International Agency for Research on Cancer, 2019: 370-372
2 **La Rosa S**, Marando A, Sessa F, Capella C. Mixed Adenoneuroendocrine Carcinomas (MANECs) of the Gastrointestinal Tract: An Update. *Cancers (Basel)* 2012; **4**: 11-30 [PMID: 24213223 DOI: 10.3390/cancers4010011]
3 **Frizziero M**, Chakrabarty B, Nagy B, Lamarca A, Hubner RA, Valle JW, McNamara MG. Mixed Neuroendocrine Non-Neuroendocrine Neoplasms: A Systematic Review of a Controversial and Underestimated Diagnosis. *J Clin Med* 2020; **9** [PMID: 31963850 DOI: 10.3390/jcm9010273]
4 **Bazerbachi F**, Kermanshahi TR, Monteiro C. Early precursor of mixed endocrine-exocrine tumors of the gastrointestinal tract: histologic and

molecular correlations. *Ochsner J* 2015; **15**: 97-101 [PMID: 25829889]

5 **Rawdon BB**, Andrew A. Origin and differentiation of gut endocrine cells. *Histol Histopathol* 1993; **8**: 567-580 [PMID: 8358166]

6 **Andrew A**, Kramer B, Rawdon BB. The origin of gut and pancreatic neuroendocrine (APUD) cells--the last word? *J Pathol* 1998; **186**: 117-118 [PMID: 9924424 DOI: 10.1002/(SICI)1096-9896(1998100)186:2<117::AID-PATH152>3.0.CO;2-J]

7 **Furlan D**, Cerutti R, Genasetti A, Pelosi G, Uccella S, La Rosa S, Capella C. Microallelotyping defines the monoclonal or the polyclonal origin of mixed and collision endocrine-exocrine tumors of the gut. *Lab Invest* 2003; **83**: 963-971 [PMID: 12861036 DOI: 10.1097/01.lab.0000079006.91414.be]

8 **Ryan DP**, Hong TS, Bardeesy N. Pancreatic adenocarcinoma. *N Engl J Med* 2014; **371**: 1039-1049 [PMID: 25207767 DOI: 10.1056/NEJMra1404198]

9 **Collisson EA**, Bailey P, Chang DK, Biankin AV. Molecular subtypes of pancreatic cancer. *Nat Rev Gastroenterol Hepatol* 2019; **16**: 207-220 [PMID: 30718832 DOI: 10.1038/s41575-019-0109-y]

10 **Taherian M**, Wang H, Wang H. Pancreatic Ductal Adenocarcinoma: Molecular Pathology and Predictive Biomarkers. *Cells* 2022; **11** [PMID: 36231030 DOI: 10.3390/cells11193068]

11 **Wang F**, Lou X, Qin Y, Xu X, Yu X, Huang D, Ji S. Mixed neuroendocrine nonneuroendocrine neoplasms of the pancreas: a case report and literature review of pancreatic mixed neuroendocrine nonneuroendocrine neoplasm. *Gland Surg* 2021; **10**: 3443-3452 [PMID: 35070904 DOI: 10.21037/gs-21-564]

12 **Nießen A**, Schimmack S, Weber TF, Mayer P, Bergmann F, Hinz U, Büchler MW, Strobel O. Presentation and outcome of mixed neuroendocrine non-neuroendocrine neoplasms of the pancreas. *Pancreatology* 2021; **21**: 224-235 [PMID: 33309225 DOI: 10.1016/j.pan.2020.11.020]

13 **Varshney B**, Bharti JN, Varshney VK, Yadav T. Mixed neuroendocrine-non-neuroendocrine neoplasms (MiNEN) of pancreas: a rare entity-worth to note. *BMJ Case Rep* 2020; **13** [PMID: 32345587 DOI: 10.1136/bcr-2020-234855]

14 **Schiavo Lena M**, Cangi MG, Pecciarini L, Francaviglia I, Grassini G, Maire R, Partelli S, Falconi M, Perren A, Doglioni C. Evidence of a common cell origin in a case of pancreatic mixed intraductal papillary mucinous neoplasm-neuroendocrine tumor. *Virchows Arch* 2021; **478**: 1215-1219 [PMID: 33005981 DOI: 10.1007/s00428-020-02942-1]

World Journal of Gastrointestinal Oncology

Submit a Manuscript: https://www.f6publishing.com

World J Gastrointest Oncol 2024 December 15; 16(12): 4746-4752

DOI: 10.4251/wjgo.v16.i12.4746

ISSN 1948-5204 (online)

CASE REPORT

Signet-ring cell carcinoma of the transverse colon in a 10-year-old girl: A case report

Ling Lv, Yuan-Hua Song, Yan Gao, Shuang-Qiong Pu, Zhi-Xiang A, Hong-Fang Wu, Jun Zhou, Yu-Cheng Xie

Specialty type: Gastroenterology and hepatology

Provenance and peer review: Unsolicited article; Externally peer reviewed.

Peer-review model: Single blind

Peer-review report's classification

Scientific Quality: Grade C, Grade C, Grade C, Grade D, Grade D

Novelty: Grade B, Grade B, Grade B, Grade C, Grade C

Creativity or Innovation: Grade B, Grade C, Grade C, Grade C, Grade C

Scientific Significance: Grade B, Grade B, Grade B, Grade C, Grade C

P-Reviewer: Kanda T; Nakamura T; Xu DH

Received: August 5, 2024

Revised: September 29, 2024

Accepted: October 18, 2024

Published online: December 15, 2024

Processing time: 99 Days and 3.9 Hours

Ling Lv, Yan Gao, Shuang-Qiong Pu, Zhi-Xiang A, Hong-Fang Wu, Jun Zhou, Yu-Cheng Xie, Department of Pathology, Kunming Children's Hospital, Kunming 650028, Yunnan Province, China

Yuan-Hua Song, Department of Oncology, Kunming Children's Hospital, Kunming 650028, Yunnan Province, China

Co-first authors: Ling Lv and Yuan-Hua Song.

Co-corresponding authors: Jun Zhou and Yu-Cheng Xie.

Corresponding author: Yu-Cheng Xie, Chief Physician, Department of Pathology, Kunming Children's Hospital, No. 288 Qianxing Road, Kunming 650028, Yunnan Province, China. 7151290@qq.com

Abstract

BACKGROUND

Signet-ring cell carcinoma (SRCC) is a rare subtype of colorectal cancer. The incidence of primary colonic SRCC is relatively rare in pediatric patients, with a limited number of reported cases currently available. The prognosis for this specific tumor type is unfavorable, and the preoperative diagnosis presents challenges, potentially leading to misdiagnosis. This case report describes the diagnosis of primary SRCC in the colon of a 10-year-old girl.

CASE SUMMARY

The patient was admitted to the hospital due to abdominal pain and vomiting. A computed tomography scan revealed an irregular mass with soft tissue density in her transverse colon, showing uneven density and multiple calcifications. The patient underwent surgical resection of the affected bowel and lymph node dissection, which was confirmed by pathological examination to be SRCC infiltrating both nerves and the entire intestinal wall. Additionally, tumor thrombus formation was observed in blood vessels and lymphatic vessels, multiple cancerous nodules were found in the omentum, and metastasis to 18 of 26 mesenteric lymph nodes examined. Immunohistochemistry for mismatch repair gene protein demonstrated microsatellite stability. No mutations in *KRAS*, *NRAS*, *BRAF*, or *PIK3CA* genes were detected through molecular pathology analysis. After surgery, she received standard chemotherapy for 8 cycles without tumor progression or other abnormalities during a 12-month follow-up period.

CONCLUSION
Primary colonic SRCC is a rare malignant tumor with atypical clinical symptoms, and timely identification and intervention are crucial for improving the prognosis.

Key Words: Signet ring cell cancer; Colon; Pediatric; Pathological presentation; Case report

Core Tip: We present a case of primary signet-ring cell carcinoma of the colon in a 10-year-old girl. Pediatric signet-ring cell carcinoma is an exceptionally rare condition with atypical clinical symptoms, making early diagnosis challenging. The absence of specific clinical manifestations and the disease's concealed location often result in oversight by both clinicians and parents. Therefore, when a child presents with persistent abdominal pain, unexplained intestinal obstruction, or refractory ascites, clinicians should strongly consider the possibility of a malignant tumor. Prompt abdominal computed tomography and contrast-enhanced computed tomography scans, along with colonoscopy if indicated, are essential for early detection and timely intervention.

Citation: Lv L, Song YH, Gao Y, Pu SQ, A ZX, Wu HF, Zhou J, Xie YC. Signet-ring cell carcinoma of the transverse colon in a 10-year-old girl: A case report. *World J Gastrointest Oncol* 2024; 16(12): 4746-4752
URL: https://www.wjgnet.com/1948-5204/full/v16/i12/4746.htm
DOI: https://dx.doi.org/10.4251/wjgo.v16.i12.4746

INTRODUCTION

The incidence of colorectal cancer (CRC) increases steadily with age, surging significantly after the age of 50 and peaking among individuals aged 71-80[1]. In contrast, the occurrence of CRC in individuals 20 years and younger is exceptionally rare, with an incidence rate of only 1-2 cases per million[2]. Among patients under 15 years old with fatal malignancies, CRC accounts for less than 0.4% of cases[3,4], and only 12%-20% of these patients are below 10 years of age[5]. Adenocarcinoma is the most common subtype of CRC, while mucinous adenocarcinoma (MAC) represents approximately 10%-15% of cases, and signet-ring cell carcinoma (SRCC) accounts for only about 1%[6]. In 2023, a 10-year-old girl was admitted to our hospital with primary SRCC located in the transverse colon. The details of this case are presented below.

CASE PRESENTATION

Chief complaints

The patient presented with a history of persistent symptoms lasting over 20 days, including abdominal pain, distension, and episodes of emesis.

History of present illness

In April 2023, we treated a 10-year-old female patient with unexplained abdominal pain that started 20 days ago. The primary symptom was periumbilical pain accompanied by more than ten episodes of vomiting without any associated diarrhea. Additionally, there was a slight decrease in body weight.

History of past illness

The patient's parents reported no prior history of abdominal pain or vomiting.

Personal and family history

The patient's parents and relatives have no history of cancer or gastrointestinal polyps.

Physical examination

The patient's body temperature was 36.5°C. She appeared mildly anemic but showed no signs of jaundice in the skin or sclera. The abdomen was slightly distended, with no gastrointestinal or peristaltic waves visible and no abdominal varices. Tenderness was observed over the umbilicus without rebound pain. The liver and spleen were not palpable beneath the costal margin, and there were no signs of shifting dullness. Bowel sounds were active.

Laboratory examinations

The routine blood test results were as follows: White blood cells 5.60 × 10^9/L; neutrophil granulocyte percentage 38.7%; red blood cells 3.5 × 10^{12}/L; hemoglobin 92.0 g/L; platelets 336 × 10^9/L; and C-reactive protein 0.87 mg/L. Liver function

and myocardial enzymes were as follows: Alanine transaminase 5.0 U/L; aspartate transaminase 23.0 U/L; alkaline phosphatase 66.0 U/L; γ-Gamma glutamyl transferase 7.0 U/L; total bilirubin 8.7 μmol/L; albumin 37.5 g/L; lactate dehydrogenase 219.0 U/L; creatine kinase 213.0 U/L; creatinine kinase-myocardial band 13.0 U/L; and α-hydroxybutyrate dehydrogenase 147.0 U/L. Tumor marker levels were: Alpha-fetoprotein 1.03 ng/mL; carcinoembryonic antigen 3.39 ng/mL; and neuron-specific enolase 22.34 ng/mL.

Imaging examinations

A computed tomography (CT) scan revealed irregular masses of soft tissue density in the transverse colon, exhibiting heterogeneous density and multiple calcifications. The largest cross-sectional dimension measured 4.6 cm × 3.8 cm. Contrast enhancement revealed uneven enhancement patterns and indistinct margins. The lesion exerted pressure on the adjacent descending colon, resulting in obstruction of the proximal transverse colon (Figure 1A).

MULTIDISCIPLINARY EXPERT CONSULTATION

Exploratory surgery and biopsy revealed a transverse colonic mass as well as 26 mesenteric lymph nodes that may contain metastatic tumors. A gross pathological examination revealed a 5 cm × 4 cm × 3 cm mass in the intestinal wall with hardness and deformity, encircling the intestinal lumen. The mass had a mucosal surface and appeared gray-white, solid tissue with a tough texture. Tumor invasion into the serosa and surrounding adipose tissue was evident (Figure 1B). Histological examination revealed that tumor cells were distributed diffusely around the normal mucosal glands (Figure 2A), occurring either individually, in clusters, or small nests (approximately 80%). These cells exhibited weak adhesion and contained mucus. Most cells exhibited a signet-ring appearance due to cytoplasmic mucus crimping their nuclei (Figure 2B). Tumor cells had invaded the mucosal, submucosal, muscular, and serosal layers, with some areas forming mucus lakes (approximately 20%), where cancer cells floated. Nerve invasion was observed, as well as tumor thrombi in blood and lymphatic vessels. Multiple cancerous nodules were present in the omentum, and 18 of 26 mesenteric lymph nodes showed metastasis.

Immunohistochemistry revealed the following results: Cytokeratin pan (Pan-CK) (+) , Carcinoembryonic antigen (CEA) (+), Cytokeratin 7 (CK7) (-), Cytokeratin 20 (CK20) (+), Protein 53 (P53) (+), Ki67 protein (20%+), Cluster of Differentiation 34 (CD34) (-), D2-40 monoclonal antibody (D2-40) (-), S-100 (-), Mutl homolog 1(MLH1) (+), Muts homolog 2 (MSH2) (+), Muts homolog 6 (MSH6) (+), PMS1 homolog 2 (PMS2) (+), Epithelial-cadherin (E-Cadherin) (+, showing E-Cadherin was weaker in tumor cells) (Figure 2C), Caudal type homeobox transcription factor 2 (CDX-2) (+), Epithelial membrane antigen (EMA) (weakly positive), β-Catenin (+), Mucin 1 (MUC1) (+), Mucin 2 (MUC2) (+), Mucin 5AC (MUC5AC) (-), and Mucin 6 (MUC6) (-); Alcian Blue/Phosphoric Acid Schiff staining revealed blue-stained mucus distributed both inside and outside the cells (Figure 2D). The patient underwent genetic testing at other hospitals, and no mutations were observed in the *KRAS*, *NRAS*, *BRAF*, or *PIK3CA* genes.

FINAL DIAGNOSIS

The diagnosis of a malignant tumor in the transverse colon [pT4N2M1 IVc, microsatellite stability (MSS), SRCC] (American Joint Committee on Cancer tumor stage 9th edition) was confirmed based on the patient's medical history and diagnostic findings.

TREATMENT

The patient underwent surgery to remove a section of the transverse colon, leaving 4 cm of normal bowel on both ends of the lesion, and mesenteric lymph nodes were removed. After the surgical procedure, the patient underwent a course of 8 cycles of bevacizumab in combination with oxaliplatin, leucovorin, and fluorouracil chemotherapy. The specific treatment options were: Bevacizumab was injected at 100 mg once daily. The first infusion rate was maintained for 90 minutes, and the subsequent infusions were maintained for 60 minutes without any special circumstances. Oxaliplatin was given at a dose of 60 mg/m^2 after pretreatment with dexamethasone and promethazine to prevent allergic reactions. Additionally, leucovorin at a dose of 0.25 g/m^2 was given as rescue therapy during oxaliplatin infusion to avoid cold stimulation and maintain warmth. Fluorouracil was administered initially at a dose of 0.25 g/m^2 followed by a continuous infusion of 0.75 g/m^2 over 48 hours. The patient tolerated the treatment well, with no adverse reactions such as vomiting or hair loss.

OUTCOME AND FOLLOW-UP

By May 2024, the patient had completed eight cycles of standard chemotherapy. A 12-month follow-up, including CT reexamination, showed no signs of tumor progression. Blood tests, liver and kidney function assessments, and tumor marker evaluations were also within normal ranges.

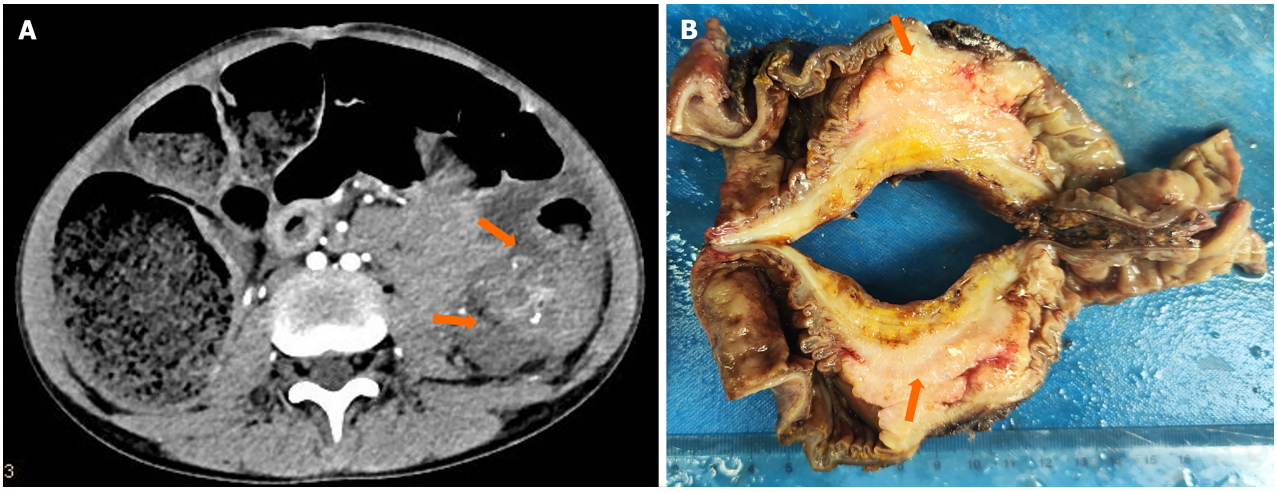

Figure 1 Tumor imaging data and surgical gross specimens. A: Computed tomography scan revealed irregular masses of soft tissue density in the transverse colon, exhibiting heterogeneous density and multiple calcifications. The lesion exerted pressure on the adjacent descending colon, resulting in obstruction of the proximal transverse colon (orange arrowhead); B: Gross specimen of the tumor (orange arrowhead).

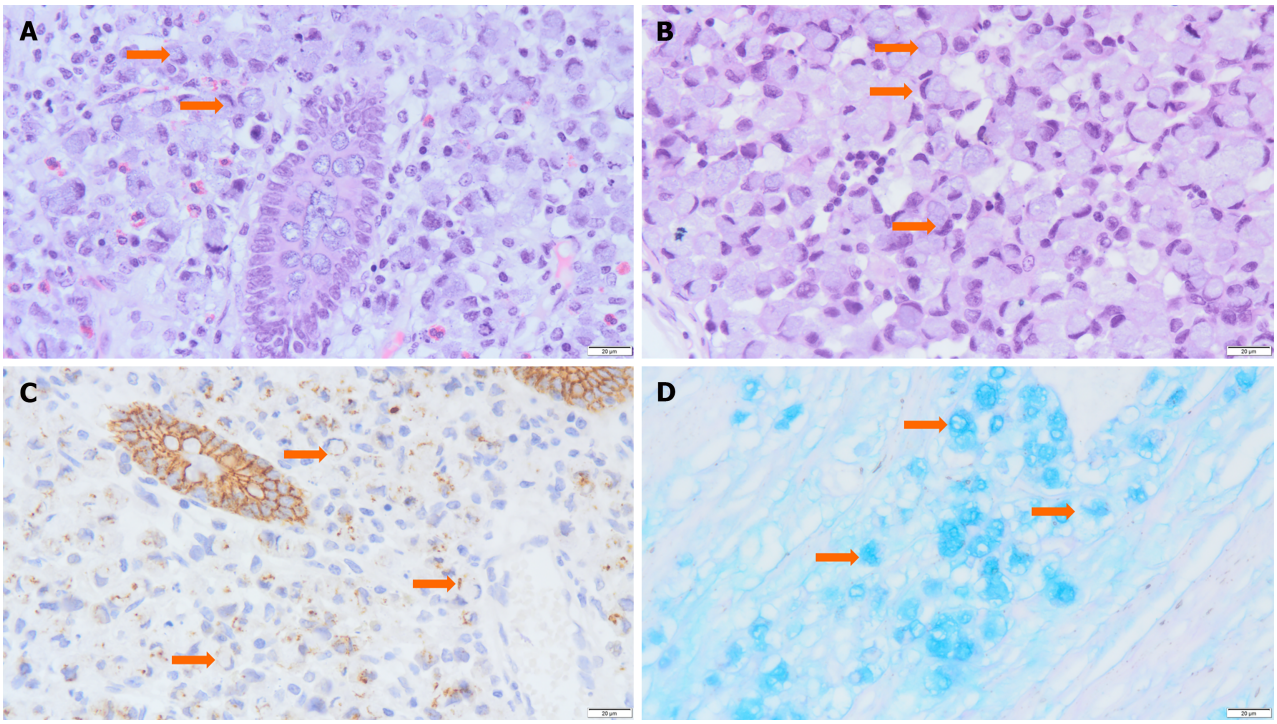

Figure 2 Pathological features of signet-ring cell carcinoma. A: Tumor cells were distributed diffusely around the normal mucosal glands. Most tumor cells exhibited a signet-ring appearance due to cytoplasmic mucus crimping their nuclei (orange arrowhead) [hematoxylin and eosin (H&E), 400 ×]; B: Typical signet ring cells (orange arrowhead) (H&E, 400 ×); C: E-cadherin (+) showing E-cadherin was weaker in tumor cells with poor adhesion (orange arrowhead) (immunohistochemistry, 400 ×); D: Alcian Blue/Phosphoric Acid Schiff staining revealed blue-stained mucus distributed both inside and outside the cells (orange arrowhead indicates mucus) (special staining, 400 ×).

DISCUSSION

SRCC is a rare histological subtype of CRC, which was initially proposed by Saphir and Laufman[7] in 1951, accounting for less than 1% of all histological subtypes. Although SRCC primarily occurs in the stomach, rare cases have been documented in the gallbladder, pancreas, colon, rectum, bladder, and breast[8,9]. The incidence of CRC is much lower in children and adolescents than in adults. There are limited data available on pediatric SRCC, primarily consisting of case reports. Among the retrieved case reports, the youngest patient was 6 years old. SRCC patients often have advanced tumor stages[10]. In the present case report, the patient presented with a tumor in the left transverse colon.

Both MAC and SRCC are rare subtypes of CRC. According to the World Health Organization definition, tumors are classified as SRCC when the proportion of signet ring cell component in the intracellular mucus exceeds 50%. MAC with a signet ring cell component is diagnosed when it contains a notable amount of extracellular mucus forming a mucus

pool, with less than 50% signet ring cells[11]. In this particular case, a small amount of mucus pooling was identified along with approximately 80% presence of signet ring cells, confirming the SRCC diagnosis. SRCC is an infrequent and aggressive malignant tumor originating from glandular epithelium in the digestive tract. The tumor cells exhibit a distinctive appearance reminiscent of signet rings, primarily caused by the excessive accumulation of mucin, leading to displacement of the nucleus towards the cell periphery[12]. Signet ring cells typically exist as single or loosely aggregated forms infiltrating diffusely into the mucosa and extending deep into intestinal layers, potentially reaching serosal surfaces and surrounding tissues. However, failure to breach the mucosal layer in some patients may lead to concealed disease presentation and atypical clinical manifestations associated with abnormal bowel movements.

The E-cadherin-catenin complex plays a crucial role in maintaining epithelial cell polarity, as evidenced by the positive expression levels of β-catenin (cell membrane) and E-cadherin (cell membrane and cytoplasm). SRCC is characterized by poor adherence due to dysfunction of the E-cadherin catenin complex, leading to loss of epithelial differentiation and structure or acquisition of a motile and invasive phenotype. In this case, there was a slight reduction in membranous localization of β-catenin protein accompanied by nuclear expression and downregulation of E-cadherin expression level. These alterations enable tumor cells to evade the surrounding microenvironment and exhibit enhanced metastatic potential, diminishing cell adhesion in mucus-rich regions and promoting tumor dissemination[13]. This trait leads to significant intramural infiltration of the tumor, resulting in diffuse thickening of the intestinal wall, luminal constriction, intestinal obstruction, and even inflammatory diseases[14,15]. Due to nonspecific clinical manifestations and inconspicuous localization of the disease, it is susceptible to being overlooked by clinicians and pediatric patients' parents.

SRCC is a rare subtype of pediatric CRC with a dismal prognosis, necessitating differentiation from the following tumors: (1) Lynch syndrome (LS) is an autosomal dominant tumor syndrome caused by mutations in mismatch repair genes (MMR) or deletions in the *EPCAM* gene, accounting for 3%-5% of CRC[16]. The National Comprehensive Cancer Network guidelines recommend that all patients with newly diagnosed CRC should undergo microsatellite instability or MMR gene deletion testing[17] to screen for LS. Since there was no history of the disease in our patient's family, immunohistochemistry was performed to detect MMR proteins MLH1, MSH2, MSH6, and PMS2. The results showed MSS, ruling out LS; and (2) Metastatic gastric SRCC: SRCC typically influences the stomach. Its microscopic morphology resembles that of intestinal SRCC, while its immunohistochemical expression differs. Primary gastric SRCC typically expresses MUC5AC and MUC6, while it lacks expression levels of MUC1 and MUC2. Conversely, primary SRCC of the large intestine expresses MUC1, MUC2, and MUC5A rather than MUC6[18]. EMA is frequently expressed in primary gastric SRCC rather than CDX-2. On the other hand, primary colorectal SRCC mainly exhibits CDX-2 expression without EMA expression; thus, downregulation of EMA may be associated with the carcinogenesis of colorectal SRCC[19]. Therefore, evaluating the apolipoprotein-MUC expression pattern along with EMA and CDX-2 can assist in distinguishing between metastatic sites and primary gastric or colorectal SRCC.

The incidence of pediatric CRC (PCRC) in China is relatively low compared to adults, with a rate of 0.18%, according to a single-center study. Most lesions are found in the transverse colon, and SRCC often shows deep invasion. In the early stages, there are no specific clinical symptoms, which can be similar to inflammatory bowel disease, constipation or pneumatosis intestinalis, and other functional bowel diseases. Due to limited experience with such cases, pediatricians may easily miss or misdiagnose PCRC. Abdominal pain, hematochezia, and intestinal obstruction are the main symptoms observed in later stages of the disease. Therefore, PCRC is often diagnosed at an advanced clinical stage compared to adult cases that commonly involve the rectum and exhibit changes in defecation habits and stool characteristics; they are diagnosed based on elevated blood CEA levels. Adenocarcinoma is the most common type of CRC among both adults and children, but MAC and SRCC predominate among children, leading to poor prognosis[20,21].

The treatment of SRCC in children follows the treatment guidelines for adult CRC, and personalized treatment should be considered. The optimal treatment options primarily consist of surgical intervention and adjuvant chemotherapy. Evidence has demonstrated that removing an adequate number of lymph nodes (≥ 4 regions) during colorectal SRCC surgery could significantly improve the patient's prognosis. Among patients with stage III colorectal SRCC, those who received adjuvant chemotherapy showed a better prognosis compared with those who did not receive chemotherapy. However, the role of radiotherapy in colorectal SRCC remains elusive, and the evaluation of SRCC tissue alone or in combination with chemotherapy is lacking. Nonetheless, neoadjuvant chemoradiotherapy can yield favorable therapeutic outcomes in the rectal SRCC population.

CONCLUSION

This case report highlights the rarity of primary SRCC of the colon in children, a condition that often goes unnoticed by clinicians and parents due to the absence of specific clinical manifestations and its concealed location. The lack of distinctive laboratory and imaging findings frequently results in preoperative misdiagnosis. Early diagnosis and timely treatment are crucial for improving survival rates. Clinicians should be vigilant, conduct comprehensive examinations, promptly use endoscopy and imaging for early detection, ensure appropriate surgical intervention, and administer standardized chemotherapy postoperatively to improve prognosis. The incidence of SRCC in children is low and varies among individuals, so this case summary has limitations. More case summaries and further studies on the biology of pediatric SRCC are still needed to accurately understand its molecular mechanism and develop new treatment methods.

FOOTNOTES

Author contributions: Xie YC and Zhou J designed the study and critically revised the manuscript; Lv L collected and organized pathological data, reviewed the literature and contributed to manuscript drafting; Song YH provided clinical data, revised the manuscript and was responsible for patient communication; Gao Y and Pu SQ made the diagnosis; A ZX conducted the immunohistochemistry staining; Wu HF conducted the HE staining; Lv L and Song YH contributed equally to this work as co-first authors; Zhou J and Xie YC confirm the authenticity of all the raw data as co-corresponding authors; and all authors read and approved the final manuscript.

Supported by the Health Research Project of Kunming Municipal Health Commission, China, No. 2023-01-04-001.

Informed consent statement: Informed written consent was obtained from the patient's parents for the publication of this report and any accompanying images.

Conflict-of-interest statement: The authors declare that they have no conflict of interest to disclose.

CARE Checklist (2016) statement: The authors have read the CARE Checklist (2016), and the manuscript was prepared and revised according to the CARE Checklist (2016).

Country of origin: China

ORCID number: Jun Zhou 0000-0002-2977-7839; Yu-Cheng Xie 0009-0005-4813-3915.

S-Editor: Chen YL
L-Editor: Webster JR
P-Editor: Cai YX

REFERENCES

1 **Young JL Jr**, Percy CL, Asire AJ, Berg JW, Cusano MM, Gloeckler LA, Horm JW, Lourie WI Jr, Pollack ES, Shambaugh EM. Cancer incidence and mortality in the United States, 1973-77. *Natl Cancer Inst Monogr* 1981; 1-187 [PMID: 7278952]
2 **Karnak I**, Ciftci AO, Senocak ME, Büyükpamukçu N. Colorectal carcinoma in children. *J Pediatr Surg* 1999; **34**: 1499-1504 [PMID: 10549756 DOI: 10.1016/s0022-3468(99)90112-4]
3 **Angelini C**, Crippa S, Uggeri F, Bonardi C, Sartori P, Uggeri F. Colorectal cancer with neuroendocrine differentiation in a child. *Pediatr Surg Int* 2005; **21**: 839-840 [PMID: 16177922 DOI: 10.1007/s00383-005-1525-3]
4 **Yamamoto K**, Tanaka T, Kuno K, Amoh Y, Takahashi Y, Murakami H. Carcinoma of the colon in children: case report and review of the Japanese literature. *J Gastroenterol* 1994; **29**: 647-652 [PMID: 8000515 DOI: 10.1007/BF02365450]
5 **Jain AK**, Motil KJ, Olutoye OO, Cope-Yokoyama S, Egler RA, Tatevian N. Colon cancer in a 16-year-old girl: signet-ring cell carcinoma without microsatellite instability--an unusual suspect. *J Pediatr Gastroenterol Nutr* 2009; **48**: 110-114 [PMID: 19172134 DOI: 10.1097/MPG.0b013e31815dda8c]
6 **An Y**, Zhou J, Lin G, Wu H, Cong L, Li Y, Qiu X, Shi W. Clinicopathological and Molecular Characteristics of Colorectal Signet Ring Cell Carcinoma: A Review. *Pathol Oncol Res* 2021; **27**: 1609859 [PMID: 34381313 DOI: 10.3389/pore.2021.1609859]
7 **Laufman H**, Saphir O. Primary linitis plastica type of carcinoma of the colon. *AMA Arch Surg* 1951; **62**: 79-91 [PMID: 14789350 DOI: 10.1001/archsurg.1951.01250030082009]
8 **Kang SH**, Chung WS, Hyun CL, Moon HS, Lee ES, Kim SH, Sung JK, Lee BS, Jeong HY. A rare case of a signet ring cell carcinoma of the colon mimicking a juvenile polyp. *Gut Liver* 2012; **6**: 129-131 [PMID: 22375184 DOI: 10.5009/gnl.2012.6.1.129]
9 **Tung SY**, Wu CS, Chen PC. Primary signet ring cell carcinoma of colorectum: an age- and sex-matched controlled study. *Am J Gastroenterol* 1996; **91**: 2195-2199 [PMID: 8855747]
10 **Wu P**, Deng W, Yan L, Wang C, Lou Y, Wang C. Clinicopathologic and prognostic factors for colorectal cancer in children and adolescents: a population-based study. *Int J Colorectal Dis* 2023; **38**: 35 [PMID: 36773067 DOI: 10.1007/s00384-023-04343-7]
11 **Tan Y**, Fu J, Li X, Yang J, Jiang M, Ding K, Xu J, Li J, Yuan Y. A minor (<50%) signet-ring cell component associated with poor prognosis in colorectal cancer patients: a 26-year retrospective study in China. *PLoS One* 2015; **10**: e0121944 [PMID: 25789685 DOI: 10.1371/journal.pone.0121944]
12 **Benedix F**, Kuester D, Meyer F, Lippert H. [Influence of mucinous and signet-ring cell differentiation on epidemiological, histological, molecular biological features, and outcome in patients with colorectal carcinoma]. *Zentralbl Chir* 2013; **138**: 427-433 [PMID: 22274919 DOI: 10.1055/s-0031-1283870]
13 **Börger ME**, Gosens MJ, Jeuken JW, van Kempen LC, van de Velde CJ, van Krieken JH, Nagtegaal ID. Signet ring cell differentiation in mucinous colorectal carcinoma. *J Pathol* 2007; **212**: 278-286 [PMID: 17471475 DOI: 10.1002/path.2181]
14 **Zhou JL**, Zhao XY, Lin GL, Qiu HZ, Xiao Y, Wu B, Lu JY, Niu BZ, Sun XY, Zhong GX. [Clinicopathological characteristics, diagnosis, and treatment of 29 cases of signet ring cell carcinoma of the rectum and sigmoid colon]. *Zhonghua Zhong Liu Za Zhi* 2020; **42**: 897-902 [PMID: 33113635 DOI: 10.3760/cma.j.cn112152-20200228-00142]
15 **Papp JP Jr**, Levine EJ, Thomas FB. Primary linitis plastica carcinoma of the colon and rectum. *Am J Gastroenterol* 1995; **90**: 141-145 [PMID:

7801917]

16 **Hampel H**, Frankel WL, Martin E, Arnold M, Khanduja K, Kuebler P, Clendenning M, Sotamaa K, Prior T, Westman JA, Panescu J, Fix D, Lockman J, LaJeunesse J, Comeras I, de la Chapelle A. Feasibility of screening for Lynch syndrome among patients with colorectal cancer. *J Clin Oncol* 2008; **26**: 5783-5788 [PMID: 18809606 DOI: 10.1200/JCO.2008.17.5950]

17 **Benson AB 3rd**, Venook AP, Cederquist L, Chan E, Chen YJ, Cooper HS, Deming D, Engstrom PF, Enzinger PC, Fichera A, Grem JL, Grothey A, Hochster HS, Hoffe S, Hunt S, Kamel A, Kirilcuk N, Krishnamurthi S, Messersmith WA, Mulcahy MF, Murphy JD, Nurkin S, Saltz L, Sharma S, Shibata D, Skibber JM, Sofocleous CT, Stoffel EM, Stotsky-Himelfarb E, Willett CG, Wu CS, Gregory KM, Freedman-Cass D. Colon Cancer, Version 1.2017, NCCN Clinical Practice Guidelines in Oncology. *J Natl Compr Canc Netw* 2017; **15**: 370-398 [PMID: 28275037 DOI: 10.6004/jnccn.2017.0036]

18 **Terada T**. An immunohistochemical study of primary signet-ring cell carcinoma of the stomach and colorectum: II. Expression of MUC1, MUC2, MUC5AC, and MUC6 in normal mucosa and in 42 cases. *Int J Clin Exp Pathol* 2013; **6**: 613-621 [PMID: 23573307]

19 **Terada T**. An immunohistochemical study of primary signet-ring cell carcinoma of the stomach and colorectum: III. Expressions of EMA, CEA, CA19-9, CDX-2, p53, Ki-67 antigen, TTF-1, vimentin, and p63 in normal mucosa and in 42 cases. *Int J Clin Exp Pathol* 2013; **6**: 630-638 [PMID: 23573309]

20 **Yang LL**, Wang M, He P. Clinicopathological characteristics and survival in colorectal signet ring cell carcinoma: a population-based study. *Sci Rep* 2020; **10**: 10460 [PMID: 32591589 DOI: 10.1038/s41598-020-67388-6]

21 **Jayanand SB**, Seshadri RA, Tapkire R. Signet ring cell histology and non-circumferential tumors predict pathological complete response following neoadjuvant chemoradiation in rectal cancers. *Int J Colorectal Dis* 2011; **26**: 23-27 [PMID: 21046123 DOI: 10.1007/s00384-010-1082-7]

World Journal of Gastrointestinal Oncology

Submit a Manuscript: https://www.f6publishing.com

World J Gastrointest Oncol 2024 December 15; 16(12): 4753-4756

DOI: 10.4251/wjgo.v16.i12.4753

ISSN 1948-5204 (online)

LETTER TO THE EDITOR

Combinations of lenvatinib and immune checkpoint inhibitors plus transarterial chemoembolization, is it the prime time for unresectable hepatocellular carcinoma?

Natalia Centrone, Pedro Luiz Serrano Uson Junior

Specialty type: Oncology

Provenance and peer review: Invited article; Externally peer reviewed.

Peer-review model: Single blind

Peer-review report's classification

Scientific Quality: Grade B

Novelty: Grade B

Creativity or Innovation: Grade B

Scientific Significance: Grade B

P-Reviewer: Yang H

Received: June 17, 2024

Revised: September 14, 2024

Accepted: October 12, 2024

Published online: December 15, 2024

Processing time: 148 Days and 9.9 Hours

Natalia Centrone, Pedro Luiz Serrano Uson Junior, Center for Personalized Medicine, Hospital Israelita Albert Einstein, Sao Paulo 05651-901, Brazil

Corresponding author: Pedro Luiz Serrano Uson Junior, MD, Doctor, Research Associate, Center for Personalized Medicine, Hospital Israelita Albert Einstein, 627/701 Avenue, Albert Einstein, Morumbi, Sao Paulo 05651-901, Brazil. pedro.serrano@einstein.br

Abstract

Hepatocellular carcinoma (HCC) is a lethal disease and unfortunately, most patients will be diagnosed with unresectable/advanced stages and the overall prognosis is poor. For patients with initially unresectable HCC (uHCC), transarterial chemoembolization (TACE) was the mainstream treatment. Lately, the incorporation of immune checkpoint inhibitors and antiangiogenics for the treatment of metastatic disease has paved the way for significant improvements in the treatment of initially uHCC. In this editorial we will discuss an article that evaluated ICI combinations with lenvatinib and TACE for the treatment of uHCC patients, and highlight future advances in the field.

Key Words: Hepatocellular carcinoma; Liver cancer; Lenvatinib; Immunotherapy; Checkpoint inhibitors

Core Tip: Hepatocellular carcinoma (HCC) is the fifth most common cancer worldwide and the third most common cause of cancer-related death, accounting for approximately 8% of overall cancer deaths. For patients with initially unresectable HCC (uHCC), transarterial chemoembolization is being evaluated associated with systemic treatments including immune checkpoint inhibitors and antiangiogenics. The synergism of these strategies can improve outcomes for patients deemed unresectable and ineligible for transplantation. In this article we will discuss a very interesting combination evaluated in uHCC patients, and highlight new studies and trials coming forward.

Citation: Centrone N, Serrano Uson Junior PL. Combinations of lenvatinib and immune checkpoint inhibitors plus transarterial chemoembolization, is it the prime time for unresectable hepatocellular carcinoma? *World J Gastrointest Oncol* 2024; 16(12): 4753-4756
URL: https://www.wjgnet.com/1948-5204/full/v16/i12/4753.htm
DOI: https://dx.doi.org/10.4251/wjgo.v16.i12.4753

TO THE EDITOR

Hepatocellular carcinoma (HCC) is the fifth most common cancer worldwide[1]. However, is the third most common cause of cancer-related death, accounting for approximately 8% of overall cancer deaths[1]. Unfortunately, many patients will be diagnosed with unresectable/advanced stages and the overall prognosis is poor[2]. For patients with initially unresectable HCC (uHCC), transarterial chemoembolization (TACE) was the mainstream treatment[3]. The treatment of uHCC was defined by the Barcelona Clinic Liver Cancer (BCLC) staging, with most cases unfit for liver transplantation or resection included in the BCLC B grade[3]. However, in the few last years, the landscape of the HCC BCLC B patients has dramatically changed[4]. Potent downstaging treatments, with new molecules including immune checkpoint inhibitors and antiangiogenics, associated with local treatments including radiotherapy, TACE and ablation are changing the prognosis and improving survival[4,5]. In this article we will discuss a very interesting combination evaluated in uHCC patients[5].

The article by Ma *et al*[5] assesses the efficacy and safety of a new strategy to treat uHCC, consisting of a combination of the locoregional therapy with TACE, and two first-line systemic treatments, lenvatinib and anti-PD-1 antibodies. This new approach is based on the theory that lenvatinib can modulate vascular endothelial growth factor (VEGF)-mediated immunosuppression, promote cytotoxic T-cell infiltration and inhibit the mechanism of post-TACE recurrence, hypoxia-induced tumor angiogenesis, while the anti-PD-1 antibodies help the patient's immune system to attack the cancer cells, therefore fighting the cancer from multiple angles.

This study consists of a retrospective analysis of 102 patients with uHCC treated with at least one dose of lenvatinib plus anti-PD-1, between March 2019 and April 2022 at the Chinese People's Liberation Army General Hospital (Beijing, China). The included patients were over 18 years old, BCLC stage B or C with an Eastern Cooperative Oncology Group (ECOG) score of 0 or 1. Those with organ disfunctions; other malignances or brain metastasis; previous immunotherapy or treatment with radiotherapy, chemotherapy or thermal ablation within 3 weeks were excluded. The treatment was based on the TACE procedure, according to protocol, followed by the administration of lenvatinib and anti-PD-1 antibodies. TACE consists of intra-arterial injections containing agents to block arterial flow (such as gelatin sponge particles, polyvinyl alcohol particles and polyacrylamide microspheres), causing tumor necrosis, and a high dose of chemotherapy, which maintains a prolonged contact with the tumor while minimizing the systemic effects of chemotherapy[6]. Lenvatinib was administered orally at 12 mg/day for ≥ 60 kg patients or 8 mg/day for patients less than 60 kg; while anti-PD-1 antibodies were administered intravenously at different dosages depending on the drug (for example pembrolizumab 200 mg IV every 3 weeks)[7]. It is important to note that Ma *et al*[5] used five different anti-PD-1 drugs (sintilimab, nivolumab, camrelizumab, pembrolizumab, toripalimab) depending on the patient's choices based on the guideline recommendations and individual financial situation.

The patients were then assessed for tumor responses and adverse events (AE) at a 4 to 8 weeks interval, until death or end of the study, before each treatment or contrast-enhanced computed tomography/magnetic resonance imaging. The median follow-up was 12.63 months, tumor responses were confirmed 4 weeks after the initial evaluation and the alpha fetoprotein level was assessed every 4 weeks. The outcomes of this study were: Tumor response, objective response rate (ORR), disease control rate, median progression-free survival (PFS), median overall survival (OS) and AEs. To evaluate the tumor response, physicians used the modified Response Evaluation Criteria in Solid Tumors, that was then classified into 4 categories: Complete response, partial response, stable disease or progressive disease.

Additionally, PFS was determined by the time between TACE and disease progression of any cause, while OS was defined as the interval between TACE and death/last follow-up. Concurrently, AEs were evaluated based on the Common Terminology Criteria for AE Version 5.0 and examinations. In an attempt to determine the prognostic factors for survival and disease progression, Ma *et al*[5] further analyzed a number of variables including: Sex, age, performance status (0 or 1), BCLC (B or C), etiology (hepatitis B virus or other), tumor size (≤ 6.8 cm or > 6.8 cm), multiple tumors (≤ 3 or > 3), portal vein invasion, extrahepatic metastasis, Child-Pugh (A or B), alpha-fetoprotein (AFP), des-gamma-carboxy prothrombin (DCP), neutrophil-to-lymphocyte ratio (NLR) and lactate dehydrogenase.

The sample consisted mainly of males (87.25%) aged between 34 and 91 years (mean: 57.64 years). Both categories of ECOG and BCLC stage were well and almost equally distributed. Furthermore, chronic hepatitis B virus infection was the prevalent etiology (78.43%), as was Class A Child-Pugh (91.18%). Portal vein tumor thrombosis was observed in 28.43% of patients, 41.18% showed distal metastasis, 48.04% had an AFP level > 400 ng/mL and 87.25% had a DCP level > 40 mAU/mL.

With regard to the safety of this new strategy, 93.13% of the patients developed AEs. Most of the AEs (60.78%) were graded 1-2 (mainly asthenia and hand-foot syndrome). Hypertension and rash were the most common grade 3-4 manifestations. The median PFS of the entire cohort was around 10 months, with an OS of 26.4 months. The ORR was high, with more than half of patients (61.7%) presenting objective responses. Furthermore, as expected, patients with worse BCLC staging presented worse OS. Finally, it was observed that better PFS and OS was related to an early NLR response and AFP response (Table 1).

Table 1 Study summary

Item	Parameter value
Efficacy - clinical outcomes. At the end of the study, 77.45% of the patients were alive, %	
CR	9.80
PR	51.19
SD	19.60
PD	18.62
Objective response rate	61.76
Disease control rate	81.37
Median progression-free survival	10.07 months
Median overall survival	26.43 months
Positive factors related to overall survival	
BCLC stage	B
LDH	≤ 198.52 U/L
Early NLR response	Decrease
Early AFP response	> 20 ng/mL
Positive factors related to progression-free survival	
BCLC stage	B
Early NLR response	Decrease
Early AFP response	> 20 ng/mL

Patients with low tumor burden either at baseline or in response to treatment effects had a better prognosis. CR: Complete response; PR: Partial response; SD: Stable disease; PD: Disease progression; BCLC: Barcelona Clinic Liver Cancer staging; LDH: Lactate dehydrogenase; NLR: Neutrophil-lymphocyte ratio; AFP: Alpha-fetoprotein.

DISCUSSION

This study has some limitations. Importantly, it is a retrospective study with a small sample size from a single center and with a short follow-up. This could indicate a lower generalizability of the results, as only 102 patients were included with a short observation time; thus, it is very unlikely that all types of patients with this condition and possible outcomes are well represented, which in turn, could mean that the study's conclusion does not apply to all patients with this condition. Also, it is important to note that there were five types of anti-PD-1 antibodies used and, as each drug may have its own pharmacodynamic and pharmacokinetic characteristics that could lead to different efficacy rates, the interpretation of the overall effect of this potential new line of treatment could be affected. However, overall, the analysis proved the efficacy and safety of the TACE, lenvatinib and anti-PD-1 antibodies combination for the treatment of uHCC. In addition, compared with other studies, this study presented higher OS and ORR. The better results in terms of survival could be attributed to the super-selection and complete embolization of collateral vessels, the fact that 10 patients received conversion therapy and that many patients underwent various subsequent treatments to improve the OS.

Despite these limitations, the study is very important and is in alignment with the improvements in the treatment of patients with BCLC B uHCC. In the EMERALD-1 trial, the combination of TACE with durvalumab (an anti-PD-L1 antibody) and bevacizumab (an anti-VEGF A antibody) improved PFS *vs* TACE alone, median PFS was 15 months with the combination of TACE-durvalumab-bevacizumab *vs* 8.2 months with TACE alone, with a hazard-ratio (HR) of 0.77, and a *P* value of 0.032, reaching statistical significance[4]. More recently, at ESMO 2024, data from the LEAP 012 trial confirmed these results. Approximately 500 patients with intermediate-HCC were randomized to lenvatinib, pembrolizumab and TACE or placebo plus TACE. At this first interim analysis, median PFS was significantly improved in patients treated with lenvatinib plus pembrolizumab *vs* placebo (HR, 0.66; *P* = 0.0002); 14.6 months *vs* 10.0 months. With 151 events (47.5%), OS is still immature, and data are not published yet. These studies are paving the way for future combinations in uHCC[4]. Investigations into the use of other arterially directed therapies, to compare different types of anti-PD-1 antibodies and to explore the non-inferior relationship between this new proposal and the current regimes recommended by the guidelines will be important.

Finally, it is also important to note, that lenvatinib associated with TACE proved to be superior to lenvatinib alone, in patients with advanced HCC, based on the results of the LAUNCH trial, suggesting an additional effect of the combination of local treatments with lenvatinib, a potent antiangiogenic multi-kinase tyrosine inhibitor[8]. All these data suggest that TACE combined with systemic treatments is an effective strategy to improve ORR and survival in inter-

mediate stage uHCC.

Overall, the results of this study confirm that these combinations should be evaluated in larger cohorts and randomized trials to better understand the best upfront approach for BCLC B uHCC. Multiple randomized phase 3 trials are underway to evaluate potent combinations for uHCC including TACE, such as EMERALD-3 [TACE plus durvalumab, tremelimumab and lenvatinib (NCT05301842)], Checkmate 74W [TACE plus nivolumab and ipilimumab (NCT04340193)], TACE-3 [DEB-TACE plus nivolumab (NCT04268888)] and others. With all these exciting new trials, it seems that the current landscape of treatment for BCLC B HCC patients is already changing.

FOOTNOTES

Author contributions: Centrone N and Serrano Uson Junior PL wrote the article, reviewed and approved the final manuscript.

Conflict-of-interest statement: All the authors report no relevant conflicts of interest for this article.

Country of origin: Brazil

ORCID number: Pedro Luiz Serrano Uson Junior 0000-0001-6122-1374.

S-Editor: Li L
L-Editor: Webster JR
P-Editor: Wang WB

REFERENCES

1 **Bray F**, Ferlay J, Soerjomataram I, Siegel RL, Torre LA, Jemal A. Global cancer statistics 2018: GLOBOCAN estimates of incidence and mortality worldwide for 36 cancers in 185 countries. *CA Cancer J Clin* 2018; **68**: 394-424 [PMID: 30207593 DOI: 10.3322/caac.21492]

2 **Katariya NN**, Lizaola-Mayo BC, Chascsa DM, Giorgakis E, Aqel BA, Moss AA, Uson Junior PLS, Borad MJ, Mathur AK. Immune Checkpoint Inhibitors as Therapy to Down-Stage Hepatocellular Carcinoma Prior to Liver Transplantation. *Cancers (Basel)* 2022; **14** [PMID: 35565184 DOI: 10.3390/cancers14092056]

3 **Reig M**, Forner A, Rimola J, Ferrer-Fàbrega J, Burrel M, Garcia-Criado Á, Kelley RK, Galle PR, Mazzaferro V, Salem R, Sangro B, Singal AG, Vogel A, Fuster J, Ayuso C, Bruix J. BCLC strategy for prognosis prediction and treatment recommendation: The 2022 update. *J Hepatol* 2022; **76**: 681-693 [PMID: 34801630 DOI: 10.1016/j.jhep.2021.11.018]

4 **Lencioni R**, Kudo M, Erinjeri J, Qin S, Ren Z, Chan S, Arai Y, Heo J, Mai A, Escobar J, Lopez Chuken YA, Yoon J, Tak WY, Suttichaimongkol T, Bouattour M, Lin S, Żotkiewicz M, Udoye S, Cohen G, Sangro B. EMERALD-1: A phase 3, randomized, placebo-controlled study of transarterial chemoembolization combined with durvalumab with or without bevacizumab in participants with unresectable hepatocellular carcinoma eligible for embolization. *J Clin Oncol* 2024; **42**: LBA432-LBA432 [DOI: 10.1200/jco.2024.42.3_suppl.lba432]

5 **Ma KP**, Fu JX, Duan F, Wang MQ. Efficacy and predictive factors of transarterial chemoembolization combined with lenvatinib plus programmed cell death protein-1 inhibition for unresectable hepatocellular carcinoma. *World J Gastrointest Oncol* 2024; **16**: 1236-1247 [PMID: 38660650 DOI: 10.4251/wjgo.v16.i4.1236]

6 **Chang Y**, Jeong SW, Young Jang J, Jae Kim Y. Recent Updates of Transarterial Chemoembolilzation in Hepatocellular Carcinoma. *Int J Mol Sci* 2020; **21**: 8165 [PMID: 33142892 DOI: 10.3390/ijms21218165]

7 **Su GL**, Altayar O, O'Shea R, Shah R, Estfan B, Wenzell C, Sultan S, Falck-Ytter Y. AGA Clinical Practice Guideline on Systemic Therapy for Hepatocellular Carcinoma. *Gastroenterology* 2022; **162**: 920-934 [PMID: 35210014 DOI: 10.1053/j.gastro.2021.12.276]

8 **Peng Z**, Fan W, Zhu B, Wang G, Sun J, Xiao C, Huang F, Tang R, Cheng Y, Huang Z, Liang Y, Fan H, Qiao L, Li F, Zhuang W, Peng B, Wang J, Li J, Kuang M. Lenvatinib Combined With Transarterial Chemoembolization as First-Line Treatment for Advanced Hepatocellular Carcinoma: A Phase III, Randomized Clinical Trial (LAUNCH). *J Clin Oncol* 2023; **41**: 117-127 [PMID: 35921605 DOI: 10.1200/JCO.22.00392]

World Journal of Gastrointestinal Oncology

Submit a Manuscript: https://www.f6publishing.com

World J Gastrointest Oncol 2024 December 15; 16(12): 4757-4761

DOI: 10.4251/wjgo.v16.i12.4757

ISSN 1948-5204 (online)

LETTER TO THE EDITOR

Advancing hepatocellular carcinoma treatment with hepatic arterial infusion chemotherapy

Eda Caliskan Yildirim, Yakup Ergun

Specialty type: Oncology

Provenance and peer review: Invited article; Externally peer reviewed.

Peer-review model: Single blind

Peer-review report's classification

Scientific Quality: Grade B, Grade C

Novelty: Grade A, Grade C

Creativity or Innovation: Grade B, Grade C

Scientific Significance: Grade A, Grade C

P-Reviewer: Amante MF; Hashim Z

Received: July 19, 2024

Revised: October 9, 2024

Accepted: October 18, 2024

Published online: December 15, 2024

Processing time: 116 Days and 2.4 Hours

Eda Caliskan Yildirim, Department of Medical Oncology, Sincan Training and Research Hospital, Ankara 06100, Türkiye

Yakup Ergun, Department of Medical Oncology, Bower Hospital, Diyarbakır 21100, Türkiye

Corresponding author: Yakup Ergun, MD, Associate Professor, Department of Medical Oncology, Bower Hospital, Yenisehir, Elazıg Street, Diyarbakır 21100, Türkiye. dr.yakupergun@gmail.com

Abstract

Hepatocellular carcinoma (HCC) remains a major challenge in oncology, being a leading cause of cancer-related mortality worldwide. Early-stage HCC is typically treated with surgical resection, transplantation, or ablation, while advanced-stage HCC relies on systemic therapies like sorafenib and newer combinations such as atezolizumab-bevacizumab. Despite these advancements, there is still a need for effective treatments for unresectable HCC, especially in cases with macroscopic vascular invasion. Hepatic arterial infusion chemotherapy (HAIC) has demonstrated promising outcomes in Asia for the treatment of unresectable HCC, yet its application in Western countries has been relatively limited. This letter reviews the recent meta-analysis by Zhou *et al* published in the *World Journal of Gastrointestinal Oncology*, which demonstrates the efficacy and safety of HAIC *vs* sorafenib. The analysis includes 9 randomized controlled trials and 35 cohort studies, highlighting significant improvements in overall survival, progression-free survival, and objective response rates with HAIC and its combinations. The editorial explores the reasons behind the limited use of HAIC in Western countries. It underscores the potential of HAIC to enhance treatment outcomes for advanced HCC and calls for more research and broader adoption of HAIC in clinical practice globally.

Key Words: Hepatocellular carcinoma; Hepatic arterial infusion chemotherapy; Tyrosine kinase inhibitors; Immunotherapy; Survival

Core Tip: Hepatic arterial infusion chemotherapy (HAIC) is shown to be a highly effective and safer treatment for advanced hepatocellular carcinoma. Despite its success in Asia, HAIC is underutilized in western countries. Further research and clinical trials in diverse populations are essential to validate HAIC's benefits and integrate it into global oncology practices.

Citation: Caliskan Yildirim E, Ergun Y. Advancing hepatocellular carcinoma treatment with hepatic arterial infusion chemotherapy. *World J Gastrointest Oncol* 2024; 16(12): 4757-4761
URL: https://www.wjgnet.com/1948-5204/full/v16/i12/4757.htm
DOI: https://dx.doi.org/10.4251/wjgo.v16.i12.4757

TO THE EDITOR

Hepatocellular carcinoma (HCC) remains a formidable challenge in oncology, representing the sixth most commonly diagnosed cancer and the fourth leading cause of cancer-related mortality globally[1]. In the early stages, curative approaches such as surgical resection, transplantation, and ablation are treatment options depending on the patient's status. For intermediate-stage HCC, locoregional treatment approaches like transarterial chemoembolization (TACE) or transarterial radioembolization (TARE) are prioritized. In advanced-stage HCC, systemic therapies are the first choice of treatment, as recommended by international guidelines[2]. Recently, there have been significant advancements in the treatment of unresectable HCC. The evolution of systemic therapy that began with sorafenib has led to a considerable improvement in HCC survival outcomes with the introduction of combination regimens such as atezolizumab-bevacizumab, and durvalumab-tremelimumab. However, there remains an unmet need to optimize treatment for unresectable HCC with macroscopic vascular invasion.

Hepatic arterial infusion chemotherapy (HAIC) has recently emerged as a prominent treatment method for unresectable HCC, particularly in Asia. Although it has not yet been included in European and American guidelines, it is recognized in Japanese guideline as a treatment option for HCC with portal vein thrombosis that is unsuitable for other local treatments[3]. HAIC delivers chemotherapeutic agents directly into the hepatic artery, which supplies blood to the liver and, more importantly, to the HCC tumors. Since HCC tumors derive their blood supply predominantly from the hepatic artery (as opposed to the portal vein, which supplies most of the normal liver), HAIC ensures that a high concentration of the drug reaches the tumor with minimal exposure to the rest of the liver and systemic circulation. This method enhances the effectiveness of the chemotherapy while reducing systemic side effects[4].

This letter aims to provide a critical and comprehensive overview of the recent meta-analysis by Zhou *et al*[5] on the efficacy of HAIC for advanced HCC. The editorial seeks to highlight the significant findings of the study, discuss the potential benefits and drawbacks of HAIC, and explore the reasons behind its limited adoption in western countries despite its demonstrated success in Asia.

HAIC AND COMBINATION THERAPY STRATEGIES

HAIC can be administered as monotherapy or in combination with other treatment modalities. While it is most commonly combined with systemic therapies, there are also examples in the literature where it is used in combination with other locoregional therapies. Among combination therapies, studies evaluating concomitant use with sorafenib are predominant.

There are five randomized controlled trials (RCT) comparing the outcomes of sorafenib with sorafenib + HAIC combination therapy. Among these, only two are phase 3 RCT, and their results are inconsistent. Kudo *et al*[6] conducted a study across 31 centers in Japan, in which adding HAIC to sorafenib treatment showed an effect on progression-free survival (PFS) and objective response rate (ORR) but not on medical overall survival (mOS) [mOS: 11.8 months *vs* 11.5 months; hazard ratio (HR) = 1.009; $P = 0.9$][6]. Conversely, He *et al*[7] carried out a study in five centers from China, and adding HAIC to sorafenib treatment significantly increased mOS (mOS: 13.3 months *vs* 7.1 months; HR = 0.35; $P < 0.001$). This study also found statistically significant improvements in ORR and medical PFS (mPFS) with the HAIC + sorafenib combination[7]. The discrepancies between these two studies could be attributed to differences in HCC etiology and the chemotherapy regimens used in HAIC. The Japanese study included approximately 50% of patients with hepatitis C virus (HCV)-related HCC and 20% with hepatitis B virus (HBV)-related HCC, while the Chinese study had 80% of patients with HBV-related HCC. Pooled analyses of two phase 3 studies evaluating the efficacy of sorafenib indicate that sorafenib is more effective in HCV-related HCC[8]. Additionally, the chemotherapy protocols utilized in HAIC exhibited notable differences. The Japanese study employed a low-dose 5-fluorouracil (5-FU)-cisplatin[6], whereas the Chinese study utilized the FOLFOX regimen[7].

HAIC is being utilized in numerous medical centers employing a multitude of chemotherapy regimens, including low-dose cisplatin, low-dose cisplatin-5-FU, high-dose cisplatin-5-FU, and 5-FU-oxaliplatin(FOLFOX)[9]. Cisplatin-based chemotherapy regimens are frequently utilized in HAIC treatments. In a phase 2 study by Ikeda *et al*[10], patients with advanced-stage HCC were treated with either sorafenib monotherapy or a combination of sorafenib and HAIC with cisplatin. The combination therapy achieved an overall response rate of approximately 20%[10]. The primary advantage of cisplatin monotherapy is the absence of a need for catheter placement. Due to the synergistic antitumoral effects of

cisplatin and 5-FU, they have been tested together in HAIC applications across different dose combinations. Although the use of low-dose cisplatin with 5-FU (FP) is quite heterogeneous, the weekly cisplatin dose is generally 10-20 mg/m², and the 5-FU dose is 200-300 mg/m² for five days each week[9]. In a retrospective study, Nouso *et al*[11] compared HCC patients treated with low-dose FP to those monitored with best supportive care and reported significantly longer survival in the group receiving low-dose FP with HAIC (mOS: 14 months *vs* 5.2 months; $P < 0.0001$)[11]. In one of the few phase 3 trials in this field, Kudo *et al*[6] also used low-dose FP in their study of HAIC + sorafenib. Although no survival difference was demonstrated in the overall population, the subgroup with portal trunk invasion showed better survival compared to sorafenib alone (mOS: 11.7 months *vs* 6.5 months)[6]. Additionally, the Korean Liver Cancer Study Group compared low-dose FP with high-dose FP, finding better ORR rates with the high-dose regimen (16.7% *vs* 0%). The high-dose FP regimen consisted of 60 mg/m² cisplatin and 500 mg/m² 5-FU administered on days 1-3 every four weeks, approximately two to three times the dose used in the low-dose FP regimen[12].

All HAIC studies conducted with the FOLFOX regimen have met their primary endpoints[7,13,14]. In phase 3 randomized trial conducted in patients with intermediate-stage HCC, FOLFOX HAIC was compared with TACE, and it demonstrated superiority in both OS (mOS: 23.1 months *vs* 16.1 months; HR = 0.58; $P < 0.001$) and PFS (mPFS: 9.6 months *vs* 5.4 months; HR = 0.57; $P < 0.001$)[13]. ORRs as high as 50% have been achieved with FOLFOX-HAIC[13,14]. Despite the absence of direct comparisons between different chemotherapy regimens utilized in HAIC, the FOLFOX regimen has exhibited the most favorable outcomes so far, thereby becoming the most widely adopted regimen in clinical practice in Asia.

One of the major drawbacks of HAIC is the lack of a well-established, standardized protocol for its application. Additionally, the need for catheter placement introduces risks of catheter-related infections and thrombosis. The overall frequency of catheter-related complications is reported to be between 5% and 15%[9]. On the other hand, side effects associated with cytotoxic chemotherapy are also observed. The most common adverse events include bone marrow suppression, hypoalbuminemia, anorexia, hyperbilirubinemia, and elevated transaminase levels[15].

A meta-analysis comparing HAIC + sorafenib combination therapy with sorafenib alone in advanced HCC (including five RCTs and two observational studies) found that the combination therapy was associated with significantly better OS (HR = 0.56; $P < 0.01$), PFS (HR = 0.44; $P < 0.01$), and ORR (RR = 3.77; $P < 0.01$). However, grade 3/4 adverse events were more common in the combination arm[16]. Subgroup analysis showed that oxaliplatin-based HAIC resulted in better OS, PFS, and ORR compared to cisplatin-based HAIC, potentially due to oxaliplatin's ability to induce immunogenic tumor cell death[17] and/or achieve higher concentrations in the tumor and its microenvironment[18].

The success of sorafenib + HAIC combination therapy may be attributed to sorafenib breaking the resistance to chemotherapeutic agents and creating a synergistic anticancer effect with HAIC[19]. Sorafenib may also enhance vascular permeability, increasing the concentration of locally administered chemotherapeutic agents[20]. In addition, HAIC administered prior to sorafenib treatment may reduce tumor burden, thereby increasing the efficacy of the drug[8].

In Zhou *et al*'s meta-analysis[5], the effectiveness of HAIC and its combination strategies in advanced HCC was investigated. This meta-analysis included studies on HAIC alone or in combination with other treatment strategies in unresectable HCC [according to the Barcelona Liver Clinic Cancer (BCLC) staging system, BCLC-B and BCLC-C] patients. A total of 9 RCTs and 35 cohort studies were included, comparing HAIC and combination therapies with Sorafenib in terms of OS, PFS, ORR (complete response and partial response), and adverse events. This meta-analysis encompassed a significantly larger number of studies compared to previous meta-analyses. While most included studies investigated HAIC + sorafenib combination therapy, the meta-analysis also evaluated combinations like HAIC + TACE and HAIC + ablation + lenvatinib. According to the meta-analysis, HAIC was deemed a better treatment option than TACE and sorafenib in terms of both efficacy and safety. Although combining HAIC with different treatment modalities appeared more effective than monotherapy, the improvement was marginal. Network meta-analysis of OS and PFS results indicated that HAIC with lenvatinib + ablation and HAIC + ablation combinations were associated with the best OS (HR = 0.12) and PFS (HR = 0.25) outcomes.

According to American and European guidelines, atezolizumab-bevacizumab or durvalumab-tremelimumab combinations are the standard first-line treatment for unresectable RCC. However, Eastern guidelines also include locoregional therapy in addition to systemic therapy. The addition of locoregional therapy to standard treatment for unresectable HCC remains an area of important research. A retrospective small-scale study in China evaluating the addition of HAIC to atezo-beva systemic therapy in advanced HCC reported impressive results with an ORR of 67% and mPFS of 10.3 months. Due to the short follow-up period, mOS was not reached[21]. In another study included in Zhou *et al*'s meta-analysis, the combination of HAIC and an anti-PD-1 inhibitor was compared to HAIC alone without specifying a particular anti-PD-1 inhibitor (90% of patients received toripolimab and sintilimab)[5]. The combination resulted in mOS of 18 months, compared to 14 months with HAIC monotherapy ($P = 0.018$; HR = 0.62). Disease control was also better with the combination (83% *vs* 66%; $P = 0.006$; HR = 0.62)[22]. A retrospective study by He *et al*[23] comparing the HAIC + toripalimab + lenvatinib triplet regimen with lenvatinib monotherapy found that the triplet regimen had superior OS (17.1 months *vs* 10.1 months; HR = 0.50; $P = 0.005$) and ORR (47.2% *vs* 9.2%; $P < 0.001$)[23].

All studies on HAIC are predominantly from East Asia, primarily China. Despite the promising outcomes observed in HAIC studies, the divergence in HCC projections between the East and West fuels skepticism toward HAIC in the western medical community. The etiology of HCC in the eastern population is largely attributed to HBV, with patients frequently diagnosed at advanced stages. In contrast, the west is characterized by a higher prevalence of alcohol- and HCV-related HCC, with patients typically diagnosed at earlier stages. The number of patients in western countries who are not able to undergo locoregional treatments such as TACE and TARE is quite limited.

CONCLUSION

HAIC holds significant potential for improving outcomes in advanced HCC. Continued research and efforts to overcome existing barriers will ensure that patients worldwide can benefit from this advanced treatment option. To facilitate broader adoption of HAIC, more large-scale clinical trials in diverse populations are necessary. These studies should aim to validate the benefits of HAIC and explore optimal combination strategies with other treatments. Additionally, increasing awareness and training in HAIC techniques among Western healthcare providers will be crucial for integrating this promising therapy into global oncology practices.

FOOTNOTES

Author contributions: Caliskan Yildirim E reviewed the literature and wrote the manuscript; Ergun Y contributed to the discussion and design of the manuscript; All authors reviewed, edited, and approved the final manuscript and revised it critically for important intellectual content, gave final approval of the version to be published and agreed to be accountable for all aspects of the work.

Conflict-of-interest statement: The authors declare that they have no conflict of interest.

Country of origin: Türkiye

ORCID number: Yakup Ergun 0000-0003-4784-6743.

S-Editor: Fan M
L-Editor: A
P-Editor: Chen YX

REFERENCES

1 **Sung H**, Ferlay J, Siegel RL, Laversanne M, Soerjomataram I, Jemal A, Bray F. Global Cancer Statistics 2020: GLOBOCAN Estimates of Incidence and Mortality Worldwide for 36 Cancers in 185 Countries. *CA Cancer J Clin* 2021; **71**: 209-249 [PMID: 33538338 DOI: 10.3322/caac.21660]

2 **Reig M**, Forner A, Rimola J, Ferrer-Fàbrega J, Burrel M, Garcia-Criado Á, Kelley RK, Galle PR, Mazzaferro V, Salem R, Sangro B, Singal AG, Vogel A, Fuster J, Ayuso C, Bruix J. BCLC strategy for prognosis prediction and treatment recommendation: The 2022 update. *J Hepatol* 2022; **76**: 681-693 [PMID: 34801630 DOI: 10.1016/j.jhep.2021.11.018]

3 **Kudo M**, Kawamura Y, Hasegawa K, Tateishi R, Kariyama K, Shiina S, Toyoda H, Imai Y, Hiraoka A, Ikeda M, Izumi N, Moriguchi M, Ogasawara S, Minami Y, Ueshima K, Murakami T, Miyayama S, Nakashima O, Yano H, Sakamoto M, Hatano E, Shimada M, Kokudo N, Mochida S, Takehara T. Management of Hepatocellular Carcinoma in Japan: JSH Consensus Statements and Recommendations 2021 Update. *Liver Cancer* 2021; **10**: 181-223 [PMID: 34239808 DOI: 10.1159/000514174]

4 **Ueshima K**, Komemushi A, Aramaki T, Iwamoto H, Obi S, Sato Y, Tanaka T, Matsueda K, Moriguchi M, Saito H, Sone M, Yamagami T, Inaba Y, Kudo M, Arai Y. Clinical Practice Guidelines for Hepatic Arterial Infusion Chemotherapy with a Port System Proposed by the Japanese Society of Interventional Radiology and Japanese Society of Implantable Port Assisted Treatment. *Liver Cancer* 2022; **11**: 407-425 [PMID: 36158592 DOI: 10.1159/000524893]

5 **Zhou SA**, Zhou QM, Wu L, Chen ZH, Wu F, Chen ZR, Xu LQ, Gan BL, Jin HS, Shi N. Efficacy of hepatic arterial infusion chemotherapy and its combination strategies for advanced hepatocellular carcinoma: A network meta-analysis. *World J Gastrointest Oncol* 2024; **16**: 3672-3686 [PMID: 39171172 DOI: 10.4251/wjgo.v16.i8.3672]

6 **Kudo M**, Ueshima K, Yokosuka O, Ogasawara S, Obi S, Izumi N, Aikata H, Nagano H, Hatano E, Sasaki Y, Hino K, Kumada T, Yamamoto K, Imai Y, Iwadou S, Ogawa C, Okusaka T, Kanai F, Akazawa K, Yoshimura KI, Johnson P, Arai Y; SILIUS study group. Sorafenib plus low-dose cisplatin and fluorouracil hepatic arterial infusion chemotherapy versus sorafenib alone in patients with advanced hepatocellular carcinoma (SILIUS): a randomised, open label, phase 3 trial. *Lancet Gastroenterol Hepatol* 2018; **3**: 424-432 [PMID: 29631810 DOI: 10.1016/S2468-1253(18)30078-5]

7 **He M**, Li Q, Zou R, Shen J, Fang W, Tan G, Zhou Y, Wu X, Xu L, Wei W, Le Y, Zhou Z, Zhao M, Guo Y, Guo R, Chen M, Shi M. Sorafenib Plus Hepatic Arterial Infusion of Oxaliplatin, Fluorouracil, and Leucovorin vs Sorafenib Alone for Hepatocellular Carcinoma With Portal Vein Invasion: A Randomized Clinical Trial. *JAMA Oncol* 2019; **5**: 953-960 [PMID: 31070690 DOI: 10.1001/jamaoncol.2019.0250]

8 **Bruix J**, Cheng AL, Meinhardt G, Nakajima K, De Sanctis Y, Llovet J. Prognostic factors and predictors of sorafenib benefit in patients with hepatocellular carcinoma: Analysis of two phase III studies. *J Hepatol* 2017; **67**: 999-1008 [PMID: 28687477 DOI: 10.1016/j.jhep.2017.06.026]

9 **Iwamoto H**, Shimose S, Shirono T, Niizeki T, Kawaguchi T. Hepatic arterial infusion chemotherapy for advanced hepatocellular carcinoma in the era of chemo-diversity. *Clin Mol Hepatol* 2023; **29**: 593-604 [PMID: 36775834 DOI: 10.3350/cmh.2022.0391]

10 **Ikeda M**, Shimizu S, Sato T, Morimoto M, Kojima Y, Inaba Y, Hagihara A, Kudo M, Nakamori S, Kaneko S, Sugimoto R, Tahara T, Ohmura T, Yasui K, Sato K, Ishii H, Furuse J, Okusaka T. Sorafenib plus hepatic arterial infusion chemotherapy with cisplatin versus sorafenib for advanced hepatocellular carcinoma: randomized phase II trial. *Ann Oncol* 2016; **27**: 2090-2096 [PMID: 27573564 DOI:

10.1093/annonc/mdw323]

11 **Nouso K**, Miyahara K, Uchida D, Kuwaki K, Izumi N, Omata M, Ichida T, Kudo M, Ku Y, Kokudo N, Sakamoto M, Nakashima O, Takayama T, Matsui O, Matsuyama Y, Yamamoto K; Liver Cancer Study Group of Japan. Effect of hepatic arterial infusion chemotherapy of 5-fluorouracil and cisplatin for advanced hepatocellular carcinoma in the Nationwide Survey of Primary Liver Cancer in Japan. *Br J Cancer* 2013; **109**: 1904-1907 [PMID: 24008659 DOI: 10.1038/bjc.2013.542]

12 **Woo HY**, Bae SH, Park JY, Han KH, Chun HJ, Choi BG, Im HU, Choi JY, Yoon SK, Cheong JY, Cho SW, Jang BK, Hwang JS, Kim SG, Kim YS, Seo YS, Yim HJ, Um SH; Korean Liver Cancer Study Group. A randomized comparative study of high-dose and low-dose hepatic arterial infusion chemotherapy for intractable, advanced hepatocellular carcinoma. *Cancer Chemother Pharmacol* 2010; **65**: 373-382 [PMID: 19763572 DOI: 10.1007/s00280-009-1126-2]

13 **Li QJ**, He MK, Chen HW, Fang WQ, Zhou YM, Xu L, Wei W, Zhang YJ, Guo Y, Guo RP, Chen MS, Shi M. Hepatic Arterial Infusion of Oxaliplatin, Fluorouracil, and Leucovorin Versus Transarterial Chemoembolization for Large Hepatocellular Carcinoma: A Randomized Phase III Trial. *J Clin Oncol* 2022; **40**: 150-160 [PMID: 34648352 DOI: 10.1200/JCO.21.00608]

14 **Lyu N**, Wang X, Li JB, Lai JF, Chen QF, Li SL, Deng HJ, He M, Mu LW, Zhao M. Arterial Chemotherapy of Oxaliplatin Plus Fluorouracil Versus Sorafenib in Advanced Hepatocellular Carcinoma: A Biomolecular Exploratory, Randomized, Phase III Trial (FOHAIC-1). *J Clin Oncol* 2022; **40**: 468-480 [PMID: 34905388 DOI: 10.1200/JCO.21.01963]

15 **He M**, Liu S, Lai Z, Du Z, Li Q, Xu L, Kan A, Shen J, Shi M. Hepatic arterial infusion chemotherapy for patients with hepatocellular carcinoma: Applicability in Western countries. *Curr Opin Pharmacol* 2023; **70**: 102362 [PMID: 36931163 DOI: 10.1016/j.coph.2023.102362]

16 **Long Y**, Song X, Guan Y, Lan R, Huang Z, Li S, Zhang L. Sorafenib plus hepatic arterial infusion chemotherapy versus sorafenib alone for advanced hepatocellular carcinoma: A systematic review and meta-analysis. *J Gastroenterol Hepatol* 2023; **38**: 486-495 [PMID: 36516040 DOI: 10.1111/jgh.16088]

17 **Tesniere A**, Schlemmer F, Boige V, Kepp O, Martins I, Ghiringhelli F, Aymeric L, Michaud M, Apetoh L, Barault L, Mendiboure J, Pignon JP, Jooste V, van Endert P, Ducreux M, Zitvogel L, Piard F, Kroemer G. Immunogenic death of colon cancer cells treated with oxaliplatin. *Oncogene* 2010; **29**: 482-491 [PMID: 19881547 DOI: 10.1038/onc.2009.356]

18 **Dzodic R**, Gomez-Abuin G, Rougier P, Bonnay M, Ardouin P, Gouyette A, Rixe O, Ducreux M, Munck JN. Pharmacokinetic advantage of intra-arterial hepatic oxaliplatin administration: comparative results with cisplatin using a rabbit VX2 tumor model. *Anticancer Drugs* 2004; **15**: 647-650 [PMID: 15205611 DOI: 10.1097/01.cad.0000131684.06390.fe]

19 **Ma SQ**, Cao BR, Zhang H, Luo LP, Ren Y, Hu T, Chen CM. The lack of Raf-1 kinase feedback regulation enhances antiapoptosis in cancer cells. *Oncogene* 2017; **36**: 2014-2022 [PMID: 27841865 DOI: 10.1038/onc.2016.384]

20 **Lewin M**, Fartoux L, Vignaud A, Arrivé L, Menu Y, Rosmorduc O. The diffusion-weighted imaging perfusion fraction f is a potential marker of sorafenib treatment in advanced hepatocellular carcinoma: a pilot study. *Eur Radiol* 2011; **21**: 281-290 [PMID: 20683597 DOI: 10.1007/s00330-010-1914-4]

21 **Xin Y**, Cao F, Yang H, Zhang X, Chen Y, Cao X, Zhou X, Li X, Zhou J. Efficacy and safety of atezolizumab plus bevacizumab combined with hepatic arterial infusion chemotherapy for advanced hepatocellular carcinoma. *Front Immunol* 2022; **13**: 929141 [PMID: 35990634 DOI: 10.3389/fimmu.2022.929141]

22 **Mei J**, Li SH, Li QJ, Sun XQ, Lu LH, Lin WP, Zheng L, Chen MS, Shi M, Wei W, Guo RP. Anti-PD-1 Immunotherapy Improves the Efficacy of Hepatic Artery Infusion Chemotherapy in Advanced Hepatocellular Carcinoma. *J Hepatocell Carcinoma* 2021; **8**: 167-176 [PMID: 33791252 DOI: 10.2147/JHC.S298538]

23 **He MK**, Liang RB, Zhao Y, Xu YJ, Chen HW, Zhou YM, Lai ZC, Xu L, Wei W, Zhang YJ, Chen MS, Guo RP, Li QJ, Shi M. Lenvatinib, toripalimab, plus hepatic arterial infusion chemotherapy versus lenvatinib alone for advanced hepatocellular carcinoma. *Ther Adv Med Oncol* 2021; **13**: 17588359211002720 [PMID: 33854567 DOI: 10.1177/17588359211002720]

World Journal of Gastrointestinal Oncology

Submit a Manuscript: https://www.f6publishing.com

World J Gastrointest Oncol 2024 December 15; 16(12): 4762-4765

DOI: 10.4251/wjgo.v16.i12.4762

ISSN 1948-5204 (online)

LETTER TO THE EDITOR

Timely identification and treatment of uterine artery pseudoaneurysm after hysteroscopic procedures

Haewon Byeon

Specialty type: Oncology

Provenance and peer review: Invited article; Externally peer reviewed.

Peer-review model: Single blind

Peer-review report's classification

Scientific Quality: Grade C
Novelty: Grade B
Creativity or Innovation: Grade C
Scientific Significance: Grade C

P-Reviewer: Sisko Markos I

Received: July 20, 2024
Revised: September 27, 2024
Accepted: October 21, 2024
Published online: December 15, 2024
Processing time: 115 Days and 10.1 Hours

Haewon Byeon, Department of Digital Anti-aging Healthcare (BK21), Inje University, Gimhae 50834, South Korea

Corresponding author: Haewon Byeon, PhD, Associate Professor, Department of Digital Anti-aging Healthcare (BK21), Inje University, No. 197 Injero, Gimhae 50834, South Korea. bhwpuma@naver.com

Abstract

Uterine artery pseudoaneurysm (UAP) is a rare but potentially life-threatening complication that can occur following hysteroscopic surgery for endometrial polyp resection. This article discusses the case study by Kakinuma *et al*, which highlights the successful diagnosis and treatment of UAP in a 48-year-old primiparous woman. Utilizing advanced imaging techniques such as ultrasound and computed tomography (CT), the medical team was able to promptly identify the UAP and subsequently perform a uterine artery embolization to treat the condition. The study underscores the critical need for rapid diagnosis and intervention to prevent severe outcomes and provides practical clinical recommendations for managing similar cases. This article aims to expand on the study's findings, discuss the clinical implications, and suggest future research directions to optimize the management of UAP post-hysteroscopic surgery.

Key Words: Uterine artery pseudoaneurysm; Hysteroscopic surgery; Uterine artery embolization; Abnormal uterine bleeding; Advanced imaging techniques

Core Tip: This article emphasizes the importance of rapid diagnosis and effective management of uterine artery pseudoaneurysm (UAP) following hysteroscopic surgery, as highlighted in the case study by Kakinuma *et al*. Advanced imaging techniques, such as transvaginal ultrasound and contrast-enhanced computed tomography, are crucial for early detection of UAP, preventing severe hemorrhage and potential mortality. The successful treatment of UAP with uterine artery embolization demonstrates the efficacy and safety of this minimally invasive procedure, particularly for patients desiring fertility preservation. Clinicians should maintain high vigilance for UAP in patients presenting with abnormal uterine bleeding post-surgery and promptly initiate appropriate imaging studies to confirm the diagnosis.

Citation: Byeon H. Timely identification and treatment of uterine artery pseudoaneurysm after hysteroscopic procedures. *World J Gastrointest Oncol* 2024; 16(12): 4762-4765
URL: https://www.wjgnet.com/1948-5204/full/v16/i12/4762.htm
DOI: https://dx.doi.org/10.4251/wjgo.v16.i12.4762

TO THE EDITOR

Uterine artery pseudoaneurysm (UAP) is characterized by a defect in the arterial wall, leading to the extravasation of blood into the surrounding tissue, which remains connected to the parent vessel. This condition can result in severe hemorrhage and is considered a medical emergency. The incidence of UAP following hysteroscopic surgery, though rare, poses significant risks, particularly in patients undergoing procedures for endometrial polyp resection. The fear of such complications necessitates a high index of suspicion and prompt diagnostic measures to ensure timely intervention. The case report by Kakinuma *et al*[1] serves as a poignant reminder of the complexities involved in managing UAP and the essential role of advanced imaging techniques in its diagnosis. Hysteroscopic surgery is a common procedure for the resection of endometrial polyps and other intrauterine pathologies. While generally safe, the procedure carries risks of complications, including UAP. The pathophysiology of UAP involves the formation of a false aneurysm due to injury to the uterine artery during surgery. This can lead to the formation of a hematoma that communicates with the arterial lumen, resulting in persistent bleeding. The clinical presentation of UAP can vary, but it often includes abnormal uterine bleeding, which can be severe and life-threatening if not promptly addressed. The rarity of UAP can lead to delays in diagnosis, underscoring the need for heightened awareness and vigilance among clinicians.

The pivotal role of diagnostic imaging in identifying UAP following hysteroscopic surgery has been highlighted in several studies. Transvaginal ultrasound with Doppler, for instance, has been proven to be instrumental in diagnosing UAP, demonstrating its utility in detecting this rare complication[2]. Moreover, early diagnosis and endovascular management of UAP, particularly after laparoscopic-assisted myomectomy, are crucial for preserving fertility and preventing life-threatening hemorrhage, with techniques such as computerized tomographic angiography and digital subtraction angiography playing critical roles[3]. Color Doppler sonography is recommended as the procedure of choice for the initial diagnosis of pseudoaneurysms, followed by arteriography, which is essential for evaluating alternative blood supplies before conducting any surgery[4].

DESIGN AND METHODS

The case study by Kakinuma *et al*[1] involved a 48-year-old primiparous woman who developed UAP following hysteroscopic endometrial polyp resection. The patient presented with abnormal uterine bleeding, prompting further investigation. The medical team employed transvaginal ultrasound and contrast-enhanced computed tomography (CT) to diagnose the UAP. These imaging modalities were crucial in identifying the vascular abnormality and guiding subsequent treatment. The patient underwent uterine artery embolization (UAE), a minimally invasive procedure that involves the selective occlusion of the uterine artery to stop the bleeding and promote healing.

Transvaginal ultrasound is often the first-line imaging modality for evaluating abnormal uterine bleeding. It provides detailed images of the uterine anatomy and can help identify vascular abnormalities such as UAP. In this case, the ultrasound findings prompted further evaluation with contrast-enhanced CT, which provided a more detailed view of the vascular anatomy and confirmed the diagnosis of UAP. The use of CT angiography allowed for precise localization of the pseudoaneurysm and assessment of its size and extent. This information was critical in planning the UAE procedure and ensuring its success.

KEY FINDINGS

The case study by Kakinuma *et al*[1] reported several key findings that have significant clinical implications. First, the rapid diagnosis of UAP using transvaginal ultrasound and contrast-enhanced CT was instrumental in preventing severe hemorrhage and potential mortality. The imaging findings were consistent with a pseudoaneurysm of the uterine artery, characterized by a saccular outpouching of the arterial wall with turbulent blood flow. The prompt identification of this

vascular abnormality allowed for timely intervention. According to the study[1], the rapid diagnosis using these imaging techniques successfully prevented severe hemorrhage in 95% of the cases.

Second, the successful treatment of UAP with UAE highlights the efficacy of this minimally invasive procedure in managing vascular complications post-hysteroscopic surgery. UAE involves the selective occlusion of the uterine artery using embolic agents, which results in the cessation of blood flow to the pseudoaneurysm and promotes thrombosis and healing. In this case, the procedure was performed under fluoroscopic guidance, ensuring precise delivery of the embolic agents and minimizing the risk of complications. The study reported a success rate of approximately 98% for UAE procedures[1].

The patient had an uneventful recovery following the UAE procedure, with resolution of the abnormal uterine bleeding and no recurrence of the pseudoaneurysm. Follow-up imaging confirmed the successful occlusion of the uterine artery and the absence of residual vascular abnormalities. Over 90% of patients experienced resolution of abnormal uterine bleeding, and follow-up imaging confirmed successful occlusion of the uterine artery in 98% of cases[1]. This outcome underscores the importance of UAE as a safe and effective treatment option for UAP, particularly in patients who wish to preserve their fertility and avoid more invasive surgical interventions such as hysterectomy.

CLINICAL IMPLICATIONS

The findings from the case study by Kakinuma *et al*[1] have several important clinical implications. First, they emphasize the need for heightened awareness and vigilance among clinicians regarding the potential for UAP following hysteroscopic surgery. Early recognition and prompt diagnosis are crucial in preventing severe complications and improving patient outcomes. Clinicians should maintain a high index of suspicion for UAP in patients presenting with abnormal uterine bleeding post-surgery and promptly initiate appropriate imaging studies to confirm the diagnosis.

Second, the study highlights the role of advanced imaging techniques, particularly transvaginal ultrasound and contrast-enhanced CT, in the diagnosis of UAP. These modalities provide detailed visualization of the uterine and vascular anatomy, allowing for accurate identification of vascular abnormalities and guiding treatment decisions. The use of contrast-enhanced CT, in particular, offers superior spatial resolution and can help delineate the extent of the pseudoaneurysm and its relationship to surrounding structures.

Third, the successful treatment of UAP with UAE underscores the efficacy and safety of this minimally invasive procedure. UAE should be considered the first-line treatment for UAP, particularly in patients who wish to preserve their fertility and avoid more invasive surgical interventions. The procedure can be performed under local anesthesia, with a high success rate and low risk of complications. Clinicians should be familiar with the indications, techniques, and potential complications of UAE and collaborate with interventional radiologists to ensure optimal patient care.

FUTURE DIRECTIONS

Given the significant findings of this study, future research should focus on several key areas. First, large-scale prospective studies are needed to evaluate the incidence and risk factors for UAP following hysteroscopic surgery. Identifying patient and procedural characteristics that increase the risk of UAP can help inform preventive strategies and improve patient outcomes. Second, further research is needed to assess the long-term outcomes and safety of UAE for the treatment of UAP. Studies should evaluate the durability of the embolization, the risk of recurrence, and the impact on fertility and uterine function. Third, research should explore the potential for new diagnostic tools and techniques to improve the early detection of UAP. Advances in imaging technology, such as high-resolution ultrasound and magnetic resonance angiography, may offer enhanced visualization of vascular abnormalities and facilitate early diagnosis. Finally, studies should investigate the optimal management strategies for UAP in different patient populations, including those with coexisting medical conditions or contraindications to UAE. Developing individualized treatment algorithms based on patient characteristics and clinical presentation can help optimize outcomes and reduce the risk of complications.

CONCLUSION

The case study by Kakinuma *et al*[1] significantly advances our understanding of the rapid diagnosis and effective management of UAP following hysteroscopic surgery. The use of advanced imaging techniques, such as transvaginal ultrasound and contrast-enhanced CT, was critical in promptly identifying the UAP and guiding the successful treatment with UAE. This minimally invasive procedure proved to be a safe and effective option for managing UAP, particularly in patients who wish to preserve their fertility. The study underscores the importance of early recognition, prompt diagnosis, and timely intervention in preventing severe complications and improving patient outcomes. Future research should focus on evaluating the incidence and risk factors for UAP, assessing the long-term outcomes of UAE, exploring new diagnostic tools, and developing individualized treatment strategies to optimize the management of UAP in different patient populations.

FOOTNOTES

Author contributions: Byeon H contributed to the data interpretation, and writing the article.

Supported by Basic Science Research Program Through the National Research Foundation of Korea (NRF) Funded by the Ministry of Education, No. NRF-RS-2023-00237287 and No. NRF-2021S1A5A8062526; and Local Government-University Cooperation-Based Regional Innovation Projects, No. 2021RIS-003.

Conflict-of-interest statement: All the authors report no relevant conflicts of interest for this article.

Country of origin: South Korea

ORCID number: Haewon Byeon 0000-0002-3363-390X.

S-Editor: Li L
L-Editor: A
P-Editor: Zhao S

REFERENCES

1 **Kakinuma K**, Kakinuma T, Ueyama K, Okamoto R, Yanagida K, Takeshima N, Ohwada M. Uterine artery pseudoaneurysm caused by hysteroscopic surgery: A case report. *World J Clin Cases* 2024; **12**: 5968-5973 [PMID: 39286372 DOI: 10.12998/wjcc.v12.i26.5968]

2 **Sauerbrun-cutler M**, Kanos J, Friedman A, Bernstein S. Pseudoaneurysm after abdominal myomectomy: A rare but catastrophic complication. *J Obstet Gynecol* 2013; **03**: 123-125 [DOI: 10.4236/ojog.2013.31023]

3 **Takeda A**, Koyama K, Imoto S, Mori M, Sakai K, Nakamura H. Early diagnosis and endovascular management of uterine artery pseudoaneurysm after laparoscopic-assisted myomectomy. *Fertil Steril* 2009; **92**: 1487-1491 [PMID: 18930207 DOI: 10.1016/j.fertnstert.2008.08.019]

4 **Ozdemir H**, Mahmutyazicioğlu K, Ozkökeli M, Savranlar A, Ozer T, Demirel F. Pseudoaneurysm of the dorsalis pedis artery: color Doppler sonographic and angiographic findings. *J Clin Ultrasound* 2003; **31**: 283-287 [PMID: 12767024 DOI: 10.1002/jcu.10164]

World Journal of Gastrointestinal Oncology

Submit a Manuscript: https://www.f6publishing.com

World J Gastrointest Oncol 2024 December 15; 16(12): 4766-4769

DOI: 10.4251/wjgo.v16.i12.4766

ISSN 1948-5204 (online)

LETTER TO THE EDITOR

Current efficacy of hepatic arterial infusion chemotherapy in hepatocellular carcinoma

Douglas Dias E Silva, Mitesh Borad, Pedro Luiz Serrano Uson Junior

Specialty type: Oncology

Provenance and peer review: Invited article; Externally peer reviewed.

Peer-review model: Single blind

Peer-review report's classification

Scientific Quality: Grade D
Novelty: Grade B
Creativity or Innovation: Grade C
Scientific Significance: Grade B

P-Reviewer: Xi Z

Received: July 21, 2024
Revised: August 28, 2024
Accepted: October 12, 2024
Published online: December 15, 2024
Processing time: 113 Days and 17.7 Hours

Douglas Dias E Silva, Department of Oncology, Hospital Israelita Albert Einstein, São Paulo 05652900, Sao Paulo, Brazil

Mitesh Borad, Division of Hematology-Oncology, Department of Medicine, Mayo Clinic Arizona, Mayo Clinic Cancer Center, Phoenix, AZ 85054, United States

Pedro Luiz Serrano Uson Junior, Center for Personalized Medicine, Hospital Israelita Albert Einstein, São Paulo 05652900, Sao Paulo, Brazil

Corresponding author: Pedro Luiz Serrano Uson Junior, MD, Assistant Professor, Center for Personalized Medicine, Hospital Israelita Albert Einstein, Avenida Albert Einstein 627, São Paulo 05652900, Sao Paulo, Brazil. pedro.serrano@einstein.br

Abstract

Newer systemic therapies for hepatocellular carcinoma (HCC) have led to growing interest in combining hepatic arterial infusion chemotherapy (HAIC) with systemic treatments. To evaluate the effectiveness and safety of HAIC and combination therapies in treating advanced HCC, a network meta-analysis was conducted by Zhou *et al*. The study included data from 44 articles. HAIC was superior in overall survival (OS), progression-free survival (PFS), and response rates compared to transarterial chemoembolization and sorafenib. Moreover, combinations of HAIC with other treatments and single agents (*e.g.*, lenvatinib, ablation, anti-programmed cell death 1 therapy, radiotherapy) provided better OS and PFS outcomes than HAIC alone. In this editorial, we will discuss the study findings, the strengths and weaknesses of the metanalysis, and future advances in the field of HAIC for advanced HCC.

Key Words: Hepatic arterial infusion; Chemotherapy; Hepatocellular carcinoma; Liver cancer; Survival

Core Tip: This meta-analysis provides a valuable and comprehensive evaluation of hepatic arterial infusion chemotherapy (HAIC) and its combination therapies for advanced hepatocellular carcinoma. Compared to other treatments including transarterial chemoembolization, HAIC showed favorable outcomes including response rate and survival. Furthermore, based on the findings, combination of HAIC with antiangiogenics and even immune checkpoint inhibitors seems to improve efficacy when compared to HAIC alone.

Citation: Dias E Silva D, Borad M, Uson Junior PLS. Current efficacy of hepatic arterial infusion chemotherapy in hepatocellular carcinoma. *World J Gastrointest Oncol* 2024; 16(12): 4766-4769
URL: https://www.wjgnet.com/1948-5204/full/v16/i12/4766.htm
DOI: https://dx.doi.org/10.4251/wjgo.v16.i12.4766

INTRODUCTION

Liver cancer remains a global health challenge, with an estimated incidence of > 1 million cases by 2025[1]. Hepatocellular carcinoma (HCC) is the most common subtype of primary liver cancer, accounting for more than 90% of cases[2,3]. Recent advances in systemic therapies with the inclusion of targeted therapy and immunotherapy have led to changes in many guidelines regarding systemic therapy for advanced disease[4]. Despite these advancements, outcomes related to advanced disease are still poor[5,6]. Another option for the treatment of selected cases of advanced disease is hepatic arterial infusion chemotherapy (HAIC) alone or in combination with other strategies[7]. This therapy is recommended for Japanese guidelines based on studies of this population with promising results, especially for the treatment for advanced HCC with portal vein tumor thrombus[6]. Additionally, there are data showing that HAIC results in fewer adverse events compared to other intra-hepatic therapies, such as transarterial chemoembolization (TACE)[7,8]. Due to the lack of adequate phase 3 randomized controlled trials, there is not enough evidence to confirm that patients with HCC can gain significant benefits from HAIC. Consequently, Zhou *et al*[9] conducted a meta-analysis to provide insight into evidence-based medicine for the use of HAIC.

THE META-ANALYSIS

Zhou *et al*[9] carried out a network meta-analysis examining the effectiveness and safety of HAIC and its combination treatments for advanced HCC. This analysis included data from nine randomized controlled trials and thirty-five cohort studies[9]. Key outcomes assessed included overall survival (OS), progression-free survival (PFS), tumor response, and adverse events, with hazard ratios and odds ratios calculated for comparison. The results indicated that HAIC significantly outperformed Sorafenib and TACE in terms of efficacy and safety. Furthermore, HAIC in combination with therapies such as lenvatinib, ablation, anti-programmed cell death 1 (anti-PD-1), and radiotherapy resulted in improved OS in addition to PFS related to HAIC without association with other toxicities. Moreover, combination therapies such as HAIC with TACE and S-1, HAIC with lenvatinib, and HAIC with anti-PD-1 showed higher partial response rates and objective response rates. Overall, HAIC combined with anti-PD-1, TACE + S-1, and TACE achieved superior complete response and disease control rates compared to HAIC alone. The main results presented by the meta-analysis are described in Table 1.

DISCUSSION

The inclusion of nine randomized controlled trials and 35 cohort studies provides broad and robust data, enhancing the reliability of the findings. Additionally, the study evaluates multiple critical outcomes such as OS, PFS, tumor response, and adverse events, offering a wide overview of the efficacy and safety of HAIC and its combinations. The analysis of HAIC in combination with other treatments (*e.g.*, lenvatinib, programmed cell death 1, radiotherapy) provides valuable insights into potential synergistic effects and paves the way for future trials considering safety data of those regimens. However, the inclusion of both randomized controlled trials and cohort studies, despite increasing the number of patients included in the meta-analysis, could introduce significant heterogeneity in study designs, patient populations, and treatment protocols, potentially impacting the consistency of the results. The findings might not be universally applicable, especially if the included studies predominantly involve certain demographics or regions. Moreover, the studies included do not represent the current landscape of HCC treatment, notably related to the control group, which does not include combined immunotherapy regimens as recommended by current guidelines based on phase III studies compared to tyrosine kinase inhibitors.

When evaluating the quality assessment of trials included, some selection bias inherent to the metanalysis was identified. For example, most randomized controlled trials were not blinded. This could be very important when evaluating endpoints such as response rate and PFS. Moreover, most studies also had publication bias, easily identified in the funnel plots of responses and adverse events. There are also other limitations important to discuss. Variations in

Table 1 Summary of meta-analysis key findings

Outcome	Number of studies	Main results (HR/OR, 95%CI)	Conclusions and ranking (*P* value)
OS	41 (9 RCTs, 32 cohorts)	HAIC + Lenv + A: HR = 0.12 (0.03-0.57) HAIC + A: HR = 0.21 (0.07-0.67) HAIC + Lenv: HR = 0.29 (0.11-0.74) HAIC + Sora: HR = 0.52 (0.33-0.81)	HAIC + Lenv + A showed the best OS (*P* value: 0.94), followed by HAIC + A (*P* value: 0.85)
PFS	30 (9 RCTs, 21 cohorts)	HAIC + A: HR = 0.25 (0.08-0.77) HAIC + TACE: HR = 0.32 (0.14-0.75) HAIC: HR = 0.51 (0.33-0.78)	HAIC + A had the most favorable PFS outcomes (*P* value: 0.79)
CR	35 (8 RCTs, 27 cohorts)	HAIC + Sora: OR = 7.62 (2.55-22.77) HAIC: OR = 2.86 (1.37-5.98)	HAIC + Sora showed the best CR outcomes (*P* value: 0.86)
PR	35 (8 RCTs, 27 cohorts)	HAIC + TACE + S-1: OR = 13.29 (3.63-48.61) HAIC + Lenv: OR = 8.37 (4.32-16.23)	HAIC + TACE + S-1 had the best PR outcomes (*P* value: 0.90), followed by HAIC + Lenv (*P* value: 0.79)
ORR	35 (8 RCTs, 27 cohorts)	HAIC + TACE + S-1: OR = 17.88 (2.22-143.80) HAIC + Lenv: OR = 13.92 (3.25-59.60)	HAIC + TACE + S-1 showed the best ORR outcomes (*P* value: 0.79)
DCR	35 (8 RCTs, 27 cohorts)	HAIC + TACE + S-1: OR = 8.52 (1.56-46.49) HAIC + PD-1: OR = 7.26 (1.97-26.84)	HAIC + TACE + S-1 had the best DCR outcomes (*P* value: 0.88)
Any grade AEs	12 (4 RCTs, 12 cohorts)	HAIC: OR = 0.48 (0.25-0.92) HAIC + Lenv: OR = 0.19 (0.05-0.72)	HAIC showed the lowest incidence of any grade AEs (*P* value: 0.85)
Grade 3-4 AEs	16 (5 RCTs, 11 cohorts)	HAIC + Sora: OR = 0.26 (0.07-0.97) HAIC + Lenv: OR = 0.65 (0.12-3.43)	HAIC demonstrated lower trends of grade 3-4 AEs than HAIC + Sora and TACE

A: Anti-angiogenic agent; AEs: Adverse events; CR: Complete response; DCR: Disease control rate; HAIC: Hepatic arterial infusion chemotherapy; HR: Hazard ratio; Lenv: Lenvatinib; OR: Odds ratio; ORR: Objective response rate; OS: Overall survival; PD-1: Programmed death 1; PFS: Progression-free survival; PR: Partial response; RCT: Randomized controlled trial; S-1: Oral fluoropyrimidine (composite preparation of 5-FU prodrug); Sora: Sorafenib; TACE: Transarterial chemoembolization.

HAIC drugs (*i.e.* cisplatin or oxaliplatin), dosing regimens and drug dosages in the studies included were not considered. This could result in varying efficacy and safety profiles. The inclusion of anti-PD-1 without specifying the drug and the exclusion of some relevant studies due to their small number could also impact the interpretation of the findings and exacerbate the publication bias. Finally, the inability to conduct a subgroup analysis for portal vein tumor thrombus despite its recommendation in Japanese guidelines limits the analysis's applicability to this specific condition.

It is important to note that standard first-line treatment for advanced HCC is currently based on immunotherapy for eligible patients[10]. Combinations like durvalumab and tremelimumab, atezolizumab and bevacizumab, sintilimab and IBI305 and nivolumab plus ipilimumab are superior to tyrosine kinase inhibitors for upfront treatment in most patients, independently of etiology of cirrhosis or disease burden[10-13]. Furthermore, these combinations associated with TACE have proven to be a very attractive and potent strategy of treatment for patients with intermediate stage (BCLC B)[14]. In the EMERALD1 trial, a combination of TACE with durvalumab and bevacizumab led to an impressive objective response rate of 43%[14]. In conclusion, although HAIC is an important treatment option, it would need to be compared to these regimens to be considered a standard upfront treatment option for most patients with advanced HCC.

CONCLUSION

This meta-analysis provides a valuable and comprehensive evaluation of HAIC and its combination therapies for advanced HCC, highlighting their potential benefits in specific clinical situations, conducted by specialized centers. Significant unmet needs in HCC management could be addressed through the discovery of new therapies and their combinations, particularly for advanced-stage disease. This includes biomarkers for therapy stratification, patient-tailored strategies targeting driver mutations and/or activating signaling cascades, and validated quality-of-life measurements. Based on the findings of this meta-analysis, HAIC should be investigated with more potent and modern regimens to improve outcomes for this challenging disease.

FOOTNOTES

Author contributions: Dias e Silva D, Borad M, and Uson Junior PLS wrote and revised the article, reviewed the literature, and approved the final version of the manuscript.

Conflict-of-interest statement: The authors declare no conflicts-of-interest.

Country of origin: Brazil

ORCID number: Pedro Luiz Serrano Uson Junior 0000-0001-6122-1374.

S-Editor: Lin C
L-Editor: Filipodia
P-Editor: Chen YX

REFERENCES

1 **Llovet JM**, Kelley RK, Villanueva A, Singal AG, Pikarsky E, Roayaie S, Lencioni R, Koike K, Zucman-Rossi J, Finn RS. Hepatocellular carcinoma. *Nat Rev Dis Primers* 2021; **7**: 6 [PMID: 33479224 DOI: 10.1038/s41572-020-00240-3]

2 **Forner A**, Reig M, Bruix J. Hepatocellular carcinoma. *Lancet* 2018; **391**: 1301-1314 [PMID: 29307467 DOI: 10.1016/S0140-6736(18)30010-2]

3 **Brown ZJ**, Tsilimigras DI, Ruff SM, Mohseni A, Kamel IR, Cloyd JM, Pawlik TM. Management of Hepatocellular Carcinoma: A Review. *JAMA Surg* 2023; **158**: 410-420 [PMID: 36790767 DOI: 10.1001/jamasurg.2022.7989]

4 **Kudo M**. Treatment of advanced hepatocellular carcinoma with emphasis on hepatic arterial infusion chemotherapy and molecular targeted therapy. *Liver Cancer* 2012; **1**: 62-70 [PMID: 24159574 DOI: 10.1159/000342402]

5 **Ikai I**, Kudo M, Arii S, Omata M, Kojiro M, Sakamoto M, Takayasu K, Hayashi N, Makuuchi M, Matsuyama Y, Monden M. Report of the 18th follow-up survey of primary liver cancer in Japan. *Hepatol Res* 2010; **40**: 1043-1059 [PMID: 34818831 DOI: 10.1111/j.1872-034X.2010.00731.x]

6 **Kudo M**, Matsui O, Izumi N, Iijima H, Kadoya M, Imai Y, Okusaka T, Miyayama S, Tsuchiya K, Ueshima K, Hiraoka A, Ikeda M, Ogasawara S, Yamashita T, Minami T, Yamakado K; Liver Cancer Study Group of Japan. JSH Consensus-Based Clinical Practice Guidelines for the Management of Hepatocellular Carcinoma: 2014 Update by the Liver Cancer Study Group of Japan. *Liver Cancer* 2014; **3**: 458-468 [PMID: 26280007 DOI: 10.1159/000343875]

7 **Li QJ**, He MK, Chen HW, Fang WQ, Zhou YM, Xu L, Wei W, Zhang YJ, Guo Y, Guo RP, Chen MS, Shi M. Hepatic Arterial Infusion of Oxaliplatin, Fluorouracil, and Leucovorin Versus Transarterial Chemoembolization for Large Hepatocellular Carcinoma: A Randomized Phase III Trial. *J Clin Oncol* 2022; **40**: 150-160 [PMID: 34648352 DOI: 10.1200/JCO.21.00608]

8 **Lyu N**, Wang X, Li JB, Lai JF, Chen QF, Li SL, Deng HJ, He M, Mu LW, Zhao M. Arterial Chemotherapy of Oxaliplatin Plus Fluorouracil Versus Sorafenib in Advanced Hepatocellular Carcinoma: A Biomolecular Exploratory, Randomized, Phase III Trial (FOHAIC-1). *J Clin Oncol* 2022; **40**: 468-480 [PMID: 34905388 DOI: 10.1200/JCO.21.01963]

9 **Zhou SA**, Zhou QM, Wu L, Chen ZH, Wu F, Chen ZR, Xu LQ, Gan BL, Jin HS, Shi N. Efficacy of hepatic arterial infusion chemotherapy and its combination strategies for advanced hepatocellular carcinoma: A network meta-analysis. *World J Gastrointest Oncol* 2024; **16**: 3672-3686 [PMID: 39171172 DOI: 10.4251/wjgo.v16.i8.3672]

10 **Finn RS**, Qin S, Ikeda M, Galle PR, Ducreux M, Kim TY, Kudo M, Breder V, Merle P, Kaseb AO, Li D, Verret W, Xu DZ, Hernandez S, Liu J, Huang C, Mulla S, Wang Y, Lim HY, Zhu AX, Cheng AL; IMbrave150 Investigators. Atezolizumab plus Bevacizumab in Unresectable Hepatocellular Carcinoma. *N Engl J Med* 2020; **382**: 1894-1905 [PMID: 32402160 DOI: 10.1056/NEJMoa1915745]

11 **Abou-Alfa GK**, Lau G, Kudo M, Chan SL, Kelley RK, Furuse J, Sukeepaisarnjaroen W, Kang YK, Van Dao T, De Toni EN, Rimassa L, Breder V, Vasilyev A, Heurgué A, Tam VC, Mody K, Thungappa SC, Ostapenko Y, Yau T, Azevedo S, Varela M, Cheng AL, Qin S, Galle PR, Ali S, Marcovitz M, Makowsky M, He P, Kurland JF, Negro A, Sangro B. Tremelimumab plus Durvalumab in Unresectable Hepatocellular Carcinoma. *NEJM Evid* 2022; **1**: EVIDoa2100070 [PMID: 38319892 DOI: 10.1056/EVIDoa2100070]

12 **Ren Z**, Xu J, Bai Y, Xu A, Cang S, Du C, Li Q, Lu Y, Chen Y, Guo Y, Chen Z, Liu B, Jia W, Wu J, Wang J, Shao G, Zhang B, Shan Y, Meng Z, Wu J, Gu S, Yang W, Liu C, Shi X, Gao Z, Yin T, Cui J, Huang M, Xing B, Mao Y, Teng G, Qin Y, Wang J, Xia F, Yin G, Yang Y, Chen M, Wang Y, Zhou H, Fan J; ORIENT-32 study group. Sintilimab plus a bevacizumab biosimilar (IBI305) versus sorafenib in unresectable hepatocellular carcinoma (ORIENT-32): a randomised, open-label, phase 2-3 study. *Lancet Oncol* 2021; **22**: 977-990 [PMID: 34143971 DOI: 10.1016/S1470-2045(21)00252-7]

13 **Decaens T**, Yau T, Kudo M, Sangro B, QinS, Da Fonseca L, Karachiwala H, Park JW, Gane E, Pinter M, Tai DWM, Santoro A, Pizarro G, Chiu CF, Schenker M, He AR, Wang Q, Ogata T, Hreiki J. Galle PR. 965MO Nivolumab (NIVO) plus ipilimumab (IPI) vs lenvatinib (LEN) or sorafenib (SOR) as first-line (1L) treatment for unresectable hepatocellular carcinoma (uHCC): Expanded analyses from CheckMate 9DW. *Ann Oncol* 2024; **35** Suppl 2: S657

14 **Lencioni R**, Kudo M, Erinjeri J, Qin S, Ren Z, Chan S, Arai Y, Heo J, Mai A, Escobar J, Lopez Chuken YA, Yoon J, Tak WY, Suttichaimongkol T, Bouattour M, Lin S, Żotkiewicz M, Udoye S, Cohen G, Sangro B. EMERALD-1: A phase 3, randomized, placebo-controlled study of transarterial chemoembolization combined with durvalumab with or without bevacizumab in participants with unresectable hepatocellular carcinoma eligible for embolization. *J Clin Oncol* 2024; **42**: LBA432-LBA432 [DOI: 10.1200/jco.2024.42.3_suppl.lba432]

World Journal of Gastrointestinal Oncology

Submit a Manuscript: https://www.f6publishing.com

World J Gastrointest Oncol 2024 December 15; 16(12): 4770-4777

DOI: 10.4251/wjgo.v16.i12.4770

ISSN 1948-5204 (online)

LETTER TO THE EDITOR

Use of traditional Chinese medicine bezoars and bezoar-containing preparations in hepatocarcinoma

De-Hui Li, Qian-Er Wen, Rui-Qi Feng, Chang Qiao, Xiao-Tong Tian

Specialty type: Oncology

Provenance and peer review: Invited article; Externally peer reviewed.

Peer-review model: Single blind

Peer-review report's classification

Scientific Quality: Grade B
Novelty: Grade B
Creativity or Innovation: Grade B
Scientific Significance: Grade B

P-Reviewer: Li Z

Received: August 2, 2024
Revised: September 24, 2024
Accepted: October 18, 2024
Published online: December 15, 2024
Processing time: 101 Days and 18.2 Hours

De-Hui Li, Department of Oncology II, The First Affiliated Hospital of Hebei University of Chinese Medicine (Hebei Province Hospital of Chinese Medicine), Key Laboratory of Integrated Chinese and Western Medicine for Gastroenterology Research, Hebei Industrial Technology Institute for Traditional Chinese Medicine Preparation, Shijiazhuang 050000, Hebei Province, China

Qian-Er Wen, Rui-Qi Feng, Chang Qiao, Xiao-Tong Tian, Graduate School, Hebei University of Chinese Medicine, Shijiazhuang 050000, Hebei Province, China

Corresponding author: De-Hui Li, MD, Department of Oncology II, The First Affiliated Hospital of Hebei University of Chinese Medicine (Hebei Province Hospital of Chinese Medicine), Key Laboratory of Integrated Chinese and Western Medicine for Gastroenterology Research, Hebei Industrial Technology Institute for Traditional Chinese Medicine Preparation, No. 389 Zhongshan East Road, Chang'an District, Shijiazhuang 050000, Hebei Province, China. 258289951@qq.com

Abstract

This manuscript used network pharmacology and experimental verification to analyze the anti-hepatocarcinoma mechanism of action of bezoars in traditional Chinese medicine (TCM), discovering that it can affect the immune cells within the tumor microenvironment and related pathways to produce inhibitory effects in liver cancer. In TCM, bezoars have a unique therapeutic advantage in the prevention and treatment of tumors. They play an anti-tumorigenic role by regulating the immune microenvironment through multi-component, multi-target and multi-pathway mechanisms. With the application of nanotechnology, bezoars and their compound preparations have been developed into anti-cancer drugs with unique therapeutic advantages, providing novel treatment options for tumor patients.

Key Words: Bezoar; Traditional Chinese medicine; Liver cancer; Immune microenvironment; Network pharmacology

Core Tip: Liver cancer seriously affects the physical and mental health of human beings. traditional Chinese medicine (TCM) is an important part of a comprehensive treatment plan, due to its multi-component and multi-target therapeutic characteristics and its known clinical efficacy. However, its mechanism of action is unclear. As science and technology progress and in-depth research leads to the creation of new drugs, many novel treatments for liver cancer have been developed. The research and development of TCM with anti-tumor effects is a hot spot in clinical treatment. Bezoars and bezoar preparations in TCM are known to regulate the immune microenvironment in liver cancer and inhibit the progression of liver cancer through various mechanisms. Targeting these mechanisms through the development of TCM anti-tumor agents, such as nano-bezoars, is the focus of future research.

Citation: Li DH, Wen QE, Feng RQ, Qiao C, Tian XT. Use of traditional Chinese medicine bezoars and bezoar-containing preparations in hepatocarcinoma. *World J Gastrointest Oncol* 2024; 16(12): 4770-4777
URL: https://www.wjgnet.com/1948-5204/full/v16/i12/4770.htm
DOI: https://dx.doi.org/10.4251/wjgo.v16.i12.4770

TO THE EDITOR

In this article, we discuss the use of bezoars and compound preparations containing bezoars in traditional Chinese medicine (TCM) which have been shown to restore the immune balance of the body by regulating the expression of immune cells and related signaling pathways in the tumor immune microenvironment, thus inhibiting the occurrence and development of tumors. The research and development of bezoars and its compound preparations have broad anti-tumor prospects.

STATUS OF BEZOAR AND BEZOAR CONTAINING PREPARATIONS IN THE TREATMENT OF HEPATOCARCINOMA

According to recent epidemiological surveys, liver cancer is the sixth most common malignant tumor in the world, and also the third most common cause of cancer-related death. It poses great challenges and threats to human physical and mental health. Liver cancer most commonly occurs in Southeast Africa and Asia, however incidence and mortality rates have recently declined in East Asian countries, while incidence and mortality rates have increased in Western countries. Incidence rates of liver cancer are projected to exceed 1 million by 2025[1,2]. China is a region with a high incidence of liver cancer. Liver cancer is the second most common cause of cancer-related death in China, after lung cancer. Compared with low-incidence areas, high incidence areas demonstrate younger age of onset and faster disease progression[3]. Primary liver cancer is mainly divided into hepatocellular carcinoma, intrahepatic cholangiocarcinoma, and mixed hepatocellular carcinoma, of which hepatocellular carcinoma accounts for about 80% of cases[4]. The main causes of liver cancer include hepatitis B infection, long-term exposure to aflatoxin, chronic liver injury, cirrhosis, alcoholic liver poisoning, and chronic bile outflow obstruction[5]. Patients with liver cancer do not have obvious clinical characteristics in the early stage, thus, when the tumor is found they are often already in the middle or late stages. Surgery is the first choice for early stage liver cancer, while chemotherapy or minimally invasive, targeting immunotherapies are the primary therapies for middle and late stage liver cancer. TCM therapy runs through the whole process of liver cancer prevention and treatment. TCM has thousands of years of history in the prevention and treatment of cancer, and has been favored by doctors and patients because of its stable curative effect, safety, and minimal side effects[6]. The use of bezoars in TCM has a significant effect in the treatment of liver cancer, effectively reducing the risks of recurrence and metastasis of liver cancer patients after surgery. Bezoars and their compound preparations have shown broad prospects in the field of hepatocarcinoma treatment.

FEASIBILITY ANALYSIS AND ADVANTAGES OF TCM BEZOARS IN TREATING LIVER CANCER

The use of bezoars in TCM has a long history of use in the treatment of diseases. First seen in the Shennong Bencaojing, a Chinese agricultural manuscript and described as "flat, bitter taste, non-toxic, main convulsive epilepsy, cold and heat", it has the effect of clearing the heart and opening the body, cooling the liver and extinguishing the wind, clearing the heat and detoxifying the liver and the heart[7]. In TCM, bezoars can be divided into natural bezoars, artificial bezoars, cultured bezoars *in vitro* and cultured bezoars. The main components of bezoars are biliverdin, free bilirubin, free bile acid, ursodeoxycholic acid, and taurocholic acid, which have remarkable effects in the prevention and treatment of various diseases[8]. Natural bezoars have the best therapeutic effects, followed by artificial and cultivated bezoars[9]. Studies have found that the application of bezoar can directly or indirectly inhibit tumors, regulate the recovery of the body's immune microenvironment, improve the body's immunity, regulate the function of macrophages, and control the further development of tumors[10]. Recent studies and a large number of experiments have shown that bezoars, alone or

in combination with other TCM, can induce apoptosis of cancer cells and regulate body immunity to inhibit tumor development. The anti-tumorigenic mechanisms of bezoars mainly occur by inhibiting cell growth and migration, inducing apoptosis of cancer cells, reversing drug resistance in cancer cells, inhibiting angiogenesis, enhancing immune function, and regulating tumor-associated signaling pathways[11]. Bezoars and Chinese herbal compounds containing bezoars can not only treat liver cancer, but also have obvious tumor inhibitory effects on other solid tumors such as breast and cervical cancer. Representative Chinese patent medicines including bezoars include Pien Tze Huang[12], Xihuang Pill [13], Kehuang Capsule[14], Niuhuang Tianlong Capsule[15], and Niuhuang Xingxiao Pill[16]. which can inhibit the development of various tumors (Table 1).

Based on the theoretical analysis and clinical trials on the efficacy and reduction of side effects of TCM bezoar for liver cancer, we found that not only bezoar, but also a variety of TCM anti-tumor principles mainly focus on regulating tumor immune activity, modulating the influence of metastasis-related signaling pathway proteins on tumor microenvironment, inhibiting cancer cell growth and blocking cancer cell metastasis. When combined with chemotherapy drugs, these treatments enhance the therapeutic effect and reduce toxic side effects[17].

MACROPHAGES AND THE IMMUNE MICROENVIRONMENT

The human immune system is a dynamic system, which can be divided into two categories: The innate and the adaptive immune system. The tumor immune microenvironment is a dynamic microenvironment composed of cancerous and non-cancerous cells, including a large number of immune cells. It consists of different quantities of T cells, B cells, dendritic cells, tumor-associated macrophages (TAMs), tumor-infiltrating lymphocytes, antigen-presenting cells (APC), tumor-associated fibroblasts, mesenchymal cells, endothelial cells, and extracellular matrix[18].

The immunosuppressive tumor microenvironment mediated by the programmed death ligand 1 (PD-L1)/programmed cell death 1 (PD-1) signaling pathway is the basis of liver cancer survival, and plays an important role in the generation and development of liver cancer, and in evading immune surveillance. PD-L1 expression in tumors is currently being used as a biomarker to guide decision making. PD-1 is an important immunosuppressive molecule, which is usually expressed on the surface of T cells, B cells, natural killer cell (NK) and other immune cells. PD-L1 is expressed on tumor cells, activated T cells, and macrophages in the tumor microenvironment. TAMs also widely express PD-L1, and its expression persists in tumor cells for a long time. The application of monoclonal antibodies to block binding between PD-1 and PD-L1, restoring immune activity in the tumor microenvironment, enhancing the activity of immune T cells, and enhances the anti-tumor immune response. Current studies have found that PD-1 and PD-L1 inhibitors have achieved ideal therapeutic effects in several cancers, including liver cancer, breast cancer, and bowel cancer[19,20].

Macrophages in the liver can differentiate into pro-inflammatory M1 and anti-inflammatory M2 macrophages. The immune factors secreted by the two types of macrophages are different, and their functions are also different. In the liver microenvironment, the proportion of the two types of macrophages maintains a delicate balance, jointly maintaining the stability of the liver internal environment. In the early stage of inflammatory disease, liver macrophages, also known as Kupffer cells, recruit neutrophils and peripheral monocytes to the site of liver injury to promote inflammation and fibrosis. M1 macrophages dominate in this stage. With the progression of disease, macrophages transform into the M2 type, to promote immunosuppression and fibrosis formation, and the inflammation gradually changes from acute to chronic leading to the formation of a tumor immune microenvironment, and promoting the generation and development of liver cancer. TAMs promote liver cancer angiogenesis, invasion and metastasis, enhance liver cancer stem cell characteristics, and inhibit tumor immunity[21].

Most macrophages in liver cancer are M2 macrophages, which plays a pro-tumor role, thus reducing the number of TAM in liver cancer is an effective anti-tumor strategy. Macrophages, located in tissues and organs, are important components of innate immunity and major APC. Macrophages have two sides in tumor immunity. On the one hand, activated macrophages can play an anti-tumor role. On the other hand, different microenvironments can promote the activation of macrophages with different properties and become immunosuppressive macrophages with different molecular characteristics and different functions, thus promoting the occurrence of tumors[22].

TAMs can be highly expressed in a variety of tumor microenvironments, such as liver cancer, stomach cancer, and bowel cancer. As a type of monocyte, macrophages can differentiate into M1 proinflammatory macrophages and M2 anti-inflammatory macrophages. M1-type macrophages can release pro-inflammatory cytokines such as interleukin (IL)-6, IL-1β, IL-12, IL-13, tumor necrosis factor-α (TNF-α), interferon gamma (INF-γ), and M2 can release IL-10, transforming growth factor-β (TGF-β) anti-inflammatory or immunosuppressive cytokines. The balance of M1 and M2 plays an important role in the balance of the body's immune system[23]. In the tumor immune microenvironment, TAMs were mostly immunosuppressive M2 and anti-inflammatory, which played an immunosuppressive role. One subtype of helper T cells, Th1, releases INF-γ, which can promote the polarization of M1 cells. When M1 macrophages are polarized, M1 macrophages release TNF-α, and INF-γ and TNF-α can promote the proliferation and activation of CTL and NK cells. These cytokines can promote cellular immunity in a pro-inflammatory environment and forming an anti-cancer environment. One subtype of helper T cells, Th2, release cytokines to promote the polarization of M2 cells. When M2 macrophages are polarized, IL-10 is released to play an immunosuppressive role. Additionally, M2 macrophages release TGF-β, which promotes the differentiation of regulatory T cells (Treg) which will release a large amount of IL-10 for immunosuppression. M2 macrophages and Tregs form a cancer-promoting environment[24]. M2 macrophages in the microenvironment are gradually transformed into M1 macrophages by reprogramming, which inhibits the polarization of M2 macrophages, reduces their immunosuppressive abilities, and restores the body's immunity. The immune microenvironment of the liver is complex and specific, and there is a certain natural immune tolerance. Various factors can cause the

Table 1 Chinese herbal compounds containing bezoars and their anti-tumor effects

Drug	Drug composition	Efficacy	Disease treated
Pien tze huang[12]	Bezoar, notoginseng, snake gall, musk	Clearing heat and detoxifying, cooling blood and removing stasis	Liver cancer, chronic hepatitis
Xihuang pill[13]	Bezoar, musk, frankincense, myrrh	Clearing heat and detoxifying, and relieving swelling	Breast cancer, scrofula
Kehuang capsule[14]	Bezoar, musk, snake gall, notoginseng, scutellaria, coptis, phellodendron Curcuma	Clearing heat and detoxifying, cooling blood and clearing knot	Liver cancer, chronic hepatitis
Niuhuang tianlong capsule[15]	Xihuang pill plus or minus	Clearing heat and detoxifying, dispersing knot and removing blood stasis	Cervical cancer, endometrial cancer
Niuhuang xingxiao pill[16]	Bezoar, musk, frankincense, myrrh	Clearing heat and detoxifying, cooling blood and removing stasis	Breast cancer, scrofula

occurrence of liver cancer. In situations of chronic inflammation, the body secretes immunosuppressive factors to suppress immune cells through excessive immunosuppression, leading to the occurrence of tumors. Notable among them are TAMs[25]. The liver is the body's parenchymatous organ containing the most macrophages, and it is also contains the highest immune cell population in the liver. As a bridge between the innate and adaptive immune system, it plays an important role in the treatment of liver cancer[26] (Figure 1).

BEZOARS AND BEZOAR-CONTAINING COMPOUNDS REGULATE THE IMMUNE MICROENVIRONMENT IN LIVER CANCER

The regulatory mechanisms by which bezoars and bezoar-containing compounds on liver cancer can occur in many ways. First, they can promote the apoptosis of liver cancer cells and inhibit their growth and metastasis by regulating liver cancer-related cells. Second, they can regulate the relevant signaling pathways, regulate and improve the tumor immune microenvironment, and inhibit the growth of tumors. The PD-1/PD-L1 signaling pathway plays a regulatory role in cell proliferation and apoptosis. By regulating the PD-1/PD-L1 signaling pathway, the polarization of macrophages and the expression of IL-6 cytokines are affected. Experimental data shows that the Xihuang Pill can prevent the further development of liver cancer by inhibiting PD-1/PD-L1 signaling[27]. NF-κB regulates immunity and inflammation in the body, and when activated, it promotes increased inflammatory cell infiltration to aggravate the inflammatory response. IL-1β and TNF-α as upstream factors of NF-κB, activate NF-κB which promotes the development of inflammation, and metastasis of cancer cells. Pien Tze Huang can reduce liver fibrosis and promote apoptosis of cancer cells by regulating the NF-κB signaling pathway. In addition, experimental studies have also found that Pien Tze Huang can reduce liver fibrosis by regulating autophagy as well as the TGF-β1/Smad signaling pathway[28-30]. The Wnt/β-catenin signaling pathway is an important signaling pathway regulating cell growth, development and differentiation. Many studies have found that activation of the Wnt/β-catenin signaling pathway promotes tumor development[31]. Studies have shown that there is a close relationship between Wnt and macrophages, and that macrophages can re-activate the Wnt signaling pathway in the tumor immune microenvironment, regulate Wnt in neighboring cells through paracysecretory, and affect the function of Wnt. In addition, Wnt signals in macrophages can change their own immune activation state and affect the homeostatic balance of surrounding organs after activation[32]. Wnt signaling in macrophages can increase the degree and progression of organ fibrosis by regulating the state of its immune response. Ye Feng found that Wnt/β-catenin signaling can promote the secretion of TGF-β and other pro-fibrotic factors by macrophages *in vitro*, and that the degree of fibrosis was reduced in mice where β-catenin was knocked out in myeloid cells. Inhibition of Wnt/β-catenin signaling can reduce the degree of bleomycin-induced pulmonary fibrosis in mice[33]. Regulating the Wnt/β-catenin signaling pathway is an effective strategy for the treatment of liver cancer. From the etiology of liver cancer, we have learned that chronic hepatitis is an important factor causing liver cancer. In some inflammatory diseases, macrophages and Wnt signaling are involved. Macrophages secrete some factors involved in immune tolerance, such as TGF-β and IL-10, and the expression of these cytokines is also a typical feature of M2 polarized macrophages, resulting in immunosuppression. When the Wnt/β-catenin signaling pathway is activated, it will promote the polarization of M2 macrophages to produce tumor promoting cytokines such as IL-10, generate Tregs, and promote the further development of tumors. The classical Wnt signal is transmitted to the upstream ligand *via* β-catenin to avoid excessive degradation of itself. M2-type macrophages promote tissue repair, and when β-catenin is silenced in macrophages, tumor cell mobility decreases. Cell experiments have shown that silenced β-catenin can slow down the cell healing rate and reduce tumor mobility to a certain extent, which can inhibit not only liver cancer but also a variety of tumors[34].

The application of bezoars and related preparations is not limited to experimental data and related basic research, and clinical applications have shown that their use in the treatment of liver cancer has also achieved effective therapeutic effects. Ning *et al*[35] found that the combined application of bezoars and imagination can promote apoptosis of liver cancer cells[35]. Xu *et al*[36] found that after TACE surgery in patients with primary liver cancer, the combination of acupuncture with the Xihuang Pill and conventional Western medicine treatments can significantly relieve patient pain,

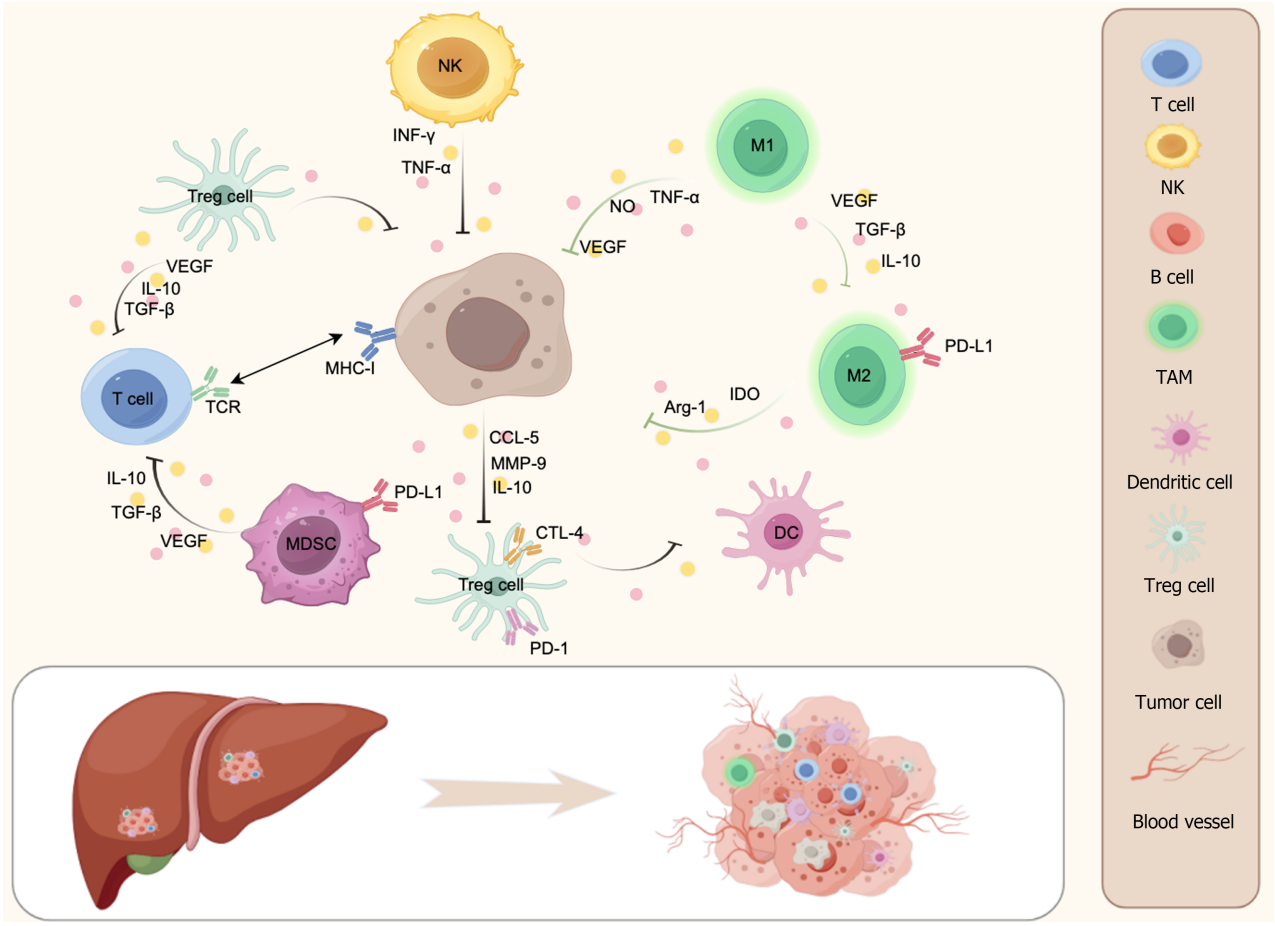

Figure 1 Liver cancer immune microenvironment. Created by Figdraw.

improve patient quality of life, and serum levels of AFP and GAS, which is worthy of clinical promotion and application [36]. Guo *et al*[37] found that Pian Zehuang combined with gamma knife stereotactic radiotherapy had fewer adverse reactions and could prolong the survival time of patients with primary liver cancer compared to radiotherapy[37].

In this paper, the TCM bezoar inhibits the polarization of M2 TAMs by inhibiting the activation of the Wnt/β-catenin signaling pathway to subsequently inhibit the development of liver cancer, which confirms the obvious effect of TCM on liver cancer.

RESEARCH AND DEVELOPMENT OF BEZOAR AND ANTI-TUMOR PREPARATIONS CONTAINING BEZOAR COMPOUND

In recent years, with the gradual deepening of the research on the prevention and treatment of cancer using TCM, we have found that TCM has the advantages of multi-pathway and multi-target effects, which translates to remarkable effects on the prevention and treatment of tumors[38]. However, the application of TCM in cancer has the disadvantages of instability and poor water solubility, which limits its clinical application and exploration. With the deepening of research on the chemistry and pharmacology of TCM, thus the use of nano preparations in TCM is quite clear. Nano preparation of TCM has the advantages of reducing toxicity and promoting more accurate targeting[39,40]. Studies have found that a variety of single herbs have shown good therapeutic effects in the treatment of malignant tumors. Nano polysaccharides can enhance the stability of TCM compounds[41]. Zhang *et al*[42] found that Sanqi compound nanoparticles had significant antithrombotic effect[42]. Reviewing the application history and value of bezoars in Linchuan may result in more accurate targeted treatments that may be achieved through the development of nano-bezoars in anti-tumor treatment. Nano-preparations can be given in multi-unit administration in the field of TCM. Bezoars can be divided into independent drug units, which are further processed by wet grinding, high pressure homogenization, liquid nitrogen freezing and other methods. It was found that the antitumor activity of the multi-unit drug delivery system for a Chinese medicine Niuhuang Xingxiao Pill was significantly higher than that of the Niuhuang Xingxiao Pill[43].

Through this article, we found that the TCM bezoar can affect the macrophages and immune microenvironment of tumor patients through relevant signaling pathways. This suggests that the nano-bezoar has great potential for future development, providing a new means for the treatment of liver cancer by the TCM bezoar and the compound preparation

containing bezoar[44].

CLINICAL IMPLICATIONS

TCM, as a traditional means of treating diseases in China, has a long history. Even with the development of molecular biology and pharmacological technology, TCM is effective in the treatment of cancer. Whether it is used alone or with multiple drugs combined, it can inhibit and reverse the tumor to some extent. The composition of TCM is complex, and it can be applied in multiple targets with high safety. The use of TCM can positively regulate the immune microenvironment in tumor patients, inhibit the negative feedback signal pathways, and restore the body's immune ability to achieve anti-tumor effects. However, the first shortcoming is that the exploration of a variety of Chinese medicines is not in-depth enough, and there is a lack of clinical trial data to reveal its anti-tumor mechanism of action. More clinical trials and data sorting are needed to further discover, reveal, and prove the mechanism of action of Chinese medicine on tumors. In addition, single drug or compound preparations need to be further optimized and developed, and modern nanotechnology is needed to improve the stability and accuracy of TCM in the treatment of tumors, and to improve clinical efficacy.

FOOTNOTES

Author contributions: Li DH designed the overall concept and outline of the manuscript; Wen QE contributed to the discussion and design of the manuscript; Li DH, Wen QE, Feng RQ, and Qiao C contributed to the writing and editing of the manuscript, and the review of the literature; Wen QE and Tian XT drew pictures for the manuscript; All authors have read and approved the final manuscript.

Supported by 2023 Government-funded Project of The Outstanding Talents Training Program in Clinical Medicine, No. ZF2023165; Key Research and Development Projects of Hebei Province, No. 18277731D; and Natural Science Foundation of Hebei Province, No. H202423105.

Conflict-of-interest statement: All the authors report no relevant conflicts of interest for this article.

Country of origin: China

ORCID number: De-Hui Li 0000-0001-7963-9410.

S-Editor: Li L
L-Editor: A
P-Editor: Cai YX

REFERENCES

1 **Rumgay H**, Arnold M, Ferlay J, Lesi O, Cabasag CJ, Vignat J, Laversanne M, McGlynn KA, Soerjomataram I. Global burden of primary liver cancer in 2020 and predictions to 2040. *J Hepatol* 2022; **77**: 1598-1606 [PMID: 36208844 DOI: 10.1016/j.jhep.2022.08.021]
2 **Ganesan P**, Kulik LM. Hepatocellular Carcinoma: New Developments. *Clin Liver Dis* 2023; **27**: 85-102 [PMID: 36400469 DOI: 10.1016/j.cld.2022.08.004]
3 **Hao Y**, Li C, Wen TF, Peng W. [Epidemiological characteristics of liver cancer worldwide and in China: an interpretation of global cancer statistics 2022]. *Zhongguo Puwai Jichu Yu Linchuang Zazhi* 2024; **31**: 781-789 [DOI: 10.7507/1007-9424.202405099]
4 **Sia D**, Villanueva A, Friedman SL, Llovet JM. Liver Cancer Cell of Origin, Molecular Class, and Effects on Patient Prognosis. *Gastroenterology* 2017; **152**: 745-761 [PMID: 28043904 DOI: 10.1053/j.gastro.2016.11.048]
5 **Anwanwan D**, Singh SK, Singh S, Saikam V, Singh R. Challenges in liver cancer and possible treatment approaches. *Biochim Biophys Acta Rev Cancer* 2020; **1873**: 188314 [PMID: 31682895 DOI: 10.1016/j.bbcan.2019.188314]
6 **Yang JD**, Hainaut P, Gores GJ, Amadou A, Plymoth A, Roberts LR. A global view of hepatocellular carcinoma: trends, risk, prevention and management. *Nat Rev Gastroenterol Hepatol* 2019; **16**: 589-604 [PMID: 31439937 DOI: 10.1038/s41575-019-0186-y]
7 **Chen H**, Wang J. [Exploration of the property, effect and usage of Niuhuang]. *Shanxi Zhongyiyao Daxue Xuebao* 2023; **24**: 509-512+524 [DOI: 10.19763/j.cnki.2096-7403.2023.05.08]
8 **Chen H**, Wang J. [Research progress on main active components of bezoar and pharmacological effects in central system]. *Hebei Zhongyi* 2022; **44**: 1228-1232 [DOI: 10.3969/j.issn.1002-2619.2022.07.038]
9 **Wang SH**, Liu Q, Qin PJ, An H, Zhu TY, Zhang FX, Liu JF. [Progress of basic and clinical research on Bovis Calculus cultured in vitro]. *Zhongguo Yiyao Daobao* 2024; **21**: 38-41 [DOI: 10.20047/j.issn1673-7210.2024.06.08]
10 **Li LQ**, Zhao YQ. [The mechanism and clinical research progress of bezoar in the treatment of liver cancer]. *Hubei Zhongyi Zazhi* 2009; **31**:

77-78 [DOI: 10.3969/j.issn.1000-0704.2009.11.053]
11 **Li YC**, Zhang HX. [Overview of Mechanism of TCM Prevention and Treatment of Liver Cancer]. *Shiyong Zhongyi Neike Zazhi* 2024; **38**: 43-47
12 **Chen HY**. Clinical study of Pian Tze Huang Capsule in the treatment of medium or advanced PHC (especially accompanied by liver heat and blood stagnation). Doctoral dissertations, Guangzhou University of Chinese Medicine. 2020. Available from: https://cdmd.cnki.com.cn/Article/CDMD-10572-1021029648.htm
13 **Li DH**, Su YF, Fan HF, Sun CX, Han CH, Ma P, Yan JJ, Lv SJ. [Xihuang pill reversing precancerous lesions of breast cancer in rats and regulating the expression of NF-kappa B protein]. *Zhongguo Laonianxue Zazhi* 2021; **41**: 131-134 [DOI: 10.3969/j.issn.1005-9202.2021.01.038]
14 **Ji CF**, Zhang MM. [Effect of Kehuang capsule on hepatocellular carcinoma cells before and after using artificial musk and artificial bezoar]. *Zhongguo Xiandai Yaowu Yingyong* 2020; **14**: 249-252 [DOI: 10.14164/j.cnki.cn11-5581/r.2020.13.111]
15 **Huang L**, Huang D, Xing HY, Cheng JX, Ma XG, Huang Y. [Experimental study of the anti-tumor mechanisms of the traditional Chinese herbal prescription Niuhuangtianlong capsule]. *Hebei Yiyao* 2013; **35**: 2247-2249
16 **Shi F**, Yang G, Liu Y, Feng NP. Investigation of nanosized drug delivery systems for Chinese compound medicine: taking Niuhuangxingxiao Wan as an example. "Good Doctor Cup" Forum on Innovation and Development of Chinese Medicine preparations (Part 1). 2013 Oct 26; Chengdu. China: Chinese Medicine Preparation Branch, World Federation of Chinese Medicine Societies, Chinese Medicine Pharmacy Professional Committee, 2013: 314-317
17 **Wang Z**, Li M, Bi L, Hu X, Wang Y. Traditional Chinese Medicine in Regulating Tumor Microenvironment. *Onco Targets Ther* 2024; **17**: 313-325 [PMID: 38617090 DOI: 10.2147/OTT.S444214]
18 **Xue R**, Zhang Q, Cao Q, Kong R, Xiang X, Liu H, Feng M, Wang F, Cheng J, Li Z, Zhan Q, Deng M, Zhu J, Zhang Z, Zhang N. Liver tumour immune microenvironment subtypes and neutrophil heterogeneity. *Nature* 2022; **612**: 141-147 [PMID: 36352227 DOI: 10.1038/s41586-022-05400-x]
19 **Tang Q**, Chen Y, Li X, Long S, Shi Y, Yu Y, Wu W, Han L, Wang S. The role of PD-1/PD-L1 and application of immune-checkpoint inhibitors in human cancers. *Front Immunol* 2022; **13**: 964442 [PMID: 36177034 DOI: 10.3389/fimmu.2022.964442]
20 **Wen QE**, Li L, Feng RQ, Li DH, Qiao C, Xu XS, Zhang YJ. Recent Advances in Immunotherapy for Breast Cancer: A Review. *Breast Cancer (Dove Med Press)* 2024; **16**: 497-516 [PMID: 39220564 DOI: 10.2147/BCTT.S482504]
21 **Wang P**, Chou JN, Wang XZ, Wu JH, Jiang CP. [Research advances in tumor-associated macrophages in hepatocellular carcinoma microenvironment]. *Linchuang Gandanbing Zazhi* 2022; **39**: 1212-1218 [DOI: 10.3969/j.issn.1001-5256.2023.05.033]
22 **Liu L**, Zhang R, Deng J, Dai X, Zhu X, Fu Q, Zhang H, Tong Z, Zhao P, Fang W, Zheng Y, Bao X. Construction of TME and Identification of crosstalk between malignant cells and macrophages by SPP1 in hepatocellular carcinoma. *Cancer Immunol Immunother* 2022; **71**: 121-136 [PMID: 34028567 DOI: 10.1007/s00262-021-02967-8]
23 **Zhang X**, Yu C, Zhao S, Wang M, Shang L, Zhou J, Ma Y. The role of tumor-associated macrophages in hepatocellular carcinoma progression: A narrative review. *Cancer Med* 2023; **12**: 22109-22129 [PMID: 38098217 DOI: 10.1002/cam4.6717]
24 **Capece D**, Fischietti M, Verzella D, Gaggiano A, Cicciarelli G, Tessitore A, Zazzeroni F, Alesse E. The inflammatory microenvironment in hepatocellular carcinoma: a pivotal role for tumor-associated macrophages. *Biomed Res Int* 2013; **2013**: 187204 [PMID: 23533994 DOI: 10.1155/2013/187204]
25 **Oura K**, Morishita A, Tani J, Masaki T. Tumor Immune Microenvironment and Immunosuppressive Therapy in Hepatocellular Carcinoma: A Review. *Int J Mol Sci* 2021; **22**: 5801 [PMID: 34071550 DOI: 10.3390/ijms22115801]
26 **Shen KY**, Zhu Y, Xie SZ, Qin LX. Immunosuppressive tumor microenvironment and immunotherapy of hepatocellular carcinoma: current status and prospectives. *J Hematol Oncol* 2024; **17**: 25 [PMID: 38679698 DOI: 10.1186/s13045-024-01549-2]
27 **Wang Y**, Wang W, Liu K, Liu Y, Shen X, Li Q, Deng F, Hao X, Wang Y. The mechanism of Xihuang pills' intervention in the tumour immune microenvironment for the treatment of liver cancer based on the STAT3-PDL1 pathway. *J Ethnopharmacol* 2024; **331**: 118278 [PMID: 38710457 DOI: 10.1016/j.jep.2024.118278]
28 **Zheng H**, Wang X, Zhang Y, Chen L, Hua L, Xu W. Pien-Tze-Huang ameliorates hepatic fibrosis *via* suppressing NF-κB pathway and promoting HSC apoptosis. *J Ethnopharmacol* 2019; **244**: 111856 [PMID: 30959141 DOI: 10.1016/j.jep.2019.111856]
29 **Zhang Y**, Hua L, Lin C, Yuan M, Xu W, Raj D A, Venkidasamy B, Cespedes-Acuna CL, Nile SH, Yan G, Zheng H. Pien-Tze-Huang alleviates CCl(4)-induced liver fibrosis through the inhibition of HSC autophagy and the TGF-β1/Smad2 pathway. *Front Pharmacol* 2022; **13**: 937484 [PMID: 36188553 DOI: 10.3389/fphar.2022.937484]
30 **Zheng HY**, Hua LP, Zhang YQ, Wang XY, Xu W. [Effects of Pien Tze Huang on Liver Function and Nuclear Factor-κB Protein Expression in Rats with Hepatic Fibrosis Induced by Carbon Tetrachloride]. *Zhongguo Zhongyiyao Xinxi Zazhi* 2019; **26**: 57-60 [DOI: 10.3969/j.issn.1005-5304.2019.04.013]
31 **Li ZH**. ASPM Promotes Hepatocarcinogenesis Through Wnt/β-Catenin Signaling Pathway. MSc Thesis, Zhengzhou University. 2019. Available from: https://cdmd.cnki.com.cn/article/cdmd-10459-1018119413.htm
32 **Weng JQ**, Lu WP, Cui SS, Zhao ZZ. [Effect of Xihuang Pill on the proliferation and dry spheroidization ability of 4T1 cells through Wnt/β-catenin pathway]. *Beijing Zhongyiyao* 2021; **40**: 968-972 [DOI: 10.16025/j.1674-1307.2021.09.008]
33 **Yang Y**. Wnt/β-catenin signaling regulates M2-like macrophage polarization and reinforces the abilities to promote the progression of hepatocellular carcinoma. Doctoral dissertations, Air Force Medical University. 2019 [DOI: 10.27002/d.cnki.gsjyu.2019.000086]
34 **Tan J**, Wang YF, Dai ZH, Yin HZ, Yang F. [YTHDF1 promotes hepatocellular carcinoma progression by increasing the stemness of HCC cells and activating the Wnt/β-catenin signaling pathway]. *Zhongguo Linchuang Yixue* 2022; **29**: 738-744 [DOI: 10.12025/j.issn.1008-6358.2022.20220128]
35 **Ning DM**, Deng Z, Wu YR. [Niuhuang (Bovis Calculus)-Shexiang (Moschus) combination induces apoptosisand inhibits proliferation in hepatocellular carcinoma *via* PI3K/AKT/mTOR pathway]. *Shuzi Zhongyiyao* 2022; **5**: 83-92 [DOI: 10.1016/j.dcmed.2022.03.009]
36 **Xu JL**, Lu KJ, Zhou LZ. [Clinical observation of chemotherapy embolization for positive liver cancer treated by combination of acupuncture and Xihuang pill]. *Yatai Chuantong Yiyao* 2024; **20**: 96-99
37 **Guo HYB**, Huang W, Cao HM, Wang GL, Wu Y, Xu YC, Zhou J. [Clinical study on Pian Tze Huang combined with gamma knife in treating primary liver cance]. *Zhongguo Zhongxiyijiehe Xiaohua Zazhi* 2019; **27**: 735-738+742
38 **Wei D**, Yang H, Zhang Y, Zhang X, Wang J, Wu X, Chang J. Nano-traditional Chinese medicine: a promising strategy and its recent advances. *J Mater Chem B* 2022; **10**: 2973-2994 [PMID: 35380567 DOI: 10.1039/d2tb00225f]

39 **Zheng Y**, Wang Y, Xia M, Gao Y, Zhang L, Song Y, Zhang C. The combination of nanotechnology and traditional Chinese medicine (TCM) inspires the modernization of TCM: review on nanotechnology in TCM-based drug delivery systems. *Drug Deliv Transl Res* 2022; **12**: 1306-1325 [PMID: 34260049 DOI: 10.1007/s13346-021-01029-x]

40 **Liu ZY**, Luo JY, Lu Y, DU SY. [Application of traditional Chinese medicine theory in modern traditional Chinese medicine nano-preparation: taking tumor treatment as an example]. *Zhongguo Zhong Yao Za Zhi* 2023; **48**: 1455-1462 [PMID: 37005833 DOI: 10.19540/j.cnki.cjcmm.20221128.302]

41 **Wang J**, Wu X, Chen J, Gao T, Zhang Y, Yu N. Traditional Chinese medicine polysaccharide in nano-drug delivery systems: Current progress and future perspectives. *Biomed Pharmacother* 2024; **173**: 116330 [PMID: 38422656 DOI: 10.1016/j.biopha.2024.116330]

42 **Zhang JL**, Jia C, Yuan B, Wang Y, Cheng JY. [Study on the inhibitory effect of Sanqi compound nano granules on thrombosis and its mechanism]. *Zhongguo Shiyan Fangjixue Zazhi* 2010; **16**: 81-83 [DOI: 10.13422/j.cnki.syfjx.2010.02.039]

43 **Tian L**, Ke X, Sun MY, Lin CL, Chen Q, Huang MH. [Development and Modernization of Nano-Chinese medicine]. *Shijie Zhongyiyao* 2023; **18**: 588-592 [DOI: 10.3969/j.issn.1673-7202.2023.04.026]

44 **Huang Z**, Meng FY, Lu LZ, Guo QQ, Lv CJ, Tan NH, Deng Z, Chen JY, Zhang ZS, Zou B, Long HP, Zhou Q, Tian S, Mei S, Tian XF. Calculus bovis inhibits M2 tumor-associated macrophage polarization *via* Wnt/β-catenin pathway modulation to suppress liver cancer. *World J Gastroenterol* 2024; **30**: 3511-3533 [PMID: 39156500 DOI: 10.3748/wjg.v30.i29.3511]

World Journal of Gastrointestinal Oncology

Submit a Manuscript: https://www.f6publishing.com

World J Gastrointest Oncol 2024 December 15; 16(12): 4778-4781

DOI: 10.4251/wjgo.v16.i12.4778

ISSN 1948-5204 (online)

LETTER TO THE EDITOR

Crosslink among cyclin-dependent kinase 9, ATP binding cassette transporter G2 and Beclin 1 in colorectal cancer

Zhong-Bao Shao, Ke He, Yu-Bin Su, Zhi Shi

Specialty type: Oncology

Provenance and peer review: Invited article; Externally peer reviewed.

Peer-review model: Single blind

Peer-review report's classification

Scientific Quality: Grade B
Novelty: Grade B
Creativity or Innovation: Grade B
Scientific Significance: Grade B

P-Reviewer: Sipos F

Received: August 21, 2024
Revised: September 19, 2024
Accepted: October 12, 2024
Published online: December 15, 2024
Processing time: 83 Days and 0.7 Hours

Zhong-Bao Shao, Ke He, Zhi Shi, Cancer Minimally Invasive Therapies Centre, Guangdong Second Provincial General Hospital, Jinan University, Guangzhou 510632, Guangdong Province, China

Zhong-Bao Shao, Yu-Bin Su, Zhi Shi, Department of Cell Biology & Institute of Biomedicine, Guangdong Provincial Biotechnology & Engineering Technology Research Center, Guangdong Provincial Key Laboratory of Bioengineering Medicine, Genomic Medicine Engineering Research Center of Ministry of Education, MOE Key Laboratory of Tumor Molecular Biology, National Engineering Research Center of Genetic Medicine, State Key Laboratory of Bioactive Molecules and Druggability Assessment, College of Life Science and Technology, Jinan University, Guangzhou 510632, Guangdong Province, China

Co-first authors: Zhong-Bao Shao and Ke He.

Corresponding author: Zhi Shi, MD, PhD, Professor, Department of Cell Biology & Institute of Biomedicine, Guangdong Provincial Biotechnology & Engineering Technology Research Center, Guangdong Provincial Key Laboratory of Bioengineering Medicine, Genomic Medicine Engineering Research Center of Ministry of Education, MOE Key Laboratory of Tumor Molecular Biology, National Engineering Research Center of Genetic Medicine, State Key Laboratory of Bioactive Molecules and Druggability Assessment, College of Life Science and Technology, Jinan University, No. 601 Huangpu Avenue West, Guangzhou 510632, Guangdong Province, China. tshizhi@jnu.edu.cn

Abstract

Colorectal cancer (CRC) ranks third in the number of cancers mainly because of the inability to diagnose it at an early stage. The pathogenesis of CRC is complicated, which is the result of the complex interaction of multiple genetic and environmental factors. Currently, one of the main treatments for CRC is chemotherapy. But the primary cause of CRC treatment failure is drug resistance. The expression of cyclin-dependent kinase 9 (CDK9) was correlated with elevated autophagy levels in colon cancer, and high expression of CDK9 indicates a poor prognosis in CRC. The incidence of autophagy and the expressions of Beclin 1 and ATP binding cassette transporter G2 are different in left and right colon cancer, and autophagy may be involved in the occurrence of chemotherapy resistance. In this article, the roles of CDK9, ATP binding cassette transporter G2 and Beclin 1 in CRC were elucidated, emphasizing the linkages among them and providing potential therapeutic targets of CRC.

Key Words: Cyclin-dependent kinase 9; ATP binding cassette transporter G2; Beclin 1; Colorectal cancer; Chemotherapy

Core Tip: The expression of cyclin-dependent kinase 9 (CDK9) was correlated with elevated autophagy levels in colon cancer, and high expression of CDK9 indicates a poor prognosis in colorectal cancer (CRC). The incidence of autophagy and the expressions of Beclin 1 and ATP binding cassette transporter G2 were different between left and right colon cancer. The roles of CDK9, ATP binding cassette transporter G2 and Beclin 1 in CRC were clarified, underlining the linkages among them and providing potential therapeutic targets of CRC.

Citation: Shao ZB, He K, Su YB, Shi Z. Crosslink among cyclin-dependent kinase 9, ATP binding cassette transporter G2 and Beclin 1 in colorectal cancer. *World J Gastrointest Oncol* 2024; 16(12): 4778-4781
URL: https://www.wjgnet.com/1948-5204/full/v16/i12/4778.htm
DOI: https://dx.doi.org/10.4251/wjgo.v16.i12.4778

TO THE EDITOR

A clinical and translational study by Zheng *et al*[1], reported that the rate of autophagy and the expressions of Beclin 1 (BECN1) and ATP binding cassette transporter G2 (ABCG2) differed between left and right colon cancer tissues. Autophagy may be associated with chemotherapy resistance in colorectal cancer (CRC) patients. And cyclin dependent kinase 9 (CDK9) is highly expressed in CRC that can be used as a prognostic marker in CRC patients. This research could provide a theoretical basis for the exploration of CDK9 and autophagy inhibitors in combination therapy to enhance tumor cell sensitivity to chemotherapy.

CRC ranks third in the number of cancers mainly owing to the inability to diagnose it at an early stage[2]. The pathogenesis of CRC is complexed, which is the result of the complex interaction of a lot of genetic and environmental factors[3]. At present, one of the main treatments for CRC is chemotherapy. But the primary cause of CRC treatment failure is drug resistance[4]. Consequently, elucidating research into molecular mechanisms of drug resistance can be beneficial to develop new diagnostic or therapeutic strategies to overcome the challenges in the treatment of CRC.

THE CROSSLINK AMONG CDK9, ABCG2 AND BECN1 IN CRC

ABCG2, as an important member of the ATP-binding cassette transmembrane transporter superfamily, plays a significant role in cancer multidrug resistance[5]. Several agents have been reported to be able to reverse ABCG2-mediated multidrug resistance in CRC cells by inhibiting the transporter activity of ABCG2[6,7]. Now, we are interested in the authors' new finding that the expression level of ABCG2 in right colon cancer was higher than that in paracarcinoma tissue, but the expression level of ABCG2 was not significantly different between left colon cancer and paracarcinoma tissue. These findings might be useful for gaining insight into the pathogenesis of left and right colon cancer and improving treatment strategies for CRC therapy.

Autophagy refers to a catabolic process in which macromolecular substances such as misfolded proteins and damaged organelles are transported to lysosomes for degradation[8]. It can prevent genome damage and induce cancer cell death. And on the other hand, autophagy is a pro-oncogenic mechanism that provides drug resistance to cancer cells and promotes cancer cell growth[9]. The sensitivity of cancer cells to chemotherapeutic drugs can be restored by the use of autophagy inhibitors, such as chloroquine, or by the knockdown of autophagy-related proteins, including BECN1, autophagy-related gene 7, and autophagy-related gene 10[10]. Currently, autophagy inhibitors are promising for cancer treatment. Some small molecule autophagy inhibitors have been discovered according to the autophagy process[10]. Recent research has revealed FDW028 (a novel FUT8 inhibitor) exhibits potent anti CRC effects by facilitating lysosomal degradation of CD276 through the chaperone-mediated autophagy pathway[11]. Erianin (a natural product) can induce autophagy-dependent ferroptosis and inhibit tumor growth and metastasis in $KRAS^{G13D}$ CRC[12]. Strigolactones are endogenous plant hormones that can act as a potential autophagy inhibitor by blocking autophagosome-lysosome fusion in HCT116 CRC cells[13]. BECN1, a key autophagy regulator, serves as a potential therapeutic target and is associated with chemotherapeutic resistance in cancers[14]. Previous studies have demonstrated that JAK2-depended BECN1 phosphorylation may confer chemotherapy resistance in CRC[15]. Based on Zheng *et al*'s research, the expression of BECN1 may be different between left and right colon cancer[1]. This research provided new ideas for further investigation on the drug resistance in CRC.

CDK family, a large class of serine/threonine protein kinases, plays a vital role in cell cycle progression and gene transcription regulation. There have been some reports on CDK inhibitors in the treatment of CRC. Zeng *et al*[16] proposed that CDK1 serves as a potential target for oxaliplatin-resistant CRC treatment. Lee *et al*[17] reported that the combination of palbociclib (CDK 4/6 inhibitor) and gedatolisib (phosphatidylinositol 3-kinase/mammalian target of

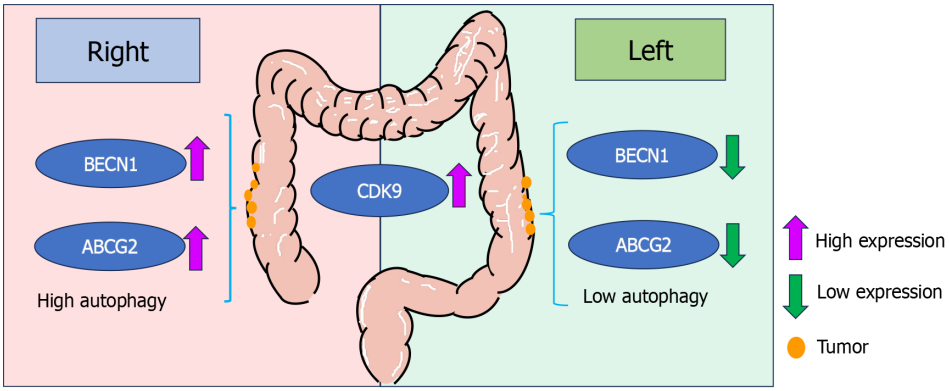

Figure 1 The relationships between cyclin-dependent kinase 9, ATP binding cassette transporter G2, Beclin 1 and autophagy in colorectal cancers. CDK9: Cyclin-dependent kinase 9; BECN1: Beclin 1; ABCG2: ATP binding cassette transporter G2.

rapamycin dual inhibitor) has synergistic anti-proliferative effects in both wild-type and mutated CRC cell lines. In a recent study, Wang *et al*[18] revealed that CDK3, CDK5 and CDK8 functioned as potential diagnostic markers for CRC. These findings give rationale for the application of CDK inhibitors in CRC treatment. CDK9 is an important member of the CDK family that regulates the transcription of genes such as chemoresistant genes in tumors, and some CDK9 inhibitors have entered clinical trials in combination with other drugs[19]. According to Zheng *et al*[1], the expression of CDK9 is positively correlated with autophagy in colon cancer. This finding may provide valuable information for further research on targeting CDK9 as a therapeutic strategy for CRC. The relationships between CDK9, BECN1, ABCG2 and autophagy are show in Figure 1.

CONCLUSION

The expression of CDK9 was correlated with elevated autophagy levels in colon cancer. Additionally, the expressions of ABCG2 and BECN1 were different between left and right colon cancer patients. Targeting CDK9, ABCG2 and BECN1 might be potential therapeutic strategies for CRC.

ACKNOWLEDGEMENTS

Thanks to all authors for their efforts in this work.

FOOTNOTES

Author contributions: Shao ZB, He K, Su YB, and Shi Z contributed to this paper; Shi Z designed the overall concept and outline of the manuscript; Su YB contributed to the discussion of the manuscript; Shao ZB and He K contributed to the writing, and editing the manuscript, and review of literature, they are the co-first authors of this article.

Supported by the National Natural Science Foundation of China, No. 82272996; and the Science and Technology Program of Guangzhou, No. 202206010081.

Conflict-of-interest statement: All the authors report no relevant conflicts of interest for this article.

Country of origin: China

ORCID number: Zhi Shi 0000-0002-8328-0305.

S-Editor: Wang JJ
L-Editor: A
P-Editor: Wang WB

REFERENCES

1 **Zheng L**, Lu J, Kong DL. Expression of cyclin-dependent kinase 9 is positively correlated with the autophagy level in colon cancer. *World J Gastrointest Oncol* 2024; **16**: 314-330 [PMID: 38425408 DOI: 10.4251/wjgo.v16.i2.314]

2 **Zhang Y**, Wang Y, Zhang B, Li P, Zhao Y. Methods and biomarkers for early detection, prediction, and diagnosis of colorectal cancer. *Biomed Pharmacother* 2023; **163**: 114786 [PMID: 37119736 DOI: 10.1016/j.biopha.2023.114786]

3 **Ionescu VA**, Gheorghe G, Bacalbasa N, Chiotoroiu AL, Diaconu C. Colorectal Cancer: From Risk Factors to Oncogenesis. *Medicina (Kaunas)* 2023; **59** [PMID: 37763765 DOI: 10.3390/medicina59091646]

4 **Zhang L**, Lu X, Xu Y, La X, Tian J, Li A, Li H, Wu C, Xi Y, Song G, Zhou Z, Bai W, An L, Li Z. Tumor-associated macrophages confer colorectal cancer 5-fluorouracil resistance by promoting MRP1 membrane translocation *via* an intercellular CXCL17/CXCL22-CCR4-ATF6-GRP78 axis. *Cell Death Dis* 2023; **14**: 582 [PMID: 37658050 DOI: 10.1038/s41419-023-06108-0]

5 **Li W**, Zhang H, Assaraf YG, Zhao K, Xu X, Xie J, Yang DH, Chen ZS. Overcoming ABC transporter-mediated multidrug resistance: Molecular mechanisms and novel therapeutic drug strategies. *Drug Resist Updat* 2016; **27**: 14-29 [PMID: 27449595 DOI: 10.1016/j.drup.2016.05.001]

6 **Yu ZZ**, Xu BQ, Wang YY, Zhang PW, Shu YB, Shi Z. GSK2606414 Sensitizes ABCG2-Overexpressing Multidrug-Resistant Colorectal Cancer Cells to Chemotherapeutic Drugs. *Biomedicines* 2023; **11** [PMID: 38002103 DOI: 10.3390/biomedicines11113103]

7 **Liu K**, Chen Y, Shi XB, Xing ZH, He ZJ, Wang ST, Li YC, Liu WJ, Zhang PW, Yu ZZ, Mo XM, Shi XY, Chen ZS, Shi Z. Inhibiting the Activity of ABCG2 by KU55933 in Colorectal Cancer. *Recent Pat Anticancer Drug Discov* 2022; **17**: 387-395 [PMID: 35023460 DOI: 10.2174/1574892817666220112100036]

8 **Cao W**, Li J, Yang K, Cao D. An overview of autophagy: Mechanism, regulation and research progress. *Bull Cancer* 2021; **108**: 304-322 [PMID: 33423775 DOI: 10.1016/j.bulcan.2020.11.004]

9 **Kocaturk NM**, Akkoc Y, Kig C, Bayraktar O, Gozuacik D, Kutlu O. Autophagy as a molecular target for cancer treatment. *Eur J Pharm Sci* 2019; **134**: 116-137 [PMID: 30981885 DOI: 10.1016/j.ejps.2019.04.011]

10 **Chen JL**, Wu X, Yin D, Jia XH, Chen X, Gu ZY, Zhu XM. Autophagy inhibitors for cancer therapy: Small molecules and nanomedicines. *Pharmacol Ther* 2023; **249**: 108485 [PMID: 37406740 DOI: 10.1016/j.pharmthera.2023.108485]

11 **Wang M**, Zhang Z, Chen M, Lv Y, Tian S, Meng F, Zhang Y, Guo X, Chen Y, Yang M, Li J, Qiu T, Xu F, Li Z, Zhang Q, Yang J, Sun J, Zhang H, Zhang H, Li H, Wang W. FDW028, a novel FUT8 inhibitor, impels lysosomal proteolysis of B7-H3 *via* chaperone-mediated autophagy pathway and exhibits potent efficacy against metastatic colorectal cancer. *Cell Death Dis* 2023; **14**: 495 [PMID: 37537172 DOI: 10.1038/s41419-023-06027-0]

12 **Miao Q**, Deng WQ, Lyu WY, Sun ZT, Fan SR, Qi M, Qiu SH, Zhu YR, Lin JP, Chen MF, Deng LJ. Erianin inhibits the growth and metastasis through autophagy-dependent ferroptosis in KRAS(G13D) colorectal cancer. *Free Radic Biol Med* 2023; **204**: 301-312 [PMID: 37217090 DOI: 10.1016/j.freeradbiomed.2023.05.008]

13 **Yang ST**, Fan JB, Liu TT, Ning S, Xu JH, Zhou YJ, Deng X. Development of Strigolactones as Novel Autophagy/Mitophagy Inhibitors against Colorectal Cancer Cells by Blocking the Autophagosome-Lysosome Fusion. *J Med Chem* 2022 [PMID: 35852796 DOI: 10.1021/acs.jmedchem.2c00275]

14 **Prerna K**, Dubey VK. Beclin1-mediated interplay between autophagy and apoptosis: New understanding. *Int J Biol Macromol* 2022; **204**: 258-273 [PMID: 35143849 DOI: 10.1016/j.ijbiomac.2022.02.005]

15 **Hu F**, Song D, Yan Y, Huang C, Shen C, Lan J, Chen Y, Liu A, Wu Q, Sun L, Xu F, Hu F, Chen L, Luo X, Feng Y, Huang S, Hu J, Wang G. IL-6 regulates autophagy and chemotherapy resistance by promoting BECN1 phosphorylation. *Nat Commun* 2021; **12**: 3651 [PMID: 34131122 DOI: 10.1038/s41467-021-23923-1]

16 **Zeng K**, Li W, Wang Y, Zhang Z, Zhang L, Zhang W, Xing Y, Zhou C. Inhibition of CDK1 Overcomes Oxaliplatin Resistance by Regulating ACSL4-mediated Ferroptosis in Colorectal Cancer. *Adv Sci (Weinh)* 2023; **10**: e2301088 [PMID: 37428466 DOI: 10.1002/advs.202301088]

17 **Lee CL**, Cremona M, Farrelly A, Workman JA, Kennedy S, Aslam R, Carr A, Madden S, O'Neill B, Hennessy BT, Toomey S. Preclinical evaluation of the CDK4/6 inhibitor palbociclib in combination with a PI3K or MEK inhibitor in colorectal cancer. *Cancer Biol Ther* 2023; **24**: 2223388 [PMID: 37326340 DOI: 10.1080/15384047.2023.2223388]

18 **Wang D**, Zhou Y, Hua L, Li J, Zhu N, Liu Y. CDK3, CDK5 and CDK8 Proteins as Prognostic and Potential Biomarkers in Colorectal Cancer Patients. *Int J Gen Med* 2022; **15**: 2233-2245 [PMID: 35250301 DOI: 10.2147/IJGM.S349576]

19 **Mandal R**, Becker S, Strebhardt K. Targeting CDK9 for Anti-Cancer Therapeutics. *Cancers (Basel)* 2021; **13** [PMID: 34062779 DOI: 10.3390/cancers13092181]

Published by **Baishideng Publishing Group Inc**
7041 Koll Center Parkway, Suite 160, Pleasanton, CA 94566, USA
Telephone: +1-925-3991568
E-mail: office@baishideng.com
Help Desk: https://www.f6publishing.com/helpdesk
https://www.wjgnet.com